

A D - 774 743

AIR FORCE CAMBRIDGE RESEARCH LABORATORIES REPORT ON RESEARCH

John F. Dempsey

Air Force Cambridge Research Laboratories
L. G. Hanscom Field, Massachusetts

February 1973

DISTRIBUTED BY:



National Technical Information Service
U. S. DEPARTMENT OF COMMERCE
5285 Port Royal Road, Springfield Va. 22151

ACCESSION	
BTB	W32c Section
DOC	Best Section
MANUFACTURED	
JUSTIFICATION	
BY	
DESTRUCTION INABILITY OF IT	
864 DATE 3-18-87	

[Handwritten signature]

This document has been approved for public release and sale;
its distribution is unlimited.

Qualified requestors may obtain additional copies from the
Defense Documentation Center. All others should apply to the
Clearinghouse for Federal Scientific and Technical Information.

Unclassified

Security Classification

AD 774743

DOCUMENT CONTROL DATA - R&D

(Security classification of title, body of abstract and indexing annotation must be entered when the overall report is classified)

1. ORIGINATING ACTIVITY (Corporate author) Air Force Cambridge Research Laboratories (CA) L. G. Hanscom Field Bedford, Massachusetts 01730	2a. REPORT SECURITY CLASSIFICATION Unclassified
	2b. GROUP

3. REPORT TITLE

AIR FORCE CAMBRIDGE RESEARCH LABORATORIES
REPORT ON RESEARCH

4. DESCRIPTIVE NOTES (Type of report and inclusive dates)

Scientific. Interim. July 1, 1970 through June 30, 1972

5. AUTHOR(S) (First name, middle initial, last name)

John F. Dempsey, Editor

6. REPORT DATE February 1973	7a. TOTAL NO. OF PAGES 374	7b. NO. OF REFS 0
8a. CONTRACT OR GRANT NO. N/A	9a. ORIGINATOR'S REPORT NUMBER(S)	
b. PROJECT, TASK, WORK UNIT NOS. 9993XXXX	AFCRL-TR-73-0384	
c. DOD ELEMENT N/A	9b. OTHER REPORT NO(S) (Any other numbers that may be assigned this report)	
d. DOD SUBELEMENT N/A	Special Reports, No. 163	

10. DISTRIBUTION STATEMENT

This document has been approved for public release and sale;
its distribution is unlimited.

11. SUPPLEMENTARY NOTES TECH, OTHER	12. SPONSORING MILITARY ACTIVITY Air Force Cambridge Research Laboratories (CA) L. G. Hanscom Field Bedford, Massachusetts 01730
--	--

13. ABSTRACT

This is the sixth in a series of Reports on Research at the Air Force Cambridge Research Laboratories. This report covers a two-year interval. It was written primarily for Air Force and DOD managers of research and development and more particularly for officials in Headquarters Air Force Systems Command, for the Director of Science and Technology (DL), and for the Commanders of and the Laboratories within DL. It is intended that the report will have interest to an even broader audience. For this latter audience, the report, by means of a survey discussion, attempts to relate the programs of the larger scientific field of which they are part. The work of each of the laboratories is discussed as separate chapters. Additionally, the report includes an introductory chapter on AFCRL management and logistic activities related to the reporting period.

NATIONAL TECHNICAL
INFORMATION SERVICE

I

Unclassified

Security Classification

14. KEY WORDS	LINK A		LINK B		LINK C	
	ROLE	WT	HOLE	WT	ROLE	WT
Upper Atmosphere Physics Upper Atmosphere Chemistry Prediction of Meteorological Extremes Microwave Acoustics Millimeter Wave Propagation Electromagnetic Wave Propagation Signal Processing and Detection Information Processes Balloon Technology Rocket Instrumentation Plasma Physics Energy Conversion Solar Plasma Dynamics Solar Astronomy Ionospheric Physics Radio Astronomy Meteorology Geology Gravity Seismology Geodesy Geokinetics Optical Physics Laser Physics Electronic Solid State Radiation Damage Crystal Growth and Characterization						

II

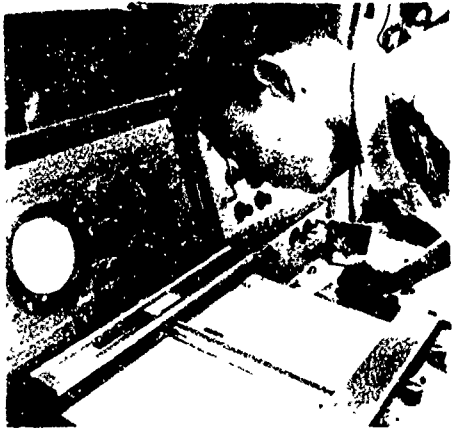
Unclassified

Security Classification

Report
on
Research | JULY 1970 - JUNE 1972
at
AFCRL

D D
FEB 1973
PAR 1
L
 SURVEY OF
PROGRAMS AND
PROGRESS

THE AIR FORCE CAMBRIDGE
RESEARCH LABORATORIES
AIR FORCE
SYSTEMS COMMAND
BEDFORD, MASSACHUSETTS
FEBRUARY 1973



Foreword

The first *Report on Research* at the Air Force Cambridge Research Laboratories covered research during the period January 1961 through June 1962. This report, the sixth in this series, covers the period July 1970 through June 1972. The research laboratory begun by the Army Air Force on September 20, 1945, with the name, The Cambridge Field Station, has grown through more than 25 years, and made contributions to Air Force operations, to technology, and to scientific knowledge out of all proportion to its size and to the Air Force investment in its programs. The broad span of research covered by this book has a single unifying theme—the Air Force missions of surveillance, detection, communications, and navigation. Although the impact of a new piece of hardware is more easily noted, and AFCRL has produced many in response to Air Force needs, the most enduring contribution from the Laboratories may well be in the field of environmental forecasting. Environmental research usually fits the classic pattern of a slowly maturing science—there are few, if any, spectacular breakthroughs, but numerous small improvements in diverse disciplines, each of which adds its small bit to improvement of Air Force capability. If environmental forecasting is realized to the full extent desired by the Air Force, it will come through the kinds of research—electromagnetic-atmospheric interactions, optical and radio astronomy, solar particle emissions, studies of atmospheric composition, chemistry and density—that engaged much of AFCRL's attention during the period of this report.

William K. Moran, Jr.

WILLIAM K. MORAN, JR
Colonel, USAF
Commander

Contents

I	The Air Force Cambridge Research Laboratories	1
	Organization and People ... Annual Budgets ... AFCRL Computation Center ... Field Sites ... Research Vehicles ... The AFCRL Research Library	
II	Aeronomy Laboratory	9
	Polar Atmospheric Processes ... Atmospheric Structure ... Upper Atmosphere Chemical Release ... Spectroscopic Studies ... Solar Extreme Ultraviolet Radiation ... Design Climatology ... Atmospheric Composition	
III	Microwave Physics Laboratory	58
	Radar Systems ... Antenna Theory ... Plasma Electromagnetics ... Millimeter Wave Propagation ... Microwave Acoustics	
IV	Aerospace Instrumentation Laboratory	98
	Research Rockets ... Research Satellites ... Free Balloon Control ... Tethered Ballooning ... Balloon Instrumentation ... Materials Research ... High Altitude, Heavy Load Parachute Tests	
V	Space Physics Laboratory	110
	Space Forecasting ... Research on Solar Dynamics ... Energetic Particle Research ... Geomagnetism ... Energy Conversion ... Plasma Physics	
VI	Meteorology Laboratory	146
	Mesoscale Weather Forecasting ... Atmospheric Modeling ... Atmospheric Boundary Layer ... Satellite Meteorology ... Clear Air Turbulence (CAT) ... Upper Level Winds ... Weather Radar Techniques ... Warm Fog Dissipation ... Cumulus Cloud Modification ... Cloud Physics ... Meteorological Instrumentation	
VII	Sacramento Peak Observatory	187
	The Sun ... Facilities and Instruments ... Instruments for Air Weather Service Solar Observatories ... Research on Solar Energy Transport ... Research on Solar Activity ... Research on Solar Magnetic Fields	

VIII	Terrestrial Sciences Laboratory	218
	<i>Seismology ... Geology ... Geokinetics ... Geodesy and Gravity</i>	
IX	Optical Physics Laboratory	245
	<i>Atmospheric Optics ... Infrared Physics ... Radiation Effects ... Radiometry ... The Remote Inference Problem ... Laser Physics</i>	
X	Ionospheric Physics Laboratory	278
	<i>Total Electron Content ... F-Layer Irregularities ... Long Baseline Interferometer ... Traveling Ionospheric Disturbances ... Ionospheric Waveguide ... Electrical Structure ... Solar Radio Astronomy ... Solar Polarization ... Arctic Program ... Polar Cap Absorption ... Auroral Investigations ... Goose Bay Ionospheric Observatory ... Dynamic Polar Ionospheric Model ... Systems Oriented Research</i>	
XI	Solid State Sciences Laboratory	324
	<i>Electromagnetic Materials ... Infrared Detector Research ... Radiation Effects and Device Hardening ... Processing Technology</i>	

Appendices

A	AFCRL Projects by Program Element	365
B	AFCRL Rocket and Satellite Program: July 1970 - June 1972	367
C	AFCRL Organization Chart	371

Air Force Cambridge Research Laboratories

The Air Force Cambridge Research Laboratories (AFCRL) serves the United States Air Force by conducting basic and applied research to meet known and anticipated military needs and requirements. This report describes the programs, activities, and accomplishments of AFCRL for the period July 1, 1970, to June 30, 1972.

The largest research laboratory in the Air Force, AFCRL covers a broad spectrum of technical programs in the environmental sciences and selected areas of electronics. AFCRL is an in-house laboratory with a professional staff of more than 600 scientists and engineers. Its in-house programs are supported by contractual research in universities and industry.

The research programs of AFCRL are summarized in the mission statement: *Conducts research in those areas of the environmental, physical and engineering sciences offering the greatest potential to the continued superiority of the Air Force's operational capability; conducts specifically assigned exploratory development efforts involving the environmental, physical and engineering sciences; participates in establishing advanced technologies whose exploitation will lead to new Air Force capabilities.*

ORGANIZATION AND PEOPLE: On July 1, 1970, AFCRL became part of the Air Force Systems Command (AFSC), when its former command, the Office of Aerospace Research (OAR), was deactivated. This organizational change was designed to make Air Force research more respon-

sive to military technology and systems requirements. AFCRL became one of 12 laboratories under the Director of Laboratories (now Director of Science and Technology), Headquarters, Air Force Systems Command, at Andrews AFB, in Maryland.

The main AFCRL laboratory complex is located at L. G. Hanscom Field, Bedford, Mass., 20 miles west of Boston. At Hanscom Field, AFCRL is a tenant of the

Electronic Systems Division of the Air Force Systems Command.

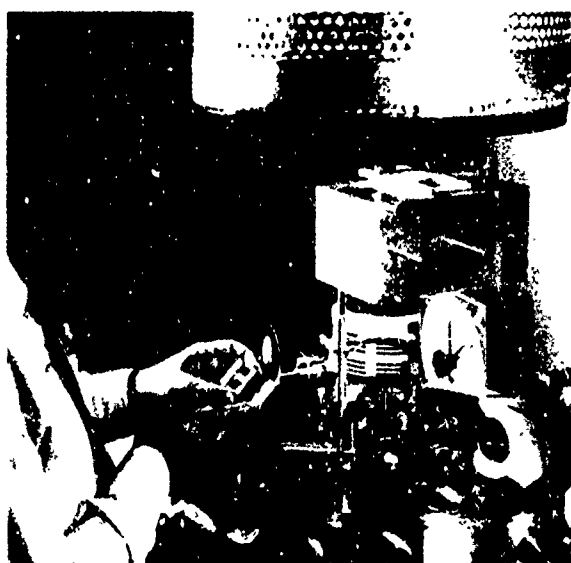
Colonel William K. Moran, Jr., assumed command of AFCRL in June 1971, succeeding Colonel Dale J. Flinders. Colonel Moran came to AFCRL from the position of Commander, Aerospace Research Laboratories, Wright-Patterson AFB, Ohio. Colonel Charles A. Smith, Vice Commander, reported to AFCRL on July 1, 1970.

As of June 30, 1972, AFCRL had an authorized complement of 1156 personnel—981 civilians and 175 officers and airmen—a decrease of 79 from the work force in June 1970. Reduction in manpower authorizations led to the abolition of the Data Sciences Laboratory, at the close of the reporting period. The continuing laboratories are: the Aeronomy Laboratory, Aerospace Instrumentation Laboratory, Ionospheric Physics Laboratory, Meteorology Laboratory, Microwave Physics Laboratory, Optical Physics Laboratory, Sacramento Peak Solar Observatory, Space Physics Laboratory, Solid State Sciences Laboratory, and the Terrestrial Sciences Laboratory. In addition, AFCRL operates a small West Coast Office to manage AFCRL support to the technology requirements and system developments of the AFSC Space and Missile Systems Organization (SAMSO) near Los Angeles.

In June 1972, 173 AFCRL employees held the doctor's degree, 221 held master's degrees, and 236 bachelor's degrees. AFCRL scientists are active in their respective professional societies. One scientist served as Editor of the *IEEE Transactions on Antennas and Propagation* for most of the reporting period. Another was Editor of *Applied Optics*, and three AFCRL scientists served as Associate Editors of the *IEEE Transactions on Antennas and Propagation*, the *Journal of Crystal Growth* and *The Moon*. AFCRL scientists also served as editorial advisors and referees for various learned journals, served on professional committees, and



Of the 1156 employees at AFCRL, more than 600 are scientists or engineers, and 173 hold the Ph.D. degree.



chaired professional meetings and symposia.

During the two years of this report, AFCRL sponsored or cosponsored six scientific conferences. AFCRL scientists and engineers authored 228 in-house reports, 567 articles in scientific and professional journals, and presented 654 papers at technical meetings. These publications and presentations are listed at the conclusion of each laboratory chapter.

ANNUAL BUDGETS The annual budgets for the two years covered in this report are shown in the accompanying tables. The indicated totals cover salaries, equipment, travel, supplies, computer rental, service contracts, and those funds going into contract research. The largest expenditure is for salaries which accounted for approximately \$20 million of the FY-1972 budget of \$59.27 million. The annual budget increased from \$55 million in FY-1970 to \$59 million in FY-1972.

Funds received from AFCRL's higher headquarters, the AFSC Director of Laboratories (DL), and, to a lesser extent, those received from AFSC organizations other than DL, are used to conduct continuing long-range programs.

AFCRL receives much support from other elements of the Air Force. The Electronic Systems Division, the host organization at Hanscom Field, provides approximately 400 manyears of support to the laboratory complex. Holloman AFB, New Mexico, provides services to the Sacramento Peak Observatory and the AFCRL Balloon Detachment No. 1. Funds from other agencies are earmarked for specific research projects.

Nearly half of the AFCRL budget during the reporting period was spent for contract research. Of the \$59.27 million FY-1972 budget, \$28.79 million was devoted to contract research. As of June 30, 1972, AFCRL had 459 contracts in effect. Of these, 160 were with U. S. industrial concerns, 167 were with U. S. universities, and 38 were with foreign universities and companies. The remainder were with research foundations and other government agencies.

Contracts let by AFCRL are usually smaller than those awarded by other government R&D laboratories, but this is not the only difference. AFCRL contracts almost always call for work in direct support of research carried out within AFCRL.

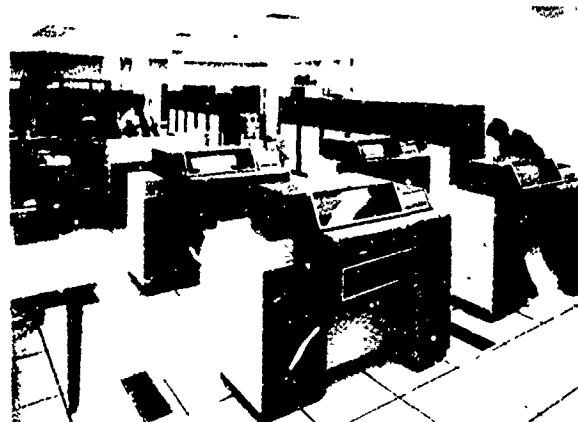
TABLE I
SOURCES OF FY-1971 FUNDS

Air Force Systems Command - DL	\$42,594,400
Advanced Research Projects Agency	5,892,917
Air Force Systems Command Other Than DL	2,560,526
National Aeronautics and Space Administration	2,159,331
Defense Nuclear Agency	2,035,000
Air Weather Service	783,699
Defense Communications Agency	700,000
National Security Agency	128,328
Department of Transportation	121,225
Army	94,445
Air Force Technical Applications Center	47,000
Air Force Logistics Command	560
Navy	142
TOTAL	\$57,117,573

They are monitored by scientists who are themselves active, participating researchers, and who plan the research, organize the program, interpret the results and share the workload of the actual research.

AFCRL COMPUTATION CENTER: A permanent, two-story structure consisting of 43,000 square feet was occupied in November 1970 by the AFCRL Computation Center. The AFCRL Command Section, the Deputy for Technical Plans and Operations, and the Deputy for Research Services were also moved to this building at that time. The first of the Computation Center's two Control Data Corporation 6600 computer systems was installed in December 1970 and the second 6600 was to be installed in July 1972.

The CDC 6600 systems consist of a modular designed multiprocessor operation with extensive input-output devices, peripheral equipment and communications equipment. The systems provide remote batch, interactive graphics and conversational capabilities through a network of approximately 50 remote stations located within the laboratory complex and at off-base locations. The decommutation facility processes data from satellites, rockets, air-



The \$2 million AFCRL computer center, completed in November 1970, and the AFCRL CDC-6600 computer.

TABLE 2
SOURCES OF FY-1972 FUNDS

Air Force Systems Command - DL	\$44,586,000
Advanced Research Projects Agency	4,201,453
Defense Nuclear Agency	4,125,853
Air Force Systems Command Other Than DL	2,804,912
National Aeronautics and Space Administration	1,598,049
Air Weather Service	1,385,480
Atomic Energy Commission	227,510
Department of Transportation	133,474
National Security Agency	91,666
Army	78,000
Air Force Technical Applications Center	30,000
TOTAL.	\$59,262,397

craft, balloons and from laboratory data collection systems, using two special purpose Honeywell computer systems.

The Computation Center also provides mathematical analysis and scientific programmer services and operates a large-scale analog/hybrid computation facility in support of simulation studies.

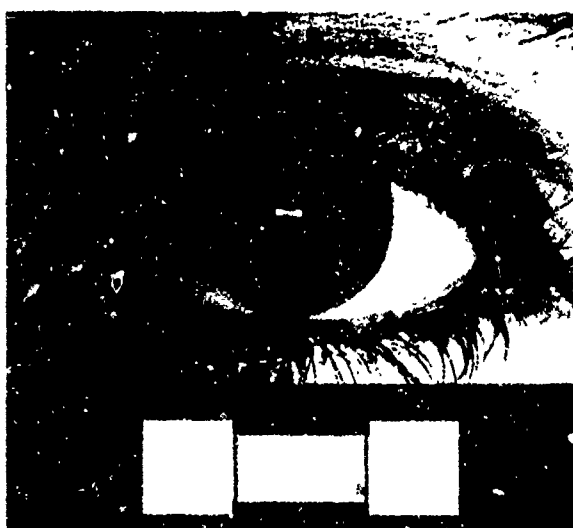
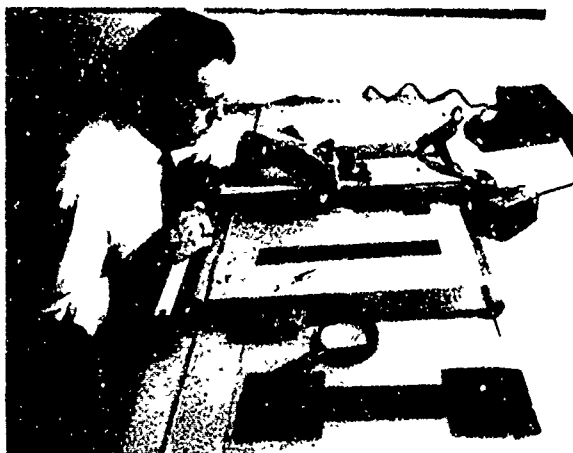
FIELD SITES: In addition to the 90 acres which AFCRL occupies at Hanscom Field, it operates several off-base sites, locally and at distant locations. The largest local site is the Sagamore Hill Radio Observatory in Hamilton, Massachusetts, which includes two large radio telescopes, one with an 84-foot dish, the other with a 150-foot dish. Other local sites are the Weather Radar Research Facility at Sudbury, Massachusetts, and a 350-acre Antenna Range in Ipswich, Massachusetts. A high precision millimeter wave radio telescope (15 to 100 GHz) is located on Prospect Hill in Waltham, Massachusetts. A former Nike Control Site in Bedford, Massachusetts, housed part of the Optical Physics Laboratory.

AFCRL has large permanent sites in New Mexico and California. One balloon launch facility is located at Holloman AFB, New Mexico, the other is at Chico, California. At Sunspot, New Mexico, overlooking Holloman from its 9200-foot elevation stands the Sacramento Peak Solar Observatory, perhaps the most completely instrumented facility in the world for solar optical astronomy. Its Vacuum Tower Telescope began operating in October 1969. The Lunar Laser Observatory which AFCRL had maintained at Mt. Lemmon, about 40 miles north of Tucson, Arizona, was closed on June 30, 1972.

The most remote permanent facility is the Geopole Observatory at Thule Air Base, Greenland, which began observations in 1958 and has yielded a 14-year continuous record of Arctic magnetic ac-



Two of the larger off-base sites are the Sagamore Hill Radio Observatory at Hamilton, Mass., and the Weather Radar Facility at the U. S. Army Natick Laboratories Annex in Sudbury, Mass. Sagamore Hill is the site of the 84-foot and 150-foot radio telescopes, as well as numerous smaller antennas. Several radar sets, including a special weather radar set, are located at the Sudbury site.



Microwave acoustics has miniaturized many components. Above, technician carefully traces and cuts out the pattern for an interdigital transducer. Below, the finished size of the device can be realized. It is less than 2 mm long, and the distance between taps on the interdigital structure has been reduced to a few microns.

tivity, auroral phenomena and ionospheric variations. Another remote station is the Goose Bay Ionospheric Observatory at Goose Bay Air Station, Labrador, where studies of a variety of arctic events are made, including Polar Cap Absorption of high frequency waves.

AFCRL occupies temporary sites on a number of military installations including the Fort Churchill, Canada, rocket range; Fort Wainwright and Eielson AFB, Alaska; Albrook AFB, Canal Zone; Eglin AFB, Florida; Travis AFB, California; Vandenberg AFB, California, and the White Sands Missile Range, New Mexico. In addition to these military sites, AFCRL has used other locations on a temporary basis. Trailers were transported each year from Hanscom Field to a five square mile field site near Liberal, Kansas, for studies of small-scale meteorological phenomena. Upon completion of these measurements in the summer of 1970, a lease was negotiated for 15 acres at Donaldson, Minnesota, for the continuation of these studies. Existing facilities at Roswell, New Mexico, and Sioux Falls, South Dakota, commercial airports and the Poker Flat, Alaska, Range are also used.



AFCRL has had many distinguished visitors. Here, a group including the Hon. Nigel H Bowen, Minister of Education and Science of Australia

RESEARCH VEHICLES: From its permanent balloon launch sites in New Mexico and California, and from temporary sites in several other locations, AFCRL launched 198 large research balloons during the two-year period. Of these, 92 were launched in FY-1971. These balloons carried test and experimental payloads for the Space and Missile Systems Organization (SAMSO), the Defense Nuclear Agency (DNA), National Aeronautics and Space Administration (NASA), the Army and university scientists with military contracts. AFCRL scientists themselves are, however, the largest users.

The AFCRL balloon group holds records for maximum balloon size (34 million cubic foot volume), maximum altitude reached (161,000 feet), and maximum payload carried aloft (seven tons) as of June 1972. AFCRL scientists are planning an R&D mission calling for the design and launch of a 47.8 million cubic foot balloon to ascend to an altitude of 170,000 feet.

During the past two years, AFCRL launched a total of 83 large research rockets, most of which were fired from Eglin AFB, Florida (32). Fort Churchill, Canada (11), the White Sands Missile Range, New Mexico (20), and Wallops Island, Virginia (14), were also important launch sites. Since the launch of its first rocket in August 1946—a German V-2—AFCRL has sent 890 large research rockets aloft (exclusive of a like number of smaller meteorological rockets), as of June 1972.

Rockets are used to examine almost every aspect of the earth's upper atmosphere and near-space environment—winds, temperatures and densities; the electrical structure of the ionosphere; solar ultraviolet radiation; atmospheric composition; the earth's radiation belts; cosmic ray activity; and airglow and aurora. The rockets most frequently used have been the Nike Iroquois (NIRO), the Nike Tomahawk, the Black Brant, and the Aerobee.

During this reporting period, AFCRL-

designed packages were carried aboard five satellites. Two satellites were exclusively instrumented by AFCRL—the Cannon Ball II and Musket Ball density-measuring satellites.

Four research instrumented aircraft—two NKC-135's and two C-130's—gather data for various projects. The NKC-135's have been part of the AFCRL inventory for more than a decade, and the C-130's for almost as long. One NKC-135 and one C-130 are instrumented for measuring the transmission, scattering and reflectance of optical radiation in the atmosphere. The other NKC-135 is used for performing ionospheric and associated observations which take the aircraft all over the world, with recent emphasis on the Arctic auroral zone. Another C-130 is instrumented for meteorological observations.

THE AFCRL RESEARCH LIBRARY: The depth and quality of the technical collection



The collection of the AFCRL Research Library is valued at more than \$15 million

maintained by the AFCRL Research Library is surpassed by few libraries in the country.

Available to AFCRL scientists are the scientific journals of Bulgaria, Czechoslovakia, Holland, France, Germany, Hun-

gary, Italy, Japan, Poland, Russia and Sweden. The collection of Chinese science journals and monographs is one of the most comprehensive in the U. S. Associated with the foreign periodical collection are translation services.

II Aeronomy Laboratory



Aeronomy is the study of the physical and chemical properties of the earth's upper atmosphere, a region that extends from the top of the stratosphere at about 50 kilometers to interplanetary space at several thousand kilometers. Although this region comprises only about a tenth of 1 percent of the earth's atmosphere, dramatic physical and chemical processes take place there that profoundly affect the earth's environment. Some of these processes are readily visible to the eye, such as the brilliant auroral displays that predominate at the higher latitudes. Other processes are invisible but no less dramatic, such as the vast upper atmosphere motions caused by energy coming from the sun.

The operation of space vehicles is affected by the vehicle's environment. To predict the future position of a satellite, we must know the density of the atmosphere, not only at the present moment, but also up to the time for which we are making the prediction. To do this, we must know what the sun will be doing and how this will affect the earth's atmosphere.

Another area of interest to the Air Force is target detection. The Laboratory is actively engaged in measuring certain radiations that are emitted by targets of interest.

Nuclear weapons effects on the atmosphere are being studied to determine the ways in which a nuclear detonation will affect the capabilities of communication and radar systems.

As another example of an application, we can sometimes modify the upper atmosphere for operational purposes. For example, the Laboratory has been able, by releasing appropriate chemicals into the

upper atmosphere, to create an artificial ionosphere for communication purposes. Recently, the possibility of using chemical releases as spoofs against anti-aircraft missiles has been investigated.

The Aeronomy Laboratory is also actively supporting the Air Weather Service Space Forecasting Program. This is being done in three areas—atmospheric density, which was mentioned previously, solar X-rays as indicators of the strength of flares erupting on the sun, and riometer, very low frequency and magnetometer measurements made at the Geopole Observatory at Thule, Greenland, and transmitted to the Solar Forecast Center in Cheyenne Mountain, Colorado.

To be able to meet these needs of the Air Force, personnel of the Aeronomy Laboratory are studying such basic parameters of the upper atmosphere as density, temperature, pressure and composition. Under composition is included the number of atoms and molecules that are present, whether they are electrically charged or neutral, whether they are in the ground state or in excited states and what the transition probabilities are in going from one state to another.

These atmospheric constituents undergo various dynamic processes. For example, winds in the upper atmosphere can be quite strong, sometimes of the order of several hundred kilometers per hour. In certain regions there is strong turbulence; in other regions turbulence is weak and molecular diffusion predominates.

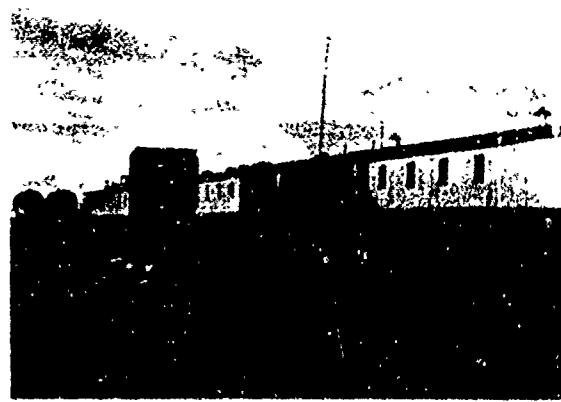
The atmospheric constituents are constantly undergoing various chemical reactions. Among the reactions being studied are ion-electron recombination, ion-ion recombination, electron attachment and detachment, ion-neutral reactions and neutral-neutral reactions.

The properties of the upper atmosphere are also affected by energy from the sun. For example, the solar ultraviolet and X-radiation which are being studied cause

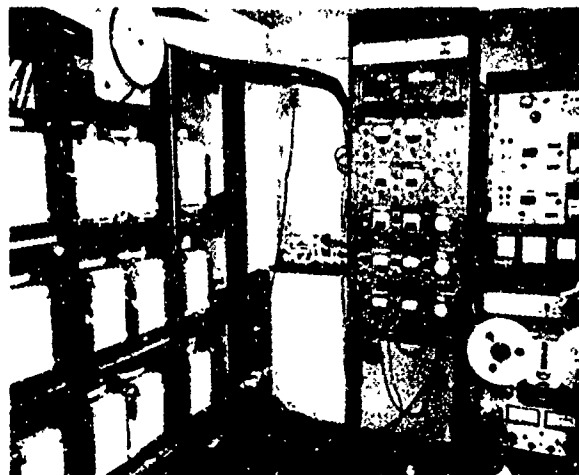
excitation, ionization and even dissociation of atmospheric constituents.

POLAR ATMOSPHERIC PROCESSES

The Polar Atmospheric Processes Branch has shifted its primary emphasis during the past two years from auroral and air-glow research to studies of the physics and chemistry of the Polar Cap upper atmosphere and the determination and characterization of geophysical disturbances originating in or best studied in the Polar Cap. The approach to the new objectives involves determining: the basic parameters of the ambient Polar Cap upper atmosphere, the energy input to and output of the Polar Cap atmosphere, and the effects of disturbance phenomena on the ambient atmosphere and energy balance. A systematic approach is being used because a variety of conditions can produce the sporadic and inhomogeneous perturbations which affect communications, warning and detection systems. The program of measuring the altitude profile of the green line atomic oxygen emission at mid-latitudes



The unusual phenomena of the polar atmosphere offer a key to the understanding of many atmospheric processes. AFCRL maintains its Geopole Observatory at Thule, Greenland, which is only a short distance from the geomagnetic pole.



VLF receivers at Thule monitor signals from many transmitters in the mid-latitudes. VLF transmissions are very sensitive to ionospheric disturbances. Riometers measure galactic noise at 30 MHz, which allows a determination of the amount of absorption occurring in the arctic ionosphere.

tude regions has been continued because the methods being developed and validated will be used in the Polar Cap region.

OBSERVATIONS OF POLAR ATMOSPHERIC PHENOMENA: Most of the observations made by the Polar Atmospheric Processes Branch are made at the AFCRL Geopole Observatory, at Thule AB, Greenland, located near the North Pole of the dipole geomagnetic field. The station is equipped to make optical, ionospheric, and magnetic measurements. A real-time data link is maintained between the Geopole Observatory and the Solar Forecast Center in Cheyenne Mountain, Colorado.

The Geopole Observatory is uniquely situated for the study of solar particle events since the magnetic field lines extend to great distances and effects of the magnetotail and/or the interplanetary field are observed. This is particularly true during the Polar Cap Absorption (PCA) events which follow some solar flares. Recently,

two such events have received considerable attention on an international scale,—those of November 1969 and March 1970. Contributions to the understanding of these events were made by branch personnel using data from Geopole.

OPTICAL MEASUREMENTS OF THE NOVEMBER 1969 PCA EVENT: In 1970, a specialized electro-optical microdensitometer system for analysis of the optical measurements made during the "PCA 69" Program was delivered and an evaluation program instituted. Initially, measurements at Geopole during the November 1969 period corresponding to the "PCA 69" intensive rocket-borne measurement program at Ft. Churchill, Canada, were evaluated. These results complemented other AFCRL optical measurements made from a KC-135 flying laboratory, providing a combination of temporal-spatial coverage during the crucial first 24 hours of the solar particle event. Other research has shown that the total energy input from polar particle fluxes which are enhanced during the solar particle event can be estimated from measurements of ionized molecular nitrogen optical emissions. During the second and third day of the solar particle event the results calculated from the optical intensities agreed within 10 percent with satellite measurements of polar particle fluxes. This indicated that optical measurements could be used as an economical, convenient, ground-based monitor of polar particle fluxes.

VLF MEASUREMENTS AS PARTICLE DETECTORS DURING THE NOVEMBER 1969 PCA EVENT: Very low frequency (VLF) radio wave propagation has been found to be a very sensitive terrestrial means of detecting disturbances of the ionosphere. It is generally accepted that VLF waves propagate in a spherical waveguide bounded by the earth's surface and the lower ionosphere, the D region. Under normal ionospheric conditions the upper boundary of

the waveguide is at 85-50 kilometers during the night and at approximately 70 kilometers during the day. During disturbed conditions this upper boundary can be as low as 50 kilometers, because of increased ionization at low altitude. Within a few minutes of a solar flare, VLF paths in daylight are disturbed by the increased ionization in the D region due to X-rays. About one hour later, paths both in daylight and darkness can be affected by the ionization caused by the arrival of protons and electrons. Because of the influence of the earth's magnetic field, the greatest flux of solar particles into the upper atmosphere is in the polar regions. Thus VLF transmission paths which cross the polar caps are the first affected and the most strongly affected by the precipitating particles. By monitoring these paths, disturbances of polar regions can be detected.

The sensitivity of VLF as a particle detector was demonstrated during the November 2, 1969 solar particle event. At that time, VLF transmission paths were monitored at the AFCRL-operated Geopole Observatory at Thule, Greenland, and in Switzerland. VLF paths in daylight were disturbed by solar X-rays at 0945 UT, a few minutes after the solar flare; however, nighttime paths were not affected by the X-rays. Disturbances on these paths were recorded at 1034 UT indicating that particle precipitation was beginning to cause ionization changes over the polar regions. Riometers (Relative Ionospheric Opacity Meters) did not detect the presence of any ionospheric disturbance until about ten minutes later. Since no polar-orbiting satellite data were available at this time, VLF provided the only record of the onset of the ionospheric disturbances. The amplitudes of the signals received at the AFCRL Geopole Observatory were strongly attenuated during the particle precipitation and the signals did not fully recover to normal levels for nine days after the initial disturbance.

During the solar particle event an Air Force satellite (OV5-6) outside the magnetosphere directly monitored the flux of electrons and protons. Data show that electrons were first detected by the satellite at the same time as ionospheric disturbances were detected by the VLF receivers. This arrival of electrons outside the magnetosphere at about the same time as they arrived in the ionosphere over the pole was unexpected, and it proves the existence of a rapid and efficient transfer between particles traveling along interplanetary field lines and the D region in the polar regions.

By monitoring many VLF stations, the AFCRL Geopole Observatory near the geomagnetic pole can detect the presence of ionospheric disturbances caused by particle precipitation in polar regions. From an understanding of the VLF effect produced by natural ionization sources it is possible to predict the effect on VLF communications of man-made ionization disturbances such as nuclear detonations.

OPTICAL MEASUREMENTS OF THE MARCH 1970 PCA EVENT: Observations of the behavior of visual aurorae and of optical emissions in regions near the geomagnetic pole have shown distinct differences from the behavior in the auroral zone and even from that in regions intermediate between auroral zone and magnetic pole. In particular, the polar glow aurora is associated with polar cap absorption events in which the sequence of the intensities of the O I and O II emissions follow that of the PCA. The period from March 6-10, 1970 was one in which a moderate PCA event occurred, and the optical emission data from a high latitude station such as Thule AB were thus of interest.

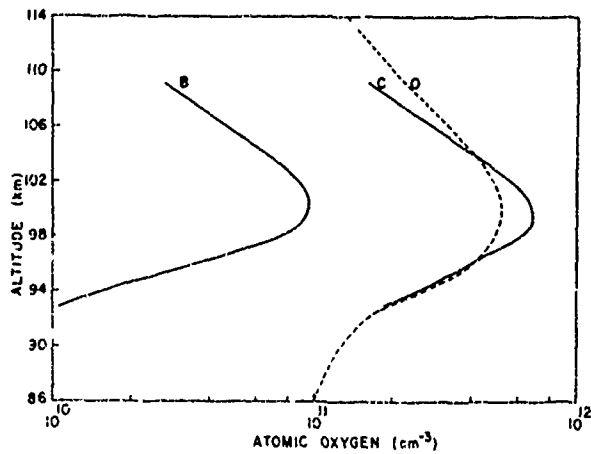
The period preceding March 6-10 was one of much activity, both solar and magnetic, so that the attribution of effects to specific causes is difficult. However, an effect of the Polar Cap Absorption event, a

possible effect of a solar flare, and the presence of luminosity fluctuations with time intervals similar to those previously observed in the auroral zone were noted.

A moderate Polar Cap Absorption event began between 1025 and 1100 UT on March 7 and lasted two days with a maximum riometer absorption of the order of 5 dB. In addition a geomagnetic storm of unusual intensity and short duration began at 1417 UT on March 8. In spite of the short duration of the PCA, the twilight conditions over much of the observational period, and the overall disturbed character of the period, it was possible to monitor the course of the PCA by means of optical observations. The observed intensities were low, indicating a low particle flux, consistent with the moderate character of the PCA shown by the riometer records. The optical intensities measured on the 8th and 9th, taken together with the riometer absorption, indicated a considerable softening of the energy spectrum from the 8th to the 9th.

The largest solar flare during the period occurred on March 7. The 6300 Angstrom and 5577 Angstrom photometric records showed an intensity increase occurring within one minute of the solar flare maximum. Although similar increases are also observed in the absence of flares, a search for flare-connected increases of intensity is of interest.

It has been proposed that periodically structured Pc 1 micropulsations originate outside the polar cap and travel in an F-layer horizontal waveguide. Other work has shown that for polar substorms, at least, no persistent relationship is found between Thule (Qanaq) micropulsations and those in the auroral oval. It has also been proposed that some types of micropulsations originate mainly on polar cap field lines or in the polar ionosphere. The period March 6-10 1970, provides a good opportunity to separate the possible sources, whether from polar field lines or by



Atomic oxygen concentrations with altitude:
Bands B and C are from [O I] 5577 Angstrom observations on the basis of the Barth and Chapman mechanisms respectively; O is from CIRA 1965 model atmosphere.

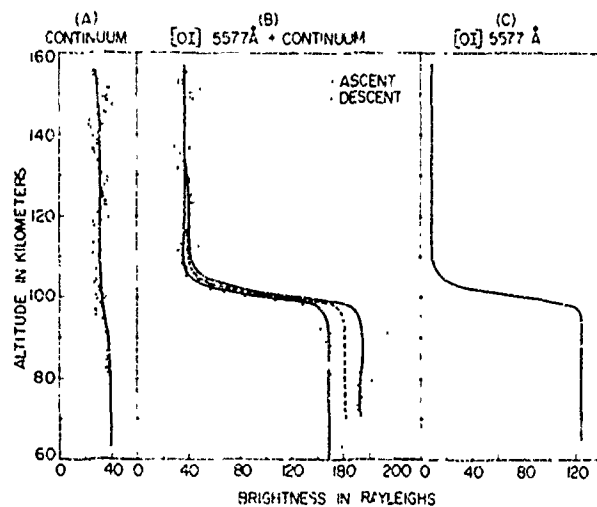
ducted travel from the oval, and to compare these with the luminosity fluctuations.

O (¹S) LIFETIMES AND HEIGHTS FROM PULSATING AURORA MEASUREMENTS: The time delay between the forbidden optical radiation of the oxygen green line (5577 Angstroms) and the allowed optical radiation of ionized molecular nitrogen (3914 Angstroms) in pulsating aurorae was analyzed as a function of the frequency of pulsations. The time delay is a function of the radiative transition probability and the collisional deactivation probability of the green line. The effective lifetimes were calculated from Ohmholz's equation, and by using known values of the quenching coefficient and number densities from a standard atmosphere, the mean lifetimes were related to the heights of the pulsating aurora.

OPTICAL MEASUREMENT OF THE GREEN LINE ATOMIC OXYGEN EMISSION: One of the important constituents of the upper atmosphere is the atomic oxygen in the altitude region of 80 to 120 kilometers. An attempt was made to develop a simple

procedure of measuring the altitude profile of the atomic oxygen green line emission and comparing it with the simultaneous independent measurement of atomic oxygen by other workers for checking the validity of the method. The other simultaneous independent methods used for determining the atomic oxygen were: 1) chemiluminescence of nitric oxide, and 2) mass spectrometer chemical technique. The procedure would enable one to: 1) determine the predominant chemical process responsible for the emission (Chapman and/or Barth), and 2) once the predominant process and the rate coefficients are known, the simple and straightforward measurement of this emission could be used for determining the atomic oxygen at any latitude. So far there has been only partial success. The airglow measurements indicate that the Chapman mechanism is adequate for explaining the emission. As yet the simultaneous measurements by independent methods have not resolved the problems because there have been partial failures of at least one of the methods in each of the coordinated attempts.

(O I) 6300 ANGSTROM AURORAL EMISSIONS: Auroral emissions are due to the bombardment of the upper atmosphere by incident electrons, protons, and particles of extra-terrestrial origin. The polar cap, auroral zone and, during severe magnetic storms, even the mid- and low-latitude regions exhibit auroral activity. One of the auroral emissions is the (O I) 6300 Angstrom line emission. The spatial and temporal variations of this emission, its dependence on solar and magnetic activity and also its dynamic movement were studied from the auroral observations from a mid-latitude station—AFCRL's Solar observatory at Sacramento Peak, New Mexico. These show a movement toward the equator and also an increase in the (O I) 6300 Angstrom emission with an increase in magnetic activity. The auroral emission



Integrated emission measured by a rocket photometer: A) continuum brightness for 5577 angstrom filter as determined from that for a 5530 angstrom filter; B) total brightness from the 5577 angstrom filter; C) [O I] 5577 Angstrom green line emission computed as the difference between B and A.

also shows a good correlation with the recurrence of the phase of the solar cycle. The method of analysis is equally valuable to the study of the polar region, where additional information on particle bombardment is now available from satellite observations and also from ground ionospheric observations.

ATMOSPHERIC STRUCTURE

The Atmospheric Structure Branch uses three major approaches to investigate the upper atmosphere. The first is to make *in situ* measurements of structure parameters by flying instruments on rockets and satellites. The second is to develop comprehensive theories and models of the properties of the upper atmosphere. The third is to make laboratory measurements of the rates of chemical reactions which are important in the normal and disturbed atmosphere and which rates are required for theoretical structure computations.

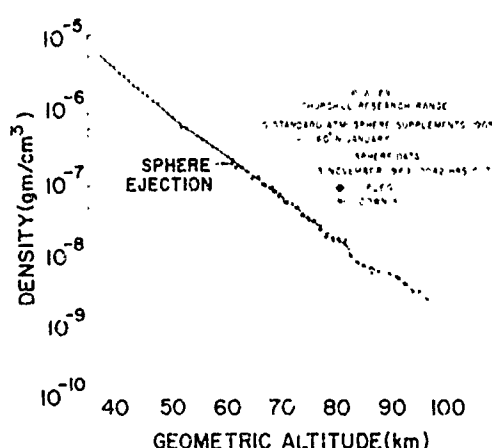
ROCKET MEASUREMENTS: Data reduction and analysis has been completed on neutral density and temperature results obtained at Churchill Research Range, Canada, during the solar proton event (PCA) of November 2-4, 1969. Density data obtained from a rocketborne falling sphere payload launched on November 3 at 0042 hours LT following commencement of the PCA event show pronounced density oscillations. Unusually large density oscillations have been observed previously by satellites (LOw G ACcelerometer Satellite (LOGACS) and OV1-15) following a proton event or intense auroral disturbance, but this was the first time that similar phenomena were reported at sounding rocket altitudes. The temperature results deduced from the sphere densities also showed an oscillatory pattern and greatly enhanced temperatures relative to the model atmospheres used for comparison. Temperature data obtained at 0632 hours LT on November 3 showed oscillations of decreased amplitude, and near normal conditions were observed in data obtained at 1708 hours LT. These results have been made available to other PCA 69 investigators who

have a requirement for *in situ* density-temperature data to be used in further quantitative studies and analyses.

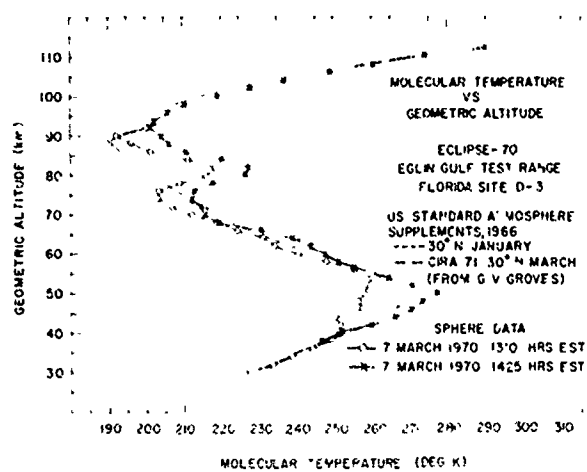
Neutral density and temperature results obtained at Eglin AFB, Florida, during the total eclipse of March 7, 1970 were analyzed and presented at the International COSPAR Eclipse Symposium held at Seattle, Washington, in June 1971. The most dramatic results were observed in a comparison of temperatures determined from density measurements made near totality (1310 hours LT) and fourth contact (1425 hours LT). Small, but measurable, differences were observed between the two sets of data. At the levels of the mesopause (90 kilometers) and stratopause (50 kilometers), the fourth contact results were warmer than those corresponding to totality by 11 and 19 degrees K, respectively. Because a total solar eclipse shuts off the energy input from the sun, it might cause a temperature decrease in the shadowed portion of the atmosphere. When the solar radiation strikes the atmosphere again, its temperature tends to increase. This effect is especially noticeable near 50 kilometers where ozone absorption of solar ultraviolet radiation causes heating. However, with only one such set of measurements, it is not possible to be sure that this is an eclipse effect. It is possible that the variation was partly or entirely due to a meteorological short-term variation.

Another measurement was made by an AFCRL 10-inch falling sphere that was launched near first contact (1151 hours LT) during the March 1970 eclipse. This new 10-inch sphere was instrumented with a triaxial MICRO-G accelerometer, which was at least two orders of magnitude more sensitive than the omnidirectional accelerometer used in the 7-inch spheres. Results obtained up to about 145 kilometers show near normal conditions.

Two sounding rockets instrumented to measure mesospheric ozone were launched during and after the solar proton event of



Density profile measured by 7-inch falling sphere at Fort Churchill at 0042 hours CST on November 3, 1969, following commencement of a Polar Cap Absorption event.



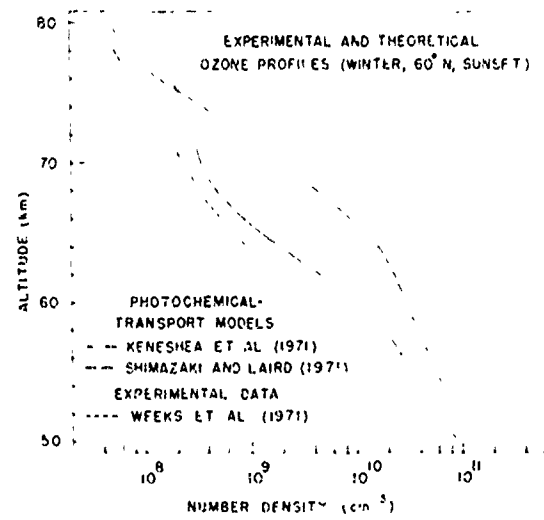
Molecular-scale temperature profiles derived from 7-inch falling sphere measurements at Eglin during the total solar eclipse of March 7, 1970.

November 2, 1969 from Ft. Churchill, Canada. The ozone distribution was found to be profoundly affected by this disturbance. A decrease in density was observed on November 2 (7 dB absorption at 30 MHz) relative to November 4 (2 1/2 dB absorption at 30 MHz) at all altitudes from 50 to 80 kilometers. This decrease amounted to a factor of 2 at 54 kilometers, 3 at 60 kilometers, and 4 at 67 kilometers. This effect is contrary to predicted ozone enhancements during certain types of particle precipitation events and shows that our understanding of the complicated photochemistry of ozone is still quite incomplete.

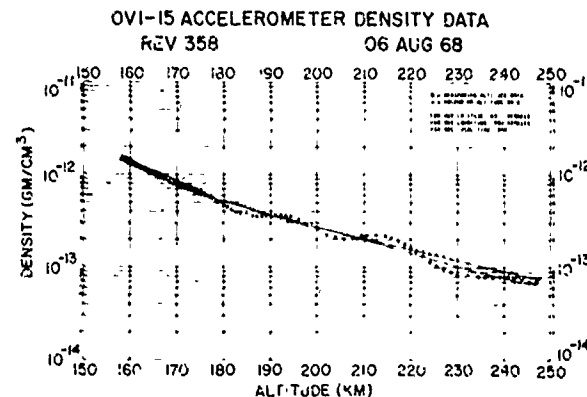
The high latitude ozone distribution on November 4, 1969, believed to be typical of undisturbed conditions, was found to be somewhat less than that represented by the most recent photochemical-vertical transport models, especially in the vicinity of 50 kilometers. The differences between experimental results and recent models provide valuable clues to certain critical parameters used in the models, some of which are presently not measurable direct-

ly. Species such as H₂O, NO, O, and H are intimately tied to the O₃ photochemistry, and the assumed turbopause altitude, for example, will significantly affect the O₃ distribution. Further measurements of this type, in conjunction with certain other critical quantities such as O₂(¹A_g), and total density will further help to determine the source of the discrepancy between the models and the observations.

Two rockets were fired near totality and at last contact of the solar eclipse of March 7, 1970 to measure changes in O₂ and O₃. Negligible changes were observed in the O₂ distribution from 70-90 kilometers and in the O₃ distribution below 60 kilometers. It is quite likely that the O₃ distribution changed above 60 kilometers. The only photochemical model of the eclipse behavior of ozone at these altitudes predicts measurable effects below 60 kilometers. The difference between our observations and the theory is believed to result from the failure to incorporate the interaction of O₃ with nitrogen and hydrogen compounds in the photochemical model.



Ozone profile measured at Fort Churchill at sunset on November 4, 1969, compared with theoretical profiles.



Density results from the accelerometer on satellite OV1-15 during revolution 358 on August 6, 1968, exhibiting wave structure at high latitudes. Circles indicate data obtained between the North Pole and perigee; crosses indicate data obtained between perigee and 34 degrees North.

SATELLITE MEASUREMENTS: Results from the accelerometer experiment flown on the low-orbiting SPADES satellite (OV1-15) have revealed new information about the nature of neutral atmospheric density variations. Wave motions were detected in density profiles obtained in the Northern Hemisphere during a period of moderate geomagnetic activity. This wave structure was most predominant near the north geomagnetic pole. An example of wave motion measured on orbit number 358, August 6, 1968, when perigee was at 62.1 degrees North is shown. The amplitude of the waves showed a latitudinal dependence, with higher amplitudes occurring at higher latitudes. The observed wave phenomena are probably atmospheric gravity waves generated by energy deposited into the auroral atmosphere during a magnetic storm.

Data were also obtained in the Southern Hemisphere during a period of very low geomagnetic activity. These measurements, made near the vernal equinox, showed a latitudinal density gradient with lower densities at the higher latitudes. At 220 kilometers, the average high latitude

density was 15 percent less than the density at 45 degrees South. Also, a longitudinal variation was revealed at high southern latitudes, with larger density values occurring in the vicinity of the south geomagnetic pole. This finding indicates that localized heating takes place in the polar region even during quiet conditions.

New characteristics of the semiannual variation in atmospheric density were also found. Present models show this effect to be worldwide with maxima and minima appearing on the same date at different latitudes and altitudes. However, comparison of OV1-15 accelerometer data taken in July and September 1968 indicate that the semiannual variation occurred at middle latitudes before occurring at high latitudes. Also, below 200 kilometers the amplitude of the semiannual variation was considerably greater than model predictions.

The Cannon Ball II and Musket Ball Satellites were launched in August 1971. Considerable accelerometer drag data were obtained from Cannon Ball II and orbital drag density data from both satellites before their re-entry.

Results obtained from satellite-borne ionization gauges have been processed and analyzed. Data analysis of gauge measurements made during the first half of 1968 has produced direct measurements of the semiannual effect. This effect, originally detected by the indirect satellite orbit decay method of atmospheric probing, is a persistent and worldwide feature of our atmosphere. Gauge measurements of the effect were obtained over a circular orbit at an altitude close to 400 kilometers, during daylight hours and over equatorial and middle latitudes. Gauge results are in good agreement with the most recent values obtained from the satellite drag techniques and, in addition, have provided a finer resolution of the semiannual effect than had previously been obtainable.

Two density gauge systems were as-

signed to Air Force Systems Satellites for flight as secondary payloads. The two density measuring systems were designed and fabricated. The sensors were cold-cathode ionization gauges designed for installation on a satellite boom which is erected after orbit is obtained. Due to a change in mission requirements, the flight of the instrument on Systems Test Program 71-4 was postponed. The second instrument was flown on Systems Test Program 71-5. Due to a partial boom malfunction, only limited data were obtained.

Two of the three sets of major models recently adopted by COSPAR for publication as the COSPAR International Reference Atmospheres 1972 were developed by the Laboratory. These included the seasonal and latitudinal models of density, temperature, pressure and winds for the altitude range 25 to 110 kilometers and the mean CIRA. The mean model is for the altitude region 25 to 500 kilometers and contains values of density, temperature, scale height, pressure, mean molecular weight and concentrations of major constituents, plus expected extreme ranges of density and temperature.

The prediction of satellite orbits is particularly sensitive to the density variability of the atmosphere. A major requirement is to provide operational systems with the most accurate possible density models of the upper atmosphere. In conjunction with model development programs, atmospheric density models are being tested at AFCRL by their performance in predicting satellite ephemerides. The Atmospheric Structure Branch has developed a computer program capable of utilizing and evaluating various atmospheric density models to determine their relative effectiveness in terms of speed and accuracy in ephemeris prediction. The objective is to determine which of the currently available atmospheric density models best meets Air Force requirements for use in satellite orbit prediction programs. Two

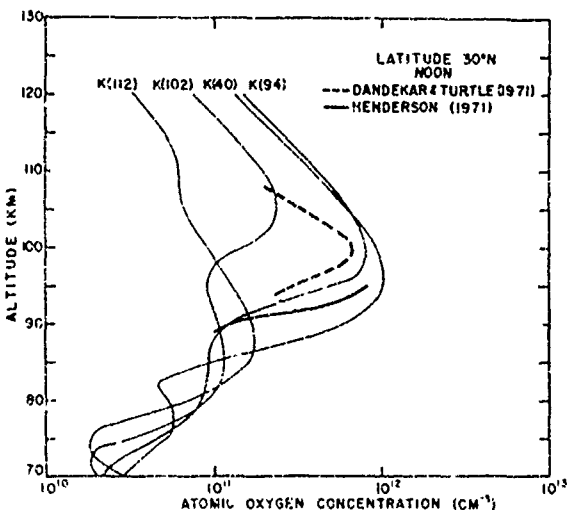
studies have been completed for Air Force agencies having mission requirements in this area.

THEORETICAL AERONOMY: The space-time distributions of certain major and minor species in the upper atmosphere have been theoretically shown to be dependent upon transport properties, such as turbulence, molecular diffusion and winds.

A set of calculations of coupled time-dependent equations of motion and continuity which utilize transport coefficients based upon measured turbulent and molecular parameters has been performed. The results of the calculations for O, O₂, O₃, OH, H, H₂, H₂O, H₂O₂ and A, for 30 degrees North equinox and 60 degrees North winter conditions, are compared to *in situ* measurements, demonstrating good correspondence where data are available over the altitude range 40 to 150 kilometers. The control by turbulence of the A, H₂O, H₂, O and O₂ distributions is demonstrated in the calculations by varying the turbopause between observed limits. This variation markedly changes the flux conditions of these species and subsequently their spatial and temporal distributions. The other species of these water vapor-oxygen calculations are photochemically tied to oxygen and thus their distributions are also changed.

Certain of the species, such as O₃, show mixed photochemical and transport control. For example, in the altitude region 40 to 70 kilometers, ozone is transport controlled at night, but during the day photochemical processes dominate. The effect of transport at night causes ozone to be displaced from the photochemical distribution by a factor of 2 to 3. The midnight measurement of ozone at Woomera, Australia, (30 degrees South latitude) confirms this shift from the photochemical distribution.

The results of theoretical computations with turbopause altitudes (the highest altitude at which turbulence exists) of 40, 94,



Atomic oxygen concentrations computed using photochemical-transport techniques, with turbopause altitudes at 112, 102, 94 and 40 km in succession, compared with experimental results. The curve with the turbopause at 94 km agrees with O profiles derived from airglow measurements.

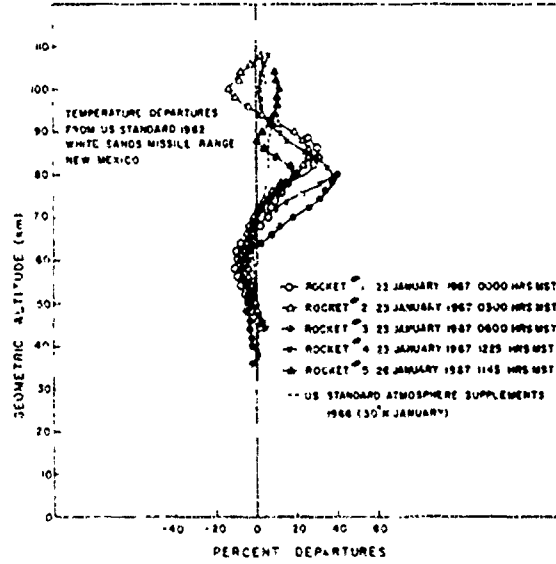
102 and 112 kilometers in succession are shown. The results obtained when the turbopause is assumed to be at 94 kilometers agree well with the O profiles derived from AFCRL airglow measurements and from measurements with a rocket-borne silver surface by NOAA, Boulder, Colorado.

Analysis of turbulence spectra, determined from photographs of chemical releases in the upper atmosphere, and application of the theory which predicts the observed spectra, will result in the determination of local rates of turbulent dissipation and thus the intensity and the diffusion and conduction coefficients of the observed turbulence. The present results of this investigation show that there is a small inertia-like ($-5/3$) subrange of the spectrum limited by viscosity at scale sizes of the order of 10 to 50 meters, and with the large scale end of the spectrum having a (-3) relation, which does not indicate a buoyancy subrange but rather the dominance of the spectrum of the mean density distribution. It has been conclusively

shown that the decay of this mean density gradient with time causes the observed decay of the contaminant spectrum while the turbulent velocity field remains invariant.

The simultaneous measurements of wind velocity and temperature between 30 and 90 kilometers at several latitudes allows the determination of a criterion of atmospheric stability, the Richardson number, as well as an estimate of the rate of local turbulent dissipation as a function of latitude. If the critical value of the Richardson number of unity or even one-half is accepted, then analysis of the above parameters shows that the winter northern mesospheric temperature is intensely turbulent with estimates of the heating rates often exceeding 10^5 ergs/gm sec in narrow layers and at altitudes as low as 50 kilometers. This contrasts with the summer northern atmosphere which is less turbulent and has lower heating rates.

The results for the mid-latitude (38 degrees N) suggest a narrow region of turbu-



Temperature departures from the U. S. Standard Atmosphere 1962, derived from 7-inch falling sphere measurements at White Sands Missile Range, exhibiting wave structure.

lence above 80 kilometers present about 50 percent of the time and with heating rates which are not as large or extensive as those of the northern and equatorial latitudes. The equatorial data suggest intensive turbulence occurring quite often, close to a fractional occurrence of unity.

At all latitudes there quite often occurs a region of marginal stability ($R_i \sim \lesssim 1$) slightly above the stratopause, which could be a source or enhancement region for internal gravity waves. Plots of AFCRI, 7-inch falling sphere data show that such waves propagate through the mesosphere.

A simple expression has been derived for the elevation error of a radar beam as a result of ionospheric refraction. A spherically symmetric ionospheric model was assumed. The formula is based upon equations in the literature which express the refraction due to a flat earth and the angular deviation at infinity caused by a spherical earth.

Studies of the nighttime lower ionosphere during PCA conditions have led to the conclusions that electrons are lost by attachment to O_2 (forming O_2^-) below 75 kilometers at night and that no detachment occurs. The attachment rate decreases in proportion to the square of the density. Thus attachment becomes less important above 75 kilometers. Furthermore, atomic oxygen is abundant above this altitude at all times, further inhibiting negative ion formation because $O_2^- + O \rightarrow O_3 + e$ is a rapid process.

Computations of the electron and positive ion chemistry during a PCA are in fair agreement with the experimental data. However, it is believed that photodetachment rates for species such as CO_4^- , CO_3^- , NO_3^- and hydrated negative ions are needed because too few electrons are calculated in the 50 kilometers region, where these ions are abundant, in comparison to the measurements.

There is at present no explanation for the existence of oxonium ions ($H_{2n+1}O_n^+$)

measured in the D region. It appears that ionization of NO by HLy alpha would provide enough electrons, but the transfer mechanism $NO^+ \rightarrow$ oxonium ions is unknown. The sequence $NO^+ \rightarrow NO^+ \cdot H_2O \rightarrow NO_2^+ \rightarrow NO_2^+ \cdot H_2O \rightarrow H_3O^+$ may provide the answer if all the necessary processes are sufficiently rapid.

LABORATORY MEASUREMENTS OF REACTION RATES: Several reactions of ions with neutral molecules are important in the properties of the normal and perturbed atmosphere. Both positive and negative ions are of interest, extending in complexity from simple atomic species, e. g., O^+ , O^- , to such polyatomic species as $H^+ \cdot 4H_2O$ and CO_4^- . The double mass spectrometer systems used in much of this research permit measurements of ion-neutral reaction cross sections and determinations of reaction mechanisms in the range of interaction energies from a few tenths of an electron volt (eV) up to several hundred eV.

In a weakly ionized gas, such as the earth's ionosphere, reactions which convert positive monatomic ions (O^+ , N^+) into diatomic ions (O_2^+ , NO^+ , N_2^+) are important because of the relatively large rate at which diatomic ions recombine with electrons, thus leading to decay of the charged particle number densities. Cross sections for several such conversion reactions have recently been measured. One of these is the process: $N^+ + N_2 \rightarrow N_2^+ + N$, which is endothermic by 1.03 eV and exhibits the expected threshold in the cross section at about this energy. Studies of the kinetic energy of the product ions have shown that there are two distinct groups of N_2^+ products, corresponding to electron transfer from N_2 to N^+ in the one case and to nitrogen atom transfer from N_2 to N^+ in the other. Indirect evidence was also obtained suggesting the formation of N_2^+ in an excited electronic state (the so-called $B^2\Sigma_u^+$ state) at interaction energies above

4 eV. The production of excited states in aeronomic reactions is important both because of subsequent collisional processes which may occur (it can result in faster conversion of species) and because such states are responsible for the optical radiation frequently observed in the perturbed atmosphere.

Of the several negative ion-neutral reactions which have recently been studied, one of the more interesting processes is $O^- + H_2O = OH^- + OH$. This reaction is endothermic by a few tenths of an electron volt, and its cross section increases rapidly with increasing interaction energy, as expected. When isotopically labeled oxygen ions ($^{18}O^-$) are used as the reactant species, both labeled and unlabeled hydroxyl ions ($^{18}OH^-$ and $^{16}OH^-$, respectively) are observed as products. The labeled ion product may be looked upon as resulting from transfer of a neutral hydrogen atom from the H_2O to the $^{18}O^-$. The unlabeled OH^- results from proton transfer to the $^{18}O^-$, which gives neutral ^{18}OH and leaves $^{16}OH^-$. Velocity analysis of the product ions confirms this interpretation of the reaction mechanism. The kinematics of these processes are such that at the high interaction energies possible in a perturbed atmosphere, O^- ions can be converted to OH^- and OH , and both the charged and neutral hydroxyl species will be energetic and able either to radiate or to react further with the ambient species.

UPPER ATMOSPHERE CHEMICAL RELEASES

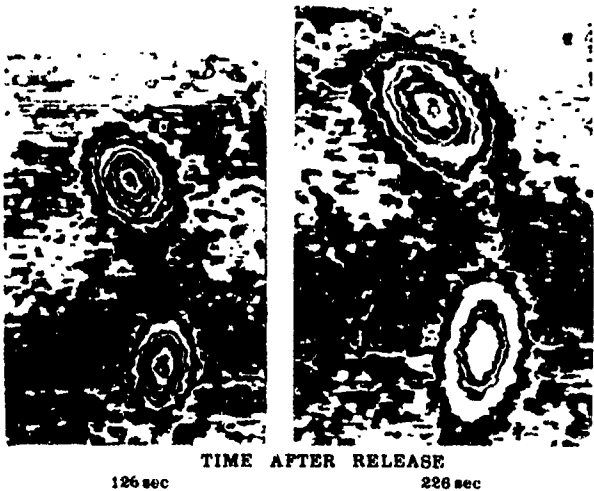
Concentrated efforts during the past two years have further refined chemical release techniques as a tool to measure and interpret the dynamic properties of the mesosphere and lower thermosphere. There are marked changes of temperature and composition with height in this region. It is perturbed by tidal and gravity waves,

by direct absorption of solar energy and by turbulent energy dissipation. A versatile technique for understanding and forecasting the dynamics of this region is the observation of the reactions, motion, dissipation and spectral histories of chemicals injected from rockets.

ATMOSPHERIC STRUCTURE FROM CHEMICAL RELEASES: Chemical releases in the lower thermosphere are useful to obtain geophysical data on diffusion coefficients, temperatures, winds, wind shears, densities, turbulence, and atomic oxygen densities. Trimethyl aluminum (TMA) has proven to be a specially versatile chemical. It can be released as trails or puffs which are fluorescent at twilight and chemiluminous at night. Winds are measured by recording the changes in cloud position as a function of the time, while diffusion coefficients can be obtained from the cloud's rate of growth. During twilight the spectral intensity of aluminum oxide fluorescence permits determination of the temperature of the ambient atmosphere. When diffusion coefficients and temperatures are known, one can utilize familiar gas-kinetic relationships to deduce atmospheric densities.

Diffusion, temperature and density were measured in the 120-180 kilometer altitude region at different seasons and times using data collected in experiments performed during 1968-1972 at Ft. Churchill (59 degrees North), Canada, Hawaii (22 degrees North), and Eglin AFB, Florida (30 degrees North). The Eglin releases include the very successful ALADDIN I and II and HAVE GENIE experiments. The ALADDIN I experiment was carried out on November 20, 1970 to determine Atmospheric Layering and Density Distribution of Ions and Neutrals. The program measured vertical profiles between 70 and 150 kilometers altitude of total neutrals, ions and electrons, individual species, temperature, density, diffusion coefficients,

cient, horizontal winds and turbulent structure. The simultaneous observation of different parameters in the upper atmosphere makes it possible to define their interrelations and to test computer code models of these interrelations. All measurements were made in a 13-minute period (1722-1735 CST) with a local solar depression of 8 to 10.5 degrees. ALADDIN II was carried out on April 12, 1972. A total of 17 rockets were flown in an 11-hour period from evening twilight, through the night, to morning twilight. This series of rocket flights combined chemical releases, mass spectrometer, falling sphere and other experimental techniques to measure winds, temperatures, density, composition and structure of the upper atmosphere. In addition, a series of experimental chemical releases was performed, including nickel and iron carbonyl, lithium at E-region altitudes, and trimethyl boron. The HAVE GENIE experiment (Geophysical Experiments for Neutral species in the Ionospheric E-region) took place May 17-18, 1971. Fifteen rockets that combined chemical release and falling sphere experiments were flown in a 10-hour period to measure wind fields and temperature and density profiles during an evening twilight and night. Simultaneous measurements were made of winds by meteor trail observations and by inflatable spheres. Chemical releases during the following morning twilight measured winds, for comparison with radar observations of meteor winds. Also included were experimental releases of strontium, lithium, and sodium metal vapors and liquid iron carbonyl to evaluate techniques for dispensing metal vapors and for studies of oxide formation as a function of release altitude. In many of the experiments the trimethyl aluminum (TMA) was released as a string of spherical puffs on the downleg of the trajectory. This procedure simplifies the triangulation, rate of growth measurements and aiming of the optical equipment. The alu-



These isodensitraces show the diffusion growth of two diborane puffs at 117 and 122 km.

minum oxide temperatures in the 130-180 kilometer region are lower than predicted by atmospheric models; they appear to increase with altitude at a rate of 60-70 degrees K per 10 kilometers. At 150 kilometers, $T_{\text{mean}} = 600$ degrees K; densities fluctuate up to 50 percent from a mean value of 2×10^{-12} gram. cm⁻³ at 150 kilometers. The U.S. Standard Atmosphere, $T_{\text{exo}} = 900$ degrees K, summer model density curve seems to fit the data best.

Some of the diffusion coefficients have been obtained from diborane ($B_2 H_6$) trails and puffs. $B_2 H_6$ is oxidized by atmospheric oxygen into BO_2 which fluoresces in sunlight. Spurious diffusion rates, obtained below 130 kilometers due to the prevailing high wind shears, are being recalculated, using mathematical formulas that take into account the distortion introduced by the wind shear.

ATOMIC OXYGEN FROM NO TRAILS: AFCRL has used nitric oxide (NO) releases since 1963 to determine atomic oxygen (O) densities in the upper atmosphere. When NO reacts with O, electronically excited NO_2 is formed with subsequent emission of

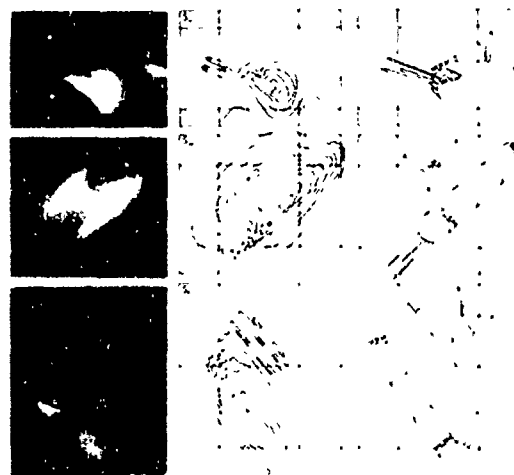
visible light. The technique consists of releasing the NO as a free jet from a sonic orifice during rocket ascent. The orifice is located on the front of the vehicle, which is exposed after nose cone ejection. The free jet expands against the ambient air as the rocket travels at supersonic speed. In these circumstances, a hemispherical mixing zone, bounded by a bow and an inner shock, is formed ahead of the rocket in which the so-called "headglow" originates. A photometer located next to the release orifice views a portion of the headglow, and telemeters measured radiances to a receiving station. Low-density wind tunnel simulation tests at Arnold Engineering Development Center, Tennessee, have revealed that the headglow radiance is independent of the NO release rate and partial pressure in the mixing zone and linearly dependent on the flux of atomic oxygen impinging on the jet. A trough in the rocket-measured atomic oxygen profile at 110-120 kilometers may be related to the peculiar convective conditions of the upper atmosphere or the large-scale meridional or zonal flow of atomic oxygen.

Since atomic oxygen measurements are necessary for a full understanding of the dynamics of the upper atmosphere, future (O) determinations must be concurrent with wind measurements and with photometric determinations of O₃, O₂(¹ Δ_g), OH, and O(¹S), all of which are intertwined in the general photochemical and dynamical behavior of the lower thermosphere.

RADIATIVE STUDIES OF CHEMICAL RELEASES: AFCRL has been active in optical measurements of barium during the ARPA SECEDE series. Barium releases are unique in that they demonstrated the possibility of making ion clouds as low as 100 kilometers altitude. The barium clouds also generate dense clouds of barium oxide. Barium ion clouds can be observed both optically and by radio frequency reflection. Radar characteristics have been

correlated with the development of spatially distributed well defined small-scale structure. This structure consists of thin rods parallel to the earth's magnetic field lines, tens of meters in diameter and tens of kilometers long. Similar structures associated with nuclear weapons have marked effects on the rf propagation characteristics of the ionosphere. Barium releases, in addition to their application to defense problems, are a useful tool in aeronomical measurements. The excitation of the energy states of metals and their oxides upon release results in the emission of resonant radiation and chemiluminescence. This radiation has been analyzed to obtain information about chemical reactions, spectroscopy, and other processes characteristic of the ionosphere. Clouds of metals that have been released, other than barium, include lithium, aluminum and iron.

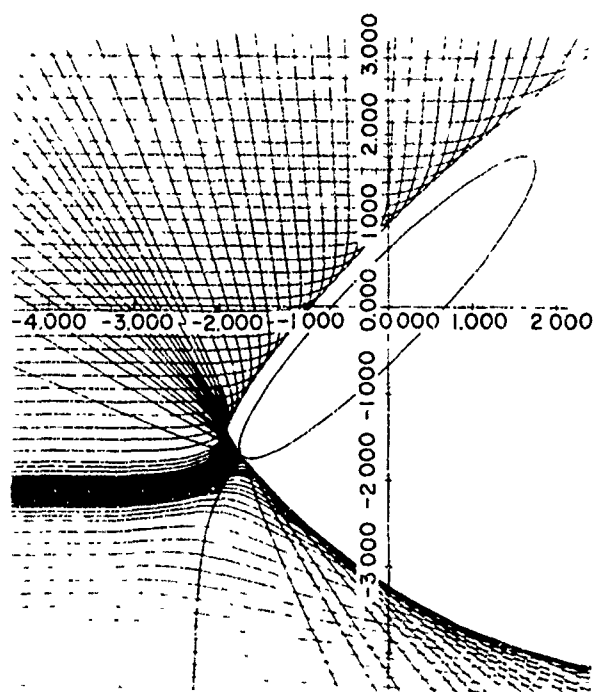
TV STUDIES OF CHEMICAL RELEASES: Rocket-released chemicals interact with ambient species or sunlight to produce visible clouds. Conventional photographic observations, photogrammetry and photometry provide the position, drift, and growth



Photographs and density contours of a barium release and computer projection of a model. Views are from three sites at 930 seconds after release.

history of the clouds. Frequently, photographic film does not have the required optical sensitivity. Therefore, a low light level TV was developed to supply data with the time resolution necessary to determine release characteristics. Growth dynamics, early spectral parameters, and fine scale structural definition have been studied with Vidicon and SEC-Vidicon TV cameras using various lenses, intensifiers, gratings, and video tape and monitor photography to provide high resolution recordings. The tapes enable real-time field evaluation of the releases. These records, as well as narrowband filtered and unfiltered film records, are analyzed on a powerful new digital color TV densitometer. This instrument is especially useful when the records show detailed structure too complex for conventional manual processing, where high spatial accuracy of individual features is required, or when frame-to-frame histories are needed to evaluate time derivatives. The instrument is capable of both high resolution and rapid scan (minutes per frame versus hours for manual analysis) with 256 discrete density levels. Machine editing retains essential data, and automated computations provide total chemical yields, peak intensities, and spatial histories.

RADIO WAVE SCATTERING FROM CHEMICAL RELEASES: A theoretical investigation of the scattering of HF radio waves by spherical electron clouds in the presence of the earth's magnetic field has been completed. The effect of the earth's field was found to be small at 30 MHz but substantial at 3 MHz. The cross section for the ordinary ray depends much more strongly on the field direction than that for the extraordinary ray. A study of clouds which decay more slowly than the Gaussian form showed that an inverse square type of density distribution has substantially higher cross sections in both the forward and back directions. Scattering investigations



Ray paths for scattering by overdense ellipsoidal plasma cloud inclined at 45 degrees to propagation direction.

were extended to ellipsoidal clouds positioned with their major axis along the earth's field lines.

WINDS AND SHEARS: The motion of a chemical vapor trail in winds of constant shear has been studied mathematically. Detailed solutions were obtained in three cases: 1) the flow has no vorticity, 2) vorticity motion predominates, and 3) the wind is stratified vertically. The history of the trail differs considerably in each case and an analysis of the three cases has been used to understand observed flow patterns in the upper atmosphere.

The differential equation governing the diffusion of a gas cloud in the presence of a constant background velocity gradient has been solved analytically. From the solutions, the infinite space Green's function for diffusion in a constant shear flow

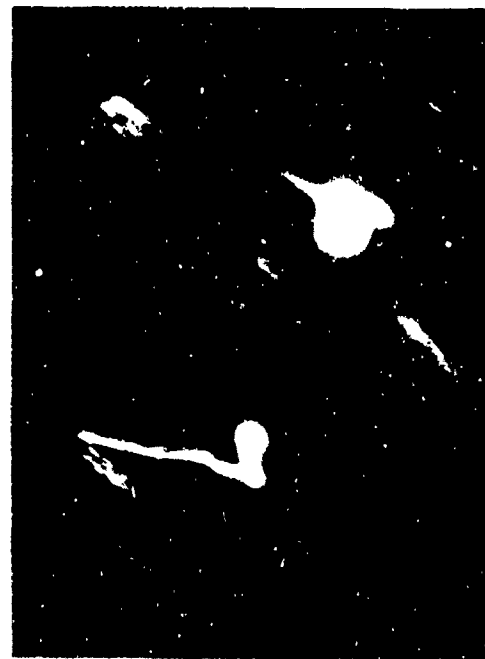
was derived and utilized to solve initial value problems appropriate to upper atmosphere chemical releases. It was shown that the presence of wind shear in the ambient flow can lead to spurious experimental diffusion coefficients and that these coefficients may differ by one order of magnitude from the longitudinal and transverse diffusion coefficients determined in the usual manner. Analytical solutions appropriate for puff and trail releases have been obtained. Horizontal shears of horizontal winds were derived from chemical trail experiments conducted at Eglin AFB, Florida. The vertical profiles of the winds and the vertical shears in the 90-160 kilometer altitude range were found to exhibit a characteristic wave structure with wavelength increasing with altitude. Vertical profiles of the horizontal shears also exhibit a wave structure, but the dominant wavelength appears to be only half that of the winds and vertical shears. Horizontal divergence and vertical vorticity were also computed and found to have amplitudes of approximately 0.001 sec^{-1} . Theoretical studies were also conducted to discover the source of these motions and to evaluate the extent of their contribution to ionization transport and thermospheric heat balance.

In February 1971, a lithium cloud was tracked in full daylight for 40 minutes with a prototype instrument developed at the Laboratory. Two daytime vapor trail trackers based on this prototype have been constructed under contract and are undergoing testing and calibration. These instruments will make possible the first 24-hour neutral wind study, planned for early 1973.

TURBULENCE STUDIES: Seventy horizontal wind profiles have been analyzed for wind shear amplitudes and altitudes ranging from 90 to 150 kilometers. Between 90 and 100 kilometers, shears above 0.03 sec^{-1} occur in 25 percent of the samples whereas

shears above 0.06 sec^{-1} occur in only 3 percent of the samples. The average energy deposition rate (erg per gram-second) could represent a 20- to 80-degrees K temperature rise per day in those samples, if typical eddy viscosities are used. This energy dissipation rate has a significant effect on local transport processes, temperature profiles and the occurrence and persistence of sporadic E layers.

The statistical significance of seasonal effects in these high shears and their associated vertical wavelengths have been reported and compared with theoretical predictions from gravity wave spectra suggested by Hines. The energy dissipation can cause sandwich-like layers of turbu-



Three vapor trails separated by 50 km horizontally after distortion by ionospheric winds, 300 seconds following release. Note the generally similar wind patterns, but the turbulent region in one corresponds to a laminar region in another at the altitude region between 102 and 106 km. In each trail the left bend is at 106 km altitude, with the lower and upper right bends at 102 and 112 km, respectively.

lent and laminar flow and abrupt thermal gradients.

AIRCRAFT DECOY SYSTEMS: Aircraft are extremely vulnerable to heat seeking missiles which home on their hot engine parts or exhaust trails. A system, to provide a semi-continuous chemical decoy has been designed and tested at the Laboratory. This system was flight tested at Eglin AFB in 1970 under AFCRL direction, and shown to provide flexibility in release sequence, rate and duration, and to give a strong IR target. A series of decoys, released continuously, can protect flights up to an hour's duration. The system can be retrofitted to existing aircraft with minimal modifications.

Chaff currently used for meteorological soundings provides an effective radar decoy over a wide wavelength region. Properly dispensed, small amounts of this chaff can form a persistent and dense radar target several miles long. A dispenser system to keep the dispensing aircraft hidden in the chaff cloud was designed and ground tested. The cloud protects following aircraft and, if necessary, it can be reinforced.

SPECTROSCOPIC STUDIES

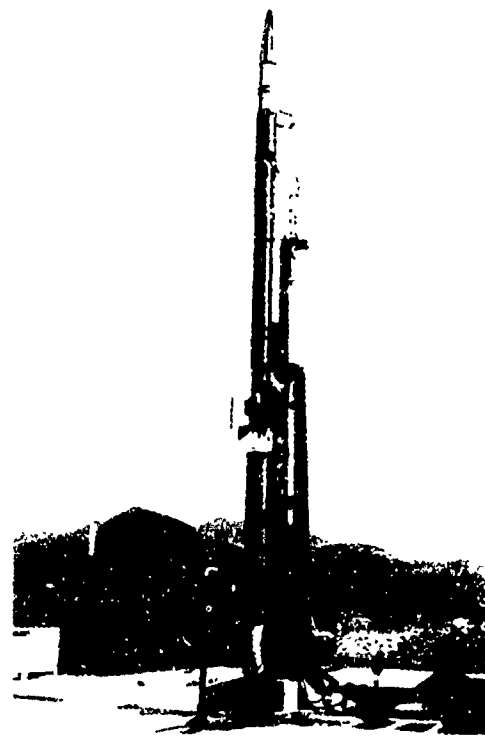
The Spectroscopic Studies Branch has continued to use ultraviolet spectroscopy and theoretical methods to measure, calculate, and interpret upper atmospheric processes and the associated atomic and molecular parameters such as cross sections and transition probabilities. The portion of the ultraviolet radiation which is absorbed by the atmosphere enters significantly not only into normal and perturbed upper atmospheric processes, but also into artificially induced situations, such as those produced by upper atmosphere nuclear detonations.

PROJECT CHASER: This major effort of the Spectroscopic Studies Branch is conducted for the Space and Missile Systems Organization. The goal of the project is to obtain measured data from large missiles launched from Vandenberg AFB, California. The purpose and associated technical details of the project are classified. The project has proceeded through the design, fabrication, calibration, testing and flight phases. The same AFCRL group has also participated in the experiment design, mission, trajectory analysis, calibration, field test, and analysis phases of the project. Several calibration units were completely designed, tested, and used at the Laboratory. The calibration of all units was the exclusive responsibility of AFCRL. Three flights have been completed. Measurements were obtained on two different target vehicles on the first and second flights, while the third flight did not achieve altitude. The report on the first flight has been completed.

A photograph of the CHASER rocket and a diagram of the trajectories and sequence of events are shown.

This is the first time such measurements have been made using this method. This technique may be refined and modified in the future to make upper atmosphere measurements needed to improve the predictability of certain USAF systems.

PHOTOIONIZATION OF $O_2(\alpha^1\Delta_g)$ IN THE D REGION: Until recently, the photoionization of this abundant metastable molecule was believed to be an important source of ionization in the D region. However, calculations reported recently showed that this photoionization is less important than previously judged. The calculations were based on 1) new photoionization cross sections for the ground state $O_2(^3\Sigma_g^-)$ molecule, 2) new photoionization cross sections for the metastable $O_2(^1\Delta_g)$ obtained from a collaborator at Boeing Aircraft Company, and 3) new solar flux data measured at



The Chaser rocket. The instruments are located in the nosecone of the rocket.

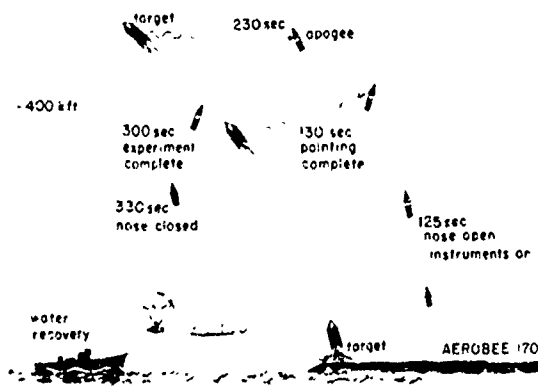
the Aeronomy Laboratory. This information showed that an important factor not previously considered, the absorption by carbon dioxide (CO_2), reduced the solar flux at the O_2 absorption minima (windows) with a consequent decrease in the importance of the photoionization of $\text{O}_2(^1\Delta_g)$. Additional calculations confirmed these results.

OSCILLATOR STRENGTHS OF ATOMIC OXYGEN: In an approximate quantum mechanical treatment of an atom placed in an external electric field, it was shown that the real atom resembles a collection of classical electrons bound to a fixed point with each electron vibrating with a frequency v_n , and associated oscillator strength, f_n , the f-values. Furthermore, it was shown that these f-values determine the intensities of the absorption lines of

the atom. These concepts are also applicable to the analysis of molecular spectra. A laboratory study of several years' duration in cooperation with Northeastern University has begun yielding oscillator strengths (or f-values) of atomic oxygen at strong autoionized lines. A continuum background source is used and the oxygen atoms are created by pyrolysis of ozone (O_3). These experimental f-values for the autoionized lines are the first measurements made, and they are needed to interpret the photoionization continuum whose shape is partially determined by these parameters.

OTHER PROGRESS ON MEASUREMENTS OF CROSS SECTIONS: Data reduction has continued on the measurements of absorption cross sections of H_2O and D_2O , and new cross sections for N_2 with higher resolution. The results for H_2O , in particular, are assuming more importance for upper atmospheric applications since various hydrates, $\text{A}_m(\text{H}_2\text{O})_n$, have been detected.

A table of cross sections at the wavelengths of strong emission lines emitted by



Diagrammatic illustrations of trajectories. The launching areas of target and Chaser are approximately 20 miles apart. The nose-cone opens 125 seconds into the flight, and records signals from the target as indicated. Since recovery is from the water, a specially designed package protects the attitude control system from water damage.

a high altitude nuclear detonation was prepared. The requirements were discussed and obtained at DASA-sponsored meetings, and the tables are based partly on measurements made by the Aeronomy Laboratory. A chapter of the *Reaction Rate Handbook* was revised, and a new chapter on atmospheric absorption of solar radiation has been completed.

ALTITUDE DISTRIBUTION OF ATOMIC OXYGEN: Work is underway on a rocketborne experiment which will determine the distribution of atomic oxygen, by measuring the attenuation of an absorption line of atomic oxygen over a known path length. Testing of the light sources and associated instrumentation for the measurement of atomic oxygen continued.

ANALYSES OF NITROGEN (N_2) AND HYDROGEN (H_2) SPECTRA: Vibration and rotation absorption spectra of nitrogen bands in the 1000 Angstrom region of the vacuum ultraviolet (VUV) have been studied for the $c \leftarrow X$ and $o \leftarrow X$ systems, the former being a member of the Rydberg series converging to the first ionization potential and the latter a series converging to the second ionization potential of N_2 . Data for this study were taken using the very accurate photographic method, a technique especially useful for determining molecular structure. Molecular constants for the states involved in these transitions were accurately determined and numerous rotational perturbations were explained. The study of the absorption spectra of H_2 and its isotopes was continued. A new Rydberg series discovered in deuterium (D_2) contains sharp rotational structures, and extends up to principal quantum number around 40. The convergence limit of this series was very accurately determined, and the limit agreed to within 1 cm^{-1} with the D_2 ionization potential obtained by the combination of the previously known values for the dissociation energies of D_2 and D_2^+ , and the ioniza-

tion potential of atomic deuterium.

ABSORPTION SPECTRA OF DIATOMIC RARE

GASES: This area of molecular research has possible application to the theory of dimers with possible subsequent application to speculated upper atmospheric processes. Absorption band analysis for the diatomic neon molecule including electronic, vibrational, and in some cases, rotational transitions, are completed. The existence of stable diatomic neon (Ne_2) was demonstrated, and its dissociation energy was determined to be about 30 cm^{-1} , i.e., about 3.7×10^{-3} eV. Numerous stable excited molecular states were also found. Evidence was obtained for the existence of heteronuclear diatomic molecules such as $HeNe$, $HeAr$, and $NeAr$. However, their dissociation energies are presently unknown.

During the study of the absorption spectra of rare gas molecules, a new emission spectrum was discovered when a mixture of He and Ar was used in the discharge as source background. The spectrum appeared as two band groups at 1426 Angstroms and 1457 Angstroms. Band groups with very similar structure to that for the (He + Ar) mixture were also discovered for the mixtures (Ne + Ar), (Ne + Kr), (Ne + Xe), and (Ar + Xe). The preliminary explanation for these band groups is that they are produced by molecular ions such as $(HeAr)^+$ and that the associated transitions occur at large internuclear distances where the molecular ions have shallow potential bowls. This suggests emission by rare gas heteronuclear ions from an upper to a lower state.

DETERMINATION OF MOLECULAR FORCES:

Research on the structure of polyatomic molecules has centered on the determination of molecular force fields from observed vibrational frequencies. The occurrence of an external diagonal force was found to correspond to the existence of a vibrational form fully characteristic of a pure stretching or pure bending mode,

while the analogous extremal off-diagonal force constant was found to correspond to a pair of completely mixed vibrational forms, which are, however, separable from all the other modes of motion in terms of the well known classical concept of stretching and bending associated with linear elastic restoring forces. Formulas for such extremal force constants and for the distribution of the potential energy among them have been derived, and are useful in providing approximate values for vibration-rotation interaction constants of molecules such as water (H_2O) and nitrogen dioxide (NO_2).

THEORETICAL ATOMIC SPECTROSCOPY: To describe a many-electron atom quantitatively with high accuracy it is convenient to express the many-electron effects in terms of two-electron contributions. This task is accomplished by the use of parentage expansions. For dipole transitions (needed for transition probabilities) each of these terms can be determined separately, but for the evaluation of the associated energy levels, complications occur in the calculations. The needed coefficients of fractional parentage, recoupling coefficients, and matrix elements have been studied during the year.

A detailed study was made of the structure of corrections to the energy and dipole transition moments of light atoms and ions. New results were found for O V and N IV (beryllium-like structures, a four-electron atom). There was striking improvement over previous work. Because of their importance to upper atmosphere effects, work will be continued on these ions.

To obtain a detailed understanding of the behavior of the atmosphere following a severe disturbance, reliable data are needed on radiative transition probabilities for the various excited levels of positive ions of atmospheric species including the ions O V and N IV. Although much theoretical

and experimental data on these transition probabilities are available, omissions still exist and some of the data are unreliable.

ATOMIC CROSS SECTIONS: The calculations of cross sections for the capture of electrons by oxygen ions from argon have been finished. Calculations of the cross sections for the capture of electrons by protons from atomic oxygen using an impact-parameter method for relatively low energies are about to be resumed. A thorough review of the theory of the polarization of light emitted from electron-impact induced excitation has been completed. A study of the feasibility of calculating the cross sections for the capture of electrons by protons from helium into magnetic substates of atomic oxygen is being made, and an attempt will be made to extend the theory of polarization of light to apply to radiation from atoms formed by electron capture.

Capture of electrons by oxygen ions from argon is one example of a possible reaction following an upper atmosphere nuclear detonation, and electron-impact induced excitation is an important auroral process. Indeed, much of the ambient radiation in the upper atmosphere originates from electron-impact induced excitation.

SOLAR EXTREME ULTRAVIOLET RADIATION

The intensity of solar radiation in the X-ray and extreme ultraviolet region of the spectrum between 1-1700 Angstroms is extremely small in comparison to the intensity of solar radiation in the visible and infrared region of the spectrum. Yet this so-called XUV radiation is the primary source of heating and ionization in the earth's upper atmosphere and it plays a dominant role in the photochemistry of the upper atmosphere. The reason for the im-

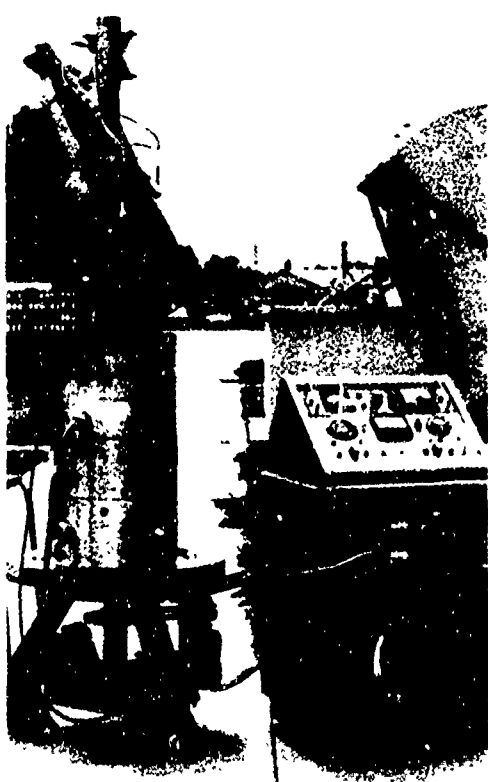
portance of solar XUV is that it is essentially completely absorbed in the upper atmosphere since it is energetic enough to dissociate, excite, and ionize the atomic and molecular constituents of the atmosphere. The longer wavelength visible and infrared radiation, on the other hand, is almost completely transmitted through the upper atmosphere.

Any detailed study of the earth's atmosphere and ionosphere therefore requires accurate experimental data on the absolute intensity of solar radiation incident at the top of the atmosphere, and the intensity as a function of altitude in the atmosphere. The study of the long term variability of the intensity of solar XUV during periods of changing solar activity and during solar flares is also of importance to aeronomy, since temporal variations in solar XUV cause important temporal variations in the parameters of the atmosphere and ionosphere.

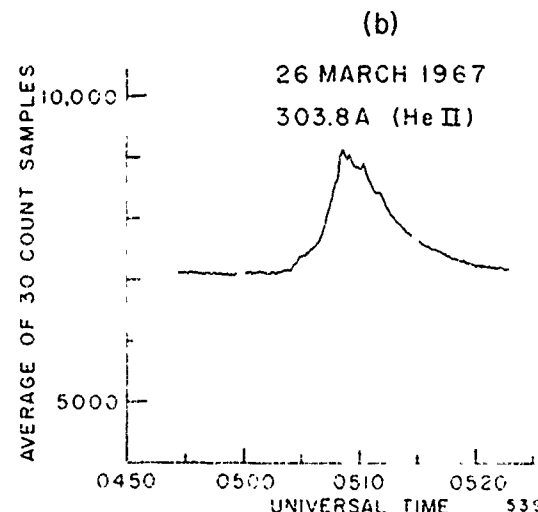
Research in solar XUV in the Aeronomy Laboratory is accomplished with the use of spectrometers flown in both rockets and satellites. The rocket experiments measure primarily the intensity of solar XUV as a function of altitude in the earth's atmosphere. The intensities of particular solar emission lines, separated by the spectrometer, vary with altitude as the emission lines are absorbed by the atmospheric constituents. These absorption data are analyzed to obtain information on the vertical structure of atmospheric densities and ionization. The satellite experiments measure the intensity of solar XUV incident at the top of the earth's atmosphere, since the altitude of the satellite orbit is usually above that part of the earth's atmosphere which absorbs the radiation. The satellite experiments are particularly valuable for a detailed study of long-term variations of solar radiation. In addition, satellite experiments provide the only means to measure solar XUV radiation continuously during the lifetime of a flare on the surface of the sun.

ROCKET OBSERVATIONS OF SOLAR XUV:

During this reporting period, the rocket program to measure solar XUV intensities has continued. The rocket payloads carry grazing-incidence grating spectrometers to measure absolute intensities in selected regions of wavelength over the total wavelength range of 30 to 1250 Angstroms. The wavelength regions covered in a particular rocket experiment depend upon the choice of diffraction grating and detector. The spectrometers are designed so that either a wide wavelength region can be scanned several times during the rocket flight, or several particular selected intense solar



Pre-flight testing of an AFCRL extreme ultraviolet spectrometer mounted on a biaxial solar pointing control



The variation with time of the intensity of the resonance line of singly ionized helium at 304 angstroms recorded during the development of a flare on the surface of the sun.

emission lines can be measured nearly continuously during the flight.

One type of XUV spectrometer now being flown at AFCRL consists of two spectrometers mounted together in a single casting. This newly designed double spectrometer is equipped with eight photoelectric detectors to record different regions of wavelength simultaneously during the rocket flight. The spectrometer permits good spectral resolution to be achieved over a wide range of wavelengths during the relatively short period of time available in a rocket experiment. The spectrometer is mounted on a biaxial solar pointing control which points the optical axis of the spectrometer at the sun during flight.

The first flight of this double spectrometer, launched on an Aerobee 150 rocket from White Sands Missile Range on April 4, 1969, was completely successful. This experiment recorded the solar spectrum in four overlapping wavelength regions, providing a complete high-resolution spectral scan between 50 and 300 Angstroms and also recorded the solar spectrum in four narrow bands of wavelengths lying between 305 and 1250 Angstroms. The data

obtained from this flight have been analyzed and published during this reporting period. The most significant results obtained from this experiment were the identification of many emission lines of highly ionized atoms abundant in the sun, and the determination of the electron temperature in the regions of the solar atmosphere in which the spectral lines of the lithiumlike ions O VI, Ne VIII, and Mg X and the berylliumlike ion O V are predominantly emitted.

Another flight of the double spectrometer was launched, also on an Aerobee 150 from White Sands Missile Range, on August 12, 1970. This experiment was instrumented to obtain accurate data on the absorption of eight pre-selected solar emission lines as a function of altitude in the earth's upper atmosphere. Unfortunately, a malfunction occurred in the nose-cone lift mechanism during this flight; however, the payload was recovered and the instrument flown again on March 16, 1971. This flight was successful, and, from the data, the atmospheric densities of molecular nitrogen and atomic and molecular oxygen between 120-270 kilometers have been determined. One other XUV experiment was flown on an Aerobee 170 from White Sands Missile Range on August 12, 1970. This instrument was equipped with a single diffraction grating and a single photoelectric detector. The experiment was successful and yielded good data on absolute intensities over the wavelength region of 225 to 1225 Angstroms. The altitude achieved by the rocket during this flight was unusually high for this payload, so that the intensity measurements correspond very nearly to the absolute intensities incident at the top of the earth's atmosphere.

An extensive analysis of the solar XUV spectrum between 30 and 128 Angstroms has also been completed. This analysis was based on recordings of the solar spectrum obtained in two previous rocket flights. One of these flights recorded the spectrum

of a very quiet sun, while the other recorded an active sun. The study clearly indicates the dependence of the intensity of the emission lines originating from highly ionized coronal ions on solar activity.

On November 9, 1971, AFCRL launched two rocket experiments simultaneously from White Sands Missile Range to obtain the absolute intensities of solar XUV with a higher spectral resolution and accuracy in the flux measurements than was possible in the past. One of the instruments was a double spectrometer designed to record the solar spectrum between 220 and 1220 Angstroms with a spectral resolution of 0.5 Angstrom and to measure the attenuation of four selected solar emission lines in this same wavelength range as a function of altitude. The line attenuation measurements enable the data of the complete wavelength scan to be corrected for atmospheric attenuation. The other experiment of the pair recorded the solar spectrum between 30 and 205 Angstroms with a spectral resolution of 0.15 Angstrom. The latter spectrometer was equipped with a gas-flow Geiger-Mueller counter having a particularly high quantum efficiency at wavelengths shorter than about 130 Angstroms. The simultaneous rocket experiments were completely successful. As a result the data recorded by each spectrometer refer to identical physical conditions in the solar atmosphere. These data are now being reduced and analyzed.

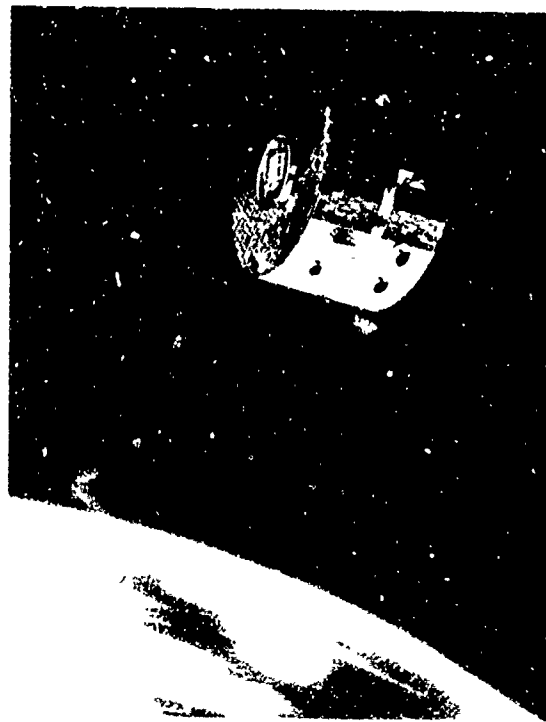
SATELLITE OBSERVATIONS OF SOLAR XUV: NASA's OSO-III, OGO-IV, and OGO-VI satellites, launched between March 1967 and June 1969 carried several of the Laboratory's XUV experiments. These experiments were generally successful and the data are still being analyzed.

During this past year, an analysis of data from OSO-III obtained during solar flares has been completed. The spectrometer aboard OSO-III covered the wavelength range of 300 to 1300 Angstroms and had a spectral resolution of about 2 Ang-

stroms. Radiation of this wavelength, which is the major cause of the formation of the ionosphere, is absorbed by the time it has reached about 100 kilometers above the earth. Changes in solar radiation due to solar activity, therefore, cause changes in ionospheric structure. Particularly violent eruptions on the sun, known as solar flares, have been observed for over a hundred years from the ground, most often in hydrogen emission lines falling in the visible region of the spectrum. However, until the advent of rockets and satellites, no direct measurements of the agent causing the ionospheric disturbance (the XUV radiation) were possible.

The measurements from OSO-III have established the magnitudes and time-dependences of flare emissions in a number of wavelengths in the extreme ultraviolet region. These XUV flare emissions have also been correlated with the familiar ground-based observations of the hydrogen emission lines. The average medium-sized flare is accompanied by an increase of about 15 percent in the total solar radiation in the XUV, the radiation increasing for about 2 minutes to its peak value and subsiding again to pre-flare level about 5 minutes after its peak enhancement. This causes detectable ripples in the ionosphere. A major event of the type which causes profound disruptions in the state of the ionosphere is characterized by a doubling and tripling of XUV emission from the sun in some wavelengths. A sample observation shows an enhancement of about 30 percent in a prominent XUV line observed during a class 2 flare.

The Laboratory will also have XUV spectrometers aboard the NASA Atmosphere Explorer satellites. The orbit of these satellites will be pointed at the sun, enabling continuous measurements of solar XUV in the wavelength range of 140 to 1850 Angstroms to be made above the earth's atmosphere and within part of the earth's atmosphere as the satellite progresses through perigee.



An artist's conception of the AFCRL extreme ultraviolet spectrometer to be flown aboard the NASA Atmospheric Explorer satellite



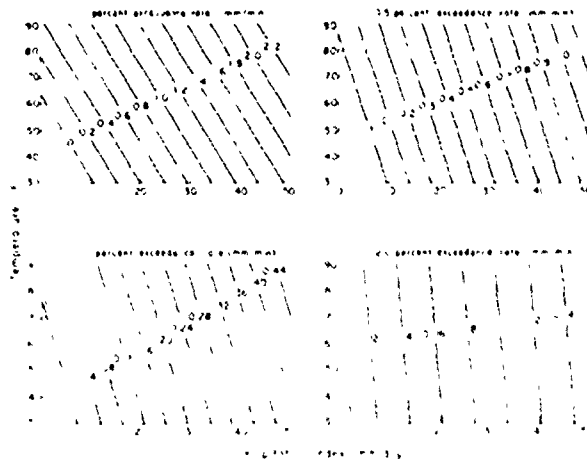
Pre-flight calibration of an extreme ultraviolet rocket spectrometer. The rocket instrument is located in the vacuum chamber of the laboratory grazing-incidence monochromator partially visible in the right-hand side of the photograph

PHOTOMETRIC CALIBRATION OF XUV SPECTROMETERS: To reduce the experimental data obtained from an XUV spectrometer to absolute intensities, the photometric efficiency of the spectrometer must be established in the Laboratory prior to flight. The accuracy of the laboratory calibration sets the ultimate limit on the accuracy of the absolute intensities derived from the space experiment. A collaborative experiment between AFCRL and the National Bureau of Standards (NBS) in Washington, D.C., is now being carried out to check the accuracy of the techniques currently used at AFCRL to calibrate XUV spectrometers. In this experiment, the NBS synchrotron will be used as a continuous source of XUV radiation of known intensity, spectral distribution, and polarization. Thus, a direct comparison of the calibration of a spectrometer obtained by using two independent techniques will be possible.

DESIGN CLIMATOLOGY

Design climatology is the study of the variation in weather elements and their presentation in statistical formats suitable for Air Force systems design and for military operations. Consultations are provided, and studies prepared, for Air Force Systems Command working level engineers and their contractors. For military operations the principal customer is the Air Weather Service.

CLIMATIC EXTREMES FOR MILITARY EQUIPMENT: During the past year a major effort to revise the DOD MIL-STD-210A, Climatic Extremes for Military Equipment, continued. Several new studies of specific weather elements and their extremes were prepared. One study attempts a much higher precision of specification of the instantaneous intensity of precipitation, the total depth of fall, and the number of days



Relation of instantaneous precipitation rates to precipitation index and monthly mean temperature based on all data.

on which it occurred, that is equaled or exceeded at 2 percent to 1/10 percent calculated risk, at any place in the world. This calculation is made from standard climatological data. It answers simple problems, such as how much water should aircraft windshield wipers be required to handle on final approach, and more complicated problems, such as the threshold sensitivity with which proximity fuses should be designed, and also, which microwave frequencies are best suited for satellite communication systems, search radars, and ground approach control radars (GCA) for aircraft. One of the models in the precipitation study is a nomograph for obtaining intensities from the monthly depth of precipitation, days of occurrence, and temperature. Further work in this area has been to specify the intensity, water content and drop size distributions for the extreme storms up to altitudes of 18 kilometers.

Two other studies were performed specifically for the MIL-STD-210 revision. Humidity extremes which equipment should be designed to withstand were specified for altitudes from sea level up to the mesopause. An in-depth analysis of wind

speed extremes in which an attempt is made to specify maximum wind gust in terms of the size of the equipment as well as the acceptable risk, is still in manuscript form. Hail extremes which aircraft in flight as well as structures on the ground should withstand have also led to a report in which tentative estimates for appropriate calculated risk suggest that aircraft in flight should be able to withstand 1 1/2 inch hailstones and ground equipment should be able to withstand hailstones of 2 to 4 inches. A hailstone 5.4 inches in diameter, such as the one observed in Potter, Nebraska, in 1928, will occur in only one hailstorm in 33,000.

ERROR ANALYSIS: In previous design climatology research, an effort had been made to relate slopes in constant pressure surfaces in the stratosphere to vertical accelerations on aircraft flying at constant pressure altitude. One of the major problems in accurately depicting the atmospheric changes in short distances and time periods is the confidence which can be placed in the meteorological instrumentation. This problem is especially difficult in analyzing upper air data, so that any data which will help to determine these errors are of great value. The special soundings taken to determine the slopes of the pressure surfaces in the stratosphere were most valuable. They showed, for example, that rms errors in atmospheric density measurements at 20 to 30 kilometers from operational radiosonde data are only about 0.5 to 0.75 percent of the actual density. These soundings have most recently been used to show that ballistic wind changes over 10-mile distances in areas of great cyclonic activity are greater than available models indicate.

DETECTION AND TRACKING: Research on the probability of visual and infrared detection and tracking at specific angles through various layers of the atmosphere

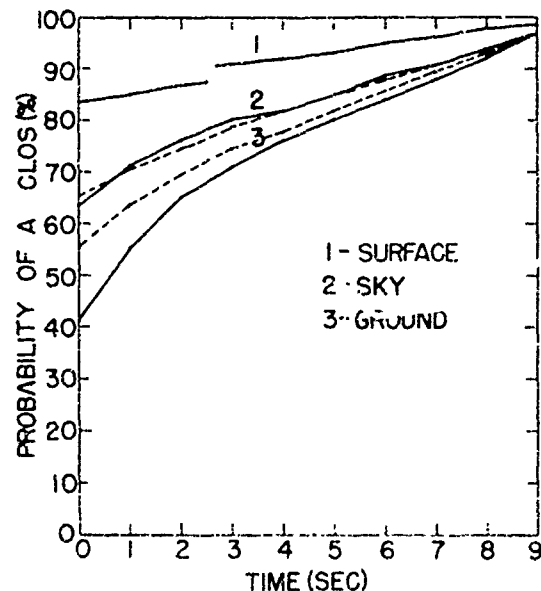
continued through expansion of the in-flight line-of-sight data gathering program. Thousands of small clinometers have been procured and given to the flight crews of as many military and commercial aircraft as can be persuaded to make and report line-of-sight observations. Observers report whether the line of sight through the instrument is clear or obscured by clouds or haze when the instrument is pointed toward the sky, toward the ground, and toward the horizon. Nearly 150,000 observations have been received, but many times this number are anticipated. One objective of this study is to get large enough sample sizes so that accurate probability distributions of clear and obscured line of sight in various areas of interest to the military can be generated. They can then be used to determine the feasibility of specific designs, and if operations are worthy of consideration. Even the sparse data now available indicate tremendous differences in the possibility of seeing along various paths depending on whether observations are made on the ground or from an aircraft.

The probabilities of optical devices working, as indicated by the in-flight observations, are considerably lower than would be inferred from standard weather observations. These probabilities have been worked out for the last 9 seconds of flight as two missiles close. Since haze can be differentiated from clouds in the data, the probability of a clear infrared line of sight can be determined separately from the probability of a clear visual line of sight.

WEATHER TYPING: Nearly ten years ago, work began on typing weather maps, using large capacity, high speed computers. Since sensible weather records are available for each station on weather maps, probabilistic statements regarding the incidence of various types of weather can be made for the typed situation. This re-

search, which had previously been published, has recently attracted the attention of both civilian and military operational weather forecasters. As a result, a new in-depth study was requested to determine the extent which prediction of some weather elements critical to aircraft landings (which frequently vary considerably in hours or even minutes) could be aided by such typing.

A study was performed to determine the feasibility of applying these procedures to estimate the probability of low visibility during the next six hours at Travis AFB, California. It revealed that local influences on visibility often dominate the effects of the large-scale weather situation being typed. Little improvement in prediction



Curve 1 gives the probabilities of a clear view from standard meteorological observations. Dashed and dotted curves 2 indicate analogous probabilities based upon processing of flight crew observations of whether or not blue sky was visible. Curves 3 provided the analogous probabilities from the in-flight observations but are based upon whether or not the ground was visible. Solid curves 2 and 3 are computed from reports in which both haze and clouds in a layer act as the obstruction. Dashed curves 2 and 3 result when clouds are the only obstruction.

was obtained since only large-scale features have been satisfactorily typed. Future typing endeavors will include analogues of significant features of local influences.

ECOLOGY PROBLEM: Due to Congressional concern over pollution of the stratosphere by SST aircraft, a climatological study was made of the water balance of the stratosphere. The Air Force is also interested in the effects military aircraft will have on the stratosphere. A report, just published, indicates from precipitation radar echoes in the stratosphere that 40.6 million tons of water in ice clouds is introduced daily from mid-latitude convective activity in addition to the half million tons of water vapor reaching the stratosphere through normal circulation. Only 1 percent of vaporization of these ice clouds would raise the stratospheric water content by 1 part in a million. Water emitted by aircraft operating in the stratosphere should be considered in relation to both natural sources, to determine its importance. Parallel calculations in this report indicate that typical SST fleet operations would add 0.5 parts per million, not nearly as important as has been speculated.

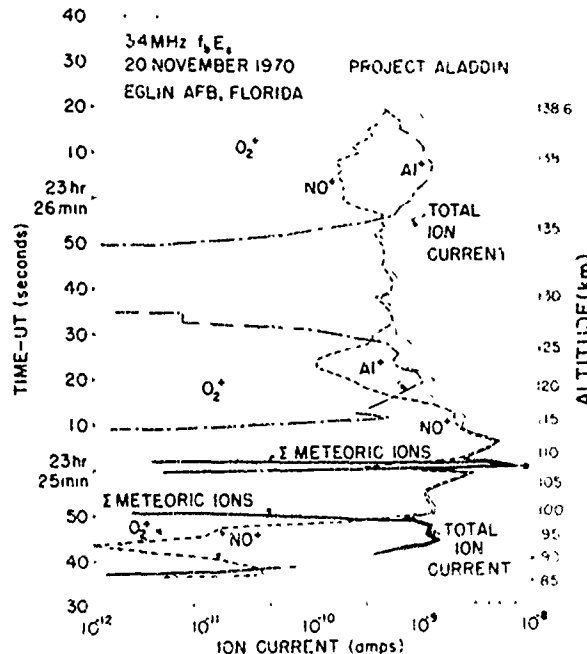
MODEL ATMOSPHERES: A set of model atmospheres has been developed that represent the vertical distributions of thermodynamic properties of the atmosphere that would be encountered by vertically rising or descending vehicles during extreme warm and cold stratospheric and mesospheric (20 to 90 kilometers) conditions in arctic and subarctic regions. Frequencies of occurrence of these warm and cold areas are given for a number of locations north of 55 degrees latitude. This information is needed for the design of reentry vehicles. It is part of a continuing study of the distribution of atmospheric properties between 30 and 120 kilometers which support the model atmosphere re-

search conducted to develop Standard Atmospheres. More recently, an effort to revise the *U. S. Standard Atmosphere Supplements, 1966* has been mounted. Preliminary monthly models for each 15 degrees latitude have been prepared for presentation to the U. S. Committee on Extension to the Standard Atmosphere, which has been reactivated.

ATMOSPHERIC COMPOSITION

The Laboratory has been concerned with the measurement of the charged and neutral atmospheric constituents above 50 kilometers and the determination of the physical and chemical processes responsible for the distributions of these constituents in the atmosphere. The effort has been directed toward understanding and predicting both the neutral and ionized structure at any time and for any natural or artificial disturbance. Measurements are performed with mass spectrometers aboard rockets and satellites and attendant atmospheric processes are studied by subsequent analysis of the flight data.

Various lower ionospheric disturbances such as polar cap absorption, aurorae, sporadic E and solar eclipses have been studied, utilizing the rocket data acquired during such events. In addition, spatial and temporal variations in the neutral composition and density between 150 and 500 kilometers were deduced from measurements obtained from the OV3-6 and OV1-15 Air Force satellites. Rocket and satellite programs were also conducted for the continued acquisition of data to determine the aeronomical properties of the mesosphere and thermosphere (neutral constituents) and of the ionospheric D, E and F regions (positive and negative ion species). Other efforts have included the further development of mass spectrometer flight instrumentation, theoretical and ex-



The positive ion composition of the E region during a sporadic E event. The sporadic E layer at 108 km was composed mainly of silicon ions and smaller amounts of sodium, magnesium, calcium, iron, nickel and silicon oxide ions. The aluminum ions above 110 km resulted from TMA ($Al(CH_3)_3$) released from a previous rocket.

Experimental studies of instrumental in-flight measurement characteristics and the initiation of a laboratory program to examine atmospheric cluster ion processes.

ROCKET COMPOSITION MEASUREMENTS:

In recent years it has been recognized that the determination of atmospheric physical properties requires the near-simultaneous measurements of many parameters which can only be obtained through coordinated rocket and ground-based programs. Project ALADDIN (Atmospheric Layering and Density Distributions of Ions and Neutrals) was conceived to study in some detail atmospheric mass transport processes and their influences on the distributions of ions and minor neutral species. The ALADDIN I program was organized and

directed by AFCRL and included nine rocket payloads from three agencies: AFCRL, NASA Goddard Space-Flight Center, Greenbelt, Maryland, and U. S. Army White Sands Missile Range, New Mexico. The rocket payloads were launched within a ten-minute period about sunset on November 20, 1970 from Eglin AFB, Florida. The measurements included positive ion and neutral composition (AFCRL); winds, turbulence, neutral particle temperature and $O_2(^1\Delta)$ concentrations (AFCRL); neutral particle densities and temperatures (NASA), and meteorological temperatures, densities and winds (WSMR).

Neutral composition measurements of molecular nitrogen (N_2), molecular and atomic oxygen (O_2 and O), argon (Ar), carbon dioxide (CO_2), and ozone (O_3) were obtained from 88 to 120 kilometers on the vehicle upleg and to 60 kilometers on the downleg. By switching the electron ionization energy between 36 and 19 eV on alternate mass scans, measurements of atomic oxygen were extended to low altitudes. This marks the first time a continuous profile of atomic oxygen has been directly measured between these altitude limits. Other, as yet unidentified, constituents in concentrations of less than 1 ppm were also detected.

An ionosonde, operated by Lowell Technological Institute, Lowell, Massachusetts, at the launch site to provide electron density profiles, detected a sporadic E layer at 108 kilometers which had an ionization density ten times greater than normal. Positive ion mass spectrometer measurements revealed a 1 kilometer thick layer composed of meteoric atomic ions near this altitude in addition to the omnipresent meteoric layer at 95 kilometers. Along with the major E-region ions of NO^+ and O_2^+ , large concentrations of aluminum ions were observed between 115 and 139 kilometers, resulting from the trimethyl aluminum ($Al(CH_3)_3$) released from two rock-

ets 5 minutes prior to the positive ion measurements. These aluminum ions served as convenient tracers of ion transport processes. A coordinated analysis of these several measurements is in progress.

The ALADDIN I program has emphasized the importance of dynamics in determining the structure of both the neutral and ionized atmosphere. The measured wind field, density and temperature have been used to calculate the structure of the atmosphere and ionosphere. The model calculations compare reasonably well with the measured structure of the neutral and ionized atmosphere.

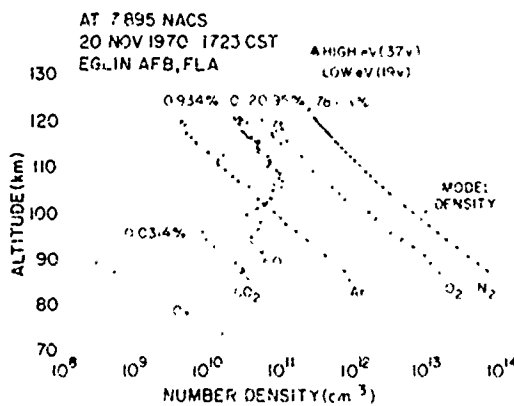
The ALADDIN II program was intended to extend the objectives of ALADDIN I and measure the atomic oxygen profile with a nitric oxide chemical release and a green-line photometer in addition to the neutral mass spectrometer. Measurements of the wind field components, atmospheric density and temperature (AFCRL) were also successfully obtained in the nine-rocket program launched on April 12, 1972 from Eglin AFB. One of the density and temperature profiles was obtained by a Sandia inflatable sphere payload. In addition, meteorological temperatures, densities, and winds were obtained by WSMR and ground-based ionosonde measure-

ments were made by Lowell Technological Institute.

Another joint program was carried out in conjunction with the Mullard Space Science Laboratory (MSSL), England, at Eglin AFB, Florida, in May 1971. The objective of this program was to compare D-region sampling methods for water cluster ions for attached (MSSL) and detached (AFCRL) shock waves ahead of the sampling probe. It is suspected that the weakly bound water cluster ions may be collisionally fragmented traversing the shock-heated gas of the detached shock wave. Daytime and nighttime measurements were obtained from two Nike-Iroquois payloads containing three instruments each: a positive or negative ion quadrupole mass spectrometer (AFCRL), and a positive ion short path length mass spectrometer and a plasma probe (MSSL). The mixed water clusters $\text{NO}_2^-(\text{H}_2\text{O})_n$, along with small amounts of $\text{CO}_3^-(\text{H}_2\text{O})_n$ ($n = 0 - 5$), were dominant in the nighttime negative ion data, but in the cold mesopause (80-90 kilometers) appreciable quantities of negative ions exceeding 160 amu were detected.

The daytime AFCRL positive ion measurements were also programmed to examine the effects of the sampling electric field. It was found that a large electric field causes extensive fragmentation of cluster ions when the instrument is sampling in the vehicle ram direction and that this effect diminishes when the instrument is directed toward the rarefied vehicle wake. The measurements are presently undergoing analysis and will be compared with MSSL results.

A coordinated rocket program was conducted from Wallops Island, Virginia, by AFCRL in October 1971; seven rockets were launched around sunset on October 5. The rocket payloads were designed to measure twilight variations in neutral composition and density and, especially, the changes in O , O_2 , and O_3 between 60 and 120 kilometers. The experimental in-



Neutral composition measurements of the mesosphere and lower thermosphere

strumentation consisted of neutral mass spectrometers, ultraviolet absorption photometers, 2 to 8 Å angstrom X-ray counters, and 7-inch falling spheres instrumented with omnidirectional accelerometers. The program was highly successful. Cryopumped quadrupole mass spectrometers were utilized to measure the neutral species between 70 and 120 kilometers. The mass range of from 4 to 110 amu was swept in about 1 second. Concentration-height profiles of O₃ and O₂ will be obtained from UV absorption measurements at 2600 Angstroms, 2750 Angstroms (O₃), Lyman alpha, and the Schumann-Runge maximum (O₂). Two rockets were launched almost simultaneously to allow correlation between the two techniques for measuring O₂ and O₃. No such correlations between absorption and mass spectroscopy have previously been made in the upper atmosphere. Neutral atmospheric density, temperature, and pressure will be determined from falling sphere drag acceleration results.

Four Nike-Iroquois rockets with ion mass spectrometers and Langmuir probes were launched around sunrise from Wallops Island on October 6, 1971. The objectives of the program were to determine D-region electron detachment processes from negative ion composition measurements and D-region ionization sources at sunrise through positive ion composition measurements. A cryopumped positive ion mass spectrometer and negative ion mass spectrometer were launched when the entire D region was in darkness. Following these, a negative ion mass spectrometer was fired at a solar zenith angle of 94 degrees, so that 4 eV radiation penetrated below 80 kilometers, and a positive ion mass spectrometer was launched at a solar zenith angle of 90 degrees. Excellent data were obtained from all instruments, except the last positive ion spectrometer that failed during excessively "hard" Iroquois burn. From an examination of the flight data,

the following observations were evident: very large negative ion clusters, up to 200 amu, were measured below 90 kilometers; mass 46⁻ amu, probably NO₂⁻, was measured before sunrise but was absent after sunrise; relatively large quantities of chlorine ions, 35⁻ and 37⁻, were seen in the D region; large positive ion clusters up to 98 ± 1 amu, the upper limit of the mass scan, were present below 90 kilometers, including mass numbers that could be identified as the H⁺(H₂O)₄ and H⁺(H²O)₅ water clusters, and a sporadic E layer comprised of meteoric ions was present in the lower E region and evident in ionograms taken during flight.

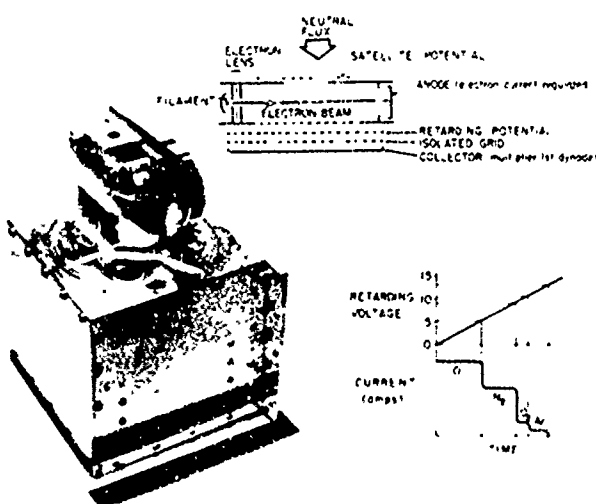
A rocket flight was conducted near midday in February 1972 from Wallops Island, Virginia, to determine the diurnal variations in D-region negative ion composition during quiescent ionospheric conditions. The measurements were made at low Mach number and indicated that most of the negative ions have very large masses exceeding 200 amu, and that in previous measurements made at larger Mach numbers these cluster ions were probably fragmented due to shock heating. Such large negative ion clusters are theoretically difficult to explain and these results have prompted new Laboratory investigations.

A rocket program, designated ICECAP 72, was performed from Poker Flat, Alaska, in March 1972 to study auroral processes. Positive ion composition measurements were made in an IBC Class II auroral form. In a preliminary analysis, the data showed large NO⁺ concentrations and O⁺ densities somewhat larger than expected.

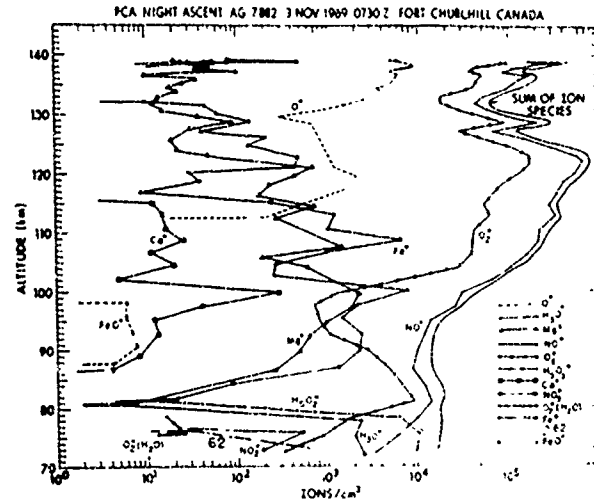
SATELLITE COMPOSITION MEASUREMENTS: Analysis of the massive volume of data obtained from the OV3-6 and OV1-15 satellites is continuing. Measurements of atmospheric composition near 400 kilometers and density by the OV3-6 satellite have shown marked departures from atmospheric models. The results have shown that

the molecular species constitute a much larger percentage of the atmosphere near local sunset than near local noon. Near local sunset, the N₂/O ratio is a few percent, and near local noon, the ratio is a few tenths of a percent or less. This indicates that the temperature maximum is nearer local sunset than the density maximum near 1400 hours LT. The results show that diffusive equilibrium models must be reconsidered with regard to dynamics and heating sources of the atmosphere. In addition, the measurements exhibit a significant dip in the density of each of the species for a large percentage of the orbits near equatorial latitudes (dips located near 10 degrees North and 10 degrees South magnetic latitude). When these dips or troughs occur, the molecular species are often affected more strongly than atomic oxygen.

A new mass spectrometer has been developed at AFCRL for measurements of the neutral composition at satellite altitudes. The instrument, referred to as the Velocity Mass Spectrometer (VMS), makes use of the high satellite velocity to separate the species by energy in a retarding field. The VMS has three main compo-



The satellite velocity mass spectrometer



The positive ion composition of the highly disturbed D and E regions during a simultaneous polar cap absorption event and intense auroral event. Energetic protons create the ionization below 90 km while energetic electrons are responsible for the ionization above 95 km.

nents: an ion source in which the incoming neutral particles are ionized by an electron beam; a retarding potential analyzer to determine the energy, and thereby the mass of the species; and an electron multiplier to measure the ion species current. The unique feature of the VMS is that it is able to discriminate against particles which have struck a surface and thus it is capable of making highly accurate measurements of reactive gas species such as atomic oxygen. The VMS was successfully launched on the OV1-21 satellite on August 7, 1971. Preliminary results have shown the technique to be valuable although the useful satellite lifetime was so short that atmospheric interpretation will be limited.

POLAR CAP ABSORPTION (PCA) EVENTS: The positive ion chemistry of the disturbed D region was determined for the first time from an analysis of rocket measurements taken during the November 24, 1969, PCA event at Ft. Churchill, Canada. The initial

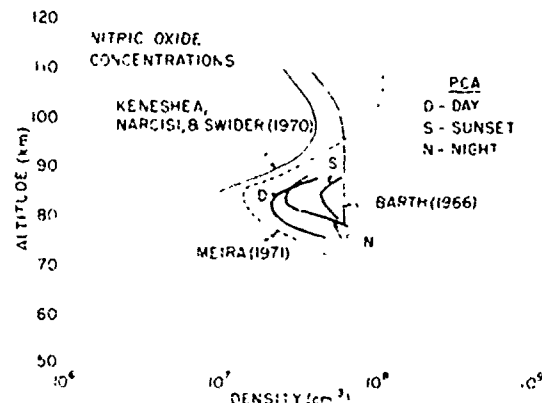
ion species, created by intense proton ionization during a PCA, undergo rapid reactions which produce O_2^+ (> 90 percent) and NO^+ (< 10 percent) in less than a millisecond. Subsequently, the O_2^- was expected to convert to water cluster ions below 85 kilometers in a matter of seconds. The PCA rocket measurements, however, revealed NO^+ and O_2^+ as the major ions while the water cluster ions became predominant only below 77 kilometers at night, somewhere below 73 kilometers during the day, and somewhere below 78 kilometers at sunset (the latter two altitudes represent the lower measurement limits). This indicated a short circuit in the O_2^- to water cluster ion conversion scheme which has since been attributed to the destruction of an intermediate by atomic oxygen. The inclusion of this atomic oxygen reaction in subsequent PCA calculations yielded ion profiles which agree quite well with the measurements. This convenient simplification of the ion composition to NO^+ and O_2^+ in the upper D region allowed the derivation of atmospheric neutral nitric oxide concentrations by using known ion chemical reactions. The derived concentrations agree with other nitric oxide measurements within the respective errors.

The negative ion composition in both the quiescent and disturbed D region remains unexplained. In quiet periods, negative cluster ions dominate, but in the PCA the major ions between 75 and 94 kilometers were O^- at night and O_2^- in the day. In light of measured associative detachment reactions which can quickly destroy O^- and O_2^- , it is not known how these ions are so rapidly produced and/or endure to become the predominant species. Additional work is clearly required in this area.

AURORAE: Positive ion composition measurements have been performed in intense aurorae during which the high latitude E region is strongly perturbed by precipitating energetic electrons. Al-

though the ion chemistry of the quiescent E region is fairly well understood, the auroral rocket measurements yielded anomalously large NO^+/O_2^+ ratios. Since increases in nitric oxide concentrations of up to ten times normal are required to explain these results, several efforts are underway at AFCRL and elsewhere to determine the processes which can produce such enhancements.

SOLAR ECLIPSES: Positive ion composition measurements in the lower ionosphere during the November 1966 solar eclipse and negative ion composition measurements during the March 1970 solar eclipse were analyzed. The D-region results provided strong evidence for the existence of a fast ionospheric reaction which converts NO^+ to water cluster ions, but the actual reaction could not be determined from the measurements. (Note: In the highly disturbed D region, the lifetime of NO^+ is apparently too small for this process to be significant.) The E-region results exhibited the expected behavior of the molecular ions during the eclipse; both the NO^+ and O_2^+ concentrations decayed while the NO^+/O_2^+ ratio increased with solar obscuration. The long-lived meteoric atomic ions were generally unaffected in the short per-



Neutral nitric oxide concentrations derived from PCA measurements compared with other measurements and determinations

iod of the eclipse. A meteoric ion layer that was submerged prior to totality became prominent after the molecular ions fully decayed at totality and produced a sporadic E layer at 105 kilometers.

Negative ion composition measurements near totality again showed the heavy negative ion clusters predominant below 92 kilometers. Relatively large concentrations of O^- , O_2^- , NO_2^- and NO_3^- were detected between 90 and 98 kilometers which were only seen in the eclipse measurements and which cannot presently be explained.

CLUSTER STUDIES: AFCRL rocket-borne mass spectrometer measurements indicate that molecular clusters, and especially water cluster ions, are responsible for some important chemical processes affecting the composition of the lower ionosphere. For example, the puzzling existence of free sulfur ions (S^+) in the D region appears to be associated with water cluster ion concentrations. It has been proposed that terrestrial sulfur-bearing sources (e.g., SO_2 , SO_3) could be associatively reacting with water to form agglomerates which are more amenable to ionization than free sulfur, or other possible sulfur compounds. Another suspected cluster-related reaction is the conversion of NO^+ to water cluster ions which was found to proceed rapidly in the absence of sunlight, as demonstrated in eclipse data. It is possible that reactions with mesospheric conglomerates are responsible for the observed fast depletion of NO^+ under these conditions.

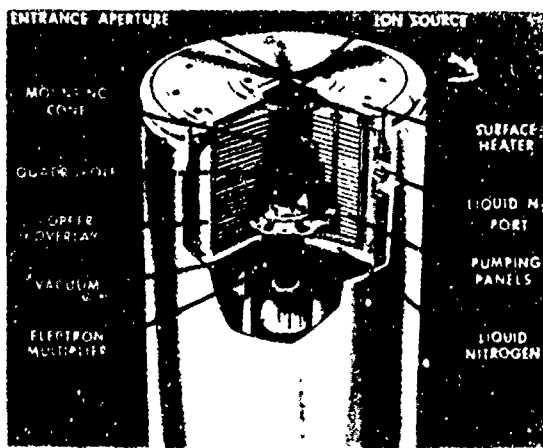
The implications of these problems in atmospheric molecular cluster chemistry have also prompted investigations into clustering reactions as pollutant sinks which are of interest to the Air Force and the Department of Transportation.

Research in these areas is presently being carried out via: 1) A molecular beam/free-jet apparatus at AFCRL to study the equilibrium characteristics of dimers of

pollutant species as molecular cluster precursors and appearance potentials of larger clusters, and 2) The Aerodynamic Molecular Beam Facility at Arnold Engineering Development Center, Tennessee, where free-jet expansions with much higher source pressures are utilized to produce high concentrations of large molecular clusters to study their chemical and physical characteristics.

ROCKET MASS SPECTROMETER SAMPLING

CHARACTERISTICS: To reduce the currents measured by rocket-borne mass spectrometers to ambient species number densities, a thorough knowledge of the instrument sampling characteristics is necessary. When this procedure concerns ion measurements, as compared to neutrals, not only mechanical kinetic effects but also the instrument electric fields influence the ion trajectories. Thus a self-consistent, unified process which solves for both the fields and trajectories is needed, and this requires a lengthy numerical calculation. For the positive ion instrument, several calculations of this nature have been performed for the collisionless case.



The cryopumped neutral mass spectrometer designed for rocket measurements in the 50 to 140 km range.

Calculations are now being made which use a Monte Carlo random sampling method to include the effects of collisions. This will aid in data reductions procedures in the D region where collisions play an important role.

Because of the presence of electrons, the collection problem for the negative ion instrument is more difficult than the corresponding problem for positive ions. A full numerical solution for the collecting characteristics, including space charge effects, has not yet been completed. However, the electric fields surrounding a circular double disk, a simple model of the actual instrument configuration, have been calculated for a zero space charge.

JOURNAL ARTICLES JULY 1970 - JUNE 1972

BEDO, D. E.

Gain Variations in Channel Electron Multipliers

The Rev. of Sci. Instms., Vol. 43, No. 1 (January 1972)

BEDO, D. E., and HINTEREGGER, H. E.

Some Preliminary Results of XUV Spectrophotometry from OGO-VI
Trans. of Am. Geophys. Un., Vol. 51 (1970)

BEST, G. T.

Daytime Tracking of a High Altitude Vapor Trail

J. of the Atm. Sci., Vol. 27, No. 6 (September 1970)

Optical Instrumentation for Tracking High Altitude Vapor Releases by Day

Appl. Opt., Vol. 9, No. 12 (December 1970)

BEST, G. T., FORSEBERG, C. A., GOLOMB, D., ROSENBERG, N. W., and VICKERY, W. K.

The Release of Iron Carbonyl into the Upper Atmosphere

J. of Geophys. Res., Vol. 77, No. 9 (20 March 1972)

BEST, G. T., GOLOMB, D., JOHNSON, R. H. (Photomet., Inc., Lexington, Mass.), KITROESER, D. F., MAC LEOD, M. A., ROSENBERG, N. W., and VICKERY, W. K.

The Release of Diborane into the Upper Atmosphere

J. of Geophys. Res., Vol. 76 (1971)

CHAMPION, K. S. W.

The Properties of the Neutral Atmosphere
Sp. Res. XII, Verlag Akad., Berlin, Ger. (1972)

CHAMPION, K. S. W., and MCISAAC, J. P.

Ionization Gauge Results from the ATCOS (OV3-6) Satellite

Sp. Res. XI, Verlag Akad., Berlin, Ger. (1971)

Direct Measurements of the Semi-Annual Variation During 1968

Sp. Res. XII, Verlag Akad., Berlin, Ger. (1972)

CHERNOSKY, E. J.

The Response of the Magnetosphere to Sunspots as Indicated by Geomagnetic Storminess Levels

Rad. Sci., Vol. 6, No. 5 (May 1971)

DANDEKAR, B. S.

Behavior of Aurora at a Midlatitude Station

J. of Atm. and Terres. Phys., Vol. 34 (1972)

DANDEKAR, B. S., and TURTLE, J. P.

Day Sky Brightness and Polarization During the Total Solar Eclipse of 7 March 1970

Appl. Opt., Vol. 10, No. 6 (June 1971)

FAIRE, A. C., and MURPHY, E. A.

Neutral Density and Temperature Measurements, PCA-69

Proc. of 1969 Solar Particle Event (July 1970)

Perturbations in Density and Temperature Height Profiles Obtained at Eglin, Florida

Sp. Res. XI, Verlag Akad., Berlin, Ger. (1971)

FAUCHER, G. A., and MORRISSEY, J. F.

Atmospheric Density Measurements in the 70-115 Kilometer Region

J. of Geophys. Res., Oceans and Atm., Vol. 76, (1971)

FORBES, J. M., CAPT.

Yield of O(¹D) by Dissociative Recombination of O₂ from Night Airglow Observations

J. of Atm. and Terres. Phys., Vol. 32, No. 12 (1970)

FORBES, J. M., CAPT., and GELLER, M. A. (Univ. of Ill.)

Lunar Semidiurnal Variation

in OI (5577 Å) Nightglow

J. of Geophys. Res., Vol. 77, No. 16 (June 1972)

FREEMAN, D. E.

Extremal Off-Diagonal Force Constants for Molecular Vibrations

Chem. Phys. Ltrs., Vol. 8, No. 3 (1 February 1971)

- FREEMAN, D. E., and ALIX, A., BERNARD, L. (Univ. of Rheims, Fr.)
Study of the Stationary Values of the Off-Diagonal Elements of the Matrices F_{-1} and Σ in the Theory of Molecular Vibrations
 Comptes, Rendus, de l'Academie des Sci., Paris, Fr., Vol. 273B (August 1971)
- FREY, J. H., FISCHER, W. L. (Sea Farm Res. Fdn., Inc., Waltham, Mass.), MAPLE, E. (Sp. Phys. Lab.), and CHERNOVSKY, E. J.
Broad Band Micropulsation Activity at a Geomagnetic Midlatitude Station
 J. of Geomag. and Geoelect., Vol. 23, No. 1 (1971)
- GEORGE, J. D., ZIMMERMAN, S. P., and KENESHEA, T. J.
The Latitudinal Variation of Major and Minor Neutral Species in the Upper Atmosphere
 Sp. Res. XII, Verlag Akad., Berlin, Ger. (1972)
- GRANTHAM, D. D., and KANTOR, A. J.
Validity of Reported Extreme Wind Speeds in the Arctic Stratosphere at SST Altitudes
 Bull. of the Am. Met. Soc., Vol. 51, No. 12 (December 1970)
- GRINGORTEN, I. I.
Modeling Conditional Probability
 J. of Appl. Met., Vol. 10, No. 4 (August 1971)
- HALL, L. A.
Solar Flares in the Extreme Ultraviolet
 Sol. Phys., Vol. 21 (1971)
Spectral Changes in the Zenith Skylight During Total Solar Eclipses
 Appl. Opt., Vol. 10, No. 6 (June 1971)
- HALL, L. A., and HINTEREGGER, H. E.
Solar Radiation in the Extreme Ultraviolet and Its Variation with Solar Rotation
 J. of Geophys. Res., Vol. 75, No. 34 (1 December 1970)
- HEROUX, L. J.
Introduction to a Discussion on Spectrometers and Detectors
 Nuc. Instms. and Meth. (North Holland Pub. Co., Amsterdam), Vol. 90 (1970)
- HEROUX, L. J., and COHEN, M.
Measurements of Electron Temperature in the Solar Chromosphere and Corona
 Philos. Trans., Roy. Soc., London, Eng., Vol. 270 (1971)
- HEROUX, L. J., COHEN, M., and MALINOVSKY, M.
The Interpretation of XUV Rocket Measurements of Intensity Ratios of
- Solar Spectral Lines of the Lithiumlike Ions O VI, Ne VIII and Mg X
 Sol. Phys., Vol. 23 (April 1972)
- HINTEREGGER, H. E.
The Extreme Ultraviolet Solar Spectrum and Its Variation During a Solar Cycle
 Ann. de Geophys. 26, No. 2 (1970)
- HOPFMAN, H. S.
Ionic Spectra of Meteors
 Astrophys. J., Vol. 163, No. 2, Part I (January 1971)
- HOPFMAN, H. S., and MOSES, H. E.
The Ultraviolet Convergence of the Electromagnetic Correction to the Ground State Energy of Hydrogen
 Nuovo Cimento Ltrs., No. 4 (1972)
- HUFFMAN, R. E., PAULSEN, D. E., LARRABEE, J. C., and CAIRNS, R. B. (Boeing Sci. Res. Lab., Seattle, Wash.)
Decrease in D-Region $O_2(^1\Delta_g)$ Photoionization Rates Resulting from CO_2 Absorption
 J. of Geophys. Res., Vol. 76, No. 4 (1 February 1971)
- INNES, F. R.
Reduced Matrix Elements and Representations of Wave Functions
 J. de Phys., Vol. 31, Suppl. C4-43 (1970)
Symmetry Methods for Correlation in Atoms
 The Structure of Matter, The Rutherford Centennial Symp. Vol., Univ. of Canterbury, Christchurch, N. Z. (1971/B. G. Wybourne, Ed.)
- KANTOR, A. J.
Sharp Slopes of Pressure Surface at SST Altitudes
 Bull. of Am. Met. Soc. (September 1970)
- KANTOR, A. J., and GRANTHAM, D. D.
Effect of Range on Apparent Height and Frequency of High-Altitude Radar Precipitation Echoes
 Mo. Wea. Rev., Vol. 98, No. 10 (October 1970)
- KENESHEA, T. J., and MAC LEOD, M. A.
Wind-Induced Modification of E-Region Ionization Profiles
 J. of the Atm. Sci., Vol. 27, No. 6 (September 1970)
- KENESHEA, T. J., and ZIMMERMAN, S. P.
The Effect of Mixing Upon Atomic and Molecular Oxygen in the 70-170 Kilometer Region of the Atmosphere
 J. of the Atm. Sci., Vol. 27, No. 5 (August 1970)

- KLEIN, M. M.
Forward and Back Scatter of RF Waves by Spherical Overdense Clouds for Several Electron Density Distributions
Rad. Sci., Vol. 6, No. 3 (December 1971)
Perturbation Calculation of the Scattering of Electromagnetic Waves by an Underdense Plasma Layer
IEEE Trans. on Ant. and Prop., Vol. AP-20, No. 1 (1972)
- KRASSA, R., and HALL, W. N.
The Aurora Borealis and the 1972 Total Solar Eclipse
Sky and Teles., Vol. 43, No. 3 (March 1972)
- LENHARD, R. W.
Accuracy of Radiosonde Temperatures and Pressure-Height Determinations
Bull. of Am. Met. Soc. (September 1970)
- LLOYD, J. W. F., and SILVERMAN, S. M.
Measurement of the Zenith Sky Intensity and Spectral Distribution during the Solar Eclipse of 12 November 1966 at Belo Horizonte, Brazil, and on an Aircraft
Appl. Opt., Vol. 10 (June 1971)
- LOMONT, J. S. (Univ. of Ariz.), and MOSES, H. E.
The Application of Ray Representations of Translation Groups to the Motion of an Electron in a Crystal Lattice
Annals of Phys. (M. P. Morse, Ed., M. I. T.), Vol. 68 (October 1971)
- LUND, I. A
Correlations Between Areal Precipitation and Geopotential Height
Mo. Wea. Rev. (September 1971)
An Application of Stagewise and Stepwise Regression Procedures to a Problem of Estimating Precipitation in California
J. of Appl. Met., Vol. 5, No. 5 (October 1971)
Sunshine and Lunations at Sapporo, Japan
J. of the Met. Soc. of Jap., Vol. 50, No. 3 (June 1972)
- MAC LEOD, M. A., and ROSENBERG, N. W.
Chemical Releases During the IQSY
Ann. of the IQSY, Vol. 9 (1970)
- MAIER, W. B., II (Univ. of Calif.) and MURAD, E.
Study of Collisions Between Low-Energy N^+ and N_2 : Reaction Cross Sections, Isotopic Compositions, and Kinetic Energies of the Products
J. of Chem. Phys., Vol. 55, No. 5 (1 September 1971)
- MAPLEYN, R. A.
Book, Theory of Charge Exchange
(John Wiley & Sons, Inc /1972)
- MARCOS, F. A., and CHAMPION, K. S. W.
Gravity Waves Observed in High Latitude Neutral Density Profiles
Sp. Res. XII, Verlag Akad., Berlin, Ger. (1972)
Variations of the Neutral Atmospheric Density at Low Satellite Altitudes
Proc. of 1st Intl. Conf. on Aerosp. and Aeronaut. Met., Wash., D. C. (May 1972)
- MARCOS, F. A., CHAMPION, K. S. W., and SCHWEINFURTH, R. A.
More Accelerometer and Orbital Drag Results from SPADES (OV1-15) and Cannon Ball I (OV1-16) Satellites
Sp. Res. XI, Verlag Akad., Berlin, Ger (1971)
- MOSES, H. E.
Vertical Shear Modes in Inertial Waves on a Rotating Earth
J. of Geophys. Res., Vol. 76, No. 9 (20 March 1971)
Eigenfunctions of the Curl Operator, Rotationally Invariant Helmholtz Theorem, and Applications to Electromagnetic Theory and Fluid Mechanics
SIAM J. of Appl. Math., Vol. 21, No. 1 (July 1971)
Exact Electromagnetic Matrix Elements and Exact Selection Rules for Hydrogenic Atoms
Lettere al Nuovo Cimento, Vol. 4 (1972)
Motions of Trails Through Fluids With Constant Velocity Shear
J. of Geophys. Res., Oceans and Atm., Vol. 77, No. 9 (20 March 1972)
- MOSES, H. E., and QUESADA, A. F.
The Expansion of Physical Quantities in Terms of the Irreducible Representations of the Scale-Euclidean Group and Applications to the Construction of Scale-Invariant Correlation Functions Part I
Archive for Rat. Mech. and Anal., Vol. 44, No. 3 (1972)
- MURAD, E.
The Reaction of N^+ with CO at Low Energies
Recent Dev. in Mass Spectr., Univ. of Tokyo, Jap. (1970)
- MURAD, E., and HILDENBRAND, D. L. (McDonnell-Douglas Corp., Calif.)
The Dissociation Energy of $NaO(g)$ and the Heat of Atomization of $Na_2O(g)$
J. of Chem. Phys., Vol. 53, No. 9 (November 1970)

- MURAD, E., and MAIER, W. B., II (Univ. of Calif.)
Production of N_2^+ in Collisions Between N^+ and N_2
Chem. Phys. Lett., Vol. 7 (December 1970)
- NAGARAJA RAO, C. R., TAKASHIMA, T. (Univ. of Calif.), and MOORE, J. G.
Polarimetry of the Daytime Sky During Solar Eclipse
J. of Atm. and Terres. Phys., Vol. 34 (1972)
- NARCISI, R. S.
D Region Composition During Disturbed Conditions
DASIAc Spec. Rpt. 116, Conf. on Appl. of Chem. to Nuc. Eff. (October 1970)
Composition Studies of the Lower Ionosphere
Chap., Upper Atm. Phys., F. Verniani, Ed.; Casa Editrice Compositori, Pub. (1972)
- NARCISI, R. S., BAILEY, A. D., DELLA LUCCA, L., SHERMAN, C., and THOMAS, D. M., CAPT.
Mass Spectrometric Measurements of Negative Ions in the D and Lower E Regions
J. of Atm. and Terres. Phys., Vol. 33, No. 8 (August 1971)
- NARCISI, R. S., BAILEY, A. D., WLODYKA, L. E., and PHILBRICK, C. R.
Ion Composition Measurements in the Lower Ionosphere During the November 1966 and March 1970 Solar Eclipses
J. of Atm. and Terres. Phys., Vol. 34 (1972)
- NARCISI, R. S., PHILBRICK, C. R., and ULWICK, J. C. (Ionos. Phys. Lab.), GARDNER, M. E.
Mesospheric Nitric Oxide Concentrations During a PCA
J. of Geophys. Res., Vol. 77 (1972)
- NARCISI, R. S., and ROTH, W. (Diagnostic Instrm., Inc., San Diego, Calif.)
The Formation of Cluster Ions in Laboratory Sources and in the Ionosphere
Adv. in Elect. and Electron Phys., Vol. 29 (1970)
- FAULSEN, D. E., HUFFMAN, R. E., and LARRABEE, J. C.
Improved Photoionization Rates for $O_2(^1\Delta_g)$ in the D Region
Rad. Sci., Vol. 7, No. 1 (January 1972)
- PAULSEN, D. E., SHERIDAN, W. F., and HUFFMAN, R. E.
Thermal and Recombination Emission of NO_2
J. of Chem. Phys., Vol. 53 (15 July 1970)
- PAULSON, J. F.
Charge Transfer Between Ar^+ and Ar: Time-of-Flight Analysis of Product Ions and Mechanisms in Some Ion-Neutral Reactions
Recent Dev. in Mass Spectr., Univ. of Tokyo, Jap. (1970)
- PAULSON, J. F., DALE, F., and STUDNIARZ, S. A. (Univ. of Pittsburgh, Pa.)
Beam Studies of Ion-Neutral Reactions
Conf. on Appl. of Chem. to Nuc. Eff., DASIAc Spec. Rpt. No. 116 (1971)
- PHILBRICK, C. R., and MCISAAC, J. P.
Measurements of Atmospheric Composition Near 400 Kilometers
Sp. Res. XII, Verlag Akad., Berlin, Ger. (1972)
- QUESADA, A. F., and MAC LROD, M. A.
The Determination of Diffusion Coefficients in a Shearing Flow by Chemical Tracer Techniques
Proc. Symp. of Air Pollution, Turb. and Diffusion, Ed. by H. W. Church and R. E. Luna, Las Cruces, N. M. (March 1972)
- ROGENBERG, N. W.
Observations of Striation Formation in a Barium Ion Cloud
J. of Geophys. Res., Vol. 76, No. 28 (1 October 1971)
- ROSENBERG, N. W., and BEST, G. T.
Chemistry of Barium Released at High Altitudes
J. of Phys. Chem., Vol. 75, No. 10 (1971)
- ROSENBERG, N. W., and ZIMMERMAN, S. P.
Ionoospheric Winds and Viscous Dissipation
Rad. Sci., Vol. 7, No. 3 (1972)
- SALMELA, H. A., and SISSENWINE, N.
A Note on Errors in Upper Air Humidity Climatology
J. of Appl. Met., Vol. 9, No. 6 (December 1970)
- SHERMAN, C., and PARKER, W. (Mt. Auburn Res Assoc., Newton, Mass.)
Potential Due to a Circular Double Disk
J. of Appl. Phys., Vol. 42 (February 1971)
- SILVERMAN, S.
Disorder in the Normal Paraffins from $8 \leq n \leq 16$
Intl. J. of Phys. and Chem. of Sol., Vol. 31 (1970)
The Polar Cap as a Distinct Geophysical Entity
J. of Franklin Inst., Vol. 290 (September 1970)
Night Airglow Phenomenology
Sp. Sci. Rev., Vol. 11, No. 2/3 (October 1970)

- SILVERMAN, S. M., and BALMER, M. K. (Pittsford Cent. High Sch. Sci. Dept., Pittsford, N. Y.) *Cell Constants for Dicalcium Silicate-Alkali Fluoride Complexes and Preparation and Phase Transformations of Dicalcium Silicate-Alkali Fluoride Complexes* J. of the Am. Ceram. Soc., Vol. 54, No. 2 (February 1971)
- SILVERMAN, S. M., and BRENTON, J. G. (Geo-Sci., Inc., Alamogordo, N. M.) *A Study of the Diurnal Variations of the 5577 Å C I Airglow Emission at Selected IGY Stations* Planet. and Sp. Sci., Vol. 18 (1970)
- SILVERMAN, S. M., LLOYD, J. W. F., and AHMED, M. (Regis Coll., Weston, Mass.) *Rocket Measurements of Sodium Dayglow* Planet. Sp. Sci., Vol. 18 (1970)
- SILVERMAN, S. M., LLOYD, J. W. F., and SHARP, W. E. (Univ. of Mich., High Alt. Eng. Lab.) *Summary of Sky Brightness Measurements During Eclipses of the Sun* Appl. Opt., Vol. 10, No. 6 (June 1971)
- SILVERMAN, S. M., and MOORE, J. G. *Optical Observations at the AFCLR Geopole Observatory, Thule AB, Greenland, from 6-10 March 1970: Descriptive Overview* World Data Ctr. A, Rpt. UAG-12, Part II (April 1971)
- STERGIS, C. G. *Aeronomy and Sferics* McGraw-Hill Encycl. of Sci. and Tech. (1971)
- SWIDER, W. *Sources for H, O⁺, (H₂O)_n Ions in the D Region* J. of Geophys. Res., Vol. 75, No. 34 (1 December 1970) *Eclipse, Astronomical and Ionosphere* McGraw-Hill Yrbk. of Sci. and Tech. (1971) *Neutral Atmospheric Dynamics* EOS. Trans. of the Am. Geophys. Un., Vol. 52, No. 7 (July 1971) *Reply* J. of Geophys. Res., Vol. 77, No. 10 (April 1972)
- SWIDER, W., NARCISI, R. S., KENESHEA, T. J., and ULWICK, J. C. (Ionos. Phys. Lab.) *Electron Loss During a Nighttime PCA Event* J. of Geophys. Res., Vol. 76 (July 1971)
- TAKEZAWA, S., and TANAKA, Y. *Absorption Spectrum of HD in the Vacuum-UV Region. Rydberg States and Ionization Energy* J. of Chem. Phys., Vol. 56 (15 June 1972)
- TANAKA, Y., and YOSHINO, K. *Absorption Spectrum of the Argon Molecule in the Vacuum-Ultraviolet Region* J. of Chem. Phys., Vol. 53 (September 1970)
- TURTLE, J. P., and OELBERMANN, E. J. (Ordnance Res. Lab., Penn. State Univ.), BLAKE, J. B., VAMPOLA, A. L. (Aerosp. Corp., El Segundo, Calif.), YATES, G. K. (Sp. Phys. Lab.), and LANCEROTTI, L. J. (Bell Tel. Labs., Murray Hill, N. J.) *Rapid Access of Solar Electrons to the Polar Caps* J. of Geophys. Res., Vol. 77, No. 4 (1 February 1972)
- WEEKS, L. H., CORBIN, J. R., and CUIKAY, R. S. (Raytheon Co., Norwood, Mass.) *Ozone Measurements in the Mesosphere During the Solar Proton Event of 2 November 1969* J. of Atm. Sci., Vol. 29 (1972)
- WEEKS, L. H., and SMITH, L. G. (Univ. of Ill.) *Lyman- α Measurements During the Solar Eclipse of 12 November 1966* Sol. Phys., Vol. 20 (1971)
- YOSHINO, K. *Absorption Spectrum of the Argon Atom in the Vacuum-Ultraviolet Region* J. of the Opt. Soc. of Am., Vol. 60, No. 9 (September 1970)
- YOSHINO, K., and CARROLL, P. K., COLLINS, C. P. (Univ. Coll., Dublin, Ireland) *The High Energy Σ_v⁺ States of N₂* J. of Phys. B, Vol. 3 (1970)
- ZIMMERMAN, S. P., FAIRE, A. C., and MURPHY, E. A. *The Measurement of Atmospheric Stability from 30 to ~ 90 Kilometers* Sp. Res. XII, Verlag Akad., Berlin, Ger. (1972)
- ZIMMERMAN, S. P., and NARCISI, R. S. *The Winter Anomaly and Related Transport Phenomena* J. of Atm. and Terres. Phys., Vol. 32, No. 7 (July 1970)
- ZIMMERMAN, S. P., and ROSENBERG, N. W. *Wind Energy Deposition in the Upper Atmosphere* Sp. Res. XII, Verlag Akad., Berlin, Ger. (1972)
- ZIMMERMAN, S. P., and TROWBRIDGE, C. A., SKY, I. L. (Photomet., Inc., Lexington, Mass.) *(U) Atmospheric Turbulent Spectra* Proc. of ARPA Entrainment Wkshp., Riverside Res. Inst., N. Y. (1971) SECRET Rpt. *Turbulence Spectra Observed in Passive Contaminant Gases in the Upper Atmosphere* Sp. Res. XI, Verlag Akad., Berlin, Ger. (1971)

PAPERS PRESENTED AT MEETINGS
JUL' 1970 - JUNE 1972

BEST, G. T., FORSBERG, C. A., GOLOMB, D., ROSENBERG, N. W., and VICKERY, W. K.

The Release of Iron Carbonyl into the Upper Atmosphere

DASA High Alt. Nuc. Eff. Symp., Stanford Res. Inst., Menlo Pk., Calif. (10-12 August 1971)

BEST, G. T., FORSBERG, C. A., HOFFMAN, H. S., and ROSENBERG, N. W.

AFCRL SECEDE II Optical Observations

SECEDE Data Rev., Stanford Res. Inst., Menlo Pk., Calif. (29 March-1 April 1971)

BEST, G. T., and ROSENBERG, N. W.

Spectroscopic Studies of Barium Releases

SECEDE Sum. Study, Stanford Res. Inst., Menlo Pk., Calif. (13-31 July 1970)

CHAMPION, K. S. W.

AFCRL Planned Satellite Density Measurements

Jt. AWS-CRI-ESD-SAMSO Wkg. Gp. on Density Forecasting, Los Angeles, Calif. (23 March 1971)

The Properties of the Neutral Atmosphere

(Invited), 14th Ann. COSPAR Mtg., Seattle, Wash. (17 June-2 July 1971)

COSPAR International Reference Atmospheres 1971

DASA High Alt. Nuc. Eff. Symp., Stanford Res. Inst., Menlo Pk., Calif. (10-12 August 1971)

Low Altitude Density Satellites

TTCP Pan. FM-13 Mtg., Bermuda (18-21 October 1971)

CHAMPION, K. S. W., and MARCOS, F. A.

Lower Thermosphere Density Variations Determined from Accelerometers on the Cannon Ball II Satellite

15th COSPAR Mtg., Madrid, Sp. (10-24 May 1972)

CHAMPION, K. S. W., MARCOS, F. A., and SCHWEINFURTH, R. A.

Atmospheric Density Values from Orbital Drag on the Cannon Ball II and Musket Ball Satellites

15th COSPAR Mtg., Madrid, Sp. (10-24 May 1972)

CHAMPION, K. S. W., and MCISAAC, J. P.

Direct Measurements of the Semi-Annual Variation During 1968

14th Ann. COSPAR Mtg., Seattle, Wash. (17 June-2 July 1971)

CHAMPION, K. S. W., and SCHWEINFURTH, R. A.

The Mean COSPAR International Reference Atmosphere

14th Ann. COSPAR Mtg., Seattle, Wash. (17 June-2 July 1971)

The Low Altitude Density Research Satellites, Cannon Ball II and Musket Ball

Fall Ann. Am. Geophys. Un. Mtg., San Francisco, Calif. (6-9 December 1971)

CHERNOSKY, E. J.

The Response of the Magnetosphere to Sunspots as Indicated by Geomagnetic Storminess Levels

1970 Symp. on Upper Atm. Currents and Elec. Flds., ESSA, Boulder, Colo. (17-21 August 1970)

Time Delays Between Solar Flare Index and Daily Levels of the Subauroral Geomagnetic Activity

52nd Ann. Am. Geophys. Un. Mtg., Wash., D. C. (12-16 April 1971)

Changes in Sunspot Area to Number Ratio and Associated Sub-Auroral Geomagnetic Activity

53rd Ann. Am. Geophys. Un. Mtg., Wash., D. C. (17-21 April 1972)

COHEN, H. A., MCISAAC, J. P., and SELLERS, B., HANSEN, F. A. (Panamet, Inc., Waltham, Mass.)

An Electron-Beam Atmospheric Density Bremstrahlung Experiment-Preliminary Results

53rd Ann. Am. Geophys. Un. Mtg., Wash., D. C. (17-21 April 1972)

COLE, A. E.

Proposed International Supplemental Atmospheres and

Proposed Interim Standard Atmosphere for Levels from 50 to 80 Kilometers

Intl. Stds. Orgn., Moscow, USSR (8-10 January 1971)

Model of Extreme Arctic and Subarctic Winter Atmospheres Between 20 and 90 Kilometers

14th Ann. COSPAR Mtg., Seattle, Wash. (17 June-2 July 1971)

CORBIN, V. V., and KLEIN, M. M.

Scattering of HF Radio Waves by Elliptical Electron Density Distributions

1972 USNC/URSI-IEEE Spring Mtg., Wash., D. C. (13-15 April 1972)

CORMIER, R. V., and SISSEKWIN, N.

Climatic Extremes for Military Equipment - MIL-STD-210B

1972 Ann. Mtg. of the Inst. of Envmt. Sci., N. Y., N. Y. (30 April-4 May 1972)

FAIRE, A. C., CHAMPION, K. S. W., and MURPHY, E. A.

Variability in Density and Temperature Measurements at White Sands During the 1971 Winter

15th COSPAR Mtg., Madrid, Sp. (10-24 May 1972)

- FAIRE, A. C., and MURPHY, E. A.**
Neutral Density and Temperature Measurements
 COSPAR Symp. on Nov. 1969 Solar Particle Event, Boston Coll., Chestnut Hill, Mass. (16-18 June 1971)
- FAIRE, A. C., MURPHY, E. A., and CHAMPION, K. S. W.**
Simultaneous Rocket Measurements of Upper Atmosphere Density, Temperature and Winds
 Natl. Fall Am. Geophys. Un. Mtg., San Francisco, Calif. (7-10 December 1970)
Neutral Density and Temperature Results Obtained During Total Eclipse of 7 March 1970
 14th Ann. COSPAR Mtg., Seattle, Wash. (17 June-2 July 1971)
- FAIRE, A. C., MURPHY, E. A., and WESTLUND, C. B.** (Univ. of Utah)
Density and Temperature Results from AFCRL 10-Inch Micro-G Falling Sphere
 14th Ann. COSPAR Mtg., Seattle, Wash. (17 June-2 July 1971)
- FORBES, J. M., CAPT.**
Evaluation of Upper-Atmosphere Density Models
 Jt. AWS-CRL-ESD-SAMSO Wkg. Gp. on Density Forecasting, Los Angeles, Calif. (23 March 1971)
- FORBES, J. M., CAPT., and GELLER, M. A.** (Univ. of Ill.)
The Lunar Semidiurnal Variation in O I (5577 Å) Nightglow
 Natl. Fall Am. Geophys. Un. Mtg., San Francisco, Calif. (7-10 December 1970)
- FREEMAN, D. E.**
Least Squares Criterion for Approximately Characteristic Normal Vibrations of a Polyatomic Molecule
 8th Aust. Spectros. Conf., Monash Univ., Clayton, Victoria, Aust. (16-19 August 1971)
- GEORGE, J. D., ZIMMERMAN, S. P., and KENESHEA, T. J.**
Calculation of the Effects of Photochemistry and Transport in a Water Vapor Oxygen Atmosphere
 52nd Ann. Am. Geophys. Un. Mtg., Wash., D. C. (12-16 April 1971)
- GOLOMB, D.**
Simulation of Rocket Plume Radiation Enhancement in Low Density Wind Tunnel
 Symp. on Plume Simulation Techniques, AFCRL (19 February 1971)
- GOLOMB, D., and GOOD, R. E.**
Atomic Oxygen Profiles Over Churchill and Hawaii from Chemical Releases
 14th Ann. COSPAR Mtg., Seattle, Wash. (17 June-2 July 1971)
- GOLOMB, D., GOOD, R. E., and BAILEY, A. B., BUSBY, M. R., DAWBARN, R.** (Arnold Eng. Dev. Ctr., Tenn.)
Dimers, Clusters, and Condensation in Free Jets
 Am. Phys. Soc. Mtg., Wash., D. C. (24-27 April 1972)
- GOLOMB, D., and KITROSSER, D. F.**
Temperature, Diffusion Coefficients and Densities Deduced from ALADDIN TMA Releases
 53rd Ann. Am. Geophys. Un. Mtg., Wash., D. C. (17-21 April 1972)
- GOLOMB, D., KITROSSER, D. F., and JOHNSON, R. H.** (Photomet., Inc., Lexington, Mass.)
Thermosphere Structure Over Churchill and Hawaii from Chemical Releases
 14th Ann. COSPAR Mtg., Seattle, Wash. (17 June-2 July 1971)
- GOOD, R. E.**
Twilight O₂(¹Δ_g) Measurements
 53rd Ann. Am. Geophys. Un. Mtg., Wash., D. C. (17-21 April 1972)
- GOOD, R. E., and GOLOMB, D.**
Atomic Oxygen Profiles in the Lower Thermosphere
 15th COSPAR Mtg., Madrid, Sp. (10-24 May 1972)
- GRANTHAM, D. D., and KANTOR, A. J.**
Probability of Encountering Thunderstorms at 50,000 and 60,000 Feet for Selected Routes Over the United States
 Intl. Conf. on Aerosp. and Aeronaut. Met., Wash., D. C. (22-26 May 1972)
- GRINGORTEN, J. I.**
Modeling Conditional Probability
 Intl. Symp. on Probability and Statistics in the Atm. Sci., Honolulu, Haw. (1-4 June 1971)
Hailstone Extremes for Design
 Intl. Conf. on Aerosp. and Aeronaut. Met., Wash., D. C. (22-26 May 1972)
- HALL, W. N.**
Polar Cap Integral Energies from N_i⁺ Intensities
 Fall Ann. Am. Geophys. Un. Mtg., San Francisco, Calif. (6-9 December 1971)
- HALL, W. N., and LLOYD, J. W. F.**
Polar Cap Optical Intensities During the 2 November 1969 Solar Particle Event
 COSPAR Symp. on the Nov. 1969 Solar Particle

- Event, Boston Coll., Chestnut Hill, Mass. (16-18 June 1971)
- HIGGINS, J. E., HALL, L. A., and CHAGNON, C. W.
Atmospheric Absorption of Solar Extreme Ultraviolet Radiation
15th COSPAR Mtg., Madrid, Sp. (10-24 May 1972)
- HINTEREGGER, H. E.
Far Ultraviolet Solar Irradiance and the Solar Cycle
Inst. of Envmt. Sci., Los Angeles, Calif. (27 April 1971)
EUV Spectral Photometry for Aeronomy
Sem. Ser. on Top. in Atm. Phys., Harvard Univ., Cambridge, Mass. (31 January 1972)
- HOFFMAN, H. S.
Lithium Chemistry in the Upper Atmosphere
53rd Ann. Am. Geophys. Un. Mtg., Wash., D. C. (17-21 April 1972)
- HUFFMAN, R. E.
Ultraviolet Absorption and Ionization Cross-Sections for Deposition Code Calculations
(invited), DASA High Alt. Nuc. Eff. Symp., Stanford Res. Inst., Menlo Pk., Calif. (10-12 August 1971)
- HUFFMAN, R. E., PAULSON, D. E., LARRABEE, J. C., and CAIRNS, H. B. (Boeing Sci. Res. Lab., Seattle, Wash.)
Decrease in D-Region $O_2(^1\Delta_g)$ Photoionization Rates Resulting from CO_2 Absorption
Natl. Fall Am. Geophys. Un. Mtg., San Francisco, Calif. (7-10 December 1970)
- INNES, F. R.
Reduced Matrix Elements and Representations of Wave Functions
CNRS Mtg. on Theory of Atomic Structure, Campus d'Orsay, Paris, Fr. (8-10 July 1970)
Symmetry Methods for Correlation in Atoms
Rutherford Centennial Symp. on the Structure of Matter, Univ. of Canterbury, Christchurch, N. Z. (7-9 July 1971)
- KATAYAMA, D. H., and HUFFMAN, R. E.
The Absorption Spectrum of H_2O and D_2O in the 600-1050 Å Region
Molecular Spectro. Symp., Ohio State Univ., Columbus, Oh. (12-16 June 1972)
- KENESHEA, T. J., GEORGE, J. D., and ZIMMERMAN, S. P.
The Vertical Distribution of Some Atmospheric Species Obtained from a Chemistry-Transport Theory
DASA High Alt. Nuc. Eff. Symp., Stanford Res. Inst., Menlo Pk., Calif. (10-12 August 1971)
- Numerically Modeling the ALADDIN I Experiment*
53rd Ann. Am. Geophys. Un. Mtg., Wash., D. C. (17-21 April 1972)
- KENESHEA, T. J., and SWIDER, W.
Diurnal D-Region Models Using a Photochemical Computer Code and Current Reaction Rates
Conf. on Theoret. Ionos. Models, Penn. State Univ., Univ. Pk., Pa. (14-16 June 1971)
- KENESHEA, T. J., ZIMMERMAN, S. P., and GEORGE, J. D.
The Latitudinal Variation of Major and Minor Neutral Species in the Upper Atmosphere
14th Ann. COSPAR Mtg., Seattle, Wash. (17 June-2 July 1971)
- KLEIN, M. M.
Scattering of Electromagnetic Waves from Stratified Plasmas at High Collision Frequencies
Am. Phys. Soc. Mtg., Wash., D. C. (26-29 April 1971)
- KLEIN, M. M., and ROSENBERG, N. W.
Scattering of HF Radio Waves by a Spherical Electron Cloud in the Presence of a Magnetic Field
52nd Ann. Am. Geophys. Un. Mtg., Wash., D. C. (12-16 April 1971)
- LUND, I. A.
An Application of Stagewise and Stepwise Regress. in Procedures to a Problem of Estimating Precipitation in California
52nd Ann. Am. Geophys. Un. Mtg., Wash., D. C. (12-16 April 1971)
Clear and Cloud-Free Lines-of-Sight Through the Atmosphere
Intl. Conf. on Aeroesp. and Aeronaut. Met., Wash., D. C. (22-26 May 1972)
- MAC LEOD, M. A.
Observations of Short-Period Ionospheric Neutral Motions
52nd Ann. Am. Geophys. Un. Mtg., Wash., D. C. (12-16 April 1971)
Horizontal Shear of Winds in the Thermosphere
14th Ann. COSPAR Mtg., Seattle, Wash. (17 June-2 July 1971)
- MAC LEOD, M. A., KENESHEA, T. J., and NARCISI, R. S.
A Comparison of Theoretical and Experimental Ion Density Profiles for Project ALADDIN
53rd Ann. Am. Geophys. Un. Mtg., Wash., D. C. (17-21 April 1972)
- MARCOS, F. A.
Accelerometer Density Results from the SPADES Satellite

- Jt. AWS-CRL-ESD-SAMSO Wkg. Gp. on Density Forecasting, Los Angeles, Calif. (23 March 1971)
Atmospheric Density Variations Between 180 and 250 Kilometers at Middle and High Latitudes
 52nd Ann. Am. Geophys. Un. Mtg., Wash., D. C. (12-16 April 1971)
Results from the AF Cannon Ball II and Musket Ball Satellites
 Jt. AWS-CRL-ESD-SAMSO Wkg. Gp. on Density Forecasting, Los Angeles, Calif. (7 March 1972)
- MARCOS, F. A., and BLOEMKER, C. F. (N. C. State Univ.), BEDINGER, J. F., CONSTANTINIDES, E. (GCA Corp., Bedford, Mass.)
Results from the PCA 69 Chemical Release Experiments
 COSPAR Symp. on Nov. 1969 Solar Particle Event, Boston Coll., Chestnut Hill, Mass. (16-18 June 1971)
- MARCOS, F. A., and CHAMPION, K. S. W.
Gravity Waves Observed in High Latitude Neutral Density Profiles
 14th Ann. COSPAR Mtg., Seattle, Wash. (17 June-2 July 1971)
Cannon Ball II Satellite Accelerometer Density Measurements
 Fall Ann. Am. Geophys. Un. Mtg., San Francisco, Calif. (6-9 December 1971)
Variations of the Neutral Atmospheric Density at Low Satellite Altitudes
 1st Intl. Conf. on Aerosp. and Aeronaut. Met., Wash., D. C. (22-26 May 1972)
- MARCOS, F. A., CHAMPION, K. S. W., and FIORETTI, R. W.
Lower Thermosphere Variations in the Southern Hemisphere
 14th Ann. COSPAR Mtg., Seattle, Wash. (17 June-2 July 1971)
- MC ISAAC, J. P., and CHAMPION, K. S. W.
Direct Measurements of the Semi-Annual Variation During 1968
 14th Ann. COSPAR Mtg., Seattle, Wash. (17 June-2 July 1971)
- MC ISAAC, J. P., and PHILBRICK, C. R.
Measurements of Atmospheric Composition Near 400 Kilometers
 14th Ann. COSPAR Mtg., Seattle, Wash. (17 June-2 July 1971)
- MC MAHON, W., HEROUX, L., and HINTEREGGER, H. E.
Measurement of the Energy and Angular Distribution of EUV Photoelectrons Emitted from Solids
 Conf. on Photoelec. and Sec. Emission, Univ. of Minn., Minneapolis, Minn. (18-19 August 1971)
- MURAD, E.
The Reactions of N⁺ With N₂
 1970 Ann. Mtg. of the Am. Phys. Soc., Div. of Elec. and Atomic Phys., Seattle, Wash. (23-25 November 1970)
- MURAD, E., and MAIER, W. B., II (Los Alamos Sci. Lab., Los Alamos, N. M.)
The Apparent Charge Exchange Reaction Between N⁺ and N₂
 7th Intl. Conf. on the Phys. of Elec. and Atomic Collisions, Amsterdam, Hol. (26-30 July 1971)
- MURPHY, E. A., ZIMMERMAN, S. P., FAIRE, A. C., and GARDNER, M. E.
A Statistical Distribution of Wind Shear and a Turbulence Criterion from ~ 30 to 90 Kilometers
 52nd Ann. Am. Geophys. Un. Mtg., Wash., D. C. (12-16 April 1971)
- NARCISI, R. S.
Ion Composition Measurements in the Mesosphere and Lower Thermosphere and Related Processes
 (Invited) Interdept. Comm. for Atm. Sci., Fed. Council for Sci. and Tech., Wash, D. C. (23 April 1971)
Mass Spectrometry in the Lower Ionosphere
 Aeron. Sem., Univ. of Ill., Urbana, Ill. (27-28 April 1971)
Aeronautical Implications from Ion Composition Measurements During a PCA
 COSPAR Symp. on Nov. 1969 Solar Particle Event, Boston Coll., Chestnut Hill, Mass. (16-18 June 1971)
O₂⁺ as a Source of Water Cluster Ions in the D Region and Negative Ion Composition Measurements in the D and Lower E Regions
 COSPAR Symp. on D- and E-Reg. Ion Chem., Univ. of Ill., Urbana, Ill. (6-8 July 1971)
The Lower Ionosphere—Its Composition, Structure, and Phenomenology
 Sigma XI Reg. Lect., Bowdoin Coll., Brunswick, Me. (12 October 1971)
Sem., Negative Ions in the D Region
 Centre for Res. in Exper. Sp. Sci., York Univ., Toronto, Can. (3 November 1971)
Sem., The State of D and E Region Theory as Viewed from Ion Composition Measurements
 Ctr. for Earth and Planet. Phys., Harvard Univ., Cambridge, Mass. (23 February 1972)
- NARCISI, R. S., BAILEY, A. D., DELLA LUCCA, L. E., and PHILBRICK, C. R.
Ion Composition Measurements in the Lower Ionosphere During the November 1966 and March 1970 Solar Eclipses

- 14th Ann. COSPAR Mtg., Seattle, Wash. (17 June-2 July 1971)
- NARCISI, R. S., PHILBRICK, C. R., GARDNER, M. E., and ULWICK, J. C. (Ionos. Phys. Lab.)
Mesospheric Nitric Oxide Concentrations During a PCA
 52nd Ann. Am. Geophys. Un. Mtg., Wash., D. C. (12-16 April 1971)
- NARCISI, R. S., PHILBRICK, C. R., MAC LEOD, M. A., and ROSENBERG, N. W.
Composition Measurements of Sporadic E and Ions from a Chemical Release
 53rd Ann. Am. Geophys. Un. Mtg., Wash., D. C. (17-21 April 1972)
- NARCISI, R. S., PHILBRICK, C. R., THOMAS, D. M., CAPT., BAILEY, A. D., WLODYKA, L. E., WLODYKA, R. A., BAKER, D. W., CAPT., FEDERICO, G., and GARDNER, M. E.
Positive Ion Composition Measurements of the D and E Regions During a PCA
 COSPAR Symp. on Nov. 1969 Solar Particle Event, Boston Coll., Chestnut Hill, Mass. (16-18 June 1971)
- NARCISI, R. S., PHILBRICK, C. R., ULWICK, J. C. (Ionos. Phys. Lab.), and GARDNER, M. E.
Mesospheric Nitric Oxide Concentrations During a PCA
 COSPAR Symp. on D- and E-Reg. Ion Chem., Univ. of Ill., Urbana, Ill. (6-8 July 1971)
- NARCISI, R. S., SHERMAN, C., PHILBRICK, C. R., THOMAS, D. M., CAPT., BAILEY, A. D., WLODYKA, R. A., BAKER, D. W., CAPT., and FEDERICO, G.
Negative Ion Composition of the D and E Regions During a PCA
 COSPAR Symp. on Nov. 1969 Solar Particle Event, Boston Coll., Chestnut Hill, Mass. (16-18 June 1971)
- PAULSEN, D. E., HUFFMAN, R. E., and LARRABEE, J. C.
Improved Photoionization Rates for O₂(¹A_g) in the D Region
 COSPAR Symp. of D- and E-Reg. Ion Chem., Univ. of Ill., Urbana, Ill. (6-8 July 1971)
- PAULSON, J. F.
Measurement of Rates of Reactions of Positive Ions and Negative Ions with Neutral Species
 ESD/AFCRL Sci. & Eng. Mtg., L. G. Hanscom Fld., Mass. (3 November 1970)
Reactions of H⁺ with D₂ and O₂
 Conf. on Neg. Ions, Liverpool, Eng. (23-26 March 1971)
Some Negative Ion Reactions With Water
 19th Ann. Conf. on Mass Spectrom. and Allied Top., Atlanta, Ga (2-7 May 1971)
Reactions of H⁺ and D⁺ with D₂, H₂, and HD
- 24th Ann. Gas. Elec. Conf., Univ. of Fla., Gainesville, Fla. (5-8 October 1971)
Some Negative Sulfur Ion-Molecule Reactions
 20th Ann. Conf. on Mass Spectrom. and Allied Top., Dallas, Tex. (4-9 June 1972)
- PHILBRICK, C. R., and FAUCHER, G. A.
Neutral Composition Measurements in the ALADDIN I Program
 53rd Ann. Am. Geophys. Un. Mtg., Wash., D. C. (17-21 April 1972)
- PHILBRICK, C. R., FAUCHER, G. A., and TRZCINSKI, E.
Rocket Measurements of Mesospheric and Lower Thermosphere Composition
 15th COSPAR Mtg., Madrid, Sp. (10-24 May 1972)
- PHILBRICK, C. R., FAUCHER, G. A., and WLODYKA, R. A.
Neutral Composition Measurements of the Mesosphere and Lower Thermosphere
 COSPAR Symp. on D- and E-Reg. Ion Chem., Univ. of Ill., Urbana, Ill. (6-8 July 1971)
- PHILBRICK, C. R., MC ISAAC, J. P., and GARDNER, M. E.
Satellite Measurements of C-Region Ion Density
 52nd Ann. Am. Geophys. Un. Mtg., Wash., D. C. (12-16 April 1971)
- PHILBRICK, C. R., NARCISI, R. S., BAKER, D. W., CAPT., TRZCINSKI, E., and GARDNER, M. E.
Satellite Measurements of Neutral Composition with a Velocity Mass Spectrometer
 15th COSPAR Mtg., Madrid, Sp. (10-24 May 1972)
- PHILBRICK, C. R., NARCISI, R. S., GOOD, R. E., HOFFMAN, H. S., KAYELOHRA, T. J., and REINISCH, B. W. (Lowell Tech. Inst. Res. Fdn., Lowell, Mass.)
The ALADDIN Experiment—Part II. Composition
 15th COSPAR Mtg., Madrid, Sp. (10-24 May 1972)
- QUERADA, A. F., and MAC LEOD, M. A.
Diffusion in a Shear Flow: Theory and Observations
 14th Ann. COSPAR Mtg., Seattle, Wash. (17 June-2 July 1971)
The Determination of Diffusion Coefficients in a Shearing Flow by Chemical Tracer Techniques
 Symp. on Air Poll., Turb. and Diff., Las Cruces, N. M. (7-9 December 1971)
The Determination of Diffusion Coefficients and Shears from Chemical Trails in Regions of High Wind Shear
 15th COSPAR Mtg., Madrid, Sp. (10-24 May 1972)

- RAO, N. C. R., and TAKASHIMA, T. (Univ. of Calif., Los Angeles), Moore, J. C.
Polarimetry of the Daytime Sky During Solar Eclipses
 14th Ann. COSPAR Mtg., Seattle, Wash. (17 June-2 July 1971)
- ROSENBERG, N. W.
Morphology of Striation Development
 SECEDE Sura. Study, Stanford Res. Inst., Menlo Pk., Calif. (13-31 July 1970)
Observation of Striation Onset in a Ba Release
 52nd Ann. Am. Geophys. Un. Mtg., Wash., D. C. (12-16 April 1971)
Chemical Releases in Aeronomy
 Ctr. for Earth and Planet. Phys., Harvard Univ., Cambridge, Mass. (17 January 1972)
Ionospheric Wind Fields During the ALADDIN I Experiment
 53rd Ann. Am. Geophys. Un. Mtg., Wash., D. C. (17-21 April 1972)
- ROSENBERG, N. W., and BEST, G. T.
Chemistry of High Altitude Barium Releases
 52nd Ann. Am. Geophys. Un. Mtg., Wash., D. C. (12-16 April 1971)
- ROSENBERG, N. W., GOLOMB, D., MAC LEOD, M. A., ZIMMERMAN, S. P., and THEON, J. S. (NASA Goddard Sp. Flt. Ctr., Greenbelt Md.)
The ALADDIN Experiment—Part I. Dynamics
 15th COSPAR Mtg., Madrid, Sp. (10-24 May 1972)
- SALMELA, H. A., SISSENWINE, N., and LENHARD, R. W.
Preliminary Precipitation Exceedance Rates for 1, 0, 0.5 and 0.1 Percent Risks Over Europe, Asia and the Contiguous United States
 Int'l. Conf. on Aeroesp. and Aeronaut. Met., Wash., D. C. (22-26 May 1972)
- SHERMAN, C., and NARCISSI, R. S.
Mass Spectrometric Measurements of Auroral Positive Ions
 53rd Ann. Am. Geophys. Un. Mtg., Wash., D. C. (17-21 April 1972)
- SILVERMAN, S. M., and MOORE, J. G.
Optical Observations at the AFCRL Geopole Observatory, Thule AB, Greenland, from 6-10 March 1970
 IUGG 15th Gen. Assem. Mtg., Moscow State Univ., Moscow, USSR (30 July-14 August 1971)
- SILVERMAN, S. M., and TUAN, T. F. (Univ. of Cincinnati, Cincinnati, Ohio)
Auroral Audibility and Traveling Ionospheric Disturbances
- 82nd Mtg. of the Acoust. Soc. of Am., Denver, Colo. (19-22 October 1971)
- SISSENWINE, N.
Evaluation of Design Climatology
 Am. Met. Soc., Boston, Mass. (17 February 1971)
Climatic Data, In-Flight Observations and Seeing Through the Atmosphere
 (Invited) Envmt. Tech. Appl. Ctr., Wash., D. C. (5 March 1971)
- SWIDER, W.
E-Region Model Parameters
 Conf. on Theoret. Ionos. Models, Penn. State Univ., Univ. Pk., Pa. (14-16 June 1971)
Chemical Excitation of O₂(¹A_g) and O₂(¹S_g) in Auroras
 53rd Ann. Am. Geophys. Un. Mtg., Wash., D. C. (17-21 April 1972)
- SWIDER, W., and GARDNER, M. E.
Atmospheric Ionization by Precipitation
Protons and Alpha-Particles
 COSPAR Symp. on Nov. 1969 Solar Particle Event, Boston Coll., Chestnut Hill, Mass. (16-18 June 1971)
- SWIDER, W., and KENESHEA, T. J.
Electron Concentration Profiles for PCA Events
 1970 Int'l. IEEE/G-AP Symp. and Fall USNC/URSI Mtg., Ohio State Univ., Columbus, Oh. (14-17 September 1970)
The Ratio of Negative Ions to Electrons in the D-Region
 52nd Ann. Am. Geophys. Un. Mtg., Wash., D. C. (12-16 April 1971)
Diurnal Variations in the D-Region During PCA Events
 COSPAR Symp. on Nov. 1969 Solar Particle Event, Boston Coll., Chestnut Hill, Mass. (16-18 June 1971)
Ionization and 30 MHz Absorption Generated in the Lower Ionosphere During a Solar Proton Event
 IUGG 15th Gen. Assem. Mtg., Moscow State Univ., Moscow, USSR (30 July-14 August 1971)
- TAKEZAWA, S.
Absorption Spectrum of D₂ in the Vacuum-UV Region Below 540 Å
 Symp. on Molecular Structure and Spectros., Ohio State Univ., Columbus, Oh. (14-18 June 1971)
Rydberg Series of the HD Molecule
 3rd Int'l. Conf. on Vacuum UV Rad. Phys., Tokyo, Jap. (30 August-2 September 1971)
- TAKEZAWA, S., and TANAKA, Y.
The Absorption Spectrum of NO in the Vacuum-UV Region
 Molecular Spectro. Symp., Ohio State Univ., Columbus, Oh. (12-16 June 1972)

- TANAKA, Y., and YOSHINO, K.
Rydberg Absorption Bands of Nitrogen
 Symp. on Molecular Structure and Spectrosc., Ohio State Univ., Columbus, Oh. (8-12 September 1970)
- Emission Spectra of Hetero-Nuclear Rare Gas Molecular Ions*
 Molecular Spectrosc. Symp., Ohio State Univ., Columbus, Oh. (12-16 June 1972)
- THOMAS, D. M., CAPT., NARCISI, R. S., BAILEY, A. D., and WLODYKA, L. E.
Composition Measurements of the Pre-Sunrise D and E Regions
 53rd Ann. Am. Geophys. Un. Mtg., Wash., D. C. (17-21 April 1972)
- TURTLE, J. P., and OELBERMANN, E. J. (Ordnance Res. Lab., Penn. State Univ.)
Discussion of the Polar VLF and Particle Precipitation Data for the November 2, 1969 Solar Particle Event
 COSPAR Symp. on Nov. 1969 Solar Particle Event, Boston Coll., Chestnut Hill, Mass. (16-18 June 1971)
- WEEKS, L. H., CORBIN, J. R., and CUIKAY, R. S. (Raytheon Co., Norwood, Mass.)
Ozone Measurements in the Mesosphere During the Solar Event of 2 November 1969
 COSPAR Symp. on Nov. 1969 Solar Particle Event, Boston Coll., Chestnut Hill, Mass. (16-18 June 1971)
- WEEKS, L. H., and SHERIDAN, W. F.
Ozone and Molecular Oxygen Measurements During the Solar Eclipse of 7 March 1970
 14th Ann. COSPAR Mtg., Seattle, Wash. (17 June-2 July 1971)
- YOSHINO, K., and TANAKA, Y.
Absorption Spectrum of N_2 in the Vacuum-UV Region, the b' - X System
 Symp. on Molecular Structure and Spectrosc., Ohio State Univ., Columbus, Oh. (8-12 September 1970)
- Absorption Spectrum of N_2 in the Vacuum-UV Region, the a - X System*
 Symp. on Molecular Structure and Spectrosc., Ohio State Univ., Columbus, Oh. (14-18 June 1971)
- Emission Band Spectrum of Mixtures of He and Ar in the Vacuum-UV Region*
 3rd Intl. Conf. on Vacuum Ultraviolet Rad. Eff., Tokyo, Jap. (30 August-2 September 1971)
- ZIMMERMAN, S. P., FAIRE, A. C., and MURPHY, E. A.
The Measurement of Atmospheric Stability from 30 to ~ 90 Kilometers
 14th Ann. COSPAR Mtg., Seattle, Wash. (17 June-2 July 1971)
- ZIMMERMAN, S. P., GEORGE, J. D., and KENESHEA, T. J.
Calculation of the Latitudinal Variation of Major and Minor Neutral Species Using Measured Transport Coefficients
 COSPAR Symp. on D- and E-Region Ion Chem., Univ. of Ill., Urbana, Ill. (6-8 July 1971)
- ZIMMERMAN, S. P., PEREIRA, G. P., MURPHY, E. A., and THRON, J. (NASA Goddard Sp. Flt. Ctr., Greenbelt, Md.)
Internal Gravity Waves and Turbulence as Observed in the ALADDIN I Experiment
 53rd Ann. Am. Geophys. Un. Mtg., Wash., D. C. (17-21 April 1972)
- Internal Gravity Waves and Turbulence in Simultaneous Upper Atmosphere Temperature and Wind Measurements*
 15th COSPAR Mtg., Madrid, Sp. (10-24 May 1972)
- ZIMMERMAN, S. P., and ROSENBERG, N. W.
Wind Energy Deposition in the Upper Atmosphere
 14th Ann. COSPAR Mtg., Seattle, Wash. (17 June-2 July 1971)
- ZIMMERMAN, S. P., and TROWBRIDGE, C. A. (Photomet., Inc., Lexington, Mass.)
Turbulence Spectra Observed in Passive Contaminant Gases
 Natl. Fall Am. Geophys. Un. Mtg., San Francisco, Calif. (7-10 December 1970)
The Measurement of Turbulent Diffusion Coefficients in the Altitude Region 90 to ~ 105 Kilometers
 15th COSPAR Mtg., Madrid, Sp. (10-24 May 1972)
- ZIMMERMAN, S. P., TROWBRIDGE, C. A., and KOPSKY, I. L. (Photonet, Inc., Lexington, Mass.)
(U) Atmospheric Turbulent Spectra
 ARPA Entrainment Wkshp., Riverside Res. Inst., N. Y. (12 October 1970) (SECRET Paper)

TECHNICAL REPORTS JULY 1970 - JUNE 1972

- BEST, G. T.
Optical Observations of Chemical Releases in the Upper Atmosphere During 1969, With Description of Instrument Used for Daytime Vapor-Trail Tracking
 AFCRL-70-0692 (October 1970)
- BEST, G. T., and CORBIN, V. L.
Photo-Equilibrium of Barium
 AFCRL-71-0600 (30 November 1971)

- BEST, G. T., FORSBERG, C. A., NOEL, T. M., and ROSENBERG, N. W.
Photographic Studies of Barium Releases
 AFCRL-70-0687 (November 1970)
- COLE, A. E.
Extreme Temperature, Pressure, and Density Between 30 and 80 Kilometers
 AFCRL-70-0462 (12 August 1970)
- CORBIN, V. L., and KLEIN, M. M.
Scattering of HF Radio Waves by Elliptical Electron Density Distributions
 AFCRL-72-0047 (17 January 1972)
- FAIRE, A. C., CHAMPION, K. S. W., and MURPHY, E. A.
ABRES Density Variations
 AFCRL-72-0042 (7 January 1972)
- FORBES, J. M., CAPT.
Upper Atmosphere Density and Deep River, Canada Neutron Monitor Counting Rates
 AFCRL Sp. Forecasting Wkg. Paper No. 5 (November 1971)
(U) Low-Altitude Satellite Ephemeris Prediction
 AFCRL-72-0428 (SECRET/17 July 1972)
- FORBES, J. M., CAPT., and BRAMSON, A. S. (IBM Corp., Burlington, Mass.)
(U) Evaluation of Upper Atmosphere Density Models for Predicting Satellite Ephemerides
 AFCRL-71-0515 (SECRET) (September 1971)
- GRANTHAM, D. D., and SISSENVINE, N.
High Humidity Extremes in the Upper Air
 AFCRL-70-0563 (6 October 1970)
- GRINGORTEN, I. I.
Hailstone Extremes for Design
 AFCRL-72-0081 (27 December 1971)
- GRINGORTEN, I. I., and TATELMAN, P.
Point and Route Temperatures for Supersonic Aircraft
 AFCRL-70-0420 (28 July 1970)
- GROVES, G. V
Atmospheric Structure and Its Variations in the Region from 25 to 120 Kilometers
 AFCRL-71-0410 (27 July 1971)
- HALL, W. N.
Polar Cap Particle Integral Energies from N_{α}^+ Intensities
 AFCRL-72-0400 (28 June 1972)
- HOFFMAN, H. S., and MOSES, H. E.
The Ultraviolet Convergence of the Electromagnetic Correction to the Ground State Energy of Hydrogen
 AFCRL-72-0080 (27 January 1972)
- HUFFMAN, R. E., PAULSEN, D. E., LARRABEE, J. C., LE BLANC, F. J., SHERIDAN, W. F., and RICH, W. D. Y. (Opt. Phys. Lab.), AMMGNS, R. L. (Sp. Gen. Co.)
(U) Project Chaser Flight No. 1 Report
 AFCRL-72-0315 (SECRET) (28 May 1972)
- KANTOR, A. J.
Objective Estimate of the Climatology of Very Tall Convective Clouds - A Negative Report
 AFCRL-70-0611 (6 November 1970)
- KLEIN, M. M.
Perturbation Calculation of the Scattering of Radio Frequency Waves by an Underdense Ionospheric Layer
 AFCRL-70-0538 (5 October 1970)
Forward and Back Scatter Characteristics of Spherically Symmetric Overdense Clouds for Several Electron Density Profiles
 AFCRL-70-0686 (November 1970)
A Study of the Scattering of Microwaves by a Stratified Overdense Plasma at High Collision Frequencies
 AFCRL-71-0400 (27 July 1971)
- KLEIN, M. M., and ROSENBERG, N. W.
Scattering of HF Radio Waves by a Spherical Electron Cloud in the Presence of a Magnetic Field
 AFCRL-71-0371 (30 April 1971)
- LENHARD, R. W., COLE, A. E., and SISSENVINE, N.
Preliminary Models for Determining Instantaneous Precipitation Intensities from Available Climatology
 AFCRL-71-0168 (5 March 1971)
- LUND, I. A.
Climatology as a Function of Map Type
 AFCRL-72-0173 (6 March 1972)
- MARCOS, F. A., and BLOEMKER, C.
Chemical Release Results During PCA 69
 Proc. of Mtg. on Op. PCA 69, AFCRL-70-0625 (October 1970)
- MOSES, H. E.
Exact Vorticity Solutions of the

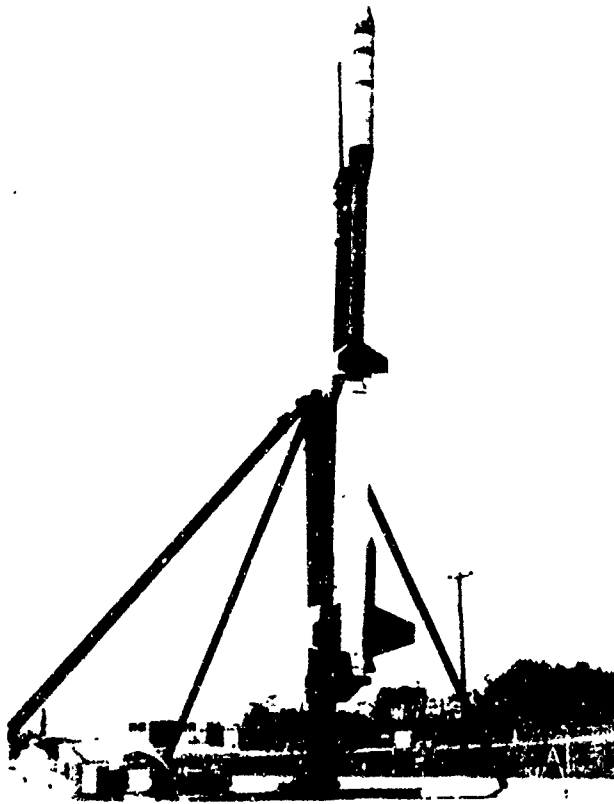
- Incompressible Navier-Stokes Equations*
AFCRL-70-0421 (30 July 1970)
- The Motion of Trails Through Fluids With Constant Velocity Shear*
AFCRL-71-0412 (30 July 1971)
- Exact Electromagnetic Matrix Elements and Exact Selection Rules for Hydrogenic Atoms*
AFCRL-71-0604 (13 December 1971)
- The Expansion of Electromagnetic Fields and Potentials in the Wave Functions of the Photon. The Exact Electromagnetic Matrix Elements and Selection Rules for Hydrogenic Atoms*
AFCRL-72-0279 (27 April 1972)
- MOSES, H. E., and QUESADA, A. F.
A Hydrostatic Approximation for the Flattening of the Planets
AFCRL-70-0668 (December 1970)
- The Expansion of Physical Quantities in Terms of the Irreducible Representations of the Scale-Euclidean Group and Applications to the Construction of Scale-Invariant Correlation Functions*
AFCRL-71-0313 (1 June 1971)
- PAULSON, J. F.
Negative Ion-Neutral Reactions
Proc. of the L. G. Hanacom Fld. Sci. and Eng. Awards Mtg., 3 Nov. 1970, AFCRL-70-0706 (15 December 1970)
- PHILBRICK, C. R., FAUCHER, G. A., and WLODYKA, R. A.
Neutral Composition Measurements of the Mesosphere and Lower Thermosphere
AFCRL-71-0602 (6 December 1971)
- QUESADA, A. F.
Some Solutions of the Diffusion Equation for an Expanding Gas Cloud in a Constant Shear Flow
AFCRL-71-0111 (12 February 1971)
- Application of Vector and Matrix Methods to Triangulation of Chemical Releases in the Upper Atmosphere*
AFCRL-71-0233 (23 April 1971)
- QUESADA, A. F., and MAC LEOD, M. A.
Line-of-Sight Integration of Density Distribution for Discrete Chemical Releases Diffusing in a Constant Shear Flow
AFCRL-71-0574 (10 November 1971)
- ROSENBERG, N. W., and VICKERY, W. K.
Materials Tested for IRCM Applications
AFCRL-70-0624 (October 1970)
- Aircraft Protection and Penetration Aid*
AFCRL-71-0254 (April 1971)
- SALMELA, H. A., SISSENNINE, N., and LENHARD, R. W.
Preliminary Atlas of 1.0, 0.5, and 0.1 Percent Precipitation Intensities for Eurasia
AFCRL-71-0627 (7 October 1971)
- SHERMAN, C.
Ion Collection by a Positive Ion Mass Spectrometer
AFCRL-72-0038 (21 January 1972)
- SHERMAN, C., and PARKER, L. W. (Mt. Auburn Res. Assoc., Newton, Mass.)
Potential Due to a Circular Double Disk
AFCRL-70-0568 (12 October 1970)
- SILVERMAN, S. M.
AFCRL Scientific Research in Greenland: 1967-1970
AFCRL-71-0489 (17 September 1971)
- SILVERMAN, S. M., and MOORE, J. G.
Optical Effects of the March 1970 Geophysical Event at the AFCRL Geopole Observatory, Thule Air Base, Greenland
AFCRL-72-0259 (18 April 1972)
- SILVERMAN, S. M., and TUAN, T. F. (Univ. of Cincinnati, Ohio)
Note on a Traveling Ionospheric Disturbance
AFCRL-71-0603 (16 December 1971)
- SISSENNINE, N.
Extremes of Hydrometeors at Altitude for MIL-STD-210B
AFCRL-72-0369 (5 June 1972)
- SISSENNINE, N., KANTOR, A. J., and GRANTHAM, D. D.
How Dry is the Sky? A Decade Later and the SST
AFCRL-72-0294 (27 April 1972)
- SWIDER, W.
Refraction and Range Errors for VHF Due to the Mid-Latitude Ionosphere
AFCRL-71-0169 (February 1971)
- SWIDER, W., and GARDNER, M. E.
Ionization Rates Due to the Absorption of

*Solar Protons and Alpha Particles in
the Upper Atmosphere*
AFCRL-71-0059 (22 January 1971)

SWIDER, W., and KENESHEA, T. J.
*Diurnal Model of the D-Region During a
PCA Event*
Proc. of Mtg. on Op. PCA 69, AFCRL-70-0625
(October 1970)

VICKERY, W. K.
*Characteristics of Upper Atmosphere
Barium, Trimethylaluminum, Diborane
and Lithium Releases, 1969*
AFCRL-70-0691 (26 October 1970)

ZIMMERMAN, S. P., and FAIRE, A. C.
*Internal Gravity Waves Observed in
Mesospheric Temperature Measurements*
AFCRL-70-0383 (7 July 1970)



The Trailblazer II on its launch pad at Wallops Island, Virginia. These heavily instrumented rockets measure radio transmission through the plasma sheath as the final stage achieves reentry velocities.

III Microwave Physics Laboratory



The work of the Microwave Physics Laboratory is concentrated in several areas in the field of electromagnetics which are linked to well identified Air Force technological objectives in surveillance, reconnaissance, communication and countermeasures. To provide new electromagnetic and electroacoustic technology to improve Air Force operational systems, the Laboratory performs research in antenna theory, electromagnetic field theory, microwave scattering and diffraction, radar sensor design, millimeter wave probing and mapping of the terrestrial and solar atmospheres, plasma physics and microwave acoustics.

Teams of scientists are working directly with the Space and Missile Systems Organization on strategic defense problems. Recent in-house work in acoustic surface waves is presently being tapped to provide false radar target generators for use as missile penetration aids. Other efforts in the control of missile radar cross sections using new theories of electromagnetic diffraction and scattering, and alteration of the reentry ionization gases surrounding the vehicle, are also underway.

The AFCRL Synthetic Aperture Dual Frequency Radar (SADFRAD) radar system provides detection and location of stationary tactical targets in a foliage background while radar target identification can be accomplished through use of the Laboratory-developed phase signature concept. These radar efforts together with the development of a new antenna for station-keeping radars are in answer to technical requirements of the Aeronautical Systems Division, Wright-Patterson AFB, Ohio. The use of millimeter forward scat-

ter radar to measure wind speeds and air turbulence has bearing on the problems of the Air Weather Service (AWS). Daily mapping of the sun with high resolution millimeter radiometry will aid in solar flare prediction and directly applies to the Space Forecasting Program. Technical needs of the Electronic Systems Division, Hanscom Field, Bedford, Mass. have spurred laboratory research into flush-mounted antennas designed for aircraft-to-satellite communication links and for space surveillance. The antenna problems associated with over-the-horizon radars are being studied because of the possible enormous dividends in performance improvement and cost savings.

Such solutions for Air Force mission problems can come only from the reservoir of knowledge and experience accumulated during investigations in the high risk research areas of basic physics and applied electromagnetics. For example, early laboratory studies of thin resistive films have recently turned out to have direct application to a new radar camouflage technique. The Laboratory maintains strong efforts in all those fields that provide the scientific base for order of magnitude advancements in the state of the art.

RADAR SYSTEMS

The electromagnetic scattering properties of a radar target are very complicated functions of the frequency and polarization of the incident signal and the orientation of the target itself. Three distinct scattering regions are usually defined: They are the optical, the resonant and the Rayleigh regions. These regions occur, respectively, when the scatterer is much larger in size than the wavelength of the incident signal, when the scatterer is about the same size as the wavelength and when

the scatterer is much smaller than the incident wavelength.

Most radars operate in the optical region, where target scattering properties are most complicated and most difficult to interpret. The Microwave Physics Laboratory has found that the lower radar frequencies and the resonant region are the key to the airborne detection of stationary or slowly moving military targets near the earth's surface. At these lower frequencies, the ground appears smooth and reflects less interfering clutter energy back to the airborne radar. Further, many military tactical targets exhibit a resonance effect at the longer wavelengths which selectively improves the radar detectability of such targets. The lower radar frequencies are also more effective in penetrating any natural foliage canopy that might ordinarily be used by the enemy for radar camouflage. HF and VHF frequencies have in fact been successfully used in two Laboratory-designed radar reconnaissance systems, the Resonant Region Radar and the Synthetic Aperture Dual Frequency Radar.

LONG WAVELENGTH RADAR TECHNIQUES:

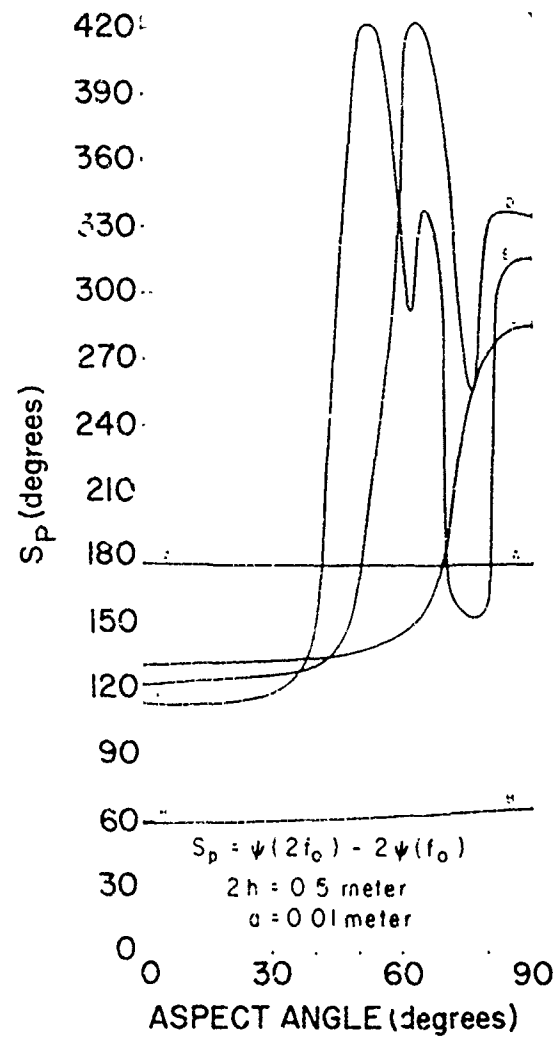
When lower frequencies are used in airborne radar systems, the reflecting properties of targets are greatly influenced by the presence of the nearby earth. Both the amplitude and phase of the signal back-scattered from the target depend on the electrical conductivity and permittivity of the earth, the height and orientation of the target above the earth, and the depression angle through which the radar views the target. An accurate understanding of these target-earth interactions is essential to the design, development and effective utilization of low-frequency airborne radar reconnaissance systems.

The dipole serves as an analytically convenient and physically reasonable model for many tactical targets at the lower radar frequencies. This stems from the

fact that at these resonant frequencies, only the overall length and gross shape of the target affect the radar return signal. Detailed features of the target's shape, being much smaller than the radar wavelength, are unimportant. Recently completed studies of the reflecting properties of dipole targets near the earth's surface have isolated those low frequency radar operating conditions that optimize the multiple frequency detection of ground targets such as missiles and trucks. These analyses also provide a convenient tool for interpreting multiple frequency amplitude and phase signature characteristics such as those presently being collected by the SADFRAD system.

Another result of some importance in low frequency radar detection theory is that the phase of the electromagnetic fields scattered by cylindrical targets is independent of the radar-target aspect angle as long as the cylinder length is less than a half-wavelength. The cylinder can be quite thick, up to half-wavelength. For thin cylinders, however, the phase over a particular part of this scattering region is a simple but very sensitive function of the cylinder length. This means that accurate measurements of phase in the radar return signal can be used to estimate the length of such thin scattering cylinders or targets. Experiments at the Laboratory's Ipswich Test Site and Scattering Range have shown that as frequency is varied, the

PHASE SIGNATURE OF THIN RODS



The dual frequency phase signature of a thin rod with the incident field polarized parallel to the rod. The phase signature is shown as a function of the aspect angle of the rod. Curves A and B are nearly straight lines, showing that when the rod is less than a half wave in length at the highest frequency, the dual frequency phase signature is essentially independent of the aspect angle of the rod. The dual frequency phase signature thus represents a measurable quantity that is related to the physical characteristics of the scatterer regardless of the viewing angle.

CURVE	f_0 MHz	ROD LENGTH			λ_0 meters
		f_0	$2f_0$	λ_0	
A	75	$\lambda/8$	$\lambda/4$	4	
B	150	$\lambda/4$	$\lambda/2$	2	
C	300	$\lambda/2$	λ	1	
D	600	λ	2λ	1/2	
E	900	$3\lambda/2$	3λ	1/3	

shape of the amplitude of the field back-scattered from thin cylinders is also independent of aspect angle, not only in the Rayleigh region, but right through the first resonance maximum. These two new pieces of information on the amplitude and phase characteristics of thin cylinders are important in radar design not only because they provide quantities that characterize the size and shape of the scatterer but also because they are not dependent on the target-radar aspect angle.

The Resonant Region Radar was the first of the two low frequency reconnaissance radars originated by this Laboratory. Basically, the system consisted of an HF monopulse phase comparison radar that yielded target azimuth versus range information as a display output. Two frequencies were used to provide a characteristic phase signature as a separate target parameter. The entire radar system was designed in-house, ground tested at the Ipswich test site, and finally flight tested for over 100 hours of airborne time. Flights over the KADC Underbrush range at Eglin AFB, Florida, proved the validity of the long wavelength detection philosophy on which the radar had been based. A similar radar system is now installed at the Ipswich site where it is being evaluated as a ground-based aircraft detection system.

One distinctive characteristic of the Resonant Region Radar was its use of the target phase signature. This concept originated at AFCRL but was developed for stationary or slowly moving targets. The question was whether the phase signature characteristic of a moving aircraft target would be adversely affected by the target motion and induced doppler shift. An analysis showed that even for such targets, the phase signature is independent of motion effects and remains as a unique target parameter. In the present test arrangement, targets are displayed so that they not only appear at their proper angular and range coordinates, but in a color that depends on their phase signature.

A series of tests on the ground-based RRR at Ipswich with Cessna type aircraft helped define the system capabilities. The aircraft flew in pre-arranged complicated flight patterns so that the observed scope data could be correlated with the aircraft orientation. Observers felt that the phase signature color display, coupled with the normal azimuth-range information, made it possible to determine the target's physical appearance and materially aided in the more sophisticated task of target identification. In addition, the color display proved to be a sensitive indicator of any deviation of the aircraft from its track. Laboratory scientists feel that the radar could have applications in Air Base defense against low flying helicopters and other attack aircraft.

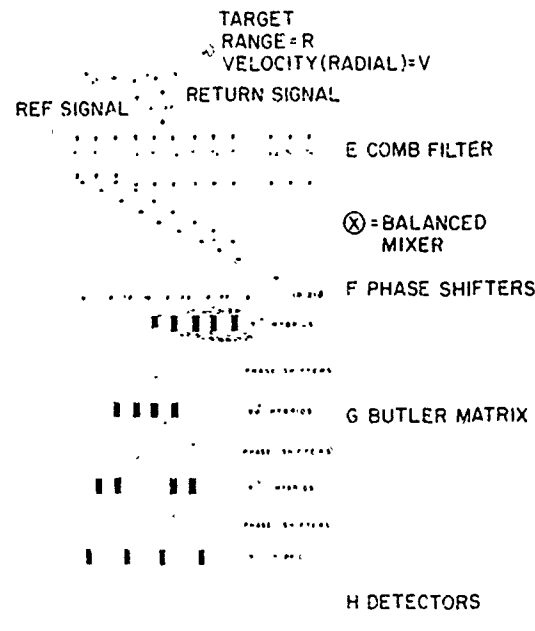
CONTROL OF RADAR CROSS SECTION: An understanding of the manner in which various objects scatter radar energy provides the basis for controlling the back-scattered energy. The Laboratory has long had an interest in impedance loading as a means for controlling the radar cross sections of targets. Some applications, such as telemetry-tracking, require an enhancement of radar cross section. Other applications call for significant reductions in radar cross sections so that an object is invisible to searching radars.

Generally speaking, control can be achieved by adding an auxiliary antenna to the object. The antenna is then impedance loaded in a manner that alters the overall scattering properties of the object-antenna combination. One limitation of this method is that the frequency bandwidth, over which the loading is effective as a cross section control, is rather restricted. This is because the loading reactances must have a negative slope as a function of frequency whereas reactive networks composed of the usual linear, passive, lossless, bilateral, lumped elements all have a positive slope with frequency. One method of avoiding these difficulties and attaining

wideband control of radar cross sections has been demonstrated during this reporting period. The new method is based on a self-adaptive load that senses the incident radar frequency and adjusts the loading to some predetermined value at that frequency. In this way, a narrower control band is centered at the desired frequency. The tuning is accomplished electronically, readjustment is rapid, the loads and associated control circuits are lightweight and compact, and the power requirements are small. All of these are distinct advantages for missile or aircraft applications.

ANALYSIS AND MODIFICATION OF THE SPECTRUM ANALYSIS RADAR: The concept of the spectrum analysis radar was developed in this laboratory and discussed in the previous *Report on Research*. A quasi-monochromatic noise generator serves as a transmitting source. The sum of the echo signal from the target and a delayed reference signal from the transmitter carries all the relevant target information. The power spectrum of this sum signal exhibits a modulation whose period is inversely proportional to target range. Peak detecting, filtering, and again spectrum analyzing leads to an A-scope type range display. This system is simple to implement and possesses advantages especially in those applications where the user is already radiating a noise signal for other purposes such as jamming. Laboratory tests of the Spectrum Analysis Radar demonstrated that the system provides high range resolution of closely spaced multiple targets, high accuracy and the capability of measuring range even at very close distances between transmitter and target.

In an effort to make maximum practical use of this promising new radar principle, scientists from both the Microwave Physics and the Data Science Laboratories set out to probe its deficiencies and define the limits of its applicability. The team analysis outlined several areas and applications in which problems could arise. These in-



RANGE GATE OUTPUTS

Among the many Spectrum Analysis Radar processing schemes developed by the Laboratory is this configuration that aids in the detection of high speed targets at long range. It uses a new type of spectrum analysis technique for the non-stationary random signals returned from the target and provides both range and range rate

clude 1) ghost targets when the radar is viewing an extended multiple target environment, 2) ghost targets when the target range is less than the equivalent range of the delay in the reference signal, 3) internally generated self noise that reduces the overall sensitivity of the system, 4) signal masking by direct coupling of transmit and receive antennas, and 5) inability of the system to detect rapidly moving targets.

Scientists from the two laboratories have already proposed solutions for several of these deficiencies. With some modifications in the spectrum analysis theory, the noise radar can have all the properties of a true correlation radar. This means that 1) ghost targets and self-noise effects can be eliminated, 2) the system can use any signal source and modulation (including

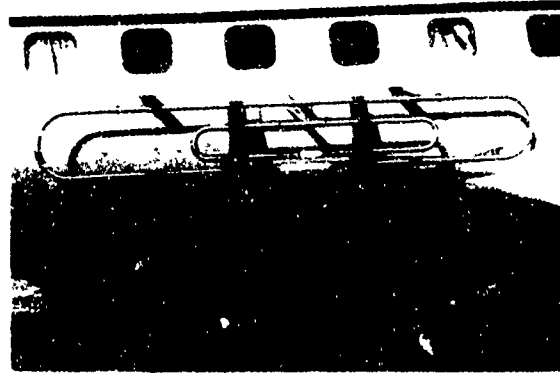
pulsed), 3) CW counter-jamming can be reduced, and 4) the system response to adjacent targets can be carefully controlled, balancing resolution against ambiguities. These improvements have also made it possible both to detect and to determine the range and range rate of rapidly moving targets. Another result of these studies is a new sum signal processing technique incorporating multiple offset filters. This will aid in detecting fast-moving targets at long range and in accurately determining both their range and range rate. The scheme also provides some suppression of system self noise.

It is clear from these studies that if one wishes to extend the use of the Spectrum Analysis Radar into some of the traditional pulsed radar areas, he must be prepared to develop new kinds of data processing components. For example, the signal processing needed to handle rapidly moving targets must be done in parallel rather than in the series arrangement used in most spectrum analyzers. The capability to deal with a range of target velocities requires either multiple-offset local-oscillator frequencies or multiple pairs of filter banks connected with different offset frequencies. Elimination of ghosts and suppression of a considerable amount of self noise can be accomplished by adding circuitry and doubling the number of filter-detection banks. Progress in integrated circuit development will undoubtedly determine the ultimate usefulness of the several new signal processing techniques proposed by this investigation.

A unique feature of the Spectrum Analysis Radar is its utilization of electromagnetic emissions that are of a random or noisy nature. Laboratory scientists have investigated the manner in which these noisy electromagnetic waves interact with standard radar targets. There is particular emphasis on developing a new description of the polarization properties of wide bandwidth stochastic plane waves—the

type of waves emitted by the Spectrum Analysis Radar. One result of these studies is that under certain conditions, these waves can be thought of as the superposition of two independent waves. The first wave is one whose vector direction is known with certainty but whose magnitude is a random quantity. The second wave is characterized by the fact that it has no measurably defined vector direction. This decomposition of the random plane waves will be used to study those properties of the reflected wave which are solely dependent upon the depolarization characteristics of the target.

THE SYNTHETIC APERTURE DUAL FREQUENCY RADAR SYSTEM (SADFRAD): The SADFRAD system, partially described in an earlier *Report on Research*, is a unique airborne experimental radar reconnaissance sensor designed and fabricated by this Laboratory in response to Air Force needs. It may come to be cited as one of the most significant solutions to a difficult tactical problem—the radar detection of stationary military targets hidden in a high clutter or densely foliated environment. Many of the radar studies mentioned earlier in this report come to bear on this problem. Terrain backscatter as a function of frequency, attenuation of electromagnetic energy as it propagates through foliage, and the radar cross section of a general class of tactical targets are just three of the interrelated parameters that were thoroughly considered in the SADFRAD design. The SADFRAD system makes maximum use of the environmental properties to maximize target-to-clutter ratios. Theory and experiment both show that the energy backscattered from terrain diminishes as the radar operating frequency decreases. The attenuation of electromagnetic waves passing through foliage also decreases with decreasing frequency. At these lower frequencies, a general class of targets which



A C-121 flight test aircraft provided the airborne test bed for the Laboratory-developed SADFRAD Radar System. These HF-VHF antennas were designed and tested in-house and represent an optimum design.

includes those of tactical interest are resonant sized and therefore produce maximum radar cross sections. All these reasons led to the selection of HF and VHF frequencies for the SADFRAD. The use of such low frequencies for foliage penetration is a bold step undertaken by AFCRL and is approximately four octaves lower than other Air Force foliage penetration radars.

SADFRAD uses a focused synthetic aperture to achieve high azimuthal resolution, two operating frequencies, and a new signal processing technique developed at AFCRL. An unusual feature of the SADFRAD system is the capability to acquire and display three separate pieces of radar information for each target examined. These three parameters, produced by the first, all digital, *focused* synthetic aperture processor ever to be placed on board an aircraft are: signals proportional to both the high and low frequency response of the target and the target dual harmonic differential phase signature. This latter is a new, Laboratory-developed radar observable and is used to assist in target identifica-

tion. The target amplitude response at the two frequencies is presented to the operator on two separate black and white TV monitors, while the phase signature data is displayed on a color monitor. These displays provide continuous radar strip imagery as a function of the azimuth and range from the aircraft. The complete SADFRAD system consists of transmitters, receivers, synthetic aperture processor, displays, inertial navigation systems and magnetic tape recorders, all installed on an Air Force Avionics Laboratory C-121 flight test aircraft.

A comprehensive flight test program was initiated in August 1970 and completed in December 1971. It had the following four objectives: 1) to demonstrate system feasibility, 2) to determine the SAD-



The synthetic aperture processor is the heart of the SADFRAD System and is the first airborne real-time digital focused processor. Target amplitude and phase data are recorded on magnetic tape recorders.

FRAD's effectiveness in detecting tactical military targets, 3) to measure differential phase signatures for a variety of targets, and 4) to obtain backscatter or clutter data at frequencies for which there is no such data.

Based on the flight test results, the feasibility of the system has been conclusively demonstrated. Quantitative radar data (low and high frequency and differential phase) of selected calibrated targets have been obtained in the following situations: 1) various clutter conditions including desert, flat open, flat scrub, woods (foliated and unfoliated), single and multiple layer foliated canopy, and 2) various target orientations, ranges and depression angles.

To determine the effectiveness of the system in detecting tactical military targets, a series of experiments have been conducted at White Sands Missile Range, New Mexico; Wright-Patterson AFB, Ohio; Jefferson Proving Ground, Indiana; Eglin Underbrush Range, Florida; St. Marks National Wild Life Refuge, Florida, and Fort Hood, Texas. It has been demonstrated that the system can detect a variety of tactical targets including: trucks, truck parks, surface-to-air missiles, mobile radars, tanks, self propelled howitzers, artillery, POL dumps, aircraft, and mobile command posts under various clutter environments, target orientations, ranges and elevation angles. The clutter environments have ranged all the way from desert and flat open areas to pine woods and hardwood forests (medium to heavy density) and the multiple layer jungle type canopy typically found at Eglin Underbrush and St. Marks National Wildlife Refuge.

Early results indicate that the radar system is performing better than expected and that the complementary aspects of the dual frequency radar philosophy greatly enhance tactical target detection. Throughout the entire test program, target differential phase signature radar data has been obtained for the general class of

tactical targets previously mentioned. The utility of this parameter in target classification and identification is being investigated. Since the use of backscatter data is extremely useful in the design and analysis of new radar systems, a series of terrain backscatter measurements have been undertaken with the SADFRAD System. New scientific data have been obtained at frequencies not previously investigated. Also, the backscatter data have been obtained for the variety of terrains mentioned above as well as open sea, rolling hills, farmland and mountains.

These test results indicate that the technology associated with the SADFRAD radar has made a significant contribution to solving current problems and provides the Air Force with a new technique for detecting concealed targets in foliage in real time under all weather conditions.

All airborne synthetic aperture radars of the SADFRAD type are unable to locate fast-moving targets of military interest



The SADFRAD display is a unique application of the use of color to determine target amplitude and differential phase. The display consists of two black and white monitors, located at the top, and a color monitor located on the bottom. Target amplitude and phase are displayed as a function of azimuth and range from the aircraft.

such as low flying aircraft. New concepts that will exploit the wide-angle search capabilities of VHF synthetic aperture radars are under active investigation in the Laboratory. Expectations are that a new technique for air-to-air surveillance, capitalizing on the advantages of VHF resonant region, multi-frequency, phase discriminant radars, can be developed and used to advantage in Air Force problems.

ANTENNA THEORY

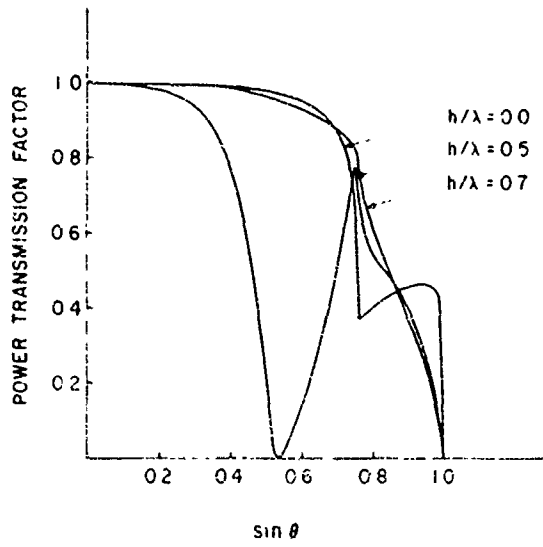
In the previous *Report on Research*, the emphasis in antenna theory was placed on information processing schemes. Processors, incorporated into the antenna design, can be made to perform a multitude of mathematical operations on the antenna signals. The result is improved performance at the cost of increased complexity. The Laboratory's 2 mm array is a case in point. Four antennas with processing perform the same functions as seven antennas without processing.

Data processing, however, does not solve all the puzzles in antenna engineering. Some of the more classic problems require new techniques in applied electromagnetic theory. One such problem is the design of small, compact, flush-mounted antennas for aircraft. A her problem area revolves about the interelement mutual coupling effects in array antennas. Techniques to include these effects and to control both the amplitude and phase distribution of array elements are always in demand. New measurement techniques and component development go hand in hand with new antenna designs. Laboratory Scientists have made several significant advances in these areas of classical antenna research.

PHASED ARRAY ANTENNAS: Phased array radars are used in many defense applica-

tions. They are quite costly, complicated, and their reliability must be unquestioned. During the past several years, engineers responsible for their development have noted that, at particular angles, the array radiation pattern exhibits nulls—that is, regions with no radiation. These nulls or blind spots in the radar coverage were not predicted by the design theory and their occurrence represents an anomaly that can seriously degrade the radar system performance. Laboratory scientists are approaching this blind spot problem from two directions. One approach seeks to understand the basic physical reasons for blind spots and includes mathematical studies of array mutual coupling. (The blind spots are known to be caused by the effects of interelement mutual coupling on the radiation patterns of the individual elements in the array.) The second approach seeks to alleviate the blind spot problem by physically modifying existing phased array antennas. This means developing methods to provide better element-to-array impedance matching.

Progress to date in this latter area includes the use of single and stratified dielectric layers and the placement of several types of metallic fence structures in the antenna structure itself, between the elements. The purpose of these fences is to change the interelement mutual coupling and thereby control the blind spot effect. The laboratory has studied the matching achievable with these metallic fence structures in a parallel plate array of open end waveguides. Results show that the height of the fence clearly affects the pattern null causing it to vary in depth and move about within the pattern structure. It is possible to use such fences to move the blind spot to a region of the radiation pattern where it has only a minimal effect on radar system performance. With a fence height greater than about half a wavelength, the blind spot can even be totally eliminated from the element pattern. The fences have



Metallic fence structures can be used to change the element pattern shape of phased array radars thereby removing blind spots in the radar coverage. With no fence ($h/\lambda = 0.0$) the element pattern has a 4 dB dip at $\sin \theta = 0.8$. When a fence half-a-wavelength high is installed ($h/\lambda = 0.5$), the dip becomes more pronounced and moves to the left. With a fence seven-tenths of a wavelength high ($h/\lambda = 0.7$), the dip or blind spot is completely removed from the element pattern.

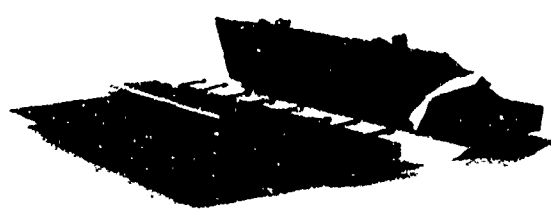
an additional advantage in that the phased array, so modified, can be scanned over a wider range of angles, thus providing increased radar coverage.

Another new development in phased arrays is a contractual investigation of conformal phased arrays. The requirement here is for high gain arrays that can be flush-mounted in a cylindrical metallic surface, such as an aircraft or missile skin. In addition, such an antenna must operate in a conventional phased array mode for broadside and near broadside directions but must also provide high gain beams in the endfire directions. Thus, this dual-mode phased array provides hemispheric coverage. The endfire beams are provided by covering the antenna and the adjacent metal surface with a dielectric layer that

produces surface wave radiation and a high gain pattern in the endfire directions.

ANTENNAS FOR STATION KEEPING RADARS: Cargo aircraft and helicopters often fly in groups or formations in which individual planes may be as far apart as 20 miles. Each aircraft must maintain a fixed position with respect to other aircraft in the group and, under poor visibility conditions, such capability must be provided by a station keeping radar set on board each aircraft. These radar systems require a directional antenna whose beam is continually rotated in the azimuth plane. In this way, each aircraft derives relative position information from all other aircraft with cooperative equipment. The antenna beamwidth in the azimuth plane must be relatively narrow but, on the other hand, the pattern in the vertical plane must be quite broad to allow communication with aircraft in the group at different altitudes. The Air Force presently uses the AN/APN-169 radar set with an antenna consisting of eight flared waveguide horns. Although this set provides the beam shape and gain requirements for station keeping, the antenna and its enclosing radome are quite large and can be used only on low performance aircraft. An Air Force need exists for a smaller antenna suitable for higher performance aircraft.

Laboratory scientists have developed a new antenna array of eight copper-plated channel guide antennas which functions as a surface wave radiating system. The array provides 17 dB of gain and each element is about 1 inch in height. Including proper spacings for mounting the arrays, the antenna projection is reduced from more than 5 inches for the AN/APN-169 to about 1.9 inches for the AFCRL array. This difference in height results in considerable streamlining and reduces wind resistance. Even though the new antenna is smaller, it has all the electrical performance of the larger antenna and, in addi-



The low-profile channel guide antenna (foreground) was developed at AFCRL as a replacement for the AN/APN-169 Station Keeping Radar antenna (background). The channel guide antenna is 3 inches lower and can be more easily streamlined for mounting on high performance aircraft.

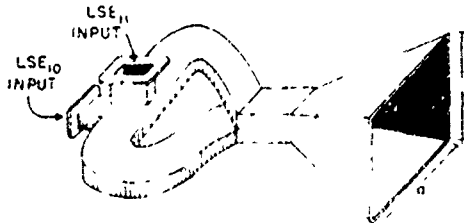
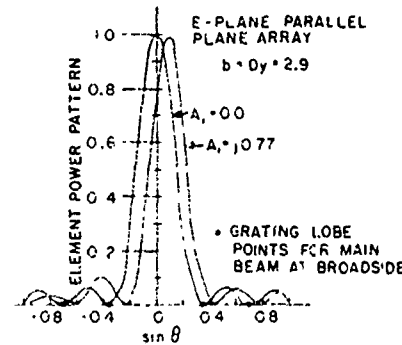
tion, this particular design provides maximum gain at the horizon as well as nearly constant gain over the whole station keeping angular sector. Previous surface wave antennas mounted on cylindrical aircraft structures could not provide proper coverage all the way to the horizon. The AFCRL channel guide antenna is the first to do so and thus serves both as a solution to this long standing puzzle in antenna technology as well as an experimentally verified answer to the station keeping antenna problem.

LIMITED SCAN ANTENNAS: Ground control approach radars and synchronous satellites require high gain antennas that can be electronically steered through relatively small cones (8-10 degrees half-angle). Such antennas are called limited scan antennas. A number of schemes have been proposed which would couple the beam scanning speed advantages of phased arrays with the high gain properties of reflector type antennas. So far, the only viable solutions have used phased arrays to scan reflector antennas and these systems have been inefficient or unduly restricted in their scanning coverage. Laboratory scientists are studying several alternate approaches to these limited scan antennas.

One approach consists of a contractual study of the limited cone scanning ob-

tained when a phased array is placed at the focal region of a reflector antenna or a microwave lens. Phase shifters and a distribution network will provide the required amplitude and phase control at the array face. This effort promises to give the efficiency and power distribution over the scan volume which were missing in the early designs.

A variation of this approach can be used to provide high gain antennas capable of multibeam and rapid scanning operations. Large arrays require costly circuitry while large parabolic dishes suffer from aberration and mechanical inertia. A Laboratory contractor is investigating a compromise



Waveguide higher order modes can be used to obtain scanned element patterns with suppressed grating lobe radiation. This figure shows that the addition of a waveguide odd mode (LSE 11) to the fundamental waveguide mode (LSE 10) shifts the horn element pattern peak and the position of its nulls. The addition of this odd mode whose amplitude increases with scan angle can more than double the allowed scan limits while maintaining tolerable grating lobe levels. A magic tee hybrid (bottom) can be used to excite the higher order waveguide modes.

solution using a large parabolic torus reflector with a small number of clustered feeds. This approach has the advantage of small aperture blocking and provides two dimensional scanning. A second design uses a double-spherical Cassegrain reflector. Geometric optics are used to examine the aperture blocking, the spread of the field and the phase and amplitude distributions. Scientists feel that although there is no single optimum condition, a proper combination of the subreflector and main reflector sizes, together with the correct positioning of the feed, can indeed produce a promising antenna.

A design for limited scan antennas presently being tested in-house uses relatively high gain horn antennas as the elements in a phased array. Even though such an array produces the desired high gain, the radiation pattern structure has many grating lobes and these are undesirable. A suppression technique that consists of exciting the horn elements with higher order modes in addition to the fundamental mode, causes a reduction in the amplitude of the unwanted grating lobes. This laboratory-developed technique provides relatively wide-angle, limited scan cones at high efficiency and with a number of antenna elements which is far less than that required for the conventional phased array approach.

LOG-PERIODIC ANTENNAS: The Air Force currently uses large ground-based antennas for over-the-horizon detection radars. AFCRL was intimately involved in the early research efforts that led to these structures. Such antennas must have high gain, good resolving power and should be broadband in operation. This latter requirement is a difficult one and has spurred antenna research in log-periodic dipole antennas. These antennas are characterized by the fact that their circuit and radiating properties remain essentially unchanged for all frequencies within the radar's oper-

ating band. For example, the shape of the radiation pattern and its beamwidth are two characteristics of log-periodic antennas which are relatively insensitive to frequency.

Although a single log-periodic antenna has desirable broadband properties, it lacks gain and resolving power. To provide these, one must consider large arrays of log-periodic antennas in two dimensional structures. Current laboratory efforts center about optimization schemes for such arrays—that is, finding ways to reduce the number of elements, to maximize the gain and resolving power and to broaden the operating frequency range. Direct application of conventional numerical methods in this optimization rapidly leads to saturation of available computer facilities. New methods of linear antenna analysis have been specially developed for the optimization of large arrays of log-periodic antennas. These methods, combined with approximate analytical methods, allow the antenna designer to make a thorough study of the array radiation properties as a function of, for example, the spacing between the dipole elements, the dipole heights and the spacing between the individual log-periodic antennas in the array. Such theoretical studies will provide the basis for new design philosophies leading eventually to better operational antennas that will make use of self-adaptive elements, providing compensation for the phase front distortion and polarization changes caused by the ionosphere.

NULL STEERING IN ARRAY ANTENNAS: Antennas used in missile defense radars and on military aircraft and satellites must be secure against enemy jamming efforts. Such problems are not restricted to military applications however. Antennas for civilian use such as those aboard commercial aircraft and at airports must be designed so as to minimize their interference with other antennas and nearby electro-



Antenna arrays can be designed to have radiation patterns with maximum gain and a controlled radiation level over some angular region. In this example, each pattern has a 30 dB dip, maintained in the same location while the main beam is scanned from broadside to endfire. Multiple independent nulls can be created and steered by amplitude and phase control of the antenna elements.

magnetic equipment. One of the methods used in these Electronic Counter Measure (ECM) and Electromagnetic Compatibility (EMC) problems is control of the antenna radiation pattern. Array antennas are much more versatile than reflector antennas in this respect. The pattern control usually consists of reducing or eliminating the jamming from a particular direction by controlling the radiation intensity of the antenna in the angular sector that includes the jamming source. One would like to accomplish this pattern control without seriously degrading the overall array performance.

Laboratory scientists have developed a technique for designing arrays of wire elements which provides the maximum gain and, at the same time, places one or several independent nulls in the radiation pattern. For example, the designer can use two closely spaced nulls to reduce the radiation level over some angular sector and hold this null region fixed in space even while a maximum gain main beam is scanned all the way from the broadside to endfire directions. A practical application

of this design is to a search or tracking array being jammed by a source whose angular location is not accurately known. Only the amplitude and phase of the array elements need be varied in this method, making it attractive for those applications in which the pattern structure must be rapidly reconfigured.

Arrays with steerable nulls also have applications in radio direction finding and navigation. In these cases, the pattern null, being usually much narrower than the main beam, is used to locate an aircraft and indicate its azimuthal position. An earlier version of this work received the Lord Brabazon Award in Radar and Navigational Aids from the Institution of Electronic and Radio Engineers in London.

SHORT BACKFIRE ANTENNAS: Short backfire antennas are efficient radiators of electromagnetic energy and are attractive to antenna systems designers because they are simple and compact. This novel antenna concept was first demonstrated by AFCLR in 1962. In 1969 the backfire antenna was placed in production as the primary transmitting and receiving antenna for the Tactical Satellite Communications System (TACSATCOM). During this reporting period, continuing research on this type of antenna has produced several valuable new array designs. The new array antennas are built around the highly directive short backfire array element. Used as a replacement for the more conventional dipoles or slots, it offers several distinct advantages: 1) the number of feed elements in the array can be reduced without any loss in array directivity or pattern quality. Arrays of dipoles or slots require four to eight times as many elements to provide the same performance characteristics, 2) the insertion loss of an array of short backfires is reduced because fewer elements are used; this results in an effective increase in array gain, 3) the array construction cost decreases since less ma-

terial is used, and 4) the weight of the structure is reduced, a decided advantage in airborne applications.

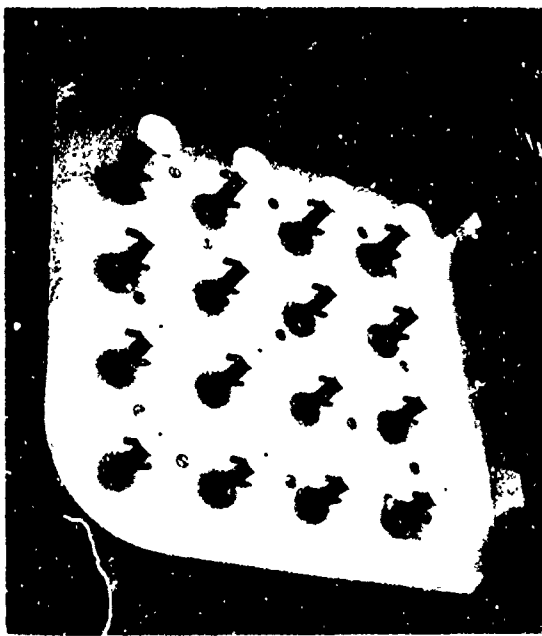
Two arrays, one with 4 short backfire elements, the second with 16, were constructed in the experimental phase of the laboratory program. By varying the element parameters, the arrays were optimized for maximum gain, or for lowest side and backlobe level, or for equal half-power beamwidths in the E- and H-planes, or for equal beam shapes in the two principal pattern planes. The four element array develops a gain of 20.2 dB and can replace a conventionally constructed multielement array of 32 dipoles. With design data furnished by AFCRL, the U. S. Navy Underwater Sound Laboratory has constructed the first UHF 4-element short backfire array for telemetry and satellite communication. It serves as receiving and

transmitting antenna in a satellite telemetry link between a research ship in the Pacific and the Navy Laboratories at New London.

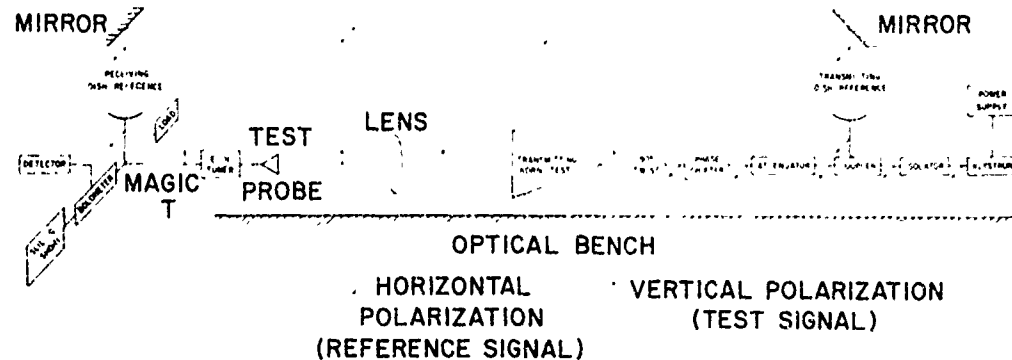
The gain of the 16-element short backfire array was measured as 25 dB. A conventionally constructed array with the same gain would require more than 100 separately fed dipoles with a complicated feed system and high cable losses. Based on this AFCRL design, several VHF arrays with the same configuration were constructed and are now in use in NASA's world-wide tracking network.

THE MILLIMETER WAVE ARRAY: Described in earlier reports, this 28-foot linear array of four parabolic reflector antennas operates at a wavelength of 2 mm (140 GHz) and represents a laboratory thrust to the frontiers of antenna technology. Data from the four elements are signal processed by a computer which both restores and enhances the antenna output information. The feed system for the parabolic dishes uses lenses and mirrors so that the millimeter wave energy is in fact treated in much the same way as visible light. There are no tried and true design methods in this frequency range. Laboratory research, therefore, encompasses both new component development and measurement techniques. Two advances, whose success was essential to the design and refinement of the beam waveguide launchers and lenses used in the millimeter wave array are discussed below.

The first advance is in the measurement of the phase of millimeter waves in free space. Using a reference signal of varying phase, the new technique is a significant improvement over the methods used at lower frequencies. It has the advantage of simple fabrication and requires none of the local oscillators, mixers, IF amplifiers and other equipment usually associated with phase measurement schemes. The varying phase reference signal is necessary be-



A 16-element short backfire antenna array. A conventionally constructed array with the same gain would require more than 100 separately fed dipoles. AFCRL pioneered in the development of this antenna type now finding widespread use throughout the world.



A schematic diagram of a new phase measurement technique for millimeter waves developed at AFCRL. The method uses a variable phase reference signal propagating in free space and orthogonal polarizations to reduce interference between the test and reference signals. Construction is simple and requires no local oscillators, mixers or IF amplifiers.

cause a flexible or movable waveguide whose phase characteristics can readily be measured is simply not available at millimeter wavelengths.

The antennas for both the test and reference signals are located on movable platforms. As the test probe antenna is moved, the reference antenna also moves and its phase changes at a rate that can either be calculated or measured. The difference between the total measured test phase and the reference phase is the phase to be determined. In this novel arrangement, the reference signal propagates over a free space path with the outputs of the reference and test antennas connected in a magic tee. This mixing of the two signals produces an interference pattern type signal with nulls whose position, when accurately measured, leads to a determination of the desired signal phase.

Experimentally verified at 140 GHz, the AFCRL phase measuring technique is sufficiently accurate to design and test antennas and lenses at millimeter and even submillimeter wavelengths. It can be made

more convenient and faster by adapting it for use on automatic measuring and plotting devices. Laboratory scientists are currently using it for the design of beam waveguide components in the 2 mm band.

The second new development in the millimeter wave antenna program is a component, a conical horn using dielectric inserts to provide wavefront correction. Important requirements for efficient beam waveguide launchers or antenna feeds are that the E- and H-plane patterns be symmetric, equal in width and have low sidelobes. Standard methods for achieving these pattern properties include corrugating the feed-horn sides or designing special mode launchers within the horn throat itself. Unfortunately, however, as frequency increases, the mechanical tolerances required in these methods are extremely difficult to obtain in practice. A new laboratory technique uses a simple conical horn and dielectric inserts to provide the desired pattern shape. This design has yielded unusually good results for a 2 mm wavelength and does not have any high toler-

ance requirements. The new feed horn assembly is now being used as the basic element on the beam waveguide launcher of the millimeter antenna array.

PLASMA ELECTROMAGNETICS

The plasma sheath that forms around reentering aerospace vehicles creates a highly conductive and reflective barrier to radio waves. It seriously disrupts various electromagnetic radiating and receiving systems on board the spacecraft. Solution of the plasma sheath problem is a goal of considerable priority in terms of projected Air Force capabilities in ballistic missile technology, space transportation systems and proposed hypersonic aircraft that travel at velocities above Mach 8. Disruptive effects of the plasma sheath include radio signal attenuation, pulse distortion, antenna voltage breakdown, radio noise generation and channel cross-modulation.

Research efforts, ranging all the way from rocket flight tests to laboratory studies of plasma media, are underway. Any investigation of the plasma sheath entails an intimate commingling of these theoretical and experimental research efforts. The basic physical processes occurring in the sheath are not perfectly known. Theories are advanced, but of necessity are incomplete. Each rocket flight, in providing expected and unexpected data, serves both to verify and extend existing theories.

Major emphasis in the laboratory program centers on developing alleviation techniques (principally through the use of chemical additives) and designing diagnostic instruments to measure the in-flight characteristics of the plasma sheath. The successful Trailblazer rocket flight of November 1970, which carried the third of the laboratory's plasma diagnostics payloads, provided data against which theoretical speculation and data from future flights on plasma alleviation techniques will be compared.

In response to Air Force needs, the laboratory is intensifying research into plasma sheath turbulence and its effects on radio wave propagation. Turbulence effects are encountered on ballistic missiles at altitudes below 100 thousand feet. In this regime the flow fields around the vehicle change from laminar to turbulent and the electron density, gas pressure and temperature in the flow fields greatly increase over their values at higher altitudes. Laboratory facilities will be modified and upgraded to provide the capability of simulating these low altitude reentry effects.

The Laboratory's dual approach of ground testing and flight testing has proved fruitful for the design and pre-flight checkout of novel plasma diagnostic techniques, the prediction of plasma sheath effects on antenna systems and the development of promising alleviation schemes. A better understanding of the plasma sheath will lead to more realistic design data for the systems engineer and more dependable aerospace communications for the Air Force.

ROCKET PROGRAM: The rocket flight test program provides plasma sheath data under actual flight conditions. Results are compared with theoretical predictions and simulation experiments with the ultimate objective of developing techniques that will alleviate the blackout effect on radio transmissions to and from reentry vehicles. An associated objective is to develop and flight test a variety of dependable diagnostic devices that will provide accurate information on the ionized plasma properties during reentry.

The test vehicle is the Trailblazer II four-stage solid fuel rocket. The first two stages drive the vehicle to an apogee of about 900 thousand feet; the remaining two stages accelerate the vehicle back down into the atmosphere in a steep trajectory at a velocity of about 17,500 feet per second.

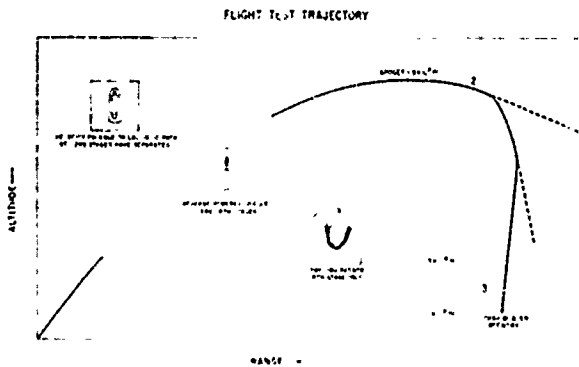
The altitude range of present interest is 100 to 300 thousand feet, and represents two different plasma regimes. In this altitude range, there is sufficient atmosphere so that the passage of a hypersonic blunt body produces a shock wave. The air flowing across this shock wave and around the vehicle undergoes large heating effects, and in the descent to about 100 thousand feet, undergoes various changes. At the lower altitudes the dense external air causes high temperatures and ionization levels in the shock layer. In addition, the effects of heat conduction and viscosity are restricted to a thin layer over the vehicle surface. At the initial high altitudes, however, the low ambient density results in a weak shock wave with little ionization, and viscous effects are not confined to the immediate reentry body area. This diversity in the reentry plasma properties requires a variety of diagnostic techniques and experiments. The rocket flight program consists of two phases: 1) extensive measurements of plasma properties during reentry together with the measurement of plasma effects on both high and low power signals; and 2) utilization of the flight data from phase 1 to select and design a system for alleviating the blackout of radio transmissions during reentry.

Phase 1 was completed with the third Trailblazer rocket flight. The plasma diagnostic data collected from this and two previous flights included the outputs from electroacoustic, electrostatic, conductivity and stripline probes. Measurements of antenna impedance mismatch, inter-antenna coupling, antenna pattern distortion, and plasma sheath attenuation on both high and low power signals were also carried out. Most of these measurements were made at three different locations on the reentry vehicle so that one can compare the effects of the thin high temperature plasma that exists at the stagnation point of the reentry vehicle with the cooler expanded plasma at the vehicle base. One result of this comparison was the observa-

tion that the plasma-caused distortion of the antenna pattern varied from point to point along the vehicle. There was no pattern deterioration at the stagnation point but there was considerable distortion at the base of the vehicle.

Some nonlinear effects were also observed. For example, antenna mismatch, decrease in mutual antenna coupling, and signal attenuation all occur at a higher altitude for high power signals than for low power signals. This high power signal attenuation was so pronounced that, in certain cases, the magnitude of the received lower powered signal was actually greater than that for the high power signal. Using a sophisticated flow field analysis that includes not only the usual chemical nonequilibrium effects but also viscous and vibrational factors, laboratory scientists were successful in predicting the signal attenuation effects observed on the test flight.

The three plasma diagnostics rocket flights have also served to flight test various probes that will be a necessary part of the future plasma alleviation test flights. These devices include voltage switchable



The flight trajectory of Trailblazer II. After separation of the launch vehicle, the reentry nosecone follows a typical trajectory to apogee, where it is propelled back down through the atmosphere at a velocity of 17,500 feet per second. Plasma effects begin to develop below 300 kilofeet.

electrostatic probes that are capable of directly collecting both electron and positive ion currents. The ability to distinguish between these currents is important because planned alleviation techniques will lower the electron density while leaving the positive ion density unchanged. The switchable probes also enable one to measure the boundary layer density at three different points above the surface of the vehicle. In this fashion, the effects of the various alleviants can be measured directly.

The first alleviation technique consists of injecting certain chemicals into the plasma sheath and was flight tested in June of 1972. The selection of the additive was based on extensive laboratory experimentation with a large number of possible injectants. Screening of potential alleviants entailed use of the in-house plasma-jet facilities complemented by a wind tunnel flight simulation with a plasma covered model of the Trailblazer nosecone. The additive finally selected was a high vapor pressure, polyhalogenated Freon. This chemical has superior electron attracting and holding ability and is also physically suited for spacecraft use. Early results indicate that the injection chemical and technique were highly successful.

SIMULATION AND ALLEVIATION: Plasma effects are studied on the ground by simulation, both the electromagnetic and gas dynamic properties of the reentry plasma sheath. Laboratory scientists currently use three separate facilities to model the various aspects of the plasma sheath which are of interest to the Air Force mission.

One plasma simulator uses no plasma at all. The device consists of a large number of lumped inductors and capacitors and represents a reasonable approximation to a uniform transmission line. It is used to study the propagation of electromagnetic waves in a dispersive medium, and in this sense, simulates a one-dimensional, linear,

homogeneous, lossless plasma. The transient response of the electrical line, together with its filtering properties, are measured and related to the simulated plasma properties. To date, the predicted and measured plasma properties agree quite well. Future work will include the effects of lossy, inhomogeneous and time varying plasmas.

A second reentry simulator utilizes an afterglow plasma. A pulsed discharge produces a plasma layer over a number of flush-mounted antennas and probes. These include a nonradiating microstrip plasma probe, an electroacoustic probe, single and double Langmuir probes and flush-mounted, cavity backed antennas. The planar geometry in this laboratory experiment allows scientists to calibrate new plasma diagnostic devices such as the AFCRL-developed microstrip probe, against more standard devices such as the Langmuir probe. Such experiments often lead to discoveries of anomalous or unsuspected behavior in the probes themselves. One such discovery, a nonlinear behavior in the electroacoustic probe, will be described in detail later.

A third simulation scheme uses a direct current arc-jet operating in pure nitrogen and produces a high temperature gas flow. Oxygen is added to the hot nitrogen in the throat of a nozzle and the synthetic air is then expanded to supersonic speeds. The resulting gas temperature is typical of reentry conditions. Microwave diagnostics are then used to determine the plasma properties. In addition, various chemicals can be injected into the flow field to determine their effectiveness as electron alleviants. Recently the effects of ablation upon electron density were measured. Samples of heat shield material were fabricated and the resulting matrix of carbon cloth and binder was doped with potential electron alleviants. The ablative samples were "burned" in the synthetic air flow field and their effects on electron density

measured downstream. Pure tungsten and Teflon were found to be the ablators that best reduced electron density.

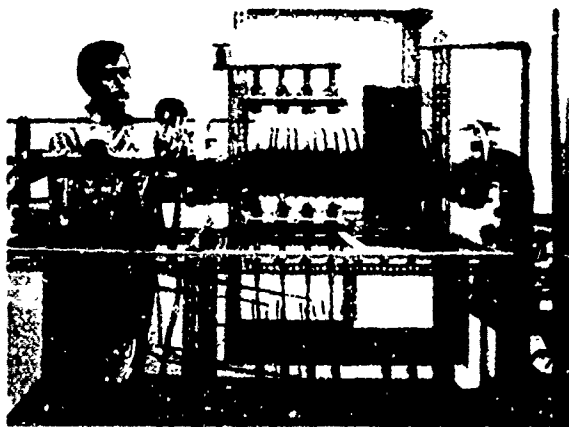
PLASMA DIAGNOSTICS: Reliable diagnostics are a prime requirement in all laboratory and applied plasma studies. Promising new techniques and standard diagnostic methods under unusual conditions are studied to complement the laboratory's rocket flight program. Many times, diagnostic methods must be used in situations where their performance is unknown. The scientist finds himself trying to measure the properties of the plasma medium, whose basic processes are not perfectly understood, with diagnostic devices whose behavior cannot be perfectly predicted. For example, the use of chemical additives to alleviate the communication blackout can result in plasmas with large negative ion populations. Even though it was not developed for this purpose, the electrostatic probe is used to measure such negative ion concentrations. Few investigations of probe response in such plasma environments have ever been carried out.

In laboratory experiments, electrostatic probe response is calibrated against microwave cavity perturbation measurements. When there are no negative ions present and the two diagnostic techniques are each used to measure electron decay characteristics, there is good agreement in the results. In electronegative gaseous plasmas, however, the two techniques give electron decay time constants that differ by factors of 4 to 8. Scientists attribute these differences to the influence of negative ions on the response of the electrostatic probe. The phenomena involved are under study using mass and optical spectrometry.

Laboratory scientists have also discovered a new technique for measuring electron density distributions. It is built around the microwave cavity perturbation method but uses two or more simultaneous probing fields. The approach involves cor-

relating measured frequency shift functions with computer generated functions for a variety of assumed electron distributions. In pulsed plasmas, including electronegative gases, agreement between experiment and theory within a factor of two has been achieved.

Another probe type that has been successfully used to measure plasma properties surrounding the Trailblazer reentry vehicle is the electroacoustic probe. The probe resonances are generally explained by the trapping of electron waves between a physical boundary, such as the rocket vehicle skin, and a critical plasma density layer. The shape, position and amplitude of the resonant signal are strongly dependent upon the power density of the incident probe signal. During a simulation experiment in the laboratory, scientists noted a nonlinear behavior in the electroacoustic probe. When the input signal power exceeded a certain threshold, high frequency oscillations were superimposed on the normal probe resonances. (This was the first time that such probe behavior had been observed with the planar button-discharge simulation scheme.) An experimental program is now in progress to explain these



A reentry plasma simulation device. It provides partially ionized, h^{-1} temperature, synthetic air and measures the efficiency of the chemical additives used to reduce electron density in the plasma.



A double probe technique measures the time dependent electron density during a nonlinear plasma interaction with a high power microwave field. This technique, together with microwave perturbation methods, measures plasma parameters during laboratory simulations of reentry.

nonlinearities. Scientists believe that either simple electronic heating or violent local ionization caused by trapped radiation could be the causative factor.

A plasma-clad antenna may produce local communication blackout conditions at much lower power levels than simple theory predicts. This is caused by the presence of local ionization that can drastically reduce the threshold power at which microwave breakdown occurs. The mechanisms of this lowered microwave threshold for a spatially dependent breakdown phenomenon, are under study. A microwave signal is propagated through a waveguide section containing a test gas. This signal causes no breakdown until it interacts with a distant, underdense plasma. Breakdown then occurs—first at the plasma, and then progressively in time and space, toward the source of the microwave signal. The nonlinear time dependence of the electron density at a given position is measured with a variety of electrostatic and microwave cavity probes. A grasp of the physical mechanisms involved will bring a greater

understanding of the signal loss and distortion that occurs during the reentry phase.

WAVE PROPAGATION IN A HOT MAGNETOPLASMA: A hot magnetoplasma is a plasma that is immersed in a magnetic field and in which the current density at one point depends on the electromagnetic field intensity at neighboring points. In addition, there is attenuation of propagating electromagnetic waves even though electron-charged particle collisions (the usual attenuation mechanism in plasmas) are nonexistent. This collisionless wave damping is a distinctive phenomenon of hot magnetoplasmas. It is caused by phase mixing that produces a transfer of energy from the electromagnetic wave to a resonant group of particles. In addition, energy dependent electron-neutral particle collisions cause changes in the plasma attenuation characteristics while the coulomb forces between charged particles have a pronounced effect on wave propagation characteristics. Hot magnetoplasmas exist naturally on the sun and in nuclear fusion reactions. However, the Laboratory's interest stems from Air Force application-related considerations. A possible alleviation technique for reentry communications blackouts consists of creating a magnetoplasma about the reentry vehicle. When this occurs, transmission windows open through the sheath allowing communications at particular frequencies.

The Appleton-Hartree equation, with a few modifications, is the usual means for determining the propagation characteristics of electromagnetic waves in such magnetoplasmas. Laboratory scientists have obtained the dispersion relations by solving the Boltzmann and Fokker-Planck kinetic equation using a variety of Fourier transform techniques and perturbation schemes. Five elaborate computer programs have been developed. The attenuation constant and phase shift for plane

electromagnetic wave propagation can be readily evaluated from a series of useful graphs. Results of this study show that for certain regimes, the theoretical expressions for electrical conductivity derived from the kinetic model, differ greatly from those predicted by the usual simple, cold, constant collision frequency model of a plasma. For example, when the signal frequency of a right-hand circularly polarized wave is near the electron cyclotron frequency, the hot plasma effects, the velocity dependent collision frequency and coulomb interactions all play a major role in determining the attenuation constant and the phase shift of the wave.

MILLIMETER WAVE PROPAGATION

The Laboratory's millimeter wave research program has two principal objectives. The first is to investigate the limitations imposed by the atmosphere on propagation of electromagnetic energy at millimeter wavelengths. The second is to use the propagated wave as a diagnostic tool to obtain information on lower atmospheric structure and solar activity. Radar and radiometric systems are used for these studies with the primary instrument being the Laboratory's 29-foot millimeter wave antenna at Prospect Hill, Waltham, Mass.

Millimeter waves interact strongly with the lower atmosphere. Atmospheric oxygen, water vapor and precipitation all attenuate millimeter waves, and this has resulted in limited use of short wavelength in communications and radar. On the positive side, however, this millimeter wave-atmospheric interaction has been partially responsible for the emergence of a new branch of science called microwave meteorology. Microwave measurements of atmospheric emission lead to estimates of temperature, pressure, and water vapor profiles. Through high resolution doppler

shift and doppler spread measurements, cross path wind speeds can be inferred and turbulent regions detected.

The laboratory also monitors the millimeter wave emission from active regions on the sun. Large solar flares produce density changes in the upper atmosphere that in turn perturb satellite orbits. These solar flares also change the characteristics of the ionosphere and produce HF communications blackouts. Observations of the sun have been conducted for many years to derive criteria for predicting these solar events.

MILLIMETER WAVE COMMUNICATIONS: The rapidly increasing demand for wide-band communications with global coverage has recently led to frequency allocations in the millimeter wave spectrum for earth-satellite links. From experimental and theoretical studies already conducted by the laboratory, it is evident that the major obstacle in utilizing these wavelengths is the high signal attenuation due to rain. Earth terminals located in rainy regions would experience an unacceptably high outage time. In order to obtain a correlation between rainfall rate and the attenuation of millimeter waves, a radiometric system operating at frequencies of 15 and 35 GHz was located in Hilo, Hawaii, a region that has heavy rainfall. Two methods were used (extinction and emission measurements) to determine the total atmospheric attenuation and its dependence on zenith angle and rain rate. This AFCRL program has been recently completed and has yielded some of the most quantitative rain attenuation data that have been obtained to date. Some of the early results show that for orographic rain with rates up to 50 mm per hour, 1) zenith attenuations are well correlated with rain rate and can be accurately estimated from local rain rates, 2) attenuations at lower elevation angles are not as well correlated with rain rate, 3) attenuations up to about

10 dB can be calculated quite accurately from atmospheric emission measurements, and 4) attenuations at 15 and 35 GHz are highly correlated, making it possible to predict the attenuation at one frequency from the measured value at the other.

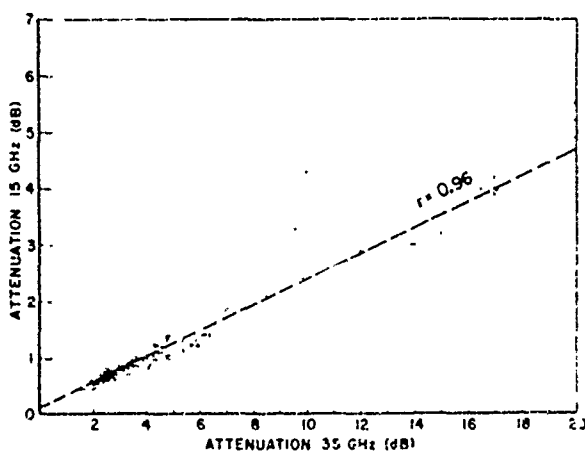
Heavy rain is generally quite localized and it may be possible to improve millimeter communication system reliability through space diversity. That is, two or more ground terminals are spaced sufficiently far apart so that the simultaneous outage time of all the terminals is acceptably low. When one terminal experiences heavy rainfall, operations are shifted to an alternate terminal. To determine the effectiveness of this approach, two radiometric sun trackers operating at 35 GHz have been installed at sites near AFCRL separated by 7 miles and are operating on a daily basis. From the data obtained thus far, it is evident that while the improvement due to space diversity is not high for the lower attenuations associated with

widespread light rain, separation of the ground stations does provide a significant improvement for the higher attenuations associated with heavy rain. A system outage occurs when signal attenuation levels reach 25 dB. With two separated ground stations, an outage can occur only when this attenuation occurs at both stations simultaneously. In the AFCRL experiment, two-station outage occurs only one twentieth as often as it does with a single ground station. The space diversity concept may well be the most direct way of providing dependable millimeter communications.

WAVE PROPAGATION IN RANDOM MEDIA:

The electromagnetic properties of the atmosphere depend on the frequency of the signal propagating through it. For signals of sufficiently high frequency, the atmosphere becomes non-uniform and takes on a structure in which the index of refraction varies slightly from one point to another in a random manner. Although the average value of these variations is zero, electromagnetic waves passing through the atmosphere can be strongly affected. Detrimental effects include loss of coherence and spreading or scattering of the radiation coupled with a fluctuation in the intensity of the signals. Such behavior is sometimes observable at optical frequencies, for example, in the propagation of laser beams and also at millimeter wavelengths.

Atmospheric scattering also limits the data rate of millimeter communications channels. A laboratory study approaches this reduced data-rate problem via the scalar wave equation. The classical approach to propagation in a random medium with small fluctuations requires the so-called infinite Born and Rytov solutions. A Laboratory scientist has succeeded in establishing a closed form relation between the two and has used this result to analyze the propagation of a plane milli-



A Laboratory program to measure the millimeter wave attenuation caused by heavy rainfall was recently completed and has yielded some of the most quantitative rain attenuation data that have ever been obtained. This scatter plot shows the high correlation of the attenuations measured simultaneously at frequencies of 15 and 35 GHz and makes it possible to predict the attenuation at one frequency from the measured value at the other.

meter or optical wave through the fluctuating atmosphere. The effects of multiple scattering are included in this analysis. It has also been possible to compare the often-used first Rytov approximation to the general solution and thereby establish the range of validity of the approximation. This work provides the basis for estimating the channel carrying capacity of a communications link as a function of the state of the atmosphere.

Another research effort provides a link between beam spreading and the assumed statistics of the turbulent atmosphere. In analyzing this problem, one must use a realistic model to describe the random nature of the atmosphere, and then find ways to solve the resulting random differential equations that describe the propagation of electromagnetic waves through the medium. Two parameters traditionally used to characterize the turbulent atmosphere are the inner and outer scales of turbulence. These bound the regions of the energy dissipation and creation mechanisms. Although some studies of laser beam propagation have included the effects of the inner scale of turbulence, this new laboratory study clearly relates the dependence of the wave-medium interaction on both the inner and outer scales of turbulence. One result of the study is that the effect of the outer scale of turbulence is quite significant in many cases and may not be neglected. The analysis can be used with a wide variety of source configurations. New calculations, based on quantum field theory, are currently underway and will complement this research as well as extend it to the case of large fluctuations in the index of refraction.

REMOTE SENSING OF LOWER ATMOSPHERIC STRUCTURE: Various Air Force functions require lower atmospheric meteorological data such as temperature-pressure profiles, humidity, cloud water content, wind speed and turbulence. The Laboratory ob-

tains information on the above parameters from radiometric and radar measurements at millimeter and short centimeter wavelengths. This technique is superior to conventional methods, such as radiosondes, for obtaining meteorological information in that data can be obtained continually over wide and inaccessible regions of space.

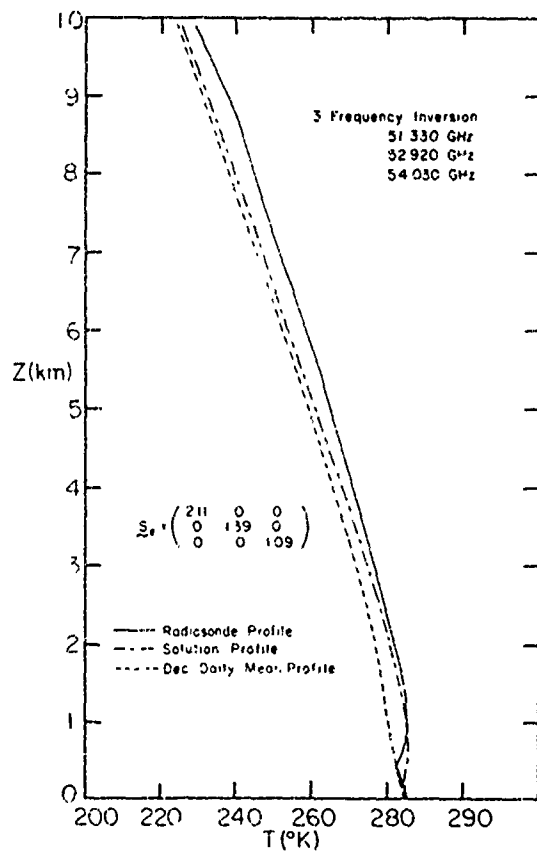
The method for obtaining temperature-pressure and humidity profiles depends on the fact that the integral form of the radiative transfer equation relates the antenna temperature to atmospheric temperature, pressure, and humidity. One simply measures antenna temperature at several wavelengths near the oxygen line centered at 5 mm, and then inverts the integral equation to obtain the temperature-pressure profile. Additional measurements can be made at the 1.35 cm water vapor line to obtain the relative humidity profile.

Initial atmospheric observations were conducted with a ground-based scanning radiometer to provide antenna temperatures over the frequency range from 50-60 GHz. Inversion of the data yielded temperature-pressure profiles which agreed very closely with radiosonde data. In some instances temperature inversions were detected. In order to obtain more accurate results, a new, more sensitive multi-channel radiometer has been constructed. It has four channels that observe and record simultaneously, three in the oxygen band and one at the water vapor line.

FORWARD SCATTER RADAR MAPPING OF THE TROPOSPHERE: The Laboratory has also investigated a new technique for remotely measuring the laminar and turbulent flow of tropospheric air. A forward scatter experiment conducted jointly by the Laboratory and the Canadian Communication Research Center has been operated over a 500 km path at a frequency of 15.7 GHz for the purpose of measuring these parameters. The scatter mechanism arises from atmos-

pheric refractive index inhomogeneities and is present at essentially all times. The cross path wind is related to the doppler shift of the received signal and the doppler spread is a measure of the degree of turbulence that is present. Wind and turbulence data can also be obtained from conventional doppler backscatter radars; however, these depend on the presence of particulate matter such as rain or clouds to obtain a detectable signal and thus cannot be used for continual monitoring.

The bistatic radar system uses narrow-beam transmitting and receiving antennas (0.15 degrees) for large volume coverage of the troposphere with high spatial resolution. Through simultaneous computer-controlled beam swinging of both antennas, measurements can be performed at any point within a volume of air 200 km long, 100 km wide, over a height range from 5 to 15 km. Systematic crosspath wind measurements over extended periods of time have been demonstrated to agree with rawinsonde data obtained in the vicinity of the radio scatter link. In a number of cases doppler fluctuations were recorded which strongly suggested that considerable turbulence (CAT) was present in the medium. These results will have to be confirmed by aircraft reports. Apart from the long range experiment a need exists to monitor winds very closely over more restricted areas such as runways, test ranges, etc. Based on the experience gained, Laboratory scientists are undertaking a new effort to develop a system that will be operationally useful to the Air Weather Service. AWS has the task of providing accurate and continuous wind measurements over such areas. A short range bistatic scatter experiment is being conducted. New equipment design utilizing path delay measurement techniques for spatial resolution is aiming at a reduction in equipment complexity, particularly a size reduction of the antennas presently used in the long range experiment. On-line

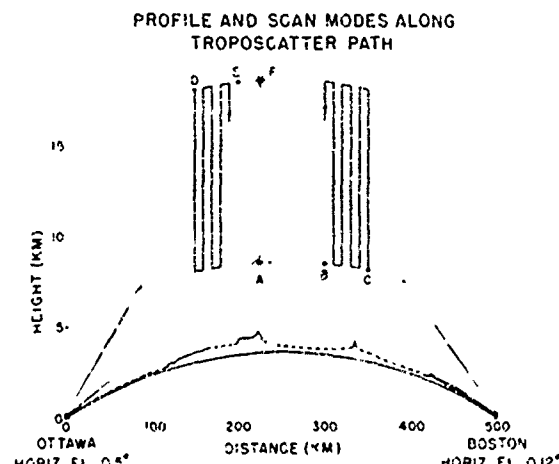


Lower atmospheric temperature profiles can be obtained from radiosondes and also from radiometric and radar measurements at millimeter wavelengths. Above, a temperature profile inferred from radiometric measurements near the 60 GHz oxygen line is compared with a temperature profile measured simultaneously with a radiosonde and the mean temperature profile for the month of December.

processing will permit a simultaneous display of wind parameters from a series of positions in space.

TROPOSPHERIC REFRACTIVE BENDING AT LOW ELEVATION ANGLES: A radio wave is bent or deflected as it passes through a medium of varying refractive index such as the troposphere. Since the refractive index of the atmosphere generally decreases with altitude, a radar target outside the lower atmosphere appears to be

slightly higher in altitude than it really is and this difference between actual and apparent altitude increases as the target approaches the horizon. In the past, angle error corrections calculated from various atmospheric models of the refractive index were sufficiently accurate for most applications. However, existing Air Force systems that utilize high resolution precision tracking radars and large antennas for satellite communications require more accurate refractive bending corrections than are presently available. For example, a radar observing a target at an elevation angle of 10 degrees would have to be corrected for a refractive bending of approximately 0.1 degree which is large compared to the millidegree capability of the more accurate radars. Failure to accurately correct for this bending could result in height errors of several miles for orbital objects. Also, synchronous orbit communication satellites operate with a large number of ground stations that are often required to point at elevation angles less than 15 degrees; satellite acquisition is a difficult task if accurate refraction corrections are not available.



A 500-km tropospheric scatter link is operated between a local Laboratory site and Ottawa, Canada. The volume common to the two antenna beams is moved in a raster scan mode to map winds and turbulence over a large region of the troposphere.

Presently, two approaches are used for obtaining refractive bending corrections. First, radiosondes are launched to provide a refractive index profile that can be used in a ray tracing computer program to calculate the corrections. This approach, while probably the most accurate available, is expensive since several radiosondes a day must be launched. The second approach is to estimate a refractive index profile based on ground level meteorological parameters. In this latter case, the obvious question is: How good are the results achieved with any particular model? This specific area is currently under investigation.

Most refractive index models are of a single or multiple exponential form and, in general, all such models give roughly the same results for elevation angles above 10 degrees. However, experimental verification of model results at low elevation angles is sparse, and does not exist for angles below 2 degrees. The Laboratory has undertaken a one-year experimental program, using the 29-Foot Millimeter Wave Antenna, to measure low angle refractive bending. With the sun as a target, accurate measurements can be made down to the horizon. The results of this experimental program will be applicable for frequencies ranging from 2 to about 50 GHz.

Very accurate data are collected at sunrise and sunset, weather permitting, over elevation angles from 0 to 20 degrees. These AFCRL results represent the only measured data below elevation angles of 2 degrees, and are the most accurately measured data up to 10 degrees. Comparing the measured data taken over the dry New England winter months with the results predicted from different refractive index models, the best fit occurs with the 1958 CRPL Exponential model profile.

SOLAR ACTIVITY: The radiation from the sun is the prime energy source for the terrestrial environment. Variations in ei-

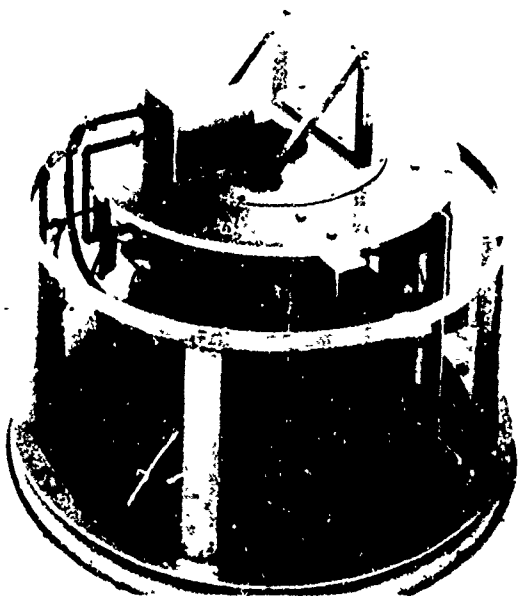
ther the intensity or the spectral character of this energy produce corresponding changes in our local environment referred to as aurora, HF communications blackouts, magnetic storms and polar cap absorptions. Because of the disruptive nature of these effects on communications systems, a world-wide program of solar observations has been in progress with the goal of developing a capability to forecast the occurrences of the major solar disturbance, the proton flare.

The proton flare is a vast explosive event occurring within the solar chromosphere. Its source of energy is the rapid collapse of a magnetic field that has been built up over a period of days or weeks. The magnetic field confines a region of the solar plasma within an ever decreasing volume until an instability results, accelerating the plasma particles to relativistic velocities, and ejecting them outward.

Since the proton flare is the final stage of the development of a magnetically confined plasma condensation within the solar chromosphere, a program for monitoring this evolutionary sequence has been in progress. Observations at millimeter wavelengths are particularly important since this wavelength radiation is emitted from the sun's chromosphere, the seat of flare activity. Millimeter wavelength radiation is emitted by the plasma involved in the magnetic containment process and propagates through the remainder of the solar atmosphere without attenuation.

High resolution spectral mappings of the solar chromosphere are now being performed with the AFCRL 29-Foot Millimeter Wave Antenna at wavelengths of 8 and 20 mm and will be extended to include 3 mm. These spectroheliograms are taken daily and used to locate and catalogue solar active centers. The use of two separate wavelengths has certain advantages. The 8-mm radiation is emitted from a region of the solar atmosphere that is

approximately 1000 km below the region emitting the 20-mm radiation. Combining both of these observations gives the relative intensity of the disturbance at two different heights and permits scientists to make a three-dimensional assessment of the structure of the active center under study. Analysis of such observations on a daily basis leads to an evolutionary profile of the disturbance which depicts the motion of the disturbance as it rises, falls, or remains stationary in the chromosphere. Preliminary analysis indicates that the proton event situation is more likely to occur when the millimeter signal intensity increases at both wavelengths simultaneously and exceeds certain statistical thresholds. The solar observations are directed toward developing a forecasting capability whose goal is the ability to predict a proton event from 6 to 24 hours prior to its occurrence.



This novel antenna feed for the Laboratory's 29-foot Millimeter Wave Antenna produces simultaneous collimated beams at frequencies of 15, 35, and 94 GHz.

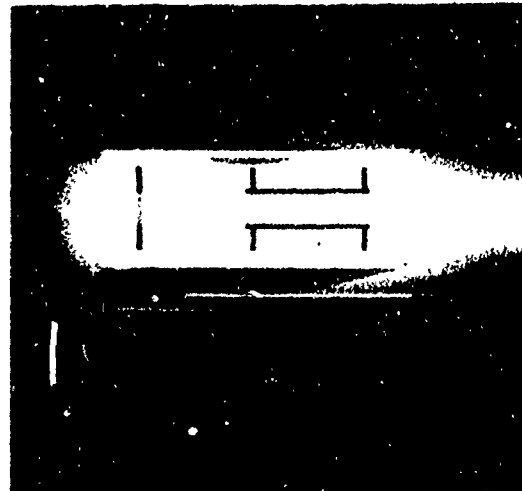
MICROWAVE ACOUSTICS

When AFCRL began its microwave acoustics program in 1958, it was almost alone in the field. At the time, microwave delay lines could be made only from piezoelectric quartz and had high insertion losses. AFCRL has pioneered in the development of better materials and thin film transducers to reduce the insertion loss of volume wave delay lines. More recently, the Laboratory has led the way in the generation and detection of acoustic surface waves at microwave frequencies.

Although the technology is relatively new, acoustic surface wave devices have progressed rapidly from their early use as delay lines to performing sophisticated signal processing functions such as correlation and convolution. In addition, these microwave acoustic components can perform many of the functions of purely electronic devices and they can do it in smaller packages, since the acoustic velocity and wavelength are 100,000 times smaller than the electromagnetic velocity and wavelength.

This new technology may well cause the replacement of a sizable percent of electronic circuitry by electroacoustic components. Several laboratory-developed devices are already under study for Air Force use in communication, navigation, surveillance, and electronic countermeasures.

ACOUSTIC SURFACE WAVE LOSSES: One of the basic objectives of the Laboratory program is to obtain acoustic surface wave delay lines and signal processing devices with the minimum insertion loss and the maximum bandwidth. Theoretical and experimental studies have already led to the discovery of two new orientations of lithium niobate which have losses lower than other known acoustic surface wave substrates. Such discoveries require a detailed understanding of the various loss mecha-



Quartz surface wave encoder or decoder designed, fabricated and tested in the Laboratory. These passive devices are generally smaller than integrated circuit devices having comparable bit rates.

nisms in the material: the conversion loss, when an electromagnetic wave is changed to acoustic energy in the transducer; the attenuation or propagation loss; the diffraction or spreading loss; and the loss due to beam steering. Laboratory efforts are underway investigating each of these loss mechanisms.

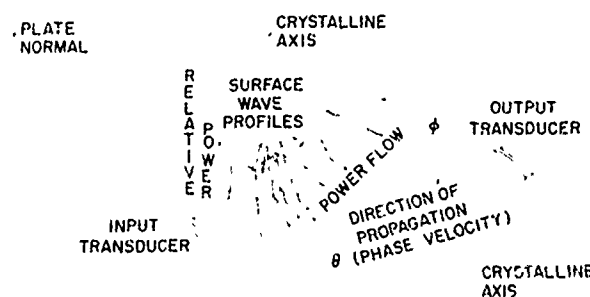
The losses have been measured with an AFCRL-developed laser probe technique. The surface wave acts as a moving diffraction grating that deflects the laser light into a number of sidelobes at angles prescribed by scattering theory. This deflected light is then detected by a photomultiplier. The exponential decay of the surface wave energy was observed by scanning the laser beam along the acoustic propagation path, while the diffraction spreading and beam steering effects were observed by scanning a finely focused laser spot perpendicular to the beam. The anisotropy of piezoelectric crystalline substrates causes beam steering although there are certain special symmetry axes along which there is no beam

steering effect. The orientation dependence of the velocity and the beam steering angle for all known acoustic materials has been computed and assembled in the *Microwave Acoustics Handbook* (AFCRL-70-0164).

One of the newly discovered orientations of lithium niobate has higher piezoelectric coupling and lower beam steering than any previously known orientation. Laboratory scientists fabricated a 1.13 GHz delay line using this orientation. The device has a bandwidth of 10 percent, and is also perfectly matched without the use of complicated external matching networks. This last feature, coupled with the fact that precision X-ray orientation of the crystal is not required, means that such a delay line can be inexpensively mass produced for Air Force ECM and signal processing applications.

Diffraction spreading effects are quite complicated in anisotropic media, much more so than in isotropic materials. Laboratory scientists have recently solved the complex mathematical problems associated with anisotropic materials and can predict the diffraction spreading effects. The laser probe technique experimentally verifies their predictions. One early result of these studies is the discovery of an orientation of lithium niobate in which the crystalline anisotropy can be used to reduce diffraction spreading effects. This second new orientation has the highest piezoelectric coupling and lowest diffraction spreading of any known material and is particularly well suited for delay lines with time delays substantially exceeding 10 microseconds.

The Air Force has need of long time delay devices at gigahertz frequencies. Propagation losses are the major impediment to their attainment. AFCRL has improved the quality of the optically polished surfaces of the substrate to the point where attenuation is limited mainly by scattering from thermal phonons. Experi-



Schematic representation of how diffraction spreading, propagation loss, and beam steering (power flow at angles other than $\phi = 0$) cause the surface wave energy generated at the input transducer to be reduced at the output transducer. A Laboratory research program is directed to understanding and measuring these losses in order to minimize their effects.

ments with quartz, lithium niobate and bismuth germanium, in which these thermal phonon effects were effectively "frozen out," verified this theory. Both the insertion and the propagation losses are, however, temperature dependent. The temperature dependence of the transducer insertion loss was eliminated in these experiments by the invention of a novel three-transducer method. This enabled scientists to measure only the temperature dependence of the attenuation loss. Such experiments with surface waves propagating along the X-axis of Y-cut quartz provided verification of a long accepted viscosity model that can now be used with confidence to find new low-loss orientations.

The energy of an acoustic surface wave is concentrated within about one acoustic wavelength (about 4 micrometers at 1 GHz) of the transducer surface. High power fluxes have been used to demonstrate non-linear effects such as harmonic generation and mixing. A theoretical analysis of the selection rules governing the interaction of two intersecting beams showed the possibility of single-sideband mixing and beam deflection. This latter effect will be

useful in building electronically variable delay lines and frequency analyzers. The low acoustic velocity attainable with bismuth germanium oxide ($\text{Bi}_{12}\text{GeO}_{20}$) makes it very attractive for compact, long delay, time delay lines.

To resolve conflicting published results concerning the values of the elastic, piezoelectric and dielectric constants of $\text{Bi}_{12}\text{GeO}_{20}$, AFCRL scientists have conducted an exhaustive study of this material. Over 45 samples of material grown by three independent sources were tested. The piezoelectric constant was determined using three different techniques. In addition, the first accurate measurements of the dielectric constant of $\text{Bi}_{12}\text{GeO}_{20}$ at microwave frequencies have been made. The material constants resulting from this survey and a detailed study of the loss mechanisms, have all been published.

SIGNAL PROCESSING WITH ELASTIC SURFACE WAVES: AFCRL has recently designed, fabricated, and tested new acoustic surface wave devices for use in encoding and decoding binary information. These devices were first requested by and subsequently delivered to the Communications and Navigation Division of RADC.

In these devices a digital pulse or information bit is used to generate, by means of an acoustic surface wave interdigital transducer, an elastic surface wave pulse that propagates on a piezoelectric Y-cut quartz substrate. This propagating pulse has a center frequency of 70 MHz or 100 MHz depending on the spacing of the lines of the transducer. As the "information bit" propagates along the X-axis of the quartz, it is detected either in phase or out of phase by pairs of interdigital transducer taps spaced 100 nanoseconds apart. This corresponds to 7 wavelengths at 70 MHz (or 10 wavelengths at 100 MHz). This detected sequence gives rise to a bi-phase modulated pseudo-random code that may then be used directly as the synchronization preamble for coordinated multiple access systems or to transmit information. In a communications application, the encoded information would be amplified and transmitted to a correlator or decoder (a mirror image of the encoder) fabricated with the same photolithographic master on a matched quartz substrate. The encoding-decoding process increases the signal-to-noise ratio and gives anti-jam protection.

These surface wave devices have the advantages of being compact and lightweight, and in addition, dissipate very little power. The 12 micrometer wide chrome-aluminum lines were etched on a quartz substrate by means of the same photolithographic techniques used to make integrated circuits. The expectation is that mass production techniques will make the cost of these surface wave devices comparable to those of integrated circuits. These 10-megabit/sec surface wave devices are generally smaller than integrated circuit devices having comparable bit rates. In addition, the latter require watts of DC power to operate, while the surface wave devices themselves require no auxiliary power supply, as they are passive. The design of these devices requires the extensive information on piezoelectric coupling, beam steering, and diffraction loss summarized in the recently compiled *Microwave Acoustics Handbook*.

The Laboratory has pioneered in the generation of surface waves at frequencies as high as 5 GHz. It may soon be possible to fabricate surface wave devices at much higher bit rates than is possible with integrated circuits. The size, speed, and power advantages of surface wave devices make them very attractive for use in satellite communications systems with or without multiple access requirements.

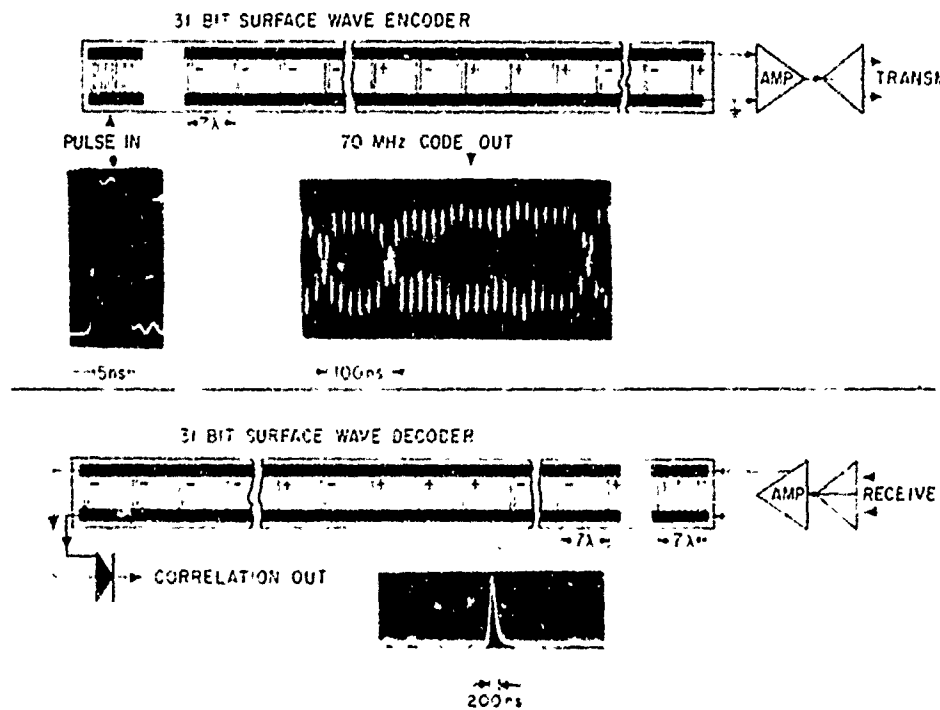
MAGNETIC SURFACE WAVES: A magnetic surface wave is defined as a magnetic disturbance along the surface of a saturated ferrimagnetic crystal--such as yttrium

iron garnet (YIG). Energy is transferred along the surface from one lattice site within the crystal to a neighboring one via the quantum mechanical exchange force between electron spins. The characteristics and properties of such a mode of propagation were predicted by AFCRL scientists in 1969. Since then, the theoretical work has been extended to include coupling of magnetic waves with acoustic surface waves. This work is being augmented with experiments.

Macroscopically, the magnetic surface wave shares certain common features with the Rayleigh acoustic surface wave. That is, wave amplitudes decay rapidly within a few wavelengths from the crystal surface while successive phase fronts lie in the

surface plane and propagate at a velocity less than that of the bulk wave velocity.

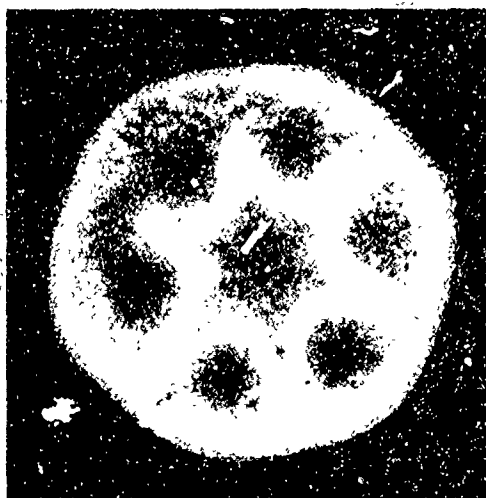
In a magnetic wave, the magnetization vector precesses about a dc magnetic biasing field with the tip of the vector describing an elliptical path in a plane perpendicular to the surface and to the biasing field. The relative elastic displacement of a lattice point, due to a propagating Rayleigh acoustic surface wave, undergoes a similar elliptical motion. Unlike surface acoustic waves, however, magnetic surface wave propagation is non-reciprocal, dispersive, and tunable via the biasing field. These properties can be used to advantage in constructing microwave signal processing devices such as isolators, circulators, switches, variable delay lines and filters.



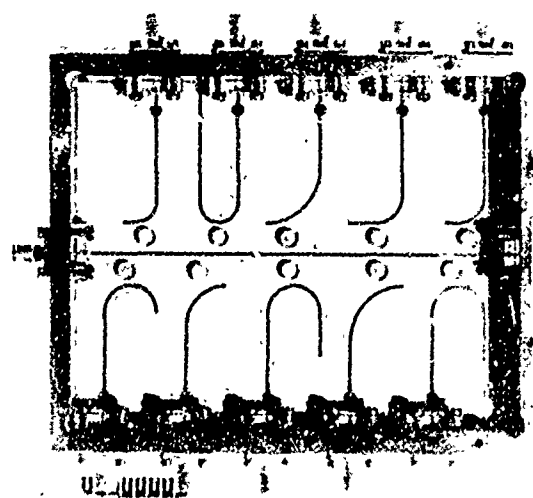
Encoding and subsequently decoding a 5 ns pulse. The device used is a multiply tapped quartz surface wave delay line. Such laboratory-developed devices were requested by and delivered to the Communications and Navigation Division of RADC.

Both magnetic and acoustic surface waves are compatible with integrated circuit technology.

DIELECTRIC RESONATORS IN MICROSTRIP CIRCUITS: Microwave integrated circuitry offers the system engineer several distinct advantages. Devices can be small, lightweight and both simple and inexpensive in construction. There are, however, some deficiencies in electrical performance. For example, microstrip resonators are subject to coupling and radiation losses and these factors result in a low quality factor (Q_L). One can use conventional cavity filters with microstrip lines but then the space and weight advantages are lost. Past *Reports on Research* have discussed the Laboratory's role in the development of high dielectric constant resonators. When these resonators are used with microstrip lines, it is possible to maintain a small package size and, at the same time, produce a high



A microwave standing wave surrounding a high dielectric resonator. A resistive backed, cholesterol, liquid-crystal film on a thin mylar substrate is used as the display mechanism. It is possible to detect either the electric or the magnetic field component by varying the conductivity of the resistive backing.



A 10-channel C-band dielectric resonator filter. Ten strontium titanate disk resonators couple microwave energy from the terminated feed line to individual output branches. The output signals are detected by small Schottky Barrier Beam Lead diodes (black pills with white dots). The substrate material is alumina giving a filter bandwidth of 60 MHz at a center frequency of 4500 MHz.

Q_L , narrow bandwidth microstrip multiplexing system.

Scientists have used this design philosophy to develop a 96-channel C-band microstrip filter. Each channel has a 3 dB bandwidth of 10 MHz; the total module has a band coverage of almost 16 GHz. The substrate material presently used is alumina; and beryllia will also be tested. This latter material has the advantage of being an excellent heat conductor and this will lend temperature stability to the microstrip filters. This type of multiplexing module is capable of fast spectral analysis, an asset that is particularly important in satisfying current Air Force needs in missile electronic countermeasures.

The dielectric resonators themselves are still under study in the laboratory. These novel devices can under certain excitation conditions, exhibit many overtone modes that may be undesirable in some applications. The mode structures can be observed with the unaided eye using a thermo-

graphic technique. A resistive-backed thin cholesterol liquid-crystal film that detects the magnetic or the electric (or both) field components is used. The conductivity of the resistive backing determines the field component that is observed. This same technique has been used in the laboratory to detect standing wave structures along microstrip circuitry and also, the complicated modes of ferrimagnetic materials. Such visualization of the dielectric resonator mode structure will aid scientists to better understand and control the overtones in the resonator devices.

JOURNAL ARTICLES JULY 1970 - JUNE 1972

ALTSHULEE, E. E., ET AL

High Resolution Millimeter Reflector Antennas
IEEE Trans. on Ant. and Prop. (July 1970)

BULLEAU, A. J., and CARR, P. H.

Performance and Applications of Microwave Photon-Phonon Double-Quantum Detection in MgO

J. of the Phys. and Chem. of Sol., Vol. 31, No. 8 (August 1970)

The Temperature Dependence of the Attenuation of Microwave Frequency Elastic Surface Waves in Quartz

Appl. Phys. Ltrs., Vol. 18 (1971)

Surface-Wave Attenuation at Microwave Frequencies: Part II-Temperature Dependence

IEEE Trans. on Son. and Ultrason., Vol. SU-18 (January 1971)

CARR, P. H.

Interaction Between Noncollinear Rayleigh Waves

IEEE Trans. on Son. and Ultrason., Vol. SU-18 (January 1971)

The Effect of Temperature and Doppler Shift on the Performance of Elastic Surface Wave Encoders and Decoders

IEEE Trans. on Son. and Ultrason., Vol. SU-19, No. 3 (July 1972)

CARR, P. H., SLOBODNIK, A. J., JR., SZABO, T. L., CAPT, DE VITO, P. A., MAJ., and FRANKLIN, S. B. (AF Acad., Colo.)

Uses and Limitations of Multiply Tapped Surface-Wave Delay Lines
IEEE Trans. on Son. and Ultrason., Vol. SU-18 (January 1971)

CLEVELAND, F. H., MAJ., and KERNWEIS, N. P.
A Technique for Measuring Phase at Millimeter Wavelengths
IEEE Trans. on Micr. Theory and Techniques, Vol. MTF19, No. 4 (April 1971)

DE VITO, P. A., MAJ.

Uses and Limitations of Multiply Tapped Surface-Wave Delay Lines
IEEE Trans. on Son. and Ultrason., Vol. SU-18 (January 1971)

DE VITO, P. A., MAJ., CARR, P. H., KEARNS, W. J., and SILVA, J. H., JR., TSGT.
Encoding and Decoding with Elastic Surface Waves at 10 Megabits Per Second
Proc. of the IEEE, Vol. 59, No. 10 (October 1971)

DRANE, C. J., and MC ILVENNA, J. F.

*Comments on the Technical Paper,
"Optimization of the Directive Gain of an Antenna Array with an Auxiliary Condition"*
Radiotekhnika i Elektronika, Vol. 15, No. 8 (August 1970)

FALCONE, V. J., JR.

Atmospheric Attenuation of Microwave Power
J. of Micr. Power, Vol. 5, Iss. 4 (4 December 1970)

FALCONE, V. J., JR., WULFSBEEG, K. N., and GITELSON, S.

Atmospheric Emission and Absorption at Millimeter Wavelengths
Rad. Sci., Vol. 6, No. 3 (March 1971)

FANTE, R. L.

Propagation of Electromagnetic Waves in a Simplified Nonlinear Gas
J. of Appl. Phys., Vol. 42, No. 11 (October 1971)

FANTE, R. L., and GAMACHE, R., YOS. J. (Avco Corp., Wilmington, Mass.)

High Power Attenuation on Reentry Vehicles
AIAA J., Vol. 10, No. 3 (March 1972)

HAYES, D. T.

The Meaning of Kato's Formulas for Upper and Lower Bounds to Eigenvalues of Hermitian Operators
Can. J. of Phys., Vol. 49, No. 2 (January 1971)

Limits to the Accuracy of the Cohen-Feldmann Bounds on Eigenvalues of Hermitian Operators
Can. J. of Phys., Vol. 49 (15 November 1971)

- HERSKOVITZ, S. B.
Liquid Additives for Blackout Alleviation: Physical Factors
 Proc. of the 4th Plasma Sheath Symp., NASA Langley Res. Ctr., Hampton, Va. (18-15 October 1970)
- JACAVANCO, D. J.
Experimental Determination of Electron Quenchant Efficiency at High Gas Temperature
 Proc. of the 4th Plasma Sheath Symp., NASA Langley Res. Ctr., Hampton, Va. (18-15 October 1970)
- KALAGHAN, P. M., and DALGARNO, A. (Harvard Coll. Obsv. /Smithsonian Astrophys. Obsv., Cambridge, Mass.)
Hyperfine Structure of the Molecular Ion H₂⁺
 Phys. Ltrs., Vol. 38A, No. 7 (27 March 1972)
- KALAGHAN, P. M., and TELFORD, L. E.
Radio Observations of Mars at 8.57 Millimeters
 The Astrophys. J., Vol. 170 (1 December 1971)
- MACK, R. B.
Phase Properties of Backscattered Fields from Thin Rods
 IEEE Trans. on Ant. and Prop., Vol. AP-19, No. 3 (May 1971)
- MAILLOUX, R. J.
Reduction of Mutual Coupling Using Perfectly Conducting Fences
 IEEE Trans. on Ant. and Prop., Vol. Ap-19, No. 2 (March 1971)
- MALONEY, L. R., MAJ.
Microwave Reentry Communication Rocket Flight Tests
 Proc. of the 4th Plasma Sheath Symp., NASA Langley Res. Ctr., Hampton, Va. (18-15 October 1970)
- MANO, K.
Interrelationship Between Terms of the Born and Rytov Expansions
 Proc. of the IEEE, Vol. 58, No. 7 (July 1970)
Symmetry Associated with the Born Rytov Methods
 Proc. of the IEEE, Vol. 58, No. 9 (September 1970)
Multiple Scattering in the Wave Propagation Through Random Media
 Proc. of the 1971 Intl. Symp. on Ant. and Prop., Sendai, Jap. (1-3 September 1971)
sF₂ Representations for Spin Projection Coefficients
 J. of Math. Phys., Vol. 12, No. 11 (November 1971)
- MAYHAN, J. T. (Univ. of Akron, Oh.), and FANTE, R. L.
Comparison of Various Microwave Breakdown Prediction Models
 J. of Appl. Phys., Vol. 42, No. 18 (December 1971)
- MC ILVENNA, J. F., and DRANE, C. J., JR.
Maximum Gain, Mutual Coupling and Pattern Control in Array Antennas
 The Rad. Elect. Eng., Vol. 41, No. 12 (December 1971)
- NEWBURGH, R. G.
The Thomas Precession and the Relativistic Right-Angled Lever
 The Am. J. of Phys., Vol. 38 (September 1970)
Thomas Precession as Evidence for the Non-Euclidean Nature of Atomic Orbits
 Lettere Al Nuovo Cimento, Vol. 3, No. 5 (29 January 1972)
- NEWBURGH, R. G., and DEWAN, E. M. (Data Sci. Lab.)
The Lorentz Contraction and Thermodynamic Work
 A Critical Rev. of Thermodyn., Mono Bk. Corp., Baltimore, Md. (1970)
- NEWBURGH, R. G., and PHIPPS, T. E., JR. (Nav. Ord. Lab., White Oak, Md.)
Relativistic Time and the Principle of Caratheodory
 Il Nuovo Cimento Sez. X, Vol. 67B (1970)
Brewster Angle and the Einstein Velocity Addition Theorem
 Am. J. of Phys., Vol. 39 (September 1971)
- ROTMAN, W.
Studies of Reentry Plasma Sheath Effects Upon Microwave Antenna Performance
 Proc. of the 4th Plasma Sheath Symp., NASA Langley Res. Ctr., Hampton, Va. (18-15 October 1970)
- SCHELL, A. C.
Recent Developments in Microwave Antennas
 Proc. of 1971 Eur. Micr. Conf., Stockholm, Swed. (23-23 August 1971), Vol. 1, Paper B4/S
A Millimeter Wave Interferometer with a Beam Waveguide Feed Network
 Proc. of the 1971 Intl. Symp. on Ant. and Prop., Sendai, Jap. (1-3 September 1971)
- SETHARES, J. C.
Visual Observation of RF Magnetic Fields Using Cholesteric Liquid Crystals
 J. of Appl. Opt., Vol. 9, No. 12 (December 1970)
- SLOBODNIK, A. J., JR.
Nonlinear Effects in Microwave Acoustic LiNbO₃, Surface Wave Delay Lines

- J. of the Acoust. Soc. of Am., Vol. 48, No. 1 (July 1970)
Microwave Acoustic Resonances in Thin Piezoelectric Disks
 IEEE Trans. on Son. and Ultrason., Vol. SU-17, No. 3 (July 1970)
Acoustic Surface Wave Investigations Using Laser Light Deflection
 Book, Acoust. Surf. Wave and Acousto-Opt. Devices (1971), Optosonic Press, N. Y., N. Y.
Surface-Wave Attenuation at Microwave Frequencies. Part I-Room Temperature
 IEEE Trans. on Son. and Ultrason., Vol. SU-18 (January 1971)
GaAs Acoustic Surface Wave Propagation Losses at 1 GHz
 Elect. Ltrs., Vol. 8, No. 12 (June 1972)
Attenuation of Microwave Acoustic Surface Waves Due to Gas Loading
 J. of Appl. Phys., Vol. 43 (August 1972);

 SLOBODNIK, A. J., JR., CARR, P. H., and BUDREAU, A. J.
Microwave Frequency Acoustic Surface Wave Loss Mechanisms on LiNbO₃
 J. of Appl. Phys., Vol. 41 (October 1970)

 SLOBODNIK, A. J., JR., and SETHARES, J. C.
The Elastic, Piezoelectric, and Dielectric Constants of Bi₁₂GeO₂₀
 J. of Appl. Phys., Vol. 43, No. 1 (January 1972)

 SLOBODNIK, A. J., JR., and SZABO, T. L., CAPT.
Design Data for Microwave Acoustic Surface Wave Devices
 Intl. Micr. Symp. Dig. (May 1971)
New High-Coupling, Low Diffraction Cut for Acoustic Surface Waves on LiNbO₃
 Elect. Ltrs. (England), Vol. 7, No. 10 (20 May 1971)

 STIGLITZ, M. R., and SETHARES, J. C.
Dielectric Resonators in Waveguides and Microstripl Circuits
 1971 Ann. Rpt., Conf. on Elec. Insul. and Dielec. Phen. (1972)

 SZABO, T. L., CAPT., and SLOBODNIK, A. J., JR.
Effect of Diffraction on the Design of Microwave Acoustic Surface Wave Devices
 IEEE Trans. on Son. and Ultrason., Vol. SU-18 (January 1971)

 WALTERER, F. G., and PHILLIPS, W. D., KLEPPNER, D.
 (Mass. Inst. of Tech., Cambridge, Mass.)
Effects of Nuclear Mass on the Bound Electron g Factor
 Phys. Rev. Ltrs., Vol. 28, No. 18 (1 May 1972)

 WULFSEBERG, K. N., and ALTHULER, E. E.
Rain Attenuation at 15 and 35 GHz
 IEEE Trans. on Ant. and Prop., Vol. AP-20, No. 2 (March 1972)

PAPERS PRESENTED AT MEETINGS

JULY 1970 - JUNE 1972

- ALTHULER, E. E.
New Applications at Millimeter Wavelengths
 IEEE/G-AP Mtg., Waltham, Mass. (18 May 1971)
 Sem., Univ. of N. H., Durham, N. H. (20 April 1972)
- ALTHULER, E. E., FALCONE, V. J., and WULFSEBERG, K. N.
Rain Attenuation at Millimeter Wavelengths
 1970 AGARD Mtg. on Trop. Rad. Wave Prop., Dusseldorf, Ger. (31 August-4 September 1970)
- ALTHULER, E. E., WULFSEBERG, K. N., and FALCONE, V. J., JR.
Rain Attenuation at 15 and 35 GHz
 1971 USNC/URSI-IEEE Spring Mtg., Wash., D. C. (8-10 April 1971)
- BUDREAU, A. J., and CARR, P. H.
Surface Wave Attenuation at Microwave Frequencies:
II Temperature Dependence
 1970 IEEE Ultrason. Symp., San Francisco, Calif. (21-23 October 1970)
- BUDREAU, A. J., SLOBODNIK, A. J., JR., and CARR, P. H.
Frequency and Temperature Dependence of Surface Wave Attenuation on Bi₁₂GeO₂₀
 1971 IEEE Ultrason. Symp., Miami, Fla. (6-8 December 1971)
- CARR, P. H.
Interaction Between Noncollinear Rayleigh Waves
 1970 IEEE Ultrason. Symp., San Francisco, Calif. (21-23 October 1970)
- Acoustic Surface Wave Research at AFCRL*
 Rome Air Dev. Ctr., Rome, N. Y. (21 January 1971)
- Physics and Applications of Ultrasonic Rayleigh Surface Waves*
 Sem., Mass. Inst. of Tech., Cambridge, Mass. (24 February 1972)
- Reduction of Reflections in Surface Wave Devices with Quarter-Wave Taps*
 1972 IEEE G-MTT Intl. Micr. Symp., Chicago, Ill. (22-24 May 1972)
- CARR, P. H., DE VITO, P. A., MAJ., and SZABO, T. L., CAPT.
Temperature and Doppler Shift Effects for Surface Wave Encoders and Decoders
 1971 IEEE Ultrason. Symp., Miami, Fla. (6-8 December 1971)
- CARR, P. H., FRANKLIN, S. B., SLOBODNIK, A. J., JR., SZABO, T. L., CAPT., and DE VITO, P. A., MAJ.
Uses and Limitations of Multiply Tapped Surface Wave Delay Lines

- 1970 IEEE Ultrason. Symp., San Francisco, Calif. (21-23 October 1970)
- CARR, P. H., and SLOBODNIK, A. J., JR.
Acoustic Losses of 600 MHz Surface Waves in Aluminum Interdigital Transducers
Gordon Res. Conf. on Phys. Acoust., Proctor Acad., Andover, N. H. (23 July 1970)
- CENTOFANTI, J. J., MAJ.
A Unique Dual Frequency Synthetic Aperture Radar System
CIRADS IV Symp., El Paso, Tex. (15-17 September 1970)
- (U) *Synthetic Aperture Dual Frequency Radar (SADFRAD)-Development and Airborne Test Results*
18th Ann. US Service Rad. Symp., Monterey, Calif. (6-8 June 1972)
- DE VITO, P. A., MAJ.
Uses and Limitations of Multiply Tapped Surface-Wave Delay Lines
1970 IEEE Ultrason. Symp., San Francisco, Calif. (21-23 October 1970)
- EHRENSPECK, H. W.
Reflector Antennas With High Efficiency
MGT Ant. Conf., Tech. Univ. of Darmstadt, Ger. (21-24 February 1972)
- FALCONE, V. J., JR.
Bayesian Estimation of Temperature Profiles from Passive Microwave Measurements
1971 Fall USNC/URSI Mtg. and Intl. IEEE/G-AP Symp., Univ. of Calif., Los Angeles, Calif. (21-24 September 1971)
Remote Sensing and Kalman Filtering
1972 USNC/URSI-IEEE Spring Mtg., Wash., D. C. (13-15 April 1972)
- FALCONE, V. J., JR., and MANO, K.
Statistical Methods of Indirect Probing of the Atmosphere
17th EPP/AGARD Symp., Electmg. Wave Prop. Panel, AF Acad., Colo. (21-25 June 1971)
- HAYES, D. T.
Electrostatic Probe Measurements of the Flow Field Characteristics of a Blunt Body Reentry Vehicle
5th AIAA Fluid and Plasma Dyn. Conf., Boston, Mass. (26-28 June 1972)
- HERSKOVITZ, S. B.
Liquid Additives for Blackout Alleviation: Physical Factors
4th Plasma Sheath Symp., NASA Langley Res. Ctr., Hampton, Va. (13-15 October 1970)
- JACAVANCO, D. J.
Experimental Determination of Electron Quenchant Efficiency at High Gas Temperature
4th Plasma Sheath Symp., NASA Langley Res. Ctr., Hampton, Va. (13-15 October 1970)
- JACAVANCO, D. J., and HERSKOVITZ, S. B.
Determination of Electron Quenchant Efficiency Under Simulated Entry Conditions
4th Plasma Sheath Symp., NASA Langley Res. Ctr., Hampton, Va. (13-15 October 1970)
- KALAGHAN, P. M.
Solar Mapping at Millimeter Wavelengths
Boston Section of the IEEE Gp. on Ant. and Prop., Waltham, Mass. (16 March 1971)
Spectral Characteristics of Active Centers in the Millimeter Wavelength Range
1972 USNC/URSI-IEEE Spring Mtg., Wash., D. C. (13-15 April 1972)
- LAMMERS, U. H. W.
Forward Scatter Atmospheric Mapping at Millimeter Waves
MIT Lincoln Lab. Airborne Sev. Storm Surv. Sum. Study, Barnstable, Mass. (7 August 1970)
Tropo-Structure Resolution of Backscatter and Forward Scatter Radars
1971 USNC/URSI-IEEE Spring Mtg., Wash., D. C. (8-10 April 1971)
- LAMMERS, U. H. W., and DAY, J. W. B. (Comm. Res. Ctr., Ottawa, Ont., Can.)
Comparison of Turbulent Layer Models and High Resolution Forward Scatter Results
1970 AGARD Mtg. on Trop. Rad. Wave Prop., Dusseldorf, Ger. (31 August-4 September 1970)
- LAMMERS, U. H. W., and OLSEN, R. L. (Comm. Res. Ctr., Ottawa, Ont., Can.)
Doppler Measurements on a Long Range 16 GHz Bistatic Scatter Link
1972 USNC/URSI-IEEE Spring Mtg., Wash., D. C. (13-15 April 1972)
- MACK, R. B.
Properties of the Phase of Backscattered Fields of Finite Circular Cylinders (invited)
Electmg. Gp., Div. of Eng. and Appl. Phys., Harvard Univ., Cambridge, Mass. (14 April 1971)
- MACK, R. B., and GORR, B. B.
A Self-Adaptive Method for Wide-Band Control of Radar Cross-Sections at VHF
1971 AFSC Sci. and Eng. Symp., Dayton, Oh. (5-7 October 1971)

- MAILLOUX, R. J.**
A Study of the Use of Conducting Fences for Reducing Mutual Coupling
 20th Symp. on USAF Ant. Res. and Dev., Univ. of Ill. at Urbana-Champaign, Urbana, Ill. (13-15 October 1970)
- Surface Waves and Anomalous Waves on Phased Arrays with Conducting Fences*
 1971 Fall USNC/URSI Mtg. and Int'l. IEEE/G-AP Symp., Univ. of Calif., Los Angeles, Calif. (21-24 September 1971)
- Blind Spot Occurrence in Phased Arrays - When to Expect it and How to Cure it*
 IEEE Oct. Conf., Chicago, Ill. (18-20 October 1971)
- MALONEY, L. R., MAJ.**
Microwave Reentry Communications Rocket Flight Tests
 4th Plasma Sheath Symp., NASA-Langley Res. Ctr., Hampton, Va. (13-15 October 1970)
- MANO, K.**
Multiple Scattering in the Wave Propagation Through Random Media
 1971 Int'l. Symp. on Ant. and Prop., Tohoku Univ., Sendai, Jap. (1-3 September 1971)
- MAVROIDES, W. G.**
Weather Profiles Using AFCRL 3-D Radar
 MIT Lincoln Lab. Airborne Sev. Storm Surv. Sum. Study, Barnstable, Mass. (7 August 1970)
- MC ILVENNA, J.**
Maximization of the Gain of Arrays Subject to Pattern Constraints
 Electmg. Rad. Sem., Harvard Univ., Cambridge, Mass. (13 November 1970)
Maximum Gain and Null Steering in Array Antennas
 Boston Chap. of the IEEE Mtg., Boston, Mass. (19 April 1972)
- MERRY, J. B.**
Magnetoelastic Theory of F^{19} Nuclear Acoustic Resonance in Antiferromagnetic $RbMnF_3$
 1971 IEEE Ultrason. Symp., K'لامi, Fla. (6-8 December 1971)
- NEWBURGH, R. G.**
Brewster's Angle and the Einstein Velocity Composition Law
 Seminaire de Physique Theorique, Institut Henri Poincaré, Paris, Fr. (12 October 1970)
Proposed Optical Measurement of the Brewster Angle as a Test of Special Relativity Theory
 Colloq., Nav. Ordin. Lab., White Oak, Md. (13 November 1970)
A First Order Effect in Moving Anisotropic Media
- Ann. Mtg. of the Opt. Soc. of Am., Ottawa, Ont., Can. (5-8 October 1971)**
Synchrotron Radiation as Evidence Against the Ritz Emission Theory
 N. E. Sec. Mtg. of the Am. Phys. Soc., Boston Coll., Chestnut Hill, Mass. (14-15 April 1972)
- PAPA, R. J.**
Review of Problems Associated With Communications Through Plasmas (Invited)
 1970 Int'l. IEEE/G-AP Symp. and Fall JSNC/URSI Mtg., Oh. State Univ., Columbus, Oh. (14-17 September 1970)
- RAO, K. V. N.**
Decay of Low Pressure Neon Afterglows
 2nd Arc Symp. of the Am. Phys. Soc., Hartford, Conn. (20 October 1970) 23rd Ann. Gaseous Elect. Mtg. of the Am. Phys. Soc., Hartford, Conn. (21-23 October 1970)
- Electrostatic and Microwave Probing of Low Pressure, Neon, Oxygen and Neon-Oxygen Afterglow Plasmas*
 Plasma Phys. Mtg. of the Am. Phys. Soc., Wash., D. C. (4-7 November 1970)
- ROTHMAN, W.**
Studies of Reentry Plasma Sheath Effects Upon Microwave Antenna Performance
 4th Plasma Sheath Symp., NASA-Langley Res. Ctr., Hampton, Va. (13-15 October 1970) IEEE Gp. on Ant. and Prop., Boston Sec., Boston, Mass. (19 January 1972)
Microwave Measurements of Flow Field Characteristics at the Stagnation Point of a Blunt Reentry Body
 5th AIAA Fluid and Plasma Dyn. Conf., Boston, Mass. (26-28 June 1972)
- SCHELS, A. C.**
Beam Waveguides for Millimeter Wave Antenna Feeds
 IEEE G-AP G-MTT Mtg., Ga Inst. of Tech., Atlanta, Ga. (18 November 1970)
Engineering Salary Trends
 Boston Sec. of the IEEE Gp. on Ant. and Prop., Waltham, Mass. (14 December 1970)
Recent Developments in Microwave Antennas
 1971 Eur. Micr. Conf., Stockholm, Swed. (23-28 August 1971)
A Millimeter Wave Interferometer With a Beam Waveguide Feed Network
 1971 Int'l. Symp. on Ant. and Prop., Sendai, Jap. (1-3 September 1971)
- SCHINDLER, J. K.**
A Note on the Polarization Properties of Stochastic Electromagnetic Plane Waves of Arbitrary Bandwidth

- 1970 Intl. IEEE/G-AP Symp. and Fall USNC/URSI Mtg., Oh. State Univ., Columbus, Oh. (14-17 September 1970)
Wideband Radar Camouflage
 ICBM Pen Aids Wkg. Gp., SAC Hq., Offutt AFB, Neb. (29 July 1971)
- SCHINDLER, J. K., and BLACKSMITH, P.
Wideband Radar Camouflage Properties of Absorbing Clouds
 U. S. Air Staff, Wash., D. C. (15 July 1971)
- SLETTEN, C. J.
Needed: New Techniques and Concepts in Electromagnetics
 Oh. State Univ., Columbus, Oh. (28 January 1971)
- SLOBODNIK, A. J., JR.
Surface Wave Attenuation at Microwave Frequencies: I. Room Temperature
 1970 IEEE Ultrason. Symp., San Francisco, Calif. (21-23 October 1970)
Acoustic Surface Wave Investigations and Devices for Air Force Applications
 ESD/AFCRL Sci. & Eng. Mtg., L. G. Hanscom Fld., Mass. (3 November 1970)
Acousto-Optic Light Diffraction and Devices
 (Invited Talk), Boston Sec. of the IEEE Gp. on Son. and Ultrason., Boston, Mass. (17 March 1971)
Design Curves for $Bi_{12}GeO_{20}$ Spiral Acoustic Surface Wave Delay Lines
 1972 IEEE G-MTT Intl. Micr. Symp., Chicago, Ill. (22-24 May 1972)
- SLOBODNIK, A. J., JR., and SETHARES, J. C.
The Elastic, Piezoelectric, and Dielectric Constants of Bismuth Germanium Oxide
 1971 IEEE Ultrason. Symp., Miami, Fla. (6-8 December 1971)
- SLOBODNIK, A. J., JR., and SZABO, T. L., CAPT.
Design Data for Microwave Acoustic Surface Wave Devices
 1971 IEEE G-MTT Intl. Micr. Symp., Wash., D. C. (17-20 May 1971)
- STIGLITZ, M. R.
Microstrip Filters Using Dielectric Resonators
 Intl. Filter Symp., Santa Monica, Calif. (15-18 April 1972)
- STIGLITZ, M. R., and SETHARES, J. C.
Dielectric Resonators in Waveguide and Microstrip Circuits
 1971 Ann. Mtg. of the Conf. on Elec. Insul. and Dielec. Phen., Cascades Mtg. Ctr., Williamsburg, Va. (1-3 November 1971)
- SZABO, T. L., CAPT.
Surface Wave Losses Through Aluminum Thin Film Gratings
 1971 IEEE Ultrason. Symp., Miami, Fla. (6-8 December 1971)
Anisotropic Acoustic Surface Wave Diffraction
 IEEE Reflec. Mtg., Boston Chap. of the IEEE, Boston, Mass. (11 April 1972)
- SZABO, T. L., CAPT., and SLOBODNIK, A. J., JR.
The Effect of Diffraction on the Design of Microwaves Acoustic Surface Wave Devices
 1970 IEEE Ultrason. Symp., San Francisco, Calif. (21-23 October 1970)
- TELFORD, L. E.
Low Angle Tropospheric Refraction Measurements at 8.6 Millimeters
 1971 USNC/URSI-IEEE Spring Mtg., Wash., D. C. (8-10 April 1971)
- ## TECHNICAL REPORTS JULY 1970 - JUNE 1972
- ALTSCHULER, E. E.
Corrections for Tropospheric Range Error
 AFCRL-71-0419 (27 July 1971)
- ANTONUCCI, J. D.
An Artificial Transmission Line for Studies of Transient Propagation in Plasma Media
 AFCRL-72-0055 (24 January 1972)
- BURAK, M.
Pointing Calibration of a High-Resolution Millimeter-Wave Antenna by Star Observations
 AFCRL-71-0220 (29 March 1971)
- CENTOFANTI, J. J., MAJ.
(U) Synthetic Aperture Dual Frequency Radar (SADFRAD)-A Unique Airborne Sensor
 AFCRL-70-0676 (December 1970)
- CLEVELAND, F. H., MAJ., and KERNWEIS, N. P.
A Technique for Measuring Finesse at Millimeter Wavelengths
 AFCRL-70-0893 (20 November 1970)
- DRANE, C. J., JR., and MC ILVENNA, J. F.
Null Steering and Maximum Gain in Electronically Scanned Dipole Arrays
 AFCRL-72-0083 (1 February 1972)

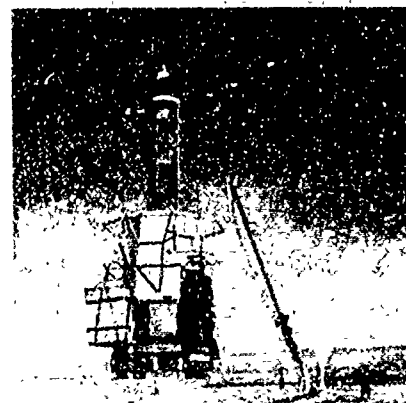
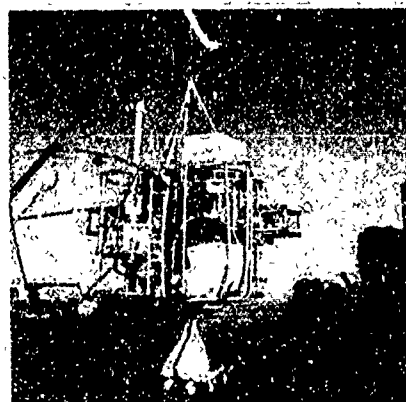
- EHRENSPECK, H. W., and STROM, J. A.
*The Short-Backfire Antenna as an Element
 for High-Gain Arrays*
 AFCRL-71-0234 (13 April 1971);
Short-Backfire Arrays
 AFCRL-71-0368 (27 May 1971)
*The Four-Element SBF Array; Variation of
 Parameters for Optimization of Performance*
 AFCRL-71-0569 (12 November 1971)
- FANTE, R. L.
*Transmission of Electromagnetic Waves
 Through a Time-Varying Dielectric Layer*
 AFCRL-72-0044 (7 January 1972)
*Analysis of Propagation in Space-Time
 Modulated Media Using Many-Space
 Scale Perturbation Theory*
 AFCRL-72-0187 (22 March 1972)
*Theory of Propagation of Electromagnetic
 Waves in Space-Time Varying Media*
 AFCRL-72-0264 (24 April 1972)
- HARSKOVITZ, S. B., and LIEGEOS, F. A.
*The Influence of Solar Illumination on X-Band
 Antenna Voltage Breakdown Phenomena*
 AFCRL-70-0472 (27 August 1970)
- JACAVANCO, D. J.
*An Experimental Study of the Interaction
 of Moderate Power Microwaves with Electron
 Density Gradients*
 AFCRL-72-0306 (16 May 1972)
- KALAGHAN, P. M., and SHORT, J.
*Tropospheric Refraction Effects and
 Their Corrections*
 Iono. and Tropo. Lmt. to Rad. Accry.,
 AFCRL-71-0169 (5 February 1971)
- MACK, R. B.
*(U) Concepts and Progress in Wide-Band
 Impedance Loading Methods*
 AFCRL-71-0372 (4 June 1971)
*Phase, Phase Signatures, and Simple Inverse
 Properties of Backscattered Fields from
 Thin Rods*
 AFCRL-71-0526 (4 October 1971)
- MACK, R. B., and GORR, B. B.
*Wideband Self-Adaptive Control of Radar
 Cross Sections*
 AFCRL-71-0506 (1 September 1971)
- MAILLOUX, R. J.
*Surface and Anomalous Waves on Phased
 Arrays of TEM Waveguides with Fences*
 AFCRL-71-0060 (28 January 1971)
- Blind Spot Occurrence in Phased Arrays -
When to Expect It and How to Cure It
 AFCRL-71-0428 (11 August 1971)
- MAILLOUX, R. J., and MAVROIDES, W. G.
*A Low Profile Antenna for Airborne Station
 Keeping Radar Applications*
 AFCRL-72-0046 (13 December 1971)
- MAVROIDES, W. G.
*Aircraft-Detection Tests Using the AFCRL
 Experimental Phase-Phase Radar*
 AFCRL-71-0140 (26 February 1971)
- NEARY, M. J., CAPT.
*Pointing Error Correction for
 Millimeter Wave Spectroheliograms*
 AFCRL-71-0236 (April 1971)
- NEWBURGH, R. G., and PHIPPS, T. E., JR. (U. S. Nav.
 Ord. Lab., White Oak, Md.)
*A Novel Rotation Sensor Based on Measurement
 of the Brewster Angle in a Moving Medium*
 AFCRL-71-0027 (8 January 1971)
- PAPA, R. J.
*Wave Propagation in a Warm Magnetoplasma
 with Coulomb Interactions*
 AFCRL-70-0419 (23 July 1970)
*Extension of Dougherty's Model Fokker-Planck
 Equation for a Plasma*
 AFCRL-70-0463 (18 August 1970)
*Wave Propagation in a Hot Magnetoplasma
 with Coulomb Collisions*
 AFCRL-70-0613 (October 1970)
- SCHINDLER, J. K., and BLACKSMITH, P.
*(U) Wide-Band Radar Camouflage Properties
 of Dipole Clouds*
 AFCRL-71-0376 (8 July 1971)
- SEAVEY, M. H., JR.
*Spinwave Relaxation in Low Anisotropy
 Antiferromagnets*
 AFCRL-70-0627 (6 November 1970)
- SLETEN, C. J., and HOLT, F. S.
*(U) Synthetic-Aperture Tracking of Moving
 Targets*
 AFCRL-71-0141 (10 February 1971)
- SLOBODNIK, A. J., JR.
*A Laser Probe for Microwave Acoustic
 Surface Wave Investigations*
 AFCRL-70-0404 (16 July 1970)
*The Temperature Coefficients of Acoustic
 Surface Wave Velocity and Delay on
 Lithium Niobate, Lithium Tantalate,
 Quartz, and Tellurium Dioxide*
 AFCRL-72-0082 (22 December 1971)

SLOBODNIK, A. J., JR., and O'BRIEN, J. V.
*Complete Theory of Acoustic Bulk Wave
Propagation in Anisotropic Piezoelectric
Media*
AFCRL-71-0601 (November 1971)

SLOBODNIK, A. J., JR., and SETHARES, J. C.
Measurement of the Elastic, Piezoelectric

and Dielectric Constants of $Bi_{12}GeO_{20}$
AFCRL-71-0570 (10 November 1971)

STIGLITZ, M. R.
*Preparation and Electrical Properties of
Some Ceramic Materials at Microwave
Frequencies*
AFCRL-70-0726 (7 December 1970)



Unlike rocket and aircraft scientific payloads which must be tailored to fit the carrier, balloon payloads have few structural or configurational constraints and can assume a variety of sizes and shapes. From top to bottom: detector for energetic particle research, air sampling equipment and an infrared measuring system.

IV Aerospace Instrumentation Laboratory



The satellites, sounding rockets, and balloons used to carry research instrumentation where data can be gathered are the special responsibility of the Aerospace Instrumentation Laboratory. In selection of the vehicle, establishment of the tracking and telemetry network, payload integration, and launch and recovery operations, this Laboratory is responsible for the successful acquisition of data. The work is performed for other AFCRL Laboratories—primarily the Aeronomy, Ionospheric Physics, Optical Physics and Space Physics Laboratories—and also for other DOD and government laboratories.

Not only does the Laboratory design and fabricate specific experimental payloads for rockets and satellites, but it also obtains the best sounding rockets available for specific flight profiles. This responsibility includes development work which leads to the upgrading of rocket performance. During the past two years, the Laboratory participated in the launching of 83 rocket probes, attaining a 90 percent success rate, and two satellites, completely instrumented by AFCRL scientists.

Balloon flight operations conducted at the Laboratory's permanent launch sites located at Holloman AFB, New Mexico and Chico, California utilize and evaluate the research and development products of the Laboratory. Thus, there is within the Laboratory a closed loop among theory, development and application, providing the setting wherein theory can be quickly tested and future research needs readily identified. The results of balloon research and development are usually manifested as a major contribution to successful acquisition of unique scientific data or as a

hardware test for an Air Force system. The major formal communication of the results of AFCRL's balloon research to the scientific community occurs during the Laboratory's Symposia which are conducted approximately every two years. The seventh in this series will be held in September of 1972.

During this reporting period, the Laboratory launched 195 free and tethered balloons. In addition, systems engineering studies and consultation services were provided to program offices considering the use of balloons for a wide range of experiments related to military systems, including three of special note. For the Army Ballistic Research Laboratories, the feasibility of using balloons in antiballistic missile dynamic blast tests was investigated. The blast sources considered included balloons inflated with detonable lifting gases and high explosives delivered by balloons. The Laboratory provided advisory support to the Air Force Weapons Laboratory concerning balloon aspects of its TORUS Electromagnetic Pulse Simulator Development. Collaborative work with the Mitre Corporation on candidate high-altitude airborne relay platforms explored the use

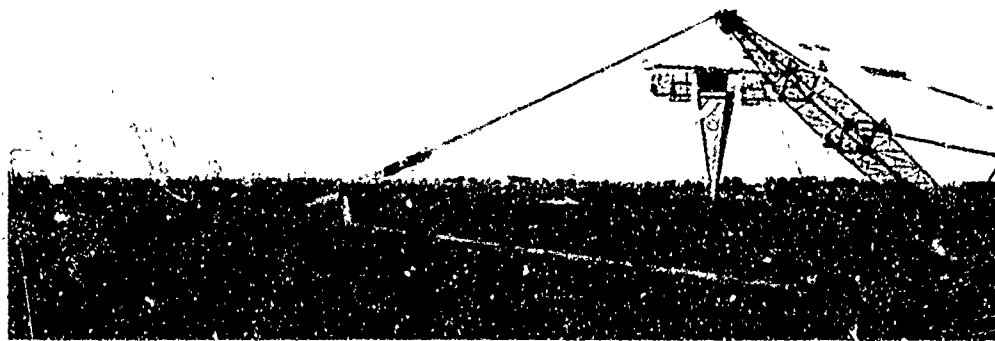
of balloons in Tactical Air Command operations.

Operational and technical support was provided by the Laboratory to the Atomic Energy Commission's (AEC) air sampling program. Balloon flights were made for the AEC from Holloman AFB, New Mexico; Chico, California; Sioux Falls, South Dakota; Panama and Alaska, with aerial recovery of the payloads accomplished at the latter two locations.

On July 3, 1971, three of the Laboratory's branches, Meteorological Observing Techniques, Vertical Sounding Techniques, and Direct Sensing Techniques were transferred, with no change of function, to AFCRL's Meteorology Laboratory. The work of these branches has been included in that laboratory's report.

RESEARCH ROCKETS

The entire AFCRL rocket program, including selection of the rocket vehicle, range scheduling, payload assembly, and data collection, is conducted by the Aerospace Instrumentation Laboratory. This Labora-



The reentry nose cone shown here was carried to 100,000 feet and released over the White Sands Missile Range. This flight, conducted in July 1970, was one of a series performed by the Laboratory during the past decade in support of a SAMSO project.

tory also conducts engineering research in several disciplines to allow new or upgraded experiments to be conducted.

CHASER: One series of experiments requiring extensions of the state of the art of launching, trajectory prediction, and recovery was conducted in support of the Chaser program. Sensors were carried to altitudes above the sensible atmosphere to measure characteristics of the exhaust trail of large rocket motors in real time, free of atmospheric extinction effects. The experiment included the launch of the target missile by the sponsoring agency, launch of the Aerobee carrying the AFCRL sensors, separation of the Aerobee payload from its propulsion, orientation of the payload to a pre-calculated look angle, opening the payload to expose the sensors, adjusting the attitude of the payload in steps to keep the target in view, rotating the payload off target to measure sky background and then the earth's atmosphere, closing the payload to a watertight condition, deploying a parachute to permit low velocity water impact, and, finally, retrieving the assembly for reuse.

A digital simulation of the two moving body problem allowed detailed assessment of the effects of the many variables of uncontrolled rocket flight on the mission. Based upon these analyses, specifications for the optical sensor were generated, and the times were determined for many functions. The experiment itself involved the first rail launch of an Aerobee 170, the first night water recovery, a new recovery system, the first use of foam-filled tins, and launch at the lowest elevation angle ever attempted for this type of vehicle. Launches at Vandenberg AFB on June 29, 1971 and November 23, 1971 were successful. A third attempt on June 20, 1972 resulted in the loss of all equipment when the Aerobee propulsion system failed.

HI-STAR: The Hi-Star program, in which IR sources in the celestial sphere are

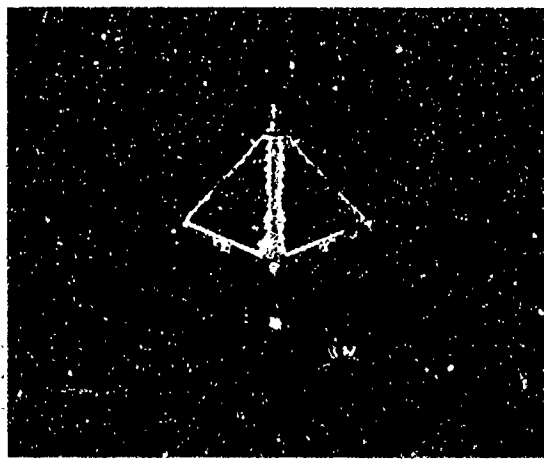
mapped with high accuracy, is also of great interest to the Air Force and requires intensive efforts by both the Optical Physics and Aerospace Instrumentation Laboratories. Seven successful experiments took place within the past two years, and recovery of the payload each time allowed reuse of the same instruments, with attendant economies. To use the full capability of the sensor, a high data rate pulse code modulation system was created, which returned the maximum amount of information that could be handled by the range-supplied receiving system.

OTHER SYSTEMS: The reentry processes related to sounding rocket payload recovery were studied under contract. The work required development of a theory which allowed analytical determinations of reentry dynamic variables. The theory will be verified by experiments and simulations at the contractor's wind tunnel facility. These studies and experiments will provide the basis for the design of systems used to recover sounding rocket payloads by aircraft.

ROCKET MOTORS: Two new rocket motors, the Ute and Paiute, were added to the AFCRL family of sounding rockets. Originally produced for other programs, they have been adapted for sounding rocket use. The Ute-Tomahawk has replaced the Nike-Iroquois vehicle, and the Paiute-Tomahawk has replaced the Nike-Tomahawk. The Nike booster, a mainstay of sounding rocket programs since the 1950's, is now an obsolete item of uncertain availability and reliability.

RESEARCH SATELLITES

The Laboratory is continuing its involvement in the Air Force's satellite research



Satellite OV5-6, launched May 23, 1969 to measure energetic particles emitted by the sun, was still in orbit and returning useful data at the end of this reporting period in 1972. A discussion of some of the data returned by this satellite can be found in the Space Physics Laboratory chapter of this report.

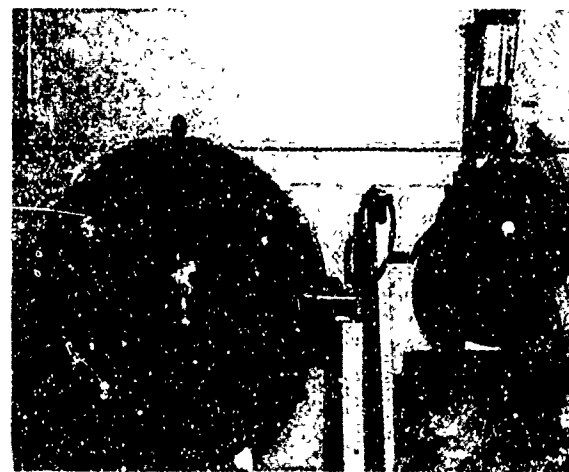
program. During the past two years, two satellites were launched for which the Laboratory had total responsibility for technical management and experiment integration. AFCRL scientists provided sensors for three additional satellite experiments which required a lesser degree of laboratory participation.

The Cannonball II and the Musketball satellites were successfully launched in August 1971. The nicknames for these satellites resulted from the unusually large mass to area ratio required to achieve a reasonable orbital life in spite of the low perigee dictated by the mission. Both of the satellites were part of the Aeronomy Laboratory's research program to provide density data for Air Force operations, including those of the Aerospace Defense Command, the Air Force Satellite Control Facility, and classified Air Force special

projects. The final design, utilizing micro-circuit techniques and other advanced methods of packaging, resulted in a 135 pound 12 inch sphere for Musketball and a 26 inch sphere weighing 800 pounds for Cannonball II. Density data were obtained from both satellites by analyzing the orbital decay and updating existing mathematical density models through an iterative process. An accurate ephemeris was made possible by the use of position data provided by the tracking system included in the spacecraft.

Additionally, the Cannonball II satellite carried a triaxial accelerometer which provided density data by the instantaneous measurement of satellite drag. Currently, these data are being analyzed by scientists of the Aeronomy Laboratory.

The OV5-6, a small satellite designed to measure solar radiation, was flown piggy-back on a Titan III in May 1969 and achieved an orbit of 10,000 by 60,000 nau-



Two AFCRL low altitude density research satellites, Cannon Ball II and Musket Ball were successfully orbited on August 6, 1971. The 12.32 inch diameter Musket Ball weighed 135 pounds, while the 26-inch diameter Cannon Ball II weighed 800 pounds. Their unusually high mass-to-area ratio gave Musket Ball a lifetime of more than a month, and Cannon Ball II, a lifetime of approximately six months, in spite of their extremely low perigees (below 140 km).

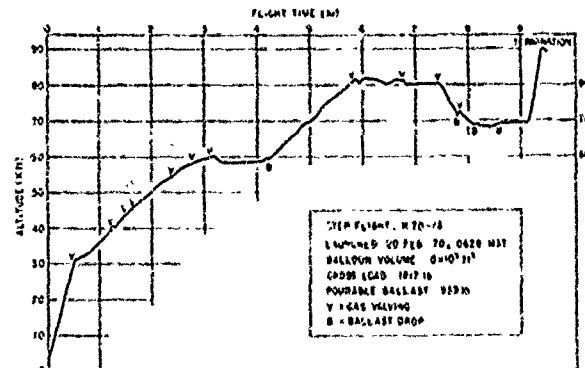
tical miles. At the time of this report, all systems were still working well, and the satellite had exceeded its 18 month design life by a factor of more than two. Scientists of the Space Physics Laboratory are analyzing the resultant data, consisting of fluxes and spectra of protons, electrons, alpha particles and gamma rays, to aid in the prediction of the effects of this radiation on the upper atmosphere and ionosphere.

FREE BALLOON CONTROL

An important element in free balloon operations is trajectory control—that is, making the balloon fly the time and space profile required to accomplish its scientific purpose or changing the trajectory for weather, payload recovery or safety reasons. While it is apparent that the winds encountered will determine its horizontal movement, the atmosphere also exerts a significant influence on the vertical motion of a balloon. A balloon is a complicated thermodynamic system with its vertical motion and equilibrium float altitude affected by ambient temperature and the various energy fluxes from the earth, atmosphere and sun.

To increase the versatility and applications of balloons, research is conducted to better understand and predict the vertical motion of balloons. Concurrently, flight experiments are conducted to determine balloon response to valving gas and releasing ballast under operational conditions.

Balloon vertical motion predictability is very much a function of atmospheric predictability, which is not very good, especially with regard to infrared flux. With this in view, multiple regression analysis studies were performed to develop information designed to predict balloon ascent rate. The predictors used consisted of balloon system parameters, such as free lift

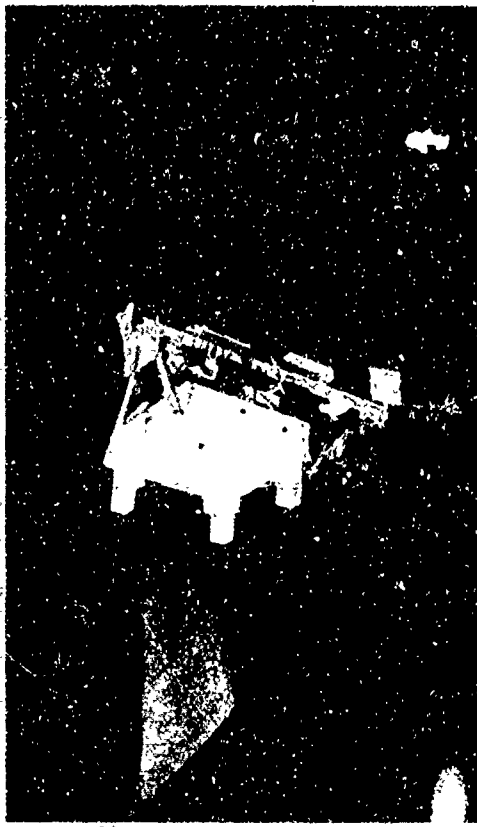


The ability to control the vertical motion of free balloons has greatly increased their efficiency and effectiveness as atmospheric platforms. By venting gas and releasing ballast by radio command from the ground, this balloon was leveled off at three different altitudes for periods of approximately one hour. Here the V and B indicate respectively when gas was vented and ballast released. In addition to providing a choice of flight profiles, this control capability is frequently used to great advantage in maneuvering the balloon to insure recovery of the scientific payload.

(the upward directed unbalanced force on a balloon) and volume, and atmospheric characteristics, such as temperature lapse rate and pressure. The results to date show that the atmospheric predictor having the best correlation with ascent rate is temperature lapse rate. While free lift, taken by itself, explains only 5 percent of the variance in average tropospheric ascent rates, it explains 47 percent of the variance in average stratospheric ascent rates. However, the analysis indicates that there are lag relationships which must be determined before accurate performance predictions will be possible.

POWERED BALLOON: A direct outgrowth of AFCRL's experience with free balloon hovering experiments is the powered balloon.

The problems involved in equipping a free balloon with a propulsion system to achieve a high altitude hovering or loiter-



Powered balloon gondola undergoing flight testing for propeller thrust, rudder control and dynamic stability. This system weighs 3500 pounds and has a 39-foot propeller. The rudder is 9 feet high and is located 13 feet behind the propeller.

ing capability have been studied. This research has indicated that the concept is feasible with present state of the art components at minimum wind field altitudes, generally near 60,000 feet, found in a number of geographical areas at selected times of the year.

Based on this feasibility study, a system design was initiated and a propeller-driven (electric motor powered) spherical balloon system was fabricated. This prototype system has a useful payload capacity of 200 pounds and will operate against a 15 knot wind for 12 hours at 60,000 feet.

Some 21 propulsion system functions, as

well as standard balloon flight functions are controlled by radio command and 18 parameters are telemetered and recorded at a specially equipped ground station.

The prototype powered balloon system will be test flown from Holloman Air Force Base, New Mexico, in September 1972 and the results of this research flight will be provided to the Air Force agencies that have expressed an interest in this capability.

TETHERED BALLOONING

Increased capabilities of tethered balloons and the unique Laboratory tethered balloon facilities have enabled AFCRL to support a wide variety of projects. System 621B (SAMSO) uses a tethered balloon to carry a navigation transmitter aloft. The balloon-borne transmitter simulates a satellite system during field tests. Air sampling sensors were flown on a tethered balloon for the Optical Physics Laboratory in support of Project 698AJ/ATOM. The first phase of a project sponsored by the AFCRL Meteorology Laboratory, in which data from wind sensors mounted on a tether cable were compared with data from tower-mounted sensors, has been completed. Future tests will include operational flights to study the earth's boundary layer using an instrumented tether cable at altitudes up to 5,000 feet.

An analytical model of a tethered balloon system has been developed. Methods employed include analysis of stability characteristics and dynamic simulation. Design parameters may be varied and the resultant effect on system stability studied. Work to date treats the balloon as a rigid structure and ignores localized motions and vibrations.

Payload platform stability and serviceability as a function of location were studied in conjunction with Laboratory sup-

port of a Defense Systems Project Group tethered balloon program. Three positions were studied: 1) in line with the tether, 2) suspended aft of the tether confluence point, and 3) snugged against the underside of the balloon. The results of this research show that each position is characterized by a different range of payload motions. Consequently, the selection of payload location must consider tradeoffs between stability and operational serviceability requirements.

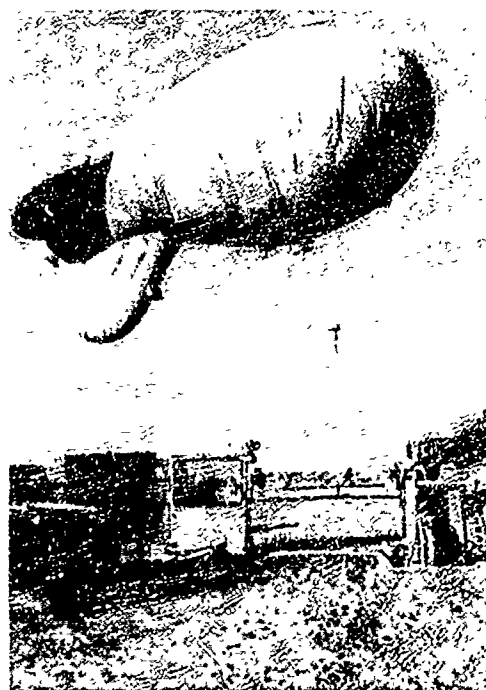
A series of tests conducted with fiber-glass tether cables shows that while their theoretical strength-to-weight ratios are high, their susceptibility to damage during routine operational handling and the difficulty of attaching end fittings make them unsuitable for tethered balloon use. Testing of Dacron cable started in July 1971. This cable consists of parallel core fibers encased in an extruded polyethylene jacket. The core fibers carry the load, and the jacket bundles the core fibers and protects

them from abrasion. Tests were designed to reveal wear modes during field operations, with the ultimate goal of establishing objective guidelines for fatigue life. To date, one failure mode related to desert use environment has been identified and corrective action taken.

The use of the AFCRL tethered balloon research facility to support USAF research and development efforts has not only ensured the availability of the latest technical advances to the user, but also provides to AFCRL, at minimum time and cost, the flight data essential to advancing the state of the art of tethered ballooning.

BALLOON INSTRUMENTATION

Flight control instrumentation, which includes data collection and transmission systems, is a necessary aspect of every operation utilizing free, tethered or pow-



A 100,000 cubic foot kite balloon ready for reel-up and at an altitude of 10,000 feet above ground.



The workhorse of AFCLR's stable of tethered balloons—a 33-foot diameter sphere—is shown here carrying an acoustic sensor experiment.

ered balloons. Positive full-time control is required by civil and military regulations for flight safety. Radio command and telemetry help satisfy regulatory requirements and inherently provide the experimenter and/or the mission controller direct and real-time access to onboard apparatus. Positive direct control and real-time readout of data permit variable trajectory profile adjustment, allowing the balloon to be flown in a specific manner to accomplish desired mission or test objectives. Data systems are essential to balloon payload housekeeping, permitting continuous observation and assessment of the operational status of the balloon-borne system. Telemetry from the balloon closes the loop between ground, ship or aircraft mission control points. In-flight adjustments, corrections or substitutions can be effectively and rapidly implemented by radio com-

mand to assure mission success if such control features have been designed into the system. By carefully tailoring the instrumentation and control system designs to meet specific mission objectives, the balloon vehicle can provide a highly stable, long duration test platform of great flexibility at minimum cost.

To accommodate the broad scope of applications possible with today's balloon technology, the Laboratory has developed an extensive array of modular flight components. These include items such as solid state timer-programmers, logic control and switching units, command receivers, command decoders, data transmitters, data encoders, signal conditioners, commutators, power sources and converters, communications relays, sensing devices, tracking beacons, transponders, homing and locating aids, automatic ballasting and gas valving devices, payload separation devices, impact-shock and vibration monitors, data recorders, navigational devices, camera systems, high intensity strobe warning lights, payload deployment devices, pyrotechnic energizers and protective devices, antennas and specialized payload attachment and release rigging hardware. The ever expanding spectrum of modular components, mostly laboratory designed and built, offers a wide choice in selection of specific equipment configurations and operating radio frequency bands from very low frequency (VLF) to super high frequency (SHF) that can be quickly assembled into new system designs.

Three different tethered balloon instrument systems of varied complexity were designed, fabricated and tested to support tethered balloon programs. All systems provide the necessary flight control and safety parameters automatically or by radio command, and two of the systems provide for multi-channel housekeeping and data telemetry.

Two special instrument systems were designed and fabricated to telemeter decel-

erator parachute performance characteristics. Parameters, such as accelerations in X, Y, Z planes in the load train and in the payload, pitch and roll on two axes, and pressure altitude, were measured in real time. A similar instrument was specifically modified to provide data during a series of launch vehicle stability measurements.

A sophisticated flight control telemetry and safety system was designed and fabricated for the powered balloon feasibility study program. The system includes both UHF and HF remote control capability and provides 18 channels of telemetered performance data on the propulsion, guidance system and housekeeping. Autopilot and manual direction control are included in the 21 command control channels employed.

Two completely instrumented mobile vans were designed, constructed and tested with electronics configured specifically to support the powered balloon program.

A new type of hygrometer was tested in the Laboratory in an effort to retain the advantage of this type sensor for accuracy at low pressures and overcome the principal drawback of present hygrometer designs, the evaporation of the basic fluid which limits the operational duration. In this design the fluid and vapor are completely enclosed. The pressure difference between the vapor and ambient air is sensed by a thin stretched diaphragm that controls the fluid heater in such a way as to bring the pressure difference to zero. Besides the advantage of no loss of fluid, the unit is much smaller than current hygrometers and provides a faster measurement response time. A breadboard model showed excessive hysteresis because of the stiffness of the only available diaphragm. A second prototype is now under construction with a new type of diaphragm.

Laboratory development work and breadboard designs have been tested successfully employing COS-MOS integrated

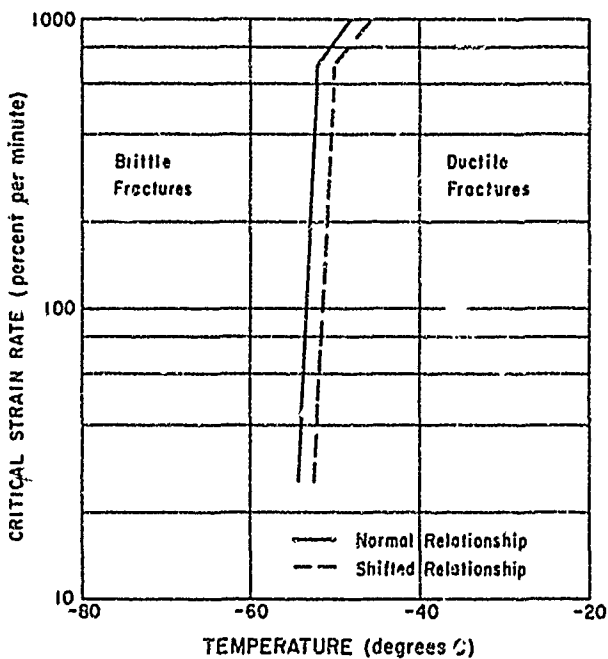
circuits in controlled phase-locked loops for command tone decoders. This development will lead to a simplified, low-cost design for ground station command intelligence generators and decoders of smaller size, increased long-term operational reliability and improved narrow-bandwidth stability, which will result in expanded remote control capabilities utilizing present HF systems. In addition, instrumentation hardware and engineering flight support services were provided to every balloon mission (195 total) conducted by the Laboratory during this period.

MATERIALS RESEARCH

Although polyethylene film has been used as the gas barrier and load bearing structure for most high-altitude constant-level balloons since the early 1950's, a complete picture of its behavior patterns under operational conditions is just emerging.

Test data on polyethylene film strength over the range of temperatures -70 degrees F to +110 degrees F are being correlated with mechanical properties on the molecular scale and provide for the first time a theoretical explanation of brittle fracture consistent with balloon flight experience. The mechanical behavior of extruded polyethylene films has long been known to be dependent on rate of straining (or stressing). It has recently been shown both analytically and experimentally that for temperatures normally experienced in the region of the tropopause, even very low strain rates will result in brittle fracture.

The rate of loading of the balloon film due to horizontal wind shears during passage through the tropopause region is magnified by the length (or height) of the balloon and by its rate of rise. It is postulated on the basis of experimental data that the maximum allowable strain rate



A slight shift in the critical strain rate-temperature relationship, due to strains produced at high launch temperatures, can produce dramatic reductions in the allowable strain rate in the tropopause temperature range, thereby increasing the probability of balloon burst during ascent.

may be significantly decreased by the launch temperature, the balloon design and the gross inflation. These complicated interrelationships appear to be reasonably consistent with balloon flight experience.

The observed complex interaction of balloon material, design, gross inflation, ascent rate and tropopause environment in the failure mechanism of ascending balloons now provides direction for rational design alterations, for improvement of extruded polyethylene and for reasonable operational constraints. Further, the adequacy of experimental nylon films, proposed for inexpensive heavy-load balloons, will be assessed largely on the basis of these research results for polyethylene film.

HIGH ALTITUDE, HEAVY LOAD PARACHUTE TESTS

One essential component of a scientific balloon system is a recovery parachute that will function reliably in the high-altitude balloon environment. The load-bearing capabilities of large plastic balloons have now far surpassed the safe limits for single parachutes of reasonable size and proven design. For several years AFCRL has been using clusters of two or three 100 foot diameter flat circular canopies to recover the heaviest balloon-borne payloads. However, to recover these payloads from higher altitudes, high-strength decelerators with appreciably reduced weight are required.

A high-strength parachute is required for the evaluation of heavy space reentry recovery systems because in the event of a premature flight termination, the parachute must recover the entire initial payload. In the normal course of events, however, most of the payload weight is released prior to flight termination. In the latter case, the high-strength parachute will then be required to recover relatively light-weight command and control instrumentation and payload support systems. The critical problem in this situation is one of descent stability and not of strength.

Parachutes normally are designed for and tested at altitudes well below balloon float levels, and no adequate criteria exist for applying scaling techniques to data obtained in wind tunnel tests using model parachutes. Consequently, the Laboratory is utilizing full-scale balloon training flights to test novel, light-weight parachute designs that show promise for high-altitude, heavy-load balloon applications.

During this reporting period, two AFCRL flights were conducted to obtain the opening and descent characteristics of large rapid inflation bowline controlled opening (RIBCO) parachutes at altitudes

above 100,000 feet. This design gives significant weight reduction, and its flight characteristics at low altitudes are reported to be equal to or superior than those of comparable conventional canopies.

On both tests, accelerations, pressure altitude and IRIG time code were telemetered and recorded, and parachute opening and descent were monitored by radar and on-board cameras.

Although neither canopy displayed unusual stability above 50,000 feet, both performed remarkably well. Considering their performance and a weight saving of approximately 400 pounds compared with a conventional cluster of three 100 foot diameter parachutes, the new RIBCO design holds considerable promise for heavy-load, high-altitude balloon applications. In view of the absence of parachute performance data at these extreme altitudes, the results of this research are expected to find practical application in other Air Force recovery system programs.

JOURNAL ARTICLES JULY 1970 - JUNE 1972

CARTEN, A. S., JR.
USAF Acts on C-5 Wakes
(Ltr. Art.) Astronaut. and Aeronaut. Vol. 8, No. 8 (8 August 1970)

Aircraft Wake Turbulence--An Interesting Phenomenon Turned Killer
Air Univ. Rev. Vol. 22, No. 5 (July-August 1971)

FAUCHER, G. A., and MORRISSEY, J. F.
Atmospheric Density Measurements in the 70-115 km Region
J. of Geophys. Res., Vol. 76, No. 18 (20 June 1971)

HERZBERG, A. F., CAPT.

Efficient Trajectory Modeling for Rocket/Moving Target Spatial Relationships
J. of Spacecraft & Rockets, Vol. 8, No. 8 (August 1971)

PAPERS PRESENTED AT MEETINGS JULY 1970 - JUNE 1972

CARTEN, A. S., JR.

The Second Symposium on Meteorological Observations and Instrumentation—Its Theme and Its Goals
2nd Symp. on Met. Obsns. and Instmn. (AMS), San Diego, Calif. (27-30 March 1972)

CARTEN, A. S., JR., and PAULSEN, W. H.

Development of Airborne Remote CAT Detection Equipment
Intl. Conf. on Atm. Turb., London Eng. (18-21 May 1971)

DOHERTY, F. X.

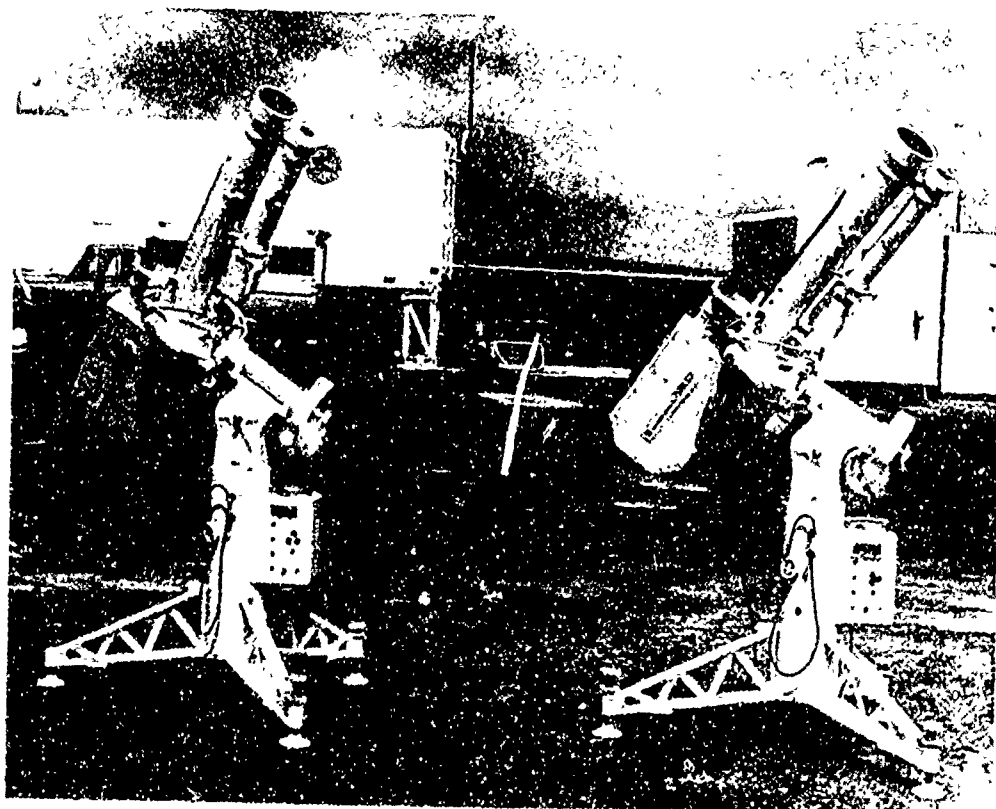
Development of a High Altitude Blast Generation System (Invited Paper)
2nd DASA Conf. on Mil. Appl. of Blast Simulators, Nav. Weap. Lab., Dahlgren, Va. (2-5 November 1970)

HERZBERG, A. F., CAPT.

Trajectory Modeling for Efficient Computation of Rocket/Moving Target Spatial Relationships
AIAA Sec. Sounding Rocket Vehicle Tech. Conf., Williamsburg, Va. (7-8 December 1970)

TECHNICAL REPORTS JULY 1970 - JUNE 1972

GRASS, L. A., ED.
Proceedings, Sixth AFCLR Scientific Balloon Symposium
AFCLR-70-0543 (27 October 1970)



Side-by-side tests with these matched telescopes have demonstrated the feasibility of obtaining standardized solar optical data.

V Space Physics Laboratory



The Air Force is active in space today, and expects to increase its operations in space in the future. The Space Physics Laboratory conducts research on the near-earth space environment and on energy conversion as applied to space missions. Most of the research is directed toward predicting variations in solar emissions, especially the development of solar flares, and studies of propagation mechanisms for solar emitted particles and the solar wind, magnetospheric phenomena involving particles and fields, and the precipitation of such particles into the ionosphere. The other portion of the Laboratory's program is the search for more efficient methods of converting energy, primarily the sun's radiant energy, into electrical power. Organic materials are studied for possible application to solar cells and the development of high energy density, lightweight batteries, and plasmas are studied for application to energy converting devices.

The research is conducted through Laboratory experimentation, through ground-based observations, and through rocket- and satellite-borne observations.

SPACE FORECASTING

The Space Forecasting Program was initiated at AFCRL in the mid-1960's to predict solar-related changes in the earth's upper atmosphere and near-space environment that have an influence on Air Force operations. It is an interdisciplinary program which draws on most of the environmental sciences—radio and optical solar

astronomy, astrophysics, radio propagation physics, and the physics and chemistry of the upper atmosphere. Its very nature requires participation by specialists in a variety of technical fields, such as energetic particles, ionospheric physics, solar physics, geomagnetism and atmospheric density.

The Space Physics Laboratory was chosen to organize, coordinate, and direct the efforts of the various contributing scientists. Because of the broad scope of the program, scientists from several of the other laboratories of AFTRL, as well as from the Space Physics Laboratory, participate.

From its inception, the Space Forecasting Program has attempted to focus strongly on the operational problems related to changing environmental conditions. To provide a convenient mechanism for coordinating the efforts of 12 to 15 scientists, with the everyday operational problems of Air Weather Service (AWS) Duty Forecasters, the Space Forecasting Workshop was established in 1966. This group, which meets four times a year, provides an ideal forum for exchanging technical information, for coupling research products with operational requirements, and for directing and coordinating the efforts of in-house scientists and contractors working in a broad spectrum of related scientific disciplines.

Space forecasters must predict the occurrence of bursts of electromagnetic radiation and energetic particles from the sun, and specify the effects of these bursts on the earth's atmosphere. These effects include absorption of radio waves in the ionosphere, geomagnetic disturbances, auroral activity, enhanced airglow levels, and atmospheric density variations. Present and projected systems such as radars, surveillance satellites, radio communications and navigation systems are all affected in varying degree by these atmospheric effects, and advance knowledge of the ex-

pected degradation of operational systems would greatly benefit the Air Force.

The most important cause of these problems is the solar flare. Since the bursts of electromagnetic energy and high energy particles from the sun are associated with solar flares, techniques for forecasting the occurrence of these flares must be developed. Related to this basic consideration are two other problems: that of predicting whether the intense flux of electromagnetic radiation and particles emitted by the flare will or will not produce near-earth effects such as magnetic storms, auroras, ionospheric disturbances, etc.; and given a geophysically significant flare, predicting the magnitude of the near-earth effect, its onset, and its duration.

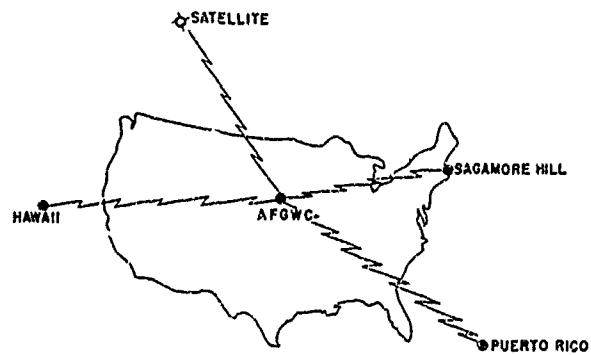
Making these predictions requires observation and measurement of the changing dynamic features in the observable solar atmosphere. These include optical, radio, and magnetic field observations. Solar data collected and recorded in past years by observatories all over the world have been obtained and have proved to be of value in developing forecasting techniques. To utilize these techniques and to study the characteristics on the visible solar surface that portend a flare, real-time world-wide observations are required.

A world-wide network of observatories was established in 1967 to provide continuous coverage of the sun. Optical and radio sites were placed in Tehran, Iran; Puerto Rico; Hawaii, and the Philippines. The decision was made in 1972 to develop a second generation solar optical observation system. A pre-production optical system is being developed which will enable the Air Force to assess what design goals can be achieved and to define the final system more clearly. New capabilities such as solar magnetic field measurements will be incorporated into this system and a strong emphasis will be placed on the standardization and automation of data collection. A matched pair of solar optical telescope-

videometer systems has been developed in an attempt to reduce to a tolerable level the differences in present solar flare measurements. Side-by-side tests have produced excellent measurements with a discrepancy of less than 6 percent in the measured area of a solar flare. It is planned to operate these systems at the various AWS observing sites to intercalibrate them and to develop standardized techniques for measuring solar parameters. Also, an effort is being made to upgrade the solar radio instrumentation at the various sites. Again, the observations will be standardized and a high level of accuracy will be maintained at all sites. The measurements made at the Sagamore Hill site, in Hamilton, Mass. will be used as the norm and AFCRL will monitor all solar radio data for conformity with these standards.

One current study in the solar radio area is the generation of maps at three different radio frequencies: 3 mm, 8.6 mm and 9 cm. With these measurements as the basis, a three-dimensional representation of the solar atmosphere will be constructed in an effort to obtain an understanding of how the solar flare process varies with height.

A complex of Univac 1108 computers, which serves as the central collection point for all world-wide solar-geophysical observations, is situated at Offutt Air Force Base in Omaha, Nebraska. These computers are linked in real time to the world-wide network of optical, radio, and ionospheric observatories. Observable radio and optical features of the sun are fed directly into this network, as well as observations from riometers, neutron monitors, ionosondes, magnetometers and satellites. The basic purpose of this program is to specify the solar and geophysical conditions that precede a burst of solar energy and to determine the terrestrial effects that follow the burst. This is analogous to the meteorological observations that are made throughout the world 24 hours a day.



AFGWC serves as the central collection, processing and dissemination point for solar-geophysical data measured by satellites as well as ground-based observatories located around the globe.

AFCRL scientists have written more than 20 data-processing programs for these computers to handle the continuous data stream, and special emphasis has been placed on improving the quality of the data through comprehensive error-checking routines. In addition to the data resulting from ground-based measurements, large numbers of satellite observations are also collected in real time, sorted, error checked, tabulated and analyzed. One example of this is the Vela X-ray program. This program has been written to accept X-ray data from several Vela satellites, and, after analysis, to provide values of the absolute X-ray flux as a function of time. Programs have also been written to process both the ground-based and the Vela satellite neutron monitor data, the Vela solar wind data and the solar particle data. These programs have been delivered to Air Force Global Weather Center (AFGWC) and have been integrated into the real-time system for operational use.

To enhance our understanding of the physical mechanism of proton-induced disturbances, the Vela proton data resulting from the real-time analysis is being utilized.

lized to analyze several unusual proton events. An attempt will be made to construct a computer model for the release of low-energy protons from solar flares, and then to predict their subsequent effect on the earth's magnetic environment.

Plans have been formulated for installing a highly sensitive, ground-based magnetometer network across the United States at a constant magnetic latitude. The purpose of this network is to monitor micropulsations of geomagnetic activity very accurately. The data collected will be used to produce short-range prediction techniques relating solar wind parameters to magnetospheric phenomena.

A study designed to test the feasibility of generating ionospheric maps from a sparse network of ionosondes in North America has been completed. This study has been instrumental in developing very valuable techniques for ionospheric forecasting as well as providing quantitative data for evaluating the increase in forecasting capability achievable with additional ionosonde stations. An ionospheric network analysis has also been performed in which the cross correlations between all pairs of stations were calculated. From these correlations a series of tables will be prepared that will provide predictions of foF₂ at any location one to six hours in advance. This is accomplished by looking up the present values at another station that has been shown to be most highly correlated for that specific time, solar activity index, and magnetic condition.

Efforts to develop improved analytical techniques for the prediction of solar radiations and their effects on the near-earth environment are continuing. A comprehensive solar-geophysical data base has been developed covering the period 1955 through 1969. Utilizing this data base, a series of statistical analyses have been performed to identify the most useful solar flare predictors and to combine these predictors into flare prediction equations.



A variety of computer programs written at AFCRL are being integrated into the AFGWC computer system to process the flood of solar-geophysical data.

Currently, solar X-ray data are being carefully analyzed. X-ray data from the satellites SOLRAD 9 (1-8 Angstroms) and Explorers 33 and 35 (2-12 Angstroms) have been acquired covering an extensive period of time. The Explorer data have been correlated with solar optical flares and hence have become part of the overall data base. These data will now be used to develop techniques to predict flares and their geophysical effects. The SOLRAD 9 data have been analyzed by means of a special computer program and the parameters of the bursts have been determined. These bursts will be associated with the 2-12 Angstrom bursts and relationships between the two sets of data will be developed for eventual use in forecasting techniques.

It is interesting to note that VLF radio data may be operationally useful as an early detector of X-ray flares. Preliminary studies indicate that the characteristics of an X-ray burst can be estimated within the first four minutes of the event. A study is presently in progress (1972) to examine

one year's VLF data in an effort to establish a procedure for systematically determining the X-ray burst characteristics from the VLF signatures.

In addition to flare forecasting technique development, a longer term type of forecasting research program has been initiated that approaches the problem from a more subtle and rigorous point of view. Theoretical-and-computational research on the interplanetary propagation of solar flare-related charged particle radiation has been instituted. Suitably realistic mathematical models are used to investigate the effects of various physical processes known to be present in the interplanetary medium on the sun-earth transport of both prompt and delayed flare particle distributions. These processes include adiabatic deceleration, Fermi acceleration, and co-rotation of magnetic sector boundaries. This research, which will contribute to a better understanding of such phenomena as Polar Cap Absorption and geomagnetic storm events, is necessary before accurate prediction techniques can be formulated.

A model of auroral activity is presently being developed. Low energy corpuscles continuously emitted by the sun maintain the aurora in the well known oval configuration, centered on the geomagnetic pole and rotating in a manner dependent on the sun-earth relationship. Utilizing this model, techniques have been constructed to predict the varying effect of the aurora on propagation paths through the polar ionosphere as a function of frequency and path geometry.

RESEARCH ON SOLAR DYNAMICS

X-ray and ultraviolet emissions from the sun are highly variable in time. The emission of particulate matter is also variable in time. These variable emissions are produced in conjunction with centers of activ-

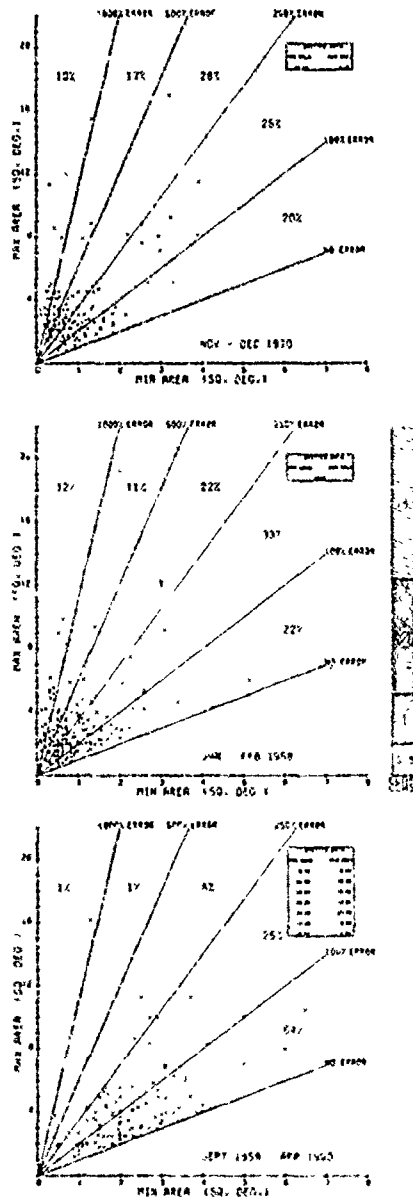
ity which rotate with the solar surface but which develop and decay over periods of days or weeks. The emissions produce many effects in the upper terrestrial atmosphere, on the terrestrial magnetic field, and in the surrounding space.

Attempts to forecast near-earth variations ultimately depend on a knowledge of the processes which cause these solar regions to develop and decay and on an understanding of the mechanisms which transfer the energy into and through space. Work in solar plasma dynamics falls into three categories: understanding the development and decay of the solar regions, determining mechanisms for the emissions and radiation from these regions, and work to develop the calibration constants for solar measurements.

Research is divided into three main areas: The Solar General Circulation; Theoretical Studies of Solar Terrestrial Relations; and Physical Processes in Solar Phenomena. The development and decay of solar active regions is being studied along two lines within the framework of the general circulation task. First and foremost is a long-range program to obtain a homogeneous time series of measurements of the characteristic life cycles of the regions. Allied with this is a comprehensive study of the energy processes of the large-scale solar circulation and its relation to the life cycles of the active regions.

SOLAR ACTIVE REGIONS: The study of active region life cycles appears at first to be a straightforward collection of the various data in the literature, and an analysis of them. There is, for example, a century of data describing sunspot characteristics and their changes. Flare data extend back for four decades, and more data were taken in the last ten years than in the previous thirty.

Radio emission characteristic data has been collected for less than two decades. Data concerning many other characteris-



Illustrative of the uncertainties in flare data is the maximum and minimum areas reported for each confirmed (two or more observatories reporting) flare, during three sample periods. The maximum and minimum areas are plotted as ordinate and abscissa respectively and percent error is defined as the (maximum error minus the minimum area) divided by the minimum area.

tics of the regions extend back over varying periods of time and include the entire range of quality and quantity. The most recent measurements of these regions are being collected from satellites, and while these are of very high quality, unfortunately they cover only the most recent few years.

As an example of the variable quality and quantity of one of the vital parameters used to measure activity, the area of a flare, which would seem to be a straightforward and easily measured quantity, can have an error in excess of 1000 percent.

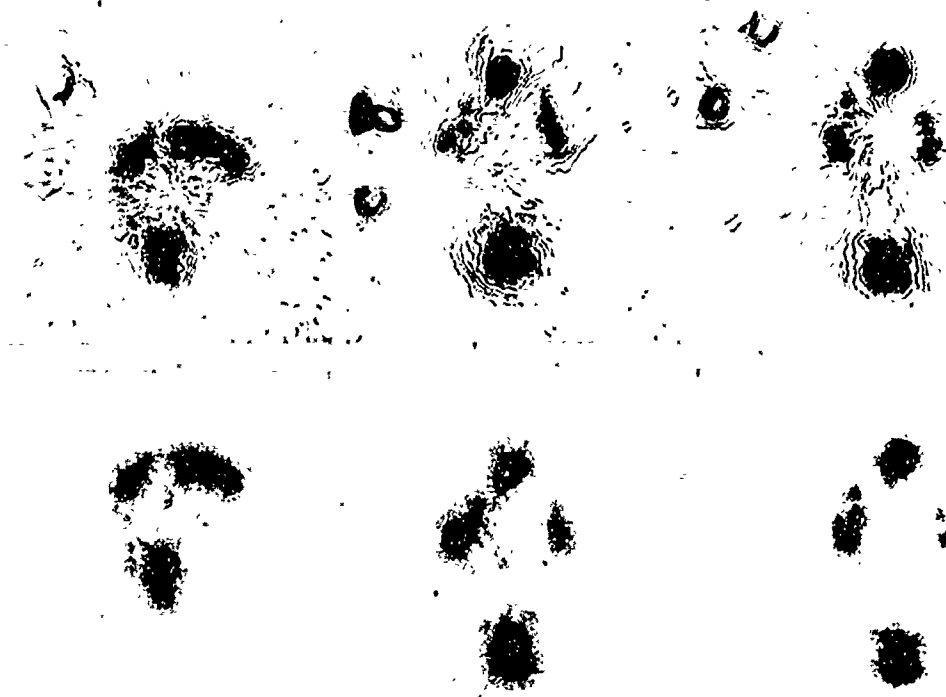
The construction of the life history of any one active region requires careful selection and analysis from this vast library of data. Many single examples of such life histories have been published in the literature. These examples, however, are invariably extreme cases, either in the amount of their activity or the extent of their peculiarity. The value of such examples to the problem of forecasting solar activity is questionable unless one is concerned with forecasting the decay of active regions once it is established that they are extreme or peculiar. Forecasting if and how incipient or tiny solar regions will develop depends on an analysis of the life history of a whole range of regions, any one of which may develop to interesting size. From the known spectrum of developmental possibilities an analysis can be made to determine the observable differences in either the behavior of these regions in their early life or the characteristics of the circulations into which they are born.

There have been many descriptions of the characteristic behavior of a single active region parameter (e.g. sunspots) but the limitations of such simple studies come to the fore when attempts are made to utilize them in the complex business of forecasting. Furthermore, the forecaster finds himself using information from more than one such simple study and these stud-

ies characteristically produce conflicting trends. Since it has yet to be proved that there is one parameter which describes the essence of a solar region or its future development, such analyses must include the behavior of the total variety of possible measurements. It might very well be that the seemingly contradictory time be-

havior of the different measurements of individual regions contains the information which is necessary to distinguish the future development of the region and hence yields the forecasting scheme.

It is much easier to describe the necessary analytical steps than to carry them out. The execution requires a carefully



The white light photograph and corresponding isodensometric trace for three different stages of a sunspot group are shown. The closed contours of the tracings are areas of constant photographic density, which is directly related to the temperature of the spot. The number of contours is a measure of the variation of the spot temperature. The outermost contour defines the extent of the spot group enabling a more precise area determination. Recently, the isodensitometer output has been digitized and interfaced with a computer which will enhance the reliability of the measurements and increase the number of sunspots handled.

standardized series of measurements of the individual parameters and objective procedures of collating these parameters into a time series of comprehensive active region descriptions. Both of these steps are extremely difficult. Over the past two years considerable progress in constructing a foundation of sunspot measurements on which to build the entire active region structure has been made in the Space Physics Laboratory. A time series of event data including flares, plages, short-wave fadeouts, radio flux measurements, and sunspot magnetic classifications has also been made. An attempt has been made to introduce a new parameter describing the integrated light deficit of sunspots to avoid the difficulties commonly associated with the measurement of sunspot umbrae and penumbrae. While this study is in its early stages, some interesting preliminary results have been obtained:

The data appear to indicate that more spots are born in the eastern half of the visible disk than on the western half. In addition, spots born on the back of the sun appear to reach a larger size than those born on the front. However, these variations are probably the result of viewing the solar surface from the earth and are not real variations in the spots themselves. These observationally induced anomalies are being removed to insure accurate region histories.

RADIO BURSTS: A major in-house theoretical effort is to investigate plasma radiation processes occurring in solar flares and/or radio bursts. The run-away or supra-thermal electrons and protons produced by lower chromospheric flares interact with the coronal plasma to produce Cerenkov plasma waves.

The phase velocity of the plasma waves emitted by this process always falls between the stream velocity and the ion thermal velocity. However, as the phase velocity approaches the ion thermal velo-

city, the emitted wave intensity increases while the damping decreases. As a result, weakly damped large amplitude and long plasma waves can propagate in the corona creating a large number of pockets in which the number of electrons and protons fluctuate as the wave progresses.

These conditions continue as long as the supra-thermal beam of electrons and/or protons persists. The slow fluctuation of ion number density from these pockets scatters the progressive plasma waves at their own frequency, changing them into electromagnetic radiation. This is the Rayleigh scattering process. On the other hand, the electron density fluctuations from these pockets (which far exceed the ion density fluctuations) scatter the plasma waves at frequencies combining (sum and difference) those of the incident plasma waves and the electron current density fluctuation. The simplest combination of frequencies in the radiation is the Raman scattering process.

Other combinations of radiation frequency involving higher harmonics of the fundamental plasma frequency are also excited, but their intensity is too low to be detectable. On the other hand, the occurrence of very high harmonics is forbidden by the energy conservation in the scattering process. This actually depends on the energy flux of the incident plasma waves and on the density fluctuation called "power spectrum of the radio noise." However, only a small fraction of the plasma wave energy is transformed into electromagnetic radiant energy by the scattering processes. Since there are large numbers of pockets, or small bubbles all simultaneously scattering plasma waves into radio frequency radiation, it is possible, under certain favorable conditions, that a very high intensity of radio waves could be generated. These waves are the solar radio bursts and their harmonics. It is postulated that the electric fields of the large amplitude plasma waves accelerate stochastically

flare-induced particles resulting in proton events which adversely affect Air Force communication and ground-based radio systems.

SOLAR FLARES: Another theoretical effort is concerned with the production of solar flares. The solar atmosphere is only partially ionized in the photosphere and in sunspots, while it is fully ionized elsewhere. In the photosphere and particularly in the vicinity of sunspots, the lack of ionization allows relative motion between the fluid and the magnetic field producing dynamo currents. Material flowing horizontally out of spots (Evershed effect) interacting with the vertical spot field should produce a circular current system around the spot. When these circular current systems (known as Hall currents) exceed a certain critical value, determined from the condition for two-stream instability, there will be a sudden release of energy in the form of Joule heating. Currents below the critical level may be responsible for the plage areas.

Advantages of this theory are: Sufficient convective energy and Joule dissipation is available to produce the largest observed flares; the close association of sunspots and flares is accounted for; production of runaway electrons and protons (by photospheric electric fields conducted upward along magnetic field lines) which in turn are able to produce X-rays in the upper chromosphere and cosmic rays at inner coronal heights; the same photospheric electric field conducted upward, coupled with the chromospheric magnetic field can produce a motor action resulting in possible surge prominence motion of 100 km per second as observed; a similar motor action in the corona may account for observed shocks of 1000 km per second, and, the enhanced hydrogen alpha emission identified with optical flares is explained qualitatively.

Physical processes in solar phenomena

are being determined by the direct measurement of basic atomic and molecular parameters.

ABSOLUTE F-VALUES: Absolute transition probabilities (f-values) are one example of an atomic parameter which has wide applications for determining species concentrations and temperatures in plasma diagnostics and solar and stellar abundances in astrophysics. The pressure-driven shock tube is a preferred thermal light source for f-value measurements since the shock-heated gas is in a well defined equilibrium state over a wide range of controllable operating conditions and uniform in the line of sight.

The AFCRL shock tube has been used to produce gas samples which are hot enough to emit atomic and molecular spectra of astrophysical interest. The gas in the driven (test) section of the tube contains argon or neon carrier gas to which has been added a trace of the gas to be investigated. The driver gas is helium at pressures of several hundred psi. Temperatures achieved behind the reflected shock are



The shock tube laboratory where f-value measurements are being obtained.

varied between 3,000 and 10,000 degrees K. Spectral radiation by atoms, ions, and molecules is recorded photographically and photoelectrically from steady states of known population in local thermodynamic equilibrium. The observed spectral intensities are correlated with the directly measured thermodynamic state of the gas (temperature, pressure, concentration) to allow determination of the absolute f-values for the spectral transitions.

Subsequent applications of these f-values are often found in astrophysics, i. e., the experimental values are used to determine abundances of elements observed in solar or stellar spectra. Space Physics Laboratory measurements of Cr and Fe f-values have resolved the paradox of the iron group elements being deficient by an order of magnitude in the solar photosphere relative to the corona and meteorites.

Additional applications include the use of a set of known f-values to infer plasma characteristics from the observed line intensities generated by manmade plasmas such as nuclear detonations, fireballs, and debris clouds, reentry sheaths and wakes, and chemical releases.

Sunspots are little understood regions in which a very critical balance of temperature and pressure determines whether elements will exist as atoms or molecules, for example, as Ti or TiO. Accurate f-values are needed to analyze new sunspot spectroscopic studies to derive accurate temperatures as a first step in deriving realistic sunspot models. With this in mind, absolute f-values for 90 Ti and 10 Ti II lines have been determined. TiO f-values are being measured.

ENERGETIC PARTICLE RESEARCH

Energetic particle fluxes place limitations on space operations. Also, they deposit

energy in the earth's atmosphere, ionizing and heating the ambient gases, particularly at high latitudes. This degrades, and sometimes inhibits, the operation of systems which involve the long distance propagation of electromagnetic radiation such as communications, detection, tracking and surveillance systems, or those which require knowledge of the drag effects produced by the ambient atmosphere.

Energetic particles include charged and uncharged particles. The significant fluxes of charged particles consist of electrons, protons, and occasionally alpha particles. Various other atomic nuclei provide much smaller fluxes. Particles with energy less than 100 keV cannot penetrate a significant thickness of material to cause direct effects, but they may be indicative of the behavior of higher energy particles. Flux intensity decreases rapidly with energy so that the total energy of the flux above a few hundred MeV is negligible although individual particles may be severely damaging. Thus, primary interest is devoted to electrons and protons with energies from 0.1 to 100 MeV. Alpha particles in this energy range are also of interest. Although the alpha intensity is usually much less than that of protons, it is still of sufficient magnitude for accurate measurement. The ratio of alpha to proton fluxes may be significant in analyzing and forecasting solar effects. Hydrogen and helium isotopes and heavier nuclei, as well as strange particles, are of environmental interest to the extent that study of these particles yields information on the production, propagation and interaction of the particles of primary interest. Human cells and ultra-miniature electronic components are two examples of systems which are vulnerable to the severe localized damage caused by high energy heavy nuclei.

SOLAR ENERGETIC PARTICLES: Most energetic particle fluxes originate at the sun. Galactic sources, outside the solar system,

contribute a background flux. Both of these particle fluxes create secondary reaction products when they interact with the earth's atmosphere. Time variations in the outflow of solar particle fluxes and fields modulate the influx of galactic particles. The production of secondary particles in the atmosphere depends on the intensity, energy and species of the incident flux. Thus, solar activity, and particularly the 11-year solar cycle, regulates the temporal variations in all particle fluxes.

The sun emits high energy particles irregularly during solar proton events. The enhanced fluxes from such events reach earth orbit within hours and persist for a day or more.

The evaluation of these solar events and their effects on the near-earth radiation environment requires the correlation of various data taken during a particular event and of data from various events. Such correlations cannot be performed unless the size of the event is defined on a quantitative, standardized scale. The Space Physics Laboratory has developed a quantitative classification system which has been accepted as the international standard by the IUCSTP (Inter-Union Commission on Solar-Terrestrial Physics) and COSPAR.

The system classifies a solar event with a three-digit index. The first digit represents the flux of protons with energy of more than 10 MeV as measured by a satellite within the earth-moon system. The second digit represents the 30 MHz absorption as measured by a sunlit riometer, i. e., a riometer on the day side of the earth. The third digit represents the response of a sea level neutron monitor at high latitude. The system provides a positive index for an event measurable at ground level, a zero index for an event of no significant geophysical effect (such as a PCA), and a negative index for particle fluxes so small as to be unmeasurable with ground-based equipment. The required data are usually

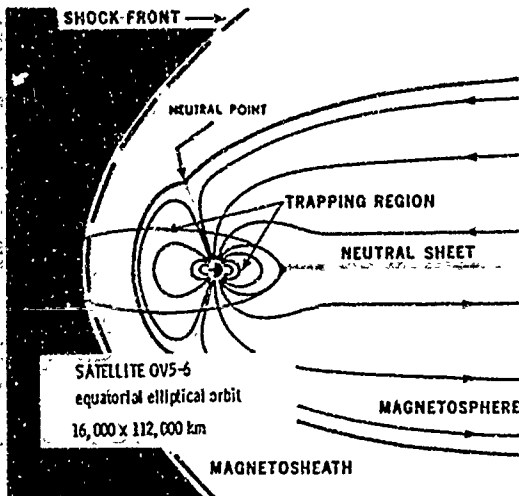
available rather quickly during an event and are not dependent on sophisticated interpretation of other types of geophysical measurements.

The Space Physics Laboratory is now preparing a complete catalog of solar proton events, using this system.

SOLAR PARTICLE MEASUREMENTS: Computer programs have been prepared and delivered to the Air Weather Service for the detection, evaluation and extrapolation of the solar proton event profiles based on data from ground and satellite detectors. These routines automatically identify significant fluctuations in the near-earth particle flux and prepare displays of appropriate data for the AWS Solar Forecast Facility. Data processing includes basic error checking and removal of erroneous points, indexing of data, and the computation of ten-minute, hourly, and daily averages. The event maximum is detected even in the presence of complex sub-structure. The rate of decay of the event is determined and the end of the event predicted. This prediction is periodically updated. The programs have been specifically designed to operate correctly, although with decreased accuracy, even if the data supplied are incomplete.

A realistic inclusive model for propagation of particles, after their initial acceleration during the event, has been developed in a form suitable for numerical solution. The model is in qualitative accord with known phenomena and experimentally determined parameters. The model was specifically tested for flare particle propagation under a variety of solar boundary conditions. It was found that for most times of interest, the choice of boundary condition does not significantly alter the flux intensity versus time results in interplanetary space, aside from a constant factor.

The interplanetary magnetic field is a stochastic field which extends outward



Satellite OV5-6 travels in an elliptical orbit $12,000 \times 75,000$ kilometers monitoring particle fluxes within and without the magnetosphere. These results obtained from this vehicle provide insight into the mechanisms of particle propagation from interplanetary space through the magnetosphere to the earth's atmosphere. This insight will be used to develop real-time systems to monitor solar particle fluxes and to predict their effect on sensitive Air Force systems.

from the sun in the average form of an Archimedean spiral. This field controls not only the outward flow of solar particles but also the inward flow of galactic particles. The radial gradient in the flux of inward flowing particles in the energy range from 50 to 200 MeV was calculated using a slightly modified form of the assumed propagation model. These theoretical results were compared to experimental measurements, onboard Mariner 4, of the energy dependent flux gradient between earth and Mars to demonstrate the validity of the theoretical model.

Satellite OV5-6, a small octahedral satellite measuring 11 inches on each side, was placed in a highly elliptical $12,000 \times 75,000$ km orbit in May 1969 and has transmitted useful information continuously since that time. It carries instruments to measure electrons, protons, alpha par-

ticles, and X-rays and gamma rays through and out of the magnetosphere. The solar fluxes monitored by these instruments have been correlated with polar observations of ionospheric and atmospheric perturbations by other laboratories of AFCRL and SAMSO. These results are being applied to the problem of predicting atmospheric and ionospheric conditions from real-time observations of solar fluxes. The excellent results obtained from this satellite far exceeded the greatest hopes for it.

The major geomagnetic storm of March 8, 1970, was analyzed using data from this satellite. This event was accorded exceptionally widespread coverage due to the eclipse of March 7. The OV5-6 data for protons and alpha particles shows a slow rise in both fluxes to a maximum of about 3×10^2 larger than ambient. The alpha to proton ratio at 6.6 MeV/nucleon remained at a constant value of 0.015. The proton spectrum had an energy dependence of about $E^{-2.4}$.

Because Polar Cap Absorption measurements by other AFCRL Laboratories were available for correlative analysis, the event of November 2, 1969, was also analyzed. In this event, the particle fluxes rose rapidly. The maximum alpha to proton ratio at 6.6 MeV/nucleon was 0.07. The proton spectrum had an energy dependence of about $E^{-1.8}$, harder than the March 8, 1970 event. These observations were compared to VLF measurements and other satellite (SAMSO satellite OV1-19) measurements taken at lower altitude over the poles. It was found that the electrons reach the Polar Cap less than a minute after their arrival at earth orbit. This implies nearly direct access of electrons to the Polar Cap without an extended entry path through the magnetospheric tail.

On the basis of these results, other events are now being analyzed. Particular emphasis is being given to the use of alpha

to proton ratios to predict physical phenomena of interest.

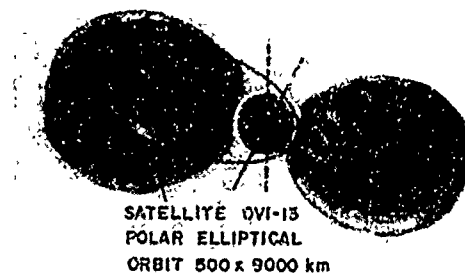
PARTICLE-MAGNETIC FIELD INTERACTIONS: The geomagnetic field allows energetic charged particles to reach the earth only over limited regions, the extent of these regions being determined by the rigidity—that is, the momentum of the particle. For example, protons with energies of ~ 10 MeV are able to penetrate to the earth only over the Polar Caps, while 18 GeV protons can be vertically incident at the surface anywhere. In principle, at least, access regions for particles with specific rigidities can be determined. The quantity used to describe the limit of particle accessibility is called the geomagnetic cutoff rigidity. For some time, a program has been conducted in the Space Physics Laboratory to calculate the cutoff rigidities by numerically calculating particle trajectories through theoretical models of the geomagnetic field. The current work particularly concerns the access of solar particles to the Polar Caps.

Particle trajectory calculations have also been used to calculate the direct access of particles from the interplanetary medium to the orbit of a satellite. This involved calculating, for each hour of the day, the possible trajectories of particles from the position of a synchronous orbit satellite through the magnetosphere to the interplanetary medium. It required the calculation of the geomagnetic cutoff rigidities and their daily variation in the vertical and west directions in a model magnetosphere. Evaluation of these results produced a means to distinguish, experimentally, whether solar particles measured by satellites in the magnetosphere arrived at their detection point directly or by a diffusive mode of propagation. If the propagation is diffusive, then the intensity at a pitch angle of 90 degrees to the magnetic field direction will be independent of azimuth. However, if the particles arrive di-

rectly, then geomagnetic cutoff effects will cause intensity differences, at a pitch angle of 90 degrees to the magnetic field lines, between particle fluxes arriving vertically, from the east, and from the west.

The magnetic poles are several hundred kilometers from the rotational poles. Therefore, magnetic coordinates are considerably displaced from the usual geographic coordinates. Magnetic field lines diverge from the earth's Southern (magnetic) Hemisphere. Near the pole these magnetic lines may be swept back into the magnetospheric tail or otherwise dispersed by the continual outward flow of low energy charged particles known as the solar wind. The resulting geometry is complex and not suitable for the long-time retention of charged particles. Below about 60 degrees magnetic latitude, the lines bow out into space, then return to enter the earth at their conjugate point in the opposite hemisphere. This closed geometry traps charged particles.

Coordinates along these lines are nor-



Satellites, such as OV1-13, in elliptical orbits through the trapped radiation region, map the energetic particle environment. Data from these satellites are used to determine source and loss mechanisms to define the time variations of the natural environment. These results are also applicable to determining the perturbation to be expected from high altitude nuclear detonations.

mally given as L , the distance of the line from the magnetic center of the earth at the magnetic equator, and B , the strength of the magnetic field. B has its minimum value, for a given line, at the equator and increases along the line toward the earth as the lines become crowded together forming cusps.

A charged particle on the equator will circle about a magnetic field line as in a cyclotron at a fixed frequency defined by the particle charge and the magnetic field strength. The radius of the circle is defined by the field and the energy of the particle. If the particle moves north or south, it will be guided by the magnetic field in a spiral motion about the line. The pitch angle of this spiral will increase as the field increases until the motion along the line is stopped. At this mirror point, the particle reverses direction, returns to the equator and repeats this motion in the other hemisphere. Due to the outward gradient in the magnetic field, the particles also slowly precess around the earth. These motions, cyclotron, mirroring and precessing, are defined by the conservation of three adiabatic invariants of the motion.

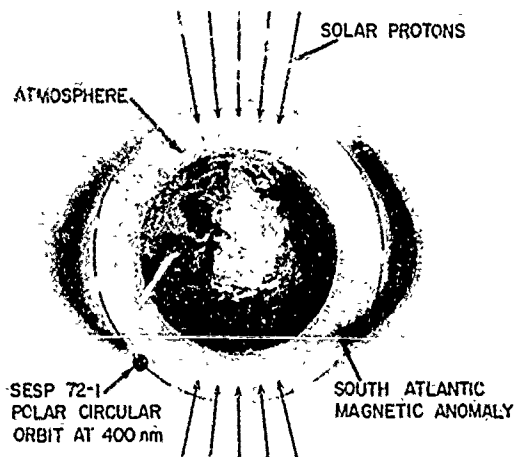
Thus, the earth's field, which is essentially a magnetic bottle, will contain charged particles indefinitely. The exact mechanism by which charges are naturally injected into this trapping region is unknown. Particles may be artificially injected by high altitude nuclear detonations such as the Starfish explosion in 1962. Such a detonation both injects new particles and distorts the magnetic field in such a way as to accelerate ambient low energy particles into the energy range of interest.

The problem is to define source and loss mechanisms as well as redistributive mechanisms. Changes in the flux can then be predicted for any future time based on a current or past observation.

A significant portion of this flux in the inner portion of the trapped region is high energy (> 50 MeV) protons. More than a

complete solar cycle has elapsed since their discovery in the radiation belt in 1959. The experiments and theories can now be evaluated to explain these protons. Since 1961, the trapped proton fluxes have been measured periodically by Space Physics Laboratory scientists with nuclear emulsions exposed in the South Atlantic anomaly on recoverable satellites. More than 50 exposures are now available. During the 1964-1965 period, the 55 MeV proton fluxes were in equilibrium and did not change. Thus, the source and loss terms were equal. Since the loss rate is determined by the known atmospheric density at this time, the magnitude of the source is determined. This source strength can be utilized to predict the expected time variation in trapped proton fluxes. Measured fluxes for 1968 and 1969 showed sharp decreases from previous years. This was due to the increased atmospheric ionization losses during the solar cycle maximum. The increased heating during the maximum of the solar cycle causes the atmospheric density above 200 kilometers to increase. In the regions of interest (a few hundred kilometers altitude), this increase is a factor of 10 or more.

The experimental data thus agree with calculations of proton fluxes based on a constant source and losses which depend on atmospheric density changes induced by solar activity. To fully define the inner zone trapped particles, it is now necessary to determine the source intensity and correlate it with the measurements of the loss processes reported here. Two possible theories to explain the source of these protons are cosmic-ray albedo neutron decay and solar neutron decay. The cosmic-ray albedo neutron decay theory hypothesizes that the protons are the decay products of neutrons ejected back up from the atmosphere after high energy galactic cosmic rays cause nuclear reactions there. The solar neutron decay theory postulates that the protons are the decay product of solar-



Satellites such as S72-1 travel in low circular orbits. They are used to observe solar fluxes which have ready access to the polar regions and vary with solar activity. They are also used to observe fluxes at the inner edge of the trapped region which vary rapidly with latitude, longitude and altitude. These trapped fluxes are particularly intense near certain magnetic field anomalies as in the South Atlantic and near Hawaii. These fluxes interfere with various Air Force missions both as a direct radiation hazard and through their effect on the atmosphere.

emitted neutrons traveling through the region. Both theories depend on the decay of a neutron into a proton and an electron. The half life for this decay is 12 minutes. Because of variations of cosmic-ray protons, the cosmic-ray albedo neutron decay source would vary by 12 percent from its mean over the solar cycle; these variations were neglected. The solar neutron decay source should increase at the peak of the solar cycle. If such an increase occurred, it was negligible. Further work is required to test these source theories.

The energetic electrons which predominate in the outer portion of the trapped region present a different set of problems. Analysis of OV1-13 data has shown that their population increases during the geomagnetic disturbance following a solar storm. Results from satellite OV1-13 indicate that during such an event, electrons diffuse inward across field lines from a

source outside the trapped region. This diffusion conserves the electron's magnetic moment and thus increases their energy. The intensity of the electrons trapped in this way is limited by wave-particle interactions. Above a certain critical flux density, interaction occurs between the electrons and self-generated whistler waves (so named because their frequency-dependent velocity of propagation produces a whistle on radio receivers). These waves accelerate the excess electrons down into the ionosphere in polar regions, causing patches of enhanced ionization. Data obtained from OV1-13 showed that these waves transfer energy from low energy particles on the equator to high energy particles further down the field lines. Electron losses at low altitudes, like proton losses, occur at high mirroring latitudes and small equatorial pitch angles, and are dominated by atmospheric effects. Particle distributions observed on OV1-13 are in good agreement with Jacchia's atmospheric model.

HEAVY NUCLEI: Because they can cause intense localized damage to human cells and ultra-miniature electronic components, heavy nuclei have been the subject of a variety of secondary investigations. Astronauts on the Apollo flights have reported seeing a variety of light flashes in darkened or semi-darkened conditions. Research in the Space Physics Laboratory has shown that many of these flashes are due to Cerenkov radiation produced when heavy, relativistic, cosmic-ray nuclei pass through the retina.

The biological effect of heavy, slow particles in human tissues is not well established. The ionizing power of such particles near the end of their range is believed to be sufficient to destroy the functioning of a sensitive cell with a single hit. The end of track effects for heavy galactic cosmic rays predominate at the level of high altitude flight. Nuclear emulsions have been ear-



In the LAPES experiment, 30 square meters of corpuscular photographic material was carried by balloon to 37 km altitude. In a 21-hour exposure, 57 tracks of relativistic nuclei heavier than iron were recorded confirming the existence of these highly damaging unshieldable radiations.

ried aloft by balloons and exposed to evaluate the magnitude of this threat and to confirm previous calculations on this subject.

In order to detect heavy (charge greater than that of iron) nuclei of relativistic energies at flight altitudes, a balloon flight was made from Holloman Air Force Base in May 1971. Thirty square meters of corpuscular photographic materials were exposed above 37 kilometers for 21 hours and between 29 and 36 kilometers for eight hours. A sliding plate mechanism permitted time discrimination of track detection. Existence of these highly damaging, non-shieldable radiations was thus confirmed.

GEOMAGNETISM

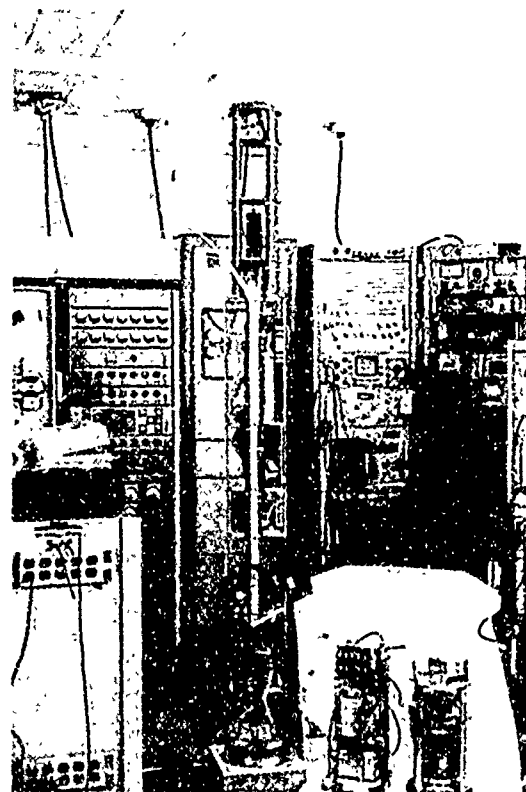
Increased levels of magnetic activity adversely affect communications, navigation, surveillance and detection systems. The

degradation of these functions is especially acute when the area or path of operation is a portion of the polar regions where radio signals are blacked out by substorms and Polar Cap Absorption events. These events have also been known to produce spurious signals capable of generating false alarms. The maximum and minimum useable frequencies of a high frequency communications network are dependent on the magnetic activity and advance assignment of a given channel requires a knowledge of the expected activity levels. Magnetic compasses become less useful at higher latitudes and of no value in polar regions during periods of high activity. The detection of high altitude nuclear detonations is also made more difficult. Aeromagnetic detection systems, perimeter safeguards and other magnetic devices must be operated at reduced sensitivity when their detection bandwidth corresponds to the natural frequency components of magnetic disturbances. Another example of the effects of geomagnetic activity that should be noted is the variation in atmospheric drag experienced by artificial satellites which is related to enhanced levels of activity. As a consequence, the orbital parameters of the satellites can be changed significantly, thus changing the predicted position of the satellite as a function of time.

Scientists in the Space Physics Laboratory undertake relevant measurements of particles and fields to construct and verify a model of the coupled earth-ionospheric-magnetosphere-solar wind system, and to use the model and the various data collected to develop techniques for predicting magnetic activity. A valid prediction system, giving advance warning of increases in magnetic activity levels will then permit the optimization of the various Air Force functions most likely to be affected.

MAGNETIC STORM RESEARCH: During the reporting period, two rockets were

launched at the Churchill Research Range, Canada, into a very intense magnetospheric substorm. The X-component of the magnetic ground station went to -1150 gammas and the 5577 Angstrom photometer showed the intensity of the aurora to be greater than 100 kilorayleighs. These rockets carried alkali-vapor magnetometers, aspect magnetometers and electron-proton detectors. The purpose of the experiments was to measure particle energies, fluxes and pitch angles during the most intense phase of the substorm. Of particular interest is the height, extent, intensity and composition of the current system associated with the substorm. These rockets were launched 80 seconds apart in order to



Payload for the measurement of component magnetic fields and charged particles within an auroral disturbance showing main instrumentation section, telemetry package, and gyro attitude reference system.

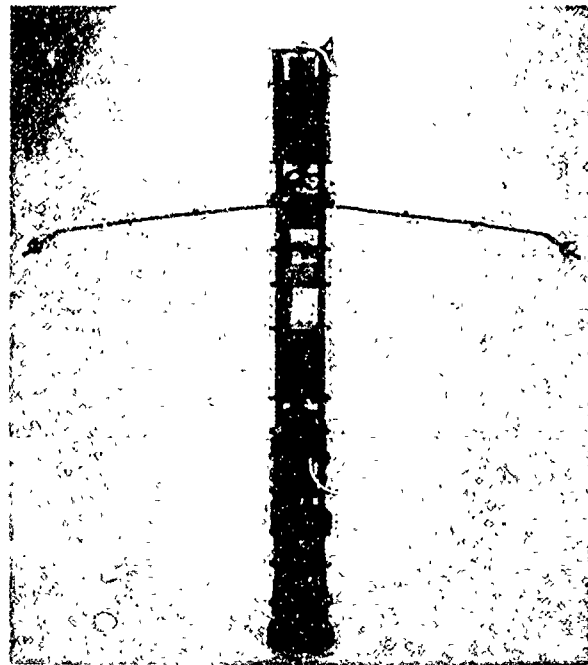
study the spatial and temporal characteristics of the disturbance.

Data from past launches through June 1970 have been completely reduced and analyzed. They show that the electrojet current system is more complex than a single line current. Either a sheet current, or multiple line currents, or both are present (at different times). Particle data show that the electron spectra in an intense substorm may be composed of two components. One, an intense, low energy (6-10 keV) component which rises slowly to peak intensity and falls off rapidly, has an intensity proportional to its peak energy. The second component has a lower intensity (by several orders of magnitude) and has a flat spectrum, thus indicating the possibility of more than one source for these auroral electrons. In addition, one flight indicated that the proton flux increased as the rocket passed over the current. Further investigation of this phenomenon is needed, but it would indicate that protons may be associated with the electrojet, and electrons with the aurora.

To complement the rocket study of the electrojet current, a ground station experiment has been developed and is in use. It employs the three-axis fluxgate magnetometer data from the Churchill Auroral Observatory, and also data from two ground stations each consisting of a portable three-axis magnetometer. One ground station is 250 kilometers south of Ft. Churchill, the other 250 kilometers north. The three stations send in X-, Y-, and Z-component data each minute to a computer programmed to determine the height, intensity, position relative to the Auroral Observatory, orientation and motion of the electrojet current. These results, coupled with descriptions of the visible aurora, aid in determining the optimum launch time and are also used to interpret the rocket magnetic field and particle data.

Two Nike Tomahawk sounding rocket payloads were launched 70 seconds apart

on May 1, 1972 into a magnetospheric substorm. The X-component of the magnetic ground station went to -450 gammas and the 5577 Angstrom photometer showed the auroral intensity to be about 40 kilorayleighs. This disturbance moved from the south and into the predicted rocket trajectories. The first payload was designed to measure field-aligned currents which are considered to be an integral part of a three-dimensional current system associated with polar substorms since they provide a means of transferring the driving potential for the auroral electrojet down to the ionosphere from a source region deep in the magnetosphere. The field-aligned currents can be detected by the magnetic field they create, which will be normal to the much larger ambient geomagnetic field. This requires an accurate vector measurement of the magnetic field which is made with a triaxial fluxgate magnetometer used in conjunction with an automatic ranging current source incrementally biasing out the major portion of the background magnetic field in 127 discrete steps of 1000 gammas each. This gives high resolution to the magnetic field measurement without limiting the dynamic range. Additional instruments included a digital-output gyroscope capable of an angular resolution of 0.3 degree to determine the absolute attitude of the magnetometer axes in space relative to an earth-centered coordinate system; an electrostatic analyzer to detect the flux and energy spectrum of electrons with energies from 0 to 20 keV that are typically found precipitating down magnetic field lines above the auroral zone; a photometer, sensitive to the 3914 Angstrom line of the aurora, which is used to determine the position of the aurora relative to the rocket; a rubidium magnetometer to provide a near-absolute value of the total intensity of the ambient field, and two coarse magnetic aspect sensors mounted along and transverse to the rocket axis. Special pre-



Tomahawk sounding rocket payload with electric field sensors in extended position.

cautions were required to maintain "magnetic cleanliness" of the payload, including a non-conducting nose cone over the forward section to reduce eddy current effects at the magnetometer position. A despin mechanism was required to lower the rocket roll rate so that the transverse magnetometer could "track" the ambient field.

The second payload was designed to measure charged particle fluxes and energy spectra, magnetic field perturbations and quasi-stationary electric fields during a substorm. A proton electrostatic analyzer and an electron electrostatic analyzer measured the fluxes and energy spectra of these particles in the energy range of 1 to 16 keV; a scintillation detector measured electrons in the range of 16 to 200 keV; a rubidium magnetometer measured the total intensity of the magnetic field from which perturbations can be determined; and a high-impedance differential voltmeter with a high common-mode rejection

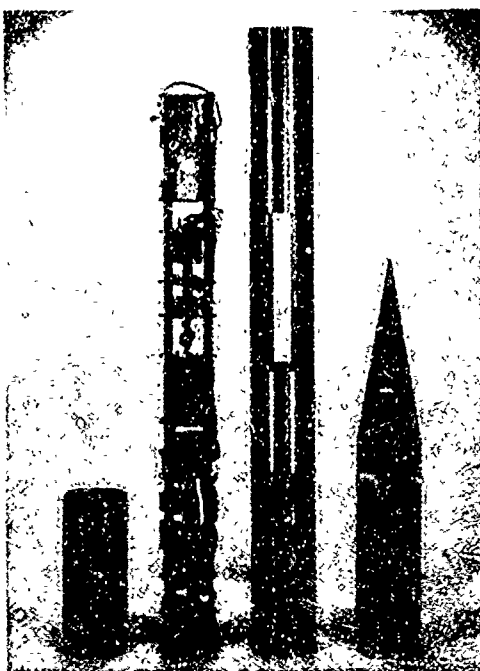
ratio measured the potential difference between two spherical sensors extended on booms from the rocket body and immersed in the auroral ionospheric plasma. Analysis of the measurements and observations is in progress.

The ground station experiment with a triaxial fluxgate magnetometer at the Churchill Auroral Observatory and two portable stations, one at Gillam, 250 km south, and one at Eskimo Point, about 300 km north, gave very good data on several nights. Just prior to flight, results from the stations indicated that there were two different substorms occurring simultaneously, one slightly south of Churchill and one about 800 km south.

MICROPULSATIONS: Low frequency, small amplitude fluctuations of the earth's magnetic field are called micropulsations. Their periods range from about 1 to 1000 seconds and their amplitudes are generally a gamma (10^{-5} Oersteds) or less. Auroral zone events of 10 gammas or more are occasionally observed. Geomagnetic micropulsations are considered to be hydromagnetic waves propagating within the magnetosphere. Hydromagnetic waves are low frequency electromagnetic waves modified by their passage through, and interaction with, the highly conducting medium, principally ionized hydrogen, filling the magnetosphere. When micropulsation frequencies are at the resonant frequencies of the magnetosphere or its various components, e.g. the plasmasphere, the neutral sheet, the plasma sheet and geomagnetic tail, these waves should transmit information on the structure and conditions in the magnetosphere. At other frequencies they would provide information on the sources producing such signals, whether natural, such as variations of the solar wind and particles entering the magnetosphere, or man-made, through modification of the local environment at high altitudes. The understanding of either

kind of micropulsation would result in a specification of magnetic activity and indicate its future development, and may afford a means of forecasting unusual levels of activity, such as magnetic storms.

Scientists conduct advanced theoretical projects in the study of micropulsations. At present, the effort is concentrated on the calculation of the resonant spectrum of the inner magnetosphere or plasmasphere. The plasmasphere is that volume of space bounded within by the ionosphere and without by the shell of dipole field lines, whose equatorial distance is from 4 to 7 earth radii, depending on the level of geomagnetic activity. These distances would encompass phenomena occurring at latitudes up to 60 to 68 degrees on the surface



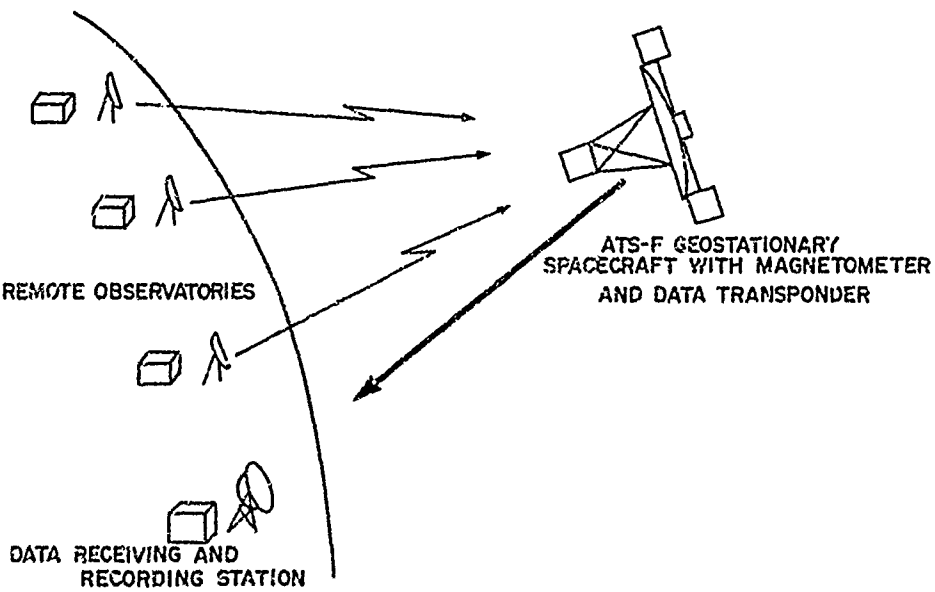
Sounding rocket payload for the study of auroral disturbances showing instrumentation for the measurement of electric and magnetic fields and charged particles.

of the earth. Substantial progress has been made in developing the theory of hydromagnetic wave propagation in geometries representative of the plasmasphere. Only a few years ago the problem of hydromagnetic waves in the magnetosphere was considered too difficult to be solved. The physical parameters and the geometry resulted in a strong coupling of the basic propagation modes. Now, due to in-house research, a successful solution of the problem is anticipated. The principal milestones in this theoretical study of geomagnetic micropulsations have been: the discovery and correction of untenable simplifying assumptions in previous studies of the problem; the demonstration that more tractable geometries could be substituted for the difficult dipole geometry without changing the nature of the basic hydromagnetic modes or their interaction; the formulation of a particularly relevant cylindrical geometry, and, the determination of the various forms of steady state oscillations. These represent the first solutions

of any type ever obtained to the problem of coupled hydromagnetic oscillations relevant to geomagnetic micropulsations.

The study of the properties of geomagnetic micropulsations (which originate in the magnetosphere) provides information on the generation and propagation of hydromagnetic waves. Three-component magnetic tape recordings of the micropulsations are made at the AFCRL field site in Sudbury, Mass. Three and one-half years of an hourly, broad-bandwidth micropulsation index, M , for periods of 20 to 200 seconds have been used in a published statistical study of the relationships of the micropulsations to other geophysical and solar phenomena.

The reduction of five months of the three-component recordings to hourly field strength values for six contiguous octave frequency bands covering the period range 16 to 1024 seconds has recently been completed. Data from high-and low-sensitivity tracks on the original tapes have been merged to form a single sample which



ATS-F geophysical data collection system.

accommodates the wide dynamic range (more than 70 dB) of the natural field variations. This large statistical sample is now being used to extend previous studies of the micropulsations. The sample yields, for example, six-point frequency spectra for each hour which display the diurnal frequency and amplitude trends of the data and also the similarities and differences between the three components. Specific examples of the interesting trends revealed by the large octave-bandwidth sample may then be studied in more detail by means of high-resolution frequency spectra.

An empirical study of geomagnetic micropulsation activity will be made using an array of surface magnetometers and a magnetometer onboard a geostationary satellite, the ATS-F. The surface observatories will be linked to the satellite by an active RF command and data relay link where ground data will be formatted, combined with the satellite measurements and then sent back to the ATS data tracking and command station. The records produced by this system will be computer-compatible magnetic tapes containing magnetic field measurements made simultaneously at the satellite and all of the surface observatories in the network. The difficulties normally encountered in obtaining useful sets of micropulsation measurements due to timing uncertainties, the multiplicity of recording techniques and differences in measuring instruments will be avoided, permitting participating agencies to devote the greater part of their effort to productive scientific work.

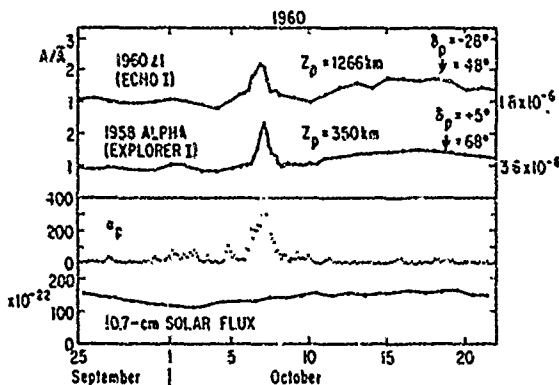
MAGNETIC ACTIVITY PREDICTIONS: The interaction of the interplanetary medium with the earth's magnetosphere provides many measures or indicators of geomagnetic activity. Examples of these indicators are K_p and AE. K_p is called a planetary index and is representative of worldwide geomagnetic activity. AE is the au-

toral electrojet index and is a measure of substorm activity. These and other indices are scaled from magnetograms from selected geomagnetic stations. While it is clear that the interplanetary medium is the driving force for geomagnetic activity as well as other magnetospheric phenomena, the exact nature of the cause-and-effect relationships among the various parameters involved in this interaction is far from being understood. One way of looking for cause-and-effect relationships is through statistical studies. Usually, a study of this type requires large quantities of data for the results of the study to be meaningful.

In addition to the current ground station data collection program and the planned ground station-satellite data collection system, a third source of data for theory verification and activity prediction is being utilized. Data from the satellites and deep space probes, Explorers 18, 21, 28, 33, 34, 35, Vela 3 and Mariners 2, 4, and 5 are analyzed by a statistical technique known as multiple correlation analysis where earth-based measures of magnetic activity such as the K_p index are related to conditions in interplanetary space. Detailed conclusions based upon the multiple correlation analysis of the Explorer 18 data are:

The single variables most highly correlated with K_p are the solar wind speed, the variability of the interplanetary magnetic field (IMF) and the magnitude of the IMF, in that order; Multiple correlation yields significant improvement over the best single correlations; Correlation coefficients increase with averaging time up to about 18 hours, and, the most appropriate index of magnetic activity for correlating with interplanetary conditions is K_p .

From July 1967 to June 1968 the satellites Explorer 33, an eccentric earth orbiter, and Explorer 35, a lunar orbiter, made coincident solar wind measurements for a total of about 1500 hours. The excellent agreement of the bulk velocity and num-



Atmospheric drag of two satellites during the October 6-7, 1960, magnetic storm compared with the geomagnetic planetary index K_p .

ber density measurements of the two satellites was used to show that the solar wind is homogeneous over a time scale of hours and a distance scale of about 60 earth radii. Since the two satellites measure essentially the same solar wind, the two sets of observations were combined to yield about 9000 hours of interplanetary observations. Multiple correlation analysis strengthened the earlier conclusion that K_p is the best index of magnetic activity and that multiple correlation is significantly better than the best single correlation.

Further detailed studies were made using data from the twin satellites called Vela 3. Again, K_p turned out to be the best index and multiple correlation yielded distinct advantages, e.g., a correlation of 0.63 with two variables compared to 0.53 with the best single one—bulk speed.

Explorer 34 measured both IMF and solar wind parameters during approximately 3200 hours. The correlation coefficient increased from 0.52 to 0.80 using seven variables.

Another approach to the magnetic activity prediction problem is through statistics compiled from historical magnetic activity data. Some constraints applicable to short-range predictions were obtained from the

investigation. For example, the present degree of magnetic activity will be followed by a level of activity either less than, equal to, or greater than, the present level. From historical data, the distribution of magnetic activity which occurred, given an initial level, can be determined and used to test proposed predictive schemes.

Finally, investigations have begun on the geomagnetic indices themselves. Semiannual and diurnal variations and persistence have been observed in the K_p index. Studies are being conducted to determine if these effects also occur in the AE and Dst indices. Relationships among the various indices are also being investigated. This should lead not only to a better understanding of the indices themselves, but also how to use them best in studying interplanetary effects and in predicting geomagnetic activity.

ENERGY CONVERSION

Energy conversion research supports Air Force requirements for electrical power used in spacecraft and satellites. The lifetimes of satellites, and the power levels needed indicate that the most desirable methods for obtaining electrical power are solar and chemical primary energy sources. Solar cells can generate enough energy from sunlight to charge secondary batteries for use while a satellite is in shadow as well as operate the equipment. For short-duration spacecraft experiments, primary batteries and fuel cells can be used for life support, operation of instruments, telemetry, etc. Thermal energy, from the sun or from other heat sources, can be used for power generation in a thermionic diode and for direct temperature stabilization of instrumentation and controls. Research on controlled thermonuclear reactions and plasma magnetohydrodynamic generators

may point the way to generation of very high power levels on future flights.

SOLAR ENERGY CONVERSION: Presently, solar power generation utilizes the silicon solar cell almost exclusively. The Space Physics Laboratory has investigated several classes of organic and metal-organic materials as possible materials for cells which can overcome the weight and cost limitations of silicon solar cells. Silicon solar cells must be supported in heavy arrays, and the utilized fabrication techniques used in manufacturing the cells is costly.

Organic materials have a special problem; their characteristic high resistivity causes low efficiency in devices using them. Photoconductive materials can solve this problem, since the device is required to operate only in sunlight. Thin-film prototype solar cells have demonstrated the feasibility of using new organic materials. Substituted aromatic hydrocarbons and their charge-transfer complexes lend themselves best to this effort. Examples of the classes of materials analyzed include

tetracene, dicyanomethylenefluorene derivatives and a series of arylidene-indandione compounds. These solids, suitably purified, are vacuum-deposited to form thin-film sandwich-type cells. The cells are analyzed for conductivity response in the solar spectral region and the photovoltaic characteristic curves are measured. The performance of the cell material is improved by modification of substituent groups on the "backbone" molecular structure. The modifications made are determined on the basis of spectrophotometric and crystallographic studies of the relationship of substituents to photoconductive and photovoltaic response. A different technique under development involves the use of porphyrin derivatives in photoelectrochemical cells. Porphyrin derivatives can be transformed to an excited electronic state by optical absorption processes in the visible region. These excited molecules can inject electrons into the conduction band of a suitably chosen semiconductor electrode, thus generating a useful current. The effects of electron-donor materials in enhancing this photocurrent are being established.

In addition to this work a program has been defined to improve the quality of the silicon cell as well as to study other inorganic photovoltaic materials. Custom cells are fabricated on a pilot-plant line and their performance is evaluated relative to the best solar cells now available. Areas for research include precise control of lithium doping to offset radiation damage and materials analysis for the application of thin-film gallium arsenide to higher efficiency solar energy conversion.



Evaluation of the photoconductive response in the visible spectral region assists in the selection of materials for photovoltaic energy conversion.

THERMAL ENERGY CONVERSION: Direct ion injection to neutralize the emitter electrode space charge is being attempted, as a means to improve existing thermionic converters. Experiments have demonstrated that a single injected ion can neutralize as many as 4,000 space-charge electrons be-

fore it recombines or migrates into the emitter. Because this effect is much larger than that predicted by simple linearized plasma sheath theory, a computer analysis of a more complete nonlinear theory will be made. If sufficient space-charge neutralization by direct ion injection is possible, the use of cesium (with its attendant corrosion problems) in thermionic converters will be obviated.

Two new mechanisms for energy conversion are also being investigated. The first is plasma electrophoresis which pumps gas from one end of a discharge tube to the other causing sizable pressure gradients to develop. A complete theory for this phenomenon was developed in the Space Physics Laboratory and this theory has been verified experimentally for quiescent and striated dc discharges. To determine the feasibility of applying the theory, flowing plasmas are probed to determine whether or not reverse electrophoresis can generate large enough potential gradients and currents to warrant its use for energy conversion.



The temperature of the DC discharge in this thermal energy conversion experiment is an important parameter in calculating the energy of the particles in a plasma.



Analysis of intermolecular approach distances in the structure of complex crystals contributes to the understanding of the electronic properties of materials.

The second new energy conversion mechanism will be studied in a program to demonstrate both the feasibility of extracting power from rocket exhausts, and also the possibility of electrically controlling their combustion and flow characteristics. Preliminary experiments on diffusion flames in propane-air mixtures indicate that a turbulent flame can be made laminar (and vice-versa) by the application of electric fields with a total power consumption of only a few milliwatts.

ELECTROCHEMISTRY: The need for substantially greater energy density in storage cells has stimulated evaluation of a range of lithium-organic electrolyte systems with theoretical energy densities an

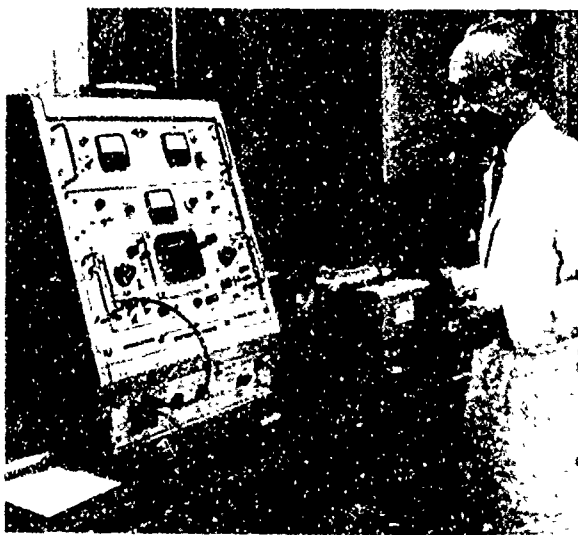
order of magnitude or more higher than the current state of the art. However, the containment and utilization of the energetic chemical reactions involved in these systems is difficult. Lithium electrodes require a hydrogen-free electrolyte which must be rigorously cleansed of impurities (for example, water), which tend to react with the electrode. Unfortunately, many of the hydrogen-free solvents which are otherwise suitable give solutions of low conductance which impairs the performance of the battery. Much of the electrochemistry program is concerned with the physical chemistry of these systems and especially such properties as viscosity, dielectric constant and specific ionic solvation which are related to the conductance problem. In addition, the program addresses the problem of the positive electrode, which is presently the limiting factor in the performance of lithium cells. The problem of low electronic conductance in typical positive plate active materials such as cadmium fluoride and zinc fluoride has been approached through new preparation

methods in which the material is doped with a rare earth element to convert it to an n-type semiconductor. The conductance of cadmium fluoride has been increased in this way by eight orders of magnitude, resulting in a material that can be discharged electrochemically with negligible ohmic loss. New positive electrode materials based on compounds of nickel and sulfur have been developed and have shown considerable promise in experimental cells.

The electrochemistry program also responds to the requirements of the technology laboratories for research into problems of immediate importance—for example, the requirement for a method of determining the state-of-charge of secondary alkaline batteries used for power storage in satellite applications.

PLASMA PHYSICS

Temperatures so high that any element will be a gas, so highly ionized that it conducts electricity better than any conventional material, and high energy densities: these are properties of plasmas, which make them of great interest to the Air Force. Plasmas make possible the magnetohydrodynamic generator, which has higher efficiency because of its high operating temperature, and a power output comparable to a conventional generator. Other applications of plasmas utilize specific molecules; for example, a gas laser uses electrons and the ionized gas to excite molecular constituents in a non-equilibrium manner for the generation of light. Another application is the use of the plasma for the controlled thermonuclear reactor. The high electrical conductivity of plasmas and their interaction with magnetic fields is used to localize and contain the plasma, while self-excited nuclear reactions can take place and generate energy.

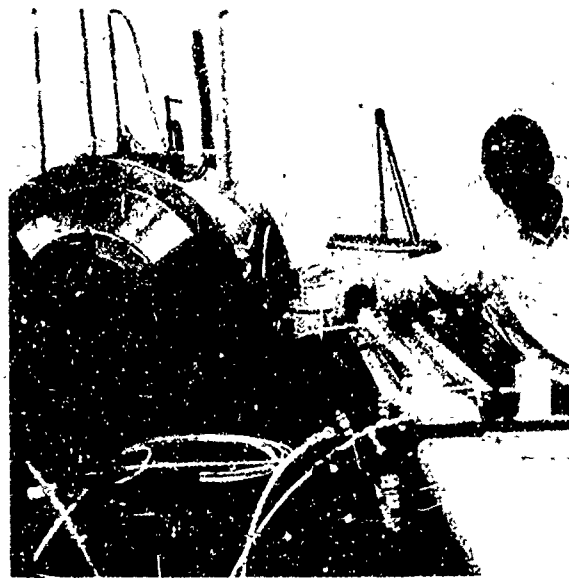


Very small changes in the concentration of chemical reactants can be measured accurately with this sensitive differential spectrophotometer.

Unfortunately, the problems of handling plasmas have prevented them from being used to solve Air Force technological problems. If a plasma is pictured as simply a collection of ions and electrons subject to the classical laws of physics, the problem is simple, but as the density of particles is increased, a single particle begins to interact with other particles. The distance over which this interaction can occur, called the Debye length, sometimes includes the entire plasma. Each particle within the plasma senses and reacts to the position and behavior of every other particle in the vessel at the same time. This gross interaction of particles with each other not only gives rise to certain conceptual difficulties, but also allows waves and oscillations of many different modes to propagate, which can make containment difficult.

In discussing problems in plasma physics, it is natural to divide plasmas into two temperature regions. In the lower temperature region, atomic collisions, degrees of ionization, degrees of excitation of atoms, electron-ion collisions and atomic spectral emission are all important processes. In the higher temperature region, particle-particle collisions become less important, and few of the wave modes are damped. Thus, at high temperatures, acoustic waves, magnetohydrodynamic waves, cyclotron waves, density waves, temperature waves, and the deviations from equilibrium which can generate these waves all must be considered.

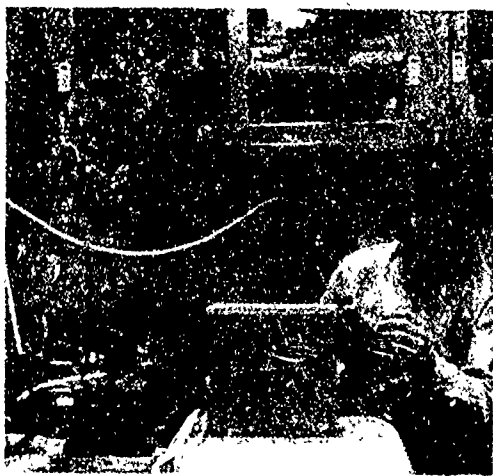
LASER APPLICATIONS: A continuing Space Physics Laboratory program in low temperature plasmas has been concerned with applications to lasers. At the present time, the only high power lasers available are in the infrared. A search has been conducted to find suitable atomic transitions so that a high power laser in the visible or shorter wavelengths can be built. Among the possibilities are the so-called molecular dissociation states. Diatomic molecules in excit-



Spectroscopic studies of a plasma for a high power short wavelength laser.

ed states decay into two separated atoms and emit laser light in the process; hence, the name molecular dissociation transitions. A very promising candidate for such a laser is the excited state of hydrogen.

In this program to develop such a laser, it has first been necessary to calculate the energy levels of the excited states of hydrogen, and determine transition probabilities between these states. For example, the cross section for an excited state of hydrogen to be photoionized had never been calculated. Using a new quantum mechanical theory suitable for these calculations, Space Physics Laboratory scientists have determined these cross sections and reported them in the literature. Another problem was determining the cross section for the transitions from excited states down to the ground state; these two cross sections determine the gain of a laser. Cross sections and transition probabilities existing in the literature were found to be inaccurate and unreliable. A new computer program was set up in the laboratory and the calculation of the tran-



Aligning an interferometer for gain measurements in a new laser plasma.

sition probabilities for the hydrogen was completed.

The next step in the program was to design a plasma which would suitably excite the desired transitions without destroying the hydrogen molecules. To do this, a new medium consisting of hydrogen, helium, and xenon was considered. Calculations have been carried out to determine the degree of ionization of such a medium under the influence of applied electric fields, the electron temperature, and the population of excited states to be expected. In this effort, careful consideration has been given to the effects of xenon on a discharge. It was found that as little as 1 percent xenon could dramatically change the density profile of ions within the medium. Theoretical calculations have now been extended to indicate that as little as one part in 10^3 of xenon could alter the discharge and optimize hydrogen for use as a lasing medium. At this time a hydrogen molecular dissociation laser has not been developed. However, optimum proportions of gases for a laser have been determined, and the addition of xenon has been shown to enhance the ionization and eliminate unwanted complex ion states. In addition, an almost complete theoretical

picture of molecular hydrogen has been calculated and published in the literature for application to MHD generator design.

PLASMA DIAGNOSTICS: In probing the optical radiation from a high density hydrogen plasma, Space Physics Laboratory scientists noted an anomaly in the green H-beta radiation from hydrogen. This anomaly was thought to be due to the presence of high frequency oscillations with large fields in the plasma. However, standard theory did not predict all of the observed variances; therefore, a series of experiments was performed using helium-hydrogen mixtures. Because a helium atom has two protons and two neutrons in a single nucleus, while a hydrogen molecule has no neutrons and a relatively large distance between the two protons, the theories of radiation for the two are very different. Experimental results for radiation from helium agreed with the theory, and on the basis of these findings a new theory of radiation for hydrogen has been constructed which better reflects actual plasma behavior, by accounting for the influence of particle collisions when coupled with a high frequency field.

Electric fields in plasmas not accessible to any other experimental technique can be measured by this new method. Preliminary measurements using this technique have now been made in an attempt to verify the theoretical predictions of the behavior of nonlinear waves in plasmas. This basic problem concerns the Air Force because turbulent nonlinear waves not only affect the behavior of lasers and MHD generators, but also form a basis for the phenomenological observations of plasmas in the ionosphere and in the sun.

JOURNAL ARTICLES JULY 1970 - JUNE 1972

- BEN-YOSEF, N., and RUBIN, A. G.
A Static Model for the Nanolight Discharge
J. of Appl. Opt., Vol. 9, No. 7 (July 1970)

- Forbidden Optical Transitions Stimulated by Plasma Turbulence in Helium**
J. of Quant. Spectros. and Rad. Transfer, Vol. 11 (1971)
- BESSE, A. L.**
Shock Front Detection by Fraunhofer Diffraction
Rev. of Sci. Instrn., Vol. 42, No. 5 (May 1971)
Theoretical Performance of Arc Driven Shock Tubes
Rev. of Sci. Instrn., Vol. 42 (1971)
- CHATTERJEE, S.**
Studies of Charge-Transfer Complexes of 1,4-Naphthaquinone Acceptors
J. Chem. Soc. (B) (London), p. 2194 (1971)
- COHN, A.**
Self-Consistent Analysis of the Effect of Radiation Escape on the Atomic State Densities and Electron Distribution Function
Phys. Ltrs., Vol. 33A, No. 8 (December 1970)
- COHN, A., and BAKSHI, P., KALMAN, G.**
Linear Stark Effect due to Resonant Interactions of Static and Dynamic Fields
Phys. Rev. Ltrs., Vol. 29 (1972)
- DIMOND, N., and MUKHERJEE, T. K.**
Chromophoric Conditioning of Photoelectric Response in Polar Molecules
Discussions of the Faraday Soc., Vol. 51 (1971)
- ENGE, W., and BARTHOLOMA, K. P.** (Institut für Reine und Angewandte Kernphysik, Kiel, Ger.), and FUKUI, K., FILZ, R. C.
Preliminary Results of Measurements on Track of Heavy Cosmic Rays in Plastic Detectors
Acta Physica Academiae Scientiarum Hungaricæ, Vol. 29, Suppl. 2 (1970) *Rad. Effects*, Vol. 5 (1970)
- ENGLADE, R. C.**
The Effect of the Solar Boundary Condition on Flare Particle Propagation
Ltr., J. of Geophys. Res., Vol. 76, No. 25 (1 September 1971)
The Radial Gradient of Galactic Protons in the Inner Solar System
J. of Geophys. Res., Vol. 76, No. 34 (1 December 1971)
- FAIRBAIRN, A. R.**
Band Strengths in Forbidden Transitions: The Cameron Bands of CO
J. of Quantitative Spectros. and Rad. Transfer, Vol. 10 (1970)
- FILZ, R. C., and MACY, W. W., WHITE, R. S.** (Univ. of Calif., Riverside, Calif.)
Time Variations of Radiation Belt Protons
J. of Geophys. Res., Vol. 75, No. 22 (1 August 1970)
- FOUGERE, P. F.**
The IGRF Competition
World Mag. Survey, 1857-1969, IAGA Bull. #28 (1971)
- Magnetic Dipole in a Stationary Plasma**
Phys. of Fluids, Vol. 14, No. 3 (March 1971)
- FREY, J. H., FISCHER, W. L.** (Sea Farm Res. Fdn., Inc., Waltham, Mass.), and MAPLE, E. CHERNOVSKY, E. J. (Aeron. Lab.)
Broad Band Micropulsation Activity at a Geomagnetic Midlatitude Station
J. of Geomag. and Geoelec., Vol. 23, No 1, (1971)
- FUJIMORI, E.**
pH-Induced Reversible Changes in the Absorption Spectrum and Photoactivity of Bacteriochlorophyll in Photosynthetic Bacteria Chromatophores
Biochim. Biophys. Acta, Vol. 223 (December 1970)
On the Fluorescence of Indole Compounds Induced by Ketone-Sensitized Photoreactions
Photochem. and Photobiol., Vol. 16 (1972)
- FUJIMORI, E., and PECCI, J.**
pH-Dependent Association of the Phycoerythrin Subunit
Biochim. Biophys. Acta, Vol. 207 (1970)
Circular Dichroism of Single - and - Double-peaked Mercurial-Induced Changes
Biophys. Biochem. Acta, Vol. 221 (1970)
Changes in Circular Dichroism and Absorption Spectrum of Phycoerythrin Chromatophores by Organic Mercurial
Photochem., Vol. 10 (1971)
- GALL, R.** (Univ. of Mex.), SMART, D. F., and SHEA, M. A.
The Direct Mode of Propagation of Cosmic Rays to Geostationary Satellites
Planet. and Sp. Sci., Vol. 19 (November 1971)
The Daily Variation of Cosmic-Ray Cutoff at the Altitude of a Geostationary Satellite
Sp. Res. XI, Vol. 2 (1971)
- GALLAGHER, C. C., COMBES, L. S., and LEVINE, M. A.**
Plasma Behavior in a Toroida. High-Beta Device
The Phys. of Fluids, Vol. 13, No. 6 (August 1970)
- GALLAGHER, C. C., and LEVINE, M. A.**
Observation of H_β Satellites in the Presence of Turbulent Electric Fields
Phys. Rev. Ltrs., Vol. 27, No. 25 (20 December 1971)
- KRUUKONIS, A. P., SILVERMAN, J., and YANNONI, N. F.**
The Crystal Structure of π,π -Dicyanovinyl-ferrocene
Acta Crystallogr., Sec. B, Vol. 28, Pt. 4 (April 1972)

- LEIBY, C. C., JR.
Gas Pumping by Striations in dc Discharges
 Bull. of the Am. Phys. Soc., Vol. 17 (1972)
- LEVINE, M. A., BOOZER, A. H., CAPT., and KALMAN, G., BAKSHI, P. (Boston Coll., Chestnut Hill, Mass.)
Particle Loss in a Toroidally Symmetric Cusp
 Phys. Rev. Ltrs., Vol. 23 (15 May 1972)
- MACKEN, N. A., BESSE, A. L., and LEVINE, M. A.
Shock Tube Boundary Layer in Ionized Argon-Helium Mixtures
 AIAA J., Vol. 10 (1972)
- MC CLAY, J. F.
On the Resonant Modes of a Cavity and the Dynamical Properties of Micropulsations
 Plan. and Space Sci., Vol. 18 (December 1970)
- MUKHERJEE, T. K.
Photoconductive and Photovoltaic Effects in Dibenzothiophene and Its Molecular Complexes
 J. of Phys. Chem., Vol. 70 (1970)
- MUKHERJEE, T. K., DIMOND, N. A., and PITTMAN, C. U., SASAKI, Y. (Univ. of Ala.), COWAN, D. O., and PARK, J. (Johns Hopkins Univ., Baltimore, Md.)
Semiconducting Polymers, Mixed Valence Ferrocene-Ferricinium Polymers
 J. of the Am. Chem. Soc., Vol. 94 (1972)
- O'FRIEL, Z., FR., and FILZ, R. C.
The Time Dependence of the Trapped Proton Energy Spectrum at Low Altitudes
 Bull., Am. Phys. Soc., Vol. 16, No. 12, (December 1971)
- PARSIGNAULT, D. R., CHASE, R. C., and KATZ, L.
Low-Energy (12-48 keV) Electrons and Protons in the Magnetosphere at Solar Activity Maximum
 Sp. Res. XI, Vol 2 (1971)
- PAYNE, R.
Application of the Method of Time Domain Reflectometry to the Study of Electrode Processes—Reply to the Critique of Schuldiner et al
 J. of Electroanal. Chem., Vol. 25 (1970)
- PYNE, R., and THEODOROU, I. E.
Coaxial Cell for Liquid Dielectric Measurements from 300-3000 MHz
 Rev. of Sci. Instrm., Vol. 42, No. 2 (February 1971)
- PECCI, J., and FUJIMORI, E.
The B-Phycoerythrin Chromophore
 Photochem., Vol. 9 (1970)
- PRASAD, B., SEN, H. K., and BAKSHI, P., KALMAN, G. (Brandeis Univ., Waltham, Mass.)
Non-Linear Collisionless Plasma Waves and Intensity of the Electric Field of the Ionospheric Irregularities
 Rad. Sci., Vol. 6, No. 2 (February 1971)
- QUINLAN, K. P.
An ESR Study of the Light-Induced Interaction Between Porphyrins and Quinones in Amide Solvents
 Photochem. and Photobiol., Vol. 261 (1970)
The Effect of Oxygen and Quinone Concentration on the Reversible Light-Induced Proton Uptake of the Chlorophyll b - Benzoquinone System
 J. of Phys. Chem., Vol. 74 (1970)
Proton Movement Accompanying the Light-Induced Electron Transfer in the Chlorophyll α -Quinone Systems
 Photochem. and Photobiol., Vol. 13 (1971)
Reversible Spectrophotometric Changes Accompanying the Light-Induced Proton Uptake of Porphyrin-Benzoquinone Systems
 Photochem. and Photobiol., Vol. 267 (1972)
- RADOSKI, H. R.
The Resonance Barrier Theory of Hydromagnetic Waves
 J. of Geomag. and Geoelec. (Jap.), Vol. 22, No. 3 (1970)
Coupled Resonances of Hydromagnetic Waves in a Cold Plasma
 J. of Geomag. Geoelec. (Jap.), Vol. 23, No. 1 (1971)
A Note on the Problem of Hydromagnetic Resonances in the Magnetosphere
 Planet. and Sp. Sci., Vol. 19 (August 1971)
- RUBIN, A. G.
Optical Investigation of Electrostatic Turbulence in Plasma
 Phys. Ltrs., Vol. 33A, No. 4 (27 January 1971)
- SEN, H. K., DUBS, C. W., and PRASAD, B.
Non-Linear Longitudinal Waves in a Hot, Collisional Magneto-Plasma with Applications to Ionospheric Irregularities
 Rad. Sci., Vol. 6, No. 4 (April 1971)
- SEN, H. K., and WHITE, M. L.
A Physical Mechanism for the Production of Solar Flares
 Bull. Am. Astronom. Soc., Vol. 2 (1970)

- SHEA, M. A.**
- Annals of the IQSY, Vol. 3, The Proton Flare Project (Book Review)*
J. of the Franklin Inst., Vol. 290, No. 2 (August 1971)
- Changes in Neutron Monitor Response and Vertical Cutoff Rigidities Resulting from Secular Variations in the Geomagnetic Field*
12th Intl. Conf. on Cos. Rays, Hobart, Conf. Pap. (Univ. of Tasmania), Vol. 3 (1971)
- SHEA, M. A., and SMART, D. F.**
- On the Application of Trajectory-Derived Cutoff Rigidities to Cosmic-Ray Intensity Variations and the Effect of the Asymmetric Magnetosphere on the Response of High-Latitude Neutron Monitors to Solar Particle Events*
Acta Physica Academiae Scientiarum Hungaricae, Vol. 29, Suppl. 2 (1970)
- Secular Variations in Cosmic-Ray Cutoff Rigidities*
Ltr. to J. of Geophys. Res., Vol. 75, No. 19 (1 July 1970)
- Calculations of the Seasonal Dependency of Neutron Monitors to an Anisotropic Flux of Solar Cosmic Rays Propagating in the Ecliptic Plane*
12th Intl. Conf. on Cos. Rays, Hobart, Conf. Pap. (Univ. of Tasmania), Vol. 2 (1971)
- Calculation of Cosmic-Ray Trajectories for Palestine, Texas, USA - Cutoff Rigidities and the Origin of the Reentrant Albedo and Calculation of the Magnitude of the Daily Variation of Vertical Cutoff Rigidities and Associated Changes in the Neutron Monitor Response for Selected North American Neutron Monitors*
12th Intl. Conf. on Cos. Rays, Hobart, Conf. Pap. (Univ. of Tasmania), Vol. 3 (1971)
- SHUMAN, B. M.**
- Rocket Measurement of the Equatorial Electrojet*
J. of Geophys. Res., Vol. 75, No. 19 (July 1970)
- SILVERMAN, J., SOLZBERG, L. J., YANNONI, N. F., and KRUKNIS, A. P.**
- Perchlorodiphenylmethyl Stable Free Radical: X-Ray Analysis of a Disordered Mixed Crystal*
J. of Phys. Chem., Vol. 75, No. 9 (29 April 1971)
- SMART, D. F.**
- Calculation of the Daily Variation of Cosmic-Ray Cutoff Rigidities at Ft. Churchill, Canada*
12th Intl. Conf. on Cos. Rays, Hobart, Conf. Pap. (Univ. of Tasmania), Vol. 3 (1971)
- SMART, D. F., and SHEA, M. A.**
- Solar Proton Event Classification System*
COSPAR Inf. Bul., No. 55 (September 1970)
- Solar Proton Event Classification System**
Solar Phys. (Res. Note), Vol. 16 (1971)
- Proposed Solar Proton Event Classification System**
S. & Terres. Phys. Notes, No. 8 (January 1971)
- 12th International Proton Event Classification System**
IUGG Circular, No. 82 (April 1971)
- SMART, D. F., SHEA, M. A., and GALL, R.**
(Universidad Nacional Autonoma de Mex. and Comm. Nacional de Energia Nuc., Mexico City, Mex.)
- Iso-Rigidity Contours in the Polar Regions Interpolated from Trajectory-Derived Vertical Cutoff Rigidities*
Acta Physica Academiae Scientiarum Hungaricae, Vol. 29, Suppl. 2 (1970)
- SMART, D. F., SHEA, M. A., and TANSKANEN, P. J.**
(Univ. of Oulu, Oulu, Finland)
- A Determination of the Spectra, Spatial Anisotropy, and Propagation Characteristics of the Relativistic Solar Cosmic-Ray Flux on November 18, 1968*
12th Intl. Conf. on Cosmic Rays, Hobart, Conf. Pap. (Univ. of Tasmania), Vol. 2 (1971)
- TSACOYEANES, C., and LEVINE, M. A.**
- Electronic Enhancement of Photodetector Performance*
J. of Appl. Opt., Vol. 9, No. 11 (November 1970)
- TURTLE, J. P. (Aeron. Lab.), OELEREMANN, E. J.**
(Ordnance Res. Lab., Penn State Univ.), BLAKE, J. B., VAMPOLA, A. L. (Aerospace Corp., El Segundo, Calif.), YATES, G. K., and LANZEROTTI, L. J. (Bell Tel. Labs., Murray Hill, N. J.)
- Rapid Access of Solar Electrons to the Polar Caps*
J. of Geophys. Res., Vol. 77, No. 4 (1 February 1972)
- WARES, G. W.**
- Absolute gf-Values for Fe I*
Trans. of Intl. Astronom. Un., Vol. 14B (1971)
- WARES, G. W., WOLNIK, S. J., and BERTHEL, R. O.**
- Shock-Tube Measurements of Absolute Fe I g f Values and Their Implications*
Bull. Am. Astronom. Soc., Vol. 2 (1970)
- Temperature Errors in Plasma Diagnostics and their Possible Effects on Absolute Transition Probabilities*
Modern Opt. Meth. in Gas Dyn. Res., Plenum Press, N. Y. (1971)
- Oscillator Strength Measurements for Fe I and Fe II*
Bull. Am. Astronom. Soc., Vol. 3 (1971)
- WHITE, M. L.**
- An Asymmetrically Rotating Fluid Disc with Applications*
Astrophys. and Sp. Sci., Vol. 16, No. 2 (May 1972)

- WOLNIK, S. J., BERTHEL, R. O., and WARES, G. W.
Shock-Tube Measurements of Absolute Fe I gf-Values
Astrophys. J., Vol. 162 (December 1970)
Oscillator Strength Measurements for Fe I and Fe II
The Astrophys. J. (15 May 1971)
- YATES, G. K., KATZ, L., KELLEY, J. G., and SELLERS, B., HANSER, F. (Panamet, Inc., Waltham, Mass.)
Proton, Alpha and Bremsstrahlung Fluxes Measured Aboard OV5-6
World Data Ctr. A-Upper Atm. Geophys. Rpt. UAG (April 1971)
- YOUNG, P. (Miss. State Univ., State Coll., Miss.) and FUKUI, K.
Thindown Intensities and Energy Deposit in Emulsions Around SST Altitudes
Proc. of Council of Eur. Wkg. Party on Sp. Biophys. (October 1971)
- ZAWALICK, E. J., and CAGE, A. J., CAPT.
Frequency Tables of the Geomagnetic Index K_p, 1932-1970
J. of Geophys. Res., Vol. 76, No. 28 (October 1971)
- PAPERS PRESENTED AT MEETINGS JULY 1970 - JUNE 1972**
- ALLER, L. H., POLIDAN, R., RHODES, E. (Univ. of Calif. at Los Angeles), and WARES, G. W.
The Spectrum of RR Telescopii, A Study of Iron
137th Mtg. of the Am. Astronom. Soc., Univ. of Wash., Seattle, Wash. (8-12 April 1972)
- BOOZER, A. M., CAPT., LEVINE, M. A., and BAKSHI, P., KALMAN, G. (Boston Coll., Boston, Mass.)
Plasma Confinement in Cusp Geometry—A New View
N. Eng. Sec. of the Am. Phys. Soc., Am. Assoc. of Phys. Teach. Spring Mtg., Boston Coll., Boston, Mass. (14-15 April 1972)
- CHATTERJEE, S.
Reactions of Dicyanomethylvinene Derivatives with Amidines
3rd Intl. Cong. of Heterocyclic Chem., Sendai, Jap. (23-27 August 1971)
- CHREST, S. A., CARNEVALE, R. F., RYAN, T. G., SRIVANEK, R. A., and WILHELM, N., WITT, G. (Univ. of Stockholm, Stockholm, Sweden)
- Rocket-Borne Particle Collection and Photometric Measurement of Noctilucent Clouds
15th COSPAR Mtg., Madrid, Sp. (10-24 May 1972)
- COHN, A.
Bistable Electron Temperature in vibrationally Excited Gases
23rd Ann. Gaseous Elec. Mtg. of the APS, Hartford, Conn. (21-23 October 1970)
- DIMOND, N. A., and MUKHERJEE, T. K.
Photoconductivity Spectral Response and Related Phenomena in Substituted Divinylbenzenes
162nd Natl. Mtg. of the Am. Chem. Soc., Wash., D. C. (12-17 September 1971)
- ENGLADE, R. C.
A Computational Study of the Radial Gradient of Galactic Cosmic Rays
Am. Phys. Soc. Mtg., Wash. D. C. (26-29 April 1971)
Energy Changes of Solar Cosmic Rays
Am. Phys. Soc. Mtg., Wash., D. C. (24-27 April 1972)
- FAIRBAIRN, A. R.
Rates of Excitation and Ionization in Arcs
2nd Arc Symp. of the APS, Hartford, Conn. (20 October 1970)
- FILZ, R. C.
Satellite Recovered Nuclear Emulsion Study of Solar Cycle Variations in Trapped Proton Fluxes
7th Intl. Colloq. of Corpus. Photog. and Vis. Sol. Detectors, Universidad Autonoma Facultad de Ciencias, Barcelona, Spain (7-11 July 1970)
A Balloon Exposure of 30 M² of Corpsecular Photographic Materials in Search of Super Heavy Cosmic Radiation
Am. Phys. Soc. Mtg., Mass. Inst. of Tech., Cambridge, Mass. (27-29 December 1971)
- FILZ, R. C., and HOLEMAN, E. (Franklin Pierce Coll., Rindge, N. H.)
Observation of the Solar Cycle Variation of 115 MeV Inner Zone Trapped Protons
52nd Ann. Am. Geophys. Un. Mtg., Wash., D. C. (12-16 April 1971)
- FILZ, R. C., and MC NULTY, P. J.
Interactions of High Energy ²⁰Ne with Emulsion Nuclei
Am. Phys. Soc. Mtg., Wash., D. C. (24-27 April 1972)
- FOUGERE, P. F.
Multiple Regression Analysis of Satellite Data with Terrestrial Activity
52nd Ann. Am. Geophys. Un. Mtg., Wash., D. C. (12-16 April 1971)

Comparisons of Solar Wind Results from the Satellites, Explorer 33 and 35
 Fall Ann. Mtg. of the Am. Geophys. Un., San Francisco, Calif. (6-9 December 1971)

FUKUI, K., and BEAUJEAN, R., ENGE, W. (Institut für Reine und Angewandte Kernphysik, Univ. of Kiel, Ger.)

Z-Coordinate Measurements in Plastic Detectors

7th Intl. Colloq. of Corpus. Photog. and Vis. Sol. Detectors, Universidad Autonoma Facultad de Ciencias, Barcelona, Spain (7-11 July 1970)

FUKUI, K., and ENGE, W., BARTHOLOMA, K. P. (Institut für Reine und Angewandte Kernphysik, Univ. of Kiel, Ger.)

Measurements of Tracks of Heavy Cosmic

Rays in Polycarbonate Plastic Detectors
 7th Intl. Colloq. of Corpus. Photog. and Vis. Sol. Detectors, Universidad Autonoma Facultad de Ciencias Barcelona, Spain (7-11 July 1970)

Charge Determination of Tracks of Heavy Cosmic Rays in Polycarbonate Plastic Detectors

Winter Mtg. of the Am. Nuc. Soc., Wash., D. C. (15-19 November 1970)

Charge Composition of Low Energy Cosmic Ray Nuclei of Elements Neon to Nickel

12th Intl. Conf. on Cosmic Rays, Univ. of Tasmania, Hobart, Tasm. (16-26 August 1971)

FUKUI, K., and YOUNG, P. S. (Miss. State Univ.)

Cosmic Ray Heavy Nucleus Enders at the Level of SST Flight

Wkg. Pty. or Biophys., Cnsl. of Eur., Frankfurt, Ger. (21 November 1970)

Evaluation of the Density of Cosmic Ray Enders in Human Tissue from Solar Minimum to Maximum at the Level of SST Flight
 Intl. Cong. on Protection Against Accel. and Space Rad., Geneva, Switz. (26-30 April 1971)

Low Energy Iron Nuclei in Galactic Cosmic Rays Detected in 1968

Am. Phys. Soc. Mtg., Wash., D. C. (24-27 April 1972)

HENDL, R. G., CAPT., CARNEVALE, R. F., and WARD, F. W., JR.

The Results of Matched Patrol Telescope Systems

1972 Am. Astronom. Soc. Sol. Phys. Div. Mtg., Univ. of Md., Coll. Pk., Md. (4-6 April 1972)

KATZ, L., KELLEY, J. G., and ROTHWELL, P. L. (Emmanuel Coll., Boston, Mass.)

Electron Pitch Angle Distributions (.1-2.70 MeV) During Quiet and Disturbed Times

Natl. Fall Mtg. of Am. Geophys. Un., San Francisco, Calif. (7-10 December 1970)

KELLEY, J. G., KATZ, L., and ROTHWELL, P. L. (Emmanuel Coll., Boston, Mass.)

Inner Belt Pitch Angle Distributions for Electrons Between .1-2.0 MeV
 52nd. Ann. Am. Geophys. Un. Mtg., Wash. D. C. (12-16 April 1971)

LEIBY, C. C., JR.

Gas Pumping by Striations in dc Discharges
 24th Ann. Gas. Elec. Conf. & 3rd Arc Symp., Univ. of Fla., Gainesville, Fla. (5-8 October 1971)

LEVINE, M. A.

Tormac, The Toroidal Cusp with a Plasma That Won't Leave
 Mass. Inst. of Tech., Cambridge, Mass. (16 April 1971) Princeton Univ., N. J. (23 April 1971)

LEVINE, M. A., BESSE, A. L., and MACKEN, N. A. (Carnegie-Mellon Univ., Pittsburgh, Pa.)
An Experimental and Analytical Study of Boundary Layers Behind Primary Shocks in Ionized Argon and Helium Mixtures
 Heat Transfer and Fluid Mech. Inst., Northbridge, Calif. (14-16 June 1972)

LEVINE, M. A., and GALLAGHER, C. C.

Spectroscopic Measurement of Turbulent Fields in the Tormac Geometry
 Plasma Phys. Mtg. of the APS, Wash., D. C. (4-7 November 1970)

Plasma Containment in the Tormac Geometry
 4th IAEA Conf. on Plasma Phys. and Controlled Nuc. Fusion Res., Univ. of Wisconsin (17-23 June 1971)

MAPLE, E., and FREY, J. H., FISCHER, W. L. (Sci. Resources Fdn., Watertown, Mass.)
Octave-Bandwidth Analysis of Mid-Latitude Geomagnetic Micropulsations (16-1024 Seconds)
 53rd Ann. Mtg. of the Am. Geophys. Un., Wash., D. C. (17-21 April 1972)

MC NULTY, P. J.

Direct Stimulation of the Retina by the Method of Virtual-Quanta for "Navy" Cosmic-Ray Nuclei
 Natl. Symp. on Nat. and Man-made Rad. in Space, Las Vegas, Nev. (1-5 March 1971)
Production of Two Pronged Events in Interactions Between 5 GeV/c⁺ and Complex Nuclei
 Am. Phys. Soc. Mtg., Wash., D. C. (26-29 April 1971)

MUKHERJEE, T. K., and DIMOND, N.

Chromophoric Conditioning of Photoelectric Response in Polar Molecules
 Intl. Conf. of Elec. Conduction in Org. Sol., Nottingham, Eng. (14-16 April 1971)

- Electronic Absorption and Fluorescence of Photoconductive Divinylbenzenes*
162nd Natl. Mtg. of the Am. Chem. Soc., Wash., D. C. (12-17 September 1971)
- O'FRIEL, Z., FR. (S. Bonaventure Univ., St. Bonaventure, N. Y.) and FILZ, R. C.
The Time Dependence of the Trapped Proton Energy Spectrum at Low Altitudes
Am. Phys. Soc. Mtg., Mass. Inst. of Tech., Cambridge, Mass. (27-29 December 1971)
- PAYNE, R.
Fundamental Problems of the Double Layer at Mercury
Conf. on the Elec. Double Layer and Its Infl. on Electrode Proc., Univ. of Ky., Lexington, Ky. (10-12 September 1970)
- Specific Adsorption of Nitrate and Chloride Ions from Formamide Solutions*
Elec. Double Layer Soc. for Electrochem. Mtg., Bristol Univ., Bristol, Eng. (17-19 April 1972)
- Adsorption of Formamide, N-Methylformamide and Dimethylformamide on Mercury*
Symp. on Adv. in Electrochem. Sci., Colo. State Univ., Fort Collins, Colo. (30 June-1 July 1972)
- POPSIADLO, R. T.
An Objective Baseline for Flare Prediction
16th COSPAR Mtg., Madrid, Sp. (10-24 May 1972)
- PRASAD, B.
Structure of Strong Non-Linear Waves in Magnetoplasma with Applications to Space Environments
Phys. Colloq., Univ. of S. Fla., Tampa, Fla. (18-20 February 1971)
- Rayleigh and Raman Scattering of Large Amplitude Plasma Waves and Solar Radio Burst*
1972 Am. Astronom. Soc. Sol. Phys. Div. Mtg., Univ. of Md., Coll. Pk., Md. (4-6 April 1972)
- PRASAD, B., and SEN, H. K.
Kinetic Theory Investigation of Non-Linear Interaction of an Electron Beam with a Magnetoplasma
Plasma Phys. Mtg. of the APS, Wash., D. C. (4-7 November 1970)
- PRASAD, B., SEN, H. K., BAKSHI, P., and KALMAN, G. (Brandeis Univ., Waltham, Mass.)
Non-Linear Collisionless Plasma Waves and Intensity of the Electric Field of the Ionospheric Irregularities
1970 Symp. on Upper Atm. Cur. and Elec. Flds. ESSA, Boulder, Colo. (17-21 August 1970)
- RADOSEK, H. R.
Magnetohydrodynamic Oscillations and Currents (Problems, Solutions, and Conjectures)
- 1970 Symp. on Upper Atm. Cur. and Elec. Flds., ESSA, Boulder, Colo. (17-21 August 1970)
The Effect of Asymmetry on Toroidal Hydromagnetic Waves in a Dipole Field
Fall Ann. Mtg. of the Am. Geophys. Un., San Francisco, Calif. (6-9 December 1971)
- Hydromagnetic Waves and Eigenmodes of the Magnetosphere*
Ctr. for Sp. Res., Mass. Inst. of Techn., Cambridge, Mass. (29 February 1972)
- RUBIN, A. G.
Satellites to Forbidden Line in Helium
Plasma Phys. Mtg. of the APS, Wash., D. C. (4-7 November 1970)
- SEN, H. K., DUBS, C. W., and PRASAD, B.
Non-Linear Longitudinal Waves in a Hot, Collisional Magneto-Plasma with Applications to Ionospheric Irregularities
1970 Symp. on Upper Atm. Cur. and Elec. Flds., ESSA, Boulder, Colo. (17-21 August 1970)
- SEN, H. K., WHITE, M. L., and WYLLER, A. A. (Bartel Res. Fdn., Franklin Inst., Swarthmore, Pa.)
A Physical Mechanism for the Production of Solar Flares
14th Gen. Assem. of the IAU, Brighton, Eng. (18-27 August 1970)
- SHEA, M. A.
Changes in Neutron Monitor Response and Vertical Cutoff Rigidities Resulting from Secular Variations in the Geomagnetic Field
12th Intl. Conf. on Cosmic Rays, Univ. of Tasmania, Hobart, Tasm. (16-25 August 1971)
- SHEA, M. A., and SMART, D. F.
Computer Simulation of Neutron Monitor Response to an Anisotropic Flux of High Energy Solar Cosmic Radiation
52nd Ann. Am. Geophys. Un. Mtg., Wash., D. C. (12-16 April 1971)
- Calculation of Cosmic-Ray Trajectories for Palestine, Texas, USA—Cutoff Rigidities and the Origin of the Re-Entrant Albedo; Calculation of the Seasonal Dependency of Neutron Monitors to an Anisotropic Flux of Solar Cosmic Rays Propagating in the Ecliptic Plane; and Calculation of the Magnitude of the Daily Variation of Vertical Cutoff Rigidities and Associated Changes in the Neutron Monitor Response for Selected North American Neutron Monitors*
12th Intl. Conf. on Cosmic Rays, Univ. of Tasmania, Hobart, Tasm. (16-25 August 1971)
- Cutoff Rigidities and Re-Entrant Albedo Calculations for Palestine, Dallas, and Midland, Texas*
Am. Phys. Soc. Mtg., Wash., D. C. (24-27 April 1972)

- Prediction of the End of Solar Proton Events*
15th COSPAR Mtg., Madrid, Sp. (10-24 May 1972)
- SHEA, M. A., SMART, D. F., and TANSKANEN, P. J.
(Univ. of Oulu, Oulu, Finland)
Deductions Regarding the Propagation of Relativistic Protons in the Interplanetary Magnetic Field During the November 18, 1968 Solar Cosmic-Ray Event
2nd Eur. Symp. on Cosmic Rays: Modulation Effects, Amsterdam, The Neth. (31 August-4 September 1970)
- SILVERMAN, J., and YANNONI, N. F.
The Crystal Structure of 9-Dicyanomethylene-2,4,5,7-Tetranitrofluorene: Comparison with Two Related Fluorene Derivatives
Am. Crystallogr. Assoc. Mtg., Univ. of N. M., Albuquerque, N. M. (4-7 April 1972)
- SILVERMAN, J., YANNONI, N. F., KRUOKONIS, A. P., and SOLTZBERG, L. J.
Analysis of a Disordered Crystal Containing the Free Radical Perchlorodiphenyl-Methyl
ACA Sum. Mtg., Carleton Univ., Ottawa, Ont., Can., (16-22 August 1970)
- SMART, D. F.
Calculation of the Daily Variation of Cosmic-Ray Cutoff Rigidities at Ft. Churchill, Canada
12th Int'l. Conf. on Cosmic Rays, Univ. of Tasmania, Hobart, Tasmania. (16-25 August 1971)
- SMART, D. F., and SHEA, M. A.
Calculation of the Daily Variation of Cosmic-Ray Cutoff Rigidities at Ft. Churchill
52nd Ann. AGU Mtg., Wash., D. C. (12-16 April 1971)
Predicting the End of Solar Proton Events from Real-Time Data Observations
53rd Ann. Mtg. of the Am. Geophys. Un., Wash., D. C. (17-21 April 1972)
- SMART, D. F., SHEA, M. A., and TANSKANEN, P. J.
(Univ. of Oulu, Oulu, Finland)
A Determination of the Spectra, Spatial Anisotropy, and Propagation Characteristics of the Relativistic Solar Cosmic-Ray Flux on November 18, 1968
12th Int'l. Conf. on Cosmic Rays, Univ. of Tasmania, Hobart, Tasmania. (16-25 August 1971)
- VANCOUR, R. F., and HANSER, F., SELLERS, F. B.
(Panametrics, Inc., Waltham, Mass.)
Some Results of a Rocket Measurement of keV Electron Spectra in an Aurora Accompanied by a Magnetic Bay
53rd Ann. Mtg. of the Am. Geophys. Un., Wash., D. C. (17-21 April 1972)
- WARES, G. W., WOLNIK, S. J., and BERTHEL, R. O.
Shock Tube Absolute gf-Values for Fe I, and Temperature and Wavelength Errors in the Corliss and Bozman NBS Monograph No. 53 (1962)
14th Gen. Assem. of the IAU, Brighton, Eng. (18-27 August 1970)
Oscillator Strength Measurements for Fe I and Fe II
184th AAS Mtg., La. State Univ., Baton Rouge, La. (29 March-1 April 1971)
- WEBB, V. H., CART, and KATZ, L.
Proton Pitch Angle Distributions Measured During June 1968
52nd Ann. Am. Geophys. Un. Mtg., Wash., D. C. (12-16 April 1971)
- WESTON, E. B., (Opt. Phys. Lab.) WARES, G. W.
Some Effects of Molecules in Solar Phenomena
1972 Am. Astronom. Soc. Sol. Phys. Div. Mtg., Univ. of Md., Coll. Pk., Md. (4-6 April 1972)
- WHITE, M. L.
On the Production of Solar Flares
1972 Am. Astronom. Soc. Sol. Phys. Div. Mtg., Univ. of Md., Coll. Pk., Md. (4-6 April 1972)
- WOLNIK, S. J., BERTHEL, R. O., and WARES, G. W.
Oscillator Strength Measurements for Ti I and Ti II
187th Mtg. of the Am. Astronom. Soc., Univ. of Wash., Seattle, Wash. (8-12 April 1972)
- YANNONI, N. F.
Organic Photovoltaic Materials
Int'l. Colloq. on Solar Cells, Toulouse, France (6-10 July 1970)
- YANNONI, N. F., KRUOKONIS, A. P., and SILVERMAN, J.
The Crystal and Molecular Structure of Ferrocenylidene Malononitrile
ACA Sum. Mtg., Carleton Univ., Ottawa, Ont., Can. (16-22 August 1970)
- YATES, G. K., and KATZ, L., ET AL
Observations Aboard OV5-6 and OV1-19 Satellites
COSPAR Symp. on Nov. 1969 Solar Particle Event, Boston Coll., Chestnut Hill, Mass. (16-18 June 1971)
- YOUNG, P. S. (Miss. State Univ.) and FUKUI, K.
Density of Stopping α -Particles at SST Flight Level
Am. Phys. Soc. Mtg., Wash., D. C. (24-27 April 1972)
- ZAWALICK, E. J.
Micropulseation Spectra
63rd Ann. Mtg. of the Am. Geophys. Un., Wash., D. C. (17-21 April 1972)

**TECHNICAL REPORTS
JULY 1970 - JUNE 1972**

CARRIGAN, A. L., ED.

Geophysics and Space Data Bulletin,
Vol. VII, No. 2
AFCRL-70-494 (September 1970)

FILZ, R. C., ENGE, W. (Institut fur Reine und
Angewandte Kernphysik, Kiel, Ger.), and DAVIS, A.
(Franklin Pierce College, Rindge, N. H.)

*A Balloon Exposure of 30 M² of Corpuscular
Photographic Materials in Search of Super-Heavy
Cosmic Radiation*
AFCRL-72-0229 (6 April 1972)

HENDL, R. G., CAPT., PODSIADLO, R. T., and
CHISHOLM, D. A., ENGER, I. (Geomet, Inc., Rockville,
Md.)

*The Objective Construction of a Solar-Geophysical
Data Base*
AFCRL-71-0142 (26 February 1971)

HUTCHINSON, R. O.

(U) Project EGAD, *Exploratory Geophysical
Anomaly Detection (Secret)*
Air Force Surveys in Geophys. No. 233,
AFCRL-71-0221 (1971)

MANSON, J. E., and BENCH, P. M.

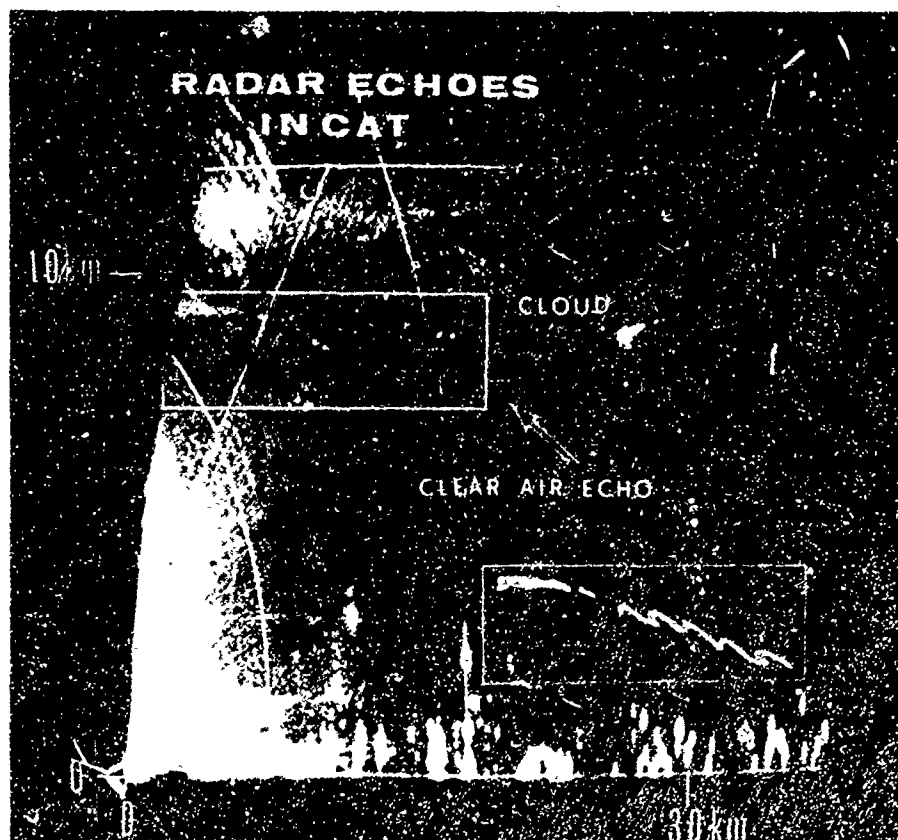
*Continuous Monitoring of Solar X-Rays
Part I. Development of a Program for
AWS Use With the Vela Satellite Data*
AFCRL-72-0140 (1 March 1972)

MC NULTY, P. J.

*Visual Sensations Induced by Relativistic
Muons*
AFCRL-71-0377 (9 July 1971)

ROTHWELL, P. L.

*Comparison of Electron Fluxes with the
Whistler Self-Excitation Limit During a
Magnetic Storm*
AFCRL-72-0036 (21 January 1972)



A portion of a long wave is detected at a height of about nine kilometers with a 16.7 cm radar at Wallops Island. The photograph and the inset show secondary waves or hollows superimposed on the principal wave. Aircraft turbulence at hollow height was reported as severe.

VI Meteorology laboratory



In spite of man's enormous strides in many fields of technology, much of his day-to-day activity continues to be significantly affected or restricted by the weather. The same is true of organizations like the Air Force. When we examine its mission and responsibilities, we are soon impressed with the impact of weather on its activities.

It is important that some Air Force systems be operable in virtually all types of weather. To accomplish this objective, the Air Force must act on two fronts. Its first responsibility is to design systems that are operable over a broad range of weather conditions. The second is to supplement these designs by modifications of the weather affecting the success of the operations. Of course, there are many other Air Force activities which can be delayed on the basis of a weather observation or a weather prediction. But whether the deficiencies are in data needed in design, methods for significantly modifying critical weather elements, or techniques for improving observations or predictions, the need for an Air Force program in meteorological research and development has been clearly established. The major responsibility for this program rests with AFCLR's Meteorology Laboratory.

During the period covered by this report the program of the Meteorology Laboratory included: research to improve short-term forecasting of terminal weather conditions; the modeling of large-scale atmospheric circulations; the definition of turbulent transport processes in the atmospheric boundary layer, and the application of data from meteorological satellites to analysis and forecasting. Also included

were research efforts to improve the forecasting and detection of clear air turbulence, the specification of high level winds through indirect sensing, and the exploitation of weather radar techniques in studies of thunderstorm development and motion and of attenuation in precipitation.

The Laboratory program in cloud physics included the development of techniques of warm fog dissipation and of cumulus augmentation to increase precipitation, research on the nature of thunderstorm electricity, and specification of the characteristics of precipitation fields in studies of the erosion of rockets.

Responsibility for the development of meteorological instrumentation for eventual use at weather stations of the Air Weather Service and at the Air Force's test ranges was transferred to the Meteorology Laboratory during this reporting period. The principal development items described in this report include instrumentation for measuring ceiling and visibility; equipment providing remote weather observations; a fog detecting radar, a lightning warning set; improved sensors for use in radiosondes, dropsondes, and rocketsondes; and improved sounding rockets, balloons, and systems to provide meteorological measurements to altitudes of about 100 km.

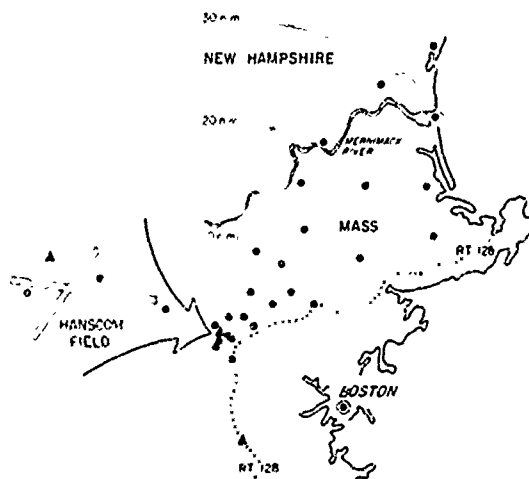
Although all the permanent quarters of the Meteorology Laboratory are located within 15 miles of L. G. Hanscom Field, Bedford, Massachusetts, climatic considerations and the existence of unique support facilities elsewhere led Laboratory scientists and engineers to conduct field programs at distant locations, ranging from Maine to California and Minnesota to Florida. Success in these experiments is due in large measure to the splendid cooperation and technical support and collaboration received from many Air Force, Army, Navy, National Oceanic and Atmospheric Administration, National Aeronautics and Space Administration, and Department of

transportation units and teams from Canada and the United Kingdom.

MESOSCALE WEATHER FORECASTING

"Ten degrees cooler in the suburbs." Such a phrase in the daily weather forecast is the most familiar example of the general fact that weather conditions are not always uniform, even within a small area. This phenomenon is known as mesoscale variability, and it can occur in time as well as in space. Few air travelers have escaped the frustration of stacking up over a terminal while landing traffic is slowed to a dribble because the runway ceiling and visibility are fluctuating above and below landing minimums.

Besides troublesome conditions at terminals, many of the meteorological obstacles to military activities are intrinsically mesoscale phenomena—severe local storms,



The AFCRL Mesonet. Solid circles denote locations of surface weather stations. Triangles denote locations of two towers, one at Hanscom Field, for observations up to a height of 275 feet, the other south of Hanscom Field, for observations up to a height of 850 feet.

hail, and violent winds, to name a few. An ability to predict the mesoscale variability of weather would add substantially to the safety and efficiency of a wide variety of military operations.

Unfortunately, the electronic computer that is supposed to be solving all of the forecaster's headaches does not even address the problem of mesoscale variability. Instead, it aims to predict merely the average weather conditions for a sizable area and interval of time. One reason for this is quite straightforward: even a computer can't forecast what it can't see! The conventional weather observing network consists of stations separated by distances of tens to hundreds of miles, reporting at intervals of 1 to 12 hours. Such a network simply cannot detect variations that occur on a scale of miles and minutes.

But suppose weather were observed on the mesoscale. Could it then be forecast on the mesoscale? One of AFCRL's newest research programs faces up squarely to this important question which has withstood all prior attacks. The question the researchers here specifically seek to answer is: What spatial and temporal density, of what kind of weather observations, leads to how much improvement in the predictability of short-period fluctuations in airport weather? Their approach is to establish a mesonet of observing stations with L. G. Hanscom Field, Bedford, Mass., as its focus, and to conduct a systematic program of forecasting experiments, the emphasis being on the zero to four-hour forecast.

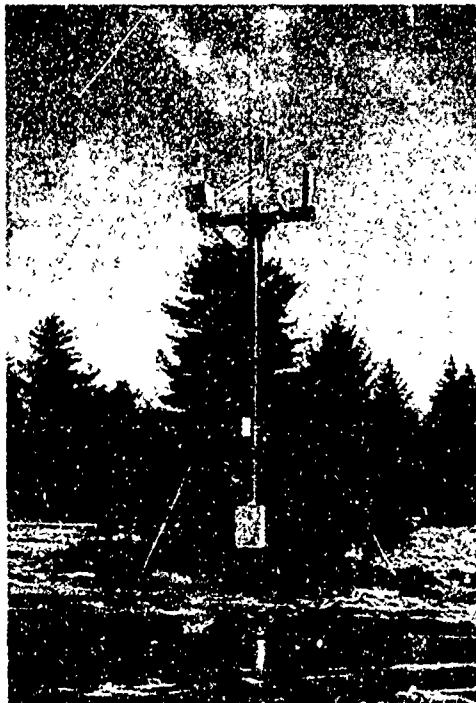
THE MESONET: For economy's sake the mesoscale observing network is confined to a 40-degree sector extending 35 miles to the northeast of Hanscom, the most frequent wind direction during periods of low ceiling and visibility. The basic net consists of 25 automatic stations, with separation ranging from 1/2 mile near Hanscom to 5 miles at the outer edge. These stations will

report visibility, wind direction and speed, temperature, dew point, and precipitation rate. In addition, vertical profiles of these measurements, except precipitation, will be reported from two towers, the taller of which provides data up to 850 feet. The other important features of the observing network are the two radars located at Hanscom. The FPS-77 surveys the entire mesonet and well beyond. The vertically pointing TPQ-11 provides a continuous record of cloud structure directly overhead.

The heart of the Mesonet is a computer, which controls operation of the entire system—collecting, processing, and displaying the data. It can scan all sensors in the network once every five seconds, and various modes of processing are at the command of the human operator. For example, the station data can be displayed as maps of either 1-minute or five-minute running averages.

THE STATIONS: Although the Mesonet sensors are not the standard instruments used by the weather services, they are all commercially available devices which were selected after careful testing and intercomparison. They are packaged in a rugged and weatherproof station mounted on a telephone pole at 25 feet above the ground. This design makes the station easily movable, reasonably vandal-proof, and readily accessible from a cherry-picker for maintenance. The station measures 4 by 4 by 6 feet with an 8-foot mast for the wind sensors.

The most radical departure from standard instrumentation is the device used to measure visibility. Conventionally, airport visibility is measured with a transmissometer which senses the extinction of light over a path of 500 feet or more. Because of its long path length this instrument is impractical for general use in the Mesonet. The search for a substitute converged on several promising candidates, which were extensively tested on the coastal fogs of



One of the Mesonet stations. The sensors, from left to right, measure visibility, wind direction and speed, temperature and dew-point, and precipitation rate.

Maine in the summer of 1970. One was found to give results that correlate well with transmissometer readings. This device senses the forward-scattered light from a path length of about 3 feet. To permit its further comparison with the standard instrument, three transmissometers are also positioned in the Mesonet.

The stations of the Mesonet are all linked to the central computer via conventional telephone lines.

THE RADAR: The FPS-77 is the same radar that is widely employed by the Air Weather Service, but here it has been provided with two novel capabilities. The controls of the radar are remoted to the forecast center, thus allowing the forecas-

ter himself to focus the radar on the sector and altitudes of his main interest. Also, the radar's output is fed directly into the computer, which produces in real time fully calibrated and range-normalized maps of echoes in true horizontal perspective. This contrasts with the conventional radar display (PPI) where the echoes are not normalized for range, and their altitude increases with range. PPI displays are also remoted to the forecast center, to serve as a yardstick for assessing the practical value of the constant-altitude PPI (CAP-PI) displays.

THE OPERATIONAL PLAN: Except for radar, the Mesonet is expected to be operational by February 1972. Radar will follow in about three months. Subject to limitations due to the size of the project's staff, the forecast center will be manned around the clock during periods of bad weather at Hanscom. Forecasts will be made for periods ranging from 15 minutes to three hours. Ideally, two forecasters will compete in these real-time experiments, one of them using conventional data, the other drawing also on the resources of the Mesonet.

Once a norm has been established for utility of the complete net, experiments will be conducted with fractional data to determine how forecasting performance depends on type and density of the mesoscale data.

Forecasting techniques to be tested initially are those generally conceded to be useful for short-period forecasting—persistence, extrapolation, and the like. It is reasonable to expect that with experience the project staff will begin to evolve novel techniques of improved performance.

Their general aim will be to develop not purely objective methods, but mixed methods which preserve the maximum useful role for the subjective skills and judgment of the experienced forecaster.

The ultimate goal of the program is to

assess definitively the practical value of automated radar and mesoscale observations of varying type and station density. It would be unrealistic to expect the Hanscom Field results to apply precisely to other locations with markedly different climatic or terrain characteristics. Nonetheless, the Hanscom experiments should establish guidelines of general validity.

ATMOSPHERIC MODELING

In many problems, particularly those involving small scale-sizes, the atmosphere is treated as a laboratory and is studied directly. For problems where the interplay of forces and processes from the entire global atmosphere must be considered, the prototype cannot be studied directly. Therefore, simplified systems must be constructed which can be studied under controlled laboratory conditions. These simplified atmospheric systems are known as atmospheric models and they have proved to be extremely useful in predicting the behavior of the complex prototype system. The application of wind tunnel experiments to the design of airfoils and entire airframes is well known. Although models of large-scale atmospheric flows have been investigated in fluid channels, we are concerned here with the use of mathematical models of the atmosphere.

All of the forces and processes operating in the atmosphere can be expressed in mathematical form in terms of time and space as independent variables. The time-dependent equations permit the prediction of a future state from some present or initially known state of the system. The distributions of the meteorological elements at some instant in time define the system. If we can construct a valid, independent equation for each of these elements, and if we know their distribution in space at some moment in time, then, in

principle, we can predict the state of the system for any time in the future. Furthermore, if the system of equations truly represents the important physical processes in the atmosphere, the future state of the model system should bear some relationship to the future state of the atmosphere itself. There are, however, three basic sources of error which cause the time development of the model to diverge from the time evolution of the real atmosphere. These sources of error are: errors in the observed initial state which include errors due to lack of resolution as well as instrumental errors; errors produced by the numerical approximations required for the solution of the system of equations, and errors arising from the inevitable inadequate representation of some of the relevant physical processes. All of these sources of error have interacting effects and degrade the quality of the prediction. However, AFCRL's efforts have been devoted primarily to improving numerical procedures and physical representation.

RESEARCH ON NUMERICAL PROCEDURES:

The current practice of all operational numerical weather prediction groups makes use of the space network approach in the solution of the system of equations which constitute the mathematical model. In this approach, observations of the dependent variables are interpolated onto a regular array of gridpoints in space, and differential quantities are represented in terms of finite difference approximations. Since the entire system of equations must be solved at each gridpoint before the variables can be extrapolated in time, the limits of the capacity of the computer and the time available for the forecast restrict the number of gridpoints in the network. Naturally, the fewer the number of gridpoints, the greater the growth of error due to truncation and lack of resolution. Therefore, it is vitally important, given the available capacity and speed of a computer, to use the

most rapid and efficient means of solving the system of equations. Greater efficiency of solution will permit finer resolution and increased accuracy, or, with the same resolution, will produce a saving in machine costs.

The operational large-scale model of the Air Force Global Weather Central (AFGWC) at Offutt AFB, Nebraska, makes use of a three-dimensional iterative procedure known as relaxation to obtain the predicted wind field. This procedure is costly in machine time and has therefore been a subject of study at AFCRL with the aim of improving the efficiency of solution.

By means of a simple modification of the model equations being used by AFGWC it is possible to simplify the method of solution and at the same time avoid the need for a three-dimensional relaxation. The method of solution permits a decoupling in the vertical so that a time-consuming three-dimensional relaxation is replaced by a series of much simpler two-dimensional relaxations—one for each level in the vertical. A number of test computations carried out at AFCRL have shown that this method of solution requires only one fourth the machine time as the conventional method, but produces essentially identical forecasts. Furthermore, the machine storage requirements are smaller; this feature by itself could result in a considerable improvement in efficiency. AFGWC is now carrying out its own tests of the new method of solution to determine whether or not it is feasible to employ it in operational analysis and forecasting.

The above procedure is geared to a non-rectangular domain of integration, such as the octagonal domain in which the AFGWC macro-scale model is solved. However, if the computational domain is rectangular and if we can assume that the map scale factor is a constant over this domain, it is possible to solve the trans-

formed system of equations directly—without the requirement for a series of two-dimensional relaxations. Such rectangular computational domains with constant map scale factor are suitable for AFGWC's fine-mesh, limited area model. Test computations in limited area rectangular domains have been carried out and have proven that the method of direct solution is not only feasible but results in an additional saving in machine time by about a factor of 2, thus reducing the machine time required in the conventional method of solution by a factor of 8.

MODELING OF OZONE DYNAMICS: A major aspect in the improvement of the physical reality of mathematical models lies in the incorporation of additional processes. Thus, although a dry atmospheric model may be adequate for predicting the broad-scale atmospheric circulation for one or two days in advance, it would hardly be adequate to predict cloudiness or precipitation. Since the Air Force operates at levels in the stratosphere where ozone is an important trace element and since AFCRL has had a long standing interest in ozone and stratospheric circulations, the Laboratory has designed a mathematical model to study the complex, nonlinear interactions among the relevant processes of ozone photochemistry, ultraviolet and infrared radiation flux-divergence, and atmospheric circulation. That these processes have important nonlinear interactions is clearly evident from the fact that in a static model, photochemical equilibrium predicts a maximum of ozone near the equator with a monotonic decrease toward the poles. Observations, however, show larger amounts of ozone at high latitudes than near the equator. Furthermore, because of its photochemical and radiative properties, ozone affects the temperature of the atmosphere, which in turn alters the circulation. The circulation not only affects the temperature distribution but through var-

ious transport mechanisms changes the ozone distribution. To complete the circle of interlocking effects we note that the reaction rates which control the photochemical production and destruction of ozone are temperature-dependent. To describe this process the AFCRL model contains equations governing the horizontal motion, mass continuity, the first law of thermodynamics incorporating radiation and ozone photochemistry, an ozone production and dynamics equation, and the hydrostatic equation. To simplify the computations, the system is transformed by averaging over longitude and parameterizing the stress terms. The vertical and north-south meridional wind components are combined into a stream function, which, with the remaining dependent variables of ozone and potential temperature, is determined at a network of 22 levels in the vertical (from the earth's surface to a height of 66 kilometers) and 18 points distributed in latitude from pole to pole.

Model calculations have been carried out for a variety of model states in time steps of two hours for periods of up to two years. It is found, not unexpectedly, that transport processes, with no diffusion, tend to increase the amount of ozone at high latitudes at the expense of the low latitudes, but are incapable of actually reversing the distribution. When eddy diffusion processes are incorporated, the calculated ozone distributions are much more realistic. The predicted ozone amounts at low latitudes are very close to the observed values. However, the high latitude amounts obtained from the model are too low.

The results to date indicate a number of improvements which should be made in the model. It is apparent that eddy diffusion is important, but a linear eddy diffusion is incapable of producing counter-gradient flux, which is probably necessary to explain the observed ozone distribution. Furthermore, the model is dry and photochem-

ical processes are known to be affected by water vapor. In addition, a major improvement can be made by designing a model with three full dimensions in space. With such a model it is not only possible to study the complex processes described above, but it becomes a relatively straightforward matter to determine the effects of atmospheric contaminants on the normal behavior of the stratosphere.

TREATMENT OF DIFFUSION BY LINEAR FILTERING: An important problem in numerical modeling of the atmosphere is that of adequately representing the sub-grid-scale atmospheric processes in terms of the larger-scale features which can be resolved by, and are explicitly treated by, the model's grid system. Although this problem is shared by all numerical models of the atmosphere, it is particularly important in extended range solutions with global models, the so-called General Circulation Models.

During the past year substantial effort was devoted to incorporating numerical filtering procedures as an integral part of large-scale numerical-dynamical models of the atmospheric circulation. These filtering procedures had recently been developed and used at AFCRL as a means of maintaining computational stability in numerical experiments. It was possible to show that the same procedures could be used very effectively to represent the physical process of atmospheric diffusion in numerical models.

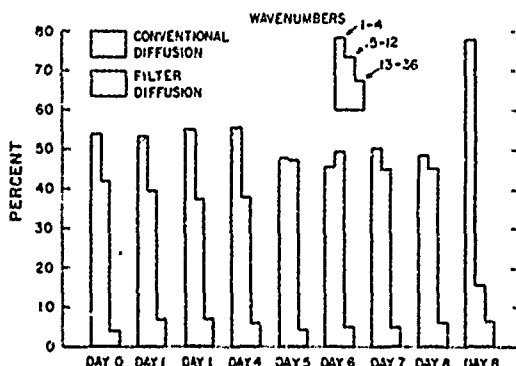
The principal difficulty with conventional representations of diffusion is that they damp the medium-scale eddies which in the atmosphere perform the important function of transferring energy from potential to kinetic. As a consequence, these models develop too much energy in the mean flow and very long waves. After about 30 model days, however, the model produces medium-scale waves. Although we see the development of cyclone wave

disturbances, the energy of the mean flow is unrealistically high as compared with the atmosphere's.

The filter was developed to permit a greater discrimination between the short waves which must be strongly damped and diffused and the medium scale waves which should remain relatively unaffected by the diffusion operator. This filter is based on the simple concept of first applying a smoothing operator which removes two-grid-interval waves and strongly damps three-grid-interval waves. The smoothing operator is then modified by a series of inverse operators which restore almost all of the amplitude damped by the smoothing at middle and long waves.

A test of the filter was carried out jointly with the Meteorological Office of the United Kingdom, Bracknell, England, to whom we are indebted for making their circulation model available and for their efforts in carrying out the integrations. The results of this test are summarized in a comparison of the integrations obtained with the filter with an earlier set of integrations in which the Meteorological Office's conventional nonlinear diffusion was employed.

In experiments with a two-level version



Mean energy spectra as a function of time when conventional and filter diffusion techniques were applied to the British Meteorological Office's model of the general circulation. The more realistic results obtained for the medium and long wave energy are very marked at the end of eight days.

of the British model, the spectral distribution of energy in the filter technique was compared with those in the conventional technique. The fraction of the total variance of the wind was calculated for each of three wave-number categories. Wave numbers 1-4 represented the very long planetary waves, wave numbers 5-12 the middle waves, and wave numbers 13-36 the short waves. Computations with both techniques started from the same initial data on day 0. As the computations proceeded, it soon became apparent that by day 8 conventional diffusion had produced a significant increase in the energy of the planetary waves at the expense of the energy of the middle waves. After only eight days, the model atmosphere, with conventional diffusion techniques employed, had lost the ability of the real atmosphere to maintain the important middle waves.

The integrations with the filter diffusion showed a completely different development. Between days 5 and 6 the middle waves actually had more energy than the long waves. After day 6, there was a tendency for the spectrum to return to the distribution shown on day 0, but there was still more energy in the middle waves than on day 0. This variation of energy in the middle waves is consistent with variations occurring in the real atmosphere. The results of this experiment clearly show conventional nonlinear diffusion damps the middle waves far too much, with the result that the model atmosphere after a relatively short time no longer resembles the real atmosphere, and filter diffusion maintains the important middle waves much as they are maintained in the real atmosphere.

ATMOSPHERIC BOUNDARY LAYER

When meteorologists refer to the atmospheric boundary layer, they may be refer-

ring to a fairly shallow layer of atmosphere extending from the surface to heights of about 50 to 100 meters. Or they may be referring to a much deeper layer extending from the surface to a height of about 1500 meters. The first layer, often referred to as the surface boundary layer, is one in which the wind velocity is determined by the vertical temperature gradient and the roughness of the underlying surface, while vertical transfers of heat, momentum, and water vapor are essentially constant with height. The deeper layer, usually called the planetary boundary layer, shows the effect of the earth's rotation in a turning of the wind vector with height, while vertical transfer rates of heat, momentum, and water vapor decrease with height.

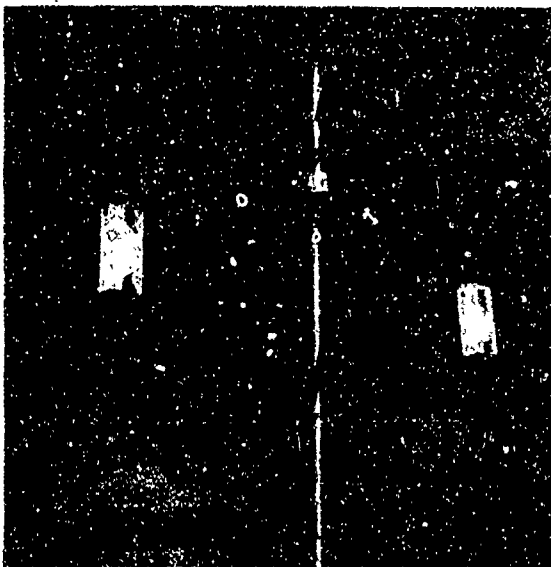
It is important to the Air Force that the structure and dynamics of these layers be understood since so many Air Force systems are operated within the planetary boundary layer and are thus dependent during the design stage and in eventual operation on the degree to which meteorological parameters in the lower atmosphere can be specified or predicted. But, in addition, many systems operating in the free atmosphere above the planetary boundary layer are dependent on weather forecasts, some of these for periods greater than 24 hours. For such forecasts to be improved, the numerical weather forecasting models used in operational forecasting must incorporate the effects of processes occurring within the planetary boundary layer.

EXPERIMENTAL RESULTS: One of the principal hypotheses formulated to describe atmospheric motions in the surface boundary layer is one which states that the vertical heat and momentum transfers, prevailing buoyancy, and height above the surface are sufficient to characterize the flow when steady-state and horizontally uniform conditions prevail. Experiments were conducted over the flat plains of

southwestern Kansas in 1968 to provide the data necessary for an examination of this hypothesis. The data included wind and temperature profiles to a height of 32 meters above ground, measurements of wind and temperature fluctuation at heights of 5.66, 11.23, and 22.6 meters, and direct measurements of the earth's frictional drag on the overlying atmosphere. Analyses of the data were on a wide variety of subjects within the general framework of the basic hypothesis, the objective being to relate average properties of the turbulent flow to a "universal" similarity parameter derived from the quantities mentioned above.

The analyses showed that the vertical transfers of heat and momentum were indeed constant with height within at least the first 32 meters, a demonstration which provided the basis for further applications of the similarity analyses. A derivation of expressions for wind and temperature profiles in terms of similarity coordinates was accomplished. A detailed analysis of each term in the equation expressing the budget of turbulent energy was completed, the result being the most complete description of the processes of turbulent energy production and dissipation to date. A similar budget was prepared for temperature fluctuations. A rational, systematic description of the spectral properties of the wind and temperature fluctuations was developed, suggested in large measure by the analyses of profiles and energy budgets concluded earlier. In summary, every analysis performed supported the basic similarity hypothesis. Thus, the Kansas field program has provided the first experimental evidence of the validity of the hypothesis.

The next step in the research program has been an extension of the region of interest to include not only the surface boundary layer but the remainder of the planetary boundary layer. In-house scientists elected to begin this effort by embarking upon a joint program with colleagues in the Meteorological Office of the United

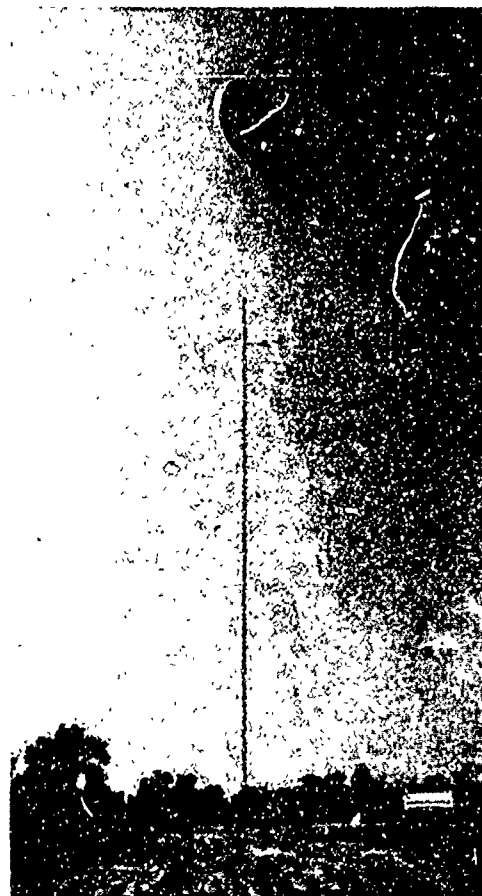


In a comparison test, AFCRL and BMO sensors were mounted on a mast at Eglin AFB. The AFCRL sensor is a three-component sonic anemometer with a fast-response platinum temperature sensor mounted near the rear post of the sonic. The British sensors consist of cups for measuring total wind speed, hot wires for wind inclination angle, and platinum wires for temperature. The wind vane keeps the British sensors continuously oriented into the wind.

Kingdom. The British scientists have developed a technique in which captive balloons are used to carry wind and temperature sensors to heights of several thousand feet. In 1969 and 1970 comparison tests were conducted in which the AFCRL and the British sensors were mounted side-by-side on a tower.

Since the tower tests showed a satisfactory matching of response characteristics, attention shifted to another area of concern. Since the British sensors were eventually to be mounted on the tethering cable, how significant is the motion of the sensor package induced primarily by the motion of the balloon? A field program was conducted at Eglin AFB, Florida, in September and October of 1971 to obtain the answer to this question. The AFCRL sen-

sors were mounted at heights of 500 and 1000 feet on a 1200-foot tower while the British sensors were flown close by at the same heights. Fifty experiments were conducted, each providing one hour of turbulence data. Detailed analyses of the two sets of experimental data have begun. However, preliminary results indicate that the British techniques are admirably suited for studies of the planetary boundary



Comparison experiments were conducted at Eglin AFB in 1971. AFCRL sonic anemometers were mounted at 500 and 1000 feet on the 1200-foot tower shown here. The British sensors were mounted at similar heights on the balloon tethering cable. The balloon is identical to the barrage balloons used over London during World War II and displays exceptional aerodynamic stability.

layer. The next phase in the joint program will be conducted at a new AFCRL field site in western Minnesota in 1973. There the AFCRL techniques will be employed in the surface boundary layer while the British techniques will be used in measurements of heat and momentum flux in the remainder of the planetary boundary layer.

AIR FORCE APPLICATIONS: In-house scientists have also been active within the past two years in a joint research program in laser propagation with scientists at Rome Air Development Center (RADC), Griffiss AFB, New York. The AFCRL role is to provide expertise on the subject of atmospheric turbulence, a feature of the atmosphere which affects the propagation of laser beams. The AFCRL responsibility is to provide experimental and analytical expertise for studying the important fine-scale temperature structure of the medium through which laser beams are propagated. The most significant outcome of this effort has been the demonstration that turbulence parameters pertinent to laser propagation theory can be derived from the micrometeorological data collected in Kansas in 1968, provided that the propagation path is horizontal and the overall area is reasonably homogeneous.

An interesting meteorological problem arises when it becomes necessary to know how meteorological measurements at one point of an Air Force base differ from simultaneous measurements made elsewhere on the same base. At Edwards AFB, California, where aircraft testing is done, it is important to know how wind and temperature affect test aircraft during take-offs and landings. But if these meteorological elements vary significantly along its 15,000-foot runway, then it may become necessary to have measurements made at a number of points. Such is the case at Edwards AFB. AFCRL scientists have assumed responsibility for the design,

procurement, and installation of a system which will provide simultaneous measurements of wind and temperature at a number of locations alongside the Edwards AFB runway. In order to determine the spacing between sensors, they conducted an experiment at Edwards in May of 1971, in which sensors were mounted at twelve positions along the test runway with separation distances ranging from a few feet to a mile. The objective was to find the correlations of wind and temperature as a function of separation distance. These correlations were then used to determine the optimum sensor spacing in the design of the runway meteorological system.

SATELLITE METEOROLOGY

In recent years the satellite meteorology program has been primarily concerned with the application of meteorological satellite data to the forecasting problems in Southeast Asia (SEA). This goal has been approached from two directions. The first is to improve the quality of the data received at local readout sites in SEA. The second approach is to develop improved forecasting techniques using satellite and conventional data sources. A third area of study is the interpretation and evaluation of Direct Readout Infrared (DRIR) data.

DIRECT READOUT DATA OPTIMIZATIONS: In the direct transmission mode a satellite broadcasts the data it is sensing in real time and the signal can be received and processed by an inexpensive ground system. At high priority sites, the Air Force has installed a more sophisticated, but still relatively inexpensive, photoprocessor to convert the signal into a picture. This system has the controls to compensate for variations in the range of signal in different satellites and sensing systems. Thus it contains the means of producing a high



A comparison of size of DRIR imagery before (right) and after (left) modification is shown. The actual width of samples is 2 3/4 and 5 1/2 inches. Dark areas are regions of high thermal emission and represent surface and low cloud features. Brighter areas are clouds. The atmospheric window between 10.5 and 12.5 micrometers is used to sense these thermal data.

quality image regardless of the characteristics of the signal.

At AFCRL, techniques were developed which considerably eased the task of adjusting the controls to produce an optimum picture. These techniques have been passed on to Air Force operational units by means of reports, training classes, and visits to sites in California and SEA. During the 1970-71 period, three consultant visits were made to SEA to install modifications to the Muirhead K300A/1 recorder, tune up the equipment, and train personnel in its operation, maintenance and calibration. A week-long training class was held in Taiwan for the forces in the Pacific area, and an installation was made at the Air Force Satellite Test Center in Sunnyvale, California.

The latest improvement to the system has been to expand the DRIR presentation

to a more convenient size. Because of the nature of the scanning system which senses the temperature data, the earth is intercepted during only about 33 percent of each revolution of the scanner. This results in an image 2 3/4 inches wide on the standard 8-inch paper. In-house scientists were able to increase the size of the image by doubling the speed at which the light source traverses the photosensitive paper and blanking out the unwanted half of each revolution of the scanner.

Aside from the convenience of being able to work with a larger picture, this modification also makes practical the extraction of quantitative temperature data from the picture. The shades of gray on the picture are proportional to the temperature of the emitting surface as indicated by a step-wedge that is transmitted in the signal. By virtue of the expanded picture it is possible to measure the gray shade with a densitometer and convert it to temperature over a representatively small area. Thus, even remote sites can have the advantage of quantitative black body temperatures of the features observed by the satellite.

SOUTHEAST ASIA STUDIES: The development and improvement of techniques for forecasting weather in SEA continued through 1971. Because forecasters assigned to this area were given brief tours, emphasis was placed on the development of objective techniques which would not require extensive training or experience. AFCRL studies concentrated on the forecasting of rainfall during the showery summer monsoon period. Under such circumstances rain gauges do not provide representative precipitation data. A more reliable estimate of the precipitation was derived from the area of a weather-radar scope covered with precipitation echoes. This radar index was related statistically to the cloud cover on the satellite picture, and a technique was developed to predict

the index 24, 48 and 72 hours following the acquisition of the satellite picture. Specifically, key areas were selected on the satellite picture in which the cloudiness was related to subsequent shower activity at Saigon, Pleiku, Udon and Ubon.

The skill of this technique was enhanced by including in the regression equations pressures and/or pressure gradients from key stations. In practice, the forecaster uses the satellite picture to estimate the average cloud amount in a 4 degree latitude by 4 degree longitude box in the key area for the particular station. The cloud amount, the pressures, and the pressure gradients are entered on a nomogram to arrive at the forecast radar index. The process takes two to three minutes. This technique demonstrated measurable improvement over climatological and persistence-type forecasts.

INFRARED STUDIES: Previous studies at AFCRL have disclosed that the assumption on which infrared thermometry is based,—that clouds emit as black bodies in the 11.5 micrometer band—does not apply generally to ice-crystal or cirrus clouds. Aircraft measurements disclosed values of emissivity ranging from 0.10 to 0.95 for cirrus clouds. This means that these clouds will transmit heat from below and will appear warmer to the radiometer than the temperature of their environment. In May of 1970 the opportunity arose to participate in a program to compare the temperatures of cirrus clouds as sensed by the satellite's 11.5 micrometer radiometer with those measured from an Air Force reconnaissance aircraft. The program ran into two difficulties. One was the inability to find optically dense cirrus outside of thunderstorm areas. The other was sporadic programming of the DRIR mode in the reconnaissance areas, which prevented collection of sufficient satellite data to perform a quantitative analysis of the temperature comparisons.

Nevertheless, interesting results were achieved by the experiment. The identification of cirrus clouds, even those barely detectable in satellite visual data, presents no problem in infrared imagery. Their shape and texture is easily recognizable as is their "brightness" when compared to other clouds in low and middle latitudes. However, except for cumulonimbus anvils and small patches, their temperatures are not representative of their altitude because of their emission characteristics.

Data collected on the aircraft flight of May 14, 1970 illustrate some of the difficulty in determining cirrus temperatures. The flight was conducted over the eastern Pacific, the northbound and southbound legs being at altitudes of 33,000 and 36,000 feet respectively. Wind conditions along the flight were variable, generally consisting of several layers of cirrus, the highest of which was above the aircraft even at 36,000 feet. At times these layers merged into one thick layer which obscured both the sky and water. Over the aircraft track, satellite-measured temperatures, based on



An aircraft track, in white, is superimposed on an 11.5 micrometer DRIR image. Satellite-measured temperature of cirrus cloud tops are shown in black numerals and are in degrees C. Aircraft-measured temperatures near or below cloud tops ranged from -51 to -58 degrees C. This shows that relatively dense jet stream cirrus cannot be treated as a black body.

the assumption that a cirrus cloud radiates as a black body, were between -41 degrees C and -43 degrees C while aircraft-measured temperatures were between - 51 degrees C and - 58 degrees C. Since the cloud tops were higher than the aircraft, their temperatures were even colder than the aircraft-measured temperatures. Thus we see that in the 11.5 micrometer band even relatively dense jet stream cirrus can emit at a temperature at least 15 degrees C warmer than the true cloud-top temperature.

Another important result of this aircraft experiment was the verification that another satellite IR sensor, the 6.7 micrometer radiometer, is capable of providing the basis for improving the temperature data sensed in the 11.5 micrometer band. The atmosphere contains extensive areas of very thin cirrus clouds. These clouds cannot be identified in the satellite video or 11.5 micrometer data and cannot be detected by the eye except at the very low viewing angles provided by an aircraft-based observation. The importance of these clouds is that they contribute errors to the temperature values sensed by the 11.5 micrometer radiometers. Therefore, the identification of these thin cloud areas in the 6.7 micrometer band will provide the basis for correcting the cloud-top and earth-surface temperatures under such clouds.

CLEAR AIR TURBULENCE (CAT)

American jet airliners still encounter severe turbulence some three to four times a month, and turbulence continues to be at least a contributing factor in about 20 percent of all aircraft accidents. During 1964-1969, turbulence was involved in 97 air carrier accidents, in which 228 persons were killed and five aircraft destroyed. For just one of these years, the direct cost of turbulence accidents exceeded \$18 million.

Accidents are not the entire story. While severe turbulence is encountered only about once every 35 million miles, airliners daily experience the lesser intensities of turbulence which extract penalties in such terms as efficiency and comfort. Military aircraft are at least as susceptible to the full range of turbulence problems. Even though passenger comfort *per se* is not a major consideration, turbulence of only modest intensity adds to fatigue of an airframe and can degrade the performance of the military crew member. Furthermore, a stable platform is essential to military operations such as aerial photography and mid-air refueling.

Clear air turbulence, which was responsible for more than one third of the accidents cited above, is the more insidious threat. Thunderstorm turbulence is unlikely to take an experienced pilot by surprise, even at night or when the convective cells are imbedded in general cloudiness. Airborne radar provides adequate warning in these cases. But for forewarning of CAT, a pilot can at present look only to forecasts or to reports from preceding flights. Because of the peculiar nature of CAT, neither source affords flawless warning.

Both the cause and the nature of CAT are still conjectural. Most likely, several mechanisms are individually capable of generating CAT, but Kelvin-Helmholtz (K-H) wave instability is thought to be the most common cause. This type of wave instability results from strong variations of the wind in the vertical occurring along thermally stable layers in the atmosphere. These stable layers, sometimes referred to as internal fronts, are relatively shallow layers in which the temperature is nearly constant or even increases with height. Therefore, one would expect CAT to be associated with both large vertical wind shear and strong thermal stability.

Regardless of the particular mechanism, all CAT appears to be a mesoscale phenomenon, characterized by space and time scales that are below the detection limit of

the weather observing network. This is why so much is still unknown about the nature of CAT and why forecasts of its occurrence are so limited in accuracy.

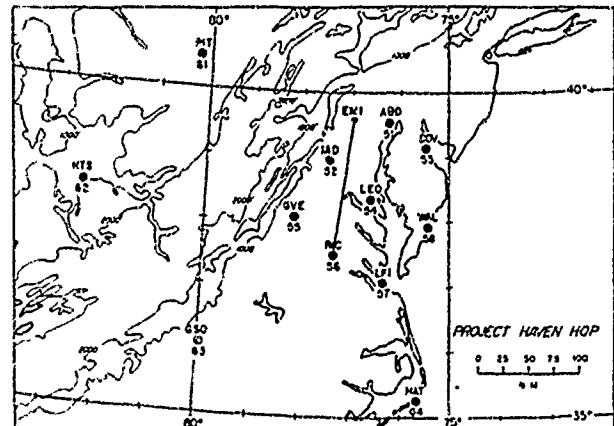
For some years now, AFCRL has been making a three-pronged attack on the CAT problem aiming to develop improved forecasting techniques and to explore the limits to which ground-based radar can detect CAT.

FORECASTING TECHNIQUES: The first step toward improved forecasting techniques is to identify and investigate the mesoscale atmospheric structures associated with the occurrence of CAT. Among other things, we must know what causes these structures to develop, their typical size, shape, and life cycle, and whether they can be predicted from standard weather observations.

Project HAVEN HOP was designed to provide such information. The field phase was conducted during a six-week period, beginning in January 1970, over an area in the vicinity of Wallops Island, Virginia, chosen for its proximity to appropriate radars.

The observational network consisted of eight mesoscale radiosonde stations surrounded by four synoptic scale stations. During operational periods, the mesoscale stations released rawinsondes every two hours and the peripheral stations every six hours, if needed. Turbulence was detected by RB-57 aircraft traversing the ground network at a succession of altitudes along a fixed ground track between Westminster, Maryland, and Richmond, Virginia. For the latter half of the six-week period, the aircraft were instrumented to record standard meteorological variables as well as turbulence.

Turbulence situations developed over the experimental network on 14 occasions during the field phase. Intensity was moderate or greater in about half of these cases. All told, more than 600 rawin soundings were made, and 80 hours of B-57 time



This network of radiosonde stations was used in Project HAVEN HOP. The line from Westminster, Maryland (EMI), to Richmond, Virginia (RIC), denotes the track of the RB-57 aircraft flown in the CAT study.

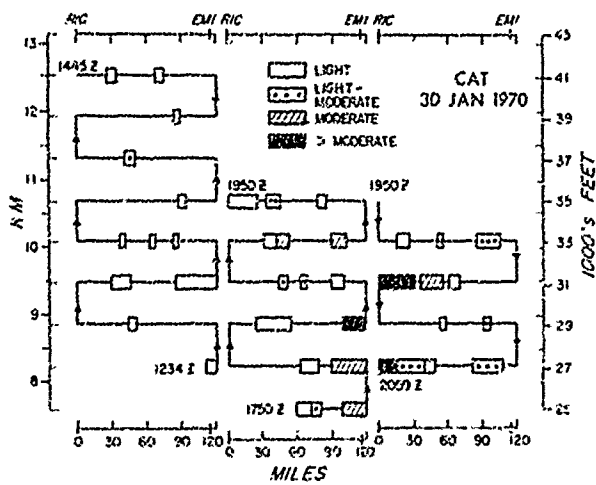
were logged, including some 35 hours with instrumented aircraft. Reduction of this enormous mass of data to a computer-compatible format has only recently been completed.

Although analysis of the 14 cases is not yet complete, certain conclusions have begun to emerge. Regions containing CAT often have a crosswind extent of 100 miles or more, but individual patches of moderate-or-stronger CAT seldom exceed 35 miles in width. A generally turbulent region may retain its identity for two to four hours, but the individual patch of CAT is much shorter lived. Consequently, while a forecast of the location of individual patches seems quite hopeless, there is promise that forecasts will be able to delineate successfully the general regions of CAT and to state the probability of encounter therein. CAT is associated with thermally stable layers containing strong vertical wind shear. The HAVEN HOP observations are consistent with the view, expressed earlier, that CAT is a manifestation of Kelvin-Helmholtz instability.

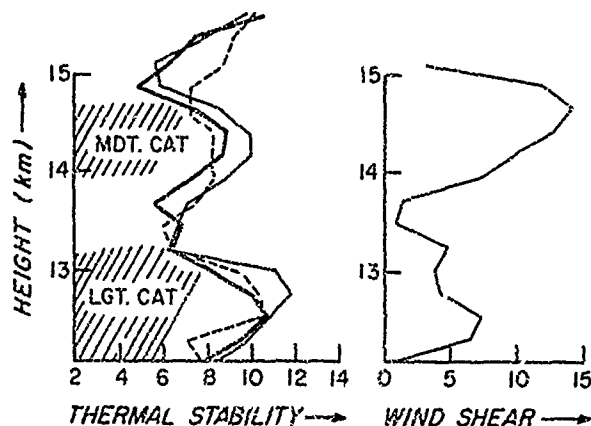
To test this hypothesis further, the field phase of HAVEN HOP II was conducted in northwest Texas in February-March

1972. Since the data for this purpose had to be more accurate and on a finer scale than in HAVEN HOP I, the observations incorporated some new features. The rawin soundings were made at intervals of 90, rather than 120 minutes, and the balloons were launched upwind of the tracking station to preclude loss of wind data when speeds were high.

RADAR TECHNIQUES: It was noted earlier that the choice of sites for HAVEN HOP I had something to do with radar. The particular radars are three exceptionally powerful and sensitive sets at Wallops Island which AFCRL, in a cooperative program with NASA, has been using since the mid-60's to study radar "angels"—the occasional echoes from clear air that have puzzled radar meteorologists for years. An early result was to prove that one class of angels is due to tiny point targets, such as insects, whereas another is due to inhomogeneities in the atmospheric field of micro-



Time and space variations of CAT are shown for three aircraft profiles. Each profile consists of a succession of horizontal passes at 2000-foot intervals over the fixed track, which was roughly perpendicular to the wind direction. The first aircraft, in its ascent, found little CAT. The second, in descent and decent a few hours later, found a number of areas with at least moderate CAT.



Height profiles of thermal stability at Dulles Airport (thin line), Leonardtown, Maryland (thick line), and Wallops Island, Virginia (dashed line), and of wind shear at Dulles Airport during a period of clear air turbulence are shown. Note that the CAT layers, moderate and light, are near the peaks in thermal stability and wind shear.

wave index of refraction. It seemed plausible that turbulence is the source of these inhomogeneities, but it was initially an open question whether this is turbulence in the aircraft sense, for the scale length of inhomogeneities that a radar sees is several orders of magnitude smaller than the wavelengths of turbulence that affect aircraft.

About five years ago, it was first verified at Wallops that an aircraft does experience turbulence when flying through a layer marked by the second class of clear-air radar echoes. Additional data have since been taken, particularly in 1969 and in 1970, the latter in conjunction with HAVEN HOP I. By now, the accumulated total of 763 simultaneous radar and aircraft observations has been fully analyzed, and the conclusions are definitive. All clear-air echo layers are turbulent to small jet aircraft of the fighter class, and on the other hand, not all turbulent regions are visible to radar. The strong CAT is the more likely to be detected by radar. Specific probabilities are shown in the following table:

Percentage of Observed CAT Detected by Wallops Island Radars During 1969 and 1970

CAT INTENSITY	ALTITUDE (km)				
	0.5-3	3-6	6-9	9-12	12-15
LESS THAN LIGHT	100	88	44	67	100
LIGHT OR GREATER	100	100	81	93	92

From the large number of detailed radar observations of CAT, it is clear that sensitive ground-based radars are reliable sensors of CAT regions. A ground-based CAT detection system is within the realm of present technology, although at present the system would probably be prohibitively expensive.

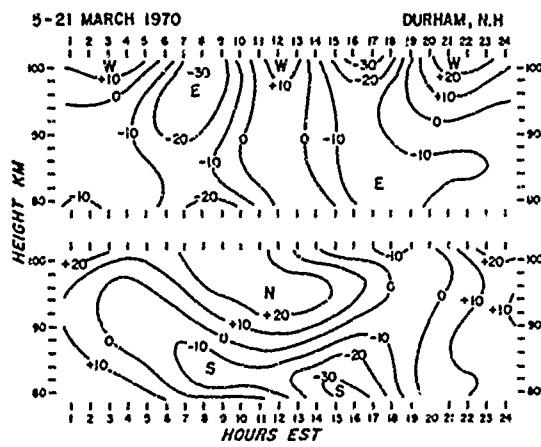
In addition to their use as CAT detectors, high power radars permit us to view or map a variety of wave structures in the clear air. Occasionally long waves are detected by such radars. The wavelengths may be a few tens of kilometers and the wave amplitude about one kilometer. From time to time, AFCRL scientists have detected large secondary K-H waves or billows occurring on the up slopes of long waves. The billows have wavelengths of about 1 kilometer and amplitudes of about 100 meters. Experience in AFCRL's CAT research program has shown that flight through these billows can be quite turbulent.

UPPER LEVEL WINDS

Meteors entering the earth's atmosphere leave ionized trails. One of the programs in the Meteorology Laboratory has been to observe these trails with radar to obtain information on wind variations in the 80 to 100 km altitude region.

The equipment development program was dominated by two requirements: automatic data reduction and unattended operations. Even though the second requirement was not fully met since full-time operation would require daily inspection and twice weekly preventive maintenance as well as tape changes, the Stanford Mark II set, developed by Stanford University in an AFCRL program, was recommended as an international prototype standard by Working Group 10 of the Inter Union Council on Solar Terrestrial Phenomena at the 1971 COSPAR meeting in Moscow. This success can be directly attributed to the philosophy of using an on-line computer in the initial AFCRL system and placing the computer as far forward in the system as possible so that changes in the system can be made by changing software (computer programs) rather than by changing hardware (tubes, circuits, etc.). The design experience gained from the AFCRL system was incorporated in the computerless, solid-state Stanford Mark II system.

A small beacon in satellite OV1-17 was used to calibrate the AFCRL set at Durham, New Hampshire, and the Stanford Mark II set at Eglin AFB, Florida. Interferometer techniques were incorporated into the AFCRL set by the University of New Hampshire to obtain height measurements. The beacon calibration showed that this method was more accurate than the method previously employed, and that all



An example of the mean diurnal horizontal wind field obtained by the AFCRL radar meteor trail set at Durham, New Hampshire, between March 5 and March 21, 1970. Altitude was determined by newly incorporated interferometer equipment, and the data reduction and analysis were done on AFCRL's central computer. Speeds are given in meters per second, and positive values are to the East and North.

of the calibrations could be made at ground level, thereby eliminating the need for future satellite-borne calibration beacons.

Meteor wind observations were taken at Eglin AFB during three periods when winds were also obtained from chemical trails released by rockets. The few observations obtained indicate that the two methods measure the same neutral wind of the atmosphere.

Winds at Stanford, California, and Durham, New Hampshire, reconfirmed previous results obtained at AFCRL and at other mid-latitude, northern hemisphere stations. Recent analyses at AFCRL show that there are rapid phase changes of the semi-diurnal wind component during periods near the equinoxes when the prevailing wind temporarily becomes easterly. During three separate periods the diurnal wind component rotated in a counterclockwise direction, indicating that there was a

downward propagation of energy from the thermosphere by the diurnal mode. In all cases the semi-diurnal mode propagated energy upwards and the sum of the propagation of energy by both the diurnal and semi-diurnal modes was always upward.

There are two methods of determining the height of the meteor return. The most accurate and difficult is to measure the range and elevation angle to the trail. The indirect method is to obtain the height from the rate-of-decay of the radar return of "underdense" trails. Since this technique is dependent on the validity of some unproved assumptions, these decay-heights should not be used on an individual basis. However, when monthly mean harmonic analyses by both methods were applied to data from the same set during the same month, they showed very similar variations with height. Hence, there is height information contained in the decay-rate of underdense trails. In particular, this means that simple radar meteor trail systems, which do not provide for measurements of range and elevation angle, may provide information on the climatological variation of the winds with height in the 80-100 km region.

WEATHER RADAR TECHNIQUES

The weather radar program at AFCRL is centered at two locations. The primary site is at Sudbury, Massachusetts, where work is focused on the observation of precipitation systems and on the development of better weather radar and display systems. Here, local thunderstorms and large convective systems are observed to learn more about their structure and dynamics and to deduce the fields of vertical and horizontal winds, wind variability, and moisture content. Four weather radars are in operation at Sudbury. Three of these, a 10-cm FPS-6, a 3.2-cm CPS-9, and an 0.86-cm TPQ-11,

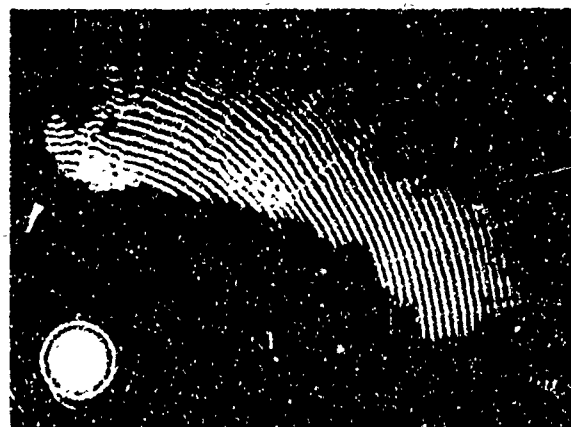
are standard radars although experimental modifications have been made to each. The fourth radar is a nonstandard radar, designated the Porcupine Doppler radar, and it provides information on the radial wind component. A fifth weather radar used by the Meteorology Laboratory is the FPS-77 located at L. G. Hanscom Field. The output from this radar will be processed digitally, and the information will be incorporated with other data in the Mesoscale Weather Forecasting Program, described elsewhere in this report.

The second site is located at Wallops Island, Virginia. The program at this site is sponsored jointly by AFCRL and NASA and is carried out with the help of the Applied Physics Laboratory, Johns Hopkins University. At the site are three high-resolution radars operating respectively at wavelengths of 71.5, 10.7, and 3.2 cm. Dish size for the first two is 60 feet, for the third, 34 feet. The very sensitive Wallops Island radars are used to investigate structures and phenomena in the clear atmosphere, the most important of these being clear air turbulence (CAT). Results utilizing these radars are included in the description of CAT research.

SEVERE THUNDERSTORM WARNING BY DOPPLER RADAR: The remote identification of tornadoes and other hazardous manifestations of severe thunderstorms is a task particularly well suited to Doppler radar, which can measure velocities of objects moving toward or away from the radar. Until recently, however, no convincing demonstration of this capability has been possible, because acquisition as well as processing of complex Doppler spectral information was much too slow for adequate surveillance of rapid developments in an array of thunderstorms. The job can now be done with the aid of a recently developed display technique called the Plan Shear Indicator (PSI).

The key to the PSI display is a sharing

of range and velocity information on the same radial coordinate. As the radar antenna rotates, the location of any precipitation echo is marked by a series of narrow concentric arcs, in distinction from the solid pattern of the conventional PPI. The arcs represent consecutive range gates spaced 855 meters apart. The distance of each arc from the center of the PSI display is the sum of a large term which corresponds to range, plus a small term, utilizing the normal allotment of space between arcs, which represents velocity. Consequently, a smooth, even-spaced pattern of narrow arcs indicates a homogeneous wind field throughout the storm echo, with no appreciable velocity gradients. A disturbed wind pattern, on the other hand, is easily recognized by the irregular appearance of its PSI arcs. They are wrinkled, indicating intense shear. Abnormal broadening of the



The plan shear indicator (PSI) display of the AFCRL meteorological Doppler radar at Sudbury, Massachusetts, shows a severe thunderstorm at a 9-degree elevation angle. The bull's-eye pattern in the lower left is side-lobe return from ground targets surrounding the radar. North is toward the top and east toward the right. The nearest edge of the storm echo to the north of the radar is at a range of 16 km and a height of 2.5 km. Disturbances in the wind field within the storm, indicated by sharp wrinkles in some arcs and enlarged widths of others, are especially prominent in the vicinity of the echo hole.

arcs indicates wind disturbance in the form of small-scale turbulence. The appearance of an echo hole is indicative of a pronounced disturbance.

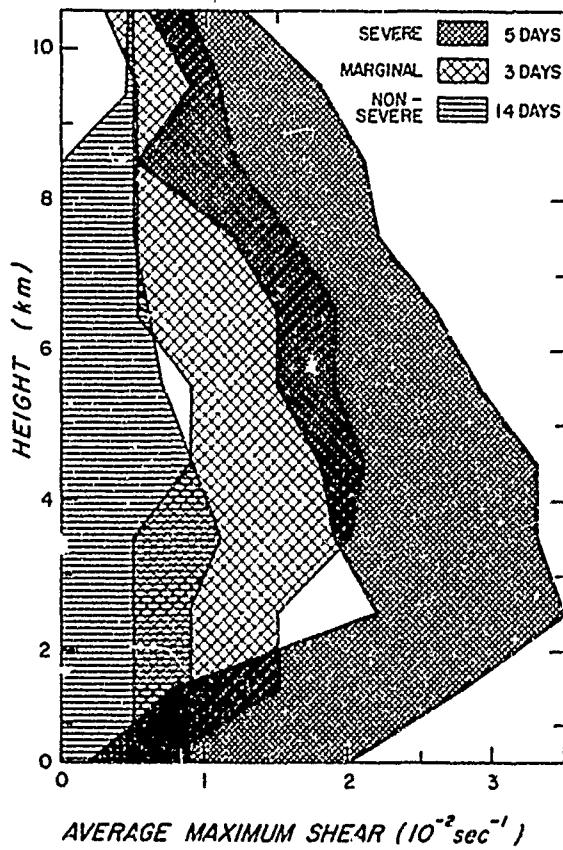
The PSI currently in use with the Laboratory's meteorological Doppler radar at Sudbury, Massachussets, obtains its velocity signals from a coherent memory filter. This is an analog device which produces waveforms representative of Doppler velocity spectra at all range gates in a small fraction of a second. In terms of a scanning antenna, the nearly simultaneous processing of spectra permits rotation of the antenna at speeds comparable to those employed with conventional storm surveillance radars (five or six revolutions per minute) without compromise of angular resolution beyond the limits imposed by the antenna beam width. Such speed enables the Doppler radar operator to monitor the entire volume of all storms surrounding the radar, except those passing overhead, once every three to five minutes, which provides plenty of opportunity to pick up any fast-breaking new developments in the velocity structure of the storms.

PSI records analyzed so far include 22 storm days during four summers. Five of the days were considered as severe storm days on the basis of reports of heavy wind damage or large hail. Three days were labeled "marginal" because the damage was only minor, or, if severe, had ceased in all storms before radar observations commenced. The remaining 14 storm days were considered to be clearly non-severe.

Disturbances in the wind field within storms are very easy to recognize on the PSI display, but not readily amenable to a complete description. In this preliminary study, a Doppler-sensitive vorticity parameter, maximum tangential shear, was selected for analysis. This parameter, defined as the gradient of Doppler velocity in a direction normal to this velocity, is proportional to the maximum slope of any arc

with respect to its tangent circle. Since it has high visibility on the PSI display and is quite easy to measure, it may be closely related to the manner in which the PSI eventually may be used operationally.

The maximum value of tangential shear was determined as a function of height for each sequence of storm observations. Averaging all observations on a given day yielded a characteristic vertical profile of maximum tangential shear for the day. There is a spread of values in the characteristic profiles within each of the three classes of storms, and the profiles demon-

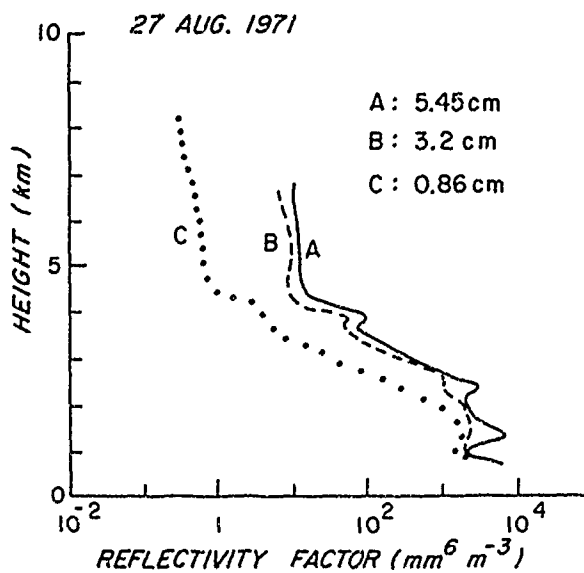


Vertical profiles are shown of the spread of maximum tangential shear, averaged over all Doppler PSI observations taken during each of 22 storm days, and categorized as severe, marginal, and non-severe.

strate a clear distinction between severe and non-severe days.

A detailed examination of the data showed that storms characterized by relatively smooth Doppler PSI patterns throughout their volume, with measured shear everywhere less than 10^{-2} sec^{-1} , were invariably free of damaging winds and large hail at the ground. High shear values were necessary but not, however, a sufficient condition for severe surface weather. At times a great deal of wind disturbance may exist aloft without manifesting itself at the ground. For this reason, the PSI display appears to be particularly well recommended as a technique to warn aircraft in flight against hazards to safe penetration of clouds which contain regions of disturbed wind field. There are preliminary indications also that the PSI technique, or equivalent alternative Doppler processing methods, may provide a warning of 40 to 60 minutes of the eventual descent of tornadoes or similar well organized damaging winds to the ground.

ATTENUATION IN RAIN: In recent years, the increased use of communication satellites and microwave links has emphasized the importance of the effect of intervening zones of precipitation on signal strength. Accurate measurements of attenuation in rain are difficult to obtain at a single wavelength. If the path is short so that the rain field can be considered homogeneous, the total attenuation between transmitter and receiver is generally small and the percentage error in measuring the attenuation coefficient is intolerably high. If, on the other hand, the transmission path is long enough so that the attenuation will be large compared with the error in power measurement, there will generally be fluctuations in rainfall intensity along the path length which are difficult to measure, and the correlations between attenuation and measured rainfall rate may be unrepresentative. Measuring drop-size distribu-



Height profiles of radar reflectivity taken sequentially at three wavelengths. The difference in reflectivity at each wavelength is a measure of the attenuation at each altitude.

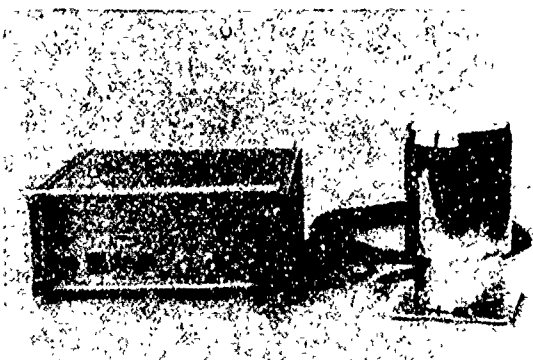
tions at the ground and computing the attenuation and rainfall rate theoretically from these distributions has the disadvantage that the results are valid only at a point and may not be applicable to the situation aloft.

Many of these problems have been overcome in an experimental program at the AFCRL Weather Radar site in Sudbury. The key to the program is the availability of radar observations at three wavelengths: 5.45, 3.2, and 0.86 cm. The three radars are pointed vertically, and observations of received power are obtained at altitude increments of 150 meters. The return signals are digitized, and processing is carried out on a computer. Because only incremental changes in the received power are considered, precise calibration of the radars is not necessary, provided the radar calibration remains constant over the interval of the measurements. Attenuation is obtained by appropriate comparisons of the received powers from one altitude to

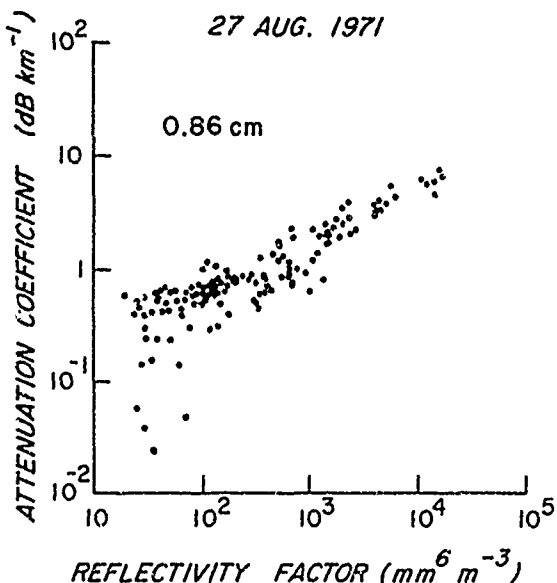
another and between different wavelengths. It is well known that attenuation is larger at the smaller wavelengths. The attenuation at 5.45 cm is generally less than the uncertainty in the power measurement and can be neglected. Thus, the measurements at three wavelengths yield the attenuation coefficients at 3.2 cm and 0.86 cm as functions of the radar reflectivity factor at 5.45 cm.

Measurements of drop size distribution at the ground are provided automatically by means of a distrometer. This device transforms the mechanical momentum of a raindrop impinging on the sensor into an electric pulse. Momentum is a function of size, so the number of electric pulses of each magnitude is a measure of the number of raindrops in each size interval. The distrometer results can be used to calibrate the 5.45 cm radar.

In addition to measuring radar reflectivity, the 5.45 cm radar has a Doppler capability which allows it to measure the velocity distribution of the raindrops. When the radar is vertically pointing, this velocity distribution can be converted to a size distribution, thus yielding the drop-size distribution as a function of height. In this



A raindrop distrometer. The momentum of a drop impinging on sensor (right) is converted to an electric impulse which is stored in the processor (left). Analysis of the number of impulses of each magnitude interval provides measurement of drop size distribution.



Reflectivity versus attenuation coefficient as measured by radar during a five-minute interval in moderate to heavy rainfall.

case, also, the distrometer measurements serve as a calibration of the radar data.

Future work will include a more detailed analysis of the drop-size distributions aloft and their relation to attenuation, and a statistical analysis of the relation between reflectivity and attenuation in several storm situations.

WARM FOG DISSIPATION

Ever since the early days of aviation, the presence of widespread areas of fog has severely limited air operations. In spite of the growth of fairly sophisticated technologies in the past 70 years, take-off, landing, and rescue operations in fog situations have remained hazardous, while the diversion of traffic due to fog has become more and more expensive. It is not surprising that scientists have sought to go beyond

the development of techniques of observing and forecasting fog to the development of fog dissipation techniques. By the mid-60's, researchers had provided operational methods of clearing cold fog, the term used to denote a fog made up of droplets at temperatures below the normal freezing point. The artificial dissipation of warm fog, however, has been a more difficult problem.

At AFCLR, three approaches have been followed in attempts to develop operationally useful techniques of dissipating warm fog. Most field experiments have been based on and have benefited from the calculations made with numerical models simulating the important physical processes involved.

HELICOPTER TECHNIQUES: By 1968, the fog-clearing capabilities of helicopters had been demonstrated by scientists of the Meteorology Laboratory in pilot experiments conducted at Eglin AFB, Florida, and Smith Mountain Lake, Virginia. In 1969, the laboratory performed a more extensive set of experiments at Lewisburg, West Virginia, in a joint program with the U.S. Army. The latter experiments were designed to provide quantitative information about the capabilities and limitations of the helicopter clearing technique. A report describing these experiments and conclusions was published in October 1970. It revealed that large helicopters were consistently capable of producing clearings with diameters ranging from 500 to 1500 feet when the depth of the warm radiation fog did not exceed 400 feet. Such clearings were suitable for helicopter landings. Moreover, it was shown that in certain wind and turbulence conditions, one or more helicopters can clear an airport runway 6000 feet long if the fog depth does not exceed 300 feet.

The Lewisburg data were investigated further to determine the climatology of radiation fog of the Appalachian type and



Helicopters were flown at Lewisburg, West Virginia, to clear a 6000-foot runway of warm fog. The swath was produced by a single CH-47 (Chinook) helicopter in a fog which was 125 to 150 feet deep.

to determine diffusion coefficients that were typical of the fog as helicopter-produced clearings filled following the cessation of active clearing efforts. The Laboratory has established the types of helicopter flight paths and the modes of flight which will provide the most effective clearing of an airport runway under varying conditions of wind speed, wind direction, and turbulent diffusion.

AIRBORNE HYGROSCOPIC PARTICLE SEEDING TECHNIQUES: During the past four years, the Meteorology Laboratory has been pursuing a research program to develop the technology for dissipating warm fog by airborne hygroscopic particle seeding. When hygroscopic particles such as pulverized salt are injected into a fog, they absorb water vapor from the air, thereby causing the fog droplets to evaporate. The approach has been to conduct an interactive program of field experimentation and computer modeling of the treatment effects.

The results of early experiments resulted, in particular, in the recognition of the importance of turbulent mixing on the effectiveness of the salt seeding and per-

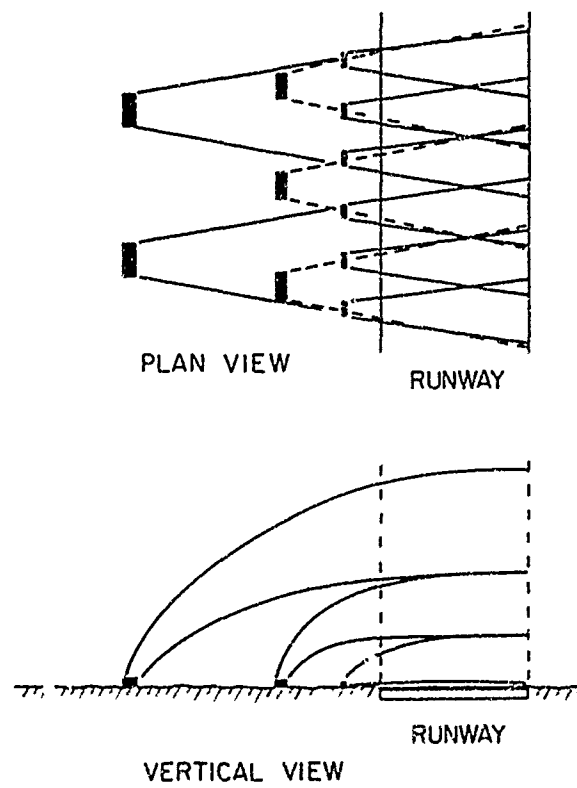
mitted it to be included in the model and treatment considerations. Field experiments to test the more realistic model were conducted on California valley fog in the fall of 1969. Good agreement was found between the model predictions and the results of these experiments. The technical feasibility of clearing warm fog by salt seeding from aircraft was established by these experiments.

Before proceeding with other experiments, Laboratory scientists used a computer model to evaluate the fog clearing capability of numerous, potentially effective hygroscopic materials. Since salt is corrosive to metals and detrimental to plant life, it is not practical for use in populated areas or over airport runways. Urea was found to be most practical since it is neither corrosive nor caustic; it is highly beneficial to plant life, and it is relatively inexpensive. Microencapsulation technology, in which dry crystals or solution droplets are chemically packaged inside thin, harmless coating shells, was exploited to provide for the sizing and stabilization of the otherwise friable urea particles, thereby optimizing its efficiency as a warm fog seeding agent.

Another series of field experiments was conducted at McClellan AFB, California during January of 1971 to investigate the practicability of using the microencapsulated urea particle seeding technique to improve the visibility in fog at an airfield to operationally useful levels. Although significant clearing of the fog was produced by the seeding, the lack of constancy of the wind field made targeting of the cleared zone a difficult problem. The technique cannot be employed reliably on an operational basis until satisfactory procedures for positioning the cleared area over the desired location are developed. More accurate wind information than is provided by currently used instrumentation is required to properly design warm fog dissipation operations. The use of area-wide

seeding patterns to overcome the targeting problem and to extend the usable lifetime of the clearings is being investigated.

GROUND-BASED HEATING TECHNIQUE: In the spring of 1971, the Laboratory undertook the development of a thermal fog dissipation system that is efficient, yet noiseless, smokeless, and safe for landing aircraft. In this technique, the temperature of the fog environment is raised by approximately 4 degrees F, supplying enough heat to evaporate the fog droplets and sustain the additional water vapor. The technical feasibility of the ground-based heating technique has been adequately



A conceptual schematic of the merging heat plume system of warm fog dispersal. By the time the heat from the individual burners is transported over the runway, the plumes have merged and the heat is nearly uniformly distributed.

ly demonstrated in the past. Thermal fog dissipation systems that have been developed to date, however, suffer from inefficient heat distribution and pollution, noise, and turbulence problems.

The thermal fog dissipation system being developed by this Laboratory is based on the controlled merging plume concept. In this concept, the fluid mechanics of bent-over heat plumes in a wind field is used to determine the intensity and the spatial distribution of burners that are required to produce a uniformly heated mass of clear air over a runway. The required heat is produced by burning a relatively clean burning fuel such as propane. A model is being developed to determine the burner intensities and spacings that are required to clear fog under various meteorological conditions.

A pilot-scale heating system which is capable of improving the visibility to at least 1/2 mile over a 400-foot length of runway is being designed. It will be tested at Vandenberg AFB, California, during July of 1972. The objectives of these tests are to demonstrate the feasibility of the controlled merging plume concept and to acquire data for designing and estimating the cost of a full-scale operational system.

CUMULUS CLOUD MODIFICATION

Techniques to modify cumulus clouds either to augment their growth and increase precipitation or to diminish their growth and decrease precipitation have been actively pursued as technical goals for more than 20 years. Today there is greater understanding of the basic physical processes involved, and the technologies of aerosol modification are more refined. In the past few years AFCRL scientists have investigated the potential for successful modification of both warm and cold cumulus clouds through modification experiments in the

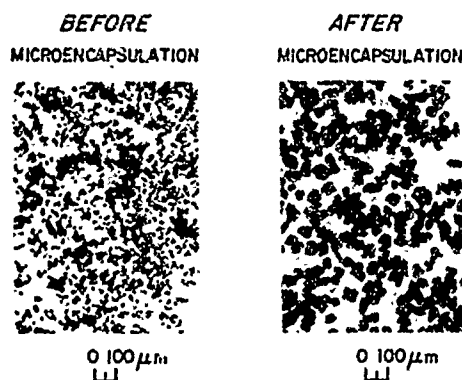
field and more recently through numerical modeling of cumulus evolution and of the effects of aircraft seeding. Recently conducted experimental and theoretical work on the modification of warm cumulus clouds is described in this section.

MODIFICATION EXPERIMENTS: In the 1950's AFCRL sponsored experiments conducted by the University of Chicago that showed positive statistical evidence that warm convective clouds can be modified when they are sprayed with water. The recent successful development of a technique of microencapsulating urea has encouraged AFCRL scientists to take another look at the potential for modifying warm cumulus clouds. The encapsulation technique has provided us with a new and effective class of seeding particles that are medium in size, have a narrow size distribution, are non-corrosive, and are easily handled.

Therefore, when AFCRL experiments in warm cumulus modification were conducted in September of 1971, the seeding material used was microencapsulated urea. Furthermore, though the chances of successful modification of maritime cumuli are somewhat less than for continental cumuli, the availability of air space over ocean areas led to the selection of an ocean location east of the Florida peninsula.

The seeding of cumuli was done on a random basis. Half the cloud sample on each day was seeded, while half served as controls. The urea was dispensed from an instrumented C-130 aircraft at the rate of 80 pounds per second from a dispenser filled with 1200 pounds of the agent. A contractor-operated light aircraft made measurements of updraft velocities beneath the cloud bases, of heights of cloud bases, and of raindrop size distributions when rainfall occurred. Since the life span of warm cumulus clouds and associated rain development appear to be strongly influenced by weak mesoscale circulations

AP-384 MICROENCAPSULATED UREA



The photographs show how microencapsulation provides a narrower size distribution of urea particles with a sharp lower size limit.

in the lower troposphere, photographs of the history of cumulus development were taken at an altitude of 45,000 feet, the platform being an RB-57F flown by an Air Weather Service crew.

Only after the analysis of all the data is completed will the scientists know which of the clouds were treated with urea and which were not. This procedure will help insure that the stratification of the experimental data on the basis of such parameters as cloud water content and cloud dimensions will be done objectively.

CUMULUS MODELING: Parallel to the experimental program is one in which mathematical-physical models of warm cumulus convection are constructed. The purpose of this numerical modeling has been to determine which processes affect the development of precipitation and to evaluate modification techniques based on alterations of the cloud droplet spectrum. The model, a time-dependent one, is basically one-dimensional, but is designed for continuity in two dimensions. When the cloud nucleus spectrum and the atmospheric sounding

are specified, the computation results in a cloud droplet distribution at the condensation level. The droplet spectrum continues to change with time as a result of condensation and coalescence processes at every level where condensate forms or to which droplets are advected. The combined physical and thermodynamic processes determine the eventual distribution of raindrop sizes as well as the ultimate cloud height. With respect to artificial cumulus modification, the model is also designed for studies of seeding effects. A spectrum of seeding nuclei can be inserted at any level and any time and the cloud growth calculated. Computer studies of this type will continue to aid us in designing and evaluating field experiments.

CLOUD PHYSICS

When we draw up a list of Air Force problems which depend for their solution upon meteorological research, we soon conclude that cloudiness, particularly when accompanied by strong turbulence, lightning, hail, and other large hydrometeors, is a subject which merits attention. In summarizing recent AFCRL progress in weather modification in the preceding sections of this report, we touched upon some of the cloud physics research conducted in the Meteorology Laboratory. But we also study the physics of cloud structure and dynamics to provide background data for improved techniques of weather observation and prediction as well as for better design of Air Force systems that are weather-sensitive.

THUNDERSTORM ELECTRICITY: Many modern aircraft and missile systems can be adversely affected by lightning and static electrical effects associated with clouds. Radomes and external stores may be des-

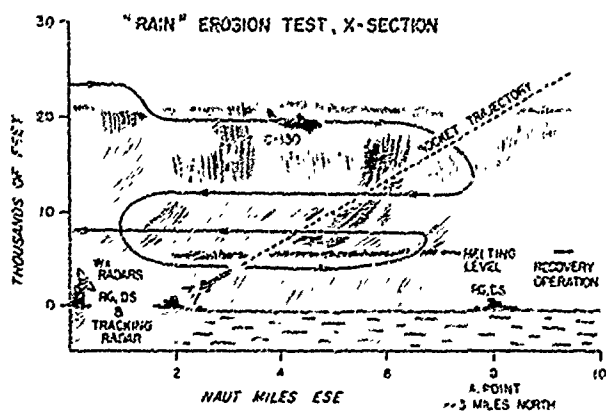
troyed in lightning strikes, while computers and navigational aids are known to fail when lightning and static electricity phenomena are present. Annual damages are sufficiently high to warrant a research program in electrical activity associated with cloud structures. The Laboratory's effort has been oriented toward techniques which will permit the pinpointing of regions within clouds where maximum electrical activity will be found and the formulating of guidelines and prototype instrumentation that will aid in in-flight avoidance of these zones.

A recent analysis of thunderstorm data collected in flights with instrumented aircraft showed that most of the lightning strikes to the aircraft occurred in transition zones where the electric field was changing from a positive-above-negative charge configuration to the reverse polarity. It was found that these changes generally occurred on the boundary of an intense negatively charged area. The latter area has a diameter of about 500 to 1000 meters. Its location and intensity are closely linked to the draft and precipitation patterns in the cloud, so there may be a number of such centers in an active storm. During the storm's development, these centers are well correlated with the areas of maximum echo intensity seen on an airborne radar set. Later on, however, the radar core disappears, but sufficient charge remains to constitute lightning hazard if the aircraft then enters the immediate area.

To be able to locate these regions and to follow the time history of the cloud-charging events, scientists are developing techniques in which data from electrostatic field and radio noise sensors will be presented in conjunction with radar echo patterns. If these efforts are successful, the results will be applicable to in-flight use as well as to the improvement of lightning warnings that are provided by the national

weather services for such locations as air bases and rocket launch facilities.

EROSION STUDIES: To what extent is a rocket eroded as it travels at supersonic speed through a field of raindrops or ice crystals? To answer this question, the Air Force's Space and Missile Systems Organization (SAMSO) has fired special instrumented rockets into precipitating clouds east of Wallops Island, Virginia. In support of this program, two teams in the Meteorology Laboratory have undertaken to provide a detailed definition of the particulates encountered by the vehicles. One team of radar specialists, employing the NASA-AFCRL radar facility at Wallops Island, has made quantitative measurements of radar returns from droplets and crystals in the region traversed by the rocket. The other team has flown in an instrumented C-130 aircraft and made measurements of the type, size, and number concentration of particles in the general area of the rocket's path both before and after the firing. The two sets of measurements have been studied for relationships between them. Such relationships will be useful in converting the radar



A schematic drawing of the erosion experiment. In addition to aircraft and radar sensors the array included recording rain gauges (RG) and sensors of raindrop size (PS).

return at launch time to the mass of material encountered by the rocket along its trajectory. In addition to the radar and aircraft data there were ground measurements made of drop size and rain rate. These data are used to calibrate the radar and serve as a check on the aircraft measurements.

METEOROLOGICAL INSTRUMENTATION

Members of the Meteorology Laboratory conducting research on the physical and dynamical nature of the lower atmosphere often find that they need special observations which, unfortunately, are not provided by the national weather services in their normal operations. So, as pointed out in earlier sections of this chapter, Laboratory scientists and engineers have had to develop research instrumentation to enable them to conduct their in-house studies.

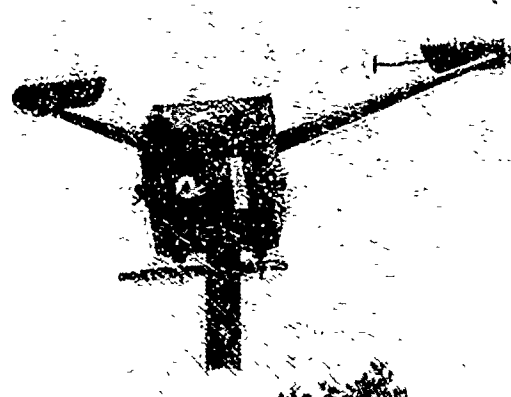
On the other hand, there are extramural requirements for instrumentation and data handling techniques. For example, the Air Weather Service, which provides weather information to operational commands and test ranges, has requirements for new or improved instruments to enable it to provide a better weather service. To meet such requirements, the Meteorology Laboratory conducts a program in which instrumentation is developed in the expectation that successful testing will be followed by procurements for operational use. The major elements of this development program are described in this section.

MEASUREMENT OF CEILING AND VISIBILITY: In spite of the fact that aviation has made enormous strides since the days of Kitty Hawk, the hazards presented by low ceilings and poor visibilities are still with us today, and the search for ever-improved

methods of measuring and displaying ceilings and visibilities continues.

In 1970, a study was initiated to obtain data on the light attenuation properties of fog from the backscatter signal of a pulsed neodymium lidar. The objective was to establish a theoretical and practical basis for measuring slant range visibility conditions for aircraft landing operations. Initially, single-ended lidar data were obtained along horizontal paths adjacent to a 500-foot baseline transmissometer. The atmospheric extinction coefficients derived from a consideration of the "slope" of the lidar traces were compared with the transmissometer data for a variety of low-visibility conditions. The results were encouraging. A correlation coefficient of 0.97 was found for these data. The investigation was expanded to obtain comparative measurements of atmospheric extinction coefficients over a slant range using the single-ended lidar and elevated reference targets. These measurements are currently being evaluated.

A visibility instrument has been developed that is based on measuring the fraction of projected light that is scattered in the forward direction. In comparison with the transmissometer, it is small, inexpen-



A prototype forward scatter instrument used for measuring horizontal runway visibility.

sive, does not have an alignment problem, and has significantly better resolution in low visibility conditions. Installed in a multiple configuration, these instruments will provide the more accurate and representative visibility information that is needed during periods of low visibility.

A ruby laser optical lidar was evaluated for use as a ceilometer. The lidar determines the cloud height by measuring the transit time of the laser pulse to the cloud and its return. This approach avoids the requirement for the extensive baseline of the standard rotating beam ceilometer (RBC) and thus could greatly simplify installation and maintenance. The system performed significantly better than the RBC. It measured clouds at a further range and detected visibility obscurations, such as pollutants trapped by an inversion, that the RBC could not "see." The ruby laser does, however, constitute an eye hazard which may preclude its routine use at airfields. Since other lasers, such as gallium arsenide and erbium, are considered eye safe, they are being investigated as possible candidates for use in a laser ceilometer.

EXPENDABLE, REMOTE-OPERATING WEATHER STATION (EROWS): In the late 1960s a program was begun to develop a system to fill the military requirement for obtaining measurements of basic meteorological parameters from remote areas where such data are not normally available or are sparse. Air-droppable automatic weather stations were developed which measure the wind speed and direction, temperature, dew or frost point, pressure, rainfall amount, and sky cover. The three other components of the total system used in conjunction with these basic EROWS units operate as follows: a control-recorder provides the means to interrogate and extract the meteorological data from one to ten EROWS units that constitute a deployed network of stations; a receiver-transmitter



An EROWS unit with its rotor blades collapsed above the battery case. The sensor package is on the top. The impact spear supports the unit. The aircraft repeater unit is shown on the left.

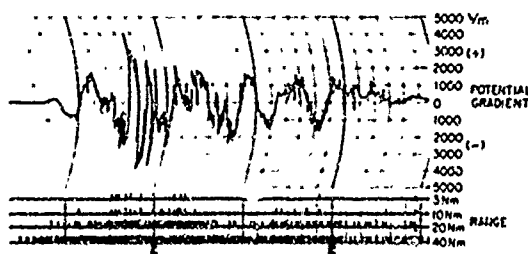
serves as an airborne repeater for the reception, amplification, and retransmission of all the radio signals between the deployed stations and the control-recorder, and a dispenser is used to launch the EROWS units from the delivering aircraft. The entire system was field tested during January 1972 at Cape Kennedy, Florida, and the basic feasibility of the system was demonstrated.

FOG DETECTING RADAR: In studying the effectiveness of fog dissipation techniques, it is often difficult in direct sensing with ground detectors to determine to what

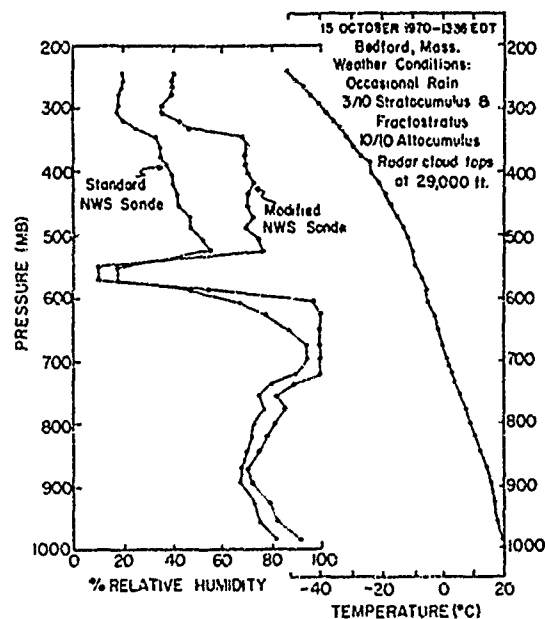
extent modification attempts have been successful. To enable Air Force personnel to make this determination, an experimental K_a band (0.86 cm) scanning radar that can detect the fog itself has been fabricated by modifying an AN/CPS-9 radar. This new set makes it possible to determine the changes that occur in the seeded area and track its motion. This radar has a very narrow antenna beam—0.3 degree—and uses an 0.5 microsecond pulse to provide high azimuthal and range resolutions. The short wavelength, the high transmitter power, and the enhancement of the receiver's signal-to-noise ratio by use of a signal integrator provides an optimum sensitivity for detection of small fog droplets. In addition to its anticipated usefulness in both warm fog and cold fog modification studies, this set provides a powerful probe for more detailed studies of clouds and fine scale atmospheric perturbations.

LIGHTNING WARNING SET: A lightning warning set has been developed for operational use on the Air Weather Service to enable AWS to determine the proximity of lightning or the presence of high electric fields that could be hazardous to refueling or munitions handling and which might cause damage to sensitive electronic equipment and computers. The set detects perturbations in the atmospheric electric field caused by lightning activity. By making use of an inverse range cubed relationship for signal amplitude and an assumption of an average change in electric moment for a cloud to ground stroke, we can determine approximate ranges to the lightning strokes. Because of the variabilities in lightning strokes and in propagation, the ranges determined have a statistical character. Ranges are presented using four range channels having thresholds set for ranges of 40, 20, 10, and 5 nautical miles based on the average change of electric moment. Finer calibrations of these thresholds are made using a weather radar

set to determine ranges to the nearest thunderstorm cell. A counter and a light are provided on each range channel to count and flash for each signal that exceeds the threshold and thus indicate how active the storm or storm complex is. In addition to the lightning ranging and counting function, the set uses a sensor with a rotating, slotted guard disc to alternately expose and shield the sensor (field mill) to determine the magnitude and polarity of the local electric field to provide a warning of hazardous conditions that may develop over the station. Both the electric field and the signals that activate each range channel are recorded to provide a graphic and easily assimilated presentation of the data. An alarm circuit is provided that can be set to operate at any given level of electric field to alert the user that a hazardous condition is developing. The criteria to be used for issuing warnings at a base will have to be determined locally since the motion and development of storms can be affected by orographic conditions or by large bodies of water. Besides, the time required to disseminate the warning and to secure threatened operations will play a large part in establishing local criteria. Tests of this equipment at Cape Kennedy during the summer of 1970 demonstrated the usefulness of the set in providing adequate warning time before the occurrence of lightning.



A Lightning Warning Set recording shows the approach and passage of two small active cells at Hanscom Field.



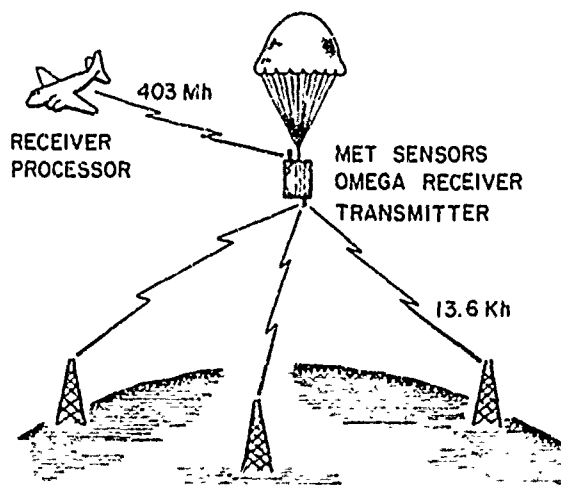
Relative humidity measurements made with the older National Weather Service sonde and with the newer, modified sonde are compared. The new sonde, with solar radiation errors greatly reduced, provides a sharper definition of cloud tops. Note the difference at about 600 mb.

RADIOSONDE/DROPSONDE/ROCKETSONDE SENSORS: A major portion of meteorological measurements made in the troposphere and lower stratosphere for Air Force use are obtained from radiosondes or dropsondes. The radiosonde is a small, lightweight instrument which is borne aloft by a balloon and which then measures the vertical profile of temperature, winds, pressure, and humidity, and telemeters the information to a receiver at the ground release site. The dropsonde is a similar package which is released from an aircraft, descends on a parachute, and telemeters similar information, with the exception of wind information, to the aircraft. The Meteorology Laboratory has sought to quantify the accuracy of the sensors involved and to improve accuracy

through the development of new sensors or new techniques of deployment and data processing.

These efforts have led to the discovery of errors as large as 40 percent in measurements of relative humidity obtained with the various radiosondes used by weather services in the United States. A patented redesign of the radiosonde case and the technique of mounting the humidity element has been completed. It has been shown in both laboratory and field tests that the greatest part of the error is eliminated with this new design. This new configuration is now being adopted for operational use by both military and civilian agencies.

The current-day dropsonde system does not have a capability of measuring the wind speed and direction beneath an aircraft. The principal reason for this is that the change in position and altitude of the aircraft with time is not known well enough for the aircraft to be used as a frame of reference to determine the motion of the dropsonde and, consequently,



An artist's conception of a wind-measuring system in which signals from Omega ground stations establish the geographical position of a dropsonde. Wind velocities are determined on a computer aboard the aircraft.

the wind field. A method of avoiding this difficulty has been under investigation at AFCRL. The technique is based on the use of navigational aids, such as Loran or Omega, the VLF navigation system accurate to 1 mile, to provide the geographical position of the dropsonde. Since Omega will have world-wide coverage by 1973, the AFCRL approach will be based on Omega signals.

First, a dropsonde is released from an aircraft. An antenna aboard the dropsonde receives signals from three Omega ground stations. These signals, together with data from the other meteorological sensors, are transmitted to a processor aboard the aircraft. The processor then provides the sonde's altitude from the pressure-temperature data as well as the sonde's geographical position. Wind velocities are then calculated in an onboard computer from the displacement of the package with time.

Above 30 km, one of the primary sources of atmospheric data is the sounding rocket. From 30 to 70 km, the meteorological sounding rocket constitutes the predominant source. The current meteorological rockets, ARCAS and LOKI, are soon to be replaced operationally by the Super-LOKI. This rocket employs a thermistor mount designed to minimize the spurious energy inputs which contaminated temperature measurements obtained with earlier operational sensors. Field testing of this sensor has demonstrated that it will reduce the temperature errors in the 30 to 60 km regime and that it will allow extension of the useful range of immersion thermometry techniques to 70 km.

SOUNDING ROCKETS: In the past year or so, a new and improved boosted dart meteorological rocket sounding system to obtain data above balloon altitudes has been successfully developed. The new system utilizes a 4-inch diameter Super-LOKI rocket motor and incorporates a family of three separate payloads. Two of these pay-



An AFCRL-developed transpondersonde, packaged in a dart sent aloft by a super LOKI rocket.

loads are of the telemetry type—a transmittersonde and a transpondersonde—both designed in-house at AFCRL. Both sondes are packaged in a 2 1/8-inch dart along with a 12-foot STARUTE retardation device. Temperature data are obtained from a 10-mil bead thermistor and wind data from a radar tracking the transmittersonde or the inherent ranging capability of the transpondersonde. The third payload, the ROBIN passive falling sphere, is packaged in a smaller 1 5/8-inch dart. The ROBIN sphere is used to obtain density and wind data from about 95 km down to 30 km when tracked by high precision radar.

The new Super-LOKI system with its transmittersonde, transpondersonde, and ROBIN payloads will replace the currently standard LOKI Dart-sonde, the ARCAS

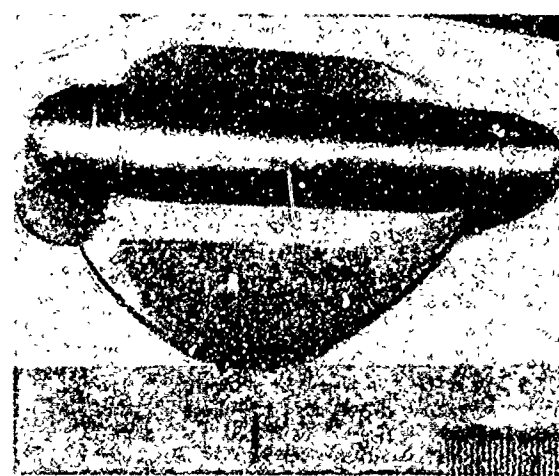
transpondersonde, and the VIPER-Dart-ROBIN systems, respectively. A very important advantage of the Super-LOKI system compared to current systems is one of economics; adoption of the Super-LOKI transponder and ROBIN configurations should result in considerable savings to the Air Force. Other significant advantages include a higher altitude capability obtainable with the telemetry payloads, 70-75 km compared to 60 km; greatly improved temperature accuracy, especially in the higher altitudes, resulting from the use of a new AFCRL-developed long wire technique of mounting the thermistor; improved meteorological data because of the slower fall rate of the new highly stable STARUTE; elimination of the need for expensive tracking radar support for the transponder payload, and simplification in handling, training, and operational procedures resulting from the use of a common rocket motor for all payloads. The R and D phases of the Super-LOKI system have been completed; the system is ready for production.

A somewhat larger meteorological rocket vehicle, the Astrobee D, was successfully evaluated for use in boosting larger,

more complex payloads to higher altitudes than are feasible with the LOKI Dart system. The relatively low-cost Astrobee D can carry payloads up to 25 pounds to a height of 130 km or more. However, the elimination of requirements for data in this altitude regime may preclude any operational utilization of this new vehicle.

SOUNDING BALLOONS: Efforts in the meteorological balloon area were concentrated on the development of improved and lower cost fast-rise balloons. Fast-rise balloons as radiosonde carriers reduce the amount of time required for a sounding, but, of more importance, they eliminate to a great extent rawin tracking errors resulting from the signal ground reflections which occur when tracking angles are low. Low angles are usually associated with high wind conditions, when the need for sensing accuracy is most important. A new fast-rise balloon, capable of attaining a height of 100,000 feet at an ascent rate of better than 1,500 feet per minute, was successfully developed and tested in temperate, arctic, and tropical climatic areas. This new fast-riser, consisting of one balloon inside of a smaller, lower modulus outer balloon, should be producible in quantity at a relatively reasonable price. High cost has been a major problem associated with previous attempts to develop fast-rise balloons.

SOUNDING SENSORS: The design and development of a new Advanced Meteorological Sounding System (AMSS) was undertaken several years ago to replace the obsolescent Rawin Set AN/GMD now in operational use. The AN GMD system, reflecting the state of the art of the late 1940's, cannot satisfy today's much more sophisticated data requirements and is becoming increasingly difficult to supply and maintain. The AMSS employs the latest technical advance in tracking, telemetry, data processing, and solid state component



The STARUTE is a retardation device carried aloft by a super LOKI. The sensor package is suspended below the STARUTE.

design. During the reporting period, fabrication of "bread-board" hardware, including a ground station as well as balloon and rocket radiosonde expendables, was accomplished. Successful flight tests demonstrated feasibility of the system.

JOURNAL ARTICLES JULY 1970 - JUNE 1972

BARAD, M. L., and IZUMI, Y.

Wind Speeds as Measured by Cups and Sonic Anemometers and Influenced by Tower Structure

J. of Appl. Met., Vol. 9, No. 6 (December 1970)

BARNES, A. A.

Temperature Sounding up to 2 Km: A Review of Techniques

Proc. of the Sec. Symp. on Met. Obsn. and Instmn., Am. Met. Soc., Boston, Mass. (27-30 March 1972)

Comparison of Winds Obtained by the Radar Meteor Trail and Chemical Release Methods

Proc. of the 53rd Ann. Am. Geophys. Un. Mtg., Wash., D. C. (17-21 April 1972)

BARNES, A. A., and MARSHALL, J. M., PETERSON, A. M. (Stanford Univ., Stanford, Calif.)

A Combined Radar-Acoustic Sounding System

Appl. Opt., Vol. 11 (January 1972)

BERKOF SKY, L.

Tropospheric Wave Motions with Baroclinic Basic Flow in Equatorial Latitudes

Tellus (June 1972)

BZRKOF SKY, L., and GYOERI, S.

A Comparison Between Total Ozone as Measured by NIMBUS III and That Computed from a Numerical Model

Sp. Res. XII (January 1971)

BOUCHER, R. J., and OTTERSTEN, H.

Doppler Radar Observation of Wind Structure in Snow

J. of Appl. Met., Vol. 10, No. 2 (April 1971)

BROUSAIDES, F. J., and MORRISSEY, J. F.

Temperature Induced Errors in the ML-476 Humidity Data

J. of Appl. Met., Vol. 9, No. 5 (October 1970)

Improved Humidity Measurements with a Redesigned Radiosonde Humidity Duct

Bull. of the Am. Met. Soc., Vol. 52 (September 1971)

BUNTING, J. T., and CONOVER, J. H.

On the Accuracy of a Precipitation Coverage Index Computed from Radar Reports

J. of Appl. Met., Vol. 10, No. 2 (April 1971)

DONALDSON, R. J., JR.

Vortex Signature Recognition by a Doppler Radar

J. of Appl. Met., Vol. 9, No. 4 (August 1970)

Mapping a Thunderstorm Anvil Flow by Doppler Radar

J. of Appl. Met., Vol. 9, No. 6 (December 1970)

DYER, R. M.

A Method for Filtering Meteorological Data

Mo. Wea. Rev., Vol. 99, No. 5 (May 1971)

Operational Comparison of Meteorological Measurements and Missile-Tracking Radio Interferometer Noise

Rad. Sci., Vol. 6, No. 12 (December 1971)

FAUCHER, G. A., and MORRISSEY, J. F.

Atmospheric Density Measurements in the 70-115 Km Region

J. of Geophys. Res., Vol. 76, No. 18 (26 June 1971)

HAFFORD, W. W., and LEVITON, R. E.

General Concepts in Rawin Systems

Met. Monographs, Vol. 11, No. 33 (October 1970)

HARDY, K. R., and REED, R. J., PROF. (Univ. of Wash.)

A Case Study of Persistent, Intense Clear Air Turbulence in an Upper Level Frontal Zone

J. of Appl. Met., Vol. 11, No. 3 (April 1972)

HAUGEN, D. A., KAIMAL, J. C., and BRADLEY, E. F. (CSIRO, Canberra, Aust.)

An Experimental Study of Reynolds Stress and Heat Flux in the Atmospheric Surface Layer

Qtr. J. of the Roy. Met. Soc., Vol. 97, No. 412 (April 1971)

KAIMAL, J. C., and BUSINGER, J. A.

Case Studies of a Convective Plume and a Dust Devil

J. of Appl. Met., Vol. 9, No. 4 (17 August 1970)

KAIMAL, J. C., and HAUGEN, D. A.

Comments on "Minimizing the Levelling Error in Reynolds Stress Measurement by Filtering"

J. of Appl. Met., Vol. 10, No. 2 (April 1971)

KEEGAN, T. J.

An Evaluation of Direct Infrared Data

Mo. Wea. Rev., Vol. 100, No. 2 (February 1972)

- KUNKEL, B. A.
Fog Drop-Size Distributions Measured with a Laser Hologram Camera
J. of Appl. Met., Vol. 10, No. 3 (June 1971)
- KUNKEL, B. A., and SILVERMAN, B. A.
A Comparison of the Warm Fog Clearing Capabilities of Some Hygroscopic Materials
J. of Appl. Met., Vol. 9, No. 4 (August 1970)
- MUENCH, H. S.
Temperature Measurements in the 30-40 Km Region
Mo. Wea. Rev., Vol. 99, No. 2 (February 1971)
- NELSON, L. D.
A Numerical Study on the Initiation of Warm Rain
J. of the Atm. Sci., Vol. 28, No. 5 (July 1971)
- OTTERSTEN, H., and EKLUND, F. (Res. Inst. of Natl. Def., Stockholm, Swed.)
Fjärranalys med Radiovagor (Radio Remote Sensing)
Forskning och Framsteg (Res. and Prog.), No. 3 (1970)
- PLANK, V. G., SPATOLA, A. A., and HICKS, J. R. (U. S. Army Cold Reg. Res. & Eng. Lab., Hanover, N. H.)
Summary Results of the Lewisburg Fog Clearing Program
J. of Appl. Met., Vol. 10, No. 4 (August 1971)
- SHAPIRO, R.
Surface Pressure Variations in Polar Regions
J. of Atm. Sci., Vol. 27, No. 7 (October 1970)
The Use of Linear Filtering as a Parameterization of Atmospheric Diffusion
J. of the Atm. Sci., Vol. 28, No. 4 (May 1971)
A Simple Model for the Calculation of the Flux of Solar Radiation Through the Atmosphere
Appl. Opt., Vol. 11, No. 4 (April 1972)
On the Response of the Lower Atmosphere to Solar Variability
Proc. of the Symp. on Sol. Corpus. Eff. on the Tropos. and Stratos. (Under Ausp. of IUCSTP/June 1972)
- SILVERMAN, B. A.
Weather Modification
McGraw-Hill Yrbk. of Sci. and Tech. (1972)
Warm Fog Modification by Airborne Hygroscopic Particle Seeding
Ph. D. Dissertation, Univ. of Chicago, Ill. (March 1972)
- SILVERMAN, B. A., and NELSON, L. D.
Optimization of Warm-Cloud Seeding Agents by Microencapsulation Techniques
Mo. Wea. Rev., Vol. 100, No. 2 (February 1972)
- WEINSTEIN, A. I.
Ice-Phase Potential for Cumulus Cloud Modification in the Western United States
J. of Appl. Met., Vol. 11, No. 1 (February 1972)
- WYNGAARD, J. C.
The Effect of Velocity on Temperature Derivative Statistics in Isotropic Turbulence
J. of Fluid Mech., Vol. 48, Part 4 (27 August 1971)
Spatial Resolution of a Resistance Wire Temperature Sensor
Phys. of Fluids, Vol. 14, No. 9 (September 1971)
- WYNGAARD, J. C., and COTE, O. R.
The Budgets of Turbulent Kinetic Energy and Temperature Variance in the Atmospheric Surface Layer
J. of Atm. Sci., Vol. 28, No. 2 (March 1971)
- WYNGAARD, J. C., COTE, O. R., and IZUMI, Y.
Local Free Convection, Similarity, and the Budgets of Shear Stress and Heat Flux
J. of the Atm. Sci., Vol. 28, No. 7 (October 1971)
- WYNGAARD, J. C., IZUMI, Y., and BUSINGER, J. A. (Univ. of Wash.), BRADLEY, E. F. (CSIRO, Canberra, Aust.)
Flux-Profile Relationships in the Atmospheric Surface Layer
J. of Atm. Sci., Vol. 28, No. 2 (March 1971)
- WYNGAARD, J. C., IZUMI, Y., and COLLINS, S. A. (Ohio State Univ.)
Behavior of the Refractive Index Structure Parameter Near the Ground
J. of the Opt. Soc. of Am., Vol. 61, No. 12 (December 1971)
- WYNGAARD, J. C., and PAO, Y. H. (Flow Res., Inc., Kent, Wash.)
Some Measurements of the Fine Structure of Large Reynolds Number Turbulence
Statist. Models and Turb. Lect. Notes in Phys., Springer-Verlag, Berlin, Vol. 12 (1972)
- WYNGAARD, J. C., and TENNER, V. H. (Penn. State Univ.)
Measurements of the Small-Scale Structure of Turbulence at Moderate Reynolds Numbers
The Phys. of Fluids, Vol. 13, No. 8 (August 1970)
- YANG, C. H., and STEINBERG, H. L., WIN-NIELSEN, A. (Univ. of Mich.)
On Nonlinear Cascades in Large-Scale Atmospheric Flow
J. of Geophys. Res., Oceans and Atm., Vol. 76, No. 36 (20 December 1971)

YEE, S. Y.
Comment on a Direct Numerical Solution to a One-Dimensional Helmholtz Equation
J. of Comp. Phys., Vol. 6, Iss. 2 (October 1970)
An Efficient Numerical Scheme for a Baroclinic Quasi-Geostrophic Model
J. of Comp. Phys., Vol. 9, No. 3 (June 1972)

**PAPERS PRESENTED AT MEETINGS
JULY 1970 - JUNE 1972**

BARNES, A. A., JR.
Temperature Sounding Up to 2 Km: A Review of Techniques
2nd Symp. on Met. Obsn. and Instrmn., San Diego, Calif. (27-30 March 1972)
Comparison of Winds Obtained by the Radar Meteor Trail and Chemical Release Methods
53rd Ann. Mtg. of the Am. Geophys. Un., Wash., D. C. (1-21 April 1972)

BERKOF SKY, L., and GYOERI, S.
The Interaction Between the Ozone and the Circulation in the Upper Atmosphere
Intl. Conf. on Met., Tel Aviv Univ., Isr. (30 November-4 December 1970)

BORRESEN, J. A.
Use of Doppler VAD-Pattern to Detect Shear Zones and Turbulence in a Snowstorm
14th Rad. Met. Conf., Tucson, Ariz. (17-20 November 1970)

BOUCHER, R. J.
Mesoscale Meteorological Structure During Radar CAT Detection
14th Rad. Met. Conf., Tucson, Ariz. (17-20 November 1970)
Shear-Induced Atmospheric Turbulence: Analysis of Simultaneous Radar, Aircraft and Meteorological Observations
1971 AFSC Sci. and Eng. Symp., Dayton, Oh. (5-7 October 1971)

BOUCHER, R. J., and GLOVER, K. M.
Radar, Aircraft and Meteorological Observations of Shear-Induced Turbulence
Intl. Conf. on Atm. Turb., London, Eng. (18-21 May 1971)

BUNTING, J. T.
Time Series Analysis of Summer Monsoon Data Over Southeast Asia

7th Tech. Conf. on Hurricanes and Trop. Met., St. Michael, Barbados, W. I. (6-9 December 1971)

CHMELA, A. C.
Propagation of the Severe Convective Storm from Doppler Observations
14th Rad. Met. Conf., Tucson, Ariz. (17-20 November 1970)

CHURCH, J. F., LT. COL.
Airborne Meteorological Sensor Development Within the United States Air Force
1971 IEEE Mtg. on Oceanog. and Atm. Tech., Wash., D. C. (6-8 October 1971)
Atmospheric Corrections for Airborne Radiation Thermometers
Conf. on the Interaction of the Sea and the Atm., Ft. Lauderdale, Fla. (1-3 December 1971)

CHURCH, J. F., LT. COL., and PRICE, R. M.
An Expendable, Remote-Operating Weather Station (EROWS)
IEEE Intl. Geosci. Electron. Symp., Wash., D. C. (25-27 August 1971)

CONOVER, J. H.
Part I. Studies of Clouds and Weather Over Southeast Asia
Part II. AFCRL and Current Work in the Meteorology Laboratory
Colo. State Univ., Ft. Collins, Colo. (27 October 1971)

CUNNINGHAM, R. M.
Aircraft Instrumentation: Measurement for a Purpose
52nd Ann. Mtg., Am. Met. Soc., New Orleans, La. (10-13 January 1972)

CUNNINGHAM, R. M., and GLASS, M.
A Warm Cumulus Modification Experiment
3rd Conf. on Wea. Mod., Rapid City, S. D. (26-29 June 1972)

DAS, P.
On the Role of Cloud Microphysics in Cumulus Dynamics
Am. Met. Soc. Conf. on Cloud Phys., Ft. Collins, Colo. (24-26 August 1970)

DONALDSON, R. J.
Severe Weather Warning by Plan Shear Indicator
14th Rad. Met. Conf., Tucson, Ariz. (17-20 November 1970)
Doppler Radar Studies of Thunderstorms
Dept. of Met. and Oceanog., N. Y. Univ. Sem., Univ. Heights Camp., N. Y. (11 December 1970)
Doppler Radar Identification of Dying Convective Storms by Plan Shear Indicator

- 7th Sev. Local Storms Conf., Kansas City, Mo. (5-7 October 1971)
- DYER, R. M.
The Distribution of Fall Speeds Within the Melting Layer
 14th Rad. Met. Conf., Tucson, Ariz. (17-20 November 1970)
- FITZGERALD, D. R.
Aircraft and Rocket Triggered Natural Lightning Discharges
 SAE/USAF Lightning and Static Elec. Conf., San Diego, Calif. (9-11 December 1970)
- GLOVER, K. M., and DUQUETTE, E. F.
A Study of Clear Air Turbulence Using Sensitive Radar
 14th Rad. Met. Conf., Tucson, Ariz. (17-20 November 1970)
- HARDY, K. R.
Radar Meteorology
 Alice G. Wallace Planet., Fitchburg, Mass. (13 March 1972)
Radar Studies of Wave Patterns and Clear Air Turbulence
 1972 USNC/URSI-IEEE Spring Mtg., Wash., D. C. (13-15 April 1972)
Studies of the Clear Atmosphere Using High Power Radar
 Rem. Sens. of the Tropos., Kittredge Sum. Conf., Cr. Univ. of Colo., Boulder, Colo. (17-30 June 1972)
- HARDY, K. R., and MATHER, G. K. (Natl. Aeronaut. Estab., Fit. Res. Sec., Ottawa, Ont., Can.)
Instrumented Aircraft Measurements in the Vicinity of Clear Air Radar Structures
 14th Rad. Met. Conf., Tucson, Ariz. (17-20 November 1970)
- JOSS, J.
Results of Experiments with Vertical Pointing Radar and Distrometers for Raindrops
 Natl. Sev. Storms Lab., Norman, Okla. (8 February 1971) Dept. of Geophys. Sci., Univ. of Chicago, Ill. (11 February 1971)
Some Cloud Physics Experiments Carried Out in Switzerland
 Sem., Inst. of Atm. Sci., S. D. Sch. of Mines and Tec'l., Rapid City, S. D. (15 February 1971) NOAA-CIRES Mtg., Boulder, Colo. (17 February 1971)
The Accuracy of Radar to Measure Rain Intensity and the Amount of Rain
 McGill Univ., Montreal, Can. (16 March 1971)
- KAIMAL, J. C.
Characteristics of Spectra and Cospectra of Atmospheric Parameters in the First 22m
- IUGG 15th Gen. Assem. Mtg., Moscow State Univ., Moscow, USSR (30 July-14 August 1971)
Turbulence Spectra, Length Scales, and Structure Parameters in the Stable Surface Layer
 Inter-Un. Commission on Radio Met. (IUCRM) Colloq. on Waves and Turb. in Stable Layers, San Diego, Calif. (6-16 June 1972)
- KAIMAL, J. C., NEWMAN, J. T., and BISBERG, A., COLE, K. (EG&G, Waltham, Mass.)
An Improved Three-Component Sonic Anemometer for Investigation of Atmospheric Turbulence
 Symp. on Flow—Its Meas. and Control in Sci. and Industry, Pittsburgh, Pa. (9-14 May 1971)
- KAIMAL, J. C., WYNGAARD, J. C., IZUMI, Y., and COTE, O. R.
Behavior of the Spectra and Geospectra of Turbulence in the Atmospheric Surface Layer
 AMS-APCA Conf., Raleigh, N. C. (5-9 April 1971)
- KEEGAN, T. J.
Interpretation and Limitations of Direct Readout Infrared Data
 52nd Ann. Mtg. of the Am. Geophys. Un., Wash., D. C. (12-16 April 1971)
- KINTIGH, E., and DAS, P.
Modification of Drop-Size Distribution in an Unsaturated Downdraft
 Am. Met. Soc. Conf. on Cloud Phys., Ft. Collins, Colo. (24-26 August 1970)
- KRAUS, M. J.
Doppler Radar Investigation of Flow Patterns Within Severe Thunderstorms
 14th Rad. Met. Conf., Tucson, Ariz. (17-20 November 1970)
A Technique for Single Doppler Radar Investigation of Horizontal Motion Within a Thunderstorm
 7th Sev. Local Storms Conf., Kansas City, Mo. (5-7 October 1971)
- KUNKEL, B. A.
Fog Drop-Size Distribution Measured with a Laser Hologram Camera
 Am. Met. Soc. Conf. on Cloud Phys., Ft. Collins, Colo. (24-26 August 1970)
A Statistical Approach to Evaluating Fog Dispersal Operations
 3rd Conf. on Wea. Mod., Rapid City, S. D. (26-29 June 1972)
- KUNKEL, B. A., SILVERMAN, B. A., WEINSTEIN, A. I., and PRICE, C. (Dyn. Sci. Div., Marshall Ind., Irvine, Calif.)

- The Design of an Efficient Thermal Fog Dispersal System for Airports*
3rd Conf. on Wea. Mod., Rapid City, S. D. (26-29 June 1972)
- LANDRY, C. R., and HARDY, K. R.
Fall Speed Characteristics of Simulated Ice Spheres: A Radar Experiment
14th Rad. Met. Conf., Tucson, Ariz. (17-20 November 1970)
- MOROZ, E. Y., and COLLIS, R. T. H., VIZZEE, W., OBLANS, J. (Stanford Res. Inst., Calif.)
Lidar Measurements of Slant-Range Visibility for Aircraft Landing Operations
Intl. Conf. on Aerosp. and Aeronaut. Met., Wash., D. C. (22-26 May 1972)
- MORRISSEY, J. F.
Atmospheric Temperature Measurements Using Balloons and Rockets
The 5th Symp. on Temp., Its Meas. and Control in Sci. and Industry, Wash., D. C. (21-24 June 1971)
- MYERS, R. F.
Improved Pictures from Weather Satellites
MIT Lincoln Lab. Airborne Sev. Storm Surv. Sum. Study, Barnstable, Mass. (7 August 1970)
- NELSON, L. D.
A Comparison of Experimental and Theoretical Condensation Growth Rates of Hygroscopic Nuclei
Am. Met. Soc. Conf. on Cloud Phys., Ft. Collins, Colo. (24-26 August 1970)
- OTTERSTEN, H.
Radar Observations of the Turbulent Structure in Shear Zones in the Clear Atmosphere
14th Rad. Met. Conf., Tucson, Ariz. (17-20 November 1970)
- OTTERSTEN, H. (Res. Inst. of Natl. Def., Stockholm, Swed.), HARDY, K. R., and LITTLE, C. G. (Env. Res. Lab., NOAA, Boulder, Colo.)
Radar and Sodar Probing of Waves and Turbulence in Statically Stable Clear-Air Layers
Scripps Inst. of Oceanogr., San Diego, Calif. (5-16 June 1972)
- PAULSEN, W. H.
Airborne CAT Detection Systems Survey
FAA Symp. on Turb., Wash., D. C. (22-24 March 1971)
Indirect Sensing of Meteorological Elements in the Terminal Area—A Survey Paper
- Joint Conf. of the Fr. Met. Soc. and Am. Met. Soc. on Aeronaut. Met., Paris, Fr. (24-26 May 1971)
- PAULSEN, W. H., and CARTEN, A. S. (Aeroesp. Instr. Lab.)
The AFCRL Program for the Development of Airborne Remote CAT Detection Equipment
Intl. Conf. on Atm. Turb., London, Eng. (18-21 May 1971)
- PENN, S., and THOMPSON, G. J., CAPT.
Stable Laminae Associated with Clear Air Turbulence
Intl. Conf. on Atm. Turb., London, Eng. (18-21 May 1971)
- PLANK, V. G.
Time-Lapse Studies of the Development and Motion of Cumulus Cloud Populations and Systems
52nd Ann. Mtg. of the Am. Geophys. Un., Wash., D. C. (12-16 April 1971)
The Fog-Clearing Capabilities of Helicopters
U. S.-Aust. Wea. Mod. Conf., Canberra, Aust. (6-15 September 1971)
- SHAPIRO, R.
Horizontal Diffusion by Linear Filter
Intl. Conf. on Met., Tel Aviv Univ., Izr. (80 November-4 December 1970)
On the Response of the Lower Atmosphere to Solar Variability
IUGG 15th Gen. Assem. Mtg., Moscow State Univ., Moscow, USSR (30 July-14 August 1971)
- SILVERMAN, B. A.
Warm Fog and Stratus Dissipation by Airborne Hygroscopic Particle Seeding
12th Interagency Conf. on Wea. Mod., Virginia Beach, Va. (27-30 October 1970)
The Role of Modelling in the Development of Warm Fog Dissipation Technology
52nd Ann. Mtg. of the Am. Geophys. Un., Wash., D. C. (12-16 April 1971)
Warm Fog Dissipation Programs in the United States
Joint Conf. on the Fr. Met. Soc. and Am. Met. Soc. on Aeronaut. Met., Paris, Fr. (24-26 May 1971)
- SILVERMAN, B. A., KUNKEL, B. A., NELEON, L. D., and WEINSTEIN, A. I.
The Practicability of Airport Fog Dispersal by Airborne Hygroscopic Particle Seeding
3rd Conf. on Wea. Mod., Rapid City, S. D. (26-29 June 1972)
- SILVERMAN, B. A., NELSON, I. D., WEINSTEIN, A. I., and CHIEN, C. W. (Met. Res. Inc., Altadena, Calif.)
Effects of Turbulence and Vertical Wind Shear on the Clearing of Warm Fog by Airborne Hygroscopic Particle Seeding

- U.S.-Aust. Wea. Mod. Conf., Canberra, Aust. (6-16 September 1971)
- SILVERMAN, B. A., and WEINSTEIN, A. I.
Warm Fog Dispersal by Airborne Wide Area Hygroscopic Particle Seeding
 3rd Conf. on Wea. Mod., Rapid City, S.D. (26-29 June 1972)
- SWEENEY, H. J.
A Turbulence Mechanism Observed in the Atmosphere
 14th Rad. Met. Conf., Tucson, Ariz. (17-20 November 1970)
- THOMPSON, G. J., CAPT., GIORGIO, P. A., and PENN, S.
Simultaneous GMD-1 Observations: Mesoscale Winds and Tracking Errors at High Levels
 2nd Symp. on Met. Obsns. and Instrmn., San Diego, Calif. (27-30 March 1972)
- WRIGHT, J. B.
The Evolution of a Standard Low Cost Meteorological Rocket System
 2nd Symp. on Met. Obsns. and Instrmn., San Diego, Calif. (27-30 March 1972)
- WYNGAARD, J. C.
Some Aspects of Stress and Heat Flux Dynamics in the Surface Layer
 IUGG 15th Gen. Assm. Mtg., Moscow State Univ., Moscow, USSR (30 July-14 August 1971)
An Atmospheric Turbulence Research Program
 Sem., Brown Univ., Providence, F. I. (22 October 1971)
The Onset of Local Isotropy in the Lower Atmosphere
 Ann. Mtg. of Fluid Dyn. Div., Am. Phys. Soc., San Diego, Calif. (22-24 November 1971)
- WYNGAARD, J. C., and COTE, O. R.
Cospectral Similarity in Stratified Turbulent Shear Flows
 Am. Phys. Soc. Mtg., Wash., D. C. (26-29 April 1971)
- WYNGAARD, J. C., IZUMI, Y., and COLLINS, S. A. (Ohio State Univ.)
Behavior of the Refractive Index Structure Parameter Near the Ground
 Ann. Mtg. of the Opt. Soc. of Am., Ottawa, Ont., Can. (6-8 October 1971)
Spatial Scales of a Turbulent Refractive Index Field
 Ann. Mtg. of the Opt. Soc. of Am., Ottawa, Ont., Can. (6-8 October 1971) Atm. Opt. Specialty Gp. Mtg., Natl. Bur. of Stds., Gaithersburg, Md. (18 May 1972)
- WYNGAARD, J. C., LYNCH, R. A., and BAUMAN, J., MAJ. (Beale AFB Calif.)
Cup Anemometer Dynamics
 Symp. on Flow—Its Meas. and Control in Sci. and Industry, Pittsburgh, Pa. (9-14 May 1971)
- WYNGAARD, J. C., and PAO, Y. H. (Flow Res., Inc., Kent, Wash.)
Small-Scale Structure of Turbulence in the Atmospheric Surface Layer
 Ann. Mtg. of the Fluid Dyn. Div., Am. Phys. Soc., Univ. of Va., Charlottesville, Va. (23-25 November 1970)
Some Measurements of the Fine Structure of Large Reynolds Number Turbulence
 (Invited Paper)
 Symp. on Statist. Models and Turb., Univ. of Calif., San Diego, Calif. (15-21 July 1971)
- YEE, S. Y.
An Efficient Numerical Scheme for Baroclinic Geostrophic Weather Prediction
 52nd Ann. Mtg. of the Am. Geophys. Un., Wash., D. C. (12-16 April 1971)
- ## TECHNICAL REPORTS JULY 1970 - JUNE 1972
- BARNES, A. A., JR.
Radar Meteor Winds at Eglin AFB, Florida
 AFCRL-72-0186 (17 March 1972)
Radar Meteor Trail Task Fincl. Report
 AFCRL-72-0190 (22 March 1972)
- BARNES, A. A., JR., and PAZNOKAS, J. J.
Results from the AFCRL Radar Meteor Trail Set
 AFCRL-72-0185 (17 March 1972)
- BERKOFSKY, L., and GYERB, S.
A Numerical Model for Investigation of Ozone Transport in the Atmosphere
 AFCRL-71-0367 (24 June 1971)
- BROWN, H. A., MUNCH, S., and HERING, W. S.
Field Test of a Forward Scatter Visibility Meter
 AFCRL-71-0315 (26 May 1971)
- CHURCH, J. F., LT. COL., and TWITCHELL, P. F. (Off. of Nav. Res., Boston, Mass.)
Atmospheric Corrections for Airborne Radiation Thermometers
 AFCRL-72-0277 (28 April 1972)

- CONOVER, J. H.
Studies of Clouds and Weather Over Southeast Asia
AFCRL-71-0078 (21 January 1971)
- DONALDSON, R. J., DYER, R. M., SCHELL, A. C. (Micr. Phys. Lab.), CRANE, R. K. (MIT Lincoln Lab., Lexington, Mass.), LAWHERN, R. A. (RADC, Rome, N. Y.)
The Detection Range of the AN/TPN-19 Radars in Heavy Rain
AFCRL-72-0368 (June 1972)
- GEORGIAN, E. J., and GRIFFIN, J. R.
Development of a Transpondersonde for the Super-LOKI Meteorological Rocket
AFCRL-72-0089 (2 February 1972)
- IZUMI, Y.
Kansas 1968 Field Program Data Report
AFCRL-72-0041 (27 December 1971)
- KUNKEL, B. A.
Physicochemical Properties of Some Hygroscopic Nuclei
AFCRL-70-0626 (10 October 1970)
- MYERS, R. F., SPRAGUE, E. D., and MAREIRO, B. A., SSGT.
Controlled Processing of Direct Readout Data from Weather Satellites
AFCRL-70-0589 (22 October 1970)
- PENN, S., THOMPSON, G. J., CAPT., and GIORGIO, P. A.
Meteorological Conditions Associated with CAT Observations in Project HAVEN HOP
AFCRL-72-0043 (7 January 1972)
- PLANK, V. G., SFATOLA, A. A., and HICKS, J. R. (U.S. Army Cold Reg. Res. and Eng. Lab., Hanover, N. H.)
Fog Modification by Use of Helicopters
AFCRL-70-0693 (28 October 1970)
- SHAPIRO, R.
Compensation of Interpolation by Linear Filter
AFCRL-71-0058 (28 January 1971)
- SFATOLA, A. A.
Climatology of Appalachian Valley Fog at White Sulphur Springs, West Virginia, and Nearby Stations During Months of Peak Fog Frequency
AFCRL-72-0054 (21 January 1972)
- THOMPSON, G. J., CAPT., GIORGIO, P. A., and PENN, S.
An Analysis of Winds Derived from Upwind Rawinsonde Releases
AFCRL-72-0189 (14 March 1972)
- WEISS, B. D., and MORRISSEY, J. F.
Investigation into Utilization of LORAN and OMEGA Wind-finding Systems for Measuring Winds Below an Aircraft
AFCRL-72-0399 (23 June 1972)

VII Sacramento Peak Observatory

Sporadic outbursts of solar activity occasionally shower the earth and its environs in space with high energy radiations. They alter the structure of the ionosphere, producing a number of highly inconvenient practical consequences for Air Force activities at all levels. As operations extend to higher altitudes, and as dependence on more sensitive electromagnetic devices increases, the effects of the solar disturbances become more troublesome, and the list of operational difficulties originating in the sun grows steadily. For example: radio propagation deteriorates and occasional complete blackouts of long distance communications occur; Over-the-Horizon electromagnetic systems are seriously cluttered and moving ionospheric waves produce radar simulations of high-level, high-speed artificial objects; density fluctuations in the upper atmosphere perturb satellite and ballistic orbits, leading to surveillance and targeting errors; showers of fast solar protons damage solid state equipment and blacken photographic film in space. In extreme cases, this radiation could kill an exposed man in space; the incoming combination of X-rays and fast particles simulate the radiations from nuclear explosions in space. They could confuse monitors of such activity in the absence of reliable solar information; perhaps less important at present, the geomagnetic field fluctuates in strength and direction, and intense aurorae occur in abnormally low latitudes, and finally, there is growing evidence of perturbations in global weather patterns due to the radiations from solar activity.

A knowledge of the solar output of X-rays and particles over the past two or

three days, and predictions of the output in the near future can provide warnings to Air Force planners that reduce or eliminate their detrimental effects. The Air Weather Service has the responsibility for distributing warnings and predictions of the aerospace disturbances that result. The terrestrial mechanisms leading to these disturbances are reasonably well understood, and AWS utilizes this knowledge to the fullest extent. The primary solar mechanisms, however, are very poorly understood. Predictions must depend on rather loose empirical correlations between observed solar events and subsequent terrestrial results, rather than physical cause and effect.

AFCRL's solar program is primarily an effort to fill this gap in our knowledge and develop more reliable prediction methods based on the physics of X-ray and particle emission from solar active features, primarily the flares. More specifically, the purpose is to pinpoint the particular observable phenomena on the sun that are the signatures of physical mechanisms leading inevitably to the emission of the disturbing radiations at predictable times and intensities. For this purpose, AFCRL probably has the most comprehensive program of solar research to be found in any single institution anywhere. This effort is distributed among five different laboratories according to the different techniques required in different wavelength bands of the solar spectrum, from the high energy X-rays to the longest radio waves that penetrate the atmosphere. Briefly, the Aeronomy Laboratory observes in the X-ray and far ultraviolet spectrum, the Sacramento Peak Observatory in the optical spectrum, the Optical Physics Laboratory in the infrared, the Microwave Physics Laboratory in the millimeter region, and the Ionospheric Physics Laboratory in the radio spectrum.

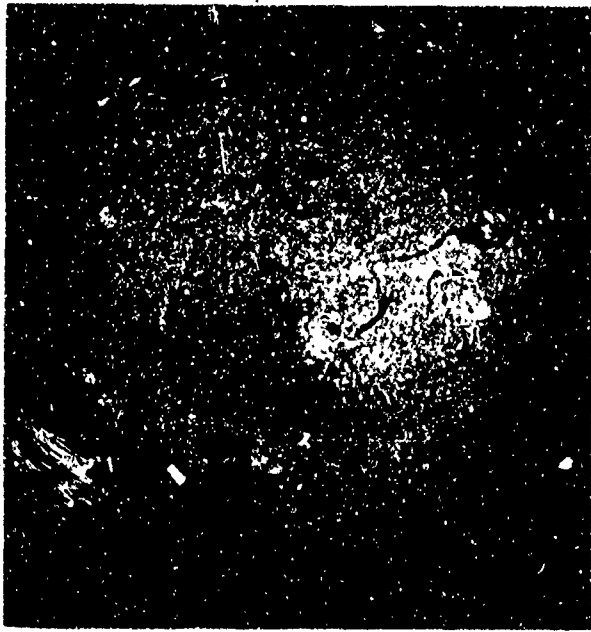
The Air Force, through AFCRL's predecessor, established the Sacramento Peak

Observatory in 1952 at Sunspot, New Mexico. The site was chosen after a lengthy examination of observing conditions in many places. Sunspot is on a peak in the Sacramento Mountains at an altitude of 9200 feet, surrounded by a dense pine forest that shades the ground and reduces troublesome low-level convective turbulence in the line of sight to the sun. The high-quality equipment which has been installed here, with the new capabilities which are presently being added, has kept Sacramento Peak one of the outstanding solar observatories in the world.

THE SUN

The sun is an undistinguished middle-aged sample of the most numerous class of stars, about midway in the stellar ranges of age, brightness, mass, size, and temperature. Because it is the only star near enough for detailed study, it is the key for decoding the relatively fragmentary observations of stars. The sun is a wholly gaseous globe, roughly 1.4 million km in diameter, of 380,000 earth masses, internally heated by nuclear fusion in the central core. The surface, at a temperature of 6000 degrees K, radiates over 6 kilowatts per square centimeter.

From the outside, we see down through a transparent atmosphere to the white visible "surface," the upper boundary of an opaque cloud of negative hydrogen ions, which we shall term the floor of the solar atmosphere. Above this floor is the 300-km thick photosphere, where most of the absorption lines of the solar spectrum are formed. Overlying it is the chromosphere, which extends upward to a sharply defined but exceedingly irregular upper boundary between the heights of 1500 and 10,000 km. This remarkable boundary, known as the "transition layer" between the chromosphere and corona, is marked



The sun photographed in the chromospheric hydrogen alpha line. The central sunspot is surrounded by bright plages that indicate the extent of the active center. The long dark filaments are prominences in projection against the disk.

by an abrupt rise in temperature, from about 10^4 degrees K in the chromosphere to 10^6 degrees K in the corona in a distance of 200 km or less. The density undergoes a corresponding drop by a factor of about 100. Resting on the chromosphere, the corona extends outward with slowly decreasing temperature and density well beyond the orbit of the earth. Beyond one or two solar radii, the corona expands at an outwardly increasing rate as the solar wind. Near the earth, it attains a velocity of about 400 km per second, a kinetic temperature of the order of 10^5 degrees K, and a typical density of 10 atoms per cubic centimeter.

From the 6000 degrees of the floor, the temperature decreases upward to a minimum of about 4200 degrees at about 500 km, and then increases gradually through the chromosphere to the transition layer.

The steady state solar atmosphere is inhomogeneous at all levels. We find marked fluctuations in all physical characteristics in neighboring surface elements less than 1000 km apart, a scale that often strains the resolving power of solar observing systems. It is now clear that these fluctuations exert a crucial influence on the basic dynamics of the solar atmosphere, the upward transport of energy, and the triggering of the disturbances we lump under the term solar activity. The main thrust of modern optical solar research is the study of these inhomogeneities in both disturbed and undisturbed regions. They complicate the theoretical interpretation of observations immeasura-



White granulation, the tops of convective elements that form the floor of the observable solar atmosphere. Average center-to-center distance of granules is about 1100 km, or 1 1/2 arc seconds.



The optical solar spectrum extends from 3000 to 9000 Angstroms. This spectrogram shows details in the short wavelength stretch around 3886 Angstroms. The line wiggles, Doppler shifts due to vertical motions, and intensity variations in the lines and continuum show the spectroscopic inhomogeneity from point to point in the solar image along the spectrograph slit.

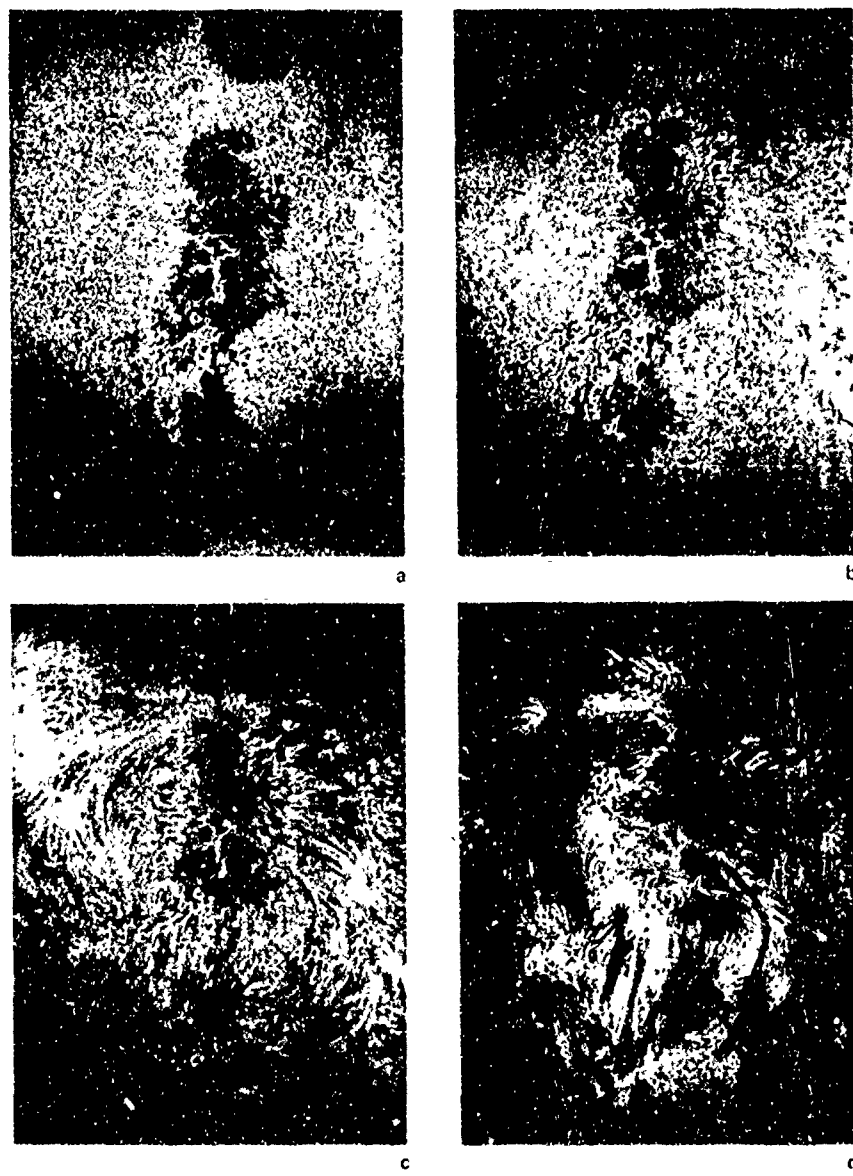
bly, but the results are very fruitful, and well worth the effort.

The white floor of the solar atmosphere has an inhomogeneous structure. Bright granules can be seen, which are the tops of convective columns, analogous to cumulus clouds. They are the principal mechanism by which the energy generated in the interior arrives at the surface. The impact of these upward-moving elements on the overlying convectively stable solar atmosphere injects mechanical energy which excites resonant oscillations and which must be the ultimate source of energy for the higher temperature chromosphere and the

very hot corona. Knowledge of this fundamental process of mechanical energy transport is still vague. It is the subject of much of the observational and theoretical research at Sacramento Peak and elsewhere. The rapid variation of vertical motion from point to point can be shown by focusing an image of the sun on a spectrograph slit. The image of the slit formed within the spectrograph will not be the straight line expected, but will show "line wiggle," which is actually wavelength displacement due to the Doppler effect in upward-and downward-moving elements in the photosphere.

The convective granulation and the disjointed motions of the photosphere are characteristic of the steady state sun, usually referred to as "quiet." This is the environment of enormous sporadic disturbances known as solar activity, a term that includes a number of slowly changing features, and a few catastrophic ones which produce the bursts of X-rays and fast particles that disturb the terrestrial aerospace. All of the active features are simply the visible manifestations of changes in a single basic physical entity, an abnormally strong magnetic field powerful enough to control the motion of the solar material.

All of the material of the sun, including its atmosphere, is a plasma, a gas of high electrical conductivity due to the presence of free electrons and ions. When a magnetic field is embedded in such a plasma, it is "frozen in." Plasma motion relative to the field is rigidly restricted to motions along the field. If the magnetic energy density, or pressure, greatly exceeds the gas pressure, the field lines are rigid tracks for gas motions, and transverse motions occur only when magnetic changes move the field lines. If the gas pressure dominates, however, mass motions powered by gravity or temperature gradients, or any other non-magnetic force, overpower the field and simply carry it along. This is the



A large complex sunspot group, about 160,000 km long, showing the characteristic dark umbra surrounded by the gray penumbra of fine radial filaments. The photographs, taken at graded distances from the center of the H alpha line, show the structures at different heights, from the white floor in *a* to the middle chromosphere in *d*. Note the numerous bright points clustered in and around this active center. Frame *d* shows the bright plage areas and dark filaments that follow magnetic flux tubes.

normal situation at the granulation level, where the ambient field is weak and the gas pressure relatively high. The turbulence of granular convection must twist the fields into unimaginably complicated figures and surely destroys any field coherence. From outside, consequently, we see little, if any, field over most of the quiet sun except for a few isolated strong "point fields" of several hundred gauss (which are presently unexplained). Occasionally, however an overpowering vertical field of 1000 gauss or more develops. It stops the normal granular convection, shutting off the flow of energy to the surface. The field area then cools off and becomes a relatively dark sunspot or spot group, the nucleus of an active center. If the field is not quite strong enough to stop convection, we often find an active center without sunspots. The strong active centers, however, are the seats of the real solar fireworks with terrestrial effects.

We classify the features of solar activity by their visible appearances rather than by their more fundamental magnetic characters, because we have not yet learned enough about the basic magnetic activities. These would, doubtless, present a far more coherent picture of solar activity than we now have, and their study is the most urgent part of the Sacramento Peak Observatory program.

In addition to the flare associated phenomena described below, the principal features of solar activity are plages, prominences, and coronal condensations.

The optical spectrum of the sun is the most important source of physical information available to us. It is an absorption spectrum consisting of a thermally generated continuum from the granulation layer, punctuated by thousands of dark lines absorbed by the atoms and molecules in the photosphere, and, for some strong lines, the chromosphere. Each atomic species has a characteristic set of lines by which the atom can be identified. The

relative intensities of the lines vary with the physical environment of the atoms, and their measurement immediately gives approximate information about the physical state of the solar atmosphere. The picture is greatly complicated, however, by the fact that a given absorption line is formed by atoms distributed over a considerable height range within which the physical parameters vary greatly. Accurately determined absorption profiles of selected lines and measurements of the continuum intensity from the center of the solar disk (vertical incidence) to the limb (grazing incidence) are the data for defining the main parameters, temperature, density and turbulent velocities, as a function of height. The spectroscopic inhomogeneities make the complexity of the problem readily apparent.

The two other most important items of information provided by the spectrum are sightline mass velocities, which result in easily measured Doppler wavelength shifts of the lines, and magnetic fields, which produce complex polarization effects in the line profiles that are not so easily measured. Both of these are complicated again by the considerable height range of line formation, within which both velocities and magnetic fields generally vary.

THE FLARE PHENOMENON: Most of the terrestrial disturbances of practical importance are the result of X-rays and fast particles generated by large flares and attendant subordinate activity, the surges, loop prominences and exceedingly hot dense coronal knots often found at the tops of the loops. All are the visible aspects of magnetic activity, and all occur in active centers, usually associated with the most complex sunspot groups marked by an intermixing of opposite magnetic polarities and consequent steep gradients.

At AFCRL, it has been determined that the optical flare starts in the chromosphere as a small bright nucleus over a satellite



A medium-sized flare of typical two ribbon form. Note the bridging arched dark filaments, actually loop prominences with foot points in the ribbons.

sunspot field surrounded by a field of opposite polarity. The flare quickly expands into an irregular patch, reaching its maximum dimensions and brightness in 15 to 30 minutes, then fading out during the next hour or two. The large ones are characteristically 50 to 100,000 km long and develop in the form of a pair of parallel ribbons which gradually drift apart. The magnetic field after the flare seems to be little different from that before the flare, but the time resolution of existing magnetographs is insufficient to define the changes that may occur during the flare. The one medium-sized flare for which sufficiently frequent magnetic observations were available did show marked changes, but more and better observations are needed to determine their typical behavior.

Magnetic loops, with roots in the two ribbons, bridge the intervening space, and are often the tracks along which material flows down, forming the loop prominences seen at the limb. Often, but by no means always, a large flare ejects one or more surges. These have the appearance of huge jets, moving out at 100 to 1000 km per second and then retracting along the same trajectory, which is defined by the magnet-

ic field. Repeating surges along the same or closely parallel paths are common. Their kinetic energy is usually comparable with the radiant energy of the flare itself.

Although a major fraction of the flare energy is in the light by which we see it, neither the X-rays nor fast particles originate in the optically visible flare itself. The X-ray pictures of flares taken from space vehicles show nearly the same configurations as the optical pictures and there is no doubt that we are seeing the same event, but at a higher level. The X-radiation often exceeds that of an equivalent black body at a temperature of about 10^9 degrees.

The fast particles ejected during a flare appear to originate in some different but neighboring site. Observations of a vigorous proton flare showed it was enclosed by a magnetic envelope that would trap any ejected particles. In this instance, at least, the protons could escape only from a nearby patch of open field lines which would guide them out into interplanetary space in a broad jet directed toward the earth.

In spite of real progress the last few



Another medium-sized flare which originated in a satellite sunspot that is covered up by the bright patch to lower right of the large spot.

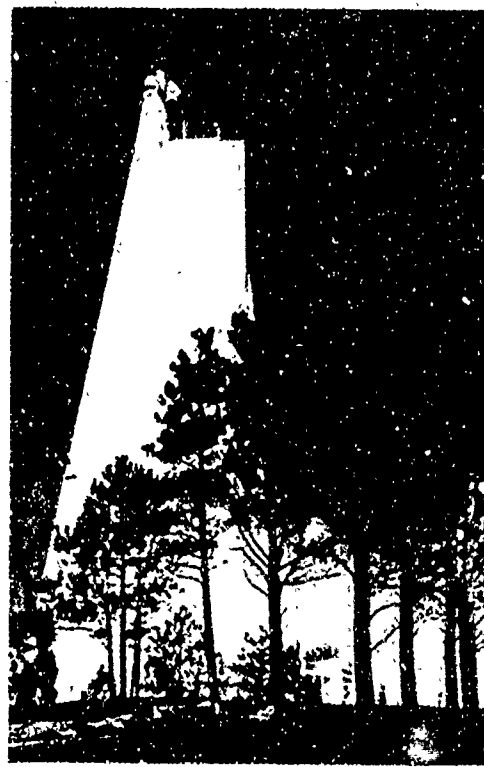
years, the physics of the flare process and the mechanisms that produce the X-rays and fast particles are still unknown. The impact of observed infalling material, lifted and guided by the magnetic field, does account for the brightness of optical flares and should theoretically produce shock waves with sufficient energy to power both the X-rays and particles. But there is no theoretical necessity for them to produce these radiations, and, indeed, no one has proposed any mechanism by which they could. There are theories, however, which appear reasonable if the rather special magnetic configurations required are granted. The Sacramento Peak Observatory will have evidence on this when the new multi-channel magnetograph catches a few flares.

FACILITIES AND INSTRUMENTS

The Sacramento Peak Observatory has an extensive array of solar observing instruments, backed by laboratory devices for analyzing photographic records and digital signals. They are most conveniently described by location.

TOWER VACUUM TELESCOPE: Completed in late 1969, this is the newest major observing facility at Sacramento Peak. Its purpose is to give the sharpest possible definition of small solar detail. To this end it incorporates four important features. It accepts light from the sun 135 feet above ground level to avoid local convection; its optical system is in an evacuated tube to avoid internal convection; all reflecting surfaces are sealed in the evacuated section where they stay clean, and the optical system is the simplest possible. The avoidance of convection anywhere in the optical path is important because convective thermal inhomogeneities in the air deflect the light rays slightly and blur the image. Light enters the vacuum through a 76 cm window at the summit of a massive concrete tower. Two flat mirrors inside the window reflect the light down an evacuat-

ed steel tube to a concave mirror of 55 meters focal length. This mirror reflects the light back up through any one of five exit windows at ground level, projecting a sharp solar image to any of the recording or spectrographic instruments. After a period of adjustment and minor modifications, the telescope achieved its full theoretical resolving power. The most troublesome defect was a slight image blurring due to temperature inhomogeneities that developed each morning in the outer zones of the entrance window, on exposure to sunlight. Temperature differences distort the optical surfaces and change the refractive index. The two effects are additive. The worst of the blurring disappeared when the aperture was diaphragmed down from 76 to 38 cm, but this procedure auto-



The tower telescope, pride of the Sacramento Peak Observatory.

matically doubled the instrumental resolution limit from 0.25 to 0.5 arc seconds, and cut the light flux by a factor of 4. After an exceedingly sensitive interference test with a laser source, and several months in careful experiment, an active refrigeration system was built and installed that blocked the conduction of heat from the surrounding metal structure into the glass at the rim of the window. This measure was completely successful. The telescope has photographed solar details as small as 0.25 arc seconds in extent, the equivalent of a dime at a distance of 12 miles. This is the best solar definition ever attained, and is a measure of the optical perfection of the instrument. Unfortunately, we have to look through the terrestrial atmosphere, which is in itself an imperfect optical element because of convection. Most of the time the image sharpness in the tower telescope is limited by these atmospheric defects, known as "poor seeing." As telescope sites go, Sacramento Peak is excellent, having hundreds of hours per year of good seeing, and an occasional period when the full theoretical 0.25 arc second resolution is actually achieved.

The finest telescope would be useless as a research tool without accessories to analyze the light and take advantage of a sharply defined solar image. The information available to the optical astronomer is that transmitted by the light entering his telescope. Measurement of the four Stokes' parameters as functions of wavelength and time at each point in the solar image would extract all of the information possible from the light. This is, of course, very difficult to do. Fortunately, we can do very well with only a selected fraction of this information, and the accessories planned for the tower telescope will provide it. At present, the two most basic instruments—a spectrograph and a filter-camera system—are in active operation. They measure the brightness parameters. A third, the magnetograph, which initially

will measure the circular polarization parameter, and eventually all three polarization parameters, is approaching active status. These three analyzers are still far from ideal, being severely restricted in coverage of wavelength, time, and area of the solar image. However, they already provide enormous amounts of data. The characteristics of these accessories are as follows:

ECHELLE SPECTROGRAPH: This is basically a 12-meter Fastie-Ebert echelle grating spectrograph, preceded by a prism spectrometer to select wavelength bands. This system, unique among solar spectrographs, allows the observer to photograph many widely separated bands in the solar spectrum simultaneously with the highest attainable spectroscopic resolution. Three cameras also simultaneously photograph the solar image on the reflecting spectrographic slit plate in white light and the calcium and hydrogen lines. Thus, the observer has a permanent record of exactly what features on the sun the spectrograph was looking at during an exposure, a most valuable capability. Dispersions up to 16 mm per Angstrom are available. The whole echelle spectrograph system is feasible only because of the superlative large gratings ruled at the Massachusetts Institute of Technology supported in part by an AFCRL contract. The grating is the determining element in the power of a spectrograph, and these gratings are by far the best ever made. The echelle spectrograph has three interchangeable gratings of different rulings for different purposes, and is undoubtedly the most versatile and powerful solar spectrograph in existence.

FILTER-CAMERA SYSTEM: This is a much less complicated instrument, but its function of photographing solar detail with the best possible definition is quite as important as that of the echelle spectrograph. The system includes two cine cameras for



A bright H alpha plage which covers much of the underlying associated spot group. Note the activity at the extreme limb (top).

70 mm and 35 mm film, fed by white light directly or through a narrow band birefringent filter. Two interchangeable filters for work in the hydrogen alpha line or the K line of ionized calcium swing into the optical path for photography in either of these lines. Three image scales are used at choice, corresponding to solar image diameters of 20, 38, and 51 cm. The quality of the tower telescope photographs taken by this simple system testify to its effectiveness.

MULTI-CHANNEL MAGNETOGRAPH: The multi-channel magnetograph is now ready for final checkout pending completion of

its data handling software. It is fed by the echelle spectrograph and will measure the sightline solar magnetic field simultaneously at 128 points along the echelle spectrograph slit. By scanning the image across the slit the observer records the magnetic field over the whole scanned area. The computer then maps the field quantitatively as a contour diagram, with a spatial resolving power of $\frac{1}{2}$, 1 or 2 arc seconds, which may be traded off against speed and area of coverage. A programmed change in the setup permits similar measurement and mapping of the distribution and magnitude of the sightline velocity of the solar material. In theory the existing point-by-point magnetograph, the Doppler Zeeman Analyzer, can perform the same functions, but the time required would be an impractical 500 times as great. The new instrument provides the spatial and time resolution necessary for the detailed study of the magnetic evolution of flares. It should be in regular operation by mid fall, 1972. When its operating characteristics and problems have been defined, the multi-channel magnetograph will be expanded in two directions. The number of points recorded will go from 128 to 256, and by a rearrangement of the sensitive elements in the focal plane, it will be possible to record in addition the plane polarization parameters at fewer points along the slit, probably about 80. This provides the raw data for mapping the whole magnetic vector over an active center.

BIG DOME: The Big Dome contains a number of special purpose instruments. The telescope room with a rotating turret houses an equatorially mounted spar, in effect an optical bench accurately tracking the sun. It consists of a rectangular steel box 27 feet long with four refracting telescopes mounted on three of its sides.

The system was painstakingly designed

to permit simultaneous operation of any or all of the telescopes. The most important of these is a 40 cm coronagraph capable of artificially eclipsing the disk of the sun and showing the surrounding corona. An ordinary telescope is hopelessly inadequate for this work because of a veil of scattered light about one thousandth as bright as the solar disk, and about 100 times as bright as the corona it overlays. To avoid this, the coronagraph must have special lenses made of the most perfect bubble free glass and polished to perfection. The optical train contains traps to catch diffracted light from the solar disk, and to dispose of the heat and light generated by the image on the eclipsing disk. Light from the coronagraph is reflected through the hollow polar axis into the observing laboratory, to be described shortly, where its apochromatic image can be directed to any one of a number of large fixed accessories. For years this coronagraph served as an all purpose telescope. The tower telescope has now taken the major part of this load, leaving the coronagraph free to concentrate on coronal observation.

The second instrument on the 27-foot spar is the magnetograph system. A 40-cm telescope forms an image of the sun on a very powerful but compact magnetograph, known as the Doppler Zeeman Analyzer, which generates an electrical signal proportional either to the sightline magnetic field or the sightline velocity on that portion of the sun seen by the entering aperture. The signal goes to a computer which constructs a contour map of the field as the magnetograph scans a raster on the sun. The best spatial resolution is 2 arc seconds, and an active center magnetic field can be mapped in about 20 minutes. The Doppler Zeeman Analyzer is one of the best existing magnetographs in the world and has been a most productive instrument. Yet it is quite impractical to use it with the $\frac{1}{2}$ arc second resolution of the multi-channel

magnetograph. An active center which the multi-channel magnetograph could scan in six minutes would require 50 hours on the Doppler Zeeman Analyzer.

A third instrument on the spar is a 22-cm coronagraph and spectrograph designed for photoelectric mapping of the corona out to heights where it is too faint for photographic detection. A photoelectric detector of high quantum efficiency detects much fainter coronal features through the bright sky background. A breadboard coronal photometer has been successfully used with this coronagraph, and a permanent version is under construction.

The fourth instrument on the spar is a chromospheric and prominence camera, consisting of a 38-cm objective lens, a birefringent filter tuned to two of the chromospheric spectrum lines due to hydrogen and helium, and a precision camera. It is essentially a coronagraph that under-eclipses the solar disk to photograph the phenomena at the extreme solar limb. It is presently used to record the appearance of limb activities over active centers that are being studied with the Doppler Zeeman Analyzer.

South of the Big Dome is a fifth apochromatic refracting telescope, a fixed horizontal instrument fed by a pair of 43-cm flat mirrors. The aperture and focal length of the objective lens are, respectively, 30 cm and 11.3 meters, and the system projects the solar image through a tube into the observing laboratory. A roll-away shed protects the external parts of the system from the weather.

The observing laboratory is the observing center of the Big Dome. Here are mounted the light analyzing instruments too bulky and too sensitive to directional changes of gravity to be carried on the moving spar. They rest on massive concrete piers going down to bedrock, free of any contact with the building. Light from

the 40-cm coronagraph and the fixed telescope enter the laboratory through a distribution center, where movable mirrors direct each of the two beams to any one of the fixed analyzing instruments, any pair of which can be used simultaneously. The principal instruments are as follows:

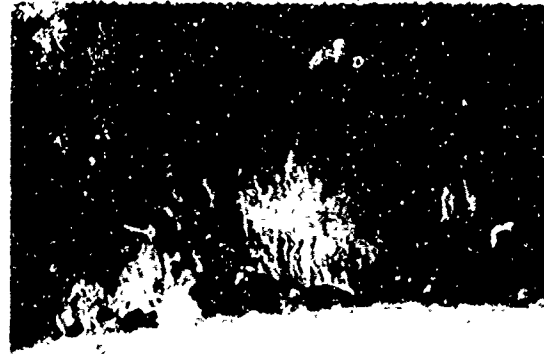
The 13-meter Littrow spectrograph is a very flexible instrument designed for operation either as a photographic spectrograph or a scanning spectrometer. Its dispersive element is one of a series of diffraction gratings of various rulings for different purposes. The photographic observer may choose any dispersion from about 1 to 18 mm per angstrom in spectrograms up to 60 cm long. A separate camera photographs the solar image on the reflecting slit jaws in either white light or the hydrogen line to record the features that were on the slit during the spectrographic exposure. While the performance of this superb spectrograph is at the limit of the state of the art, it has one serious limitation, shared by all spectrographs of its class until the advent of the echelle spectrograph. It has no provision for observing more than one region of the spectrum at a time. As a scanning photoelectric spectrometer, the Littrow spectrograph revolutionized the art of measuring solar line profiles. It introduced the principle of the double pass, now universally used. The dispersed light is reflected back to the grating through a narrow intermediate slit for a second dispersion. This procedure reduces the overwhelming scattered light at the centers of dark lines by a factor of 50 to a negligible level, and produced the first reliable profiles of the cores of the deepest solar lines. The spectrometer is still used for this purpose with the fixed telescope.

The universal spectrograph, also equipped with a slit jaw camera, is a medium instrument with dispersion of $\frac{1}{2}$ to 1 mm per Angstrom, designed for maximum luminosity to deal with the relatively

faint spectrum of the corona. Its unique virtue is the ability to cover the whole spectrum from 3200 to 8800 Angstroms in three exposures. This is invaluable for exploring the spectra of newly identified features, but the chief use of the universal spectrograph is for coronal studies with the 40-cm coronagraph.

The Sacramento Peak spectroheliograph is unique in being a double pass spectrometer with an exceedingly low level of scattered light. In standard operation, the entrance slit scans across the solar image, while three exit slits set on major lines in the solar spectrum scan across photographic films, building up an image of the sun in the light of each of the three lines. Compared with the birefringent filter, the spectroheliograph is slow and bulky. But in contrast, it can be set on any lines in the spectrum with any desired bandwidth. The freedom from scattered light has been important in revealing the instrumental origin of features that have been recorded elsewhere and analyzed as real solar features, with bizarre results.

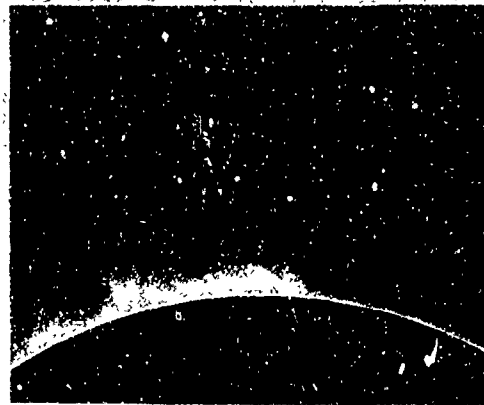
Finally, the "east bench camera" is a



A small limb prominence about 50,000 km high, showing the characteristic vertical structure, which remains static while material flows down through the magnetically defined filamentary "tubes." The picture was taken in hydrogen alpha light.

pair of twin cameras built to photograph solar structures in two different wavelengths simultaneously, with the highest resolution. It has two birefringent filters that give pictures in the hydrogen alpha line and the K line of Ca II. Either camera can be used with either filter, or take a white light picture. Even under good seeing conditions, the solar image undergoes small rapidly varying distortions. Hence in their finest details, successive pictures in different wavelengths are not exactly comparable. The east bench camcra takes simultaneous pictures in which the distortions are exactly the same, and structural differences shown by the blink comparator are genuinely solar.

HILLTOP DOME: This building houses a 12-foot spar that carries two patrol telescopes and temporarily accommodates various small experimental pieces of equipment. The hydrogen alpha patrol is a 4-inch refractor with a $\frac{1}{2}$ Angstrom bandwidth hydrogen alpha filter. On emerging from the filter, the light is divided by a beamsplitter between a 35-cm cine camera and a video receiver tube. A programmer automatically operates the camera shutter and controls the filter. It normally takes one exposure per minute whenever the sun is out, but speeds up to one every 10 seconds when fast activity like a flare is expected. The 17 mm solar image, recorded on a very fine grained film, defines details down to two arc seconds in size. The video tube is the origin of a TV picture of the sun which is displayed on screens in the tower, the Big Dome, and at several stations in the main laboratory building. Generally, one sees only a small portion of the solar surface through the large telescopes, and the TV monitors provide a full disk view of any activity which may demand instant attention. The white light sunspot patrol is similar, but lacks the birefringent filter. It uses a still finer grained film, and easily shows the solar granulation in a 20



A typical coronal condensation photographed in the light of the green line due to Fe XIV (the iron atom minus 13 of its electrons).

millimeter image. Like the hydrogen alpha patrol, it is controlled by the programmer, and runs whenever the sun is out.

GRAIN BIN DOME: This was the first permanent instrument shelter housing the first permanent instrument at Sacramento Peak. The building is a modified Sears Roebuck grain bin, erected in 1950 when the Observatory was little more than a camp. It houses a 10-foot spar on which are mounted two coronagraphs. One, a 10-cm coronagraph-spectrograph records the principal bright lines of the coronal spectrum at all positions around the solar limb at least once each clear day. The second is a 15-cm coronagraph equipped with a cine camera and a birefringent filter transmitting the green coronal line. It operates whenever the sky is sufficiently clear, and is the source of the only extensive cinematographic record of coronal activity in existence. As such, it has revealed previously unsuspected kinds of coronal activity, and their relation to the underlying activity in the photosphere and chromosphere.

OTHER INSTRUMENTS: For the quantitative analysis of all photographic material, especially spectrograms, the Observatory

built an unusually flexible microphotometer in the mid 1950's. This is a fundamental research tool for the conversion of the darkening of a photograph to quantitative measures of light intensities. Over the years it has undergone gradual modifications to take advantage of new technology as it appeared. It has acquired a reputation as the best in the world, and astronomers have come from as far away as Japan to use it. It puts out a digital signal that is recorded directly by the observatory computer on tape, or more accessibly on a disk pack.

The Recording Doppler Comparator is a device invented here for rapidly tracing the Doppler displacements of "wiggly lines" and recording them digitally on tape or disk pack. Although the same information could be derived from multiple traces with the microphotometer, the recording Doppler comparator is about ten times faster, a matter of considerable importance in the analysis of lengthy time sequences of spectra in a half dozen lines.

The Sacramento Peak Observatory requires electronic computer speed and sophistication for two classes of work, the scientific computations of theoretical astrophysical analyses, and the recording and processing of data. The computer used here is designed for scientific computations, and is capable of performing both of these functions concurrently. With an augmented core memory of 64 kilobytes, it is quite adequate for most of the observatory requirements, and the AFCRL computing center handles any problems which exceed its capabilities.

In addition to the equipment described above, the observatory has let contracts for one new system of major importance. It will provide direct photographs of the sightline magnetic and velocity fields on the sun in time lapse motion pictures, with the full spatial resolution of the tower telescope. Delivery of all components is due by October 1972. Their integration and

mounting is the responsibility of the Observatory, and should be completed by the spring of 1973.

INSTRUMENTS FOR AIR WEATHER SERVICE SOLAR OBSERVATORIES

The Air Weather Service Space Environmental Support System (SESS) is the operational agency for making and distributing warnings and forecasts of aerospace disturbances that affect Air Force operations. Since the sun is the primary cause of these disturbances, predictions of flares are a prominent part of their work. They require observational solar data 24 hours a day. To this end they have established a net of solar-observing stations distributed around the world, equipped with radio telescopes and optical patrol telescopes based on the hydrogen alpha patrol instrument at Sacramento Peak.

As we learn more about the sun, the prediction methods improve, and the observational requirements have already outrun the capabilities of these relatively simple instruments. Funds have been allocated for replacing them with more sophisticated standardized optical systems. In consultation with AFCRL's Space Physics Laboratory and Sacramento Peak Observatory, the AWS listed the desired capabilities of the new observing system. It must provide white light and hydrogen alpha photographs on an enlarged scale, a hydrogen alpha video picture, an advanced videmeter that processes the video signal to give warnings of the occurrence of a flare and chart its radiation output as a function of time, a magnetograph, and a spectrohelioscope for visual detection and viewing of the magnetic distribution. Sacramento Peak has accepted responsibility for the design of the system, monitoring of the construction of a preproduction model, and writing of an operating manual. Design of

a 30-cm solar telescope with the necessary feeds and accessories to achieve all of the requirements has been completed, and negotiations for the construction under contract of the various components are now in progress. The components will be assembled into the integrated system at Sacramento Peak. After thorough tests and optimization of the first sample, the instrument will be standardized and produced for all the AWS observing locations.

RESEARCH ON SOLAR ENERGY TRANSPORT

The nuclear power plant at the center of every star, including the sun, produces a relentless flow of energy at a rate dependent mainly on the mass of the star. All of this energy must make its way to the surface of the star and escape into outer space as electromagnetic, magnetic or kinetic particle flux equal to the nuclear power production. In the stellar interior the processes of energy flow are radiation, convection, conduction, and possibly some presently undefined magnetic mechanism, balanced in such manner that the total gravitational potential of the star is the least possible in the face of the fixed energy flux. Solar physics is concerned with the last stage of the process, the upward transport of the energy through the solar atmosphere. This looked relatively straightforward until 1940 when Edlen showed that the corona is very much hotter than the underlying photosphere, and Redman correctly concluded that the chromosphere is intermediate between the two. The simple thermal energy flow, accepted without question until then, had to go. Left to itself, heat would flow downward from the corona and chromosphere to the cooler photosphere, and, in fact, it does. Thus, the most basic physical laws require that some nonthermal processes of upward energy transport operate in the solar at-

mosphere with sufficient vigor to provide the necessary net outward flux in the face of the opposing downward thermal flux. Directly or indirectly, all the problems of solar physics are aspects of this single fundamental problem. All the features we observe in the sun are nature's provisions for disposing of an inexorable flood of energy by transmitting it to outer space with the least possible fuss (i.e., least gravitational potential). A corollary to this is that there are no truly isolated problems in solar physics. The "least possible fuss" provision is fundamental, and requires that any action in the solar atmosphere must lead to readjustments in its surroundings.

While it is difficult (and quite unnecessary) to draw sharp lines, there are some problems in solar physics that are concerned directly with energy transport. They have to do with the structure and dynamics of the solar atmosphere and such radiative problems as the formation of the lines in the solar spectrum. Because they are fundamental, problems in this area



A surge ejected by a flare. Material shoots out at about 200 km per second along magnetic field lines and then retracts along the same path. In extreme instances, surges exceed the 700 km per second velocity of escape and the material goes into interplanetary space. The picture was taken in hydrogen alpha light.

receive much attention at Sacramento Peak.

Each atomic species is tuned to a series of discrete wavelengths in the spectrum. In these wavelengths, or "lines," the solar atmosphere becomes more or less opaque, depending on the efficiency of atomic absorption and abundance of the atom. The strongest lines are those for which the atmosphere is most opaque, and the depth to which we can see is less in strong lines than weak lines because of this greater opacity, just as the limit of visibility is less in an opaque dense fog than in a light one. In the light of the continuum, the atmosphere is quite transparent at all levels down to the onset of negative hydrogen ions which are opaque at all optical wavelengths. They produce an abrupt rise in opacity, forming the white granulation layer.

For the terrestrial observer, then, strong lines tend to originate at higher levels than weak lines. Because the distribution of opacity with height is nonuniform and different for different lines, this is only a tendency. Within the inverted bell-shaped profile of a single line, however, the opacity at every level diminishes as we depart from line center, but maintains the same vertical distribution. We can be quite certain, therefore, that the light originates at steadily decreasing heights as we progress through the profile from line center to its merging with the continuum. The shape of a line profile, then, is a function of the vertical distribution of opacity, which is fixed by the vertical distributions of temperature and density. The variation of temperature and density with height is basic to an understanding of energy transport through the line forming layers. We seek to determine this through the study of line profiles and the continuum, between the center of the solar disk and the limb, where the heights of origin are greater because of the grazing incidence of the line of sight. The inhomogeneous

structure of the solar atmosphere at all levels vastly complicates the problem. The approach is to find a distribution of temperature and density, vertically and horizontally, that fits all line profiles and the continuum, from center to limb.

The magnesium line at 4571 Angstroms, due to a "forbidden" atomic transition, is especially favorable for the determination of the vertical temperature distribution. The brightness at each point in the line profile has a much simpler dependence on temperature than that for nearly all other lines. The brightness at line center indicates a low temperature of about 4200 degrees K, suggesting that the line originates near the level of minimum temperature in the lower chromosphere. The average profile of Mg 4571 from center to limb was analyzed to define the height distribution of temperature in the neighborhood of the minimum. The observed profiles were fitted at all positions on the solar disk with a temperature minimum of 4140 degrees K at a height of 540 kilometers above the floor. While this result hardly settles the lively controversy of the past five years as to whether the minimum temperature is 4600 or 4200 degrees, it strongly reinforces the proponents of the lower value, and has already won a number of converts. Unfortunately, the truth cannot be arrived at by a vote.

In the long-term effort to define the vertical distribution of temperature and density, any clues that restrict the possible range of solutions are of the utmost value. Work in this direction has been performed intermittently over the past 12 years to determine corresponding wavelength differences in the profiles of different lines. The wavelength difference in a line profile is measured between line center and any specified point of the profiles. In two lines, A and B, for each wavelength difference A there is a corresponding wavelength difference B which has the same height of origin. The radiation in the two lines at

corresponding wavelength differences must therefore originate in the same volume of space in the solar atmosphere and be the result of identical conditions of temperature, density, magnetic field, micro-turbulence, and mass motion.

An attempt was made to define corresponding wavelength differences by matching the measurable Doppler velocities and brightness fluctuations in the profiles of different lines. Although early results were inconclusive because of spectrograph limitations, they did show that the approach was sound if the lines could be photographed simultaneously to avoid the effects of imperfect seeing and tracking. The echelle spectrograph with the tower telescope has this capability, and a number of satisfactory spectrograms have been secured. The first results of an analysis of brightness fluctuations in the lines H and K of Ca II, b_1 and b_2 of Mg, and the hydrogen beta line show the expected well defined curves of corresponding wavelength differences between the Ca and Mg lines, but two significant surprises appeared. First, the hydrogen beta line has brightness fluctuations quite uncorrelated with those of the other lines. The parameters responsible for the brightness in hydrogen beta must be different from those for the Ca and Mg lines. Secondly, the Ca and Mg lines have a range of corresponding wavelength differences within which the brightness fluctuations are negatively correlated with those of the continuum. Bright granules and dark intergranular spaces reverse sign at higher levels and turn dark and bright, respectively. This peculiarity is lacking in hydrogen beta. Such a reversal poses a knotty problem in radiative transfer theory which is being explored by several investigators at Sacramento Peak and elsewhere. The program will be expanded to tie together a variety of neutral and ionized lines of different excitation potentials.

In the summer of 1970, a study was



Bright points clustered in an active center and distributed along the bases of hedge-rows of spicules near the solar limb.

begun to settle the question of systematic temperature variations with latitude of the white surface of the sun. This is an old observational problem of special interest because of its bearing on the global circulation pattern of the solar atmosphere. Earlier observations were discordant, suggesting a pole to equator temperature difference of anything from 0 to 60 degrees K.

In principle, the observations are simple measurements of differences in surface brightness, but an accuracy of 1 degree K in the temperature difference requires photometric accuracy of one part in 1500, which is not so simple. At this level of precision, the observer must correct for

the difference in atmospheric absorption between the upper and lower limbs of the sun, a changing quantity dependent on solar altitude and the momentary transparency of the atmosphere. There are also a number of small instrumental effects to be determined and eliminated.

A photoelectric detector was used with the 30-cm coelostat telescope and the tower telescope. After a long series of observations and equally long sessions with the computer, it was found that the temperature difference is 1.5 ± 0.6 degrees K at the floor of the solar atmosphere. Thus, systematic zonal temperature gradients provide very little power for global circulation.

The observations were repeated with light from the red wing of the K line of Ca II which originates at the 300-km level. Here, no temperature difference between the equator and poles was found, but the temperature in the sunspot zones was appreciably enhanced, to a maximum 8 degrees ± 2.5 degrees K, with some marked irregularities that were different in the northern and southern hemispheres, and appeared to coincide with the general level of activity in each. The 8 degree temperature difference at the low density 300-km level represents much less energy density than a 1 degree difference at the floor level.

The irregular distribution of temperature enhancements in the latitudes of solar activity suggests that they are local phenomena associated with specific active features rather than systematic latitude effects. This was investigated by comparing the observed temperature differences in detail with active features present at the time, and with the measured magnetic field strengths. A clear relation with magnetic field strength was found, which suggested that an enhancement at 50 degrees north latitude observed in both the temperature profile and magnetic flux is the precursor of the expected appearance of

sunspots of the next solar cycle at this latitude. A final conclusion is that the temperature differences could have had no detectable influence on the celebrated 1966 measurements of solar oblateness by Dicke and Goldenberg, as had been proposed by a number of theoreticians.

In addition to its own research programs, the Observatory has received numerous requests for use of the tower telescope and echelle spectrograph for studies of the strong lines of the solar spectrum that originate in the chromosphere. To avoid waste of telescope time in duplicate observation, and incidentally obtain higher quality spectrograms, the HIRKHAD program was initiated in 1971. The HIRKHAD spectrograms are simultaneous records of the H, K, and two infrared lines of Ca II, the hydrogen alpha line, and the two D lines of Na I. They are taken under best seeing conditions at graduated positions from the center of the solar disk to the limb, along with the most rigorous photometric calibrations, an item all too frequently neglected.

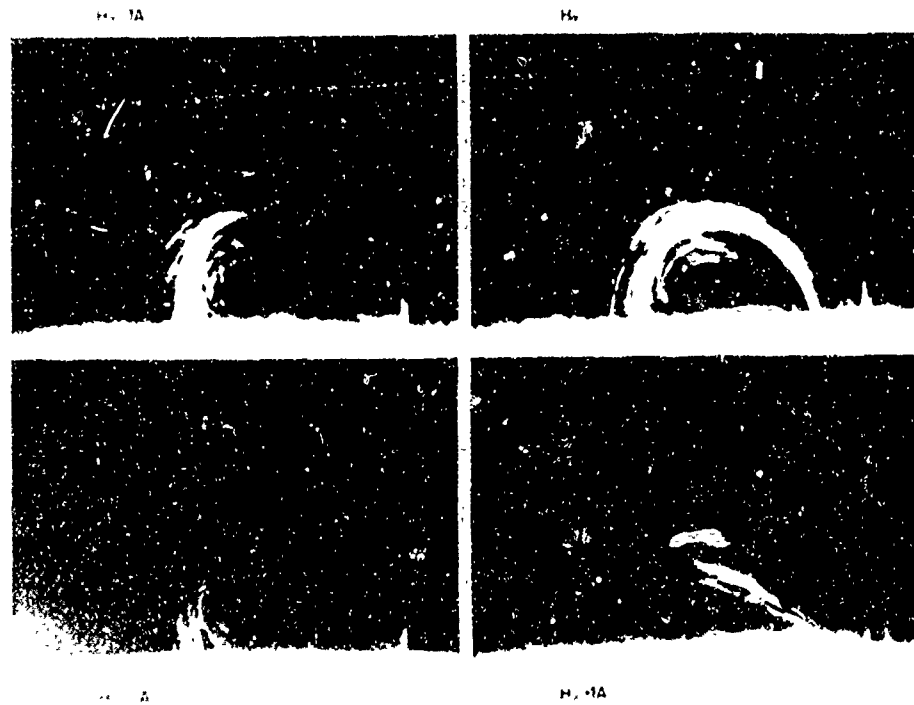
A large part of the program has been completed and the spectrograms are in the hands of several users, both at Sacramento Pea. and elsewhere. Eventually, as time and opportunity permit, HIRKHAD time sequences for evolutionary studies will be taken.

The lines of helium are practically undetectable in the solar absorption spectrum, although they are prominent in the bright line spectrum of the chromosphere at the limb where it is viewed against the dark sky. An exception is the infrared line at 10830 Angstroms, just beyond the long wave photographic limit (unless one is willing to cope with the uncertain photometry and laboratory gymnastics of hypersensitization). A birefringent filter for this line was assembled and made operational, and the sun was successfully photographed in 10830 Angstrom light with an image tube. The objective was to compare the helium

structures in and around active centers with those seen in the Ca II and hydrogen lines. The relative intensities of these lines are an indicator of the excitation conditions at chromospheric levels in active centers. The observations show weak helium emission in flares and plages, and strong absorption in prominences. A quick look interpretation indicated surprisingly low excitation, but reliable conclusions will follow data analysis.

Work has continued for several years to specify the upward mechanical energy flux through the solar atmosphere carried by the five-minute oscillations first measured

quantitatively at Sacramento Peak in 1961. The critical unknown was the upward propagation velocity of the waves. In early 1972, work was begun to settle this question with a good time sequence of spectrograms showing lines which originate at heights of 10, 150, and 300 km above the white floor of the solar atmosphere. The measured upward wave propagation, determined from the observed phase lags at the different heights, confirm the earlier rough estimate of about 40 km per second. Contrary to earlier tentative conclusions, the first analysis of the observed amplitudes and this phase velocity



A system of loops at the limb photographed in different wavelengths near the hydrogen alpha line (to show sightline velocity, about 46 km per second per Angstrom). (Hydrogen alpha -1 Angstrom shows a velocity of approach of 46 kilometers per second.) The loops follow the magnetic lines of force over an active center which guide material down from nuclei at the top into the chromosphere.

indicated that the five-minute oscillations transport more than enough energy for the heating of the chromosphere. This is an important confirmation of a previous unverified assumption that theoreticians have used for years. Because it is crucial, the analysis will be refined to include such effects as damping (which can now be measured), and possible magnetic restraints, before stating any final conclusion. This work is presently ... progress.

In a 1971 study of the low-frequency end of the power spectrum for motions at the lowest level of the photosphere, small areas of the solar surface were scanned continuously for four hours with the Doppler Zeeman Analyzer in the low-lying 5383 line of carbon. An elegant statistical analysis of the observations yielded the first detailed picture of the low-level motions, and their relation to intensity fluctuations. Strong, slowly changing velocities with varying periods, between 30 and 60 minutes long, are coherent over distances of 20 to 60 thousand kilometers. This is very much larger than the granulation size scale, and in good agreement with earlier studies of coherence lengths at higher levels. Unlike the five minute resonant oscillations, however, the motion is predominantly horizontal. The velocities are strongly correlated with brightness changes, with a four minute lag, but quite uncorrelated with the magnetic fields measured by the Doppler Zeeman Analyzer. The great size of the moving elements upsets the customary assumption that photospheric motions are the result of impacts from the upward moving granulation, and hence to the whole concept of granulation as the source of mechanical energy for the solar atmosphere.

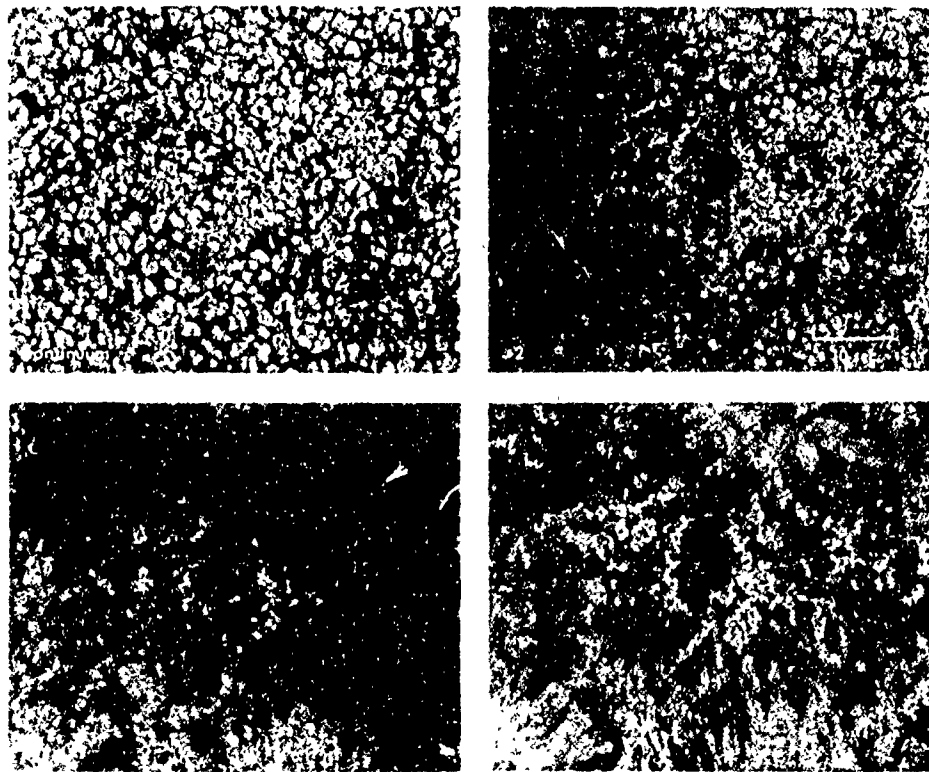
In 1970, a program was initiated to investigate systematically the small scale phenomena of solar activity at all accessible levels in the solar atmosphere. The gross magnetic changes accompanying flares, the most vigorous form of solar

activity, do not account for the energy released. This was a sort of negative confirmation of current theories of energy conversion, which state that the real action occurs in volume elements too small for resolution by the Doppler Zeeman Analyzer.

A rapid series of photographs were taken through a $\frac{1}{4}$ Angstrom bandwidth hydrogen alpha filter with the tower telescope. Exposures were made at $\Delta\lambda = 0, \pm\frac{5}{8}, \pm\frac{7}{8}$, and $+2$ Angstroms, from the center of the hydrogen alpha profile, and in the continuum. They show the structures through a descending series of levels, from the middle chromosphere down to the white floor.

It was immediately discovered that the sun is sprinkled with thousands of tiny bright points, 300-600 km in diameter, previously unrecognized. They are most conspicuous in the $\frac{5}{8}$ Angstrom frames, and tend to cluster in active centers, often beautifully arranged in a necklace along the outer boundaries of sunspot penumbrae. The points also appear in smaller numbers all over the whole solar disk, mostly along the foot points of the long hedges of vertical jets known as spicules which tend to outline the supergranule convective cells about 30,000 km in diameter. We know independently that strong magnetic knots occur along the cell boundaries, and it is suspected that they may coincide with the bright points. If so, the points are probably small Ellerman bombs, the origin of all surge prominences. Hence, it may be that the spicules emanating from the points are miniature surges. The question may be settled by the multi-channel magnetograph.

An examination of some of the pictures taken at $-\frac{7}{8}$ Angstrom showed what had been taken to be a fine scratch on one frame appeared on all frames. This discovery was not defined until some months later when work on the temperature control of the entrance window of the tower telescope yielded a modest but decisive



An island of solar filigree photographed in the continuum, and at + 2, + 7/8 and -7/8 Angstroms from the center of the hydrogen alpha line. The filigree is bright and coarse on the -7/8 Angstrom exposure (lower right), but its crinkled hair-like character is best visible in the + 2 Angstrom exposure (upper right). The granulation in the area underlying the filigree (upper left) is extraordinarily smeared.

improvement in definition. Islands were found, spotted all over the solar disk, composed of a network of hair thin, bright filaments, a feature named the "solar filigree." The measured width of the filigree strands is 200 km, but this is only an upper limit to their actual diameter, since it is right at the resolution limit of the telescope, certainly the smallest solar features ever photographed. They are observable

only rarely when the seeing is at its best. One characteristic of the filigree islands, readily seen in the figure, is a marked smearing of the underlying granular detail.

Two projects are under way to determine the significance of the filigree and the bright points, their relation with each other, with Ellerman bombs, with the granulation and spicule pattern, and with

magnetic fields. It has been predicted that oscillations at lower levels should generate upward-propagating waves in coronal condensations. They should be visible under favorable circumstances as brightness waves. An eclipse movie was taken, and multiple printed on grainless high contrast film to reduce film grain noise, but the waves could not be detected. This does not mean that they do not exist. Unless the wave fronts lie nearly parallel to the line of sight, they would be invisible because maxima and minima would be superposed. Coronal movies of the July 10, 1972 eclipse, and, if necessary, the June 30, 1973 eclipse, will be taken. Detection of these waves would be an important confirmation of the validity of the theory of plasma waves at very low densities in magnetic fields, a major component in the current efforts to explain the high energy solar radiations that stimulate terrestrial responses.

In conjunction with the search for coronal waves, Sacramento Peak motion picture footage was used to investigate coronal responses to all forms of fast activity in the chromosphere, and the relation between visible coronal activity and the many types of radio bursts recorded by AFCRL's radio and microwave telescopes. This work is still in progress, but there are already a number of interesting findings. The only chromospheric activities that provoke coronal responses are those that inject material into the corona at velocities of 50 km per second or more—all types of eruptive prominences including surges. The only flares that visibly affect the corona are those that eject surges or form loops. Events that appear to be magnetically trapped in the lower corona often emit microwaves, but have no low frequency emission. Those that reach into the upper corona, whether excited by eruptive prominences or other causes, invariably produce Type II or Type IV radio bursts.

RESEARCH ON SOLAR ACTIVITY

The preceding discussion concerns the basic steady state condition of the solar atmosphere, the environment and source of solar activity. We are accustomed to think of flares as very energetic, as indeed they are, but compared with the rate of energy output from the quiet sun, the enhancement due to even the largest flare is trivial. With the exception of the sunspots, all active features are quite invisible without the aid of refined spectroscopic devices tuned to their particular emission frequencies. Thus, solar activity has no appreciable influence on the bulk solar energy output, the power that maintains the terrestrial surface environment. How, then, can a solar flare have the strong terrestrial effects that concern us? Although the flare may enhance the solar power by only one part in one million, its energy is very different in quality. In analogy, it comes in a shower of bullets rather than as the energy of a Niagara, and these bullets affect the atoms and molecules of the ionosphere in ways that no amount of energy from the quiet sun could. The bullets are, of course, X-ray quanta and energetic particles, mostly protons and electrons. On impact, they ionize the atmospheric molecules, changing the electrical properties of the ionosphere with results that have already been described. The ionosphere is thin, about 10^{-4} as dense as sea level air. It is sensitive to very small amounts of energy, if that energy comes in sufficiently concentrated packets, i.e., in X-rays or particles energetic enough to ionize the atmospheric molecules, which are quite impervious to the floods of visible and infrared radiation put out by the quiet sun.

Small though they are, the radiations from solar activity become increasingly important in a world increasingly dependent on advancing technology, particularly in the field of Air Force operations. This is

the reason for the focus of attention on solar activity at Sacramento Peak.

The dominating force is solar magnetism, which, directly or indirectly, powers all forms of solar activity, and energizes the terrestrially effective radiations. The mechanisms by which the diffuse energy of the magnetic fields are concentrated into X-rays and fast particles are very unclear at present. Our hope for understanding lies in careful observation of the magnetic fields and their effects on solar material, interpreted in the quantitative physical terms of magnetohydrodynamics (MHD). In many instances, the sun performs hydromagnetic experiments for us on a scale far beyond any laboratory resources, and these contribute in important ways to the theoretical aspects of MHD. This is a secondary benefit, however, in the effort to find out exactly what goes on before, during, and after a flare, whose antecedents and consequences spread far beyond the flare cataclysm itself in space and time. Every form of solar activity is involved directly or indirectly.

The Sacramento Peak program in solar activity is designed to study all aspects, combining the optical observations made at the Observatory with radio observations from other AFCRL laboratories and outside sources, and data from satellites and rockets above the ultraviolet absorption of the terrestrial atmosphere.

Orbiting Solar Observatory (OSO) No. 4 observations, consisting of mosaics of the solar surface in the light of many ultraviolet lines in the 300 to 1300 Angstrom portion of the spectrum, were studied for several months. A number of these lines are radiated only at very specific temperatures, ranging from 10^4 to 10^6 degrees K in different lines. This is the temperature range from the chromosphere up into the lower corona, and a ranking of the lines according to their temperatures should rank them according to height. This is a

theoretical rationale which has been universally accepted in the analysis of XUV observations of active centers. Its validity, however, depends on a monotonic increase of temperature with height, a condition that is clearly satisfied over most of the sun, but possibly not in the less regular environment of an active center. The observations were to determine whether, in fact, the high temperature lines originate at higher levels in active centers than low temperature lines.

In the OSO pictures, active centers appear as brilliant patches on the solar disk with rather poor spatial resolution of one arc minute.

A purely geometrical method was devised to sort out the heights in an active center, based on the fact that a high level object would have a faster apparent motion due to solar rotation than a low lying object, since its radial distance from the center of rotation is greater. Hence, as an active center rotates across the disk, its image in a high level line should move slightly faster than in a low level line. Since the expected differences in height are only 1 to 2 per cent of the solar radius, the parallax effect is very small, much less than the OSO-4 image resolution. Therefore, small systematic effects in the measurements of some hundreds of OSO pictures taken in five lines of graduated temperature sensitivity had to be measured. The analysis showed that, with one explainable exception, the lines did originate in the expected order of height over a range of 17000 km. This is the first independent geometrical check that provides a reassuringly hard confirmation of the theoretical height scale of the ultraviolet lines.

The same observational material allowed measurement of the rotation rate of the sun at the heights of UV emission, well above the levels accessible to optical observation. This problem is not trivial, since

the rotation rate of the solar surface varies with latitude, from periods of 25 days at the equator to about 31 days at the poles, and appears to increase with height in the solar atmosphere. Surprisingly, at levels of about 2000 and 12000 km, the measured rotation rate is the same, within observational accuracy, as that of the sunspots at height zero in the same latitude.

The umbral flashes were discovered at Sacramento Peak in 1967. They are small bright patches, up to 3000 kilometers in diameter, that appear abruptly over the dark umbra of a sunspot in K line pictures, and migrate rapidly to the nearest umbral boundary as they fade. The entire brightness cycle is less than a minute, and a single source point often spawns a number of successive flashes at regular intervals of 120 seconds. Since the motion is directly across the strongest magnetic fields on the sun, the flashes cannot be clouds of material. Rather they are waves of excitation in a stationary medium, like a moving searchlight spot on a cloud. In 1970, a time sequence of spectrograms was secured at the tower telescope to determine what kinds of vertical mass motions along the field lines are associated with the flashes. A prominent vertical oscillation in the spot umbra with a period of 176 seconds was discovered, but apparently it is quite unrelated to the flashes. These oscillations are probably trivial in the energy balance of a sunspot, which is dominated by the magnetic field many orders of magnitude more energetic. They are important, however, as solar "experiments," significant in the theory of the interaction of magnetic fields and plasma waves, a process which is surely involved in the production of X-rays and fast particles.

RESEARCH ON SOLAR MAGNETIC FIELDS

Measurements of the sightline component of solar magnetic fields in the photosphere

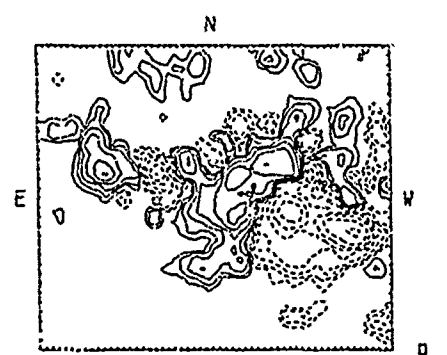
are now fairly routine. At Sacramento Peak, the computer receives the Doppler Zeeman Analyzer signals in real time and produces a contour map of the field in the scanned area which appears on a TV screen at the observing station. Thus, the observer can immediately detect areas of special interest for concentrated attention. This system is fundamental to studying the field activity associated with a number of flares. The time and spatial resolution is still not sufficient to define the important small-scale changes, but some highly significant correlations have been found that will be important in the physical explanation of flares, and also useful in flare prediction.

Solar magnetic observations depend on the Zeeman effect in a dozen sensitive lines that originate in the photosphere. Thus, a magnetic map defines the field distribution only at the photospheric level. While this is of value, the real need is for the three-dimensional field distribution in the space above the photosphere, where the flares originate. A computer program was devised in 1964 at Sacramento Peak to calculate such space field distributions from the available two-dimensional field maps. Because the maps show only the sightline component at each point instead of the full magnetic vector, it was necessary to assume that the field was free of electric currents. This was unfortunate. There was no solid information on currents in the solar atmosphere, and no reason to expect current-free fields. For lack of anything better, solar astronomers use this program, but the current-free assumption is a troublesome uncertainty.

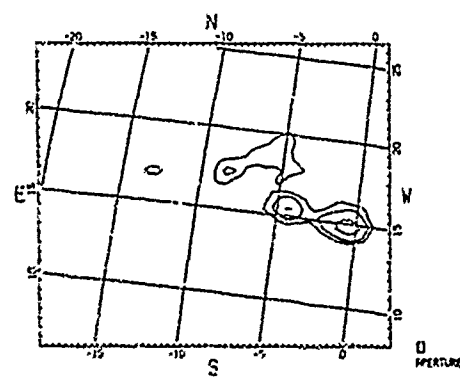
This assumption can be avoided by a vector magnetograph which maps the full magnetic vector. In the strong fields of active centers, the observations required to define the transverse components (which combine with the sightline component to define the vector) are no more difficult

than observations of the sightline component, although the volume of data is tripled. Several vector magnetographs are in operation at present, and the Sacramento

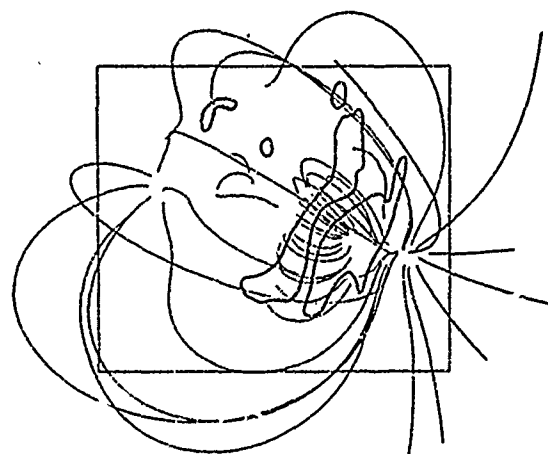
Peak Observatory plans to add the vector capability to the multi-channel magnetograph. It should be pointed out, however, that making the observations is only the



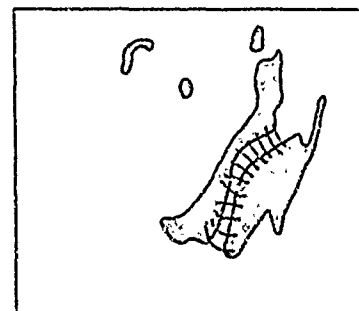
McMath Region 11128 magnetic fields at 2038 UT, January 20, 1971.



Sunspot outlines and solar coordinates for McMath Region 11128 at 2038 UT, January 20, 1971.



Lines of force computed from the magnetogram shown at top left.



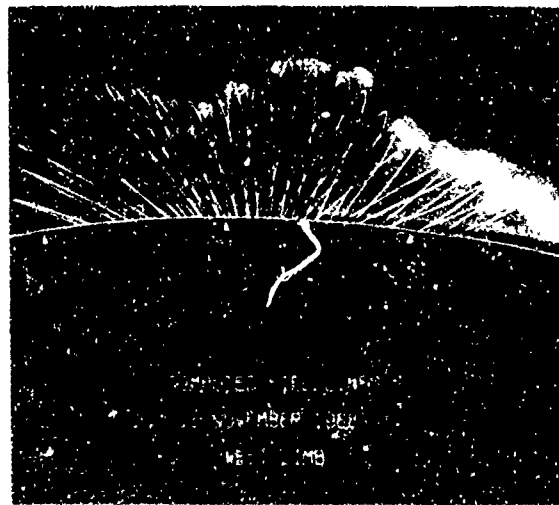
Flare patches (shaded areas) and post-flare loops at 2345 UT, January 24, 1971.

Magnetic field of the flare of January 24, 1971. Upper left: Preflare contour map of photospheric magnetic field. Upper right: Projection of three dimensional calculated field lines, and outline of flare. Note magnetic loops between the two ribbons, and the open field lines radiating from a small area to right of flare. Lower right: Diagram of post-flare loops between ribbons.

simplest part of determining magnetic vectors. The observations are measurements of the polarization of the light at selected points in line profiles. The sightline component is directly and simply related to the circular polarization, and hence is easily determined. The transverse component, however, depends on the degree and direction of linear polarization in a very complicated manner. To determine the transverse field, one must have a reasonably accurate model of the solar atmosphere in the observed region, to define the radiative transfer parameters. This is not a serious problem for the quiet sun, but in an active center, where most abnormal conditions prevail, conditioned by the field to be measured, the interpretation of the observed polarization is difficult and uncertain. Thus, the multi-channel vector magnetograph readings of the transverse field will be less definite than those for the sightline field.

In the complex sunspot groups which produce large flares, there are occasional "satellite spots," small islands or peninsulas of flux of one polarity intruding into a strong field of the opposite polarity. The flares start with bright kernels which are always in or very near such a satellite during a rapidly changing phase of its development. A flare can be reliably predicted some hours in advance by this association. After a flare has run its course, the satellite is less pronounced and the field gradients reduced. This is the most definite observational identification so far of a field configuration that invariably precedes a flare. To take advantage of this and any other magnetic flare precursors that may be discovered, magnetic observations are provided for in the design of the observing equipment for the world-wide solar monitoring net of the Air Weather Service. Meanwhile, arrangements are being made to transmit daily magnetic maps to the AWS Solar Forecasting Center by Telex, over telephone lines.

Under some circumstances, the calculated current-free field accurately represents the real field. This was shown by mapping the photospheric fields with the Doppler Zeeman Analyzer and comparing them with calculated field lines originating at the foot points of loop prominences shown in hydrogen alpha photographs. Loop prominences are rather rare, and the comparison could use only those whose fields had been mapped several days before they reached the limb and formed prominences. Five examples were found that met the requirements. All of them showed excellent agreement between the loop structure and the calculated current-free fields. This demonstration of the validity of the calculations was encouraging, and the same procedure has been used to investigate the fields in active centers that have promising looking satellites. Fortunately, the field in which the proton flare of January 24, 1971 appeared was one of those observed. When the magnetic map and the calculated field



Photograph of a coronal loop system superimposed on the current free magnetic field lines calculated from observations of the surface field. The good agreement between observed structure and calculated field confirms the validity of the current free approximation.

overlying the supposed flare location were compared, it was noted that the magnetic arches bridging the gap between the filaments coincided with a low loop structure, and that the flare as a whole was covered with a magnetic dome that would be impenetrable to outgoing protons. The fast protons, which vigorously showered the earth, are believed to have originated a short distance away in the small area of open field lines that provide a pathway extending out through the corona.

Although the current-free assumption seems to hold even around such violent cataclysms as big flares, there are a few clear instances where electric currents are present, and produce visible effects. A number of prominence pictures showing long streamers with a definite helical structure resembling a coarse screw thread have been collected. A field of this configuration can be produced only by an electric current along the helix.

In 1970, the International Astronomical Union appointed scientists from Sacramento Peak to organize an effort to determine the systematic differences between measurements by different magnetographs around the world. This is a straightforward comparison of records of the fields in the same active centers from the different observatories, complicated by the requirement that the sky must be clear at all of them at the same time. Cooperation among the observatories has been enthusiastic. At Sacramento Peak, the Doppler Zeeman Analyzer magnetic measurements in the Fe 5250 Angstrom line were compared with those in Fe 6303 Angstrom line. Fe 5250, long the standard line for magnetic measurements, has recently been suspected of systematic intensity changes induced by the magnetic fields being measured. As measured by the Doppler Zeeman Analyzer, which should be affected less than any other existing magnetograph by this effect, Fe 5250 field line strengths are approximately 20 percent

lower than those measured in the Fe 6303 line.

Surge prominences are ballistic jets of prominence material that shoot out and fall back with gravitational acceleration along a trajectory defined by the magnetic field. Typical initial velocities are about 100 to 200 km per second. Several fine movies of surges have been obtained while the magnetic fields were mapped simultaneously. Analysis of the magnetic character of the surges has been completed. With good seeing the tower telescope resolves all surges into bundles of parallel filaments along which the surge material moves. There is no sign of helical motion which would indicate the presence of electric currents, and the filaments coincide very well with the calculated fields. Each filament originates in one of the bright points or in an Ellerman bomb, usually located in the outer penumbral boundary of a sunspot.

Next, the nature of the impulse which ejects a surge filament should be determined. Since the kinetic energy is quite comparable with the radiation energy of a flare, and is expended at about the same rate, it will be important to learn whether or not the gross magnetic field changes are as small as they are for a flare.

This review describes the most significant research conducted during this reporting interval. Many minor experiments, theoretical calculations, observation, or instrumental changes that occur continually in any active observatory, have been omitted. Once a scientific objective has been determined, preliminary experimentation is required to define the most direct approach and to determine the feasibility of the project. This is particularly true of problems that strain the state of the art, and optical solar research has reached a stage where further advances depend on determining and using the best possible methods for making the observations needed.

JOURNAL ARTICLES
JULY 1970 - JUNE 1972

- ALTROCK, R. C., and CANFIELD, R. C.
Observations of Photospheric Pole-Equator Temperature Differences
Sol. Phys., Vol. 23 (1972)
- Observations of the Variation of Temperature with Latitude in the Upper Solar Photosphere*
Bull. of the Am. Astronom. Soc., Vol. 3, No. 4 (1971)
Astrophys. J., Vol. 171 (1972)
- ALTROCK, R. C., and WHITE, O. R. (High Alt. Obsv., Boulder, Colo.), BRAULT, J. W., SLAUGHTER, C. D. (Kitt Peak Natl. Obsv., Tucson, Ariz.)
Measurements of the Limb Darkening in the Forbidden Mg I Line at 4571.1 Å
Sol. Phys., Vol. 23 (1972)
- BECKERS, J. M.
The Measurement of Solar Magnetic Fields
Proc. of IAU Symp. No. 43 on Sol. Magnetic Fields, Paris, Fr. (1971)
- Achromatic Linear Retarders*
(Ltr. to Ed.) Appl. Opt., Vol. 10, No. 4 (1971)
- Solar Spicules*
Ann. Rev. of Astron. and Astrophys., Vol. 10 (1972)
- Achromatic Linear Retarders with Increased Angular Aperture*
(Ltr. to Ed.) Appl. Opt., Vol. 11, No. 3 (March 1972)
- BECKERS, J. M., and MORRISON, R. A. (AFIT, Wright-Patterson AFB, Oh.)
The Interpretation of Velocity Filtergrams III. Velocities Inside Solar Granules
Sol. Phys., Vol. 14 (1970)
- BECKERS, J. M., and WAGNER, W. J.
A Photographic Polarimeter for Solar Observations
(Ltr. to Ed.) Appl. Opt., Vol. 9 (1970)
- BRIDGES, C. A., III
Improving the Foreground Response Time of the Sigma 5 RBM Monitor
Proc. of the 18th Intl. XDS Users Gp. Mtg., Vol. 1 (1972)
- CANFIELD, R. C.
Deviations from Local Thermodynamic Equilibrium in Weak Complex Spectra and Formation of Solar Rare-Earth Lines Inside and Outside H and K
Astron. and Astrophys., Vol. 10 (1971)
- A Measurement of the Non-Thermal Velocity in the Low Chromosphere*
Sol. Phys., Vol. 20, No. 2 (1971)

- CANFIELD, R. C., and ATHAY, R. G. (High Alt. Obsv., Boulder, Colo.)
A Self-Consistent Model Atmosphere Program with Applications to Solar OI Resonance Lines
Spectrum Formation in Stars with Steady-State Ext. Atm., Groth & Wellman, Ed., NBS Spec. Pub. 3328 (1970)
- DE MASTUS, H. L., and BRUZEE, A. (Fraunhofer Inst., Freiburg, Ger.)
Flare-Associated Coronal Expansion Phenomena
Sol. Phys., Vol. 12, (1970)
- DUNN, R. B.
Computer Control of Vacuum Solar Telescope Automation in Opt. Astrophys., IAU Colloq. No. 11 (Pub. of the Royal Obsv., Edinburgh, Scotland), Vol. 8 (August 1970)
- Solar Instrumentation (Part II)*
Natl. Bur. of Stds. Spec. Pub. 353 (1971)
- High Resolution Solar Observations*
Sp. Rep. XII, Akademie-Verlag, Berlin (1972)
- EVANS, J. W.
Sacramento Peak Observatory - Annual Reports of Observatories
Bull. of the Am. Astronom. Soc., Vol. 2, No. 1 (1970)
- Solar Instrumentation, Part I*
Natl. Bur. of Stds. Spec. Pub. 353 (1971)
- GILLIAM, L. E., and WHITE, O. R. (High Alt. Obsv., Boulder, Colo.)
Photographic Isophotes of Solar Fine Structure
AAS Photo Bull. (February 1970)
- HIRAYAMA, T.
Ionized Helium in Prominences and the Chromosphere
Sol. Phys., Vol. 24 (1972)
- HYDER, C. L.
Strong Coronal Shocks and "Thermal" Solar X-Ray Bursts
Sol. Phys., Vol. 14, No. 1 (September 1970)
- HYDER, C. L., and LITES, B. (Univ. of Colo. /High Alt. Obsv., Boulder, Colo.)
Hα Doppler Brightening and Lyman-α Doppler Dimming in Moving Hα Prominences
Sol. Phys., Vol. 14, No. 1 (September 1970)
- MUSMAN, S. A.
Are Exploding Solar Granules Vortex Rings?
APS Bull., Ser. II, No. 16 (1971)
- Observations and Interpretations of Supergranule Velocity and Magnetic Fields*
Proc. of IAU Symp. No. 43 on Sol. Magnetic Fields, Paris, Fr. (1971)

- MUSMAN, S. A., and REIF, R. J. (Univ. of Colo.)
Interference of Solar Oscillations
 Bull. of the Am. Astronom. Soc., Vol. 3 (1971)
Interference in Solar Oscillations
 Sol. Phys., Vol. 20 (1971)
- MUSMAN, S. A., and RUST, D.
*Vertical Velocities and Horizontal
 Wave Propagation in the Solar Photosphere*
 Sol. Phys., Vol. 13 (August 1970)
- PARVEY, M. I. (IND. UNIV.), and MUSMAN, S. A.
*Bright-Dark Asymmetry in Solar
 Granulation*
 Sol. Phys., Vol. 18, No. 3 (1971)
- RUST, D. M.
Magnetic Fields in Solar Active Regions
 AIAA Prog. in Astronaut. and Aeronaut., Vol. 30,
 MIT Press, McIntosh and Dryer, Eds. (1972)
Magnetic Fields in McMath Region 11125
 Upper Atm. Geophys. Rpt. (UAG-20), NOAA,
 Boulder, Colo. (1972)
- RUST, D. M., and ROY, J. R. (Univ. of W. Ontario,
 Can.)
*Coronal Magnetic Fields Above Active
 Regions*
 Proc. of IAU Symp. No. 43 on Sol. Magnetic Fields,
 Paris, Fr. (1971)
- SIMON, G. W.
*Mass Motions in Solar Flares and Related
 Phenomena Book Review, Ed. by Yngve
 Ohman, Intercience, Wiley, N. Y., 1968*
 Sci., Vol. 167, No. 3926 (27 March 1970)
- SIMON, G. W., and NOYES, R. W. (Harvard Coll.
 Obsv., Cambridge, Mass.)
Observations of the Coronal Network
 Proc. of IAU Symp. No. 43 on Sol. Magnetic Fields,
 Paris, Fr. (1971)
*Observed Heights of EUV Lines Formed
 in the Transition Zone and Corona*
 Bull. of the Am. Astronom. Soc., Vol. 3 (1971) Sol.
 Phys., Vol. 22 (1972)
*Solar Rotation as Measured in EUV
 Chromospheric and Coronal Lines*
 Bull. of the Am. Astronom. Soc., Vol. 3 (1971)
- SIMON, G. W., and WEISS, N. O. (Univ. of
 Cambridge, Eng.)
On the Magnetic Field in Pores
 Sol. Phys., Vol. 13 (1970)
- TALLANT, P. E.
A Solar Flare Videometer
 Sol. Phys., Vol. 11 (1970)
- WAGNER, W. J., and BECKERS, J. M.
*The Polarization of Coronal Emission
 Lines*
 Sol. Phys., Vol. 21 (1971)
- WAGNER, W. J., and HOUSE, L. L. (High Alt. Observ.,
 Boulder, Colo.)
*Empirically Corrected Calculations of
 Coronal Visible Lines from SP5SD
 Configuration*
 Astrophys. J., Vol. 166 (1971)
- PAPERS PRESENTED AT MEETINGS**
JULY 1970 - JUNE 1972
- ALTROCK, R. C.
*An Empirical Analysis of the Infrared
 Triplet of O I*
 Mtg. of the AAS Sol. Phys. Div., Huntsville, Ala.
 (17-19 November 1970)
- ALTROCK, R. C., and CANFIELD, R. C.
*Observations of the Variation of Temperature
 with Latitude in the Upper Solar Photosphere*
 186th Mtg. of the Am. Astronom. Soc.,
 San Juan, P. R. (5-8 December 1971)
*Pole-Equator Temperature Differences
 on the Sun*
 Adelaide Conf. of the Astronom. Soc. of Aust.,
 Adelaide, S. A., Aust. (18-15 December 1971)
- BECKERS, J. M.
*The Measurement of Solar Magnetic
 Fields*
 IAU Symp. on Sol. Magnetic Fields, Paris, Fr. (31
 August-4 September 1970)
*The Response of the Helium Triplet Radiation
 in Prominences to an Increase in Ultraviolet
 Flux Resulting from Solar Flares*
 1972 AAS Sol. Phys. Div. Mtg., Univ. of Md.,
 Coll. Pk., Md. (4-5 April 1972)
- BECKERS, J. M., and SCHULTZ, R. S. (High Alt. Observ.,
 Boulder, Colo.)
Oscillatory Phenomena in Sunspots
 1972 AAS Sol. Phys. Div. Mtg., Univ. of Md.,
 Coll. Pk., Md. (4-5 April 1972)
- BIRNICK, C. A., III
*Improving the Foreground Response Time
 of the Sigma 5 REM Monitor*
 Xerox Users Gp. Mtg., Cherry Hill, N. J. (18-20 May
 1972)
- CANFIELD, R. C.
*Theory of Formation of Solar Rare-Earth
 Lines*
 Mtg. of the AAS Sol. Phys. Div., Huntsville, Ala.
 (17-19 November 1970)

Observations on the Relationship Between the Latitudinal Variations of Temperature and Magnetic Field
1972 AAS Sol. Phys. Div. Mtg., Univ. of Md., Coll. Pk., Md. (4-6 April 1972)

DE MASTUS, H. L., and DUNN, R. B.
Coronal Movies
IAU Gen. Assem., Comm. 12 - Sol. Atm., Brighton, Eng. (18-27 August 1970)

DUNN, R. B.
Computer Control of Vacuum Solar Telescope
IAU Colloq., Royal Obsv., Edinburgh, Scotland (12-14 August 1970)
Coronal Events Observed in 5303 Å (Invited)
NATO Adv. Study Inst. on the Phys. of the Sol. Corona, Athens, Gr. (6-17 September 1970)
Sacramento Peak Magnetograph
IAU Symp. No. 43 on Sol. Magnetic Fields, Coll. de France, Paris, Fr. (31 August-4 September 1970)
Optical Performance of Vacuum Solar Telescopes
Mtg. of the AAS Sol. Phys. Div., Huntsville, Ala. (17-19 November 1970)
Solar Instrumentation (Part II) (Invited Paper)
The Menzel Symp. on Sol. Phys., Atomic Spectra and Gaseous Nebulae, Harvard Coll. Obsv., Cambridge, Mass. (8-9 April 1971)
High Resolution Solar Observations
(Invited Paper) 14th Ann. COSPAR Mtg., Seattle, Wash. (17 June-2 July 1971)

DUNN, R. B., and ERSTEIN, G. L., HOBBS, R. W., MARAN, S. P.: (NASA Goddard Sp. Flt. Ctr., Greenbelt, Md.)
New Multichannel Spectrometer at Sacramento Peak
1972 AAS Sol. Phys. Div. Mtg., Univ. of Md., Coll. Pk., Md. (4-6 April 1972)

DUNN, R. B., and ZISKER, Z. B. (Astronom. Inst., Univ. of Haw.)
A Search for the Photospheric Origin of Spicules
1972 AAS Sol. Phys. Div. Mtg., Univ. of Md., Coll. Pk., Md. (4-6 April 1972)

EVANS, J. W.
Introduction to Research on the Solar Corona (Invited Paper)
NATO Adv. Study Inst. on the Phys. of the Sol. Corona, Athens, Gr. (6-17 September 1970)
Introductory Review of Solar Activity
AIAA-AAS Mtg., Huntsville, Ala. (16-20 November 1970)

Solar Instrumentation (Part I)
(Invited Paper) The Menzel Symp. on Sol. Phys., Atomic Spectra and Gaseous Nebulae, Harvard Coll. Obsv., Cambridge, Mass. (8-9 April 1971)

FISHER, R. R.
10830 Image Tube Filtergrams of Plage Activity and a Small Flare
1972 AAS Sol. Phys. Div. Mtg., Univ. of Md., Coll. Pk., Md. (4-6 April 1972)

GILLIAM, L. G., and HOLLARS, D. R.
The Temperature Dependence of the Response of 108 a-O and Tri-X at 4400 Å
AAS Mtg., Smithsonian Obsv., Cambridge, Mass. (23-24 August 1971)

MUSMAN, S. A.
Observations and Interpretations of Supergranule Velocity and Magnetic Fields
IAU Symp. No. 43 on Sol. Magnetic Fields, Coll. de France, Paris, Fr. (31 August-4 September 1970)
Are Exploding Solar Granules Vortex Rings?
APS Mtg. of Div. of Fluid Mechan., San Diego, Calif. (22-24 November 1971)
A Mechanism for Exploding Solar Granules
1972 AAS Sol. Phys. Div. Mtg., Univ. of Md., Coll. Pk., Md. (4-6 April 1972)

MUSMAN, S., and REIR, R. J. (Univ. of Colo.)
Interference of Solar Oscillations
Mtg. of the AAS Sol. Phys. Div., Huntsville, Ala. (17-19 November 1970)

RUST, D. M.
Magnetic Fields in Solar Active Regions
Mtg. of the AAS Sol. Phys. Div., Huntsville, Ala. (17-19 November 1970)
Magnetic Fields in Prominences
Symp. on the Phys. of Sol. Prom., Anacapri, Italy (28 September-2 October 1971)
Real-Time Analysis of Flare-Associated Photospheric Magnetic Fields
1972 AAS Sol. Phys. Div. Mtg., Univ. of Md., Coll. Pk., Md. (4-6 April 1972)

RUST, D. M., and ROY, J. R. (Univ. of W. Ont., Can.)
Coronal Magnetic Fields Above Active Regions
IAU Symp. No. 43 on Sol. Magnetic Fields, Coll. de France, Paris, Fr. (31 August-4 September 1970)

SIMON, G. W.
Rotation of Active Regions in the Corona
1972 AAS Sol. Phys. Div. Mtg., Univ. of MD., Coll. Pk., Md. (4-6 April 1972)
Motion and Magnetism on the Sun (Invited Paper)
Phys. Symp., Grinnell Coll., Grinnell, Iowa (14-15 April 1972)

SIMON, G. W., and LYNCH, D. K. (Univ. of Texas)
*Correlation Between the Intensity Fields
 of the Chromospheric and Coronal Networks*
 1972 AAS Sol. Phys. Div. Mtg., Univ. of Md.,
 Coll. Pk., Md. (4-6 April 1972)

SIMON, G. W., and NOVES, R. W. (Harvard Coll.
 Obsv., Cambridge, Mass.)
Observations of the Coronal Network
 IAU Symp. on Sol. Magnetic Fields, Coll. de France,
 Paris, Fr. (31 August-4 September 1970)
*Observed Heights of EUV Lines Formed in
 the Transition Zone and Corona and
 Solar Rotation as Measured in EUV Chromospheric
 and Coronal Lines*
 Mtg. of the AAS Sol. Phys. Div., Huntsville, Ala.
 (17-19 November 1970)

SIMON, G. W., and OH, Y. K. (Ohio State Univ.)
*Measurements of Supergranular Velocities
 in the Low and High Photosphere*
 1972 AAS Sol. Phys. Div. Mtg., Univ. of Md., Coll.
 Pk., Md. (4-6 April 1972)

WAGNER, W. J., and BECKERS, J. M.
Polarimetry of Coronal Emission Lines
 14th Ann. COSPAR Mtg., Seattle, Wash. (17 June-2
 July 1971)

WAGNER, W. J., and HEUSS, L. L. (High Alt. Obsv.,
 Boulder, Colo.)

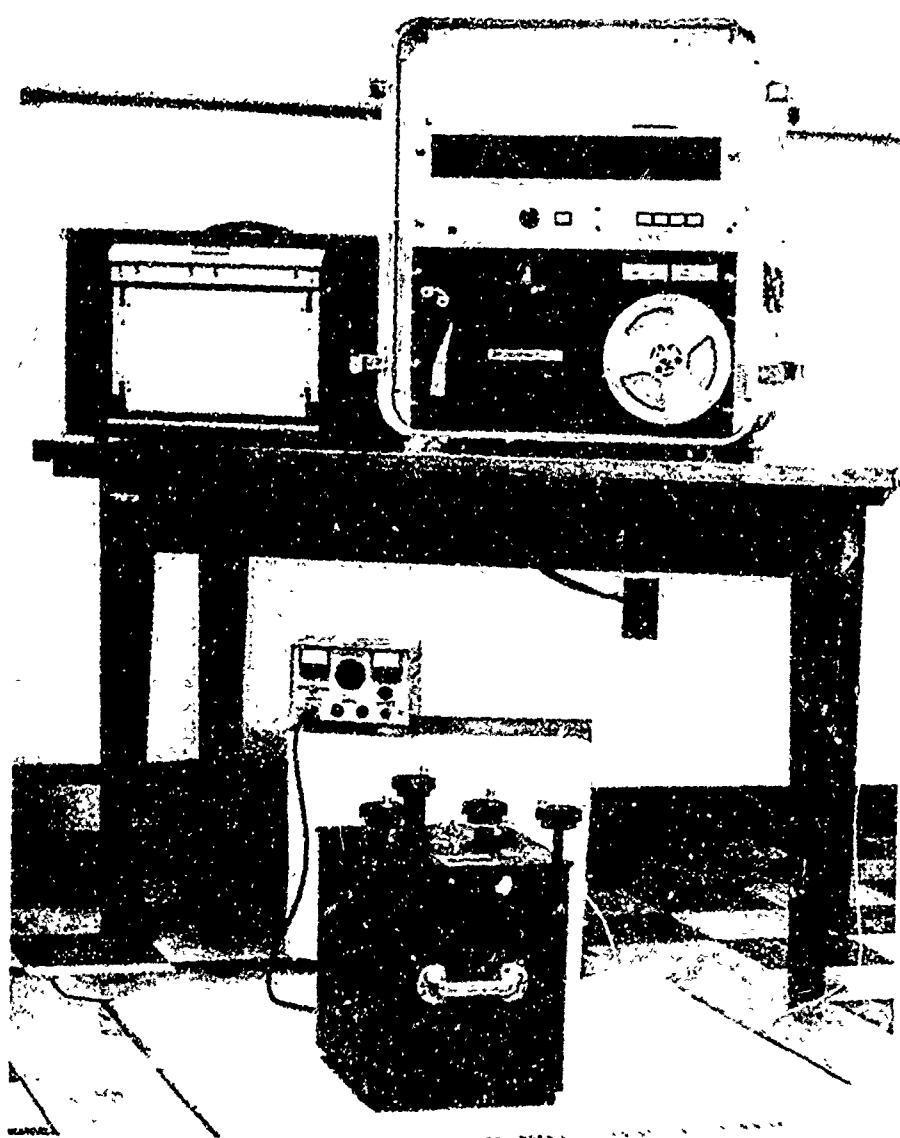
*Empirically Corrected Calculations of
 Coronal Visible Lines from the 3p² 3d
 Configuration*
 Mtg. of the AAS Sol. Phys. Div., Huntsville, Ala.
 (17-19 November 1970)

WAGNER, W. J., and NEWKIRK, G. (High Alt. Obsv.,
 Boulder, Colo.), SCHMIDT, H. U. (Max-Planck Inst.
 fur Phys. und Astrophys., Munich, Ger.)
*A Search for Compressional Waves in the
 Inner White Light Corona*
 1972 AAS Sol. Phys. Div. Mtg., Univ. of Md., Coll.
 Pk., Md. (4-6 April 1972)

TECHNICAL REPORTS JULY 1970 - JUNE 1972

FISHER, R. R.
A Search for Apochromatic Lens Systems
 AFCRL-72-0227 (8 April 1972)

RUST, D. M.
*Magnetic Fields in Solar Prominences - A
 Review*
 AFCRL-72-0048 (12 January 1972)



A LaCoste and Romberg Geodetic Gravimeter recording earth tides at AFCLR seismic-gravity observatory. Both analog and digital readout systems are shown.

VIII Terrestrial Sciences Laboratory

The Terrestrial Sciences Laboratory conducts research on the properties and environment of the earth's surface, subsurface, and near atmosphere, particularly in the areas of seismology, geology, crustal physics, spectroscopic studies and geodesy and gravity. These efforts involve the collection and interpretation of geophysical data, the application of mathematical models to actual physical phenomena, and the development and testing of new instrumentation for experimental studies.

During this reporting period, the Laboratory mission was partly redirected toward new objectives. This called for the phasing out of traditional seismology efforts and for new emphasis on geokinetic motion studies. The long-time effort in remote sensing of terrain properties was replaced by a program to determine electromechanical properties of geologic material. Expansion into spectroscopic studies of terrestrial backgrounds was begun. The programs of airborne gravity measurements and lunar distance determinations by laser reflection techniques were satisfactorily completed and the aircraft previously used for the terrain sensing and airborne gravity programs was released and reassigned.

Laboratory efforts in seismology are now oriented toward providing a better understanding of the sources and propagation characteristics of natural or manmade phenomena.

Earthquake prediction and control occupies the attention of the nation's seismologists and it is acknowledged that a more general theoretical understanding of earthquake mechanisms is needed at the present time. To improve this understand-

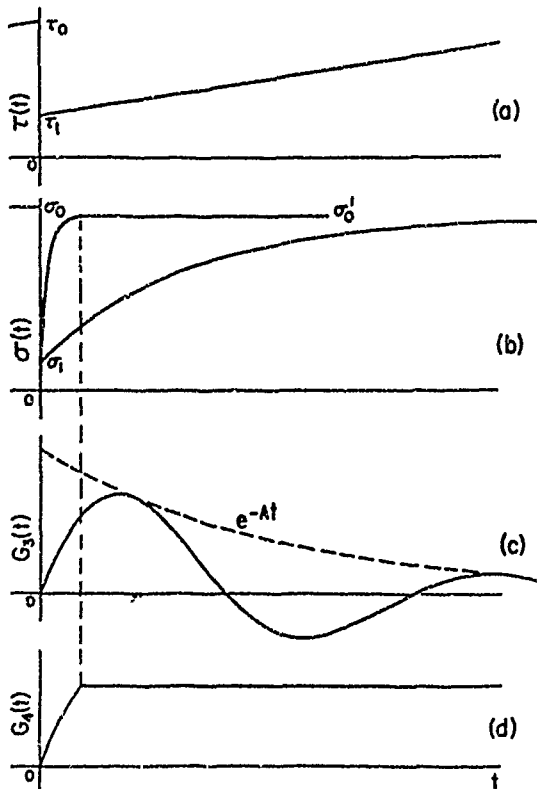
ing, the AFCRL effort in seismology is concerned with the development of more detailed quantitative theories of the earthquake focal mechanism and with direct measurement of the deformational behavior and strength of various minerals under extreme pressure and temperature.

SEISMOLOGY

EARTHQUAKE SOURCE MECHANISM: If the seismic source (explosion or earthquake) is more thoroughly understood, success in isolating and identifying unique signal characteristics radiating from each source should be enhanced. The Laboratory is pursuing this hypothesis through theoretical studies, to develop a theory applicable to seismic energy radiating from either a fault in the earth or an underground nuclear explosion.

Little is known about the actual spatial and temporal distribution of displacements along a moving fault. It is possible, however, from a mathematical viewpoint, to imagine the source replaced by a narrow "box" neatly enclosing the focal region. The seismic energy radiated from the focal region may then be described in terms of an equivalent set of displacements occurring at the box surface only. This approach has led to the development of a quantitative focal mechanism theory for the computationally difficult region very close to the source. The theory assumes both that the source dislocation function can be described temporally and that the velocity of the dislocation front along the fault can be prescribed. There are three independent possible motions of the line source. During the reporting period, the tensile and transverse shear motions were worked out to complete the work published earlier for the longitudinal shear fault.

Because of the difficulty of obtaining appropriate data from nature, these postu-



By fitting an equation to the observed data, conclusions can be drawn about the earthquake source region. Here, curve (a) gives the stress versus time. The sharp drop at time zero is assumed caused by rock fracture giving rise to an earthquake. Curve (b) shows the strength of the medium. The left curve assumes a fast recovery, the right curve, a slower recovery of strength. The curve in (c) gives the resulting motion for a slow strength recovery, the curve in (d), the motion when the recovery is very fast.

lates are being tested against physical laboratory models. The models are prefabricated to form a fault, and then slowly stressed biaxially in a pneumatic stressing machine, while the changes in the stress field are monitored optically using the photoelastic effect. The "seismic" effects resulting from model failure ("earthquakes") are recorded by strain gauge instrumentation. Disposition of the gauges throughout the model is such that the details of the propagating dislocation can

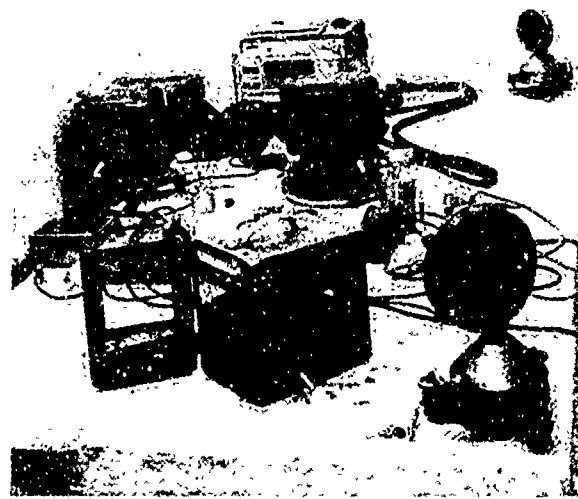
be followed from observation of the close-in seismic radiation recorded by the gauges.

ENVIRONMENTAL EFFECTS ON TEST STANDS: During recent years scientists and engineers concerned with evaluating inertial guidance devices have become increasingly aware that a limiting factor in assessing performance quality is low-level uncontrolled motion due to the test stand geophysical environment, particularly microseismic phenomena. Several approaches to analyzing and correcting for the noise problem have been attempted within the Laboratory for improved design considerations for test stands.

In the first approach, physical laboratory models are utilized incorporating the techniques of two-dimensional seismic modeling. The basic model consists of a circular disk, typically made of Plexiglas, with the model test pad isolation geometry placed on or cut into a position on the disk rim and instrumented with strain gauges. Strain gauges are also placed at the antipodal point so that the model test pad and free field response to seismic excitations can be compared. The seismic excitation source is placed on the rim halfway between the model test pad and its antipode. For a given test pad the effects of greatly differing seismic sources can readily be learned. An exploding rivet on one side gives a short transient source of surface or body waves, while sinusoidal tone bursts can be produced from a piezoelectric source on the other side. Preliminary test results indicate that some current designs for test pad isolation may be deceptive in their action, reducing undesired motion in one direction while perhaps enhancing such motion in another.

A mathematical modeling approach is also being followed, using computational techniques on the appropriate wave equations while incorporating pad designs with realistic boundary conditions. Such mathe-

matical models are also two-dimensional, assuming a rigid block of arbitrary shape welded to an elastic half-space. Seismic excitation can be either body waves or surface waves at any appropriate angle of incidence, and with any wave shape. A solution to this problem has been obtained in the form of a computer program. The program output can be in any of several convenient formats, one of which is a motion picture film showing the exaggerated motion of the test pad slowed down to appear to the eye as a continuous moving sequence.



The round device in the center of the picture is a geosensor, which uses an integrating rate gyro as the sensor to determine the alignment of the earth rotational axes. A cable runs from the instrument to a digital indicator at the rear, which reads the difference between the assumed north direction and true north. The difference can be transferred to a mirror on the outside of the sensor, and this true north reference can then be transferred to an external mirror to provide a north reference at any desired point. Here, the output is being transferred to two mirrors (round objects at right front and right rear) in a test to determine repeatability of the readings. To reduce scatter in the data, seismometers and tiltmeters are used on the pier to determine environmental motion.

EXPLOSIVE VOLCANISM: The contributions of volcanic eruptions to the dust and aerosol content of the upper atmosphere have only recently been recognized in the growing concern of scientists over general atmospheric pollution. Military significance of such phenomena lies in the evident increasing turbidity of the stratosphere and its possible detrimental effect on airborne optical, navigational, and reconnaissance sensors.

A study was conducted of the source distribution of explosive volcanism events whose effluents have likely penetrated into the stratosphere. It concluded that during the past two decades there have been two periods (1950-1956 and 1963-1970) of strongly explosive eruptions. In the latter period, two latitudinal belts of volcanoes have ejected ash and gases into the stratosphere. One belt is equatorial and the other is just below the Arctic Circle. The latter, where the tropopause is considerably lower, may have been the principal source of dust and ashes. Submarine volcanoes and volcanic eruptions producing large amounts of steam within this belt may be the source of the reported increase in stratospheric water vapor.

This reporting period saw the end of the multispectral photography and thermal infrared remote sensing, which was replaced by a program to determine soil properties by measuring electrical properties. The work in crustal studies research is becoming more closely related to the seismology program in their common interest in the deformation and plasticity of the earth's crust. These small-scale movements can cause a missile silo to become slightly misaligned from the vertical, and thus affect the targeting accuracy of a missile.

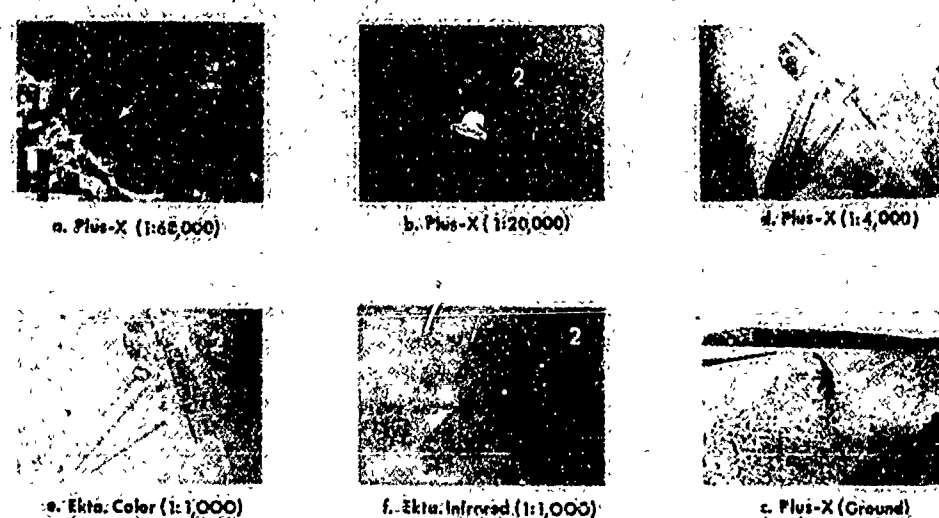
GEOLOGY

REMOTE SENSING OF TERRAIN: During the spring of 1971 the C-130 remote sensing

aircraft was reassigned from AFCRL, bringing to an end the Laboratory's use of multispectral photography and thermal infrared imaging procedures for airborne geological surveys. Prior airborne data collection flights were made, in a joint effort with the U.S. Geological Survey and the Army Corps of Engineers, over Puerto Rico and the U.S. Virgin Islands. The purpose of the surveys was to assist in analysis of lateritic soil conditions in a semitropical environment. Terrestrial radiation and reflection differences from varying soil and moisture conditions provide strong clues for terrain type identification.

One of the last airborne missions also concluded the long-term research program for evaluation of dry lakebeds as emergency unprepared airstrips. During rough-field operational tests of the new giant C-5A transport aircraft at Harper Dry Lake, California, the Laboratory obtained aerial photographic coverage of the lakebed runway. Analysis of the relative compaction and rutting of the soil by aircraft takeoffs and landings is aided by interpretation of the reflectance tone patterns seen on this multispectral imagery. Extensive ground surveys of the load-bearing properties and moisture susceptibility of the soil were conducted simultaneously to verify the interpreter's analysis.

ELECTRICAL AND MECHANICAL PROPERTIES OF TERRESTRIAL MATERIALS: After the remote sensing effort for airborne determination of the properties of terrain was terminated, Laboratory scientists turned their attention toward other means of obtaining information on the surface and subsurface geologic material through other observable signatures. The most commonly sought parameters of terrestrial materials are mechanical properties, particularly strength properties. Mechanical properties are difficult enough to measure in small sizes in the laboratory; they are exceedingly difficult to measure *in situ* in the large sample sizes usually desired or



Comparison of imagery illustrating micro-morphological characteristics at Field Station No. 2, Harper Dry Lake, California (July 1970).

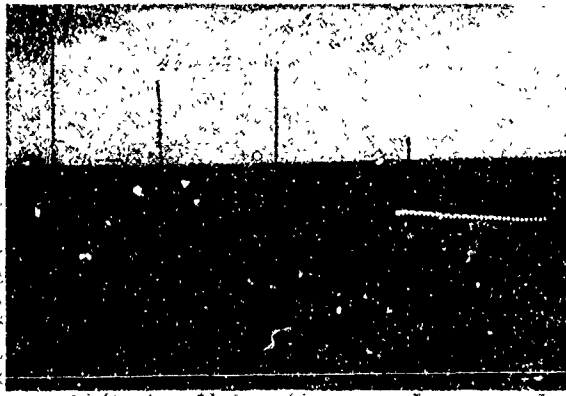
necessary. However, electrical properties of earth materials are much more easily measured, particularly in the field, and large sample sizes are measurable in many electrical techniques with as much ease as small ones. Furthermore, electrical properties of a sample can be measured both internally and externally from convenient locations without direct sample contact. The readily determined electrical parameters (dielectric constant and electrical conductivity) are believed correlated with mechanical properties (density, porosity, elasticity, and shear and tensile strength) in terrestrial materials.

Research was therefore initiated to determine: the electrical and mechanical properties of rocks and soils, correlations between these properties, and the basis of phenomena in both consolidated and unconsolidated terrestrial materials. The use of long, linear electrodes, each in a separate borehole, enables electrical measurements on any geologic sample size by providing electric definition of the sample boundary as an equipotential surface.

Field investigations are performed to identify the *in situ* mechanical properties as determined by seismic energy propagation phenomena. A full-scale field experiment utilizing a 9-position array of electrodes was prepared for deployment at a high explosive test in late 1972. Measurements of electrical conductivity before and during shock wave transit of the rock material will serve to establish both static and dynamic parameters for analysis.

Theoretical studies covering all possible correlating factors, even as fundamental as material atomic structure, are also conducted. As the understanding of the electro-mechanical relationships becomes more evident, it is planned to shift the detection technique from direct-contact electrical probes to electromagnetic wave propagation procedures which would permit subsurface measurements from a remote platform.

ROCK AND SOIL MECHANICS: Deformational behavior of poorly consolidated terrestrial material is studied in the laborato-



A nine-position array installed for determining electrical and mechanical properties of the soil. The igloo-shaped object is a stack of bricks totaling 20 tons of TNT. Detonation of this explosive caused a disturbance in the ground and the electrical changes as the disturbance moved past the sensors were measured, so that dynamic, as well as static, measurements could be made on the soil.

ry using specially designed experimental apparatus and techniques. Emphasis in the conduct of current and planned experiments is placed on such factors as amount and type of minerals, presence and pressure of pore fluids, degree of cementation, abundance of organic matter, and material fabric structure. Samples are either taken from nature or are artificially compacted from natural materials to a known porosity in either hydrostatic or uniaxial compaction machines specifically designed for these studies. The selected samples are measured in a new triaxial testing machine in which the confining pressure is applied by a gas so that observed parameters can be measured as functions of confining pressure with enough precision to determine their derivatives with respect to pressure. The confining environment can vary from 0 through 12 kilobars pressure and from room temperature to 1000 degrees C. Stress-strain curves are measured through a strain rate range of 10^{-2} to 10^{-8} per second, while internal pore pressure can vary from zero through 100 percent of the confining pressure.

The work on rocks emphasizes studies of shear strength in opposed anvil type presses which permit a pressure and temperature environment up to 150 kilobars and 1000 degrees C dependent somewhat on the sample size selected. Compressive strength is determined in a piston cylinder apparatus operating up to 30 kilobars and 1400 degrees C where selected silicate clays are studied. Deformed samples are examined by optical, X-ray, electron microscope, and other physical methods linking the microstructure to the gross sample properties to determine slip systems and mineralogy of the samples. Atomic models of the slip system are developed through the crystal structure as a function of temperature to show why a particular system is favored over competing systems. Intact and prefractured rocks are being studied with a broad spectrum of cyclic loading (fatigue testing) under effective confining pressures and temperatures that simulate the natural environments of crustal materials.

SOIL CHEMISTRY AND MINERALOGY: Air Force civil engineers need improved techniques for stabilizing soil areas affecting structures such as silos, runways, and roads, and for controlling erosion on military bases. Understanding of the chemical and mineralogical character of the interaction between soil and various chemical stabilization agents will enable their proper choice and efficient use. Previous engineering efforts have neglected the understanding of how the additive materials interact with the parent soil minerals, ideally to provide a rigid, indispersible soil mass with high load-bearing strength and resistance to weathering.

An in-house laboratory study was begun during 1971. It employs scanning electron microscopy, X-ray diffraction, petrographic, and standard chemical techniques to determine the nature, process, and mechanisms by which soil clay minerals are stabilized. Many of the physical properties of

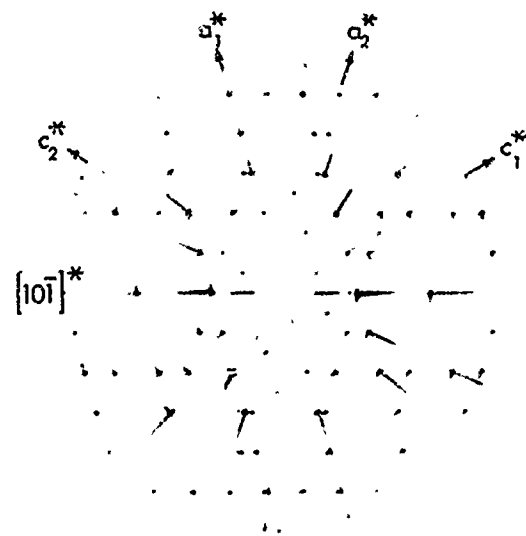
Study of an experimentally deformed mineral (amphibole).



(a) A thin section of deformed single crystal amphibole (cylinder 7.7 mm long by 2.8 mm diameter). Test conditions were 15 kb confining pressure, 400 degrees C temperature, and a strain rate of 10^{-5} per second. Deformation has induced a ductile zone (broad, light-colored band from top left to center right) and twinning (narrow, bright bands tending from upper right to center left).



(b) Magnified twin lamellae (narrow, bright bands perpendicular to the axis of the specimen in (a) show the direction of the host crystal axis.



(c) An X-ray precession photograph of the deformed amphibole single crystal shown in (a). The lower half of the photograph can be brought into coincidence with the upper half by a 180-degree rotation about the crystallographic direction $[10\bar{1}]^*$ which establishes that the crystal is twinned.

clays are determined by surface changes on the clay particles and their ionic bonding. Mixtures of pure clay mineral samples typical of natural soil conditions in various areas of the world are prepared for analysis of new compounds formed and evaluation of optimum stabilization methods.

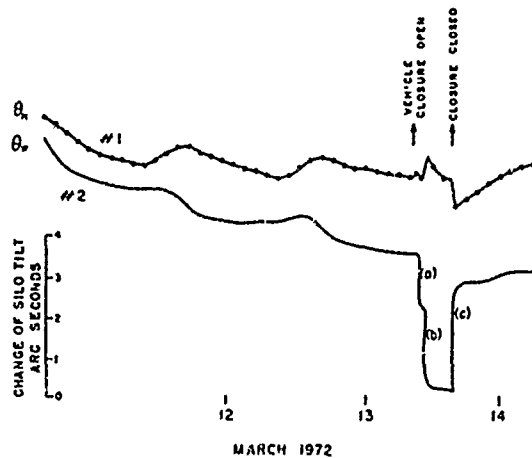
GEOKINETICS

The 1969 Ad Hoc Committee of the USAF Scientific Advisory Board recommended that with improving sensitivity of inertial guidance instruments the influence of geokinetic phenomena must be accounted for. This is predicated on studies discerning the relations between these phenomena and inertial hardware performance. The geokinetic phenomena of concern to inertial guidance testing and operations are categorized as propagating and non-propagating motions. Propagating motions include earth background noise and seismic events while nonpropagating motions include local and regional tilts, earth tides, polar wobble, earth rate irregularities, and precession. Employing data acquisition and reduction techniques developed under previous geokinetic investigations, a program was initiated to determine and define the influence of environmental noise fields on inertial hardware test components and test platforms.

ENVIRONMENTAL MOTION: Two inertial test facilities, at Honeywell Inc., St. Petersburg, Florida and Northrop Corp., Norwood, Massachusetts were used to conduct an initial environmental motion study. The program objectives were to characterize the test facilities' motion environment in terms relevant to facility design and single-degree-of-freedom performance tests. Observations of regional and facility environmental motions were described as second order statistics that

served as a basis for optimum prediction operators. These operators, in turn, were used to separate regional and facility motions, develop figure of merit for test stands, delineate intra-facility motion coherency and demonstrate gyro sensitivity to the motion environment. From these two studies a new approach to earth noise field problems in inertial component testing was developed. The approach is to describe the earth motions by determining: 1) the class of random motion, 2) the level of motion, 3) the mode of motion, and 4) the component relationships. This procedure is considered superior to accepted "quiet site" and "motion suppression structure" techniques. Application of this technique resulted in a significant removal of motion induced error from SDF gyro data.

The new methodology was applied to facility design and inertial hardware test problems at the Air Force Frank J. Seiler Research Laboratory, USAF Academy, Colorado. The response to ground motion



Tilt measurements made in a missile silo, showing the effect of a vehicle (Transporter/Erector) approaching the silo and the opening of the closure door. θ_n is the tilt toward the north and θ_w , the tilt toward the west. The changes in the tilt were caused by (a) arrival of the Transporter/Erector at the silo, (b) opening the blast doors, and (c) closing the blast doors.

and intralaboratory disturbances of a unique pneumatic spring suspension test platform were determined. The motion measurements were combined to form unambiguous estimates of platform strain, rotation and linear acceleration. These motion terms were then inserted into inertial hardware performance models to establish their impact on testing.

In these environmental noise investigations, it became increasingly evident that gyro sensitivities were influenced to some degree by seismic motions. With the cooperation of the Air Force Space and Missile Systems Organization (SAMSO), a joint program with the Northrop Corporation was originated to determine long term geophysical effects on gyrocompass testing. Major aspects of this program concerned the degree of resolution with which the gyrocompass can measure small azimuth changes, the long-term accuracy of four-position gyrocompassing when all error sources are accounted for, statistical attributes of the gyro, and the gyro as a geophysical tool. Important results to date in this program demonstrate that the gyro is sufficiently sensitive to disturbances caused by large, distant earthquakes so that there is a loss in the precision of gyrocompasses all over the world after a magnitude 6 or greater earthquake located anywhere. Since the return period of earthquakes of magnitude 6 or greater is 60 hours, the risk that an earthquake will affect test performance data depends heavily on testing duration.

Because the results of the test facility studies were good, and because there was a need to account for geokinetic factors on the performance of inertial guidance systems, a recommendation was submitted to and approved by SAMSO for determining the total motion of a Minuteman silo. Not only seismic-induced motions, but also long term motions resulting from local and regional crustal instabilities were to be monitored. The ultimate aim of this work was

to determine the effect of the operational environment on the performance of existing and planned systems, through their influence on initial azimuth and zenith estimates. The planned approach was to develop prediction operators based on in-depth studies of a few sites so that only sparse measurements would be needed at other locations. The program plan was submitted in the form of a technical summary to SAMSO.

Before a long term Minuteman silo study could begin, the feasibility of employing the methods developed for test facilities at a silo site had to be determined, and problem areas in a long-term geophysical study of the geokinetic factors that influence motion sensitive siloed systems, defined. With the cooperation of the Air Force Logistics Command, access was provided for two weeks to a test Minuteman silo site at Hill AFB, so that a short-term precursory environmental motion study could be made.

The siloed missile environmental motion study had four immediate objectives: Determine the problems of conducting a long term, total motion geokinetic study, at a Minuteman missile site; determine how well the circuitry of the prospective data acquisition system are suited to measuring the ground motion characteristics at a Minuteman missile site; test the performance of a prototype multiple-channel filter/amplification/calibration system, and identify site occupation-accessibility problems, and instrumentation capability limitations.

The field program was divided into three identifiable areas of data acquisition. First, motion measurement data were needed to help determine appropriate instrumentation for the long-term study. Second, data were needed for use in developing a theoretical treatment of the silo-missile response. Third, data which could be used to identify ground-silo-missile transmissibility characteristics to low-level inputs in-

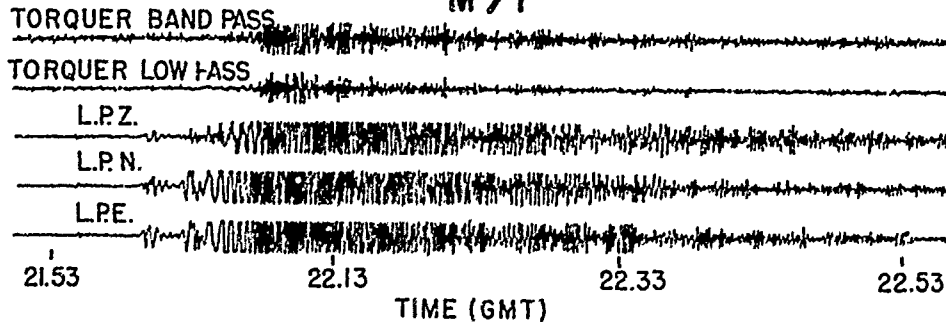
cluding silo response to loading and the missile suspension response were needed.

The study results were categorized by kind of motion, i.e., ground motion, both naturally and artificially induced, silo motion, missile motion, and site stability to load. The conclusions reached were: that existing techniques could be modified so that no substantial problem areas would prevent application of present data acquisition and reduction methods to a siloed missile site; that the multiple sensor approach for broadband coverage is reasonable; that all prototype front end circuitry performed as designed; that site motion levels were substantially larger than those measured at inertial component test sites; that silo cross-axial coupling terms are significant, and that due to everyday site operations, sparse data analysis techniques need be employed in the long-term study.

CRUSTAL STABILITY: Advanced inertial hardware performance sensitivities are not only affected by environmental seismic motions but they may also be influenced by

tectonic processes and local crustal instabilities. A program has been implemented to develop techniques for assessing the related motions caused by these mechanisms based on studies in selected regions of the upper portions of the earth's crust. These studies also provide means for determining subsurface geological and geo-physical phenomena affecting crustal stability. A three-element borehole tiltmeter array was installed to verify and extend interpretations obtained from preliminary data. Thermal noise was identified and suppressed followed by three months of virtually uninterrupted data acquisition to include local area loading tests. Data quality exceeded expectations; the borehole environment provided stability rivaling that of deep mines. Earth surface tilt in response to ocean tidal loading was routinely measured and is of sufficient magnitude to affect the long-term gyrocompass experiment in Norwood, Massachusetts. Theoretical models were developed to predict the majority of earth tide deflections at any site, given the characteristics of the

SITKA EARTHQUAKE 30 JULY 1972 M > 7



The response of a GI-T1-B gyro to a magnitude 7+ distant earthquake. The three gyro axes are labeled long period Z (vertical), N (north), and E (east). The three-component seismometer output is saturated for several minutes after the disturbance. The top two traces show the gyro output.

ocean tides and the gross crustal structure. These corrections are good to 10 percent. Solutions were obtained for the static loading problem while statistical verification was obtained for temperature fluctuations and tilt noise.

WEAPON SYSTEMS ENVIRONMENT: Once the total geokinetic environment for a given region is described, the contribution of the motion effects on motion sensitive hardware performance can be assessed. Technologies can be developed for suppressing or compensating for those motion effects which are degrading. A program was launched to identify and isolate inertial hardware systems components performance errors caused by the motion environment and to define and adapt processing schemes for minimizing the limiting effects of motion-induced errors. An Azimuth Laying Set (ALS) used in advanced Minuteman systems for pre-launch missile azimuth control was installed on a pier in the AFCRL Haskell Observatory where geokinetic and ALS data were simultaneously monitored. Evaluations were made of the GI-T1-B gyro sensitivities to earth motion; the GI-T1-B gyro is the inertial component presently employed in the Minuteman ALS systems. A frequency model for the GI-T1-B single-degree-of-freedom rate integrating gyro was derived. The transfer functions relating the gyro output angle to case motions were plotted for the GI-T1-B gyro and a "nominal" gyro. It was evident that the GI-T1-B gyro had a higher gain at most frequencies for case motions than "nominal" gyros; the conclusion is that the GI-T1-B gyro is more sensitive to seismic motions acting on the gyro case. Hence, the GI-T1-B gyro represents an instrument which is well suited for the investigation of geokinetic effects on inertial guidance instruments.

BACKGROUND RADIANCE: Survey, search and reconnaissance activities of all sorts

have in common the problem of distinguishing a target from its background. Rather than accomplish this on an empirical basis, measurements of both target and background radiative properties may be made to develop a predictive capability for the success of target discrimination.

Research within the Terrestrial Sciences Laboratory concerns itself with two aspects of this problem: 1) measurement of the magnitude and time dependence of background radiation, and 2) measurement of its wavelength dependence. Most measurements are in the thermal infrared region of the spectrum, although visible and near infrared regions are utilized where appropriate for operational requirements.

CELESTIAL BACKGROUND: The infrared background provided by stars, planets, and other celestial bodies is not well known. To define this background adequately, the Optical Physics Laboratory measures the infrared background resulting from stars, and the Terrestrial Sciences Laboratory measures the infrared radiation from planets. A balloon-borne telescope system is employed to make these observations. At the balloon float altitude of more than 100,000 feet, infrared radiation from planets is almost completely unattenuated by atmospheric absorption.

An absolute measurement of the infrared irradiance from Mars was the first objective of this program. Mars is an important target, not only because it is a relatively strong radiation source, but also because it can be used as a standard calibration reference. In April 1971, the irradiance of Mars was measured, with a 24-inch aperture telescope, using a new observational technique, to improve the statistical confidence level of the result by an order of magnitude over the previous measurements.

A similar observation of Venus in January 1972 was the second program objec-

tive, this time using a 50-inch aperture telescope carried by a high altitude balloon system—the largest balloon-borne telescope employed at that time. These absolute irradiance level observations will be followed by measurements of the wavelength dependence of these strong background sources.

TERRESTRIAL BACKGROUND: Any effort to utilize the spectral signature of a target to enhance its contrast with the background, and thus to improve target discrimination, must take into account the spectral signatures of common background materials in order to avoid false target confusion. The Terrestrial Sciences Laboratory studies the spectral signatures of common background materials, such as rocks and soils, using laboratory spectrometers that cover the spectral range from the visible through the thermal infrared. AFCRL shares this background radiance information with a number of Air Force laboratories which work together to develop new and improved reconnaissance techniques which use spectral signature information.

During the reporting period visible and near infrared spectral signatures of a complete array of minerals and rocks were determined, and a study of different soils was begun. At the same time, mid infrared emission properties of rocks and soils were measured as a function of such variables as particle size, packing, and thermal regime. It was found that there are optimum conditions which will provide maximum spectral information detectable from such materials, to increase the contrast between background and target.

GEOODESY AND GRAVITY

AFCRL's research program in geodesy and gravity is directed toward the continuing improvement of knowledge of the size,

shape and mass distribution of the earth. Improvements in these data are inputs for missile guidance systems, directly improving their accuracy.

AFCRL is continuing its participation in the National Geodetic Satellite Program, with NASA, Army, Navy, and other USAF agencies and civilian observatories. In the current phase, the Earth Physics Satellite Observing Campaign (EPSOC), geodetic laser systems deployed all over the world cooperate in observing several reflecting satellites. AFCRL is participating in this program with lasers and geodetic stellar cameras.

COMPUTER SOFTWARE: The Short Arc Geodetic Adjustment (SAGA) Program has become the most popular advanced data reduction program in the satellite geodesy community. Developed originally to accept any combination of electronic and optical observations as inputs, the program has been modified extensively to expand its program options and capabilities. Extraction of coding routines and options used for optical data reduction resulted in a much more compact program requiring less computer core.

The investigation into modeling of tropospheric refraction has been completed. During this reporting period, ray tracing through sample atmospheres has shown that a model for tropospheric scale height developed by Hopfield of the Applied Physics Laboratory yields results far superior to those obtained from the model originally employed in SAGA. As a result, the decision was made to incorporate Hopfield's model for scale height into the SAGA program. Because of these revisions, the adjustable refraction coefficients can be subjected to one sigma, *a priori* constraints that are at least five times smaller than those previously used (i.e., 0.04 meter instead of 0.20 meter).

The SAGA program treats the earth fixed minute vectors as observations and

performs a least squares adjustment to recover position and velocity at a designated epoch. The exercise of moderately accurate *a priori* orbital constraints (when available) can materially strengthen the recovery of the peripheral stations.

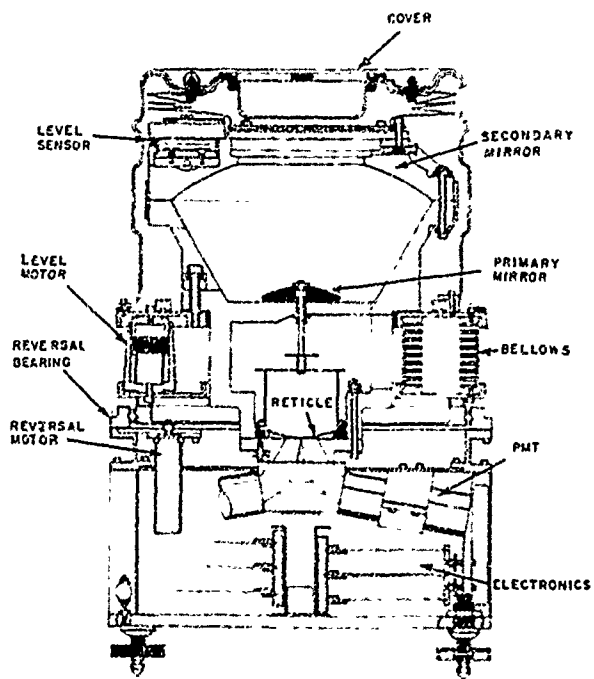
AIRCRAFT POSITIONING BY CONTINUOUSLY INTEGRATING DOPPLER (CID): Simulations were performed to check the validity of the CID approach for determining aircraft positions precisely. The assumptions of the test were influenced by AFCRL's previous studies and experience with Geociever data reductions. The error propagation of the simulations indicates that when a well designed, highly redundant tracking configuration of Geocievers of known location is exercised over a wide sweep of geometry, accuracies on the order of 0.3 meter (1 sigma) can be expected for the recovery of that portion of the trajectory intercepted by the boundary of the tracking configuration.

GEOCIEVER TEST RESULTS: Combinations of Geociever passes were employed in a short arc geodetic adjustment for the recovery of 15 observing stations. The results of this adjustment show a mean standard error of approximately 1 to 1.5 meters, and corrections to Cape Canaveral Datum Survey coordinates of about 1 to 1.5 meters.

An editing algorithm for automatically detecting and removing whole cycle count errors was developed and successfully tested in the SAGA program with simulated and actual Geociever data. To test the validity of the editing scheme a network of six stations observing one of the Navy Navigation Satellites was simulated. The sampling time interval between successive data points was assumed to be 30 seconds. At each station cycle count errors were added or subtracted from perfect measurements. Random noise was then also included. After exercising the editing scheme all

added cycle count errors and random noise were removed and the adjustment returned to the original perfect measurements.

AUTOMATED ASTRONOMIC POSITIONING SYSTEM: AFCRL, for several years, has been studying the possibility of automating astronomic position surveys. Current methods of astro observation use a moving wire system to track a star. This method relies heavily on the judgment of the observer. Studies have concentrated on instruments which would automatically record the time of a stellar transit across a



The Automated Astronomic Positioning System (AAPS). With the cover removed, light striking the diverging primary mirror is then focused by the secondary mirror on slits in the reticle to generate the signals in the photomultiplier tube (PMT). The concentric mirror system eliminates all but radial distortion. The position of the system is reversed every half hour to eliminate many possible systematic errors in the measurements.

wire or slit. Preliminary work was conducted utilizing a modified Wild T-4 theodolite. From these early efforts sufficient confidence was gained to conduct a design study. The design selected is a vertically oriented optical system. The optics consist of a concentric all-mirror system, which provides inherent freedom from astigmatism, coma, and distortion. The curved focal surface is the reticle. Stellar transits crossing the slits in the reticle are recorded by photo-multipliers. The signal from the photomultipliers is then filtered and the time of the centroid of the pulse is determined. The time of transit provides constraints at the time of transit between sensor latitude, longitude and star position. The time of transit information is then processed by a small on site fourth generation miniature computer which computes the site astronomic latitude and longitude during the observing period.

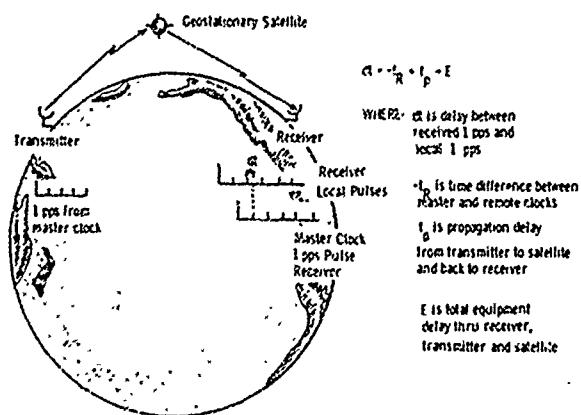
The Automated Astronomic Positioning System (AAPS) is an instrument that will provide astronomic positions in real time. It will operate under extreme temperature conditions (-35 degrees C to +48 degrees C) and over the latitude range of +70 degrees (N) to -70 degrees (S). Observations for one astronomic position are accomplished in two hours. During this interval the computer controls all operations pertaining to the AAPS. The operator will be able to manually override the system if necessary.

The high initial cost of the AAPS will be more than offset by savings in field personnel assignments and the time required at each site to acquire an astronomic position. The AAPS on one clear night will be capable of providing four astronomic positions versus current instrumentation which requires a minimum of two clear nights to acquire a single astronomic position. AFCRL is currently constructing two prototype systems which will be thoroughly tested and evaluated.

TIME SYNCHRONIZATION SYSTEM:

AFCRL has been active in a cooperative program with the National Bureau of Standards (NBS) in a series of passive time and time interval dissemination experiments. These experiments will enable geodetic field teams and other users in remote areas of the world to acquire a usable signal for time interval reference.

NBS in Boulder, Colorado, transmits the time signals to the ATS-III satellite where they are relayed to earth receiving systems. AFCRL receives the signals in a special system located at Hanscom Field, Bedford, Mass., which is tied to a cesium frequency standard. The time signals are broadcast in a format similar to the present WWV time broadcasts. The limitation to a system of this type is the ability to



Time signals broadcast from Boulder, Colorado, to a geostationary satellite are relayed to a receiver in Bedford, Massachusetts. A cesium clock checks the time difference between remote and master clocks, and the known delay as the received pulse goes through the circuitry on the satellite and then in the receiving station can be removed to calculate the propagation delay. This knowledge could be used to check the accuracy of a slide rule type calculation of the propagation delay. The position of the satellite is also broadcast, so the user has everything needed to achieve almost real-time synchronization with 10-100 microsecond accuracy.

compute accurate propagation delays to the satellite and from the satellite to the user. This was a task for a large computer. Resultant long delays were intolerable to successful remote field site operations. The NBS developed a slide rule to compute the propagation delay, given the position of the satellite during the time of the broadcast. The satellite position is computed by NBS and broadcast along with the time information. Accuracies in the 10-100 μ second region are currently predicted for the system. This system has the advantage of achieving almost real-time synchronization.

SATELLITE GEODESY: AFCRL has been active in satellite geodesy since 1962, using active satellite beacons and since 1964, using passive or reflective satellites. Recent work on passive satellite experimentation uses ground-based lasers as the active elements. Equipment development has advanced from hand-operated pointing mechanisms, with large beam angles to compensate for inaccuracies, to the present high precision tape controlled pointing mount and auxiliary electronic controls with great flexibility for various observing situations depending on conditions for the particular mode of operation and for other relevant experimentation.

The AFCRL geodetic laser system, still in the experimental stage, is capable of generating ten ranging pulses in a single pumping period of 500 microseconds for obtaining 10 independent range measurements for each stimulation period. This multipulse system has been used to observe the change in satellite range in a 500 microsecond time period as well as measuring satellite ranges with a precision of 2 parts in 10^7 .

In 1971 this system was used in the data acquisition phase of the International Satellite Geodesy Experiment (ISAGEX), a cooperative experiment in geodesy involv-

ing 15 ranging lasers and 49 camera systems located throughout the world. The system is presently being used in the Earth Physics Satellite Observing Campaign (EPSOC), a cooperative program concentrating on near simultaneous observations.

This laser system also incorporates a high energy normal mode laser for photography of the satellite-reflected pulses against stellar backgrounds for precise angular data. In preparation for these experiments investigations are being made with different film emulsions, using two USAF PC-1000 geodetic stellar cameras.

Pre-fogging and other hypersensitization experiments are being conducted toward extending system capability with various types of passive and active satellites.

A 12-inch reflecting telescope with a photomultiplier is also being employed in these studies as a means of monitoring the time and output characteristics of active satellite beacons.

The entire experiment with the AFCRL geodetic laser system is directed toward the development of a satellite observing device having the capability to produce angular observations along with real time, precise, instantaneous ranging measurements of the same satellite for the extreme precision in geodetic information required by USAF for improved missile guidance.

LUNAR LASER RANGING: The lunar laser ranging system is a potential "centimeter system" for geodesy. To extract geodetically significant data from this system, one must consider and parameterize many geophysical and astronomical effects. These include the motion of the earth's pole of rotation, the variation in the length of the day, secular motions of the earth's crust, atmospheric refraction, earth and moon tidal deformation and dissipation, the orbit

of the moon about the earth, the rotation of the moon about its center of mass and the coordinates, on the earth, of the observatory station and, on the moon, of laser retroreflectors.

A computer program, called the Planetary Ephemeris Program (PEP), which was originally written at the MIT Lincoln Laboratory serves as the basic element of "software" for providing predictions and interpreting observations in the AFCRL lunar laser experiment. The purpose of PEP is to improve planetary and lunar ephemerides using measurements from radar, laser, spacecraft telecommunications and conventional ground-based optical observations. PEP numerically integrates the differential equations of motion to determine as functions of time the positions and velocities of the planets, of the earth-moon barycenter and of the moon, and it integrates a set of variational equations to determine the partial derivatives of these positions and velocities with respect to initial conditions, masses and other parameters. The model for the moon's motion contains a parametric representation of general relativistic effects and of earth-moon tidal interactions. The effects of the planets and of the low order harmonics of the earth's and moon's gravitational potential are also included. The integrated ephemeris (including the partial derivatives which are used to set up the normal equations) is used in turn to incorporate all available observations in a least squares solution for all parameters; then the refined parameters are used to regenerate an improved ephemeris.

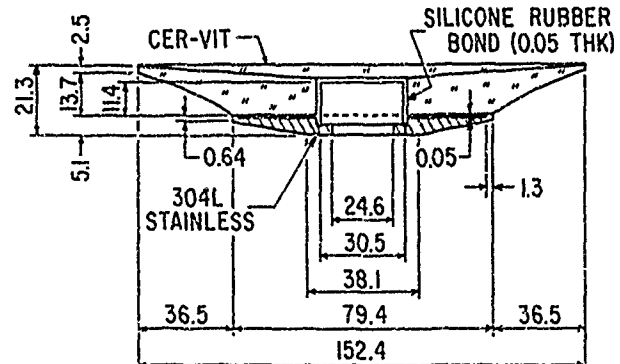
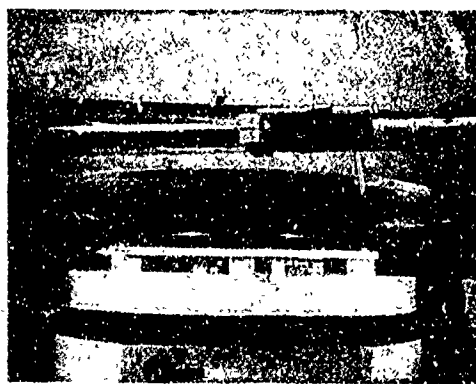
With AFCRL support, PEP has been integrated and fitted to 17,000 recent radar and Surveyor spacecraft Doppler observations and 78,000 optical observations extending as far back as 1750. Lunar Laser range gating predictions for the AFCRL experiment near Tucson, Arizona, and the Smithsonian Astrophysical Observatory (SAO) experiment in Harvard, Massachu-

sets, combined the latest MIT numerical ephemeris of the moon from PEP and the AFCRL analytic *Physica! Ephemeris of the Moon (PEM)*. Offset guidance for the AFCRL and SAO experiments are derived from PEM. AFCRL's PEM is also being used in interpreting lunar laser ranges from the McDonald Observatory, in Texas, and has found a number of other applications in the U.S. space program.

The analytic theory of the physical librations of the moon has undergone extensive investigation at AFCRL. In its present development the theory considers the following aspects: 1) the effects of the earth, sun and planets, 2) the moon's dynamical figure through the third degree spherical harmonics, 3) elasticity of the moon; 4) anelasticity of the moon, 5) nonlinear effects, and 6) secular transitions. Along this line, it was shown, recently, that lunar laser range measurements will be sensitive to the specific dissipation function of the moon for a physical libration term whose period is three years, that is, the Q of the moon is a significant parameter in the integration of its equations of motion and it may be derivable (for one frequency) from lunar laser observations.

AFCRL LUNAR LASER OBSERVATORY: The observatory was formed in July 1968 at the University of Arizona in Tucson. Lunar laser observations were made at two AFCRL sites located in the Catalina Mountains north of Tucson. The experiment began at the first site with a laser telescope having a 150-cm aperture, narrow field metal primary mirror. Thousands of ruby laser pulses were fired at the Apollo 11 retroreflector array from this site with occasional returns. It was found that the metal primary mirror was inadequate for reliable earth-moon laser range measurements. Operations at the first site were terminated in April 1971.

Observatory activities were re-directed to make extensive instrumentation modifi-



AFCRL 152 cm f/2.5 MIRROR

This 152-cm diameter mirror is the key component of the largest astronomic quality center mount glass reflecting telescope. The combination of rear tapering of the Cer-Vit mirror and stainless steel support were designed by an AFCRL scientist. The beam splitter in the center of the telescope has a maximum reflectivity at 6943 angstroms.

cations for the improvement of system performance. The most important change was in the telescope; its frame was extended and a novel Cer-Vit-steel composite mirror replaced the metal primary. The 152-cm f/2.5 hyperbolic primary was combined with a new 41-cm Cer-Vit secondary to form an f/8.0 Cassegrain optical system. This resulted in a general purpose, moderate aperture telescope, having 93 percent of the collected energy from a point source contained within a 0.7 arc-second blur image.

With the broadening of the telescope's low distortion field to about one lunar diameter, it became feasible to guide through the mainfield so the tracker was moved to the Cassegrain focus from the offset telescope on the declination cube. The heavy transmitter and receiver optical benches were moved from the Cassegrain focus to a separate box on top of the declination cube; the improved weight distribution diminished problems of flexural distortion.

The ruby laser pulse was shortened by

selecting a 2 to 7 nsec portion of the oscillator pulse with a spark gap triggered Pockels cell. The energy was maintained at 3 to 10 joules by increasing the number of laser amplifiers to four. A tunable etalon filter was added to the receiver and a real time computer was included to calculate range residuals.

At the same time as the equipment was being modified, the observatory was moved to the second Catalina site, atop Mt. Lemmon, where potential observing time was doubled. The move was completed during February 1972. The period March 1972 - June 1972 was designated as a test and evaluation phase for the modified system. System performance was successfully demonstrated using the Apollo 15 target.

After a series of successful ranging tests, particularly with the Apollo 15 reflectors on May 22 and 26, 1972, the observatory was closed on June 30, 1972.

PHYSICAL GEODESY: During the reporting period significant advancements were accomplished in theoretical and applied

studies in the area of physical geodesy. Increased requirements for more accurate and detailed geopotential data and geodetic parameters dependent on gravity gave impetus to the development of new approaches for better solutions of some classical problems and inspired new theories and practical methods.

The *Nonlinear Solution for the Boundary Value Problem of Physical Geodesy* is one example of a significant recent achievement. The classical determination of the figure of the earth and of its external gravity potential is a boundary value problem of potential theory. The classical solution to the problem offered by Molodensky *et al* consists of integrodifferential and integral equations which are extremely difficult to handle in practical work. A number of linear approximations were derived by various authors for numerical work which systematically neglected the second or higher order terms. Increasing accuracy requirements of the Air Force, especially in computations of the deflections of the vertical, could no longer be satisfied by these solutions. A new solution in the form of a series has been developed. Investigation has proved its theoretical equivalence to the original Molodensky solution but it has great advantages in simplicity and computational convenience.

The determination of the figure of the earth and its external gravity potential as a boundary value problem requires that gravity and other data are known at every point of the earth's surface. Gravity is measured at discrete points or at most along profiles only. Therefore, at other points it is determined by arbitrary interpolation or extrapolation procedures. Gravity observations are also obtained from artificial satellite observations. It is expected that second and higher order gradients of the gravity will be measurable economically over large areas in the future. The boundary value problem will not be practically applicable for these

measurements. A new method is required for the combination and processing of these various types of data. Moritz derived from Krarup's general least squares method the so called "least squares collocation theory"—an application of least squares estimation of stochastic processes which permits rigorous combination of heterogeneous data, taking into consideration random and systematic errors of the combined measurements. This method can be applied to current practical problems and will have far reaching effects in all future geodetic computations.

GRAVITY MEASUREMENTS: In 1968 and 1969 eight absolute gravity determinations were made with the Laser-Interferometric Apparatus. These eight values have now been incorporated into the International Gravity Standardization Net 1971. These eight were the last observations made with this large apparatus. At present AFCRL has contracted for design modifications to the laser-interferometric apparatus. The modified laboratory instrument will be greatly reduced in size compared to the original apparatus. It will be more portable. The design criteria of the new instrument are such that an accuracy of 0.01 mgal should be obtained. At present, various basic dropping schemes have been designed and models are being constructed to learn by experimentation which is the most practical. This contractual effort will be coupled with in-house work on both the mechanical design of the instrument and the electronics necessary for optimum utilization of the interferometer signal to arrive at a design which has been optimized for portability, economy, reliability and absolute precision.

The AFCRL airborne gravity program has been completed and the findings published, but an in-house effort investigating new and improved aerial gravimeters has continued. AFCRL has been represented on all Tri-Service panels dealing with aer-

ial gravity and aerial gravity systems and has also been a major consultant on these projects. Further, AFCRL has been closely associated with the recent helicopter airborne gravity testing.

A contractual effort to develop a charged particle absolute gravity meter was terminated and the instrument delivered to AFCRL. The instrument employs a small charged sphere which is electrostatically controlled to rise and fall in free motion between two levels whose separation can be accurately determined. The instrument did not attain its predicted accuracy and reproducibility, and further investigation by AFCRL scientists indicated that several inherent problems preclude immediate hope that the method can be used for gravity measurements with a precision of the order of 10^{-7} g. These problems, which are the result of the difficulty of removing the effects of non-gravity forces from a small particle with very high charge-to-mass and surface area-to-mass ratios, could conceivably be solved by future breakthroughs at which time the development of the instrument could be continued. Because of the small size of the instrument and its ability to acquire data very rapidly, such hope, however speculative, should not be surrendered.

A LaCoste and Romberg Earth-Tide gravimeter is in continuous operation in the seismic-gravity observatory. This instrument records the variations of the vertical component of gravity to an accuracy of one microgal. AFCRL has converted one and is presently converting a second large geodetic LaCoste and Romberg gravimeter with a capacitance pickoff of the beam position enabling the use of these gravimeters for the measurement of earth-tides. The first of these instruments is undergoing long range testing and calibration in the AFCRL seismic-gravity observatory. The data obtained from the earth-tide gravimeters will provide input data for various geodetic and inertial tests. The

converted gravity meters are to be used at field sites to complement long range inertial testing and to verify the reliability of various instruments such as the cryogenic gravimeter. The data from the AFCRL earth-tide gravimeters will also be incorporated into the United States earth-tide network under the direction of Dr. Kuo of Columbia University.

Continued support of the contractual effort toward development of a drift-free cryogenic gravimeter has been accompanied by critical in-house examination of all work being done in the field of low drift, ultra-precise, relative gravimeters. Although in-house capability for performing the research in this field is not available, AFCRL is contributing significantly to the research by providing critical, unbiased evaluation of the results and valuable independent calibration of the instruments with AFCRL portable tidal gravimeters.

THE INTERNATIONAL GRAVITY STANDARDIZATION NET 1971: The International Gravity Standardization Net 1971 (IGSN 71) was adopted by Resolution No. 11 of the XVth General Assembly of the International Association of Geodesy (IAG), held in August 1971 in Moscow. The IGSN 71 replaced the previous gravity reference system called the "Potsdam datum" adopted in 1909. The new system was developed between 1962 and 1971 by the cooperation of an international group organized within Study Group No. 5 of IAG. AFCRL was a major participant in the activities of this group, participating in the field measurement program and supporting other groups in their field activities. Nine of the 11 absolute determinations of the acceleration of gravity at key stations of the network were accomplished by AFCRL with the Hammond-Faller transportable apparatus. For the purpose of analysis, selection and final adjustment of data, in 1967 a smaller group was formed in a meeting held at AFCRL. This group deter-

mined mathematical models, scale factor treatment, observation weights and station selection criteria. Under their direction, an adjustment was performed that resulted in consistent gravity values for the 1872 stations which were finally incorporated into the IGSN 71. The completion of this network was a long sought goal of gravimetric geodesists and provides a modern world-wide framework upon which to base gravimetric surveys and studies.

GRADIOMETRY: If the gradients of the geopotential can be measured from a moving platform with sufficient accuracy, a powerful tool for the solution of a number of problems involving gravity is available. The gravity gradient is the rate of change of the gravity acceleration; mathematically it is the second derivative of the potential. The unit of the gravity gradient is the Eotvos unit (EU) one EU = 10^{-9} sec^{-2} .

Measurement of the horizontal components of the gravity gradient in a static mode was accomplished 80 years ago using the curvature variometer and the torsion balance of Eotvos. Much later, fused quartz microbalances were developed for the static measurement of the vertical gradient. Currently, several programs are in progress for the development of a moving base gradiometer. The critical problem in the measurement of gravity gradients from a moving base is the separation of gravity gradients from inertial effects caused by angular acceleration of the frame.

INSTRUMENT DEVELOPMENT: Moving base gradiometer designs have been proposed by several investigators. AFCRL investigated the feasibility and supported contractually the development of a torsionally resonant rotating sensor consisting of two rigid mass quadrupoles oriented perpendicularly to each other and connected at the center with a torsionally flexible spring. When the sensor is rotated at an

angular rate exactly one half of the torsional resonant frequency, the differential torque between the sensor arms will deflect one quadrupole with respect to the other. This angular resonant deflection is transduced into an electrical signal. The accelerations due to the motion of the sensor and other disturbing forces do not cause a differential torque or they occur at other than the resonant frequency.

In 1968 the gradiometer design theory was experimentally verified by the achievement of 1 EU at an integration time of 10 sec utilizing a soft mounted experimental sensor. The subsequent effort was the development of a sensing element mounted on an air bearing so that it could be aligned in any direction. The overall conclusion of this effort completed in November 1970 was that a hard bearing gradiometer for the measurement of gradients in any direction with an accuracy of 1 EU is feasible and practical.

After the evaluation of the results obtained by the two aforementioned efforts and the approaches proposed by other investigators, a contract was awarded for the design, fabrication and laboratory testing of a prototype hardmounted gradiometer. The contract is funded by the Advanced Research Projects Agency of the Defense Department and directed by AFCRL. Within two years this effort will produce a prototype sensor that can be used for moving base test measurements and, in turn, as the sensing element for a number of applications. The development of the prototype is scheduled to be completed and ready for airborne or shipboard testing by January 1974.

APPLICATIONS: When the basic sensor has been developed and tested the same instrument can be used in a wide variety of terrestrial and space applications. These applications include: aerial, marine, and satellite gravimetry; improvement of inertial navigation (aircraft, ship, submarine) and long-term inertial guidance; mass de-

tention for inspection and evaluation of containers, satellites, and onsite missiles; lunar and planetary potential measurements and asteroid mass determinations.

During the reporting period the Terrestrial Sciences Laboratory initiated both in-house and contractual efforts to study applications in the two most relevant categories for Air Force and DOD requirements. In the first category the geodetic and geophysical applications are studied. Gravity gradients measured by marine airborne and satellite-mounted instruments have the potential to determine quantities such as deflections of the vertical and geopotential surfaces. Required measurement accuracies and techniques for combination of gradiometer data with other terrestrial, aerial and satellite measurements will be established by this research.

A parallel but separate research effort was initiated to assess the impact of application of gradiometer techniques to inertial navigation systems. Inertial navigation system (INS) errors due to geopotential deficiencies and the achievable improvements by gradient data are studied in this research. Current operational systems, state of the art and future technologically feasible systems are being considered. Vehicles including surface, subsonic jet and supersonic velocity characteristics are included.

JOURNAL ARTICLES JULY 1970-JUNE 1972

BLIAMPTIS, E. E.

A Description of the Earthquake Source Mechanism

J. of Geophys. Res., Vol. 76, No. 26 (10 September 1971)

CARTER, W. E.

An Electro-Optical Lunar Laser Offset Tracker
IEEE Proc. of the Tech. Prog., Electro-Opt. Sys. Des. Conf. (June 1971)

Center-Mounted 152 Centimeter F/2.5, Lightweight, Cer-Vit Mirror
Appl. Opt., Vol. 11, No. 2 (February 1972)

Timing and Geodesy

Proc. of the IEEE (May 1972)

Operational Tests of the AFCRL 152 Cm Telescope

Appl. Opt., Vol. 11, No. 7 (July 1972)

CARTER, W. E., ECKHARDT, D. H., and ROBINSON, W. G.

AFCRL Lunar Laser Instrumentation Status Report

Proc. of the 14th Plenary Meeting of COSPAR (June 1971)

CRONIN, J. F.

Recent Volcanism and the Stratosphere
Sci., Vol. 172, No. 3985 (21 May 1971)

CROWLEY, F. A., and OSSING, H. A.

An Analysis of the Vibration Environment with Application to Single-Degree-of Freedom Gyroscope Performance Tests
Collection of Tech. Pap. on Guid. and Cont. Tech., AIAA Guid., Cont., and Flight Mech. Conf. AIAA 70-951 (August 1970)

DYBWAD, J. P.

Radiation Effects on Silicates (5-Kev H⁺, D⁺, He⁺, N⁺)
J. of Geophys. Res., Vol. 76, No. 17 (10 June 1971)

ECKHARDT, D. H., and DIETER, K. (Dabovich & Co., Lexington, Mass.)

A Nonlinear Analysis of the Moon's Physical Libration in Longitude
The Moon, An Intl. J. of Lunar Stud., Vol. 2, No. 3 (February 1971)

HADGIGEORGE, G.

Improvement of the GEOS 1 North American Tracking Network from Multiple Short Arc Geodetic Adjustments
Proc. of the GEOS-2 Prog. Rev. Mtg., 22-24 June 1970, Vol. 1, NASA Pub. (November 1970)

HAMMOND, J. A., and FALLER, J. E. (Wesleyan Univ., Middletown, Conn.)

Results of Absolute Gravity Determinations at a Number of Different Sites
J. of Geophys. Res., Vol. 76, No. 32 (10 November 1971)

HASKELL, N. A., and THOMSON, K. C.

Elastodynamic Near Field of a Finite Propagating Tensile Fault
Bull. of the Seismol. Soc. of Am., Vol. 62, No. 3 (June 1972)

HUNT, M. S.

The AFCRL Lunar Laser Ranging Experiment in Arizona
Sky and Teles., Vol. 43, No. 2 (February 1972)

- HUNT, G. R., and LOGAN, L. M.
An Image Selection Device for Use with a Telescope
Appl. Opt., Vol. 9, No. 12 (December 1970)
- Convenient Technique for Calibration of Radiometers Used for Low Energy Infrared Targets*
Appl. Opt., Vol. 10 (December 1971)
- Variation of Single Particle Mid-Infrared Emission Spectrum with Particle Size*
Appl. Opt., Vol. 11, No. 1 (January 1972)
- HUNT, G. R., and SALISBURY, J. W.
Visible and Near Infrared Spectra of Minerals and Rocks: I. Silicate Minerals
Modern Geol., Vol. 1, No. 4 (November 1970)
- Visible and Near-Infrared Spectra of Minerals and Rocks: II. Carbonates*
Modern Geol., Vol. 2, No. 1 (February 1971)
- HUNT, G. R., SALISBURY, J. W., and LENHOFF, C. J., 1ST LT.
Visible and Near-Infrared Spectra of Minerals and Rocks: III Oxides and Hydroxides
Modern Geol., Vol. 2, No. 3 (May 1971)
- Visible and Near-Infrared Spectra of Minerals and Rocks: IV. Sulfides and Sulphates*
Modern Geol., Vol. 3, No. 1 (November 1971)
- ILIFF, R. L.
AFTRL Laser Satellite Geodesy and Future Plans
Proc. of the GEOS-2 Prog. Rev. Mtg., 22-24 June 1970, Vol. 3, NASA Pub. (November 1970)
- LOGAN, L. M., ET AL
Microcrystals in Frozen Solutions: The Luminescence Spectra of Pyrazine
J. of Mol. Spectros., Vol. 40 (1971)
- Role of Defects and Reabsorption in the Decay of Fluorescence of Anthracene from 2-350° K*
Mol. Cryst. and Liq. Cryst., Vol. 15 (1972)
- LOGAN, L. M. and HUNT, G. R.
Infrared Emission Spectra: Enhancement of Diagnostic Features by the Lunar Environment
Sci., Vol. 169 (28 August 1970)
- Emission Spectra of Particulate Silicates Under Simulated Lunar Conditions*
J. of Geophys. Res., Vol. 75, No. 32 (November 1970)
- LOGAN, L. M., HUNT, G. R., BALSAMO S. R., and SALISBURY, J. W.
Mid-Infrared Emission Spectrum of Apollo 14 Soil: Significance for Compositional Remote Sensing
Book, Lun. Sci. III, Lun. Sci. Inst. Contribution #88 (1972)
- LUPO DEL BONO, G. (Ital. Geol. Survey, Rome, Italy)
 WILLIAMS, R. S., and CRONIN, J. F.
Photogeologic and Thermal Infrared Imagery Geologic Surveys in Italy in 1966
Bollettino Del Servizio Geologico D'Italia, Vol. 91, p. 3-44 (1970)
- MANGHANI, M. H., and FISHER, E. S. (Argonne Natl. Lab., Argonne, Ill.)
Effect of Axial Ratio Changes on the Elastic Moduli and Gruneisen γ for Lower Symmetry Crystals
J. of Appl. Phys., Vol. 41, No. 13 (December 1970)
- MOLINEUX, C. E.
Aerial Penetrometers for Soil Trafficability Determination
Proc. of Conf. on Rapid Penetration of Terres. Mats., Coll. Station, Tex. (February 1972)
- OBRIEN, P. J.
Pallmann Method for Mass Sampling of Soil, Water, or Air Temperatures
Bull., Geol. Soc. of Am., Vol. 82 (October 1971)
- PIERCE, A. D., POSZY, J. W. (Mass. Inst. of Tech.) and ILIFF, E. F.
Variation of Nuclear Explosion Generated Acoustic-Gravity Wave Forms with Burst Height and with Energy Yield
J. of Geophys. Res., Vol. 76, No. 21 (20 July 1971)
- ROBINSON, W. G., WILLIAMS, J. D. and LEWIS, T. (RCA, Lancaster, Pa.)
Quantum Enhancement of the RCA 31000E Photomultiplier
Appl. Opt., Vol. 10, No. 11 (November 1971)
- ROONEY, T. P., RIECKER, R. E., and ROSS, M. (USGS, Wash., D. C.)
Deformation Twins in Hornblende
Sci., Vol. 169, No. 173 (10 July 1970)
- SALISBURY, J. W.
Albedo of Lunar Soil
Icarus, Vol. 13, No. 3 (November 1970)
- SALISBURY, J. W., ET AL
Bibliography of Lunar and Planetary Research
Icarus, Vol. 12, No. 2, Vol. 12, No. 3, Vol. 13, No. 1, Vol. 13, No. 2 (1970)
- Bibliography of Lunar and Planetary Research - Second Quarter of 1970*
Icarus, Vol. 14, No. 2 (February 1971)
- Bibliography of Lunar and Planetary Research - Third Quarter of 1970*
Icarus, Vol. 14, No. 3 (June 1971)

- SALISBURY, J. W., and HUNT G. R.
Spectroscopic Remote Sensing of Water-Bearing Minerals
Geol. Problems in Lun. and Plan. Res. (Sci. and Tech. Ser. Pub. by AAS), Vol. 25 (1971)
- SZABO, B.
Dynamic Gradiometer (Principle, Status and Application)
Bull d'Inf. of the Intl. Grav. Bur., No. 25 (March 1971)
- SZABO, B., and ANTHONY, D.
Results of AFCRL's Experimental Aerial Gravity Measurements
Bull. Geodesique, No. 100 (June 1971)
- TERLECKY, P. M., JR., CAPT., and SPALVINS, K.,
 REPICHOWSKI, J. (AF Weap. Lab.,
 Kirtland AFB, N. M.)
Project Brickpile: A Feasibility Study on the Influence of Jointed Rock Materials On Explosion Produced Craters
AFWL Tech. Note DE-TN-71-004 (September 1971)
- THOMSON, K. C., and HASKELL, N. A.
Elastodynamic Near Field of a Finite Propagating Transverse Shear Fault
J. of Geophys. Res., Vol. 77, No. 14 (10 May 1972)
- THOMSON, K. C., and TOKSOZ, M. N. (Mass. Inst. of Techn., Cambridge, Mass.), AHRENS, T. J. (Calif. Inst. of Techn., Pasadena, Calif.)
Generation of Seismic Waves by Explosions in Prestressed Media
Bull. of the Seismol. Soc. of Am. Vol. 61, No. 6 (December 1971)
- TURNER, B. B., CAPT., and BICKFORD, M. E. (Univ. of Kansas)
Age and Probable Antarctic Origin of the Brant Lake Gneiss, Southeastern Adirondack Mountains, New York
Bull. of the Geol. Soc. of Am., Vol. 82 (August 1971)
- WILLIAMS, R. S., JR., and FRIEDMAN, J. D. (USGS, Wash., D. C.)
Satellite Observation of Effusive Volcanism
Brit. Interplan. Soc. J., Vol. 23 (1970)
Changing Patterns of Thermal Emission from Surtsey, Iceland, Between 1966 and 1969
Geol. Surv. Res. 1970, USGS Prof. Paper 700-D (Fall 1970)
- WILLIAMS, R. S., JR., and OLDALE, R. N. (USGS, Woods Hole, Mass.), FRIEDMAN, J. D. (USGS, Wash., D.C.)
Changes in Coastal Morphology of Monomoy Island, Cape Cod, Massachusetts
Geol. Surv. Res. 1971, USGS Prof. Paper 750-B (Summer 1971)
- ZINNOW, K. P., and DYBWAD, J. P.
Pressure of Light Used as Restoring Force On a Microbalance
Vacuum Microbal. Techniques, Vol. 18 (1971)
Dynamic Readout of Weight Changes on an Ultramicrobalance System
Prog. in Vacuum Microbal. Techniques, Vol. 1, T. Gast and E. Robens, Editors, Heyden & Sons, Ltd., N. Y. (1972)
- PAPERS PRESENTED AT MEETINGS JULY 1970-JUNE 1972**
- ANTHONY, D.
Gradiometer Applications and Status of Sensor Development
Geod. and Grav. Techn. Exch. Mtgs., Def. Intel. Agency, Gaithersburg, Md. (19-23 April 1971)
- BALSAMO, S. R., CAPT., and SALISBURY, J. W.
Martian Surface Temperature and Frost Deposition
AAS Mtg., Huntington Beach, Calif. (16 November 1970)
- CABANISS, G. H.
Crustal Tilt from Three Borehole Tiltmeters at Bedford, Mass.
53rd Ann. Mtg. of the Am. Geophys. Un., Wash., D. C. (17-21 April 1972)
- CABANISS, G. H., and SIMON, I. (A. D. Little, Inc., Cambridge, Mass.), MCCONNELL, R. K., JR., (Earth Sci. Res., Inc., Cambridge, Mass.)
Crustal Tilt in Coastal New England from Borehole Tiltmeters.
Natl. Fall Mtg. of the AGU, San Francisco, Calif. (7-10 December 1970)
- CARTER, W. E.
An Electro-Optical Lunar Laser Offset Tracker
Electro-Opt. Sys. Des. Conf., N. Y., N. Y. (January 1971)
- CARTER, W. E., ECKHARDT, D. H., and ROBINSON, W. G.
AFCRL Lunar Laser Instrumentation Status Report
14th Ann. COSPAR Mtg., Seattle, Wash. (17 June-2 July 1971)
- CRONIN, J. F.
Recent Volcanism and the Stratosphere
Natl. Fall Mtg. of AGU, San Francisco, Calif. (7-10 December 1970)

- CRONIN, J. F., and WILLIAMS, R. S., JR.**
Volcanism and the Upper Atmosphere
 Ann. Mtg. of the Geol. Soc. of Am., Milwaukee, Wis.
 (11-13 November 1970)
- CROWLEY, F. A.**
The Measurement of Small Motion by Earth Bound Systems
 Talcott Mtn. Sci. Ctr. for Student Involvement, Inc., Avon, Conn. (13 April 1972)
- CROWLEY, F., GRAY, R., and OSSING, H. A.**
On Motion Error in Inertial Component Tests
 AIAA Conf. on Guid., Cont. and Flt. Mech., Hofstra Univ., L. I., N. Y. (16-18 August 1971)
- CROWLEY, F. A., and OSSING, H. A.**
Environmental Noise Field Properties
 ESD/AFCRL Sci. & Eng. Mtg., L. G. Hanscom Fld., Mass. (3 November 1970)
- ECKHARDT, D. H.**
The Physical Vibrations of the Moon
 NATO Adv. Study Inst. On Lun. Stud., Patras, Gr. (14-25 September 1971)
- ECKHARDT, D. H., and ILIFF, R. L.**
Laser Geodesy at AFCRL
 Geod. and Grav. Tech. Exch. Mtgs., Def. Intel. Agency, Gaithersburg, Md. (19-23 April 1971)
- HADGIGEORGE, G.**
Results from Simulations of Continuously Integrated Doppler for Precise Aircraft Positioning
 Geod. and Grav. Tech. Exch. Mtgs., Def. Intel. Agency, Gaithersburg, Md. (19-23 April 1971)
The Geodetic Positioning Capability of the Geodimeter
 Intl. Symp. on Satel. and Terres. Triangulation, Graz, Aus. (29 May-2 June 1972)
- HERRING, J. C., MAJ., and CARROLL, J. E. (Control Data Corp., Minn. Minn.)**
The Automated Astronomic Positioning System
 Am. Cong. of Surveying and Mapping/Am. Soc. of Photogram., 1972 Conv., Wash., D. C. (12-17 March 1972)
- HUNT, M. S.**
A Lunar Laser Optical Ranging Experiment
 14th Gen Assm. of the IAU, Brighton, Eng. (18-27 August 1970)
- HUNT, G. R., LOGAN, L. M., and SALISBURY, J. W.**
Mid-Infrared Remote Sensing of Composition and Its Application to Mars
 Ann. Mtg. of the Am. Astronom. Soc., San Juan, P. R. (5-8 December 1971)
- ILIFF, R. L.**
Laser Satellite Ranging for Geodesy
 Intl. Symp. on Satel. and Terres. Triangulation, Graz, Aus. (29 May-2 June 1972)
- LOGAN, L. M., HUNT, G. R., BALSANG, S. F., CAPT., and SALISBURY, J. W.**
Mid-Infrared Emission Spectrum of Apollo 18 Soil: Significance for Competitive Remote Sensing
 Third Lun. Sci. Cong., NASA Manned Spac. Ctr., Houston, Tex. (10-13 January 1972)
- MOLINEUX, C. E.**
Aerial Penetrometers for Soil Trafficability Determination
 Conf. on Rapid Penetration of Terres. Matls., Texas A&M Univ., Coll. Station, Tex. (1-3 February 1972)
- NEEDHAM, P. E., LT. COL.**
The Formation and Evaluation of Detailed Geopotential Models Based on Point Masses
 Fall Ann. Mtg. of the Am. Geophys. Un., San Francisco, Calif. (6-9 December 1971)
- O'BRIEN, P. J.**
Soil Temperatures: A Potential Key to Shallow Aquifer Transmissivity Distribution
 52nd Ann. AGU Mtg., Wash., D. C. (12-16 April 1971)
Airborne Remote Sensor Study of Coastal Puerto Rican Hydrologic Phenomena and Will Geoscientists be Extinct by 1980?
 Ann. Mtg. of the Geol. Soc. of Am., Wash., D.C. (1-3 November 1971)
- OSSING, H. A., and CROWLEY, F. A.**
An Analysis of the Vibration Environment with Application to Single-Degree-of-Freedom Gyroscope Performance Tests
 AIAA Guid. Cont. and Flt. Mech. Conf., Santa Barbara, Calif. (17-19 August 1970)
- RIECKER, R. E.**
Amphibole Deformation and Its Geophysical Implications
 Geol. Soc. of Am. Penrose Conf. On Mantle Inclusions, Sahuaro Lake, Ariz. (30 November-4 December 1970)
- ROONEY, T. P. and WYCKOFF, C. (Appl. Photo Sci. Inc., Needham, Mass.)**
Extended Range Color Film
 ASP/ACSM Mtg., Wash., D.C. (7-12 March 1971)

- SALISBURY, J. W.
Spectroscopic Remote Sensing of Lunar Surface Composition
 NATO Lunar Sci. Inst., Patras, Gr. (20-30 September 1971)
- SZABO, B.
The Development of a Charged Particle Absolute Gravimeter and A Dynamic Moving Base Gradiometer and a Cryogenic Gravimeter; Concept, Status and Applications
 1970 Intl. Grav. Com. Assem., Paris, Fr. (7-12 September 1970)
- SZABO, B. and ANTHONY, D.
Results of AFCRL's Experimental Aerial Gravity Measurements
 1970 Intl. Grav. Com. Assem., Paris, Fr. (7-12 September 1970)
- SZABO, B. and FALLER, J. E. (Wesleyan Univ., Middletown, Conn.), HAMMOND, J. A. (Natl. Bur. of Stds. Gaithersburg, Md.)
The Laser Interferometer Absolute Gravity Apparatus and a Review of Measurements Made in 1968 and 1969
 1970 Intl. Grav. Com. Assem., Paris, Fr. (7-12 September 1970)
- TERLECKY, P. M., JR., CAPT.
The Origin, Stratigraphy, and Post-Depositional History of a Late Pleistocene Marl Deposit Near Rochester, N. Y.
 The Geol. Soc. of Am., Northeastern Sec., Buffalo, N. Y. (9-11 March 1972)
- THOMPSON, L. B., MAJ.
A Test to Determine the Geodetic and Geophysical Effects on an Inertial Grade Gyroscope
 Geod. and Grav. Tech. Exch. Mtgs., Def. Intel. Agency, Gaithersburg, Md. (19-23 April 1971)
- THOMPSON, L. B., MAJ., and DIESELMAN, J., MC LAUGHLIN, R., and MILLO, K. (Northrop Electron., Norwood, Mass.)
Recent Developments in the Testing of High Performance Gyrocompass Devices
 5th Bien. Guid. Test Symp., AFMDC Holloman AFB, N. M. (14-16 October 1970)
- THOMSON, K. C.
Near Field Observations of Focal Region Phenomena in Laboratory Models of Longitudinal Shear Faulting
 52nd Ann. AGU Mtg., Wash., D. C. (12-16 April 1971)
Mathematical and Physical Models of the Earthquake Focal Mechanism
 Geol. Soc. of Am. Penrose Conf. on Fracture Mech. and Earthquake Source Mechanisms, Aspen, Colo. (27-30 September 1971)
- THOMSON, K. C., and KUENZLER, H. W. CAPT.
Theoretical Design Criteria for Passive Test Pads
 AIAA Conf. on Guid., Cont. and Flt. Mech., Hofstra Univ., L. I., N. Y. (16-18 August 1971)
- TURNER, B. B., CAPT., and BICKFORD, M. E. (Univ. of Kansas)
Rb-Sr Geochronology of Gneisses in Structural Domes, Southeastern Adirondack Mountains, New York
 Ann. Mtg. of the Geol. Soc. of Am., Milwaukee, Wis. (11-13 November 1970)
- WILLIAMS, O. W.
Geophysical Potentials from Satellite and Lunar Laser Measurements
 AGU Mtg., St. Louis, Mo. (29 September 1970)
The Use of Lasers in Satellite and Lunar Ranging: Their Geophysical Potentials; Impressions Gained from a Teaching Experience: Science and Technology in the Soviet Union; Air Force Utilization of Research in the Terrestrial Sciences; Geopolitical Environmental Factors and Their Influence on the Management of R&D; The Role of the Military Scientist and Technician at AFCRL
 AF Acad., Colo. (23-25 November 1970)
- WILLIAMS, O. W., ECKHARDT, D. H. and SLADE, M. W. (Mass. Inst. of Tech., Cambridge, Mass.)
Phenomides Used In The Lunar Laser Range Experiment: A Status Report from MIT and AFCRL
 IL GG 15th Gen. Assem. Mtg., Moscow State Univ., Moscow, USSR (30 July-14 August 1971)
- WILLIAMS, O. W. and TYLER, S. W. (Smithsonian Astrophys. Obsv.)
Use of the SAO Star Catalog in the Reduction of PC-1000 Camera Plates
 IUGG 15th Gen. Assem. Mtg., Moscow State Univ., Moscow, USSR (30 July-14 August 1971)
- WILLIAMS, R. S., JR., and FRIEDMAN, J. D. (USGS, Wash., D.C.), THORARINSSON S. (Univ. of Iceland, Reykjavik, Icel.)
Thermal Emission from Hekla Volcano, Iceland, Prior to the Eruption of May 5, 1970
 Ann. Mtg. of the Geol. Soc. of Am., Milwaukee, Wis. (11-13 November 1970)
- WILLIAMS, R. S., JR., and PALMASON, G., JONSSON, J., SAEMUNDSSON, K. (Natl. Energy Auth., Reykjavik, Icel.) FRIEDMAN, J. D. (USGS, Wash., D. C.)
Aerial Infrared Surveys of Reykjanes and Torfajokull Thermal Areas, Iceland
 U. N. Symp. on the Dev. and Util. of Geothermal Resources, Pisa, Italy (22 September-1 October 1970)

**TECHNICAL REPORTS
JULY 1970-JUNE 1972**

ANTHONY, D.
Gradiometer Applications and Status of Sensor Development
AFCRL-71-0214 (1 June 1972)

ANTHONY, D., and PEREZ, R. M.
AFCRL's Experimental Aerial Gravimetry Program
AFCRL-71-0411 (27 July 1971)

CROWLEY, F. A., and OSSING, H. A.
Earth Environmental Noise Field
AFCRL-70-0460 (19 August 1970)

CROWLEY, F. A., OSSING, H. A., and HOGAN, J.
(Becton Coll., Chestnut Hill, Mass.)
An Analysis of the Vibration Environment at Northrop's Norwood, Mass., Test Facility with Application to Gyro Testing
AFCRL-70-0355 (July 1970)

GRAY, R. A., CABANISS, G. H., CROWLEY, F. A., OSSING, H. A., RHODES, T. S., and THOMPSON, L. B., MAJ.

Earth Motions and Their Effects on Inertial Instrument Performance
AFCRL-72-0278 (27 April 1972)

HADIGEORGE, G., BRIGGS, D., and TAOTTA, J. (D. B. A. Systems, Inc. Melbourne, Fla.)
Results from Simulations of Continuously Integrated Doppler for Precise Aircraft Positioning
AFCRL-71-0252 (23 April 1971)

JUFF, R. L.
A Laser System for Satellite Geodesy
AFCRL-70-0614 (10 November 1970)

MOLINUX, C. E., ELLAMPTIS, E. E., and NEAL, J. T., MAJ. (USAF Acad., Colo.)
A Remote Sensing Investigation of Four Mojave Playas
AFCRL-71-0235 (16 April 1971)

RHOADES, T. S.
Frequency Model for the GI-TI-B Single Degree of Freedom Rate Integrating Gyroscopes
AFCRL-71-0599 (9 December 1971)
Fundamental Geokinetic Considerations in Multiple Position Gyrocompassing
AFCRL-72-0188 (22 March 1972)

IX. Optical Physics Laboratory



The Optical Physics Laboratory conducts research on the sources, transmission, and detection of optical and infrared radiation and their interaction with the aerospace environment. Field measurements, laboratory studies, theoretical studies, and analyses are conducted to determine and understand the optical and infrared properties of sources and of the environment including the atmosphere and celestial sky. These determine how well the atmosphere transmits radiant energy and also how much energy the atmosphere radiates, both under natural and perturbed conditions.

Any optical or infrared detection or weapon system that operates in or above the atmosphere must look through the atmosphere or look against a background of either atmosphere or sky. Therefore, the need exists to know the optical properties of the atmosphere and other environments and in what manner they will enhance or limit the operation of these systems.

The Laboratory's effort on the sources of optical/infrared radiation ranges from measurements and studies of atmospheric and stellar emission as well as missile plume radiation to research into the behavior and operation of lasers, including gas and chemical lasers.

The portion of the electromagnetic spectrum studied extends in wavelength from about 2000 Angstroms in the ultraviolet to 1 millimeter where the far infrared blends into the microwave radio spectrum.

Laboratory work is divided into studies of: the visible or near visible properties of the atmosphere, where aerosol and molecular scattering is the predominant mecha-

IX. Optical Physics Laboratory



The Optical Physics Laboratory conducts research on the sources, transmission, and detection of optical and infrared radiation and their interaction with the aerospace environment. Field measurements, laboratory studies, theoretical studies, and analyses are conducted to determine and understand the optical and infrared properties of sources and of the environment including the atmosphere and celestial sky. These determine how well the atmosphere transmits radiant energy and also how much energy the atmosphere radiates, both under natural and perturbed conditions.

Any optical or infrared detection or weapon system that operates in or above the atmosphere must look through the atmosphere or look against a background of either atmosphere or sky. Therefore, the need exists to know the optical properties of the atmosphere and other environments and in what manner they will enhance or limit the operation of these systems.

The Laboratory's effort on the sources of optical/infrared radiation ranges from measurements and studies of atmospheric and stellar emission as well as missile plume radiation to research into the behavior and operation of lasers, including gas and chemical lasers.

The portion of the electromagnetic spectrum studied extends in wavelength from about 2000 Angstroms in the ultraviolet to 1 millimeter where the far infrared blends into the microwave radio spectrum.

Laboratory work is divided into studies of: the visible or near visible properties of the atmosphere, where aerosol and molecular scattering is the predominant mecha-

nism of attenuation; the infrared properties of the lower atmosphere where thermal equilibrium usually prevails; the optical and infrared properties of the upper atmosphere (including aurorae and airglow) where individual molecular interactions must be considered; the infrared properties of exoatmospheric sources—stars, nebulae, cosmic dust; the physics of lasers; measurements of the radiation from man-made sources such as missile plumes; and development of improved techniques for spectroscopic measurements.

A major area of investigation by the Laboratory concerns atmospheric attenuation or transmission of radiation by the atmosphere, particularly for laser beams. Atmospheric molecules absorb optical and infrared radiation selectively at discrete wavelengths. One objective is to determine precisely how atmospheric transmission varies with wavelength and for example, what wavelengths allow the maximum transmission of laser beams. To this end, extensive computer programs have been developed which make use of the vast collection of spectroscopic data for molecules and which permit the calculation of this transmission. Graphs and a computer program have been published and distributed widely for determining the low resolution ($\sim 20 \text{ cm}^{-1}$) transmission of the atmosphere for any path through the atmosphere for a wide range of meteorological conditions. Similarly, tables have been published for the atmospheric attenuation coefficients of various laser lines such as CO, HF and DF and CO₂.

Scattering by aerosols and molecules in the atmosphere also contributes both to attenuation and to reduction in the contrast of a target seen through the atmosphere. Extensive measurements from the Laboratory's C-130 flying laboratory, balloons and rockets have been made to determine the geographic, seasonal and altitude

variations as well as the optical properties of these aerosols and the effect of the underlying terrain, water surface or snow cover. The results of these measurements have been applied to several system problems.

Similarly, the emission of the atmosphere, insofar as it creates a disturbing or masking background against which a target must be located, is also a major concern of the Laboratory efforts. Such emissions represent interfering background noise superimposed on the optical/IR target signals that a surveillance system may be trying to detect. The emission of the lower atmosphere can be calculated from computer programs similar to those discussed previously. However, the emission from the upper atmosphere (above about 70 km) requires a much more detailed knowledge of the interactions and collisions among the individual molecules, many of which will be in excited states with excess energy, as well as how these molecules then radiate—at what wavelength and how much radiation. In addition, what happens to the upper atmosphere and thus its infrared emission when the atmosphere is disturbed by protons or electrons impinging on it, for example, during an aurora or a nuclear burst, is also being studied. Thus, there is a sizable laboratory and theoretical research program being carried out on the physics and chemistry of the atmosphere—in particular, those molecular interactions which lead to infrared emission—as well as an extensive measurement program from the Laboratory's NKC-135 optical/infrared flying laboratory, balloons and rockets. A computer program (called OPTIR) is being developed to predict and compute the optical and IR emission of the upper atmosphere, particularly under disturbed conditions. Such background emission, particularly during disturbed conditions, e.g. aurorae, could seriously impair the operation of a

surveillance, tracking, or terminal guidance system. Also, the radiation profile of the horizon determines the ultimate accuracy of horizon-sensing attitude control systems on satellites.

The measurement and study of atmospheric transmission or emission also provides a method for remotely sensing atmospheric composition and meteorological condition (including the effect or addition of contaminants, for example, from high altitude missile or jet engine exhausts).

A satellite or rocket-borne infrared system looking away from the atmosphere will still see the celestial sky as a background. Consequently, the Laboratory has mounted an extensive rocket program to survey the entire celestial sky—stars, galaxies, nebulae, etc.—in the infrared. Also, measurements of missile plumes have been obtained from rockets and aircraft. The aircraft measurements have included some of the most detailed spectroscopic data on missile plumes ever obtained.

An inseparable part of these measurements and studies is the development of more sensitive infrared sensors and spectral measuring instruments. Such a technique to which the Laboratory has contributed much is multiplex spectroscopy—which basically implies being able to analyze all wavelengths entering the spectrometer simultaneously. One form of multiplex spectroscopy—Fourier spectroscopy—has been studied and utilized by the laboratory with great success for several years.

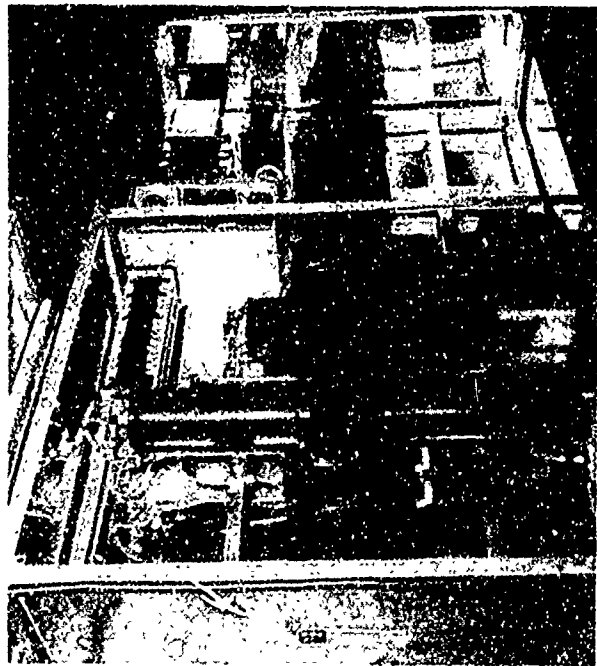
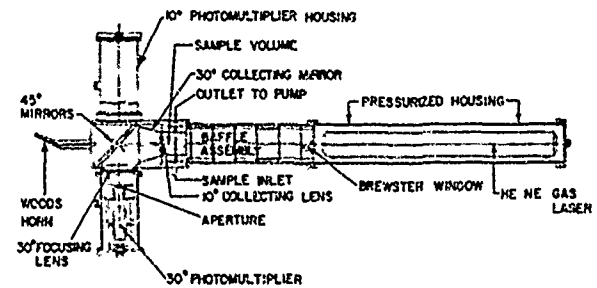
Since June 1970, in addition to the use of the two flying laboratories discussed above (an NKC-135 and a C-130A), instrumented exclusively for research by the Optical Physics Laboratory, the Laboratory has launched 12 rockets and used 28 instrumented balloon flights in its programs.

AFCRL's laser research program which is centered in this laboratory, concentrates on chemical lasers, optically induced dam-

age to laser components, tunable lasers, and non-linear optical devices.

ATMOSPHERIC OPTICS

Atmospheric Optics studies the light scattering and absorption properties of the atmosphere to determine the effect of



The optical assembly used in the aerosol particle counter. The schematic above shows the location of various components within the assembly, and the photograph below was taken by a camera looking down at the assembly.

these atmospheric optical properties on the performance of various Air Force systems and operational concepts.

One of the primary objectives of the Atmospheric Optics research is to measure the distribution of light scattering and absorbing aerosol particles in the atmosphere from the ground, from aircraft, from balloons and from rockets. These aerosol particles, ranging in size from clusters of molecules of less than one millionth of a millimeter to giant dust particles a fraction of a millimeter in size, scatter incident light in various directions as well as absorb some of the incident radiation. These optical properties of small particles depend on their number, size, chemical and physical composition, including refractive index, shape, and homogeneity.

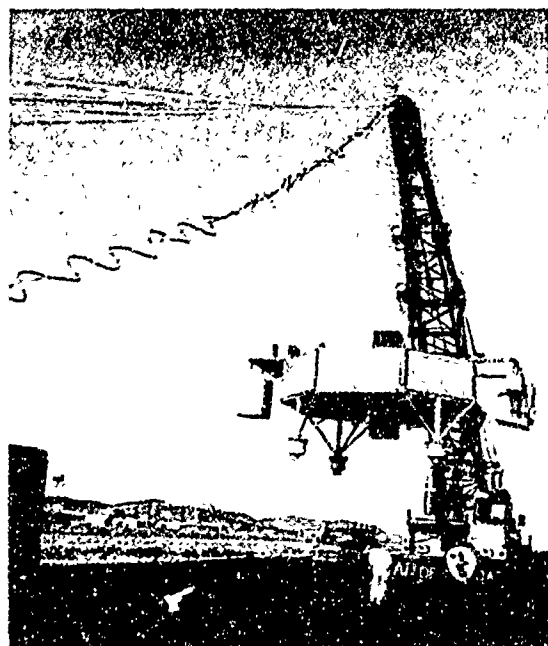
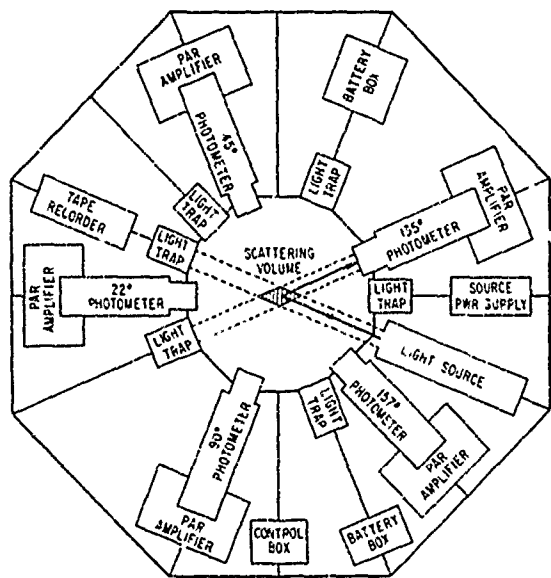
The origin of these particles is as varied as the properties of the particles themselves. Many of these particles originate from solid dust particles picked up from the ground, seaspray over the oceans, or particles ejected into the atmosphere from man-made pollution sources. Others are formed in the atmosphere from gaseous contaminants by photochemical or other processes. The aerosol particles are transported over large distances by airmass movements and are carried up into the troposphere and stratosphere by convective weather systems. In addition, it has been proven that violent volcanic eruptions can eject large quantities of volcanic dust into the stratosphere. Because of their small size and weight these particles can remain suspended in the atmosphere for long periods of time before they fall out, are washed out, or are removed otherwise. The difficulties involved in predicting the optical properties of the atmosphere at a given time and place become quite apparent from these considerations.

THEORETICAL STUDIES: Great progress has been achieved in the past in formulating theoretical concepts for calculating the

transmission of light beams through the atmosphere and the angular and spectral distribution of scattered light. Several solutions have been found within the past few years to the very difficult problem of treating multiple scattering processes, where light undergoes successive scattering processes by several aerosol particles and air molecules. A method successfully used by this Laboratory utilizes a statistical approach: Light photons are followed through the atmosphere at random through many individual scattering, absorption and ground reflection processes. This method is particularly amenable to solutions using large high-speed computers. Several programs to compute the transmission and backscattering of pulses, the contrast reduction by the atmosphere, and the radiance distribution of the twilight sky have been developed and used in the Laboratory.

BALLOON-BORNE MEASUREMENTS: Despite the great value of theoretical concepts in analyzing the effects of various parameters on practical problems, realistic model atmospheres are always required as inputs if the results are to have any applicability to real world conditions. Such input data can only be obtained from field and laboratory experiments.

Advancement in such diversified disciplines as air pollution research, cloud physics, and atmospheric optics depends largely on the capability to measure the distribution and composition of aerosol particles in the atmosphere. The number density and the size distribution are the two most important parameters. One of the methods used in determining these parameters is to measure the light scattered by these small particles. The principal advantage of this technique over other direct sampling instruments is that no mechanical contact with the particle is required and therefore the danger of changing the particles in the measuring process is greatly reduced. The



The balloon-borne nephelometer for measuring light scattering as a function of angle for various altitudes. The schematic shows the arrangement of the light source and the photometers to detect the radiation at various angles. The nephelometer is seen below hanging from the crane which will launch it on a balloon flight.

optical particle counting instruments sample the aerosol cloud with a very narrow light beam. Each time a particle moves through the light beam a pulse of scattered light can be detected. The intensity of the light pulse is related to the particle size and the refractive index of the particle. This dependence on the refractive index can cause considerable uncertainty in the size determination. The accuracy of the size determination can, however, be significantly improved if one measures the scattered light intensity in two different forward directions rather than one. For wavelengths in the 0.6 micrometer spectral region, particle size over a range from 0.1 to 1 micrometer diameter can then be measured with an accuracy of 15 percent or better.

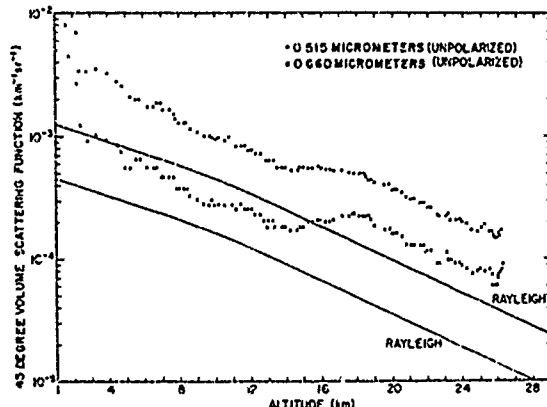
A balloon-borne instrument based on this principle has been built and a successful flight has been conducted. This aerosol counter used a helium-neon gas laser (0.6328 micrometer wavelength) as a light source. Two photometers at 10 degrees and 30 degrees with fields of view of 10 degrees measured the scattered light pulses of approximately 250 microseconds duration. The pulses were recorded on board the balloon gondola on magnetic tape. The recorded data were reduced on the ground by a computer program which counted the light pulses over predetermined amplitude ranges and altitude intervals to derive the size distribution of particles as a function of altitude.

A successful flight with this newly developed particle counter was conducted from White Sands, New Mexico, in October 1970. The balloon reached an altitude of about 23 kilometers. The results from this flight showed that the total number of particulates over the size range from about 0.2 to 1 micrometer decreased from ground level to about 11 kilometers altitude to a value of about 800 particles per liter of air. Between 18 and 22 km altitude the dust particle concentration increases

again to a value about twice as high. This "20-km maximum" has been found by many other experimenters also and seems to be worldwide. The particles follow in general a size distribution of the form $N \sim r^{-n}$ (where N is the number of particles with radius r and the exponent varies between about 3 and 5). These balloon flight results provide for the first time direct measured size distribution of aerosols at high altitudes.

Directly related to this balloon-borne aerosol counter experiment is another balloon experiment conducted by the Laboratory. A large polar nephelometer was constructed at AFCRL for the purpose of making high altitude atmospheric light scattering measurements. The instrument is balloon borne and measures the angular volume scattering function with altitude in absolute quantities. This parameter is difficult to measure accurately for it represents the amount of light an irradiated volume element of air scatters in a particular direction. Consequently, stringent requirements are placed on the measurement apparatus as to background light if reliable results are to be obtained. The angular distribution of the scattered light as well as its wavelength and polarization depends on various properties of the air molecules and aerosols contained in the volume element. These properties include molecular and aerosol number densities, aerosol particle size distribution, refractive index, and particle shape. The nephelometer detects the scattered light at five different angles, for visible and near infrared wavelengths. Moreover, it offers distinct advantages over other techniques used in atmospheric optics research in that the light transmission path is limited to approximately one meter; thus, difficulties such as multiple scattering and path attenuation of the beam are obviated. Furthermore, the unit is calibrated in absolute intensities.

The instrument consists of a xenon light source, operated in a modulated CW mode,



The value of the volume scattering function (fraction of the incident light scattered out of the beam in all directions) at 45 degrees as a function of altitude for two wavelengths. Circles and crosses are measured values for combined molecular plus aerosol scattering obtained from the balloon nephelometer. Solid lines are theoretical molecular Rayleigh scattering values. The values represent the fraction of incident light that would be scattered per kilometer in each of the 4π steradians if the scattering 45 degrees from the beam were the value at every angle.

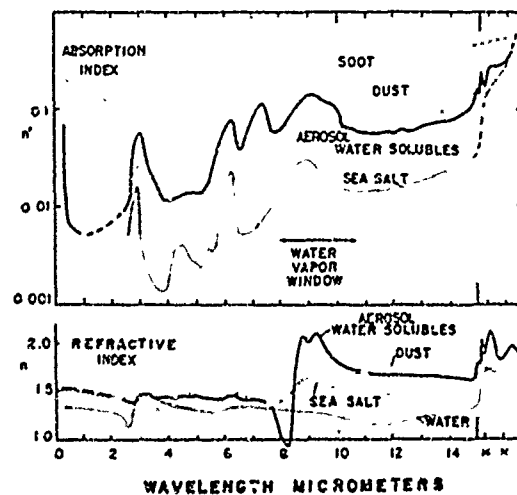
and five photometers, which view the projected beam at 22, 45, 90, 135, and 157 degrees. The volume (approximately 250 cm³) defined by the intersection of the source beam and detector field-of-view contains the atmospheric sample, the scattering properties of which are measured. In particular, the intensity and polarization of the scattered light as a function of wavelength are sensed as the balloon ascends and descends. These, in turn, provide a measure of the volume concentration and size distribution of atmospheric aerosols.

The initial flight with the equipment was made in November 1970. The results show that the nephelometer is indeed a sensitive instrument for studying optical properties of the atmosphere, even though its full capability was not realized due to some equipment malfunctions. The experimental payload went above 26 km and the

data provided profiles of the volume scattering function versus altitude for three scattering angles and four wavelengths. In addition, polarization of the scattered intensity, as a function of altitude, was measured. Aerosol scattering in the troposphere and stratosphere was quite evident from the data although the ground visibility was better than 30 km on the day of the flight. The tropospheric aerosol was closely correlated with changes in temperature profile, the vertical transport of particles being inhibited by a weak inversion. Distinct dust layers in the stratosphere (between 17 and 26 km; above the tropopause at 18 km) were identifiable. These strata appeared in the nephelometer profiles as well as in photographs of the horizon taken with time-lapse cameras mounted on top of the balloon gondola.

For many practical problems it is not only desirable to know the aerosol optical properties of relatively small atmospheric volumes as measured with the nephelometer, but also the average integrated effect over long atmospheric paths, particularly in more or less horizontal directions.

The characteristic and pronounced forward directional scattering by aerosols is a



Absorption index n' and refractive index n versus wavelength for various aerosol materials.

sensitive optical indicator for the presence of nonmolecular particles in the atmosphere. Vertical profiles of atmospheric aerosol distribution can be developed by means of optical measurements looking close to the sun and taken at different altitudes above ground level.

A high altitude balloon flight program has been developed for this purpose. There are two major components in the flight instrumentation. A biaxial sun pointer events optical radiometers continuously to the sun during the rise and float portions of the balloon trajectory. Two logarithmic amplifier radiometers which time-share a common optical filter wheel are mechanically set at fixed angles of 2 and 4 degrees from the solar vector. Spectral measurements are made at 0.34, 0.38, 0.42, 0.46, 0.50, 0.54 and 0.60 micrometers.

This system was flown at the AFCRL Balloon Flight Facility, Holloman AFB, New Mexico, most recently on August 3, 1971. The flight system rose to a float altitude of 40 kilometers. Spectral measurements of the near sun radiances were made continuously throughout the period.

The magnitudes of measured near solar scattered sunlight are significantly greater than found in a pure molecular atmosphere and, hence, demonstrate the presence of aerosol scattering even at altitudes of 30 km and above.

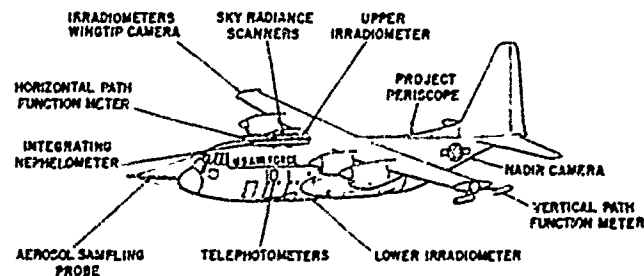
AIRCRAFT PROGRAM: To collect the data base for deriving a working concept on how the optical properties of the atmosphere vary in space and time, an aircraft measurement program has been continued to measure various optical parameters as a function of altitude up to about 6 km in various geographical areas and seasons. A C-130A Hercules has been instrumented as a flying laboratory to measure aerosol particle concentrations, scattering coefficients, sky and terrain radiance and various other parameters related to the optical properties of the atmosphere. This aircraft has been used on extensive field trips during

the time period 1970-1971 to collect data in the densely populated Central European environment, around an isolated industrial city of the midwestern United States, over the Mediterranean Sea, over the North African desert, over the desert regions of the southwestern United States, and over the snow-covered regions of northern Michigan and upstate New York, and in the New England area. During these field trips, more than 60 data packages of vertical cross sections of a variety of parameters have been obtained. The results reveal several significant features in the relationships between such parameters as surface reflectance and airmass properties on one hand, and atmospheric contrast transmittance on the other. The results also show the strong dependence of atmospheric contrast reduction on the angle between the direction of an illuminating source (for instance the sun), and the observer viewing direction. Results from these flight measurements are also in very good agreement with model computations for comparable conditions.

TWILIGHT STUDIES: Measurements of sky brightness at twilight have been used to derive information on the light scattering properties and aerosol content of the upper atmosphere. The problem is complicated

by multiple scattering of the light by aerosols and air molecules. Monte Carlo computer calculations have provided some insight into the contribution of multiple scattered light to the twilight sky radiance. The Monte Carlo calculations show that multiple scattering contributes on the order of 50 percent of the total scattered intensity and that as many as seven or eight scattering processes must be included to give total scattered intensity. Most of the multiple scattering occurs in the lower and more dense atmosphere.

LABORATORY STUDIES: Recent infrared investigations of natural aerosols in the lower atmosphere not only revealed their optical properties, but also the absorption spectra provided new data on their chemical composition over the whole world. The aerosol substances were mostly obtained from rain or snow: dust and soot by sedimentation and dry water solubles by evaporation. The samples were mostly of local origin, but results from tropical rain (Puerto Rico, Hawaii, South Pacific islands), Arctic and Antarctic snow and ice core samples were quite similar. A broad absorption maximum due to dust was noted at 10 micrometers, typical of silicate minerals. Because soot has such a high absorption index, its concentration in aer-



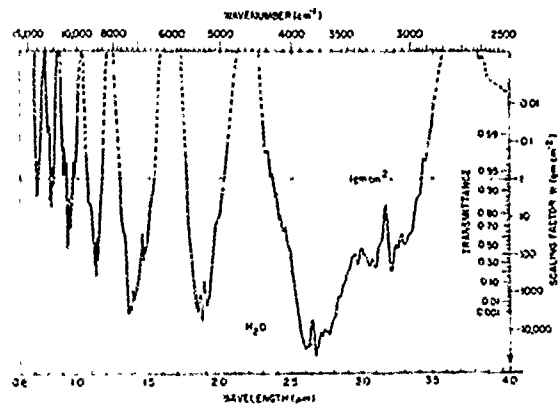
The Laboratory's C-130 flying laboratory used to investigate optical properties of the atmosphere. Placement of instruments for measuring sky radiance, atmospheric transmission, aerosol distribution, terrain reflectance, and other parameters are diagrammed in the drawing.

osol samples must be determined; its effect on the measurement of other constituents is especially strong in the visible range.

Water-soluble materials in the samples all show the same type of absorption bands, but details of peak position and band shape vary greatly. Inorganic salts (ammonium and calcium sulphate) produce bands near 9 and 17 micrometers; other bands were produced by a previously unknown alcohol soluble fraction of the water solubles, probably oxidized hydrocarbons. The importance of these was emphasized by a few samples of arctic, local, and tropical origin. They showed abnormally high concentrations of water-soluble materials, 80-90 percent of which were also soluble in alcohol and acetone. Although the acetone-soluble materials originally only showed absorption bands at 2.8 and 6.2 micrometers, wet photo-oxidation caused a slow change to more normal spectra. Smaller amounts of sea salt in aerosol cannot be detected in the infrared spectra.

INFRARED PHYSICS

The Infrared Physics program includes research on, and measurements of, the mechanisms of attenuation, absorption, transmission, and emission of infrared radiation in the aerospace environment. This includes infrared background emitted by the atmosphere and celestial sky. It also includes the attenuation by the atmosphere of the infrared radiation from natural sources, natural or man-made disturbances, or targets such as missile plumes. The results of these efforts, in addition to the data measured directly, are models and computer codes which allow the prediction of this infrared emission and transmission for any situation. Also, improved spectroscopic measurement techniques are developed.



Prediction chart for water vapor transmittance from 0.6 to 4.0 micrometers.

ATMOSPHERIC TRANSMISSION-EMISSION MODELS: Models of the transmittance and emission properties of the atmosphere have been developed. Two basically different transmittance models exist: One is a low resolution (20 cm^{-1} spectral resolution) model and covers the range from 0.25 micrometer to 28 micrometers. This model is described in *Optical Properties of the Atmosphere, Third Edition* (AFCRL-72-0497), and a computer version of the model in *Atmospheric Transmittance from 0.25 to 28.5 μm : Computer Code LOWTRAN2* (AFCRL-72-0745). This model includes effects of both molecular and aerosol scattering on atmospheric transmittance over the entire spectral range.

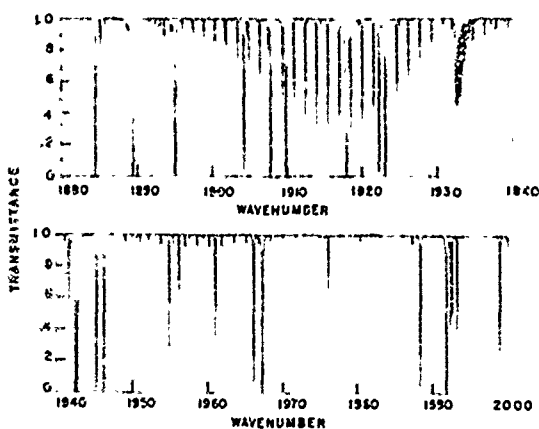
The second transmittance model uses the absorption profiles of individual molecular absorption lines and averages over these (the so-called line-by-line calculations). This approach results in synthetic spectra at either high or low resolution depending on the desired averaging spectral interval. This is the only approach capable of computing very high resolution spectra for the transmittance of laser beams through the atmosphere. It should also yield more accurate low resolution calculations when appropriately averaged over wavelength. During this past year

there has been a great increase in the development of lasers in the infrared. Such laser systems include CO, DF, and HF. A frequently asked question is: "What laser frequencies are attenuated the least by the atmosphere?" This question has been largely answered for a CO laser system in *Atmospheric Attenuation of CO Laser Radiation* (AFCRL-71-0370), and a sample synthetic spectrum from that report is included here. Similar reports for HF and DF (AFCRL-72-0312) and CO₂ (AFCRL-72-0611) laser emission regions have been published.

To attempt a calculation program of this type, it is necessary to compile the fundamental spectroscopic data (including line intensities, frequencies and half-widths) of all molecules responsible for atmospheric absorption in the spectral region of interest. The best set of absorption band constants for the atmospheric absorbing molecules are sought, and from these the required spectroscopic data are calculated.

The atmospheric gases studied so far include: CO₂, H₂O, O₃, N₂O, CO, CH₄, O₂, N₂, and HNO₃. The first six of these alone have over 90,000 rotation-vibration lines. The compilation of these lines is described in AFCRL Atmospheric Absorption Line Parameters Compilation (AFCRL-73-0096). Generally, these molecules exist in that portion of the atmosphere where local thermodynamic equilibrium can be assumed. With this assumption, a knowledge of the transmittance parameters, and a physical model of the atmosphere, the atmospheric emission can also be computed for any spectral region of interest.

The difficulty in applying the fundamental spectral data to calculate transmittance over nonhomogeneous paths such as those traversed by radiation in the real atmosphere is that a knowledge of molecular abundance and their distribution with height is needed. All the molecules studied except for H₂O, O₃, and HNO₃ have been



Atmospheric transmittance due to molecular absorption through a 10-km horizontal path at an elevation of 12 km (aerosol attenuation omitted).

assumed uniformly distributed for this purpose. There is some evidence that N₂O, CO, and NO₃ may not be uniformly mixed, and further analysis of transmittance and emission data gathered with balloons may resolve this problem. The distribution of H₂O in the stratosphere is similarly an open question. A significant source of uncertainty in these calculations results from uncertainties in line shape, which is a function of pressure, temperature, and a number of other parameters. Other uncertainties are related to departures from the usually accepted Lorentz shape in the far wings of lines, which result in uncertainties in continuum absorption on some of the "window" regions. For the present, this last problem will be solved by use of experimentally determined absorption coefficients. Significant departures from the Lorentz shape have been found even in spectral regions closer to absorption bands, and empirical data for CO₂ are now being entered into our calculations.

LABORATORY STUDIES: Instrumentation to extend infrared spectroscopic studies of upper atmospheric constituents has been designed and assembled. The program is

directed toward the measurement of vibrational band intensities—that is, the amount of absorption by a known quantity of a gas for a specific absorption band. We are particularly concerned with those molecules which occur in the upper atmosphere where upper vibrational states are well populated and play an important role in radiative transfer processes. When completed, the instrumentation will provide the capability for carrying out two distinct types of experiments. First, absorption or emission studies of atmospheric gases can be made at elevated temperatures and over long path lengths. This will allow studies to be made of those upper vibrational states which are too weak to observe at room temperature. Secondly, the Laboratory will have the capability to measure the refractive indexes of gases for wavelengths up to 25 micrometers.

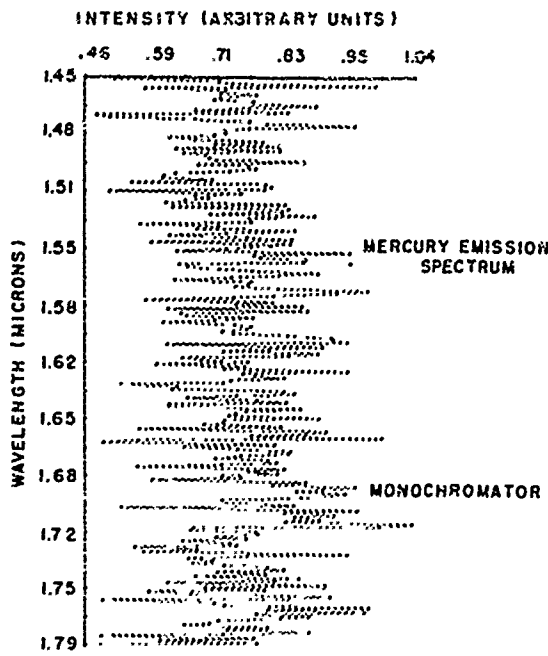
The high temperature instrumentation consists of a multitraversal cell coupled to a 2-meter Czerny-Turner spectrometer. The cell can provide a path length of 40 meters for temperatures up to 1000 degrees C. The instrumentation is designed to carry out studies of the vibrational band intensities of CO_2 and H_2O at temperatures which will provide data for the upper vibrational states. The facilities complement the present capability to carry out intensity studies at room temperature using pressure broadening techniques.

To measure refractive indexes, an asymmetric Michelson interferometer has been constructed. This instrument is designed specifically to measure the refractive index of ozone in the 3 to 25 micrometer region. These measurements will complete the earlier study in the 0.4 to 3 micrometer region. Ozone is an extremely unstable gas and cannot be studied under high pressure or elevated temperatures. Fortunately, refractive index measurements can be carried out under less severe conditions. The relationships between the refractive index curve for a molecule and its absorption

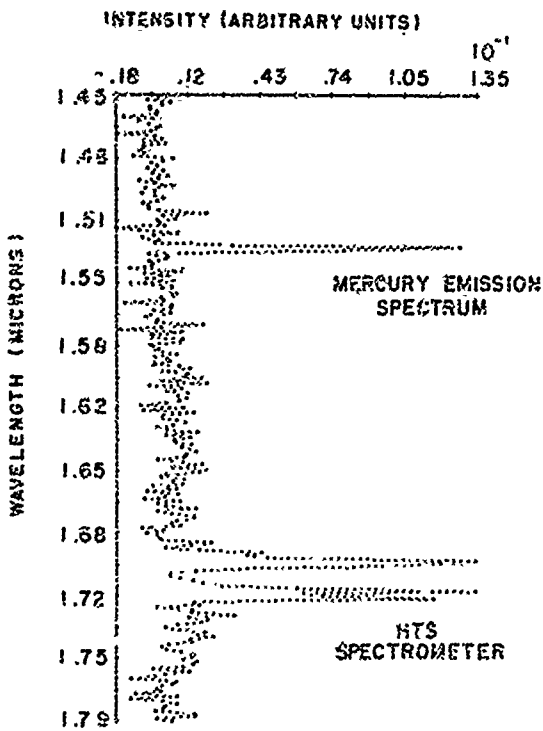
spectra are known, and from refractive index data we are able to calculate infrared band intensities.

MULTIPLEX SPECTROSCOPY: For optimum system performance, specific detailed spectral measurements must be obtained to specify such parameters as atmospheric transmission or absorption and background radiance. Conventional spectroscopic techniques are often inadequate for making many of the required measurements. Multiplex systems having high energy throughputs afford this capability.

The throughput of a spectrometer is a measure of its light-gathering capability. Multiplexing implies analyzing simultaneously all the radiation entering the spectrometer. This multiplex advantage coupled with the throughput advantage can yield increased efficiency or gains in measurement time over conventional techniques of as much as 10^8 . These gains can



Mercury emission spectrum obtained in the single slit mode with a grating spectrometer. Spectral features are masked by noise.



Mercury emission spectrum obtained using a Hadamard-coded grille on the same instrument. Large gains in signal-to-noise ratio make spectral features easily measurable.

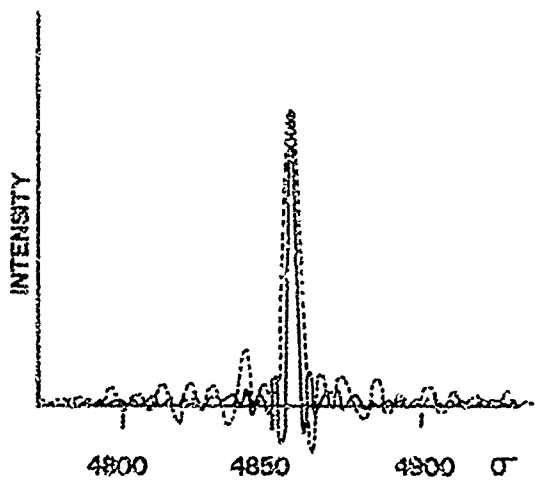
be applied to increase the S/N (signal to noise) ratio of a measurement, increase the speed of measurement (i.e., reduce measurement time T), or to obtain more detailed structural information (better resolution).

At present there are two techniques capable of yielding these advantages: Fourier spectroscopy and Hadamard spectroscopy. Fourier spectroscopy uses an interferometer spectrometer and has been developing at a rapid pace for more than a decade. Its advantages have been testified to by the presentations made at the Aspen International Conference on Fourier Spectroscopy, sponsored by the Optical Physics Laboratory of AFCRL, and appearing in the proceedings which were also published by AFCRL. Hadamard spectroscopy uses a dispersion system such as a grating or

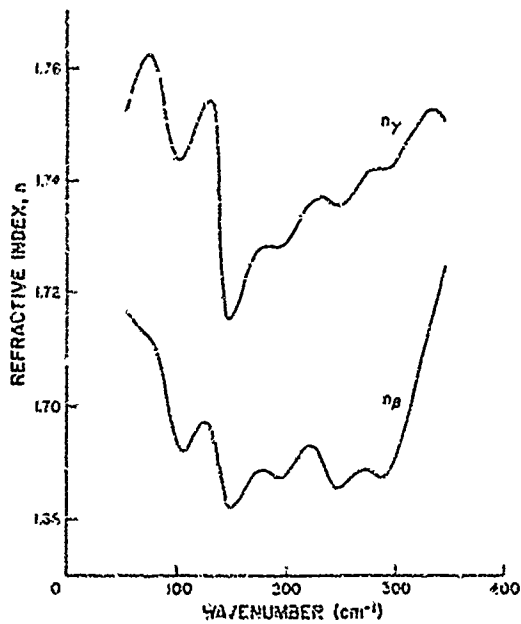
prism, is relatively new, and still must prove its practicality.

Fourier spectroscopy has the advantages of multiplexing, high throughput and large spectral coverage. Hadamard spectroscopy offers the advantages of high throughput and multiplexing. Hadamard spectroscopy alignment tolerances are microscopic and therefore may be more easily adaptable to airborne measurements of moderate spectral bandwidth than Fourier spectroscopy which requires microscopic alignment tolerances. In a laboratory environment, the Fourier spectrometer is by far the best instrument available.

A joint effort by AFCRL and industry has produced preliminary results which prove the principle of Hadamard spectroscopy. The spectrum obtained with a single-slit instrument and the spectrum obtained by Hadamard spectroscopy show the much higher signal-to-noise ratio obtainable by Hadamard spectroscopy. If a conventional spectrometer is modified by using a coded entrance aperture as well as a coded exit aperture, a doubly encoded Hadamard spectrometer results. Such a system can



Spectra obtained by numerically correcting for non-linear mirror drive motion of an interferometer corresponding to a speed fluctuation of about ± 20 percent. Dotted line is for corrected scanning motion.



Refractive index for Mylar plastic. The material is optically biaxial. The subscripts a and b refer to the two measured directions of polarization of the light.

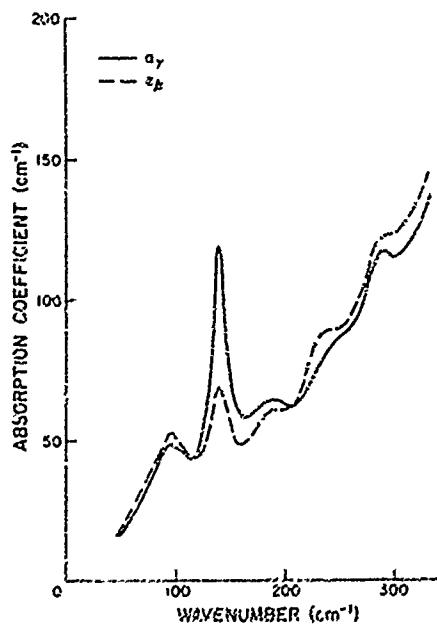
yield spatial as well as spectral information about the source.

The continuous drive interferometer systems used in Fourier spectroscopy yield unsatisfactory scanning functions (which is the impulse response of the interferometer-computer system) when the mirror drive speed is not constant. In addition to the problem of non-linearity, the interferometer yields inferior results when the movable mirror wobbles.

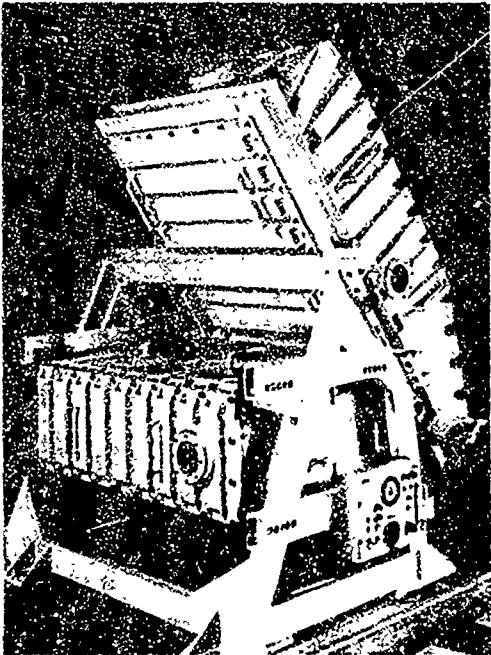
To overcome the two problems mentioned above, the new AFCRL two-meter interferometer uses cat's eyes mirror systems rather than plane mirrors, and operates in a step-integrate mode. A cat's eyes is a retroreflecting system in which the emerging beam is parallel to the entrance beam even if the whole system is tilted as much as 5 degrees. Because of this feature, the mechanical tolerances on the drive mechanism are relaxed. When a data sample is being taken, the path difference in

the interferometer is maintained to better than ± 20 Angstroms, which is adequate for satisfactory performance in the spectral region of interest.

FAR INFRARED RESEARCH: The far infrared laboratory program of optical property measurements has determined refractive indexes and absorption coefficients for a variety of materials. A typical set of data for Mylar, a plastic available in thin film form useful for beamsplitters for far infrared interferometers, shows the two sets of optical constants which can be measured on this biaxial material. Other materials have been measured both at room temperature and at pumped helium temperature (1.5 degrees K). Plastic materials do not show any significant change in optical properties (especially absorption) upon cooling. Some crystalline materials, on the other hand, undergo a dramatic change. Rutile, for example, is completely



Absorption coefficients for Mylar plastic. The material is optically biaxial. The subscripts a and b refer to the two measured directions of polarization of the light.



Vacuum chamber housing for heliostat and far infrared interferometer. This will be mounted in the KC-135 flying laboratory and used to obtain measurements of the far infrared transmission and emission of the upper atmosphere.

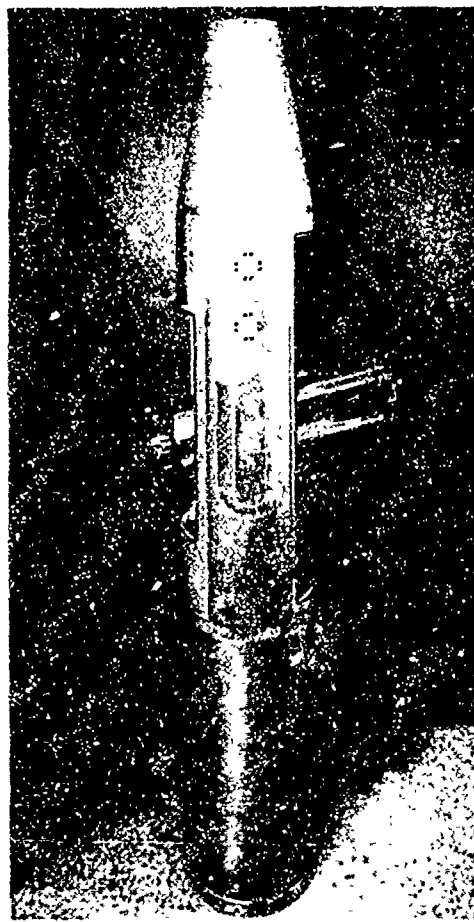
opaque at room temperature, and becomes highly transparent when cooled.

Instrumentation for measuring atmospheric transmission in the far infrared region has been installed in a KC-135 aircraft. Several checkout flights and data flights were flown in early 1972. The far infrared transmittance and emittance of the upper atmosphere will be determined for altitudes accessible to KC-135 aircraft at various latitudes.

INFRARED CELESTIAL MEASUREMENTS: The Air Force needs to detect infrared emitting targets at the greatest possible range. If these targets are viewed against the background of celestial sources, knowledge of the infrared characteristics of the background is necessary to permit discrimination of the target from the background.

A payload was developed to investigate the possibility of surveying the sky at several wavelengths in the infrared from vertical sounding rockets. A preliminary version was launched on an Aerobee 170 in July 1970. The success of this experiment resulted in the development of a full-scale sky survey payload which began a series of flights in April 1971.

To obtain precise coordinates of the celestial objects observed, the scan axis of the payload is locked to a preselected star transiting near the zenith at the time of



Rocket payload used to measure infrared emission of stars. Payload is shown with nose tip ejected to permit the star tracker to view the zenith and the infrared telescope deployed to its measurement position.

the launch. The infrared telescope is positioned at various angles with respect to the scan axis and held at this position while the rocket performs the scan maneuver. The position of the telescope along the scan plane is measured by observing star transits with a visual star aspect sensor. When the nose tip is ejected, it permits the star tracker to view the zenith and the infrared telescope to deploy to its measurement position.

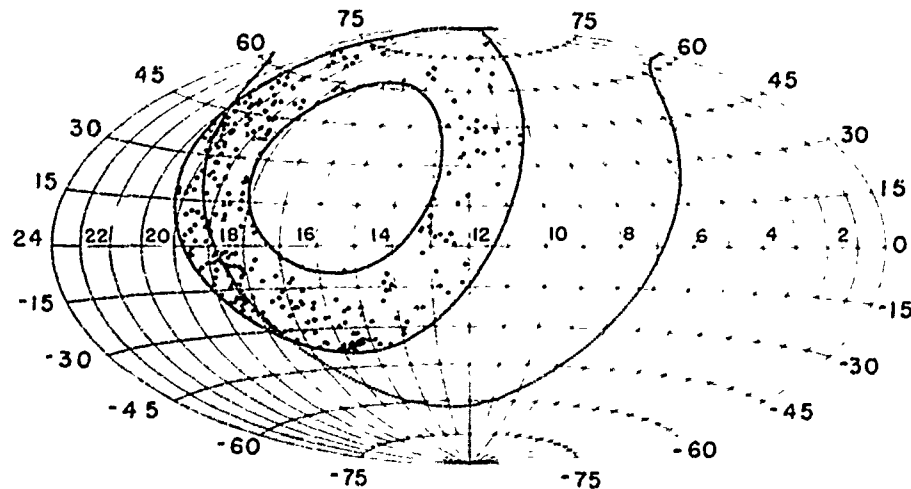
Portions of the sky have now been scanned in several infrared bands. The sources detected are not uniformly distributed throughout the scanned area, but show a concentration toward the galactic plane. This concentration of sources near the plane becomes more marked at longer infrared wavelengths. Thus, one can conclude that the majority of the sources observed are members of the Milky Way with very few extragalactic objects being detected.

The infrared sky survey will be continued for several more years. The ultimate goal is a complete set of sky maps at

wavelengths in the near, intermediate, and far infrared regions.

RADIATION EFFECTS

The primary research of this segment of the Laboratory is the optical/infrared properties of the upper atmosphere both under normal conditions and when it is disturbed by aurorae or nuclear weapons. At the altitudes considered, thermal equilibrium usually does not exist, and it is necessary to consider the collisions or interactions of individual pairs or triads of molecules, one or more of which may be in an excited state (i.e., with excess internal energy). Extensive Laboratory and theoretical studies, as well as rocket, balloon and aircraft measurements of upper atmospheric optical/infrared phenomena are being carried out. The results of these Laboratory studies and aircraft measurements also apply to missile or jet engine plume infrared radiation, and measure-



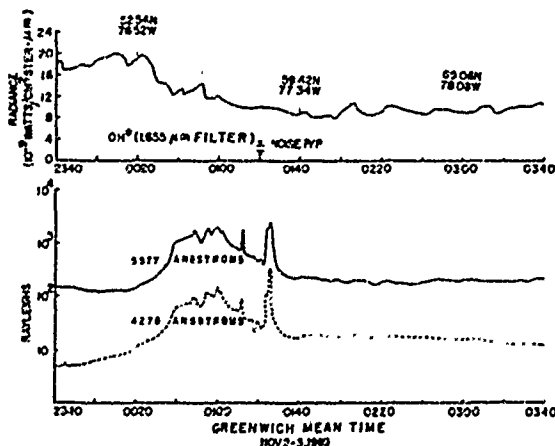
Infrared stellar sources observed at a wavelength of 4 micrometers using a rocket-borne telescope. The dotted line delineates the galactic plane.

ments of these phenomena have also been made. As in the Infrared Physics program, the goal of the research is to generate both directly measured data and also models and computer codes which permit the prediction of the optical/infrared emission of the upper atmosphere, particularly under disturbed conditions.

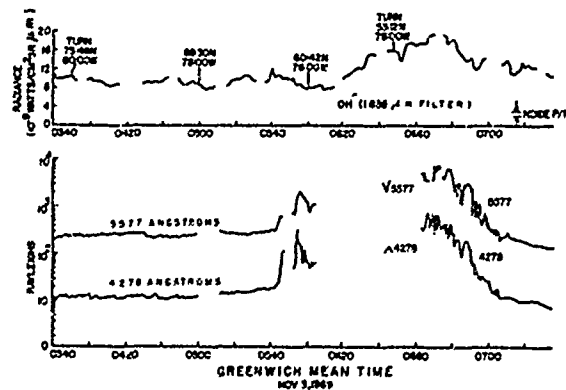
OPTICAL/INFRARED (OPTIR) CODE DEVELOPMENT: OPTIR is a computer code currently being developed to generate mathematical and physical models to calculate the optical/infrared radiation resulting from natural and/or artificial stimulation of the atmosphere. The code is designed to handle the problem of nuclear detonations in the atmosphere and their effects on optical/infrared detection systems. Progress on the OPTIR code during the past year has included: 1) a more flexible X-ray spectrum routine, 2) a routine to specify daylight/night ambient species concentrations in the atmosphere, 3) an improved model of atomic species concentrations fol-

lowing the fast "ionized chemistry" phase, 4) a 20 cm⁻¹ atmosphere transmission model, and 5) a model to compute scattering of radiation from low altitude fireballs. In addition, the following milestones were achieved: 1) preparation of a model to represent shock wave heating in the upper atmosphere and the consequent effects on the nonequilibrium chemistry in the affected region; 2) determination of the usefulness of hybrid computers in the context of the OPTIR code program; 3) development of QCHEM—an algorithm for numerical integration of some types of stiff differential equations, such as arise in models of chemical kinetics, and 4) completion of revisions in OPTIR II leading to a more complete and flexible version—OPTIR III.

An examination of existing data on PCA (Polar Cap Absorption) events suggests that the event of November 1961 is typical and will serve as an adequate basis for a model of PCA generated background in the context of the OPTIR program. This, and a routine for auroral electron energy



Enhancement of hydroxyl emission is observed from 2340 to about 0300 Greenwich Mean Time just before the aircraft crosses the auroral oval, indicated by the increased 5577 and 4278 Angstrom signals. Numbers above the curve are the position of the aircraft when the readings were taken.



Later the same night an OH enhancement occurs in the same general region as the auroral oval.

deposition, will be incorporated into an advanced version of the code.

A simple chemistry model has been implemented for the study of diurnal variation of hydroxyl airglow. Comparison with field data shows that this chemistry appears to represent adequately gross changes in the airglow intensity near sunset and sunrise. However, some nighttime features with the characteristic times of the order of a few hours seem to be associated with atmospheric motion—diffusion and convection—rather than due to a chemistry more complex than the one implemented. More work is necessary to establish the correctness of this hypothesis.

AIRCRAFT PROGRAM: The Optical/Infrared Flying Laboratory is an NKC-135 aircraft equipped with 52 viewing ports behind which are operated a variety of spectrometers, radiometers and interferometer-spectrometers. In the aircraft measurement program the infrared day and night sky backgrounds are being studied in order to provide information on the signal levels against which targets must be discernible.

The measurement of atmospheric transmission in the 2 to 6 micron region and the atmospheric emission in the 1 to 14 micron region have continued with the use of the Michelson interferometer systems. During the latitude survey from Northern Canada to the Antarctic Peninsula, the atmospheric transmission was measured near noon, and atmospheric emission was measured during the nighttime. At all latitudes, HNO_3 (nitric acid) emission was detected at 11.3 microns. The intensity of this emission, measured above 12 kilometers, exhibited no significant variations with latitude, and the intensity was consistent with earlier observations from high altitude balloons. At altitudes below 12 kilometers, emission from water molecules interferes with the observations of the HNO_3 .

A similar series of flights was made in

the Pacific from Hawaii. Here an attempt was made to measure emission from the daytime sky for comparison with atmospheric transmission measurements made at the same time by looking at the direct solar radiation. It was observed that for wavelengths greater than 4 micrometers, the solar scattered radiation is less than the thermal emission of the atmosphere. At 4.3 micrometers the solar scattered radiation is less than 1 percent of the intensity of the CO_2 emission. These measurements can be successfully made as long as the entrance aperture of the emission measuring interferometers is not directly illuminated by sunlight.

In the auroral regions, enhancements by a factor of two of the hydroxyl (OH) emission have again been observed in the general vicinity of the auroral oval. A series of flights was made from the Churchill rocket range where the aircraft was used to indicate when the desired aurorae were present at possible rocket reentry points. Once the rocket was launched into the desired aurora, infrared and visible radiometric and interferometric measurements were made in the region of the rocket reentry point for comparison with the rocket data.

Two outstanding measurements during this reporting period were the Apollo 14 and 15 missions.

In December 1970, AFCRL was requested that the aircraft be used to measure the absolute intensity and the spectral characteristics of the plume of the Apollo 14 boosters scheduled to be launched 6 weeks later. With an intensive effort, including the construction of one complete new instrument and one new trainable mount, the aircraft was test flown one month later on January 22, 1971. Following two simulated practice missions the aircraft flew within 20 miles of the Apollo 14 launch pad on January 31, 1971 and obtained an excellent set of infrared radiometric and spectral measurements of the Apollo 14 plume.

With this outstanding flight accomplished, AFCRL was again requested to measure the Apollo 15 plume spatial characteristics. A second very successful mission was flown on July 26, 1971 during the launch of Apollo 15, when excellent radiometric, spectral, and plume spatial characteristics were obtained. The data from these missions have been fully reduced with the consequent identification of the sources and behavior of the short wavelength infrared plume in considerable detail.

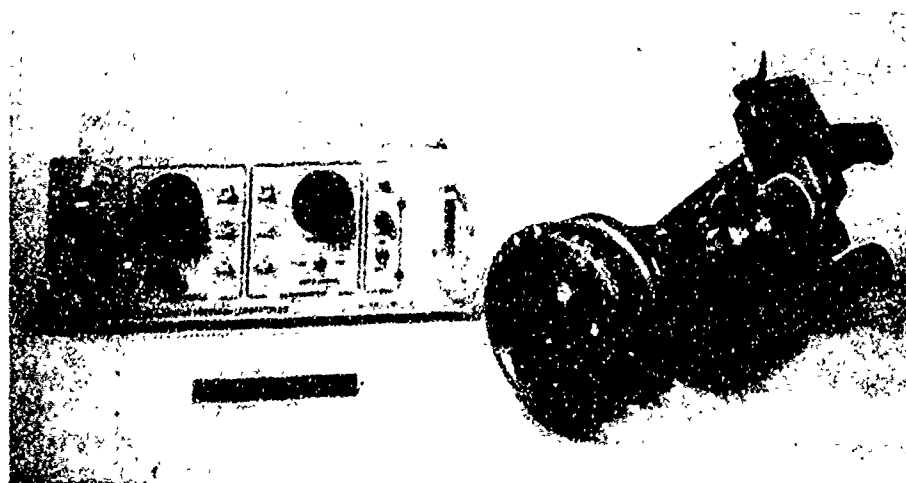
At the request of SAMSO, a further plume measurement flight was made on the Air Force Western Test Range with great success.

The development of improved instrumentation has continued. Obtaining adequate signal-to-noise ratio from some of the weakly emitting sky spectral regions in the infrared has always been a problem. One technique to improve the Laboratory capabilities involves the building of an airborne interferometer in which the detector is cooled with liquid helium and the

whole instrument, including optics and aircraft window, is cooled to liquid nitrogen temperatures. During this year an eyeball window cooled to liquid nitrogen temperatures (77 degrees K) and trainable \pm 25 degrees from its central position in all directions was successfully flown and it developed no frosting during the four-hour test.

Data reduction of interferograms has been greatly facilitated, such that it is now possible to reduce many hours of interferometric data from a single flight in almost real time.

AIRGLOW AND CHEMILUMINESCENCE: Airglow is the faint luminescence of the sky detectable on a dark, clear night. Its spectral domain extends from the ultraviolet through the visible and well into the infrared. The dominant mechanism producing airglow is chemiluminescence, the conversion of chemical energy into radiation. Prominent non-thermal sky luminescence can also be induced by nuclear detonations in the atmosphere. This chemically



Radiometer with an eyeball window fitting, trainable to view a target and background alternately to measure the difference between them. It was built in one month for the KC-135 flying laboratory mission with Apollo 14.



The KC-135 optical/infrared laboratory has many observing ports for a wide range of infrared and optical spectrometric instruments used to obtain detailed spectral and spatial measurements of atmospheric emission and transmission.

induced sky background brightness, whether natural or nuclear weapon induced, provides undesirable background noise if it should appear in the field-of-view of optical instruments intended to detect and track targets.

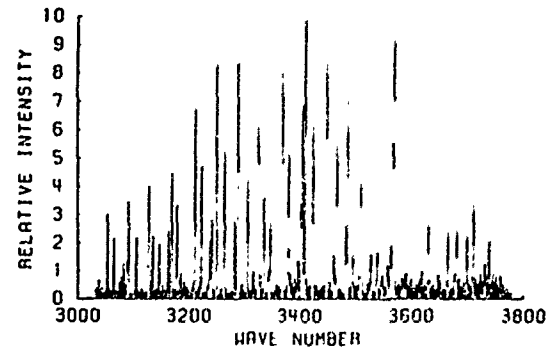
Molecules emit chemiluminescent radiation when they drop spontaneously from an excited internal state to one of lower energy following their formation in the state of higher energy. The change of internal energy may involve primarily electronic motion, with the resulting radiation typically in the ultraviolet or visible region, or the change may involve primarily vibrational and rotational motion of the molecule as a whole with the resulting radiation typically in the infrared region. In either case spontaneous light-emitting transitions characteristically are accompanied by electric dipole moment changes. The wavelength at which infrared radiation is emitted is determined by the oscillatory frequencies of the molecular vibrations, and the probability that radiation will be emitted is related to the magnitude of the moment change; thus, the interpretation of infrared chemiluminescence requires knowledge of the dipole moment function of each radiating molecular species.

Some of the more important reactions leading to chemiluminescence studied by

the Laboratory are hydrogen reacting with ozone to produce oxygen plus a hydroxyl radical, and reactions of nitrogen and oxides of nitrogen with other oxides of nitrogen or various forms of oxygen. The reactions studied leave the products vibrationally excited, and from analysis of their infrared emission spectra the dipole moments of OH, NO₂, NO and N₂O can be determined. The Laboratory's extensive study of the OH dipole moment function is of special interest. The fundamental and first overtone vibration-rotation bands of the hydroxyl radical were obtained from the study of the reaction of hydrogen molecules with ozone. The AFCRL analysis showed that the accepted value of the radiative transition probability of the band is seriously in error. The fundamental value is about 12 sec⁻¹. This result has serious implications for the interpretation of airglow spectra which are being pursued by this Laboratory.

An experimental investigation of interaction of nitrogen atoms and oxygen molecules was undertaken and completed.

It was established that NO molecules were formed in high vibrational levels.



Corrected emission spectrum of OH· from the reaction of H + O₃ vibration-rotation bands of the fundamental sequence of the ground electronic state. The rotational temperature is 540 degrees K while the vibrational distribution exceeds a temperature of 10,000 degrees K.

Dependence of infrared radiation, originating from NO molecules, upon pressure was investigated and a quantum efficiency figure was deduced. In a subsequent experiment, interferometric techniques were used and high resolution spectra of initial vibrational distribution of the NO first overtone band were obtained. The results are being compiled and interpreted for publication.

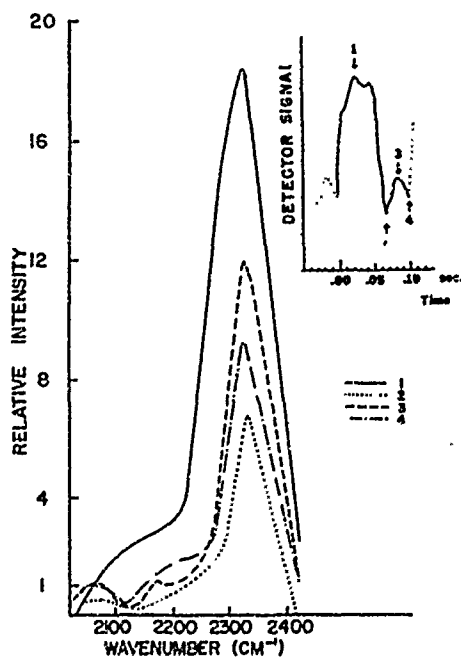
VIBRALUMINESCENCE: In addition to chemical reactions, another process whereby molecules are vibrationally excited is called "vibraluminescence." By this process, vibrational energy from a molecule which cannot radiate (due to lack of a

dipole moment) such as N₂ is transferred by collision to a molecule which can radiate. In the ionosphere E region, N₂[±] (\pm indicates vibrationally excited) is an important atmospheric constituent; since it has no dipole moment, energy is trapped and a non-equilibrium temperature is created.

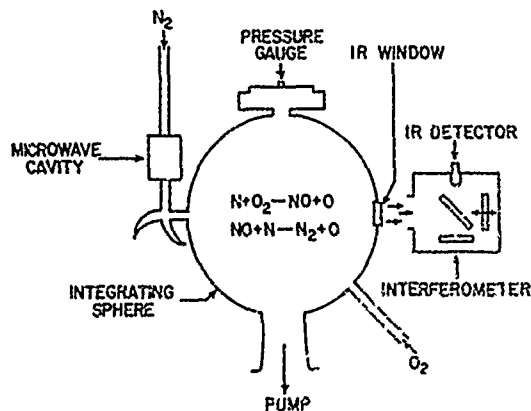
In addition to providing excitation to radiators like CO, N₂O and CO₂ whose spectra can be studied, the vibraluminescence experiments make available valuable information on the quenching of N₂^{*} (* indicates electronically excited) molecules. Analytical studies carried out under Laboratory auspices seek to model the flow of energy through N₂ molecules.

In this connection a new technique that exploits the multiplex advantage of Fourier spectroscopy has been developed to study time varying sources. The time behavior of each spectral element is observed simultaneously with each of the other spectral elements. For a source which is repeatedly excited and allowed to decay, an interferogram signal can be determined by monitoring the instantaneous value of the interferogram signal at successive times as the signal decays. For a fixed optical path difference in the interferometer, the interferogram signal is recorded from initial excitation of the source until some time later which is long compared with the overall relaxation. In this fashion, as the optical path difference is varied, a series of time separated interferograms may be recorded and the time history of all spectral elements obtained by performing the Fourier transformations. The technique has been successfully applied to the relaxation processes in a mixture of CO₂ and N₂O gases which has been excited via vibrational exchange with active nitrogen.

There has often been speculation that atoms and molecules in an excited electronic state may react with other species with a rate constant greatly different from that of their ground state. Because of the



Spectra of CO₂ and N₂O excited by N₂[±] at the four selected times as indicated on the waveform in the insert. The waveform shown corresponds to a particular optical path difference in the Fourier spectrometer and changes shape as the optical path is varied in time.



Experimental apparatus for investigation of reaction between nitrogen atoms and oxygen molecules leading to infrared radiation from NO.

great difficulty of experiments testing this notion, there are few data available to support it. In continuing experiments in this Laboratory it has been found that $O_2(b^1\Sigma)$ molecules can transfer energy to molecular hydrogen, evidently exciting it sufficiently vibrationally to allow chemical reactions which otherwise could not occur.

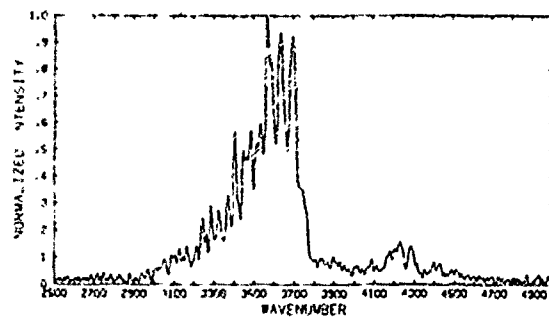
During the present reporting period a detailed survey study on the kinetics of atmospheric radiation was completed and implementation of a new low temperature, low pressure, high sensitivity facility for study of chemiluminescent reactions was begun. Conceptual design of the facility was completed and major elements of the hardware are being acquired.

MOLECULAR BEAM GENERATORS: For a chemical reaction to take place between two atmospheric molecules, the molecules must collide. Not only must they collide, but the collision must take place within a specified velocity range. If relative velocities are either too small or too great, no chemical reaction will take place. For satellite and rocket velocities the energy of atmospheric molecules in the center of mass coordinate system lies in the neighbor-

hood of a few electron volts (eV), and the range in which most chemical reactions take place is ~ 0.1 to 10 eV.

While charged particles can be accelerated to billions of electron volts, the problem of accelerating a concentrated beam of neutral particles to a few electron volts is extremely difficult. Only in recent years—during the 1960's—have techniques evolved for creating a concentrated beam of molecules in this energy range.

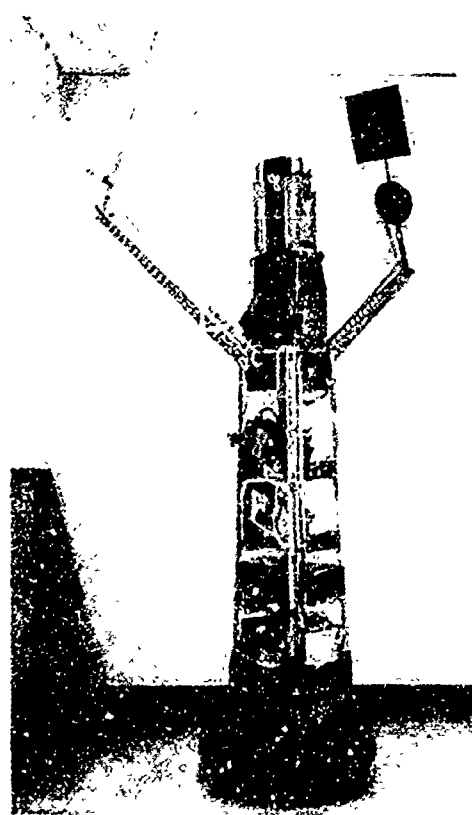
The molecular beam generator that is presently operational is based upon the principle of beam generation from a miniature supersonic nozzle. In this system, capable of producing 1–10 electron volt beams of most non-condensable gases, high pressure gas is released through a nozzle into a vacuum. An aperture in front of the nozzle blocks all particles except those traveling in an axial direction and having large velocities. The system consists of three main sections: nozzle chamber, collision chamber, and beam detector chamber. These, along with associated equipment and detectors, are installed, and beam detection and diagnostics have been completed. Of the experiments contemplated, one including vibrational excitation of CO and CO_2 molecules under the impact of high velocity particles is currently in progress. The method involves detection of



NO overtone band at 2.7 micrometers obtained with an interferometer. The spectrum reflects the vibrational distribution of NO at formation.

infrared radiation from these molecules and deduction of vibrational excitation cross sections.

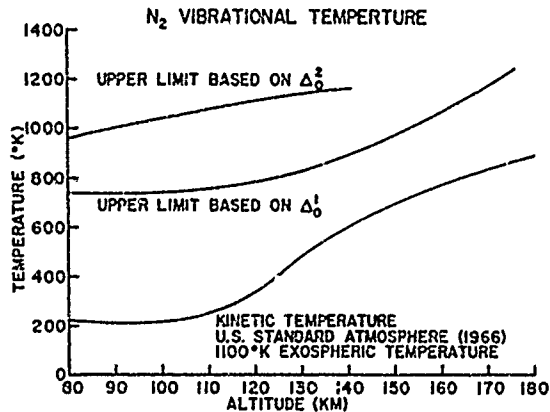
ELECTRON INDUCED EMISSION: As an energetic electron is slowed and stopped in the atmosphere, some fraction of the initial kinetic energy is dissipated by popula-



Rocket payload designed to study the temperature and density of atmospheric nitrogen by means of electron beam induced luminescence. An energetic (2.5 keV) well collimated beam of electrons is fired from the top section of the payload to a boom-mounted beam collector (circular disc). From the magnitude of specific molecular optical emissions, excited by electron impact and measured by an array of four photometers, the temperature and density of molecular nitrogen may be determined. The boom-mounted rectangular section limits the field of view of the photometers to discriminate against auroral emission.

ing excited electronic states of atmospheric molecules. The excited electronic states, in turn, may decay spontaneously with the emission of characteristic radiation. The fraction of the incident electron's kinetic energy radiated in a given transition, as the primary and higher order electrons are stopped in a gas, is defined as the electron-induced luminous efficiency. This latter process is a principal mechanism in auroral excitation and in the production of atmospheric luminescence by detonation of nuclear weapons. To interpret both auroral and nuclear-induced atmospheric emission, electron-induced luminous efficiencies must be known.

Recent auroral measurements have reported unusually bright emission from low-lying metastable electronic states, $^1\Sigma$ and $^1\Delta$ in molecular oxygen. In an effort to understand auroral excitation mechanisms, the (O-O) vibration-rotation band of O₂, $^1\Sigma$ at 7620 Å was produced in the Laboratory by energetic (50 keV) electron impact on oxygen. Using a pulsed electron beam a radiative decay time of approximately 1 millisecond was measured, in contrast to a natural radiative lifetime of 14 seconds. This implies that under these experimental conditions, approximately one in 10^4 excited O₂ $^1\Sigma$ molecules avoids collisional deactivation and relaxes by radiative decay. The luminous efficiency and collisional deactivation cross section of various molecules may be determined from the radiance of the molecular emission, the rate of luminous decay and the natural lifetime. Luminous efficiency for production by electron impact as measured under these conditions may be extended to other collisional frequencies (altitudes) assuming the number and nature of populating and depopulating processes are unchanged over the collisional frequency range. Luminous efficiency provides a measure of O₂ $^1\Sigma$ emission produced as primary energetic electrons, and their secondary and higher order electrons, are stopped in the atmos-



Upper limits for the vibrational temperature of atmospheric nitrogen measured by the electron beam luminescent technique. The symbols Δ_0^2 and Δ_0^1 refer to the population ratios of N_2^+ first negative vibrational levels 2 to 0 and levels 1 to 0.

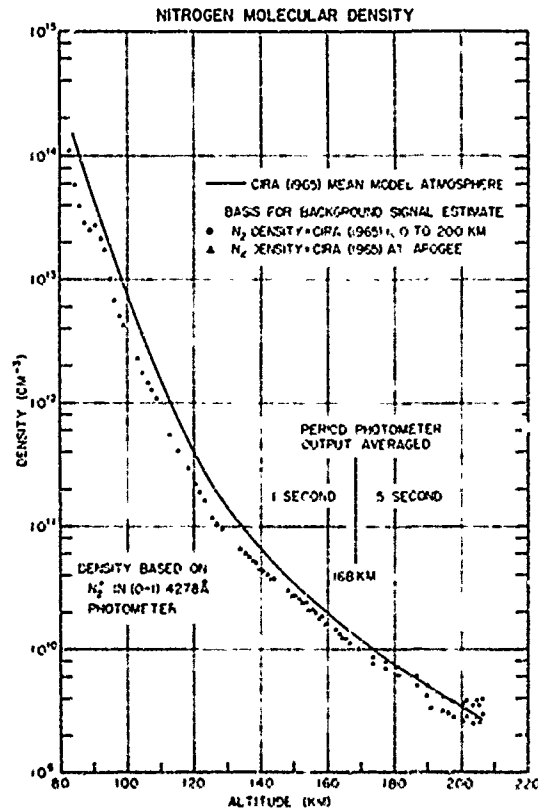
sphere, analogous to the typical electron-produced aurora.

The vibrational temperature of atmospheric N_2 has been measured using rocket-based electron-beam-induced luminescence as a remote diagnostic technique. The vibrational population of molecular nitrogen in the 80 to 175 km altitude range is inferred from the brightness of specific molecular transitions of the N_2^+ first negative band system excited by energetic (2.5 keV) electron impact.

The initial payload was launched on board an Aerobee 150, from Fort Churchill, Manitoba, Canada, March 13, 1970 at 6:18:25 GMT. Four interference filter photometers measured populations of the first three vibrational levels of the $N_2^+ B^1\Sigma$ state by observing the radiant intensity of four of the N_2^+ first negative transitions. Ground state nitrogen vibrational populations are derived from N_2^+ first negative vibrational spectra assuming relative electron excitation cross sections proportional to Frank-Condon factors. Within the experimental uncertainty, determined by the precision of the rocket instrumentation

and the nature of the experimental technique, little, if any, significant vibrational heating above kinetic temperature was measured. An upper limit of N_2 vibrational temperature was determined in the altitude range 80 to 175 kilometers (1200 degrees K at 175 km, 1000 degrees K at 150 km and less than 800 degrees K at altitudes lower than 125 km). Absolute molecular density of N_2 in the 106 to 175 km range was measured with values significantly less than the 1965 COSPAR mean model atmosphere.

A second payload was launched October 16, 1971 on an Aerobee 150 at 1:31:07 GMT from White Sands Missile Range, New



Density of molecular nitrogen in 80 to 200 km altitude range based on the electron induced luminescence technique using the rocket instrumentation shown previously.

Mexico, attaining an apogee of 214 km. The number of photometers on the second flight was increased to six. N₂ vibrational temperature was measured by observing four N₂⁺ first negative transitions, N₂ kinetic temperature by means of N₂⁺ first negative (4278 Angstroms) rotational structure, and O₂ molecular density by O₂⁺ first negative emission at 5590 Angstroms. Electron beam current was increased from 6 to 25 ma on the second payload and an in flight calibration lamp was included in an effort to provide more accurate vibrational temperatures. All instrumentation functioned successfully confirming the upper limit of vibrational temperature established in the first flight and similarly measuring molecular densities somewhat less than the 1965 COSPAR model atmosphere.

A number of the minor constituents of the upper atmosphere emit radiation in the infrared portion of the electromagnetic spectrum when excited. Measurements of these emissions, consequently, provide information concerning the identity, number and state of excitation of the emitting molecules. Knowledge of these quantities improves understanding of the chemistry of the upper atmosphere.

An instrument to measure these inherently weak infrared emissions from the airglow and aurorae has been developed under Air Force contract by Utah State University. The heart of this instrument is a cryogenically cooled circular interference filter which is rotated continuously to provide spectral scans through the desired spectral region (hence, the circular variable filter spectrometer, CVF). One of these instruments was launched from the Churchill Research Range, Manitoba, Canada, on March 23, 1971. The rocket vehicle was a Black Brant VC which achieved an apogee of 365 km; the rocket was launched into a sky that was very active with class IBC III aurora for some time prior to launch.

CALIBRATION FACILITY: A liquid nitrogen cooled collimator was constructed as an in house project and installed in a vacuum chamber. A variable aperture blackbody radiator that can be operated at temperatures from minus 195 to plus 600 degrees C serves as a collimated source. This facility has been used to determine absolute radiometer responsivity which is used to convert the read-out voltages of a radiometer to radiance values. A liquid nitrogen cooled chamber will be installed at the exit slit of a monochromator so that the radiometer spectral response can also be determined under cold environment conditions.

THE REMOTE INFERENCE PROBLEM

With the orbiting of the high resolution SIRS spectrometer in May 1970, the remote sensing of atmospheric thermal structure came of age. The instrumental demands are severe, for the deduction of vertical temperature distribution is a second order effect depending on intensity differences between neighboring frequency channels. The analysis, which involves the inversion of an integral transform, presents an even greater problem. Briefly, from a set of six or eight intensity measurements the most likely temperature profile implied by the data must be inferred.

The difficulties in inversion all ultimately stem from the incomplete character of the data and may be grouped in three categories:

- 1) Given a finite number of observations, it is possible to find an infinite manifold of temperature profiles matching the observations, and thus formally constituting solutions to the problem. The majority of these solutions are nonsensical physically, with negative temperatures and oscillat-

ing lapse-rates. The problem therefore becomes one not of finding a solution, but rather choosing one from many. Thus, the fragmentary data character with its consequent non-uniqueness forces us to introduce extraneous, external, and subjective constraints to specify and achieve uniqueness.

2) The accessible information is rendered even less valuable when we note that the observations are largely redundant. The sampling of a neighboring channel yields little that is new. The differencing of near equal data sets is a notorious source of calculational instability.

3) As if the fragmentary and redundant character were not enough, the data are beset with inherent, irreducible noise error. The majority of inversion methods seek to cope with noise by suppressing it through some *a priori* smoothing algorithm. The risk involved is that the noise discard may contain hidden information on the thermal structure.

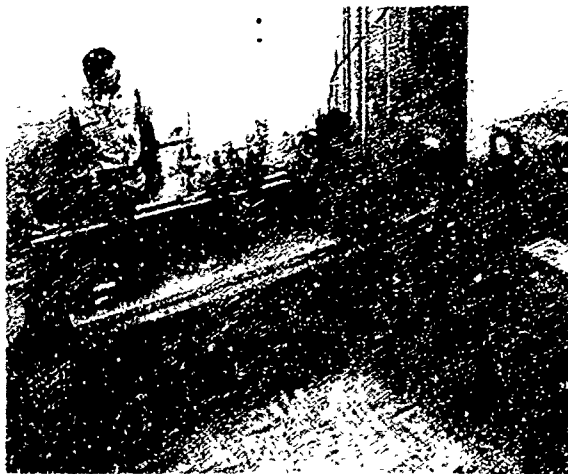
Thus, two procedures are resorted to: subjective information is added to supplement the fragmentary data to assure uniqueness, and information is subtracted by discarding intensity irregularities due presumably to noise. The danger is that although these procedures lead to an impressively smooth profile, it becomes well nigh impossible to ferret out those atmospheric features genuinely inferred by inversion from those climatological features unwittingly inserted in the processing.

These considerations dictate the approach to the problem. An algorithm is needed which will extract all the thermal information contained in the data and no more. Furthermore, the algorithm should use raw data, noise and all, for input with no resort to smoothing. Finally the method should be objective, neither requiring nor desiring climatological information.

Viewed most broadly, the problem consists in the generation of an interpolation

formula passing through the observed numbers, with a subsequent inversion of the curve to yield the temperature profile. The interpolation curve must be flexible but smooth, for the inverse operation grossly distorts structure. Because of its extreme smoothness, the Padé approximant is an attractive candidate for this role. These approximants are used in physics in two capacities: as efficient approximations to complicated functions for digital computers; and to fit resonances, phase changes and other curves exhibiting mild singularities.

The Padé approximant is completely specified by the positions of its poles and their residues. Given $2n$ arbitrarily sensed intensities, an algorithm developed in the Laboratory determines the *unique* Padé approximant of n poles and residues which fits the observations. For noise-free data the poles lie in the negative half-plane of the complex frequency plane. The corresponding temperature profile is represented by a sum of nonlinear exponential functions. Noise betrays its presence by one or



Scientist aligns instruments on test bench for laser-induced damage studies. All important laser pulse parameters are simultaneously measured.

more of the poles shifting to the real frequency axis, precisely indicating the errant channel as well as the percentage error in the channel reading.

Thus, the strength of the algorithm is revealed. Not only is the noise elimination problem facing other algorithms avoided, but the noise in the data is also inverted to determine systematic instrumental error. For a noise-free case (smooth curve), the algorithm correctly inferred the profile:

$$B(\tau) = e^{-3\tau} - 2e^{-4\tau} + e^{-5\tau}$$

For identical measurements except for a 3 percent perturbation in the fifth channel, the inference remains faithful. To a remarkable degree, the algorithm pinpoints quantitatively the culprit channel.

LASER PHYSICS

In the last ten years, laser systems have made possible great advances in military technology. Far greater advances, both foreseen and unforeseen, can be predicted for the future. Laser physics is studied at AFCLR to advance knowledge and basic technology in this vital area. Research in laser-related phenomena is initiated together with new laser applications which show potential for leading to new concept devices. Early exploratory development efforts are carried out when a research project has identified a promising new device concept. Substantial resources are also devoted to problems which have been identified in connection with existing laser systems. Exhaustive study efforts are directed toward understanding and correcting or redesigning these laser systems so that they will reliably fulfill their Air Force mission requirement.

CHEMICAL LASERS: A chemical laser derives all (or a substantial part) of its out-

put energy from a chemical reaction. It is now well known that many exothermic chemical reactions leave their product molecules in excited states. This often leads to inverted populations (i.e., more molecules in some excited state than in some lower lying state), meaning that much of the "heat of reaction" can be taken out as laser radiation. The Air Force interest in chemical lasers is due to the potentially high output power of these devices. For example, the reaction of H₂ and F₂ yielding vibrationally excited HF could produce over one megajoule of laser energy per pound of reactants.

A great deal of research data must be obtained and a great many research problems solved before chemical laser systems can be designed and operated at anywhere near their potential. Data must be obtained about the initial distributions of excited states in product molecules and about the rates at which the excited states are depopulated due to collisions with other species present during the reaction. The reactants must be mixed and the reaction take place uniformly enough to prevent optical distortion; or if the reactants are premixed, the reaction must be uniformly triggered with some comparatively low energy input. Further, the radiation emission properties of the excited state molecules of interest must be determined and correlated with atmospheric propagation phenomena. All these problems, and others, are being carefully studied within the chemical laser program of the Laboratory.

OPTICALLY INDUCED DAMAGE: One of the most serious problems in high peak power laser systems is damage to components caused by the laser radiation itself. Many different kinds of damage have been observed on material surfaces as well as within the bulk material. Conditions under which damage occurs are little known;

inconsistent and contradictory data often appear. Under these conditions, avoiding damage requires laser systems to be designed with excessively large, yet essentially unknown, safety factors.

The program in optically induced damage is aimed at correcting these problems. All of the important parameters relevant to damage phenomena have been identified. Inconsistencies and contradictions in previous work have been explained as resulting from important but uncontrolled experimental parameters.

The physical mechanisms possibly responsible for damage have been theoretically studied to understand and predict damage phenomena caused by them. These predictions are now being compared to experimental results in order to identify the actual mechanism responsible in different wavelength and pulse duration regimes. Understanding of the physical mechanisms responsible for various kinds of damage will lead to knowledge based on material properties, preparation techniques, and operating geometries for optimum laser systems design without damage.

Present activity is concentrated on laser materials, particularly ruby and glass, on nonlinear optical materials and on thin film dielectric coatings such as are used on laser mirrors and beam-splitters.

TUNABLE LASERS: Lasers have had advantages over conventional light sources in many applications because of their coherence, high spatial brightness and high spectral density. A major disadvantage of lasers had been their lack of tunability. A large number of potential laser applications require wavelength tunability, and even in applications requiring a particular fixed wavelength, luck was needed to find an appropriate laser. A number of laser devices which are capable of being tuned over significant wavelength intervals are



Scientist aligns a tunable optical parametric oscillator. From left are alignment laser, monitoring detector, passively Q-switched ruby pump laser, polarizer and parametric oscillator consisting of crystal between two closely spaced mirrors.

currently under extensive investigation. The Laboratory is actively pursuing research and exploratory development into these devices and their applications. In house research is concentrating on dye lasers and nonlinear optical devices, while contractual efforts are investigating spin-flip Raman lasers and semiconductor diode lasers.

A dye laser operates by optical pumping of dye molecules in solution into excited electronic states with high vibration-rotation energy. The vibration-rotation energy is rapidly changed to thermal energy at the solution temperature leaving the excited molecules in low lying vibration-rotation levels of the first excited (singlet) electronic state. This results in a population inversion between these levels and higher vibration-rotation levels of the ground electronic state, leading to laser oscillation between these states. Because of the large density of states and their large linewidth in solution, lasing ordinarily takes place over a very broad spectral

range (several hundred Angstroms). However, this width can be drastically reduced by the use of optical resonators with frequency-selective elements such as diffraction gratings and interferometers. Most of the available laser energy can be retained in the narrow output line due to the very tight coupling of the various energy sublevels within the excited electronic state. Tuning is accomplished by adjustments performed on the optical resonator, such as rotation of a grating or displacement of an interferometer mirror.

NONLINEAR OPTICAL DEVICES: In crystals which lack inversion symmetry, an applied electromagnetic field can generate polarization currents which depend quadratically on the applied field strength. These currents can radiate leading to second harmonic generation, or sum and difference frequency generation, if fields at two frequencies are applied. For a substantial buildup of radiation at the new frequencies, it is necessary to satisfy a condition called phase matching, which ensures that radiation generated in different parts of the crystal will add constructively.

If a tunable laser is available in one part of the frequency spectrum, second-harmonic or sum-frequency generation can be used to obtain higher frequencies and difference-frequency generation can be used to obtain lower frequencies, possibly into the very far infrared.

Closely related to difference frequency generation is optical parametric oscillation. In an optical parametric oscillator a nonlinear crystal in an optical resonator is pumped with a laser field at a frequency ω_p . Starting from thermal noise, there is a buildup of two new frequencies ω_s and $\omega_i = \omega_p - \omega_s$ which are mutually phase-matched for difference frequency generation. If the gain of the buildup exceeds the loss of the resonator, oscillation occurs resulting in a large conversion of energy

from ω_p into ω_s and ω_i . The frequencies ω_s and ω_i can be tuned by varying the index of refraction of the crystal with temperature, angle, or electric changes. This changes the conditions for phase matching.

JOURNAL ARTICLES JULY 1970 - JUNE 1972

BLISS, E. S., CAPT.

Pulse Duration Dependence of Laser Damage Mechanisms
Opto-Elect., Vol. 3 (May 1971)
The Importance of Self-Focusing in a Laser Amplifier with Large Beam Diameter
IEEE J. of Quantum Elect., Vol. 8, No. 2 (February 1972)

CLOUGH, S. A.

The Microwave Spectrum and Rotational Constants for the Ground State of D₂O
J. of Chem. Phys., Vol. 53 (1 October 1970)

DOLAN, C. P.

A Synchronizing Valve for Low Frequency (3-15 Hz) Injection of Gas into a Vacuum System
The Rev. of Sci. Instrm., Vol. 42, No. 8 (August 1971)

ELTERMAN, L.

Relationships Between Vertical Attenuation and Surface Meteorological Range
Appl. Opt., Vol. 9, No. 8 (1 August 1970)

HOPP, F. A.

Self-Induced Transparency in Two-Pass Attenuators and Related Phenomena
Phys. Rev. A, Vol. 2, No. 1 (July 1970)

HOPP, F. A., and LAMB, G. L., JR. (United Aircraft Res. Labs., East Hartford, Conn.), RHODES, C. K., and SCULLY, M. O. (Mass. Inst. of Tech., Cambridge, Mass.)

Some Results on Coherent Radiative Phenomena with Zero-Pi Pulses
Phys. Rev. A (February 1971)

HORDVIK, A., and SCHLOSSBERG, H.

Luminescence from LiNbO₃
Appl. Phys. Lett., Vol. 20, No. 5 (1 March 1972)

- HORDVIK, A., SCHLOSSBERG, H., and STICKLEY, C. M.
Spontaneous Parametric Scattering of Light in Proustite
Appl. Phys. Lett. (15 May 1971)
- HOWARD, J. N. (Off. of Ch. Sci.), and GARING, J. S.
Atmospheric Optics and Radiative Transfer
Trans. of Am. Geophys. Un., Vol. 52 (June 1971)
- HUFFMAN, P. J.
Polarization of Light Scattered by Ice Crystals
J. of Atm. Sci., Vol. 27, No. 8 (November 1970)
Formation and Growth of Ice Fog Particles at Fairbanks, Alaska
J. of Geophys. Res., Vol. 76, No. 3 (January 1971)
- HUSHFAR, F., ROGERS, J. W., and STAIR, A. T., JR.
Infrared Chemiluminescence of the Reaction
 $N + O_2 \rightarrow NO + O$
J. of Appl. Opt., Vol. 10 (August 1971)
- IZATT, J. R.
Spectral Anomalies Due to Inhomogeneous Optical Pumping in Ruby Laser
J. of Appl. Phys., Vol. 41, No. 11 (October 1970)
- LOEWENSTEIN, E. V.
Rapid-Scan Fourier Spectroscopy
Book, Far Infr. Spectros., John Wiley & Sons, N. Y. (November 1970)
- LOEWENSTEIN, E. V., and SMITH, D. R.
Optical Constants of Far Infrared Materials I: Analysis of Channeled Spectra and Application to Mylar
Appl. Opt., Vol. 10, No. 3 (March 1971)
Far Infrared
Am. Inst. of Phys. Handbook, Third Edition (1972)
- MC CLATCHIE, R. A.
Atmospheric and Surface Properties from Spectral Radiance Observations in the 4.3 Micron Region
J. of Atm. Sci., Vol. 27, No. 5 (August 1970)
- MILAM, D.
Simple, Linear Cavity, TEM₀₀ Mode, Mode-Locked Ruby Laser
J. of Quantum Elect., Vol. QE-7 (June 1971)
- MURPHY, R. E.
The Infrared Emission of OH in the Fundamental and First Overtone Bands
J. of Chem. Phys., Vol. 54 (1 June 1971)
- OSGOOD, R. M., JR., JAVAN, A. (Mass. Inst. of Tech., Cambridge, Mass.), and SACKETT, P. B.
Measurement of Vibration - Vibration Energy Transfer Time in HF Gas
Appl. Phys. Lett., Vol. 20, No. 12 (15 June 1972)
- PENDLETON, W. R. (Univ. of Utah), and O'NEIL, R. R.
Departure of N₂⁺(B²Σ⁺, V = 2 and 3)
Vibrational Populations from Franck-Condon Predictions in the Case of Energetic e - N₂(X¹Σ_g⁺, v = 0) Collisions
J. of Chem. Phys., Vol. 56 (15 June 1972)
- PICARD, R. H., and WILLIS, C. R. (Boston Univ., Boston, Mass.)
Description of Superradiant Damping by Multimode Maxwell-Bloch Equations
Phys. Lett. A, Vol. 37A (6 December 1971)
- PRICE, S. D.
Rocketborne Infrared Measurements at 12 μm
Bull. Am. Astronom. Soc., Vol. 3, No. 1 (1971)
- ROTHMAN, L. S., and CLOUGH, S. A.
Expressions for the Expanded Inverse Moment of Inertia Tensor for the Darling-Dennison Hamiltonian
J. of Chem. Phys., Vol. 54 (1 April 1971)
Perturbation Theory of Product Hamiltonians Through Fourth Order
J. of Chem. Phys., Vol. 55 (15 July 1971)
- VOLZ, F. E.
On Atmospheric Turbidity After the Agung Eruption of 1968, and Size Distribution of the Volcanic Dust
J. of Geophys. Res., Vol. 75, No. 9 (September 1970)
Spectral Skylight and Solar Radiance Measurements in the Caribbean: Maritime Aerosols and Sahara Dust
J. of Atm. Sci., Vol. 27, No. 7 (October 1970)
Synoptic Atmospheric Layers from Balloon-borne Horizon Photographs
Bull. of Am. Met. Soc., Vol. 52, No. 10 (October 1971)
Infrared Absorption by Atmospheric Aerosol Substances
J. of Geophys. Res., Vol. 77, No. 6 (February 1972)
The Infrared Refractive Index of Atmospheric Aerosol Substances
Appl. Opt., Vol. 11, No. 4 (April 1972)
- VOLZ, F. E., and SHEEHAN, L. J., MAJ.
Skylight and Aerosol in Thailand During the Dry Winter Season
Appl. Opt., Vol. 10, No. 2 (February 1971)

WALKER, R. G.
Observation of the 12 μm Background Flux
 Bull. of Am. Astronom. Soc., Vol. 3, No. 1 (1971)

WALKER, R. G., and PRICE, S. D.
*Rocketborne Celestial Measurements at
 12 μm*
 Bull. of Am. Astronom. Soc., Vol. 2, No. 4 (1970)

PAPERS PRESENTED AT MEETINGS
JULY 1970 - JUNE 1972

BLISS, E. S., CAPT.
*Damage Threshold Studies in Laser
 Crystals*
 1970 6th Intl. Quantum Elect. Conf., Kyoto, Jap.
 (7-10 September 1970)
*The Importance of Self-Focusing in a
 Laser Amplifier with Large Beam
 Diameter*
 1971 IEEE Conf. on Laser Eng. and Appl., Wash.,
 D. C. (2-4 June 1971)

BLISS, E. S., CAPT., and MILAM, D.
*Laser Induced Damage to Mirrors and
 Surfaces at Two Pulse Durations*
 1972 ASTM/NBS Laser Dam. Symp., Boulder, Colo.
 (14-15 June 1972)

ECKERG, E. E.
*The Glass High-Gain Light Integrating
 Sphere for Laboratory Investigations of
 Chemiluminescence*
 1971 Symp. of the Am. Sci. Glassblowers Soc.,
 Milwaukee, Wis. (30 June-2 July 1971)

ELTERMAN, L.
*The Role of the Aerosol Scale Height Family
 in Vertical Attenuation*
 3rd Conf. on Laser Atm. Prob., Univ. of W. Indies,
 Jam. (9-12 September 1970)

FETTERMAN, H. R. (MIT Lincoln Lab., Lexington,
 Mass.), SCHLOSSBERG, H. R., and WALDMAN, J.,
 PARKER, D. C., TANNENWALD, P. E. (MIT Lincoln
 Lab.)
*Submillimeter Lasers Optically Pumped
 Off Resonance*
 7th Intl. Quantum Elect. Conf., Montreal, Can. (8-11
 May 1972)

GRIESEN, F. W., and VOIZ, F. E.
*High-Altitude Measurements of the Optical
 Scattering Properties of the Atmosphere*

1972 Spring Mtg. of the Opt. Soc. of Am.,
 N. Y., N. Y. (11-14 April 1972)

GRIENHEISER, H. P., GOLDHAR, J., KURNIT, N. A.,
 JAVAN, A. (Mass. Inst. of Tech., Cambridge, Mass.),
 and SCHLOSSBERG, H. R.
*Experimental Investigation of the
 Transparency of a Resonant Medium
 to Zero-Degree Optical Pulses*
 7th Intl. Quantum Elect. Conf., Montreal, Can. (8-11
 May 1972) Am. Phys. Soc. Mtg., Albuquerque, N. M.
 (5-7 June 1972)
*Observation of Zero Degree Pulse
 Propagation in a Resonant Medium*
 3rd Rochester Conf. on Coherence and Quantum
 Opt., Rochester, N. Y. (21-23 June 1972)

HORDVIK, A.
*An Experimental Investigation of Thermal
 Distortion in Infrared Window Materials*
 Conf. on High Power Laser Window Mats., Bedford,
 Mass. (27-28 October 1972)

HORDVIK, A., and LIPSON, H., SKOLNIK, L. (Sol. State
 Sci. Lab.)
*Optical Evaluation of CO₂ Laser Window
 Materials at AFCRL*
 5th Class. Conf. on Las. Tech., U. S. Nav. Postgrad.
 Sch., Monterey, Calif. (25-27 April 1972)

HORDVIK, A., and SCHLOSSBERG, H.
Luminescence from LiNbO₃
 7th Intl. Quantum Elect. Conf., Montreal, Can. (8-11
 May 1972)

HORDVIK, A., SCHLOSSBERG, H., STICKLEY, C. M., and
 O'CONNOR, J. (MIT Lincoln Lab., Lexington, Mass.)
*Spontaneous Parametric Scattering of
 Light in Proustite (Ag₃PS₄)*
 6th Intl. Quantum Elect. Conf., Kyoto, Jap. (7-10
 September 1970)

HUPPI, E. R., STAIR, A. T., JR., and WALTER, T.
*Aircraft Measurements of Infrared
 Aurorae and Airglow*
 DASA High Alt. Nuc. Eff. Symp., Stanford Res.
 Inst., Menlo Pk., Calif. (10-12 August 1971)

KING, J. I. F.
*Remote Temperature Inference and
 Diagnosis of Instrumental Error Using Padé
 Inversion*
 Intl. Rad. Symp., Sendai, Jap. (26 May-2 June 1972)

MC CLATCHY, R. A.
Radiative Modeling of the Atmosphere
 1971 AFSC Sci. and Eng. Symp., Dayton, Oh. (5-7
 October 1971)

- Transmittance Functions for Satellite Temperature Sounding*
Intl. Rad. Symp., Sendai, Jap. (26 May-2 June 1972)
- MILAM, D.
Simple, Linear Cavity, TEM₀₀ Mode, Mode-Locked Ruby Laser
1971 IEEE Conf. on Laser Eng. and Appl., Wash., D. C. (2-4 June 1971)
- MURPHY, R. E., ROGERS, J. W., and BRUCE, M. H.
Energy Partition in the N + NO → N₂ + O Reaction*
DASA High Alt. Nuc. Eff. Symp., Stanford Res. Inst., Menlo Pk., Calif. (10-12 August 1971)
- O'NEIL, R. R.
Rocket Measurement of N₂ Vibrational Temperature
14th Ann. COSPAR Mtg., Seattle, Wash. (17 June-2 July 1971)
- O'NEIL, R. R., HART, A. M., STAIR, A. T., JR., and PENDLETON, W. R. (Utah State Univ.)
Rocket Measurement of N₂ Vibrational Temperature
DASA High Alt. Nuc. Eff. Symp., Stanford Res. Inst., Menlo Pk., Calif. (10-12 August 1971)
- O'NEIL, R. R., and PENDLETON, W. R. (Utah State Univ.)
Rocket Borne Electron Beam Measurement of N₂ Vibrational Temperature and N₂ and O₂ Molecular Density
15th COSPAR Mtg., Madrid, Sp. (10-24 May 1972)
- PICARD, R. H., and WILLIS, C. R. (Boston Univ., Mass.)
Master Equations for Superradiance and Coherent Propagation
Am. Phys. Soc. Mtg., Mass. Inst. of Tech., Cambridge, Mass. (27-29 December 1971)
Fluctuations in Coherent Propagation of Radiation in Resonant Media
3rd Rochester Conf. on Coherence and Quantum Opt., Rochester, N. Y. (21-23 June 1972)
- PRICE, S. D.
Rocketborne Infrared Measurements at 12 μm, Results of Flight of MAP II
133rd Mtg. of Am. Astronom. Soc., Tampa, Fla. (6-9 December 1970)
- SACKETT, P. B., and YARDLEY, J. T. (Univ. of Ill., Champaign, Ill.)
Dynamics of NO_x Electronic States Excited by a Tunable Dye Laser
27th Symp. on Molec. Structure and Spectros., Columbus, Oh. (12-16 June 1972)
- SAKAI, H., PRITCHARD, J., and VANASSE, G.
Infrared Interferometer for High Resolution Fourier Spectroscopy
1972 Spring Mtg. of the Opt. Soc. of Am., N. Y., N. Y. (11-14 April 1972)
- SANDFORD, B. P.
Optical Airborne Measurements on 2-3 November by AFCRL
COSPAR Symp. on Nov. 1969 Solar Particle Event, Boston Coll., Chestnut Hill, Mass. (16-18 June 1971)
- SANDFORD, B. P., and BURNS, J. (Gen. Elec. Co., Valley Forge, Pa.)
Infrared Measurements of Apollo 14 and 15 ARPA Plume Phys. Mtg., TRW Sys., Inc., Redondo Beach, Calif. (28 February-1 March 1972)
- SCHLOSSBERG, H.
Applications of Lasers to Basic Science
1971 IDA JASON Laser Sum. Study, La Jolla, Calif.
- SELBY, J. E. A.
Drop Size Measurements in Low Level Stratus
NCAR Part. Model. Wkshp., Boulder, Colo. (21 August 1970)
A Rapid Method for Predicting Atmospheric Transmittance at Low Resolution
Spring Mtg. of the Opt. Soc. of Am., Tucson, Ariz. (5-8 April 1971)
- STAIR, A. T., JR.
Infrared Chemiluminescence
Natl. Bur. of Stds., Gaithersburg, Md. (21 October 1971)
- STICKLEY, C. M.
The Impact of Lasers and Electro-Optics on the Federal Government
EASCON Mtg., Wash., D. C. (26 October 1970)
- VANASSE, G. A.
Multiplex Techniques in Spectroscopy
1972 Spring Mtg. of the Opt. Soc. of Am., N. Y., N. Y. (11-14 April 1972)
- VANASSE, G. A., and DESPAIN, A. M. (Utah State Univ.)
Walsh Functions in Grille Spectroscopy
Walsh Func. Symp., Catholic Univ., Wash., D. C. (27-29 March 1972)
- VOLZ, F. E.
Stratospheric Dust—Twilights and Their Colors

3rd Conf. on Laser Atm. Probing, Univ. of W. Indies, Jam. (9-12 September 1970)
The Optical Constants of Natural Aerosol Substance from 2.5 to 40 μm
 1972 Spring Mtg. of the Opt. Soc. of Am., N. Y., N. Y. (11-14 April 1972)
Return of Normal Stratospheric Turbidity and a New Short Dust Event During October 1971 and
The Complex Index of Refraction of Aerosol from 0.2 to 40 μm
 Intl. Rad. Symp., Sendai, Jap. (26 May-2 June 1972)

WALKER, R. G.
Observations of the 12 μm Background Flux
 133rd Mtg. of Am. Astronom. Soc., Tampa, Fla. (6-9 December 1970)

WESTON, E. B.
The Main Sequence of the H-R Diagram: Its Significance and Role in Stellar Evolution
 1972 Sum. Sci. Mtg. of the Astronom. Soc. of the Pacific, Univ. of Calif., Santa Cruz, Calif. (26-29 June 1972)

WESTON, E. B., and WARES, G. W. (Space Phys. Lab.)
Some Effects of Molecules in Solar Phenomena
 1972 Am. Astronom. Soc. Sol. Phys. Div. Mtg., Univ. of Md., Coll. Pk., Md. (4-6 April 1972)

TECHNICAL REPORTS JULY 1970 - JUNE 1972

BIRD, R. E.
Intensity of Scattered Light from Large Diameter Infinite Ice Cylinders in the Normal Plane
 AFCRL-72-0337 (8 June 1972)

BLISS, E. S., CAPT., and MILAM, D.
Laser Damage Study with Subnanosecond Pulses (Technical Report No. 1, Period 8 April 1969 to 31 December 1971)
 AFCRL-72-0233 (31 March 1972)

GIBSON, F. W., and DEARBORN, F. K.
Atmospheric Optics Measurements with a Balloon-Borne Nephelometer
 AFCRL-71-0455 (19 August 1971)

HOFFMAN, J., JR.
A Computer-Aided Design for an Interferometer Mirror Drive System

Aspen Int'l. Conf. on Fourier Spectros., 1970,
 AFCRL-71-0019 (5 January 1971)

LOEWENSTEIN, E. V.
Fourier Spectroscopy: An Introduction
 Aspen Int'l. Conf. on Fourier Spectros., 1970,
 AFCRL-71-0019 (5 January 1971)

MC CLATCHY, R. A.
Atmospheric Attenuation of CO Laser Radiation
 AFCRL-71-0370 (1 July 1971)

MC CLATCHY, R. A., FENN, R. W., SELBY, J. E. A., VOLZ, F. E., and GARING, J. S.
Optical Properties of the Atmosphere
 AFCRL-70-0527 (22 September 1970)
Optical Properties of the Atmosphere (Revised)
 AFCRL-71-0279 (10 May 1971)

MC CLATCHY, R. A., and SELBY, J. E. A.
Atmospheric Attenuation of HF and DF Laser Radiation
 AFCRL-72-0312 (23 May 1972)

MILAM, D., BRADBURY, R. A., and BLISS, E. S., CAPT.
Simple Linear-Cavity TEM₀₀-Mode Mode-Locked Ruby Laser
 AFCRL-72-0040 (3 December 1971)

MURPHY, R., and SAKAI, H.
Application of the Fourier Spectroscopy Technique to the Study of Relaxation Phenomena
 Aspen Int'l. Conf. on Fourier Spectros., 1970,
 AFCRL-71-0019 (5 January 1971)

PRICE, S. D.
Stellar Standards at 10 Microns
 AFCRL-70-0402 (13 July 1970)

SAKAI, H.
Consideration of the Signal-to-Noise Ratio in Fourier Spectroscopy
 Aspen Int'l. Conf. on Fourier Spectros., 1970,
 AFCRL-71-0019 (5 January 1971)

SMITH, D. R.
Optical Constants of Low Index Materials from Far Infrared Channeled Spectra
 Aspen Int'l. Conf. on Fourier Spectros., 1970,
 AFCRL-71-0019 (5 January 1971)

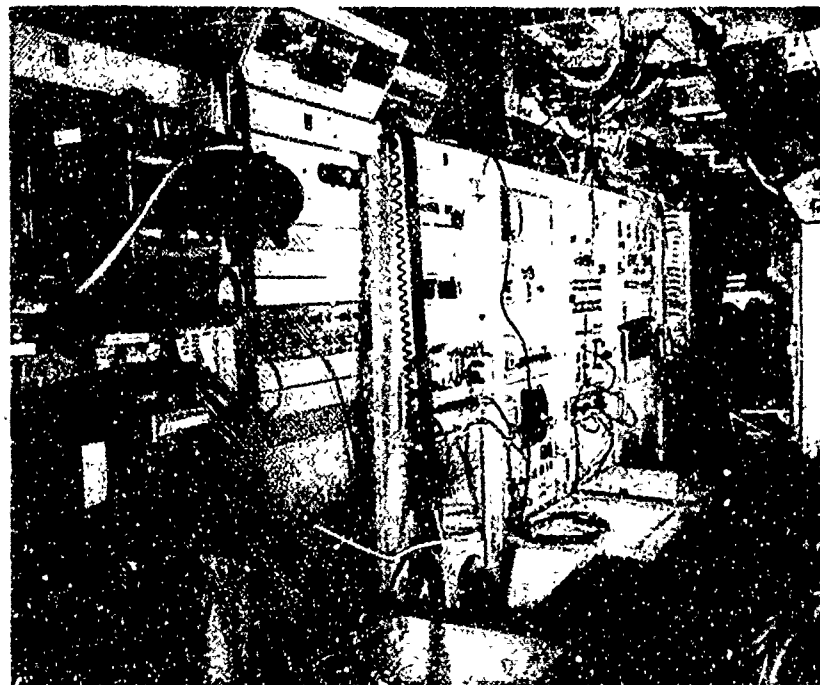
STAIR, A. T., JR.
Fourier Spectroscopy at AFCRL
 Aspen Int'l. Conf. on Fourier Spectros., 1970,
 AFCRL-71-0019 (5 January 1971)

VANASSE, G. A., STAIB, A. T., JR., and BAKER, D. J.
(Utah State Univ.),
Editors

*Aspen International Conference on Fourier
Spectroscopy, 1970*
AFCRL-71-0019 (6 January 1971)



AFCRL's NKC-135 flying ionospheric laboratory.



Part of the interior of the NKC-135 flying ionospheric laboratory.

X Ionospheric Physics Laboratory



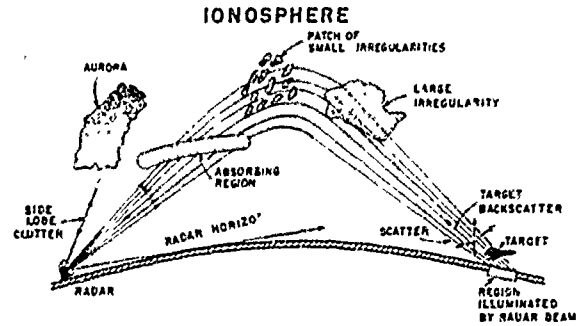
The term "ionosphere" is usually applied to that portion of the earth's atmosphere, roughly from 50 to several thousand kilometers above the surface, in which a small but significant number of the constituent particles are electrically charged (ionized). Except for a minor contribution from cosmic radiation and inter-particle collisions, these ionizations result from solar ultraviolet and soft X-radiation and from energetic solar particles, particularly those emitted during solar disturbances. Although the ions (including free electrons as well as positive and negative ions) represent a very small fraction of the total gas population, they essentially control the propagation of electromagnetic waves.

Air Force interest in the ionosphere stems from the limitations which its role as a transmission medium imposes on communication, navigation, and surveillance and detection systems. Characteristics of the ionosphere largely determine the quality of electromagnetic wave propagation, and ionospheric disturbances can have effects ranging from signal degradation to total blackout. The Ionospheric Physics Laboratory is investigating the properties, characteristics, behavior, and variations of the ionosphere (both quiet and disturbed), their causes, effects, and relationship to other observable phenomena. Important ultimate goals of the investigation are 1) the production of ionospheric models which specify parameters affecting propagation and 2) the forecasting of major ionospheric disturbances and their effects. Achievement of these goals will furnish powerful tools for the planning and design of future Air Force systems as well as for

the selection of optimum operational procedures for existing systems.

In a static, homogeneous ionosphere, interaction between the ions and a propagated signal would cause foreseeable and calculable changes in the latter—such as a decrease in signal strength as a result of energy absorption, an increase in travel time of the signal, or (in the earth's magnetic field) a change in polarization of the wave. Unfortunately, waves propagating in the ionosphere encounter both gradual and abrupt variations in ion density. Moreover, even in the quiet or undisturbed ionosphere, ion and electron densities are continuously varying as a result of charged particle drift, thermal motion, and the constantly shifting equilibrium among the various processes of ion formation and removal.

Waves traveling obliquely through a region of varying density are refracted, the amount of refraction depending not only on the electron density but also on the frequency of the waves and the angle at which they enter the region. For certain combinations of these factors the wave may actually be reflected. Both the ionospheric sounder—one of the oldest and most useful methods of probing the ionosphere—and over-the-horizon (OTH) systems, whose range of operation is much greater than that of the horizon-limited or line-of-sight systems, utilize the effects of vertical density gradients. On the negative side, these same effects are responsible for the skip-distance phenomenon, which can create blind areas in a transmitter's coverage. Horizontal density gradients must also be considered and they produce only negative consequences. By deviating a wave from a great-circle path they can cause serious errors in timing and navigation systems, or in target location by detection systems. Density inhomogeneities are also responsible for multi-path propagation. Because the various paths between the transmitter and target have different



A radar signal may be degraded by having energy reflected back into a side lobe from the aurora, may be partly absorbed as it traverses the ionosphere, and may be irregularly refracted either by a large irregularity or patches of small irregularities in electron density.

lengths, a single target produces multiple echoes, thus distorting or falsifying the picture on the radar screen. Reflections from ionized regions can also present false targets, or obscure the real target in the welter of echoes known as clutter. Variations such as these are, as yet, only partially and imperfectly predictable, usually on either a statistical or a very short-time basis.

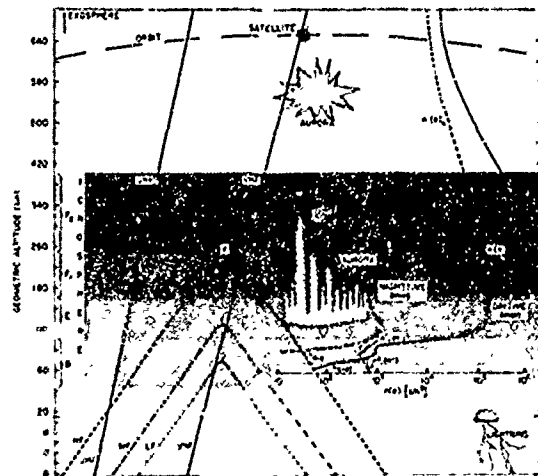
The most severe ionospheric effects are those which occur when abnormal events on the sun produce large increases in both the radiation and the corpuscular stream entering the ionosphere. Prediction of the transmission properties of the ionosphere under these varying conditions requires increased knowledge and better understanding of ionospheric variables, their effects on propagation and systems operation, their causes, and their correlation with (and possible prediction from) other observable phenomena.

Although, in general, the ionization density increases with altitude up to a maximum at approximately 300 km, the gradient (rate of change) is not uniform. Early workers in the field observed that waves were reflected from different heights and attributed the effect to the existence of

reflecting layers of peak electron density. The term is still used even though later work showed that some reflections occur not at a level where the electron density peaks, but where the density gradient has a minimum. The layers are considered to be embedded in somewhat diffuse regions, historically designated in order of increasing height, D, E, F₁ and F₂. Certain salient characteristics are relatively consistent within a region and significantly different in the other regions. The regional characteristic of most vital interest to Air Force systems planners and operators is the extent to which a given frequency band is transmitted, refracted/reflected or absorbed in passing through a region. Of equal concern is the extent to which this characteristic will be affected by ionospheric disturbances. These disturbances are almost always associated with some unusual solar activity, and may manifest themselves in relatively limited locales (e.g. Polar Cap Absorption (PCA) events) or on a world-wide or large area basis. PCAs are one of the phenomena studied in the Arctic research program. The two most important large-area events are geomagnetic storms and sudden ionospheric disturbances (SID's). Geomagnetic storms are perturbations of the earth's magnetic field which far exceed the normal range. Many of the large storms begin suddenly and simultaneously over the entire earth, and are believed to be caused by the impact of ionized gas from the sun on the earth's field. Duration of the storms may range from hours to days. SID's, on the other hand, occur only on the sunlit part of the earth following solar flares and are attributed to solar X-ray emission. They affect chiefly the lowest part of the ionosphere and generally last from 15 to 90 minutes.

The D region of the ionosphere, which normally extends from about 50 to 90 km above the earth, has the lowest electron density. Ionization in this region varies

with the solar zenith angle and the region almost disappears at night. Very low and low frequency (VLF and LF) waves are reflected by this region, medium frequency (MF) waves are absorbed and higher frequency waves pass through with partial absorption. During an SID, the lower boundary of the D region may be lowered and the ionization drastically increased, with consequent deterioration or improvement of propagation of various frequencies. At VLF the increased ionization provides better reflection of the waves, including the noise signals generated by atmospherics, causing SEA (sudden enhancement of atmospherics). The lowering of the reflection height is responsible for the SPA (sudden phase anomalies) or phase advancement in VLF waves transmitted. The increased ionization causes increased absorption of higher frequencies as they traverse the D region, commonly noted in SCNA (sudden cosmic noise absorption) and SWF's (short-wave fadeouts). The former are sudden drops in the normally steady level of noise power from cosmic sources as recorded, for example, on riometers.



This chart of the ionospheric regions includes electron density profiles and approximate reflection heights for various frequency ranges.

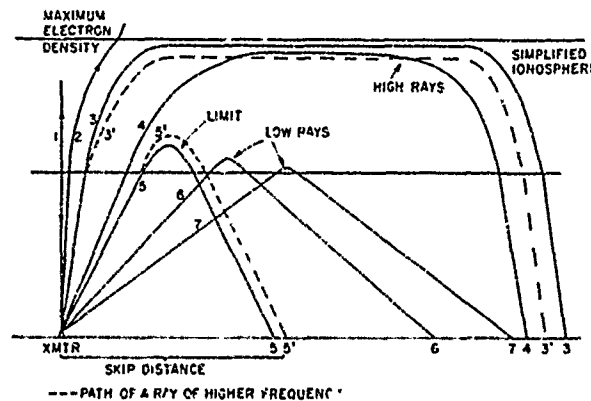
eters (Relative Ionospheric Opacity Meters). SWF's are blackouts, usually sudden and brief, of high frequency transmissions reflected in the E and F regions. Though usually only a nuisance, SWF's can be a serious problem when high reliability circuits are required.

The E region, which extends from 90 to 160 km altitude and peaks at about 110 km, is the transmitting medium for daytime propagation of HF waves up to about 1000 miles and for nighttime propagation of MF waves beyond 100 miles. Like the D region, it is chiefly ionized by ultraviolet and soft X-radiation and the ionization density is dependent on the solar elevation angle. The daytime ionization level is about an order of magnitude greater than that in the D region. The ionization level is substantially lower at night, although the E region does not disappear with the onset of darkness. Characteristic of the region is the frequent occurrence of transient irregular cloudlike patches of very high ionization known as sporadic E (E_s). E_s occurs chiefly at night in the auroral regions and in the daytime near the equator, with little seasonal variation in either locale. In the mid-latitudes it tends to occur more frequently during the local summer and in the daytime. As E_s can be either thick and opaque, effectively blanketing the higher ionospheric regions, or thin and patchy with gaps permitting penetration of waves, the effect on propagation is difficult to predict.

Also characteristic of the E region are the large electric currents which circulate horizontally above the earth's surface and cause periodic variations in the earth's magnetic field. These currents, as yet little understood, are largest in daytime, in summer and at periods of sunspot maxima. They are strongly enhanced in a narrow band along the geomagnetic equator, where they produce the "equatorial electrojet." A perhaps complementary "auroral electrojet" is sometimes formed during

periods of magnetic disturbance when additional currents are superposed on the normal currents, radically altering some of their characteristics. The effect of these currents on propagation and factors affecting it still await detailed investigation.

The ionization level is highest in the uppermost or F region, which during the day consists of the F_1 and F_2 regions. F_1 , at a height of 160-250 km, is more pronounced in summer, during ionospheric storms, and during periods of high sunspot activity. It occasionally reflects HF waves, but most waves which traverse the E region also pass through the F_1 region, with some additional absorption, to be reflected by the F_2 region. Although both the height and the ionization density of the F_2 region vary with daylight, season and sunspot cycle, it normally occurs at 250-400 km and is the principal reflection stratum for HF waves. The ionization is not strongly dependent on solar elevation angle, but the level decreases by about an order of magnitude at night, when the F_1 and F_2 layers



Effect of the angle of incidence on the path of a ray of fixed frequency. Receivers beyond the skip range will receive both high and low rays. The dashed lines show, for two angles of incidence, the path of rays of a higher frequency. As the frequency increases, the reflection height increases for the low ray, and decreases for the high ray. At the MUF for a given configuration and ionosphere, the high and low rays merge into a single ray.

merge at a height of approximately 300 km.

Patches of very high ionization also exist in the F region and are currently being studied by several groups at AFCRL. First detected by the greatly increased lengths of some pulse echoes reflected by the patches (hence the designation F_s , or "spread F"), the F-layer irregularities have subsequently been found to cause such propagation effects as scintillation of signals from satellites and radio stars, auroral backscatter and severe flutter-fading on some voice communication channels (at about 50 MHz).

Even under ideal conditions, ionospheric stratification would impose limitations on the propagation of electromagnetic waves. A vertical wave, i.e. one incident at zero degrees, is not bent but penetrates successive strata until it is reflected back to the source from some height which is determined by the frequency of the wave and the ionization density. Waves of low frequency are reflected at lower heights, and those of higher frequency, from higher altitudes (unless the frequency is high enough to penetrate the entire ionosphere). Ionosondes make use of this effect in monitoring the ionosphere. Short pulses are beamed vertically upward by a transmitter and, after reflection, are picked up by an adjacent receiver. Transmitter and receiver are slowly swept over a range of frequencies and the reflection height for each frequency is determined from the round-trip travel time of the pulse. A plot called an ionogram, of reflection height versus frequency, is used to derive a profile of the ionosphere at the site and to determine, for example, the E- or F-layer critical frequency (the frequency below which reflection occurs and above which radio waves penetrate the layer).

For angles of incidence somewhat greater than zero, the wave suffers some bending but may still traverse the layer. As the obliquity increases, however, an angle is

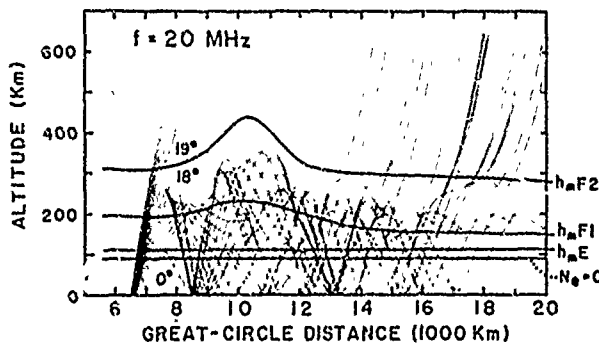
reached at which the wave is reflected back to earth at some point distant from the transmitter. As the angle of incidence continues to increase, this "return point" rapidly approaches the transmitter, reaches a minimum, then recedes again. The minimum distance between transmitter and return point is the "skip distance" for the frequency under consideration and the ionospheric conditions prevailing. It is the shortest range which the signal from the transmitter can reach by ionospheric refraction alone. It also marks the limiting, or merging, path of the so-called "high" and "low" rays. For the low rays, higher frequencies are reflected from higher levels and therefore have longer skip distances. Thus, for a given transmitter-receiver link, there is an upper limit to the frequency which can be used for reliable coverage, at any particular time. This is the MUF (maximum usable frequency) for the sites involved and is usually predictable, at least on a statistical basis. For a given layer, the MUF is related to the critical frequency f_c by the relation.

$$\text{MUF} = kf_c \sec \phi$$

where ϕ is the angle of incidence and k is a factor compensating for the earth's curvature.

The LUF (lowest useful frequency) limit for a transmitter-receiver link is less clear cut. As the frequency is lowered, the signal is increasingly absorbed and the level of background noise power increases. As a result, the signal-to-noise level decreases to such an extent that system reliability becomes unacceptable.

As both MUF and LUF are dependent on ionospheric conditions, system operating frequencies must be chosen far enough from the limits to allow reasonable safety margins during foreseeable ionospheric disturbances. In practice, determination of MUF and LUF is complicated by the fact that, instead of the clear-cut single-hop situation discussed here, there may be



Ray pattern in the vertical plane obtained by ray-tracing techniques.

multi-hop transmission, reflections from irregularities, diffuse layer boundaries, etc.

The usual scientific method of controlled variation of a single factor and observation of effects is not possible in ionospheric studies; therefore, methods have been developed to exploit models of the ionosphere and simulation of conditions and changes of conditions in the ionosphere.

One approach to simulation is the ray-tracing process. This is a method of determining the actual propagation path (energy flow) of an electromagnetic wave through a variable medium by computer solutions to the wave equation, with input data consisting of electron density profiles. The density may, in general, vary in all three dimensions. A ray pattern presents a "snapshot" view of the distribution in space of the rays emitted by a transmitter under a given set of conditions. By varying the input data, ionospheric changes can be simulated and a new pattern drawn. The method is useful in forecasting or assessing the effects of ionospheric changes on the performance of operational systems—e. g., communications systems, backscatter radars, and over-the-horizon detection systems.

Under AFCRL's continuing ray-tracing program, studies have been made of the frequencies which can be propagated under various types of prevailing ionospheric

disturbances, as well as of the distances at which appreciable levels of electromagnetic signals at those frequencies can be detected. At present, under the program, techniques are being developed for simulating very complex electron-density distributions, like those encountered in the Arctic ionosphere. Work is also underway on determining the departures of radio rays from great circle propagation paths and for determining the aspect angle between a ray of interest and the directions of magnetic-field-aligned ionization regions at high latitudes. This aspect angle governs the degree of auroral clutter in backscatter radars and depends, in part, on the refraction undergone by the ray.

Ray tracing, which essentially applies the approximations of geometrical optics to the solution of radio propagation equations, can be used at medium and high frequencies. At low and very low frequencies, however, where the scale size of vertical variations in the ionosphere is less than the wavelength, the method breaks down. For these frequencies a more rigorous and accurate solution of the wave equation must be used—the so-called "full-wave solution."

AFCRL has now developed a computer program for the full-wave solution which includes the effects of ions and employs generalized collision theory. By making a change in the input model ionosphere (for example, varying the electron density profile), the effects of fluctuations on propagation parameters in either a quiet or a disturbed ionosphere can be simulated. The solution of a typical problem (30 kHz frequency) requires five seconds on the CDC 6600 computer.

TOTAL ELECTRON CONTENT (TEC)

Almost all non-communication systems—e. g. radar tracking systems, navigation sys-

tems, position or target location systems—involve the measurement or comparison of signal travel times. While the speed of radio waves in free space is constant, waves propagating through the ionosphere encounter time delays which are proportional to the number of free electrons along the propagation paths. Unless corrected, these time delays can cause serious errors in systems using trans-ionospheric transmissions. For maximum accuracy, a correction factor must be applied which is proportional to the total electron content (TEC) along the path. The direction of polarization of an electromagnetic wave traversing the ionosphere will be rotated by an amount proportional to the integrated product of electron density and the earth's magnetic field (which decreases rapidly with increasing height above the earth's surface). Most TEC determinations are made by using this relationship. Electrons at high altitudes, because of the low magnetic field values there, do not contribute appreciably to the Faraday effect and therefore TEC values so obtained can produce errors of serious, although unknown, magnitude when applied to transmissions from satellites at geostationary or higher altitudes. To overcome this problem researchers at AFCRL and other laboratories are working on methods for directly measuring the ionospheric time delay. Perfection of these techniques is still several years in the future.

AFCRL has recently constructed, from TEC data taken at the Sagamore Hill Radio Observatory, a simple analytic model in which the range error due to the ionosphere is expressed in terms of the critical frequency $f_0 F_2$. This parameter is predicted on a world-wide basis by AWS (Air Weather Service). The TEC model, when used with a value of $f_0 F_2$ predicted by AWS, yields a significant improvement over monthly mean TEC values.

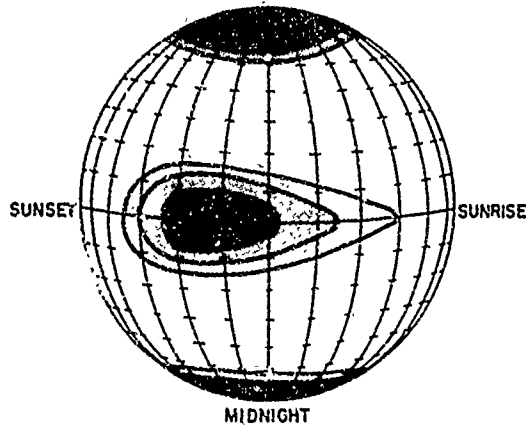
An attempt is being made to extend this first-order TEC (time delay) model to polar

and equatorial regions. To aid in this work, electronic polarimeters have been installed at Huancayo, Peru, at Jamaica, West Indies, at the Goose Bay Ionospheric Observatory, Labrador, and at Thule and Narsarssuaq, Greenland. The polarimeter, which was designed by AFCRL, is used to measure the Faraday effect. It consists essentially of an electrically spun antenna which is able to follow fast changes in polarization and is relatively insensitive to amplitude scintillations.

Comparisons are also being made with other ionospheric parameters to determine whether ground-based ionosondes can give useful estimates of TEC, and whether TEC measurements can be used to determine MUF (maximum usable frequency) along a one-hop F region path.

F-LAYER IRREGULARITIES

Patchy variations in F-layer electron density are now known to be responsible for two widely different phenomena—HF auroral backscatter and scintillation of VHF satellite signals. These F-layer irregularities are small (one to several kilometers) and aligned with their long dimension along the earth's magnetic field. They occur mainly in a belt around the geomagnetic equator and in the sub-auroral to polar latitudes, and are a source of major concern to the Air Force because of the fading and backscatter they produce. The problem is particularly acute for high latitude OTH radars on which the backscatter appears as "clutter" which both presents false targets and masks the true targets. This backscattering effect of the irregularities is highly aspect sensitive, and is most intense when the incident electromagnetic wave is nearly perpendicular to the magnetic field. This incident angle depends on the relative positions of the transmitter and the irregularity and the magnetic field, as well as the ionospheric bending of



Nighttime picture of scintillation occurrence. The density of the hatching is proportional to the occurrence of deep fading.

the wave which varies diurnally and seasonally.

Scintillations produced by F-layer irregularities on UHF-VHF waves passing through them can cause signal levels to increase temporarily to well above normal, or fade down into the background noise, thus creating a serious problem for TAC-SAT and for systems using frequencies in the VHF-UHF range, such as the proposed aircraft (ship)-to-satellite-to-ground communication systems, satellite data transmission systems, and systems for detection of missiles and satellites at altitudes above the F layer. Although scintillations of satellites and radio stars had been observed for years, it was only recently that they were linked to irregularities which, in high latitudes, cause auroral backscatter. In consequence, AFCRL is now re-examining a large collection of satellite and radio star data, originally recorded for other purposes, to determine the occurrence of F-layer irregularities, seasonal and diurnal variations and effects of magnetic storms. These results will then be compared and correlated with auroral backscatter records, to determine whether scintillation observations can be used to predict the occurrence of auroral clutter. In addition, radio star

scintillation observations taken at Sagamore Hill in Hamilton, Mass., are being compared with backscatter data recorded near Rome, N. Y., by RADC and by Polar Fox II in Maine to further determine clutter morphology.

An active data-gathering program is also underway at stations at Sagamore Hill, Thule and Narssarssuaq, Greenland, and, under contract, in Ghana and Peru, on the geomagnetic equator. A station at Goose Bay, Labrador, became operational in November 1971. Detailed studies of amplitude distribution and of the depth and rate of fading as a function of latitude, season, time of day and magnetic conditions will not only lead to better understanding of the global morphology of irregularities but will add to the data bank drawn upon by systems designers concerned with fading effects.

For example, when the ASTRA IV Panel* was faced with the problem of choosing between a VHF system in the 130 MHz range and an L-band system in the 1550 MHz range for use in international aircraft-to-satellite-to-ground communications, AFCRL data from local, equatorial and high latitude stations were used to show, for different latitudes, the percentage of time the systems would be inoperative because of fades. This information contributed to the decision which the Office of Telecommunications Policy made, choosing L-band for aircraft-to-satellite-to-ground communications for commercial aviation.

LONG BASELINE INTERFEROMETER

In addition to the F and E refractive irregularities, waves traveling through the ionosphere may also encounter patchy E-

* Application of Space Techniques Relating to Aviation, an international group acting in an advisory capacity to the International Aeronautical Organization on aircraft satellite communications—frequencies, equipment, etc.

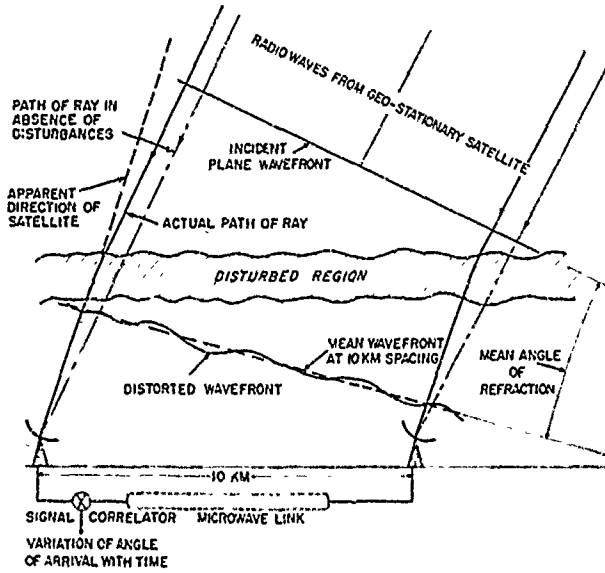


Illustration of the principle of interferometer operation.

region irregularities and moving wavelike variations in electron density, believed to be caused by gravity waves. Without extensive knowledge of these ionospheric refractive irregularities and their effects, the inherent accuracy of existing and proposed systems cannot be realized. The Long Baseline Interferometer is one of several AFCRL programs investigating these irregularities. The interferometer is used to monitor continuously, with high precision, the apparent angular position of a geostationary satellite. Small deviations in the apparent position are due to refractive changes caused by natural or manmade ionospheric perturbations having dimensions of a few hundred kilometers. It is known that the normally occurring wavelike irregularities are markedly different at high and low latitudes and that their occurrence depends in a complicated way on the degree of solar activity. By studying spectral characteristics, as well as diurnal, seasonal and other variations, it is hoped to arrive at an understanding of the physical principles involved and perhaps

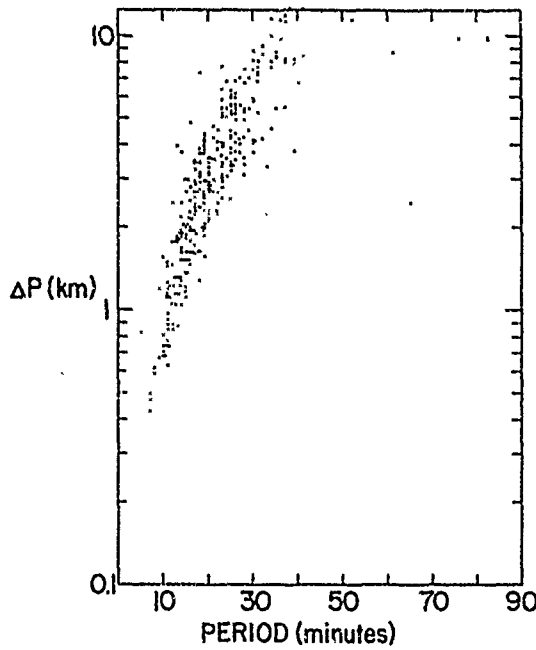
correlate the refractive irregularities with other aspects of solar-geophysical activity.

During 1970 and 1971 the interferometer was operated on 300-meter and 10-km baselines (one station is transportable), and the results have contributed to the first accurate estimates of diurnal and seasonal variations of ionospheric refraction fluctuations on a trans-ionospheric path. The baseline was then extended to 50 km (the longer the baseline, the better the angular resolution), and operations with the extended baseline covered the period September 1971 to March 1972.

The operation of the Long Baseline Interferometer at the Goose Bay Ionospheric Observatory, where geophysical phenomena are markedly different from those under which it has thus far been tested will begin in November 1972 with a 3 km baseline.

TRAVELING IONOSPHERIC DISTURBANCES

In another approach to the investigation of traveling disturbances in the ionosphere, AFCRL has since 1967 monitored the very stable high-frequency signals transmitted by CHU—the time station of the Dominion Observatory at Ottawa, Canada. These signals reach the receivers by reflection from the ionosphere, and any disturbance of the latter, in a vertical direction, shifts the level of reflection. This movement, in turn, causes a slight change in the frequency of the reflected signal—the well known Doppler shift. Wavelike disturbances of the ionosphere are detected by the recurrence of shift patterns. Data from riometer stations and from a network of ionosonde stations are used in conjunction with the Doppler information to study the characteristics of the traveling disturbances, their association with gravity waves, and their correlation with other phenomena—e.g., tropospheric storms, auroral storms, and jet stream fluctuations.



Undulation amplitudes of ionospheric waves (CHU data, 1968).

Doppler data taken in 1968 have been analyzed in a preliminary assessment of wave characteristics. A histogram of wave periods observed for the F region over New England showed that while periods ranged from 5 to 135 minutes, 90 percent fell between 5 and 40 minutes, and slightly over 50 per cent between 10 and 20 minutes. This would tend to corroborate a link with gravity waves, which typically have periods of approximately 20 minutes. When vertical phase path perturbation amplitudes were derived from the Doppler data (with an assumed mean reflection height of 250 km) and plotted against frequency, the larger perturbation amplitudes were found to be generally associated with the longer wave periods. This helps explain the "bunching" of wave periods at the lower end of the scale—small ionospheric perturbations are much more common than large ones.

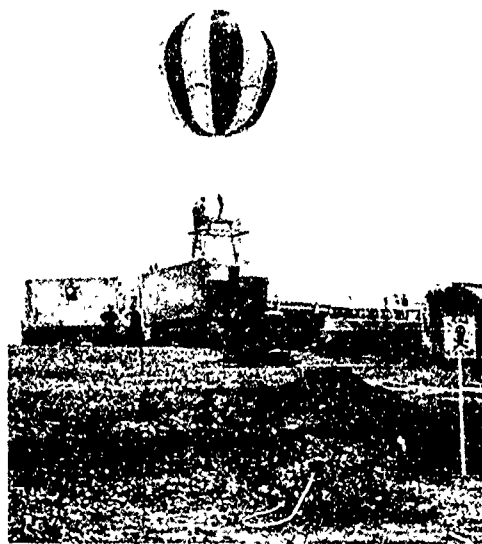
A computer program was set up to study patterns of signal characteristics obtained

by simulating variations in range, Doppler frequency and signal strength. Patterns similar to those so generated were found in the data, indicating a possibility that the simulation program could be used in predicting propagation effects.

IONOSPHERIC WAVEGUIDE

Most of the foregoing discussion has referred to high-frequency and middle-frequency waves for which the ionosphere serves as a transmission medium. At the very low frequency (VLF) end of the radio frequency spectrum, however, it is primarily a reflector. In combination with the earth's surface it forms, essentially, a giant waveguide through which VLF waves propagate in various modes with little loss. Each mode can be thought of as a combination of an ascending and a descending plane wave whose phase and amplitude are primarily determined by the properties of the earth-ionosphere boundaries.

These VLF waves, particularly suitable for communication, navigation and timing systems, as they propagate to great distances, can be received beneath the surface of the sea, are highly stable and are relatively unaffected by either natural or manmade ionospheric disturbances. However, prediction of VLF propagation, and efficient design of VLF systems, have been seriously hampered by the lack of information on the reflective properties of the lower ionosphere. The usual probing techniques involving transmission and reception of pulses cannot readily be extended to these low frequencies. Pulses generated by conventional VLF transmitters are relatively long. As a result, even at quite short distances, the reflected (sky-wave) pulse arrives at the receiver before the direct (ground-wave) pulse has ended. The superposition of signals makes it impossi-



Launch of balloon supporting the long-wire antenna at the high-precision ionosounder field site in Brazil.

ble to examine the uncontaminated sky wave, from which ionospheric reflective properties could be deduced.

To solve this problem AFCRL developed a unique, high resolution ionosounder capable of measuring reflection coefficients over the 5 kHz to 100 kHz frequency range. The sounder offers several capabilities not hitherto available. The most notable features are the clean presentation of uncontaminated, ionospherically reflected waves and the azimuthally uniform radiation pattern. The first of these features is made possible by the radiation of a VLF pulse so short that even at ranges of 400 km the early arriving ground-wave pulse has ended before the sky-wave pulse arrives. Reflection coefficients are derived by Fourier analyzing the two pulses and comparing the amplitudes and phases. A balloon-supported 1000-meter vertical antenna provides the second feature. The uni-

form pattern permits measurements to be made simultaneously over propagation paths with different magnetic orientations. As a bonus, this antenna requires very little land area, and is transportable. An early version was set up and operated from a small ship off the Florida coast.

In 1970 the ionosounder was operated in southern California in a study of mid-latitude ionospheric reflectivity as a function of frequency, angle of incidence, geomagnetic azimuth and solar zenith angle.

In May 1971 the ionosounder, set up on the geomagnetic equator in Brazil, was used to study the ionospheric reflectivity associated with a horizontal geomagnetic field. This was a cooperative research program with the Brazilian Air Force. Continuous measurements were made at a fixed receiving site 200 km east of the transmitter. In addition, sample measurements were made at 15 selected locations, using portable equipment. It had been predicted from theoretical studies that certain critical reflection situations should exist at the equator. The analysis of the data has confirmed the principal features of these predictions—e.g., a zero value for the conversion coefficient for propagation along the magnetic east-west line through the transmitter and equal values for the normal reflection coefficients to the north and to the south. Because the data covered a wide variety of frequencies, magnetic azimuths, and angles of incidence, it provided a special opportunity to test theoretically calculated reflection coefficients, using several electron density profiles, against the experimental results. As a result of these comparisons an exponential profile was found which appears to describe the daytime equatorial ionosphere with excellent agreement with the experimental data.

The ionosounder was operated from January through June 1972 to study diurnal variations in ionospheric reflection coefficients at low, and very low, frequencies. The transmitter utilized an RADC 600-

foot, vertical antenna located in Camden, New York, and the signals were received in Bethel, Vermont, over a 260-km magnetically west-to-east propagation path. Preliminary analyses of the data show that the normal reflection coefficient data are characterized by steady daytime values, but are highly variable, with deep nulls, at night and during sunrise and sunset. The conversion coefficient is much more stable at night and has a very low daytime value.

Although the earth and ionosphere form a highly efficient waveguide for VLF waves, some energy does pass through the ionosphere. Theoretical studies indicated that the amount of "leakage" would vary with geomagnetic latitude. In May 1971, the ionospheric transmissivity at high geomagnetic latitudes was measured by firing a Black Brant rocket from Fort Churchill, Canada. Receivers in the payload monitored CW transmissions from Rugby, England (GBR, 16 kHz); Cutler, Maine (NAA, 17.8 kHz); Jim Creek, Washington (NPG, 18.6 kHz); Fort Collins, Colorado (WWVL, 20.0 kHz), and Balboa, Canal Zone (NBA, 24.0 kHz). In addition, one channel monitored atmospheric noise. A preliminary survey of the data shows that intelligible VLF transmissions were received, through the ionosphere, to rocket apogee at 500 km. These results were indeed markedly different from those obtained in 1969 on the

geomagnetic equator. There, the horizontal magnetic field allowed very little VLF energy to penetrate the ionosphere.

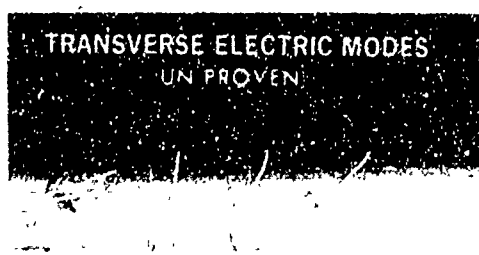
This confirmation of the theoretical prediction has stimulated military interest in the possibility of extending the highly reliable VLF communication system to include satellite-to-satellite, satellite-to-ground and satellite-to-submerged submarine links. Work in progress includes a study of the reciprocity properties of the ionosphere, and the antenna and excitation problems associated with VLF transmissions from space.

Within the earth-ionosphere waveguide, conventional VLF transmissions propagate in the Transverse Magnetic (TM) mode, which is easily excited and received at the earth's surface. In theory, the Transverse Electric (TE) mode should also exist. At the earth's surface, however, this mode tends to be shorted out, making it difficult to excite and weak for reception. At a distance from the earth, as in air-to-air communications, the situation changes and it appears that this mode would propagate with less loss than the TM mode, particularly under highly disturbed ionospheric conditions.

For some time, AFCRL has been carrying on a study of the TE mode and its properties. Preliminary data from a loop receiving antenna suspended beneath a



A standard antenna produces vertically polarized VLF waves which propagate in the Transverse Magnetic Mode. TM waves provide strong signals on the surface of the earth.



The Transverse Electric Mode appears to offer the advantage of lower attenuation for air-to-air communications.

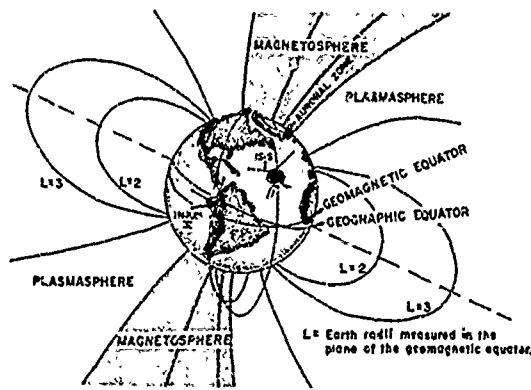
balloon indicated that signals radiated from trailing wire aircraft contain strong TE components. A new technique has been developed to circumvent the difficulty of determining the exact orientation of this swinging loop, so that accurate measurements may be made of the TE wave and the vertical TE field profile uncontaminated by undesired TM components.

The latest receiver instrumentation consists of a wide band VLF/LF receiver (5 kHz to 100 kHz) which is switched during flight between a horizontal loop antenna and a rotating vertical loop. The device is carried to altitudes up to 100,000 feet by a meteorological balloon. A pre-set barometric switch then releases the payload which falls like a dart, attaining a velocity of several hundred feet per second. The axis of the dart maintains a nearly vertical orientation because of the aerodynamic design and the distribution of mass, so that the TE antenna and the TM antenna remain horizontal and vertical, respectively, throughout the fall of the probe. This insures that the signal received from the horizontal loop is free from undesired TM contamination, and that the signal picked up by the vertical loop is free from TE contamination. The data then can be analyzed to determine the TM and TE field profiles as a function of altitude.

In April 1972 the dart was used at Swan Island (near Honduras) to obtain measurements of atmospheric noise to 70,000 feet. The TE noise was found to be on the order of 15-20 dB less than the TM noise, at 15 kHz. In the near future darts will be launched during trailing wire aircraft transmissions, to determine and compare TE and TM signal-to-noise ratios.

ELECTRICAL STRUCTURE

In addition to D, E and F regions, the Ionospheric Physics Laboratory is also investigating other parts of the atmosphere,



The earth from near space, showing the plasmasphere, magnetosphere, L shells, and some satellite orbits.

including the upper ionosphere, the exosphere, the magnetosphere and the plasmasphere. The Electrical Structure Project seeks to determine, under a wide range of atmospheric conditions, the density, energy distribution, flux and directional properties of charged particles in these regions, as well as the vector electric fields, currents and conductivity.

Research includes *in situ* experimental investigations by rockets and satellites, theoretical analysis of the physical relationships and the refinement of the theoretical foundations for the experimental techniques employed.

The spatial and temporal variations of the thermal plasma at low and mid latitudes between $L = 2$ to $L = 4$ over the altitude range 3000 to 5700 km have been studied using data obtained from two spherical electrostatic analyzers flown on the polar orbiting satellite OV3-1. Results show that during magnetically quiet periods, the ionization density characteristically decreases monotonically with increasing L and that between $L = 2$ and 3 the average electron density varies with longitude. Between April and August the maximum occurs at 150 degrees E and the minimum at 300 degrees E.

On 30 percent of the orbits, major charge density irregularities were found at $L = 4$ during periods of quiet to moderate magnetic activity. Comparison of density profiles obtained on the same day at different longitudes shows the irregularities to be of limited longitudinal extent. The results show that "filling in" of the low density regions is continually taking place, but that significant features of major irregularities are observable for up to eight days. Large-amplitude, small-scale irregularities extending over tens of kilometers are often superimposed on the major density gradients and appear to be the result of instabilities produced by inward plasma drifts. These results are directly applicable to the analysis and prediction of radio signal scintillations at low and mid latitudes and provide new data on the ionosphere at altitude regions which previously have been virtually unexplored.

Thermal positive ion densities measured with a spherical electrostatic analyzer on approximately 25 orbits of the OGO-1 satellite, apogee 149,000 km, perigee 282 km, have been studied. The charged particle distributions exhibit a highly variable character within and beyond the plasmapause boundary. The presence of the plasmapause, though quite evident in most cases, is not obvious in some, while on a few orbits more than one steep density decrease is observed. The density gradient at the plasmapause varies. Its magnitude is inversely related to the plasmapause L -position and is consistently about an order of magnitude higher for the afternoon sector orbits than for the nightside orbits. Within the plasmasphere, irregularities in the density distributions appear in the form of troughs and humps, while beyond the plasmapause they exhibit "wavelike" structures with wavelengths in the range of 0.1 to 0.3 L . These as yet unexplained irregularities do not show any correlation with the level of magnetic activity.

A delay of three to nine hours is found in the movement of the nightside plasmapause boundary following an increase in the level of magnetic activity. Similar studies in the afternoon sector show the plasmapause location in this sector correlates best with the magnetic activity that existed when the sampled plasma was in the formative nightside region, 12 to 16 hours earlier. This discovery has provided significant new knowledge on the production and maintenance of the plasmapause boundary, and new insight on the role of magnetospheric convection in the formation of the plasmasphere-magnetosphere interface.

The Injun 5 satellite, launched in August 1968 into an orbit between 666 km and 2526 km at an inclination of 80.7 degrees, carried two AFCRL plasma probes to measure the flux, density, energy distribution and temperature of electrons and positive ions with energies between 0 and 2 keV. Small-scale irregularities in the thermal plasma density are often seen between 60 and 80 degrees invariant latitude, but the most dramatic features are the large fluxes of electrons with energies in the 1 eV to 10 eV range which are observed in those regions extending over a hundred kilometers or more. These have been observed over the full height range of the satellite orbit and are most likely to be seen in the vicinity of 71 degrees invariant latitude. (Invariant coordinates are based on the use of the earth's actual magnetic field to determine latitude and longitude on the surface.)

Other instrumentation on the satellite measures electrons in the energy range 50 eV to 2 keV, and strong fluxes in this energy range are seen concurrently with the lower energy electrons seen by the AFCRL sensor. In addition, the density of thermal energy electrons falls markedly at the time of such fluxes suggesting that local acceleration is taking place, depleting

the ambient thermal plasma. These represent the first simultaneous investigations of thermal and low energy non-thermal particles in the precipitation zone. The results observed during impulsive precipitation events provide evidence for new mechanisms for thermal particle production and removal in the auroral zone.

The dynamic behavior of the topside ionosphere during the magnetic storms was studied using the Injun V, AFCRL electrostatic analyzer measurements. The ion and electron results obtained during five magnetic storms over the altitude range 500 to 2500 km show that the plasmapause and high latitude plasma trough move equatorward during periods of increasing magnetic activity. The equatorward boundaries reach a minimum value of $L = 2.5$ when the magnetic intensity K_p exceeds 7+. In the vicinity of the trough and plasmapause boundary the electron and ion temperatures exceed the normal background values by 3000 to 6000 degrees. The plasmapause location as identified by the satellite plasma probes agrees with the midlatitude red arc ground based observations and with simultaneous whistler observations of Carpenter.

The effect of magnetic storms on E-region and electron densities at low and mid latitudes was studied using the OV1-15 satellite experimental data. For the magnetic storm of October 30 to November 5, 1968 in the north latitude range 35 to 50 degrees, great changes in the ambient charged particle densities occurred with peak values corresponding to 70 times the undisturbed values. Variations in positive ions correlated well with the variations in magnetic activity index K_p , with a time lag of six to nine hours. This lag is consistent with that reported for neutral particle density changes following storms, but the magnitude of the increase is considerably greater for the charged particles. The increase results

from storm-induced changes in the thermal structure of the atmosphere with an upward expansion of ionized layers into regions where charged particle loss rates are much lower than at the normal altitudes. These results are being incorporated into disturbed-ionosphere models.

A spherical electrostatic analyzer aboard the polar orbiting ISIS I satellite measured thermal positive ions over the altitude range 580 to 3525 km. Simultaneous ISIS I measurements of low energy electrons and protons have established that soft particle fluxes observed at high latitudes on the dayside originate in the magnetosheath and enter the ionosphere via the cusp regions. The ionospheric effects resulting from this precipitation are clearly evident in the positive ion measurements which exhibit irregular enhancements in the cusp region. The peak densities, their latitudinal extent and the location of the equatorial and poleward boundaries show a strong dependence on magnetic intensity variations, and follow a diurnal pattern. In the noon sector, the location of the equatorward boundary, Λ_E , correlates better with the solar wind velocities, V (correlation coefficient ~ 0.97) than with the magnetic indices, K_p (correlation coefficient ~ 0.65). The following empirical relation is found by averaging results obtained in the time period 1000 to 1230 hours MLT: $\Lambda_E = 85.93 - 0.026V$. In the morning sector, centered around ~ 0630 MLT, Λ_E correlates better with the K_p indices (correlation coefficient 0.95) than with solar wind velocities (correlation coefficient 0.65). Upon averaging these results the following expression is obtained: $\Lambda_E = 80.16 - 2.52 K_p$.

Instruments were designed for the study of dc ionospheric electric fields and bulk ion motions including the polar wind. Final development and construction of instruments scheduled for flight on the Air Force Satellites STP S 3-2 and S 3-3 are

underway. Ionospheric electric fields will be mapped over the altitude range 300 to 1000 km and the role of electric fields in the generation of narrow band emissions, current systems and particle accelerations determined. The influence of bulk plasma motions on the ionospheric electron and ion distributions will be ascertained.

Although theories of ionospheric motion at all latitudes and a wide range of altitudes invoke the effects of high altitude electric fields, few direct measurements of these fields have ever been made. In 1968, AFCRL began developing techniques for measuring upper atmosphere dc and low frequency ac fields. In 1969-1970 four rockets carrying payloads for making both electric field and charged particle measurements were launched from Fort Churchill into regions of auroral activity, where theory predicts the existence of relatively high electric fields. Analysis of the data is still in progress, having been hampered by the necessity for precise determination of payload attitude with respect to the ambient magnetic field, and of the vehicle potential with respect to its surroundings. Methods have been developed to overcome these difficulties and a model of the ambient electric field in three dimensions has been generated.

Since most serious ionospheric disturbances have their genesis in flares and other solar phenomena, the laboratory carries on an extensive program of solar measurements and observations. The program has two goals: 1) to seek and establish correlations between solar events and ionospheric disturbances so that warnings may be issued to operational units, and 2) to investigate the mechanisms which cause, and factors which influence, the solar events themselves. The immediate results of this "pure research" part of the program is increased scientific knowledge. The insight and comprehension gained, however, will eventually lead to better and earlier warning of impending ionospheric disturbances.



The solar radio facility at Sagamore Hill. The radio telescope in the foreground is used for millimeter monitoring; the unit in the center is used for 3, 6, and 10 cm monitoring; the larger 28-foot antennas are used for decimeter and meter monitoring.

The principal observing site of the Laboratory's radio astronomy and satellite observation programs is at Sagamore Hill Radio Observatory in Hamilton, Massachusetts. The observing instruments include an altitude-azimuth mounted 150-foot antenna, an equatorially driven 84-foot parabola and various other units ranging from 28-foot parabolas to simple dipoles. With these antennas, measurements are made over a wide spectral range. The site is located at an invariant latitude of 57 degrees which places it sufficiently far north to permit auroral observations.

For the principal types of solar radio data sought (the undisturbed sun's background flux and the burst components), low-resolution radiometric systems are employed, and at Sagamore Hill a large number of radiometric systems operating between 25 and 35,000 MHz routinely monitor solar activity. Since the character

of solar emission varies greatly over frequency intervals as short as one octave, monitoring at many frequencies is required to produce valid spectral information.

Both the frequency range monitored and the geographical coverage have been greatly expanded since the program's inception in 1966. Data are presently being furnished, in addition to Sagamore Hill, by stations at Manila Observatory in the Philippines and in Athens, Greece. AFCRL has contributed equipment, advice and assistance in setting up these stations, and the laboratory maintains consultation and direction to insure the technical adequacy of the observations. A fourth station in Hawaii, is under development at present. Installation of equipment is scheduled to begin in late 1972. The addition of this fourth station will complete a world-wide network which will provide continuous (24 hours a day) observation of the sun and preclude missing any of the large radio disturbances which are most useful in forecasting proton events.

Air Weather Service SESS (Space Environment Support System) personnel handle the routine operation of the stations and channel data to DOD operational units for use in predicting and warning of solar events and geophysical effects such as Polar Cap Absorption (PCA) events, magnetic storms, and sudden increases in total electron content (TEC).

A promising line of study is the association of spectral signatures with specific solar optical events. Early in the program one such peak flux signature in the decimeter-centimeter range (the so-called U-shaped spectrum) was evaluated and associated with impending proton events and subsequent PCA. As emphasis shifted from simple "yes-no" warnings to prediction of the probable intensity of such events, it was found that integrated flux density (mean flux density times burst duration) of bursts in the centimeter range

correlated reasonably well with proton flux particles with energies greater than 10 MeV for bursts associated with disturbances on the visible hemisphere of the sun. A burst flux density integrator at 8.8 GHz has been developed and is now in operation at Sagamore Hill. The relative importance of different types of spectra, in association with geophysical phenomena, has been and continues to be tested.

Study of the spectra also furnishes insight into the mechanism of solar bursts and factors influencing the emissions. In the most common spectrum, the so-called "C" type (which actually resembles an inverted "U"), the shifting of the frequency of maximum emission along the frequency scale is related to magnetic field intensity at the height of the burst source, for the gyro-synchrotron process. The slopes, on the other hand, are determined by absorptive mechanisms, energy distribution of radiating electrons and harmonics of the gyro-frequency. It has also been established that the frequency maxima shift to higher frequencies with increasing burst intensity.

Because of the operational importance of the proton-event warning system, effort has been expended to enhance the real-time reporting capability by automating the calibration and data reporting aspects. Major additions to the Sagamore Hill solar patrol equipment are now underway with this end in view.

SOLAR POLARIZATION

As indicated in the previous section, study of the decimeter-centimeter U-shaped spectrum has led to the conclusion that the magnetic field configuration in and above the disturbed region on the sun is an important factor in shaping the signature of, and therefore in understanding the mechanisms involved in, the burst. Observation of the polarization parameters of radio emission during bursts offers

one means of exploring these fields. Instrumentation to measure the complete set of polarization parameters of an incident wave has been designed and is now operating at Sagamore Hill.

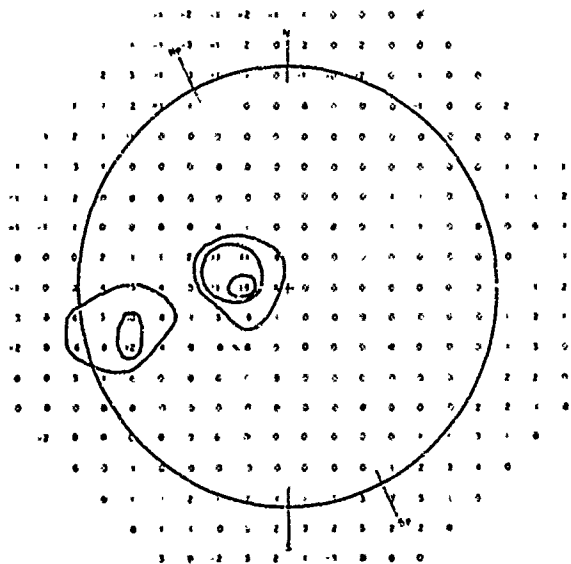
The three-antenna system will measure the four so-called "Stokes parameters" of polarization of solar radio emission at 4995 MHz. A dual circularly polarized antenna measures the total intensity and the circularly polarized component (Stokes parameters I & V); two dual linearly polarized antennas are oriented at 45 degrees with respect to each other and measure the two components of linear polarization (Stokes parameters Q & U). AFCRL is also providing support to groups at Huancayo, Peru, and Sao Paulo, Brazil, who are working on Stokes parameters I & V in the centimeter region (9.4 and 7 GHz). This effort will

complement the polarization research at Sagamore Hill.

While it is desirable to predict geophysical phenomena from observations of solar flares, another program of solar observations goes one step further by attempting to determine whether a solar flare itself can be predicted from the behavior of a solar active region. This work, which is being conducted at MIT's Haystack Observatory, involves high resolution (about 1/50 of the area of the solar disk) measurements of brightness, temperature, and circular polarization at a wavelength of 3.8 cm. Since polarization is typically at a maximum in the 3-4 cm wavelength range, the system is especially sensitive to magnetic properties of the solar regions under observation. Furthermore, work in Japan and France has shown that large flux changes at 3 to 4 cm relative to changes at other frequencies correlate with the frequency of occurrence of proton flares.

This program has produced one of the first two-dimensional polarization maps of the sun ever made in the United States. Observations have also been made of heating and polarization increases in an active solar region as early as one hour before a flare. Observations are continuing in order to build up a statistical basis for prediction which will lead to improved forecasting capability for operational units.

High resolution measurements of solar active regions, which are often the sites of disruptive solar flares, were also made during the solar eclipses of March 1970 and July 1972. The slow passage of the moon's limb across the solar disk permitted very high resolution determination of the extent of the active area. In addition, the change in solar radio emission at eight different wavelengths was monitored by accurately calibrated radio telescopes. Radio emission at different wavelengths effectively comes from different solar altitudes and depends on the electron temperature and densities at the altitude of ori-



Map of percentage of polarization (p) of the solar radio emission at 3.8 cm for October 24, 1970. The quantity p is defined as the difference in the brightness temperatures measured in left and right circular polarization modes, divided by the sum of the two brightness temperatures. This map was made using the Haystack facility and is one of the first two-dimensional polarization maps to be produced at centimeter wavelengths. On the map + is left circular and - is right.

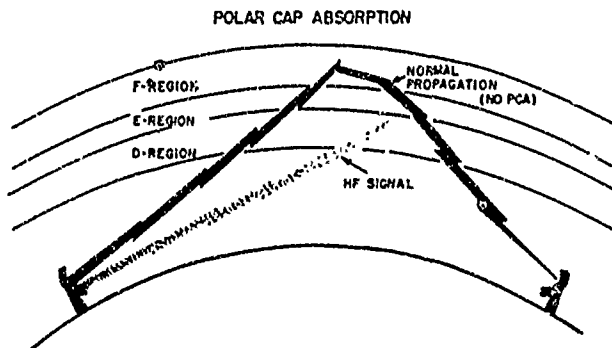
gin. From the variation in the emissions during the course of the eclipse, the electron temperature and densities at different solar altitudes were deduced and combined with the information on the source extent to produce a three-dimensional picture of the solar atmosphere over an active region.

The magnetic fields of sunspots in an active region strongly influence the emission from the region. Moreover, these fields are thought to have major control of the acceleration, trapping and escape of the solar protons which accompany a solar flare and which are largely responsible for the associated ionospheric effects. Data obtained during the March 7, 1970 eclipse showed some areas with strong magnetic fields, evidenced by increased intensity and sharper peaking in the spectrum of the source. Regions with weaker and less developed fields showed flatter emission spectra. In total, the measurements made during this eclipse have provided some quantitative measures of some vital solar parameters.

ARCTIC PROGRAM

Ionospheric disturbances are greatest, and our knowledge and understanding of these conditions is least, in the Arctic. At these high latitudes, emissions from solar events are funneled into the earth's atmosphere under the influence of the earth's magnetic field, interacting with it to produce auroras, auroral absorption, PCA's, blackouts, magnetic storms and substorms, ionospheric irregularities and plasma variations, all of which degrade or disrupt the performance of high latitude systems, and few of which are predictable with even a modicum of accuracy.

In awareness of the importance of this region, AFCRL is continuing its extensive program of Arctic ionospheric studies. In recent years, Laboratory contributions have included assumption of responsibility for the riometer program at the Geopole



During a PCA event, the greatly increased D-region ionization causes strong absorption of HF signals.

station near Thule, Greenland, programs of rocket observations from both Thule and Fort Churchill, Canada, the development and scientific staffing of the NKC-135 flying ionospheric laboratory on its numerous Arctic data-gathering flights, and in the planning of and participation in a major PCA observing expedition. AFCRL's northern riometer stations (at Thule and Godhavn, Greenland, and, since October 1971, Goose Bay, Labrador) are part of the "cooperative net"—a working arrangement with the Alaskan and Canadian riometer chains. Under this arrangement, data obtained at any station are freely available to researchers at any other station, thus avoiding duplication of effort and waste of funds and manpower.

The Laboratory's Arctic program has now been extended by the construction of the Goose Bay (Labrador) Ionospheric Observatory (to be described later in this review) which began operations in October 1971. Work is also underway on a dynamic, propagation-oriented model of the polar ionosphere which will reflect the latest developments in theory and data analysis for the high latitude regions. Publication of this model is scheduled for January 1973.

Although the AFCRL program includes research in all of the problem areas mentioned, recent major efforts have been con-

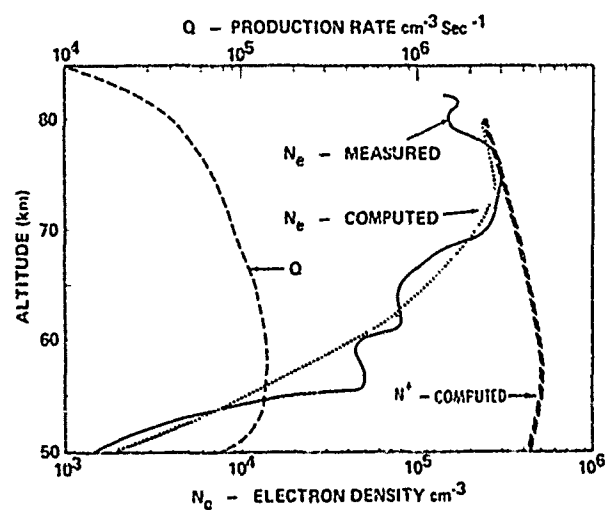
centrated on the investigation and interpretation of PCA events, and of auroral phenomena, particularly the auroral oval. The former, though infrequent, are the most devastating and long-lived of the Arctic events; the latter may prove to be of fundamental importance in correlating polar ionospheric phenomena.

POLAR CAP ABSORPTION (PCA)

The term "PCA" refers to an abnormally high degree of absorption—sometimes amounting to total blackout—of HF and VHF waves passing through the Arctic ionosphere in the aftermath of certain major solar flares. This high absorption is due to the increased ionization produced within the lower (40-85 km) level of the Arctic D region by high-energy, flare-associated particles, chiefly protons. A typical PCA commences minutes to hours after a major solar flare (which usually originates on the visible hemisphere of the sun), attains a maximum within a few hours after its onset, and then begins to decrease slowly. Its average duration is three days, though periods as short as one day or as long as ten days have been recorded. Vertical absorption at 30 MHz has, at times, exceeded 20 dB. Despite the name, PCA effects are not limited to the polar area; on occasion, they have been detected as far south as the northern United States. More commonly, however, they occur polewards of the auroral zones (magnetic latitude 64 degrees or greater), with total blackouts occurring north of the auroral oval. Except in their last stages, PCA's are not usually accompanied by noticeable increases in either geomagnetic or auroral activity. Fortunately, solar proton events, and therefore PCA's, occur relatively infrequently (approximately two per year when solar activity is at a minimum, approximately 12 per year when it is at a maximum). Never-

theless, their drastically disruptive effects on high latitude communications and detection/surveillance systems make them a matter of vital concern to military planners. The fact that similar effects accompany high altitude nuclear detonations furnishes additional impetus to Air Force investigation of PCA's.

Over the years, AFCRL has carried on both an intensive and an extensive study of PCA events, culminating in Operation PCA 69 and the PCA event of November 1969, which was the most thorough investigation of a PCA event ever conducted. As was reported in the AFCRL *Report on Research* (1967-1970), during this event AFCRL carried out a coordinated program of measurements using ground-based installations, the NKC-135 flying laboratory, and rocket and satellite-borne instrumentation. This investigation was the focus of the 1971 International COSPAR Symposium which was held at Boston College, Mass., June 16-18, 1971. AFCRL's Ionospheric Physics Laboratory organized the



Electron and ion densities computed from simplified expressions derived from Polar Cap Absorption (PCA) rocket data and the measured production rate (Q) compared to a 1962 measurement of electron density during a nuclear test conducted at night.

Symposium, and AFCRL members presented 19 of the Symposium's 53 papers.

Measurements made by the Ionospheric Physics Laboratory during PCA 69 included incident proton, electron, X-ray and Lyman-alpha fluxes, positive and negative ion densities, the electron density and temperature, and parameters of various minor atmospheric constituents. Computer codes developed from these data describe the production and loss of electrons and ions and make it possible to model ion and electron densities for an ionosphere disturbed by a PCA (or nuclear) event. Unfortunately, these codes, which contain the detailed chemistry for all the species of particles involved, require far too much time and storage capacity to be operationally useful. An approximation known as the "lumped parameter" method has therefore been developed. In this approach, the particle population is reduced to four species: electrons, neutrals, positive and negative ions; and the reactions involved to five: production by the source (UV, X-ray, etc.), shift (electron attachment to neutral, electron detachment from negative ion) and neutralization (electron recombination with positive ion, positive-ion recombination with negative ion). From this limited set of species and reactions, differential equations for species densities can be written and useful solutions obtained.

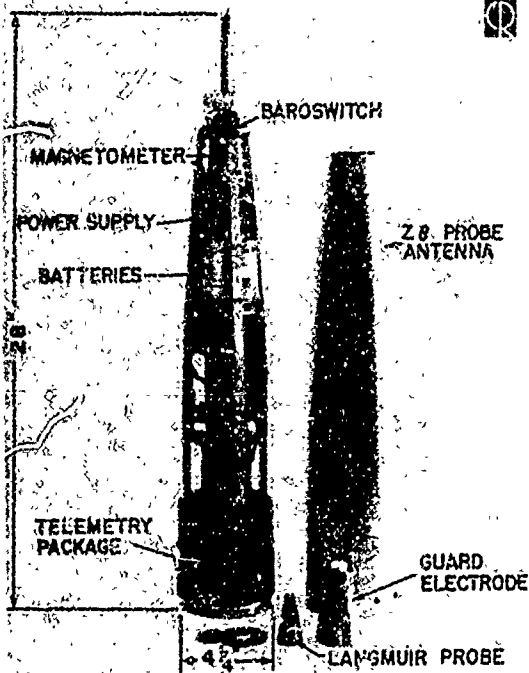
Using the lumped parameter approach with values of the lumped parameters which were developed from PCA 69 data and a production rate measured during the 1969 Atmospheric Test Series, AFCRL researchers have computed electron and ion density profiles for a nighttime (nuclear) disturbed ionosphere. The computed electron and ion densities are in excellent agreement with the measured values, and the method is now being applied to daytime and transition (sunrise and sunset) conditions.

Analysis of data obtained during PCA

69 and earlier research programs has identified and established the primary effects, causes and dominant processes of ionospheric perturbations. The development of propagation models for predicting the survivability of communications systems under ionospherically disturbed conditions still faces some unresolved difficulties. Resolution of these and other difficulties is largely dependent on *in situ* measurements by sounding rockets, as the optimum altitude for investigation is above the maximum capability of balloons and below the minimum perigee of satellites. Measurements of this type have hitherto involved the use of large multi-experiment rockets and the fielding of teams of highly trained scientists, as in PCA 69. To reduce the cost, in both funds and trained manpower, of such measurements AFCRL has developed its Small Rocket Program.

In this program small meteorological type rockets are used to conduct coordinated rocket and propagation field experiments during early-time solar proton events. The rockets, instrumented with simple "electron" or "proton" payloads, are launched by Air Weather Service personnel who are permanently stationed at Thule. The electron payloads measure the ionization parameters of interest in PCA—namely, the electron and ion concentrations as a function of altitude. Energy deposition, as a function of depth of ionospheric penetration, is derived from measurements taken by scintillation counters in the proton payloads. The optimum time for launching the rockets is determined from solar observations made by AFCRL scientists. When it is determined that a solar event is in progress, the launch site is notified by telephone and the rockets are launched at the specified time(s).

In April 1971, three small (Arcas) rockets containing payloads to measure electron and ion density profiles, as well as the energy spectrum of impinging protons, were launched into the early phases of a

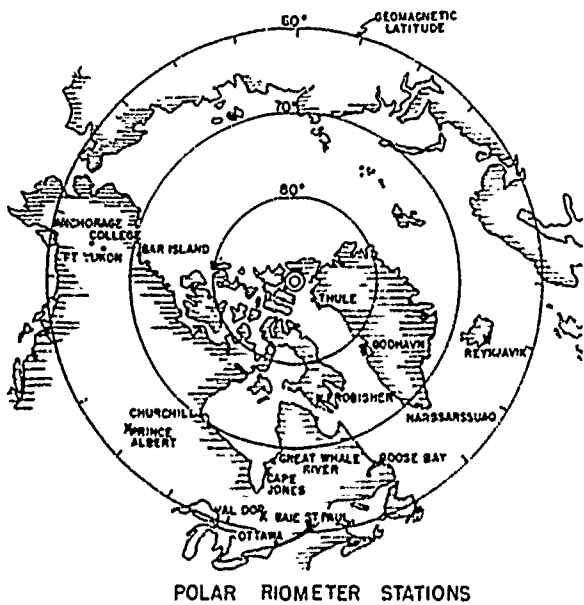


Low cost miniaturized payload for meteorological type rockets (4 1/4 inches diameter by 28 inches long) for measurement of electron and ion density profiles to 100 km utilizing Z8 impedance and modified Langmuir probes. Flight performance is monitored with magnetometer and baroswitch sensors.

PCA event by AWG personnel at Thule. All payloads performed successfully and good data were obtained on all experiments from launch to impact. The success of these launches proves that, by careful selection of experiments and by use of simplified "check-off" and recording techniques, it is possible to conduct meaningful ionospheric rocket research on a continuous basis with low level expenditure of funds and manpower. Moreover, the use of small rockets and the techniques and instrumentation perfected in this program provide opportunities for research and synoptic investigations of upper atmospheric parameters at any location where

AWS detachments exist or where it would be feasible to send in a small team of launch technicians.

The morphology (temporal and spatial variations) of PCA events is being studied as part of the Ionospheric Physics Laboratory riometer program. This aspect is of paramount importance to operational personnel who are concerned with predicting the areal extent of the absorption region, its homogeneity, its estimated duration and the probable absorption values for successive days and nights. Data for this program are collected at AFCRL-maintained stations at Thule and Godhavn, Greenland, and the Goose Bay Ionospheric Observatory, Labrador. Riometers measure and record the background galactic noise level, which can be assumed to be constant. A drop in this recorded signal



The Polar Riometer Network. Full and free exchange of data among all of the stations makes it possible to give the area fairly good coverage and let various groups pursue individual research programs at greatly reduced cost. Stations at Goose Bay (activated in October 1971), Thule and Godhavn are AFCRL-maintained.

level, therefore, indicates increased ionospheric absorption which, in turn, usually signifies increased electron density in the D region—a major PCA effect. By correlating data from high-latitude riometer stations with solar particle information—e.g., satellite proton flux measurements in different energy ranges—it may be possible to form a basis for short-range predictions of PCA magnitude, duration and peak absorption. Excellent agreement has been found between daytime riometer measurements and the square root of the proton flux for energies exceeding 10 MeV.

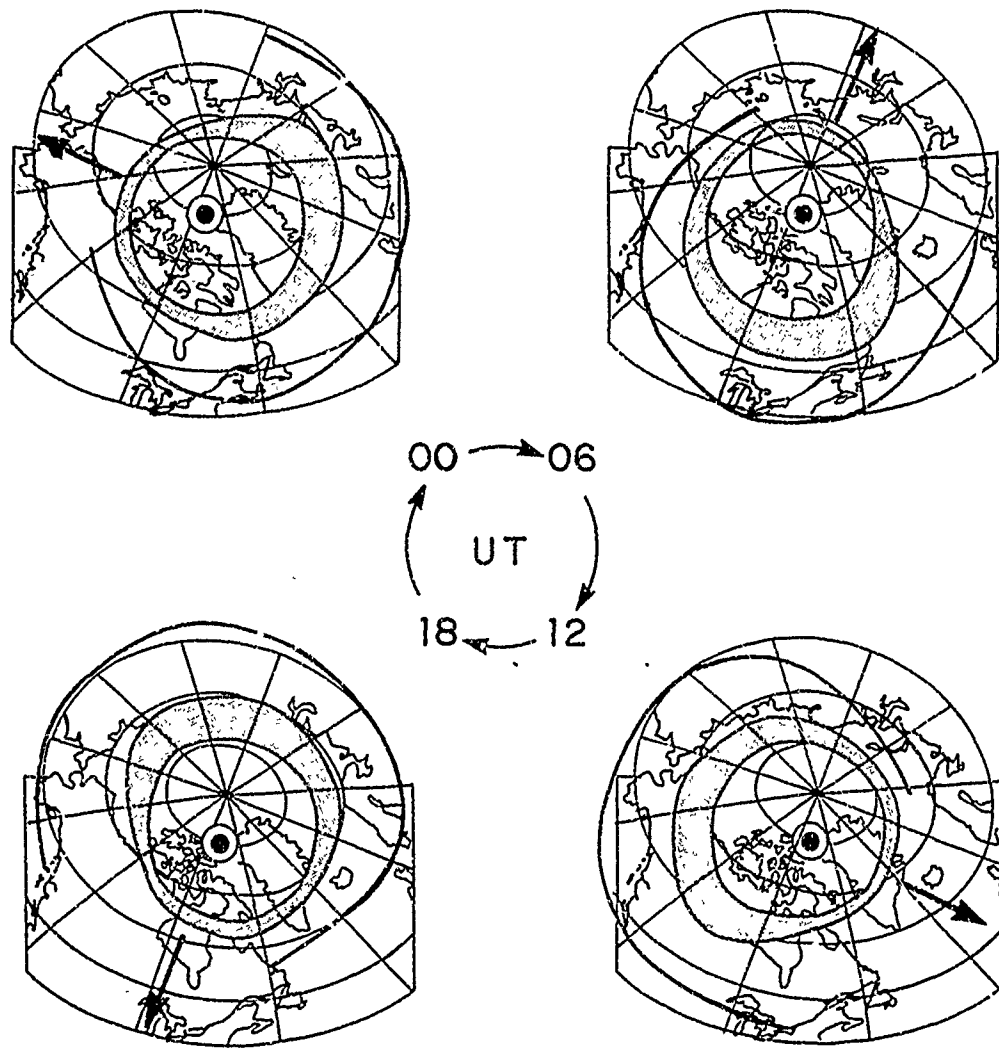
It has been observed that during a PCA event there is a marked decrease in the absorption level at night, the ratio of nighttime to daytime values ranging from 1/2 to 1/10 (average, 1.4). This decrease in absorption occurs when the solar zenith angle reaches 88-90 degrees, and the solar ultraviolet radiation in the lower levels of the ionosphere is much reduced. It was, therefore, theorized that the day-night ratio is dependent on the energy of the incident protons—i.e., on their depth of penetration (or height of energy deposition). Thus, the greater the proton energy, the greater should be the expected ratio—a prediction borne out by the data. In a study of polar cap riometer observations completed in the summer of 1971, AFCRL confirmed the importance of energy deposition height as a major factor in the nighttime recovery effect. The study also showed that not only the energy spectrum of the proton flux, but also the season and time of day (that is, the zenith angle of the sun) must be taken into account in predicting the expected absorption for a PCA event. For large zenith angles—that is, during effectively nighttime conditions—even a solar event of large magnitude may cause only a small change in the measured absorption, whereas a simultaneous measurement at a station in a daytime location would show a variation more accurately warning that a major event was in progress.

The necessity for choosing base-level criteria in accordance with solar zenith angle is particularly acute at stations like Thule where, during the winter months, this angle is always greater than 90 degrees.

AURORAL INVESTIGATIONS

Another major disruptive factor in trans-Arctic radio/radar systems is the well known aurora or northern lights. Energetic particles, probably from the magnetosphere, are guided by the earth's magnetic field and precipitate into the upper atmosphere over the polar regions. There they interact with the atmospheric constituents to produce not only the spectacular visual effects long familiar to observers in the high latitudes, but also regions of particle-caused ionization which can cause serious propagation degradation in the form of increased absorption, Doppler broadening, or deflection of waves from great circle propagation paths. Auroral events tend to have complex spatial and temporal patterns and though they occur in conjunction with geomagnetic activity, the correlation is far lower than for PCA events. Thus, they are not easily predictable, even on a short-range basis.

A fundamental entity in understanding and interpreting auroral phenomena is the auroral oval, a high latitude circumpolar belt which contains the visible discrete aurora and is the region of greatest (visible) auroral activity. The size of the oval varies with season and magnetic activity, its general shape is fairly constant, with the (north-south) thickness of the noon sector approximately 1.4 to 1.3 that of the midnight sector. The orientation of the oval is fixed with respect to the sun, and the earth rotates beneath it once every 24 hours—somewhat eccentrically, since the geographic and geomagnetic poles do not



The Auroral Oval rotates with the earth, but is centered on the geomagnetic, rather than the geographic, North Pole. The heavy line below the hatched oval shows the position of the mid-latitude trough.

coincide. The best coordinates for describing the auroral oval are geomagnetic latitude and geomagnetic local time, a coordinate system that has proved to be generally useful for ordering geophysical phenomena which depend on the solar-magnetospheric interaction. To convert geographic coordinates (e.g., of ground-based observatories, instrumented aircraft or satellites)

to geomagnetic coordinates, AFCRL developed the Auroral Oval Plotter. This simple nomographic device is now in use wherever ionospheric features are observed and described.

A major factor in AFCRL's fruitful program of Arctic studies is the NKC-135 flying laboratory. This aircraft, instrumented with an ionospheric sounder, photo-

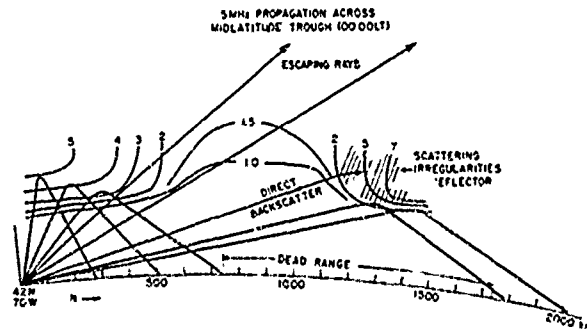
tometers, spectrometers, all-sky cameras, and HF, LF, VLF and Loran A receivers, is a versatile, mobile, maneuverable facility capable of making measurements impossible with ground stations or satellites, or combinations of the two. In investigations of the auroral oval, for example, it can make circumoval flights, passing through all local time sectors. Conversely, it can make constant local time flights, making continuous observations in a chosen sector for periods up to ten hours.

Late in 1967, AFCRL, using the all-sky cameras in the NKC-135, photographed for the first time a pulsating brightening of the polar sky whose existence had been suggested by photometers but never photographed.

Patterns of auroral sporadic E have been established and found to be very closely linked to the auroral oval. Within the oval, E_s occurs approximately 75 percent of the time, and the E_s layer always occurs in a band of about 3 degrees latitudinal width aligned along visible auroral arcs. It has also been found that intense, blanketing (but short-lived) sporadic E also occurs, but only in the sector of the oval between 2000 and 2400 CGT (corrected geomagnetic time). This sector is known to be the "spawning ground" for auroral substorms—frequent, but as yet, little understood disruptions of the normal oval pattern of visible aurora. It is probable that a sudden influx of particles is the manifestation of an auroral substorm and is linked to a "filling up" of the Van Allen radiation belts. It appears that the high latitude limit of this oval maps the boundary between the open and closed magnetic field lines. AFCRL is presently working on a program to map the high latitude limit of the closed field lines. These lines are the controlling factor in the motion of charged particles entering the atmosphere. Knowledge of their pattern and variations is crucial to the understanding of ionospheric behavior. Airborne investigations of the

noon sector of the auroral oval in darkness have shown that equatorward of the discrete aurora a continuous aurora exists and that it is associated with an extensive particle-produced E layer. The continuous aurora is subvisual in quiet magnetic periods, but is seen and photographed as a structureless, diffuse, continuous auroral form during more disturbed magnetic conditions. AFCRL also achieved, in the noon sector of the oval, the first quantitative spatial ordering of the Arctic ionosphere and found that in this sector D, E and F layer effects fall into a predictable pattern. Later studies proved the auroral E layer to be continuously present in all time sectors of the auroral oval, and therefore to form an unbroken "E-layer oval". In sunlit conditions the particle-produced E layer is superimposed on the solar E layer.

The Arctic F region is characterized by a ring of enhanced ionization, rather heavily interspersed with irregularities which cause the scintillations observed in ground recordings of satellite beacon transmissions. In addition, these field-aligned irregularities can cause strong aspect-sensitive clutter on radar at all frequencies. Measurements with a topside sounder indicated the existence of a plasma ring, with enhanced soft-electron precipitation. Observations made by the Ionospheric Physics



Effect of the F-region mid-latitude trough on propagation. The trough provides a "window" for HF radiation, and thus a dead range for HF communications or radar.

Laboratory, using the NKC-135, have now proved that this plasma ring coincides with the zone of F-layer irregularities, and that the equatorward edge coincides approximately with the equatorward edge of the auroral oval. They have also shown that there is a strong UT (universal time) control of the behavior of the F layer in this region. This control influences the extent and the position of both the polar cavity and the F-layer trough. These are two regions of decreased electron density—the former inclosed by the plasma ring, the latter south of its lower boundary—which can seriously affect the propagation paths of radio waves transmitted through the region.

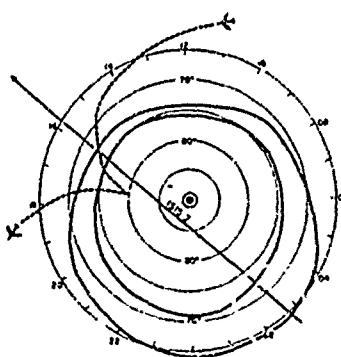
AFCRL made the first mapping of the entire extent of the region in which the solar wind interacts directly with the ionosphere and showed it to be identical in location with the dayside auroral oval. The NKC-135 is being used to establish the correlation between the optical phenomena and the Arctic ionospheric layers. The establishment of such correlations between visible and sub-visible aurora and ionospheric parameters is desirable because it is hoped that eventually important parameters of the arctic ionosphere can be inferred from optical observations.

The NKC-135 is also being used extensively in conjunction with the Goose Bay Ionospheric Observatory, for which it provided the feasibility study by operating the aircraft equipment continuously for up to four days while the aircraft was positioned at Goose Bay Air Base. This study showed that Goose Bay is suitably located for the purpose of monitoring some vital sectors of the auroral oval. The station has been established as a research tool, but may eventually be turned over to an operational unit for routine real-time observations.

An essential factor in understanding auroral events is the so-called "input-output" measurement, in which the energy of in-

coming particle fluxes is quantitatively related to the ionospheric electron densities they produce. These measurements require rendezvous between the aircraft and the sub-point of a data collecting satellite. In late May 1971, the NKC-135 and the ISIS-II satellite made the first simultaneous measurements of these quantities. Numerous additional rendezvous have been completed to date. Flight routes were planned so that ISIS-II was intercepted as its path traversed the auroral oval, thus providing additional data on ionospheric conditions in the vicinity of this focal area.

One important problem is the occurrence of auroral clutter in acquisition and over-the-horizon radar. For many years



The paths of the ISIS-2 satellite and the flight path of the NKC-135 during the satellite intercept input-output experiment.

the poor correlation between radio aurora and visible aurora has been a puzzling and disturbing fact. A number of simultaneous measurements between the Ionospheric Flying Laboratory and two HF radar installations, RADC's near Rome, New York, and Polar Fox II in Maine, have yielded some important insights. The results so far show that auroral radar returns are well correlated with the auroral E and E_s layer. Investigations to establish the correct mechanisms of HF radio aurora are continuing.

In March 1972, the first coordinated measurement program for the investigation of infrared excitation and emission processes associated with auroras was carried out at the Poker Flat rocket range near Fairbanks, Alaska. The program, called ICECAP (Infrared Chemistry Experiments for Coordinated Auroral Programs) is the precursor to more extensive and complete investigations to be made in subsequent years, which will include airborne and balloon-borne measuring systems. First order predictive models of the physical chemistry and other prominent infrared effects will be developed from the measurements for radar/infrared computer code test and development.

Rocket probe and incoherent backscatter measurements of the ionization created by deposition of energetic electrons in the atmosphere between 150 and 100 km show agreement within 15 percent. The differential flux spectra of the energetic electrons were also measured in this altitude interval. From these measurements the ion pair production rate was determined as a function of altitude using an AFCRL-developed computer code. This rate is the source function used in the radar/optic predictive codes to determine the auroral effects including ionization, heating, composition changes, emission, and excitation. First tests of the code using the measured source function gives an ionization model within 15 percent of the measured profile.

GOOSE BAY IONOSPHERIC OBSERVATORY

The Arctic's increasingly important role in Air Force systems planning and operation pointed up both our limited understanding of this highly variable and unpredictable ionospheric region and the scarcity of data-gathering stations there. Early in 1971, therefore, AFCRL began the planning and construction of the Goose Bay Ionospheric Observatory at Goose Bay, Labrador. The site chosen passes through that sector of the auroral oval in which substorms and the intense, blanketing E_s originate, thereby facilitating their study, and it is at a magnetic latitude at which there exist no sounding stations—an important consideration, as the difference of a few degrees in location can have a marked effect on the observations recorded. In addition, the site is nearly "ringed" by a chain of Loran-A stations, whose transmissions will be monitored and analyzed, and it is in a region which is in darkness during part of every day. This is essential for operation of the photometers and the all-sky cameras in the observations of airglow and auroral spectra and of visible auroras. The feasibility of establishing an observatory at the site was confirmed by stationing the NKC-135 there on two occasions while it functioned as a mobile ionospheric monitoring station.

The station was installed and is being operated under contract, with close consultation with AFCRL. The observatory's Digisonde (digital ionospheric sounder) is designed to produce not only the usual vertical-incidence ionograms, but also oblique-incidence records of backscatter (the "clutter" on radar screens). If conditions warrant, the sounder is capable of taking recordings at five-minute intervals, though initially recordings will be made every 15 minutes.

(The Digisonde, developed and built under AFCRL sponsorship, derives its name from the use of digital integration, storage

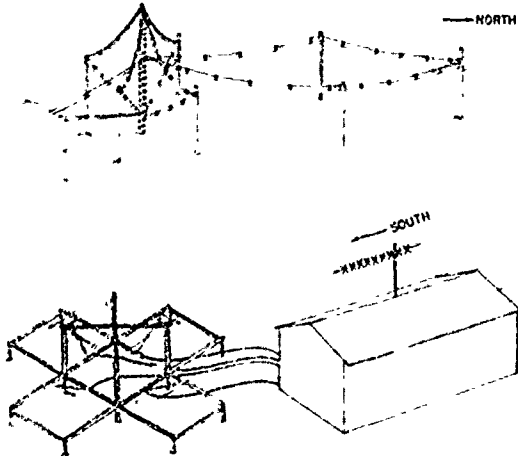


Basic Digisonde equipment.

and processing techniques. In conjunction with phase coded pulses and pulse coherent detection, these techniques yield better ionosonde records and a significant improvement in signal-to-noise ratio. This makes possible better reception of echoes through interfering noise and extends the instrument's range of operation at the low frequency end. A Digisonde has been in operation at Maynard, Mass., since mid-1971, as part of the global ionospheric sounder network.)

The Observatory's riometer utilizes a unique four-corner reflector antenna which permits observation of auroral (absorption) events in four azimuths from a single location, thus minimizing logistic requirements. It will be used to study the duration and spatial extent of auroral substorms, as a preliminary step in determining the optimum number and the best sites for riometer stations for a warning network.

The Loran-A multi-station monitor is an outgrowth of observations made during the NKC-135's ground operations at Goose Bay in April and October 1970. Transmissions from Loran-A stations in Canada's Maritime Provinces were recorded. Analysis of the data showed that it was possible to tell when high absorption was present and when spread F and sporadic E echoes were received from the various stations. As both the stations and the respective reflection points were south of Goose Bay, this indicated the possibility of observing the effects of the southward motion of the auroral oval. It was also determined that the data could be made to yield information on movement of the oval and its boundary as well as D-region absorption and possible changes in critical frequency. The observatory monitor will record transmissions from up to four stations, all at the same (1.950 MHz) frequency, on separate scopes each of which will be photographed over a 24-hour period. The vertical trace record will show the relative time differences between various ionospheric reflections. The horizontal displacement will show the time of day in 720 two-minute increments. Operation of the monitor will



Antenna configurations at Goose Bay Riometer and Digisonde stations.

be almost entirely automatic, except for film change and gain pre-setting.

Spaced Receiver Equipment and Doppler Arrival Angle Spectral Measurement (DAASM) equipment is also located at the Goose Bay Observatory. The objective of this experiment is to investigate the fine structure of ionospheric clutter signals for the purpose of improving the ability of an OTH backscatter radar to detect a target signal in the polar environment.

Also located at the Observatory are beacon satellite receivers to observe the ATS-3 Satellite at 137 MHz using an AFCRL polarimeter. This experiment measures the geographical extent of the scintillating regions as a function of time and will further refine the knowledge of the scintillation boundary. The experiment also furnishes fine grain data, necessary to integrate Sagamore Hill, Narssarssuaq, and Thule data.

In a novel attack on the problem of "clutter" as it affects OTH radar performance, AFCRL will operate at Goose Bay the DAASM (Doppler Arrival Angle Spectral Measurements) System. In its final form, this system will utilize a 3000-foot broadside receiving array to pick up signals from the backscatter transmitter at the site, and signals in the forward scatter mode transmitted from the NKC-135 flying to the north of the station. The unique feature of the system is the provision for separate processing and storing of the data from each (wide beam) element of the array. By suitably combining the stored data, it is possible to simulate an instantaneous (narrow-beam) scan of the region north of the antenna, thus obtaining, in effect, a snapshot of the Doppler structure at all northerly azimuths for a given range. A variety of gates provides for observing several ranges simultaneously. The system offers a means of studying the fine structure of ionospheric irregularities and of seeking differences in the Doppler frequency or angular structure of clutter

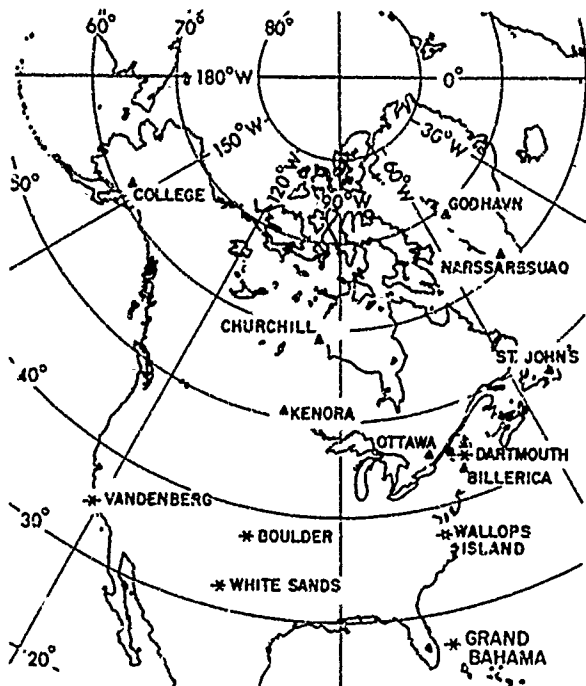
and target signals which might be used to discriminate between them and thus improve radar performance.

Pending construction of the 3000-foot array and the final version of the equipment, tests will be made with the type of spaced antenna system used in the drift experiments and probing of the fine structure of the E and F regions, as reported in the 1967-1970 issue of the *Report on Research*. HF signals in either the forward or backscatter mode are received at three separate antennas, approximately 100 meters apart, and their phases and amplitudes are recorded and compared. In the final DAASM system, a digital processor will provide real-time on-site spectral analysis and digitized printout of either original or processed data.

Plans for the Goose Bay Ionospheric Observatory also include installation of a long baseline interferometer to study the effects of irregular Arctic ionospheric refraction, and of an electronic polarimeter for TEC (total electron content) measurements. Extended and extensive studies will be made of the auroral oval, the auroral absorption band, PCA, sporadic E, spread F, the mid-latitude trough, ionospheric scintillations, great circle path deviations and time delays over satellite transmission of paths. These studies are expected to contribute significantly to the development of a new and more accurate model of the polar ionosphere.

DYNAMIC POLAR IONOSPHERIC MODEL

The need for an accurate and comprehensive model of the ionosphere is pointed up by the fact that intelligent and effective design, planning and operation of large systems, such as the OTH radars, are contingent on the availability of reasonably accurate predictions of the propagation conditions under which they will be re-



Location of ionospheric sounders providing the data used in the ionospheric mapping study. Stations marked * are providing data for the spatial variation study.

quired to operate. A truly versatile ionospheric model would not only make possible accurate short-range predictions for a specific set of operational conditions but would also, in statistical format, reduce the wide range of ionospheric characteristics and variations to a compact collection of relationships and tradeoffs. System designers and strategic planners with no specialized knowledge of the ionosphere could make effective use of such a model in deciding on site locations, operating frequencies, area coverage, safety margins, backup equipment required to insure a given level of performance, etc.

Although Air Force operations are worldwide, the most urgent and compelling model requirement is for the polar regions. The reasons are threefold: 1) Models of the mid-latitude ionosphere exist

and are quite adequate for most purposes; 2) models of the polar ionosphere are sketchy and inadequate, while ionospheric variations in the region are extreme and lack of knowledge thereof is acute; 3) increasing military operations at high latitude—in particular, the development of OTH (over-the-horizon) radars—urgently require better understanding of polar ionospheric conditions. In view of these factors, AFCRL has undertaken the development of a propagation-oriented Dynamic Polar Ionosphere Model intended to meet Air Force needs in the foreseeable future. The model is being developed with due consideration for the requirements of communications, aircraft navigation, geodesy, line-of-sight and backscatter radars, and detection of missile launches and nuclear explosions in the atmosphere. In its initial phases, however, it will be closely tied to the needs and the time schedule of the proposed 414L System.

Basically, the model will be an attempt to specify the polar ionosphere in statistical terms using data already in existence and incorporating the presently available knowledge of the physics of the region. Much of this information is qualitative in nature, and one of the major initial objectives will be its quantification insofar as is possible. A second major objective is the determination of the most effective use of existing data. Satellite observations have provided data from inaccessible regions and permit reasonably good estimates of ionospheric morphology to be formed; however, because of the altitude at which they were taken the data are not directly applicable to certain important propagation modes. On the other hand, ground-based observatories are too sparse to provide morphological information, but their data are more relevant to radio propagation conditions. Methods are being sought to adapt both types of data for inclusion in the model. Use will also be made of information available from high latitude verti-

cal incidence ionosondes for years of high (1958) and low (1964) solar activity; data from ground-based riometers are also being analyzed in statistical terms for inclusion in the model.

As this material is converted to usable form, preliminary models will be constructed, tested against suitable data and gradually refined. When a reasonably reliable statistical model has been achieved, actual propagation data from trans-polar paths will be used and comparison made with the propagation characteristics predicted by the model for similar geophysical conditions. The ray-tracing analysis procedure developed by the Ionospheric Physics Laboratory will be used in this aspect of the program.

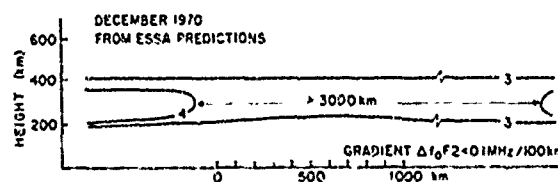
Because it is anticipated that operating problems will arise for which the statistical model is unsuitable, a parallel effort is underway to develop a real-time or instantaneous model of the polar ionosphere. This model will require that certain ionospheric properties be specified as nearly as possible in real time and will require a continuously monitoring observatory in the auroral zone—i.e., the Goose Bay Ionospheric Observatory. Both models are scheduled to be completed by January 1973.

Almost the entire program of the Ionospheric Physics Laboratory supports, directly or indirectly, the operational func-

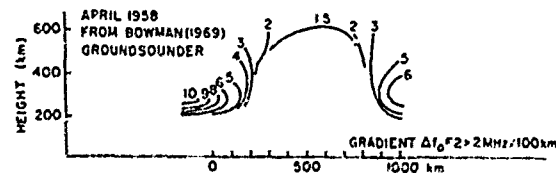
tions of the Air Force, so that even the results of basic or "pure" research find almost immediate application in the construction, modification or refinement of the models on which system designers depend for efficient planning.

Some of the support is in the form of routine information dissemination. The Air Weather Service (AWS), for example, receives a steady flow of data from AFCRL (riometer records, TEC measurements, solar patrol data, radio signatures and flare information, solar polarization measurements, notice of auroral and polar events, etc.), which it uses in formulating its DOD-wide predictions of ionospheric disturbances and their effects on systems operations. Moreover, AFCRL's ionospheric mapping program was developed in response to an expressed AWS need for a means of synoptically representing the ionosphere—a capability which could significantly improve operational forecasting of HF propagation conditions.

An initial step in the mapping program was the determination of how often the ionosphere must be sampled in order to produce usefully realistic maps. From successive electron density profiles, derived from vertical incidence ionograms taken by a network of ionosonde stations, temporal and spatial variability of the ionosphere can be assessed as a function of height. Such an assessment was made us-



Cross section of F-region mid-latitude trough based on monthly median data taken from ESSA predictions. Contours are in MHz. Because of the averaging techniques employed, the trough (region of ionization depletion) is barely visible.



A similar cross section based on ionograms taken in a single day. In contrast to the upper figure, the mid-latitude trough is pronounced.

ing data obtained at hourly intervals from mid-April through July 1970 at 16 stations on or near the North American continent. Both geomagnetically quiet and geomagnetically disturbed periods were included in the observations. Preliminary results indicate that for the mid-latitude ionosphere during undisturbed conditions one observation per hour is sufficient to specify 90-95 percent of the temporal variability, whereas during disturbed periods, the ionization varies so rapidly that observations at quarter-hour intervals are required.

The spatial variation of the ionosphere is currently under study. Using data from six of the ionosonde stations previously referred to, an attempt is being made to determine whether the correlation coefficient between data obtained at any two stations is a function of the distance between the stations. The first tentative results seem to corroborate this hypothesis.

Another form of support comes from wide adoption of AFCRL-developed methods and devices. The Auroral Oval Plotter, for example—a simple nomographic device which uses a transparent tracing of an auroral oval overlaid on a map of the high latitudes in geomagnetic coordinates—has been widely adopted by AWS, RADC, ESD, SAMSO, NASA, ESSA and in most major laboratories interested in auroral predictions or the auroral environment. In another example, Kwajalein and White Sands Missile Range, the Naval Weapons Center, the Space and Missile Test Center and the Air Force Satellite Control Facility, among others, routinely calibrate their antenna systems and check antenna parameters using methods developed by AFCRL as well as the 2695 and 1415 MHz solar flux density values supplied by the Sagamore Hill Observatory.

AFCRL's program on the physical chemistry of the E and F regions is in direct support of the NWET (Nuclear Weapons Effects Test) Program of the Defense Nuclear Agency (DNA). As part of the DNA

readiness-to-test program, the project's instrumentation and techniques must be continuously updated. The intense and rapidly changing ionization, the lower altitudes and the hostile environment in which the instrumentation is required to operate during tests demand techniques, probes and integrated payloads not utilized in geophysical research. Significant progress in the program resulted from the development of a technique and capability for testing the probes on small rockets in disturbed ionospheres, such as PCA events that simulate nuclear environments. The development of codes from PCA 69 experiments and their application to nuclear environments have already been mentioned. AFCRL is also contributing to DNA data on daily-occurring zones of auroral particle precipitation to aid in planning "input-output" experiments now in progress.

AFCRL's contributions toward the construction of accurate models have been repeatedly pointed out. Early in the development of over-the-horizon backscatter systems (OTH-B), the only models available to system planners were highly unrealistic, and unfortunately provided erroneous information in certain cases. In a recent study, using a preliminary model of the Arctic ionosphere, AFCRL researchers were able to evaluate the probability of detection (P_d) figures obtained from the averaged models and to point out their limitations and shortcomings. Subsequently, AFCRL performed a more realistic P_d study using current models. This study provided 414L with a more accurate P_d on which to base the development of the system. Ray tracing of the signals pointed up some of the problems which would be encountered. Additional studies resulted in a recommendation of a suitable site for the Polar Fox II experiment which is designed to investigate OTH-B problems.

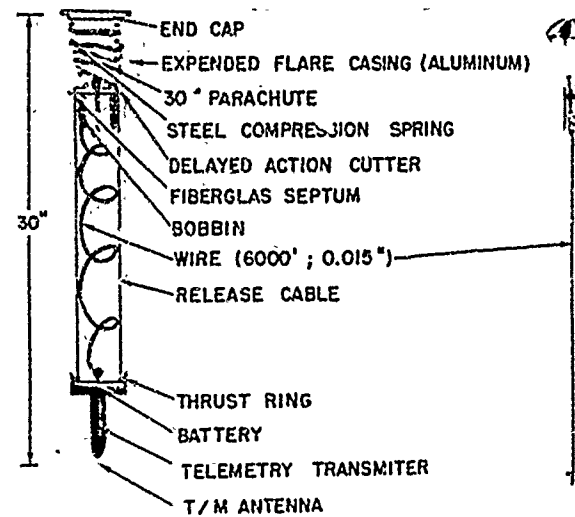
This fruitful use of a relatively crude (though the most accurate currently avail-

able) Arctic model not only emphasized the need for a more accurate and comprehensive version, but also provided valuable feedback influencing its format and enhancing its usefulness.

Further support of OTH-B systems is evidenced by the fact that many aspects of the Ionospheric Physics Laboratory's research program are oriented toward specific requirements of the 414L system. In connection with other OTH-B work, the NKC-135 will fly selected missions in Design System Verification Tests, with the goal of providing real-time radar propagation information for assessment by OTH systems operators.

AFCRL's involvement with missile and rocket launch problems originated when an early prediction that a rapidly rising rocket might initiate a lightning stroke was dramatically confirmed during the launch of Apollo 12 in November 1969. The prediction was based on previous AFCRL work which had proved that, under suitable conditions of electrification, full-scale cloud-to-ground lightning strokes can be initiated by thin steel wires rapidly paid out from grounded reels and carried to altitudes of less than 2000 feet by miniature rockets. It was reasoned that if a missile exhaust plume were conductive over a sufficiently large portion of its length it too might trigger a lightning stroke, with attendant damage to the missile.

A Laboratory Director's Fund project was initiated to evaluate the lightning threat to a missile and, if possible, to develop a capability for reducing the hazard by modifying the atmospheric electrification along the trajectory. One technique might be to deploy long wires along the planned trajectory to drain off dangerously high concentrations of electric charge, thus providing a "window" through which the missile can be launched, before the charge can again build up to a dangerously high level.



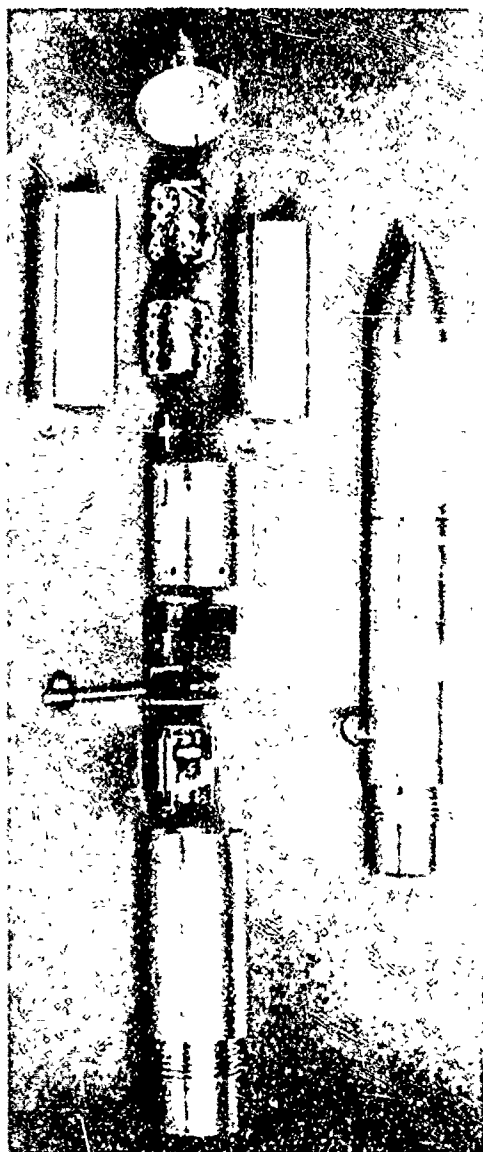
Air droppable capsules, such as illustrated here, will be used to modify atmospheric electrification by injecting long wires into thunderclouds.

Before the effectiveness of this (or any other) countermeasure can be evaluated, a statistical determination of the percentage of rocket launches which trigger lightning strokes must be made. Since it is not economically feasible to obtain this information by launching large missiles under different conditions of atmospheric electrification, long conducting wires will be used to simulate the rocket plumes. To inject these wires at the altitudes attained by thunderclouds (50,000 feet or more) a simple extension of the original experiment, using somewhat larger rockets, will not suffice. The higher velocities required generate higher aerodynamic drag forces which can exceed the strength of available materials.

Two alternative approaches were investigated. The first involved dispensing the wire gradually from a bobbin within the rocket, as the rocket flies. A preliminary design, with a cable of seven strands of #23 copper clad steel stored in the ogive section of a Little John rocket, was tested at White Sands Missile Range. The results showed it would be feasible to deploy sev-

eral thousand feet of wire by this method. The second approach involves dropping a canister from a rocket or high altitude plane. In the original design, the canister contained a spool holding 6000 feet of fine steel wire, a small parachute to slow the descent, and a telemetry transmitter to indicate actual lightning strikes. These TSAP (Thunder Storm Atmospheric Potential) devices fit into a standard dispenser for releasing illuminating flares from aircraft. Development tests of the devices were accomplished in April 1971 at the Joint Parachute Test Facility at El Centro, California. A field test program was conducted during August and September 1971 at Eglin AFB, Florida. The first rounds were dropped in clear air, and strong radar returns demonstrated that the wires had deployed. All other drops were made into clouds containing cells of precipitation located by weather radar. These cells were considered "possible thunderstorms" although there was no way of knowing if electrical activity was present. The radar returns from the wires in the clouds were masked by the returns from the clouds themselves, and it is thought that the telemetry signals may have been attenuated. The tests demonstrated that the system was mechanically feasible, but that more powerful and more stable transmitters, preferably at a lower frequency, would be desirable.

In a second generation design currently under development, a 1000-foot length of metalized Mylar tape is wound into a compact ball and stored in the nose of a small sounding rocket. When the rocket is fired and reaches the desired altitude, the ball is ejected. Aerodynamic forces rapidly slow and unwind the tape, thus introducing a long conducting filament in the cloud. It is hoped to be able to track the filament inside a thundercloud, using a VHF radar, since clouds are transparent to radio waves of these frequencies. Since the VHF radar is also capable of detecting the ionized



Two metalized Mylar tapes wound into shapes to fit into the rocket; these 1000 foot tapes will be deployed by aerodynamic drag.

paths produced by lightning strokes, the sudden appearance of such a signal simultaneously with the disappearance of the filament return would provide evidence of a triggered lightning stroke, avoiding the necessity for using a telemetry transmitter. Tests of both the ball ejection design,

and the VHF radar tracking technique, are planned in calendar year 1972.

The application of wire-derived data to the evaluation of the missile plume hazard requires knowledge of the effective conducting length of the plumes of various large rocket motors. As the variation of quasi-dc electrical parameters along typical rocket plumes was virtually unknown, a conductivity meter and a breakdown electric field device were developed to obtain experimental data. This equipment was mounted on Atlas and Minuteman launch pads at Vandenberg AFB, California, during tests conducted from October 1970 through June 1971, and the conductivity meter was installed on the launch umbilical tower and operated during the launch of Apollo 15 in July 1971. Conductivity and breakdown electric field values near the ground were obtained as functions of missile altitude, and were converted to first-order estimates of effective conducting length, using a simple electrostatic model for the action of the plume ionization.

A corollary problem in the lightning hazard evaluation work is the detection and measurement of the degree of electrification in thunderstorm clouds. Traditionally, the ambient electrostatic field strength is measured on the ground in a number of locations by so-called "field mills" and the data are analyzed to try to determine an effective charge center. However, to resolve the position and magnitude of individual charge centers within clouds requires a detailed knowledge of the field on the ground and a very large number of field mills.

In a possible new method, based on the theory that low-level electrical discharge activity occurring in cloud charge centers produces VHF radio noise, AFCRL scientists, in a joint project with NASA, utilized directional antennas at Kennedy Space Center during August 1971 to passively detect radio emissions from storm clouds

in the 100 to 1000 MHz spectral region. These tests demonstrated that VHF/UHF radio noise from clouds consists of an irregular series of very short pulses, extending over a considerable time period. The noise was detected at ranges of 50 miles or more, and can be mapped in two dimensions with a scanning antenna. In a tornado-producing thunderstorm, some of the sources responsible for the noise appear to have been at very high altitudes. Further exploration of this method is planned for the late summer of 1972. Two directional antennas spaced several miles apart will be used to try to locate charge centers in three dimensions. If successful, the technique could be used for storm tracking and warning purposes.

JOURNAL ARTICLES JULY 1970 - JUNE 1972

AARONS, J.

HF Auroral Backscatter and the Scintillation Boundary and Satellite Scintillations in the High Latitude F-Layer Irregularity Region
AGARD Conf. Proc. #97 on Rad. Prop. in the Arctic (January 1972)

AARONS, J., and ALLEN, R. S.

Scintillation Boundary During Quiet and Disturbed Magnetic Conditions
J. of Geophys. Res., Vol. 76, No. 1 (1 January 1971)

AARONS, J., and MULLANEY, H., PAPAGIANNIS, M. D
(Boston Univ., Mass.)

Quasi Periodic Fluctuations in the Scintillation Index Obtained on 8 March 1970 from Four Synchronous Satellites
Upper Atm. Geophys. Rpt. No. 12, NOAA, Boulder, Colo. (April 1971)

AARONS, J., MULLEN, J. P., WHITNEY, H. E., and STEENSTRUP, F. (Dan. Met. Inst., Copenhagen, Denm.)
Seasonal, Diurnal, and Magnetic Dependence of Ionospheric Scintillations at 64° Invariant Latitude
Conf. Rec., Jt. Satel. Stud. Gp. Mtg., Florence, Italy (October 1971)

- AARONS, J., MULLEN, J. P., and ZUCKERMAN, L. H.
*Scintillation Effects on Satellite Signals
 Observed Through the Polar Ionosphere*
*J. of the Franklin Inst., Vol. 290, No. 3 (September
 1970)*
- AARONS, J., WHITNEY, H. E., and ALLEN, R. S.
Global Morphology of Ionospheric Scintillations
Proc. of the IEEE, Vol. 59, No. 2 (February 1971)
- ABMED, M. (Regis Coll., Weston, Mass.), and
 SAGALYN, R. C.
*Thermal Positive Ions in the Outer Ionosphere
 and Magnetosphere from the OGO-1 Satellite*
J. of Geophys. Res., Vol. 77, No. 7 (1 March 1972)
- BEWERSDORFF, A. B. (Regis Coll., Weston, Mass.),
 and SAGALYN, R. C.
*Enhancements of Charged Particle Densities
 Above the Polar Cap and Their Relation to
 Geomagnetic Activity*
*Sp. Res. X (Proc. of 12th Plen. Mtg. of COSPAR,
 Prague, Czech., May 1969) (1970)*
- BUCHAU, J., WHALEN, J. A., and AKASOFU, S. I.
 (Univ. of Alaska)
On the Continuity of the Auroral Oval
J. of Geophys. Res., Vol. 75, No. 34 (1 December 1970)
- CASTELLI, J. P.
Sagamore Hill Radio Observatory
*Bull. of the Am. Astronom. Soc. (Obsv. Rpt.,
 1969-1970), Vol. 3, No. 1 (1 January 1971)*
Fixed Frequency Solar Observations
The Reflector, Vol. 19, No. 7 (March 1971)
*Report of Observatories, Sagamore Hill
 Radio Observatory, AFCRL*
Bull. of the Am. Astronom. Soc., Vol. 4, No. 1 (1972)
- CASTELLI, J. P., and AARONS, J.
Sun
 1970 McGraw-Hill Yrbk. of Sci. and Tech.
- CASTELLI, J. P., GUIDICE, D. A., and JONES, C.,
 STRAUSS, F. M., PAPAGIANNIS, M. D. (Boston Univ.,
 Mass.)
*On the Classification, Distribution, and
 Interpretation of Microwave Solar Burst
 Spectra*
Dig. of 1970 G-AP Intl. Symp. (September 1970)
- CASTELLI, J. P., and RICHARDS, D. W., CAPT.
*Observations of Solar Bursts at Microwave
 and Extreme Ultraviolet Wavelengths*
J. of Geophys. Res., Vol. 76, No. 34 (1 December 1971)
- CONLEY, T. D., and DRAPER, J. S., JARVINEN, P. V.
 (Sanders Assoc., Nashua, N. H.)
*Analysis of Radar Return from Turbulent
 High Altitude Rocket Exhaust Plumes*
AIAA J., Vol. 8 (September 1970,
- CONLEY, T. D., and HEGBLOM, E. R. (Sp. Data Anal.
 Lab., Boston Coll., Mass.)
*Successive Measurements of Positive Ion
 Concentrations During a PCA Event*
*Trans. of Am. Geophys. Un., Vol. 52, No. 11
 (November 1971)*
- CROOM, D. L.
*19 Gigahertz 1.58 Centimeter Solar Radio
 Bursts as Indicators of Proton Events*
J. of Geophys. Res., Vol. 75, No. 34 (December 1970)
*71 GHz (4.2 mm) Solar Radio Bursts in
 the Period July 1967 to December 1969*
Sol. Phys., Vol. 15, No. 2 (December 1970)
*Solar Microwave Bursts as Indicators of
 the Intensity of Solar Proton Emissions*
Astrophys. Lett., Vol. 7 (1971)
*Predicting the Intensity of Solar Proton
 Events from the Time Characteristics
 of Solar Microwave Bursts*
Sol. Phys., Vol. 19 (1971)
*Solar Microwave Bursts as Indicators of
 the Occurrence of Solar Proton Emission*
Sol. Phys., Vol. 19 (1971)
Solar Millimeter Bursts and Proton Events
Nature, Vol. 229 (1 February 1971)
- ELKINS, T. J., and PAPAGIANNIS, M. D. (Boston Univ.,
 Mass.)
Dispersive Motions of Ionospheric Irregularities
J. of Atm. and Terres. Phys., Vol. 32, No. 3 (1970)
- GASSMANN, G. J.
*(U) On the Specification of Instantaneous Arctic
 Ionospheres*
*Proc. of OHD Tech. Rev. Mtg., Stanford Res. Inst.,
 Menlo Pk., Calif., Vol. 1 (April 1971)*
Recent Airborne IR Results
*Reaction Rate Data #29, DASIAC Cr. (September
 1971)*
High Latitude Ionosphere
 1972 McGraw-Hill Yrbk. of Sci. and Tech.
On Modelling the Arctic Ionosphere
*AGARD Conf. Proc. #97 on Rad. Prop. in the
 Arctic (January 1972)*
- GASSMANN, G. J., and WAGNER, R. A.
Visible Light Flux Affecting the D-Layer
Rad. Sci., Vol. 7, No. 5 (1972)
- GUIDICE, D. A., and CASTELLI, J. P.
*The Use of Extraterrestrial Radio Sources
 in the Measurement of Antenna Parameters*
*IEEE Trans. on Aeroesp. and Elect. Sys., Vol. AES-7,
 No. 2 (March 1971)*
- HARRISON, R. P., HECKSCHER, J. L., and LEWIS, E. A.
*Helicopter Observations of VLF Radio Waves Over
 Certain Mountains and Shorelines*
J. of Atm. and Terres. Phys., Vol. 33 (January 1971)

- HOROWITZ, S.
Calculated Effects of Electron Density Irregularity on Propagation of 100 kHz Radio Waves
 AGARD Conf. Proc. No. 33 (July 1970)
- Amplitude of Phase Stability of LF Waves*
 RADC Pub., LORIG Subcom. to Invest. Eff. on Loran Envir. (23 April 1971)
- The Reflection of Radio Waves by the Lower Ionosphere at Nighttime*
 Proc. of the IEEE, Vol. 18, No. 11 (November 1971)
- HOROWITZ, S., and THOMAS, L. (Rad. and Sp. Res. Ctr., Min. of Sci., Slough, Eng.)
The Ionospheric Absorption of Downgoing Whistler Waves During Nighttime
 J. of Atm. and Terres. Sci., Vol. 33 (1971)
- KALISCH, R. B., COL.
Air Force Polar Research
 The Navigator, Vol. 18, No. 1 (1970)
- KLOBUCHAR, J. A., ET AL
The Ionospheric Storm of 8 March 1970
 J. of Geophys. Res., Vol. 72, No. 25 (1 September 1971)
- KLOBUCHAR, J. A., and MENDILLO, M. (Boston Univ., Mass.)
Model Studies of the Conversion of Faraday Rotation Measurements from a Geostationary Satellite to Total Electron Content
 Conf. Rec., Jt. Satel. Stud. Gp. Mtg., Florence, Italy (October 1971)
- MAYFIELD, E. B., and CHAPMAN, G. A. (Aerosp. Corp., Calif.), and STRAKA, R. M.
Eclipse of Radio Emission on 7 March 1970 at 10 Cm Wavelength from the Active Region Associated with McMath Plage 10618
 Sol. Phys., Vol. 21, No. 2 (December 1971)
- MENDILLO, M. (Boston Univ., Mass.), and KLOBUCHAR, J. A.
Low Elevation Angle Measurements of Total Electron Content Taken from Thule, Greenland
 Conf. Rec., Jt. Satel. Stud. Gp. Mtg., Florence, Italy (October 1971)
- MENDILLO, M., PAPAGIANNIS, M. D. (Boston Univ., Mass.), and KLOBUCHAR, J. A.
Total Electron Content Measurements During the March 7-11, 1970 Period
 World Data Ctr. A, Upper Atm. Geophys., Data on Sol.-Geophys. Act. Assoc. with the Maj. Geomag. Storm of 8 March 1970, Rpt. UAG-12, Pt. II (April 1971)
- MULLANEY, H., PAPAGIANNIS, M. D. (Boston Univ., Mass.), and AARONS, J.
Quasi-Periodic Fluctuations in the Scintillation Index Obtained on 8 March 1970 from Four Synchronous Satellites
 World Data Ctr. A, Upper Atm. Geophys., Data on Sol.-Geophys. Act. Assoc. with the Maj. Geomag. Storm of 8 March 1970, Rpt. UAG-12, Pt. II (April 1971)
- MULLEN, J. P.
Scintillation Observed During the ATS VHF Test of 11-12 November 1969
 ATS Mo. Techn. Data Rpt., NASA Goddard Sp. Flt. Ctr., Vol. 8 (December 1970)
- Ionospheric Studies in the Panama Canal Zone*
 Conf. Rec., Jt. Satel. Stud. Gp. Mtg., Florence, Italy (October 1971)
- MULLEN, J. P., and BUERKLE, C. H., JR. (N. M. State Univ., Lae Cruces, N. M.)
A Short Note on Polar Cap Scintillation Observed at Thule Using the Naval Navigation Satellite System NNSS
 Conf. Rec., Jt. Satel. Gp. Mtg., Florence, Italy (October 1971)
- PAPAGIANNIS, M. D., MENDILLO, M. (Boston Univ., Mass.), and KLOBUCHAR, J. A.
Simultaneous Storm-Time Increase of the Ionospheric Total Electron Content and the Geomagnetic Field in the Dusk Sector
 Planet. and Sp. Sci., Vol. 19 (1971)
- PFISTER, W.
The Wave-Like Nature of Inhomogeneities in the E-Region
 J. of Atm. and Terres. Phys., Vol. 33, No. 7 (July 1971)
- PIKE, C. P.
Universal Time Control of the South Polar F-Layer During the I. G. Y.
 J. of Geophys. Res., Vol. 75, No. 25 (September 1970)
A Comparison of the North and South Polar F-Layers
 J. of Geophys. Res., Vol. 76, No. 28 (October 1971)
A Latitudinal Survey of the Daytime Polar F-Layer
 J. of Geophys. Res., Vol. 76, No. 31 (November 1971)
- RAO, L. D. V. (Regis Coll., Weston, Mass.), and SAGALYN, R. C.
OGO-III Observations of the Thermal Plasma Variations During Magnetic Storms
 Trans. of Am. Geophys. Un. Mtg. (December 1970)
- RICHARDS, D. V., CART, and STRAKA, R. M.
Polarization Maps of the Sun at 7.8 GHz
 Nat. Phys. Sci., Vol. 233, No. 40 (4 October 1971)

- RUSH, C. M.
The Behavior of the F Region Above North America During the Magnetic Disturbance of 28 May 1970
 J. of Geophys. Res., Vol. 77, No. 4 (February 1972)
- RUSH, C. M., and ST. JOHN, D. E., VENKATESWARAN, S. V. (Univ. of Calif., Los Angeles, Calif.)
A Unified Description of the Tidal Effects in F_1 , F_2
 Rad. Sci., Vol. 5, No. 12 (December 1970)
- SAGALYN, R. C., and AHMED, M. (Regis Coll., Weston, Mass.)
Thermal Ions in the Dayside Auroral Zone Measured on ISIS-I
 Trans. of the Am. Geophys. Un., Vol. 52, No. 11 (November 1971)
- SAGALYN, R. C., and BEWERSDORFF, A. B. (Regis Coll., Weston, Mass.)
Evidence for an Evening Ionization Anomaly Within the Plasmasphere
 Sp. Res. XI (Proc. 18th Plen. Mtg. of COSPAR, Leningrad, USSR, May 1970) (1971)
- SAGALYN, R. C., and WAND, R. H. (Univ. of Sydney, Sydney, Aust.)
Daytime Rocket and Thomson Scatter Studies of the Lower Ionosphere
 J. of Geophys. Res., Vol. 76, No. 16 (20 June 1971)
- SAGALYN, R. C., and WILDMAN, P. J. L.
Injun V Observations of Low Energy Electrons at High Latitudes
 Trans. of Am. Geophys. Un. (December 1970)
- SLACK, F. F.
Quasiperiodic Scintillation in the Ionosphere
 J. of Atm. and Terres. Phys., Vol. 34 (1972)
- STRAKA, R. M., and CASTELLI, J. P.
Spectral Radio Observations of a Solar Eclipse
 Sol. Phys., Vol. 21, No. 2 (December 1971)
- TOMAN, K.
Frequency Variations of an Oblique 5 MHz Ionospheric Transmission
 AGARD Conf. Proc. No. 33 (July 1970)
Relationship Between Geomagnetic Index and HF Doppler Fluctuations
 Trans. of Am. Geophys. Un., Vol. 51, No. 4 (April 1970)
- TOMAN, K., CORMIER, R. J., and CORBETT, J. J.
Spatial Correlation of Auroral Radio Absorption
 AGARD Conf. Proc. No. 97 on Rad. Prop. in the Arctic (January 1972)
- TOMAN, K., and LORENTZEN, A. H.
1970 Solar Eclipse Project No. 34-F-12.00; Summary of Preliminary Results
 Sol. Eclipse 1970 Bull. F (1970)
- TOMAN, K., LORENTZEN, A. H., O'BRIEN, J. V., and WIZELMAN, L. A., JR.
Generation of Idealized Surfaces for the Simulation of Ionospheric Propagation Conditions
 Sum. of Pap., ISAP, Sendai, Jap. (1971)
- ULWICK, J. C.
Eclipse Rocket Measurements of Charged Particle Concentrations
 J. of Atm. and Terres. Phys., Vol. 34 (1972)
- WAGNER, R. A., and PIKE, C. P.
A Discussion of Arctic Ionograms
 AGARD Conf. Proc. No. 97 on Rad. Prop. in the Arctic (January 1972)
- WHALEN, J. A., BUCHAU, J., and WAGNER, R. A.
Airborne Ionospheric and Optical Measurements of Noontime Aurora
 J. of Atm. and Terres. Phys., Vol. 33, No. 4 (1971)
- WHITNEY, H. E.
Technical Note on the Conversion of Statistics on Occurrence of Scintillation Indices to Cumulative Distribution of Signal Amplitudes
 ATS Mo. Techn. Data Rpt., NASA Goddard Sp. Fit. Ctr., Vol. 8 (December 1970)
- WHITNEY, H. E., and RING, W. F.
Dependency of Scintillation Fading of Oppositely Polarized VHF Signals
 IEEE Trans. on Ant. and Prop., Vol. AP-19, No. 1 (January 1971)
- PAPERS PRESENTED AT MEETINGS JULY 1970 - JUNE 1972**
- AARONS, J.
Ionospheric Limitations on Performance on VHF Navigation and Communication Satellite Systems
 AGARD Lect. Ser. No. 41 on Appl. of Prop. Data to VHF Satel. Comm. and Nav. Sys., Eindhoven, The Netherlands, and Ottawa, Can. (June/July 1970)
The Oval F-Layer Irregularity Region
 Natl. Fall Mtg. of the Am. Geophys. Un., San Francisco, Calif. (7-10 December 1970)

- Satellite Scintillations in the High Latitude F-Layer Irregularity Region and HF Auroral Backscatter and the Scintillation Boundary*
AGARD Mtg. on Rad. Prop. in the Arctic, Max Planck Inst. fuer Aeron., Lindau/Harz, Ger. (13-17 September 1971)
- The Polar and Auroral Irregularity Regions*
Fall Ann. Mtg. of the Am. Geophys. Un., San Francisco, Calif. (6-9 December 1971)
- Amplitude Fluctuations of Satellite Beacon Signals*
Sem., Aerosp. Corp., Los Angeles, Calif. (14 December 1971)
- AARONS, J., MULLEN, J. P., WHITNEY, H. E., and STRENNSTRUP, F. (Dan. Met. Inst., Copenhagen, Den.)
Seasonal, Diurnal, and Magnetic Dependence of Ionospheric Scintillations at 64° Invariant Latitude
Jt. Satel. Stud. Gp. Mtg., Florence, Italy (4-8 October 1971)
- AARONS, J., WHITNEY, H. E., and ALLEN, R. S.
World-Wide Morphology of Scintillations
AGARD Lect. Ser. No. 41 on Appl. of Prop. Data to VHF Satel. Comm. and Nav. Sys., Eindhoven, The Netherlands, and Ottawa, Can. (June/July 1970)
- AHMED, M. (Regis Coll., Weston, Mass.) and SAGALYN, R. C.
Thermal Positive Ions in the Dayside Polar Cusp Measured on the ISIS 1 Satellite
15th COSPAR Mtg., Madrid, Sp. (10-24 May 1972)
- BASU, S.
Spectral Characteristics of Solar Radio Bursts Associated with the Emission of Energetic Electrons from the Sun
1972 Am. Astronom. Soc. Mtg., Univ. of Md., Coll. Pk., Md. (4-6 April 1972)
- BASU, S., and AARONS, J.
(U) Auroral Clutter (F and F-layer) and the Irregularity Region
OHL Techn. Rev. Mtg., Nav. Postgrad. Sch., Monterey, Calif. (3-4 May 1972)
- BUCHAU, J.
Continuity of the Auroral Oval Observed by Airborne Radio and Optical Measurements
52nd Ann. Am. Geophys. Un. Mtg., Wash., D. C. (12-16 April 1971)
- BUCHAU, J., GASSMANN, G. J., PIKE, C. P., WAGNER, R. A., and WHALEN, J. A.
Precipitation Patterns in the Arctic Ionosphere Determined from Airborne Observations
- IUGG 15th Gen. Assen. Mtg., Moscow State Univ., Moscow, USSR (30 July-14 August 1971)
- BUCHAU, J., PIKE, C. P., and WHALEN, J. A.
Ionospheric and Optical Observations in the Evening Sector of the Oval
53rd Ann. Mtg. of the Am. Geophys. Un., Wash., D. C. (17-21 April 1972)
- BUCHAU, J., WAGNER, R. A., and WHALEN, J. A.
Continuity of the Auroral Oval Observed by Airborne Radio and Optical Measurements
52nd Ann. Am. Geophys. Un. Mtg., Wash., D. C. (12-16 April 1971)
- CASTELLI, J. P.
Spectral Classification of Microwave Bursts
14th Gen. Assm. of the IAU, Brighton, Eng. (18-27 August 1970)
- Fixed Frequency Solar Observations*
Jt. Mtg. of the Ant. and Prop. Gp. Chap. of the Am. Met. Soc., GT&E Labs., Waltham, Mass. (16 March 1971)
- CASTELLI, J. P., and GUIDICE, D. A.
The Distribution of Peak Flux-Density Spectra of Solar Radio Bursts
1972 Am. Astronom. Soc. Mtg., Univ. of Md., Coll. Pk., Md. (4-6 April 1972)
- CASTELLI, J. P., GUIDICE, D. A., and JONES, C., PAPAGIANNIS, M. D. (Boston Univ., Mass.)
The Radio Events Associated with the Polar Cap Absorption Event of 2 November 1969
COSPAR Symp. on Nov. 1969 Sol. Particle Event, Boston Coll., Chestnut Hill, Mass. (16-18 June 1971)
- CONLEY, T. D.
Positive Ion Concentrations in the Lower D Region During a PCA Event Measured by a Rocket-Borne Gerdien Condenser
COSPAR Symp. on Nov. 1969 Sol. Particle Event, Boston Coll., Chestnut Hill, Mass. (16-18 June 1971)
- CONLEY, T. D., and HEGBLOM, E. R. (Boston Coll., Chestnut Hill, Mass.)
Successive Measurements of Positive Ion Concentrations During a PCA Event
Fall Ann. Mtg. of the Am. Geophys. Un., San Francisco, Calif. (6-9 December 1971)
- CORMIER, R. J.
PCA Behavior as Observed on Riometers
COSPAR Symp. on Nov. 1969 Sol. Particle Event, Boston Coll., Chestnut Hill, Mass. (16-18 June 1971)
- ELKINS, T. J.
High Resolution Measurements of Ionospheric Refraction

- 14th Ann. COSPAR Mtg., Seattle, Wash. (17 June-2 July 1971)
- (U) *A Model of Auroral Substorm Absorption and (U) Use of Magnetic Indices in Predicting High Latitude OHD Radar Performance*
OHD Techn. Rev. Mtg., Nav. Postgrad. Sch., Monterey, Calif. (3-4 May 1972)
- FIELDS, V. C.
Self-Contained Automatic Transmitter Experiments
Long Rad. Wave Prop. Discus. Gp. Mtg., Stanford Res. Inst., Palo Alto, Calif. (18-20 January 1971)
- GAßMANN, G. J.
Discussion on Cooperation of U. S. Propagation Physicists with Foreign Groups
Wkg. Pan. N-6 Symp. of Techn. Coop. Prog. (TTCP) (15 December 1970)
On the Specification of Instantaneous Arctic Ionospheres
AFSC-ARPA OHD Techn. Rev. Mtg., Arlington, Va. (17-18 March 1971)
- ARPA Experiment at Boulder
URSI Mtg., Wash., D. C. (8-10 April 1971)
Developing an Empirical Model of the Arctic Ionosphere
Conf. on Theoret. Ionos. Models, Penn. State Univ., University Pa., Pa. (14-16 June 1971)
On Modelling the Arctic Ionosphere
AGARD Mtg. on Rad. Prop. in the Arctic, Max Planck Inst. fuer Aeron., Lindau/ Harz, Ger. (13-17 September 1971)
- GAßMANN, G. J., and BUCHAU, J.
(U) *Analysis of Simultaneous Polar Fox II Backscatter and Ionospheric Sounding Data*
OHD Techn. Rev. Mtg., Nav. Postgrad. Sch., Monterey, Calif. (3-4 May 1972)
- GAßMANN, G. J., and PIKE, C. P.
Information Exchange on Arctic Ionospheric Research
Rad. and Elect. Div. of the Natl. Res. Council of Can., Comm. Res. Ctr., Ott., Can. (24-25 February 1971)
- GRIEDER, W. F., and BURT, D. A. (Utah State Univ., Logan, Utah)
Rocket Measurements of Production and Ionization at Thule, Greenland, During a PCA Event
15th COSPAR Mtg., Madrid, Sp. (10-24 May 1972)
- HARVEY, R. B.
Possibilities of Detecting and Measuring Thunderstorm Electrification
NASA Lightn. Comm. Mtg., Kennedy Sp. Ctr., Fla. (4 May 1971)
- HARVEY, R. B., LEWIS, E. A., and KOSSEY, P. A.
Rocket Measurements of TM-VLF Altitude Profiles
Sub-LF Downlink Satel. Comm. Conf., U. S. Nav. Res. Lab., Wash., D. C. (6-9 June 1972)
- HECKSCHER, J. L., and PAGLIARULO, R. P.
Measurement of Missile Plume Conductivity and Dielectric Breakdown
NASA Lightn. Comm. Mtg., Kennedy Sp. Ctr., Fla. (4 May 1971)
- KLOBUCHAR, J. A.
Total Electron Content of the Ionosphere
ESD/AFCRL Sci. & Eng. Mtg., L. G. Hanscom Fld., Mass. (3 November 1970)
Introduction to VHF Satellite Navigation and Communications Systems and World-Wide Morphology of Total Electron Content
AGARD Lect. Ser. No. 41 on Appl. of Prop. Data to VHF Satel. Comm. and Nav. Sys., Eindhoven, The Netherlands, and Ott., Can. (June/July 1970)
- KLOBUCHAR, J. A., and ALLEN, R. S.
A First-Order Prediction Model of Total-Electron-Content Group Path Delay for a Midlatitude Ionosphere
ESD/AFCRL Sci. & Eng. Mtg., L. G. Hanscom Fld., Mass. (3 November 1970)
A Simple Analytic Model of Midlatitude Equivalent Slab Thickness
Natl. Fall Mtg. of Am. Geophys. Un., San Francisco, Calif. (7-10 December 1970)
- KLOBUCHAR, J. A., and KIDD, W. C.
A Comparison of Total Electron Content Determined by the Differential Doppler and the Faraday Effects Using Radio Signals from a Geostationary Satellite
Symp. on the Future Appl. of Satel. Beacon Meas., Graz, Aus. (29 May-2 June 1972)
- KLOBUCHAR, J. A., and MENDILLO, M. J. (Boston Univ., Mass.)
Faraday Rotation of VHF Signals from Geostationary Satellites
1971 USNC/URSI-IEEE Spring Mtg., Wash., D. C. (8-10 April 1971)
Model Studies of the Conversion of Faraday Rotation Measurements from a Geostationary Satellite to Total Electron Content
Jt. Satel. Stud. Gp. Mtg., Florence, Italy (4-8 October 1971)
- LEWIS, E. A.
Lightning Strokes to In-Flight Missiles
SAMSO/AFCRL Coord. Conf., Los Angeles, Calif. (1 July 1970)

- Nonlinear Differential Equations for Ionic Motion and High Velocity Spark Gap Experiments*
NASA Lightn. Comm. Mtg., Kennedy Sp. Ctr., Fla.
(4 May 1971)
- MATSOUKAS, D., PAPAGIANNIS, M. D. (Boston Univ., Mass.), and AARONS, J., KLOBUCHAR, J. A.
Sudden Increases of Ionospheric Total Electron Content in Solar Flare Events
1971 USNC/URSI-IEEE Spring Mtg., Wash., D. C.
(8-10 April 1971)
- MENDILLO, M., (Boston Univ., Mass.), and KLOBUCHAR, J. A.
Low Elevation Angle Measurements of Total Electron Content Taken from Thule, Greenland
Jt. Satel. Stud. Gp. Mtg., Florence, Italy (4-8 October 1971)
- MULLEN, J. P.
Ionospheric Studies in the Panama Canal Zone
Jt. Satel. Stud. Gp. Mtg., Florence, Italy
(4-8 October 1971)
- MULLEN, J. P., and BUERKLE, C. H., Jr. (N. M. State Univ., Las Cruces, N. M.)
A Short Note on Polar Cap Scintillation Observed at Thule Using the Naval Navigation Satellite System NNSS
Jt. Satel. Stud. Gp. Mtg., Florence, Italy (4-8 October 1971)
- PFISTER, W.
The Wavelike Structure in the E-Region as Deduced from Drift Experiments
1971 USNC/URSI-IEEE Spring Mtg., Wash., D. C.
(8-10 April 1971)
- PIKE, C. P.
A Latitudinal Survey of the Daytime Polar F-Layer
52nd Ann. Am. Geophys. Un. Mtg., Wash., D. C.
(12-16 April 1971)
Magnetic Control of the Polar-Cusp F Layer
53rd Ann. Mtg. of the Am. Geophys. Un., Wash., D. C. (17-21 April 1972)
- RASMUSSEN, J. E., KOSSEY, P. A., and LEWIS, E. A.
Preliminary Report of High-Resolution VLF Pulse Ionosounder Measurements at the Geomagnetic Equator
Long Rad. Wave Prop. Symp., U. S. Nav. Res. Lab., Wash., D. C. (25-27 April 1972)
- RASMUSSEN, J. E., LEWIS, E. A., and KOSSEY, P. A.
Preliminary Data on the VLF Reflection Properties of the Lower Ionosphere Obtained with a High Resolution Pulse Technique

- Long Rad. Wave Prop. Symp., Inst. for Telecomm. Sci., Boulder, Colo. (14-15 January 1970)
- RICHARDS, D. W., CAPT.
Timing of Pulsar NP0527
Symp. on Intl. Astronom. Un., Manchester, Eng.
(8-7 August 1970)
- RICHARDS, D. W., CAPT., and STEAKA, R. M.
Solar Polarization Mapping at 7.8 GHz
135th Mtg. of the Am. Astronom. Soc., Univ. of Mass., Amherst, Mass. (24-27 August 1971)
- RICHMOND, A. D., and SCHIELDG, J. P., VENKATESWARAN, S. V. (Univ. of Calif., Los Angeles)
On the North-South Asymmetry of Sq Currents
53rd Ann. Mtg. of the Am. Geophys. Un., Wash., D. C. (17-21 April 1972)
- RUSH, C. M.
A Synoptic View of the Temporal and Spatial Variation of the Electron Density Above North America
1971 USNC/URSI-IEEE Spring Mtg., Wash., D. C. (8-10 April 1971)
- SAGALYN, R. C., and AHMED, M. (Regis Coll., Weston, Mass.)
Thermal Ions in the Dayside Auroral Zone Measured on ISIS-1
Fall Ann. Mtg. of the Am. Geophys. Un., San Francisco, Calif. (6-9 December 1971)
- SAGALYN, R. C., and RAO, L. D. V. (Regis Coll., Weston, Mass.)
OGO III Observations of the Thermal Plasma Variations During Magnetic Storms
Natl. Fall Mtg. of the Am. Geophys. Un., San Francisco, Calif. (7-10 December 1970)
- SAGALYN, R. C., SMIDY, M., and AHMED, M. (Regis Coll., Weston, Mass.)
Topside Polar Cap During November 1969 Proton Event
COSPAR Symp. on Nov. 1969 Sol. Particle Event, Boston Coll., Chestnut Hill, Mass. (16-18 June 1971)
ISIS-I Measurements of the Longitudinal and Temporal Behavior of the Plasmapause
Spring Ann. Mtg. of the Am. Geophys. Un., Wash., D. C. (12-16 April 1972)
- SAGALYN, R. C., and WILDMAN, P. J.
Injun V Observations of Low Energy Electrons at High Latitudes
Natl. Fall Mtg. of Am. Geophys. Un., San Francisco, Calif. (7-10 December 1970)
- SALES, G. S., and BIBL, K. (Lowell Tech. Inst. Res. Fdn., Lowell, Mass.), VARGAS-VILA, R. (Analyt. Sys., Inc., Burlington, Mass.)

A Digital Integrating Low Frequency High Power Solid State Sounder
USNC/URSI Spring Mtg., Wash., D. C.
(8-10 April 1971)

SANDOCK, J. A.

Ion Measurements Made by Collapsing the Space Charge Sheath on a Spherical Rocket Probe

52nd Ann. Am. Geophys. Un. Mtg., Wash., D. C.
(12-16 April 1971)

Preliminary Retarding Potential Measurements on Black Brant Rockets and Rocket-Borne Daytime Charged Particle Measurements on 3 November 1969

COSPAR Symp. on Nov. 1969 Sol. Particle Event, Boston Coll., Chestnut Hill, Mass. (16-18 June 1971)

STRAKA, R. M., and CASTELLI, J. P.

Spectral Radio Observations of a Solar Eclipse

14th Ann. COSPAR Mtg., Seattle, Wash.
(17 June-2 July 1971)

STRAKA, R. M., RICHARDS, D. W., CAPT., and ARORA, K. K. (Boston Univ., Mass.)

Polarization Scans of Active Regions at 3.8 Cm
1972 Am. Astronom. Soc. Mtg., Univ. of Md., Coll. Pk., Md. (4-6 April 1972)

TOMAN, K.

Morphological Features of Auroral Radio Absorption

1972 USNC/URSI-IEEE Spring Mtg., Wash., D. C.
(13-15 April 1972)

TOMAN, K., CORMIER, R. J., and CORBETT, J. J.

Spatial Correlation of Auroral Radio Absorption
AGARD Mtg. on Rad. Prop. in th. Arctic, Max Planck Inst. fuer Aeron., Lindau/Harz, Ger. (13-17 September 1971)

TOMAN, K., LORENTZEN, A. H., ET AL

Generation of Idealized Surfaces for the Simulation of Ionospheric Propagation Conditions

1971 Intl. Symp. on Ant. and Prop., Tohoku Univ., Sendai, Jap. (1-3 September 1971)

ULWICK, J. C.

Polar Cap Research Studies (Invited Paper)
Colloq., Utah State Univ., Logan, Utah
(15 September 1970)

Ionospheric Measurements During Polar Cap Absorption Events

Symp. on Outstanding Prob. of Rad./Rad. Wave Prop. in the Nuc. Envmt., Wash., D. C.
(10 December 1970)

Mesospheric Nitric Oxide Concentrations During a PCA

52nd Ann. Am. Geophys. Un. Mtg., Wash., D. C.
(12-16 April 1971)

Discussion of Black Brant Rocket Electron and Ion Density Results and Comparison of Black Brant Rocket Measurements of Charged Particle Densities During Solar Particle Events

COSPAR Symp. on Nov. 1969 Sol. Particle Event, Boston Coll., Chestnut Hill, Mass. (16-18 June 1971)

Eclipse Rocket Measurements of Charged Particle Concentrations

COSPAR Symp., Seattle, Wash. (21-25 June 1971)

Operation PCA 69 - An Investigation of the Solar Particle Event of 2 November 1969

DASA High Alt. Nuc. Eff. Symp., Stanford Res. Inst., Menlo Pk., Calif. (10-12 August 1971)

Effective Recombination Coefficients and Lumped Parameters in the D Region During Solar Particle Events

15th COSPAR Mtg., Madrid, Sp. (10-24 May 1972)

WAGNER, R. A., and PIKE, C. P.

A Discussion of Arctic Ionograms

AGARD Mtg. on Rad. Prop. in the Arctic, Max Planck Inst. fuer Aeron., Lindau/Harz, Ger. (13-17 September 1971)

WHALEN, J. A.

Auroral Precipitation Zones Applicable to Input-Output Studies

DASA High Alt. Nuc. Eff. Symp. (HANE), Stanford Res. Inst., Menlo Pk., Calif. (10-12 August 1971)

WHALEN, J. A., and PIKE, C. P.

F-Layer and 6809 Å Measurements in the Day Sector of the Auroral Oval

52nd Ann. Am. Geophys. Un. Mtg., Wash., D. C.
(12-16 April 1971)

WHITNEY, H. E., AARONS, J., and SEEMANN, D. R., SGT.

Estimation of the Cumulative Amplitude Probability Distribution Function of Ionospheric Scintillations

Symp. on the Future Appl. of Satel. Beacon Meas., Graz, Aus. (29 May-2 June 1972) 1972 USNC/URSI-IEEE Spring Mtg., Wash., D. C. (13-15 April 1972)

WILDMAN, P. J. L., SMIDY, M., SAGALYN, R. C., and RAO, L. D. V. (Regis Coll., Weston, Mass.)

Observations of Low Energy Charged Particles During the Magnetic Storm October 29 to November 7, 1968 from the Spherical Electrostatic Analyzers on Irian 5

Spring Ann. Mtg. of the Am. Geophys. Un., Wash., D. C. (12-16 April 1972)

WINNINGHAM, D. (The Univ. of Tex. at Dallas), and PIKE, C. P.

In Situ Observations of the Effects of Magnetosheath Particle Precipitation on the Dayside Ionosphere

53rd Ann. Mtg. of the Am. Geophys. Un.,
Wash., D. C. (17-21 April 1972)

WONG, M. S.

*Ray Tracing Analysis of Characteristic
HF Propagation Effects*
1972 USNC/URSI-IEEE Spring Mtg., Wash., D. C.
(13-15 April 1972)

TECHNICAL REPORTS JULY 1970 - JUNE 1972

AARONS, J., WHITNEY, H. E., and ALLEN, R. S.

*Global Morphology of Ionospheric
Scintillations*
AFCRL-70-0672 (October 1970)

BUCHAU, J.

Instantaneous Versus Averaged Ionosphere
Arctic Ionos. Modeling - Five Related Pap.,
AFCRL-72-0305 (16 May 1972)

BUCHAU, J., GASSMANN, G. J., PIKE, C. P., and
WAGNER, R. A.

*Radar Propagation Errors in the Arctic
Ionosphere*
Ionos. and Tropos. Limitations to Rad. Accuracy,
AFCRL-71-0169 (5 February 1971)

BUCHAU, J., and HURWITZ, M. G. (Logicon, Inc., Falls
Church, Va.)

*Coordinate Conversion and Other Computer
Programs for Arctic Ionospheric Research*
Arctic Ionos. Modeling - Five Related Pap.,
AFCRL-72-0305 (16 May 1972)

CASTELLI, J. P.

Microwave Burst Spectra and PCA's
Proc. of Mtg. on Op. PCA 69, AFCRL-70-0625
(28 October 1970)

CASTELLI, J. P., and GUIDICE, D. A.

*On the Classification, Distribution, and
Interpretation of Solar Microwave Burst
Spectra and Related Topics*
AFCRL-72-0049 (17 January 1972)

CONLEY, T. D.

*Preliminary Gerdien Condenser Measurements
from Black Brant Rockets*
Proc. of Mtg. on Op. PCA 69, AFCRL-70-0625
(28 October 1970)

CORNIER, R. J.

Riometer Observations During PCA's
Proc. of Mtg. on Op. PCA 69, AFCRL-70-0625
(28 October 1970)

Polar Riometer Observations

AFCRL-70-0690 (3 December 1970)

Riometry as an Aid to Ionospheric Forecasting
AFCRL-70-0689 (10 December 1970)

ELKINS, T. J.

Irregular Component of Ionospheric Refraction
Ionos. and Tropos. Limitations to Rad. Accuracy,
AFCRL-71-0169 (5 February 1971)

EVANS, D. L., COL., ET AL

*Ionospheric and Tropospheric Limitations
to Radar Accuracy*
AFCRL-71-0169 (5 February 1971)

GASSMANN, G. J.

An Ionospheric Model for the Arctic
AFCRL-70-0562 (9 October 1970)

Auroral Ionospheric Phenomenology
Proc. of Mtg. on Op. PCA 69, AFCRL-70-0625
(28 October 1970)

Model of Arctic Sporadic E
Arctic Ionos. Modeling - Five Related Pap.,
AFCRL-72-0305 (16 May 1972)

GUIDICE, D. A.

*Investigation of the 60 GHz Atmospheric
Oxygen Mantle for Application to Vertical
Sensing*

AFCRL-71-0116 (26 January 1971)

*March-April 1967 Observations of the Galactic
Spur and Their Interpretation*
AFCRL-71-0170 (5 March 1971)

HARVEY, R. B., and LEWIS, E. A.

*Radio Mapping of 250 to 925 MHz Noise
Sources in Clouds*
AFCRL-72-0078 (7 January 1972)

HOROWITZ, S.

*Numerical Solution of Wave Equations
for Long Wavelength Radio Waves*
AFCRL-71-0237 (13 April 1971)

KALAROWSKY, C. B., FIELDS, V. C., CAPT., HARRISON,
R. P., HIRST, G. C., CAPT., WHIDDEN, R. W., and
LEWIS, E. A.

*Air Droppable Wire Dispensers for Atmospheric
Electricity Studies*
AFCRL-72-0228 (28 March 1972)

KLOBUCHAR, J. A., and ALLEN, R. S.

*A First-Order Prediction Model of
Total-Electron-Content Group Path Delay
for a Midlatitude Ionosphere*
AFCRL-70-0403 (8 July 1970)

- KOSSEY, P. A., and LEWIS, E. A.
Relative Attenuation of TM-TE Waves Propagating in the Earth-Ionosphere Waveguide
 AFCRL-72-0079 (27 January 1972)
- MULLEN, J. P.
AFCRL Limited War Effort Task No. 24-Satellite Beacon Studies in the Panama Canal Zone
 AFCRL-71-0423 (6 August 1971)
- O'BRIEN, W. E., CAPT.
The Prediction of Solar Proton Events Based on Solar Radio Emissions
 AFCRL-70-0425 (23 July 1970)
- PFISTER, W.
Pulse Sounding With Closely Spaced Receivers as a Tool for Measuring Atmospheric Motions and Fine Structure in the Ionosphere. IV. Wave-Like Structure in the E-Region Derived from Drift Experiments
 AFCRL-70-0461 (11 August 1970)
Estimate of Angular Cross-Errors Due to Horizontal Gradients in the Ionosphere Iono- and Tropos. Limitations to Rad. Accuracy,
 AFCRL-71-0169 (5 February 1971)
- PIKE, C. P.
Modeling the Arctic F-Layer
 Arctic Iono. Modeling - Five Related Pap.,
 AFCRL-72-0305 (16 May 1972)
- PITTZINGER, E. W., MAJ., and GASSMANN, G. J.
High Latitude Sporadic E
 AFCRL-71-0082 (5 February 1971)
- RICHARDS, D. W., CAPT.
Sudden Frequency Deviations, Solar Extreme Ultraviolet Bursts, and Solar Radio Bursts
 AFCRL-71-0392 (9 July 1971)
Solar Mapping at the Haystack Observatory on the Wavelength of 3.8 Cm
 AFCRL-72-0090 (1 February 1972)
- RUSH, C. M.
Preliminary High Latitude Ionograms During the 2 November 1969 PCA Event
 Proc. of Mtg. on Op. PCA 69, AFCRL-70-0625
 (28 October 1970)
The Behavior of the F Region Above North America During the Magnetic Disturbance of 28 May 1970
 AFCRL-71-0425 (10 August 1971)
Improvements in Ionospheric Forecasting Capability
 AFCRL-72-0188 (28 February 1972)
A Numerical Study of the Lunar Tidal Oscillations in the Equatorial F Region
 AFCRL-72-0217 (28 March 1972)
- RUSH, C. M., and PUSTAVER, J. A. (Off. Dep. for Res. Serv.)
A Numerical Study of the Seasonal and Solar Cycle Changes of the Mid-Latitude Neutral Air Wind.
 AFCRL-70-0725 (9 December 1970)
- SALES, G. S., and GANIO, A.
Low-Frequency Ground-Wire Antenna
 AFCRL-70-0671 (December 1970)
- SANDOCK, J. A.
Preliminary Retarding Potential Measurements on Black Brant Rockets
 Proc. of Mtg. on Op. PCA 69, AFCRL-70-0625
 (28 October 1970)
- TOMAN, K.
Radio Propagation Effects Due to Ionospheric Waves
 AFCRL-70-0688 (3 December 1970)
Frequency Variations of an Oblique 5 MHz Ionospheric Transmission
 AFCRL-71-0253 (28 April 1971)
- TOMAN, K., CORMIER, R. J., and CORBETT, J. J.
Spatial Correlation of Auroral Radio Absorption
 AFCRL-71-0488 (17 September 1971)
- TOMAN, K., O'BRIEN, J. V., and WHELAN, L. A., JR. (Dabovich & Co., Inc, Lexington, Mass.)
Generation of Reflection Surfaces for Simulating Ionospheric Propagation Conditions
 AFCRL-72-0139 (17 February 1972)
- ULWICK, J. C.
Project 604 Overview
Preliminary RF Probe Measurements on Black Brant Rockets
 Proc. of Mtg. on Op. PCA 69, AFCRL-70-0625
 (28 October 1970)
- ULWICK, J. C., and BLANK, C. A. (DASA Hq., Wash., D. C.)
Operation PCA 69 - An Investigation of the Solar Particle Event of 2 November 1969
 Proc. of Mtg. on Op. PCA 69 (Ulwick and Blank, Compilers), AFCRL-70-0625 (28 October 1970)
- ULWICK, J. C., and SELLERS, B. (Panamet., Inc., Waltham, Mass.)
Rocket Measurements of Production and Ionization During 18 November 1968 PCA Event
 Proc. of Mtg. on Op. PCA 69, AFCRL-70-0625
 (28 October 1970)

WAGNER, R. A.

Modeling the Auroral E-Layer
Arctic Ionos. Modelling - Five Related Pap.,
AFCRL-72-0305 (16 May 1972)

WHALEN, J. A.

*Auroral Oval Plotter and Nomograph for
Determining Corrected Geomagnetic Local
Time, Latitude, and Longitude for High
Latitudes in the Northern Hemisphere*
AFCRL-70-0422 (27 July 1970)

WHITNEY, H. E., AARONS, J., and SEEMANN, D. R., SGT.

*Estimation of the Cumulative Amplitude
Probability Distribution Function of
Ionospheric Scintillations*
AFCRL-71-0525 (7 October 1971)

WONG, M. S.

*Ray Tracing in the Troposphere, Ionosphere
and Magnetosphere*
AFCRL-71-0317 (1 June 1971)



The scanning electron microscope is useful in studying the problem of fracture in KC1 window materials. Here, a fracture area has been magnified 2000 times.

XI Solid State Sciences Laboratory

Modern electronics, optics, magnetics, and electro-acoustics, continue to change military technology, not only in degree, but also in kind. The impact of advanced sensors, "smart" bombs, miniature microwave delay lines, reconnaissance satellites, and numerous other developments is amply recognized by the systems and operational arms of the Air Force. Not equally recognized, however, is that all these advances depend on electromagnetic materials and the sophisticated exploitation of their properties. Also not adequately recognized is that the technology advances of tomorrow cannot be derived exclusively from the electromagnetic materials of today; the discovery of new materials must come first.

An electromagnetic material is matter in any form which can generate, detect, modulate, or otherwise manipulate electromagnetic energy. While matter can be a gas, a liquid, or a solid, the AFCRL program is directed almost totally toward the latter. Solid materials, either crystalline or non-crystalline, and in bulk or thin films, are man-made in the laboratory, characterized to determine their composition, and evaluated for properties, especially those useful to the Air Force.

Many of the long-term exploratory basic research programs of the Solid State Sciences Laboratory were curtailed during this reporting period in favor of expanding research efforts fundamental to immediate Air Force problems. Among the expanded efforts are research on new optical materials for the high power laser program, materials to withstand high power operation, materials and devices that can withstand

high radiation doses with little or no performance degradation, and devices that can operate in severe temperature extremes. Infrared sensors of controlled uniformity and sensitivity that can operate in the extreme environments of space are of special Air Force interest.

This recent shift of emphasis redirected the programs of the Solid State Sciences Laboratory to three major areas: electromagnetic materials research, infrared detector research, and radiation effects and device hardening. Additionally, programs to improve device processing technology are pursued at a lower level of effort. The Laboratory is organized into the Preparation and Growth, Materials Characterization, Opto-Electronic Physics, Device Physics, and Radiation Effects Branches. Each of the three major efforts, however, cuts across organizational lines to involve several branches.

Typically, the solution of a problem involving control of electromagnetic energy requires a theoretical study to determine which crystalline system can best provide the needed properties. Frequently, the required crystal is not available. A new or special crystal must be grown to specifications, and then studied to determine its exact properties and the relation of properties to processing. The special processing and fabrication techniques frequently required must be maintained in-house because they are not commercially available. Finally, many applications require a knowledge of the effects of radiation on the device.

The Laboratory's facilities for electromagnetic materials research are unique within the Air Force. Almost any optical, semiconductor, or magnetic crystal can be produced, either as a bulk crystal or as a single crystal thin film. Coupled closely with the materials preparation facilities are analytical techniques for determining structure, purity, and properties of these materials. Phenomena exhibited by mate-

rials and devices as well as the evaluation of fabricated components are studied.

The significant advances of the past two decades in smaller size and increased reliability of devices have been, in many instances, partly offset by a greater sensitivity to radiation. For the study of the effects of ionizing radiation on materials and devices, AFCRL operates an irradiation facility with a variety of radiation sources and related analytical facilities.

The Laboratory uses a time sharing process control computer for on-line control of data collection, processing, and analysis. A high speed remote station links the Laboratory to AFCRL's CDC-6600 general computer facility. The time and manpower saved when the computer logs, scans, analyzes, and plots data has allowed more intensive investigations of many areas and has significantly improved the accuracy and timeliness of many research investigations.

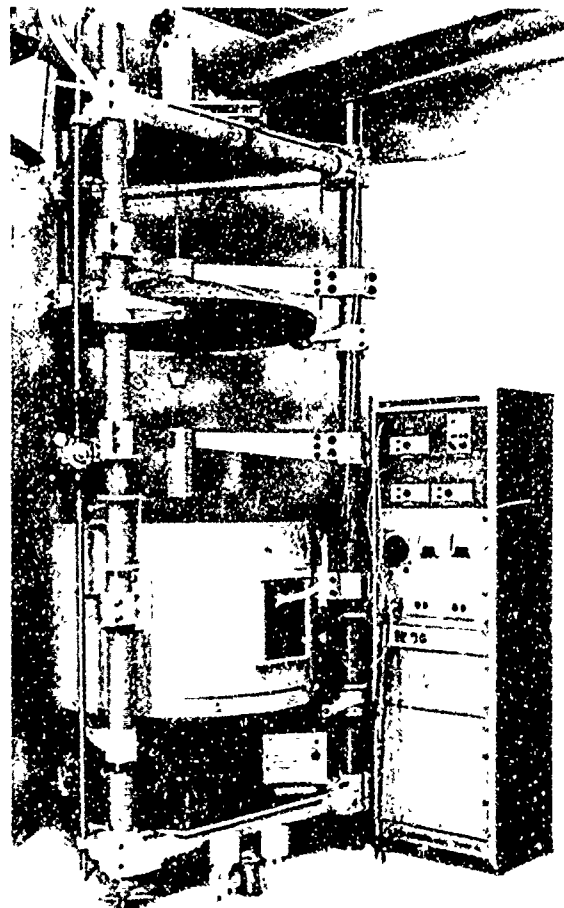
Much of the work reported in this chapter is in-house research. Because of its extensive in-house facilities, historically, the Laboratory has used very little contract assistance. During this reporting period, however, urgent military programs for the development of materials and components for high power IR lasers and for IR detector research have generated requirements best satisfied by contractual support.

ELECTROMAGNETIC MATERIALS

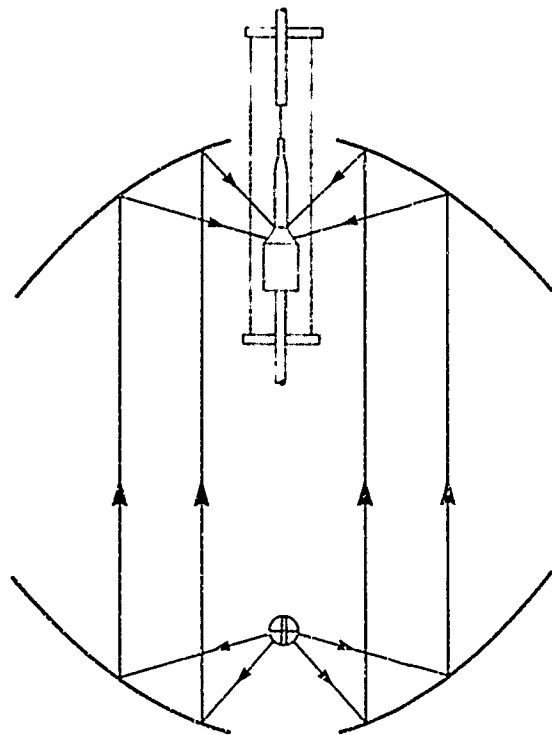
THERMAL IMAGING—A NEW CRYSTAL GROWTH METHOD: Devices such as lasers, advanced transistors, and improved magnets place stringent requirements on the types and perfection of electromagnetic crystals used. Superior crystals, which are stable under the conditions likely to be encountered in military applications, can be very difficult to produce or "grow,"

especially under carefully controlled conditions. Some can be produced only at very high temperatures. During the past two years, Laboratory scientists have devised and operated a technique called thermal imaging to produce these crystals.

The requirements to be satisfied included: a 3000 degrees C temperature capabil-



The AFCRL thermal imaging furnace. A high-pressure xenon arc lamp is placed at the focus of a parabolic mirror (these are both hidden in the bottom part of the furnace) and the light is formed into a parallel beam. The upper parabolic mirror, which is the one which can be seen, focuses the parallel beam on whatever material is in the holder, which can move vertically. The rod extending vertically through the center of the upper mirror is used to pull the crystal up from the molten material.



The thermal imaging furnace refocuses heat from one place (environment) to another. The energy generated in a high-pressure xenon arc is applied to melt a material in an oxidizing, inert, or reducing atmosphere, or a vacuum.

ity, atmospheric control, ease of growth, and cleanliness, which could best be achieved by crucibleless operation. The unique thermal imaging scheme satisfies these requirements. A high pressure xenon arc lamp is placed at the focus of a parabolic mirror, which forms the light from the lamp into a parallel beam. A second mirror directly above the first mirror focuses the parallel beam to a point. Any material placed at this point will be heated. If a cylinder of material is properly placed, the light will fall only on the top end of the cylinder. The intense light, however, will melt only a small amount of material at the top end of the cylinder, and the molten material is supported by sur-

face tension. This solves the problem of melting materials at high temperature without a crucible.

It is now possible to grow a crystal by the Czochralski technique. If a small single crystal (the "seed") is lowered to touch the molten material, it will begin to melt. If this seed is slowly pulled upward, the molten material will also be pulled upward, and as it cools it will solidify into a long crystal. By proper adjustments, the crystal can be made larger in diameter than the seed.

With improvements, the present 3000 degrees C temperature capability should be increased to 3500 degrees C. Also, the molten material and the crystal can be enclosed in a transparent quartz tube (through which the light can pass) and the crystal can then be grown in a vacuum, or in almost any gas. The gas can be under moderate pressure if required.

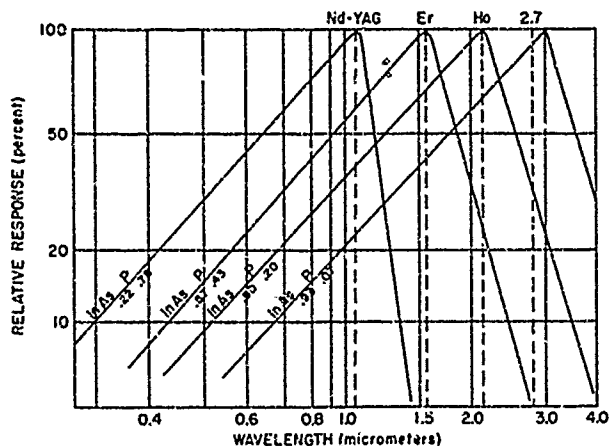
Since only light is used for heating and nothing need be in the growth region except the materials being processed, the method is extremely clean. This technique, therefore, satisfies all the requirements for very high quality crystal growth. High quality single crystals of eight different materials have been grown to demonstrate the capability of the technique, and work is now in progress on two materials of special Air Force interest, yttria (Y_2O_3) and certain rare earth-cobalt compounds.

Yttria is a tough, high temperature oxide that transmits into the infrared. It has potential use as a window for high power chemical lasers and infrared detectors, as a laser host crystal for medium gain lasers, and as a substrate for semiconductor applications. Small crystals of this material have been grown and furnace modifications are underway to permit growth of crystals large enough for characterization studies. The thermal imaging method can be used to grow even larger crystals in the future by the use of higher power.

Another material which has been grown in this furnace is in the rare earth-cobalt family. Samarium cobalt has already been developed by the Air Force Materials Laboratory, Wright-Patterson AFB, Ohio, into a permanent magnet material that is far superior in coercivity to any now available, has been applied in a traveling-wave tube for Air Force use, and has potential for lightweight magnetically focused image tubes. Such magnetic materials have many additional applications including motors, generators, and the fly-by-wire concept. In a cooperative program with AFML, AFCRL has investigated the growth of other rare earth-cobalt alloys whose characteristics are predicted to be superior to those already available. Such crystals are normally difficult to prepare because of their high chemical reactivity, but the special characteristics of the thermal-imaging technique overcame the difficulties. Several of these crystals with more complex unit cells were successfully grown, characterized, and submitted to AFML for magnetic evaluation.

IR DETECTOR MATERIALS: Many infrared systems, especially in the visible to 3 micrometer range, are still detector limited. Several AFCRL programs are focused on this deficiency.

A plot of the relative response of any given detector versus the wavelength of the light gives a curve which peaks just prior to the long wavelength cutoff. The position of this peak is a reciprocal function of the energy gap of the detector material. The energy gap of any elemental or binary compound detector material is essentially a constant. Hence, the peak response wavelength is a constant and a detector fabricated from such a material can give optimum detectivity only at that discrete wavelength. For the ternary III-V alloys, however, the energy gap is a function of the composition of the ternary.



Typical response versus wavelength curves for IR detectors. The peak sensitivity of the detector comes just before the long wavelength cutoff. By using a range of composition, indium arsenide phosphide detectors can be made to peak at any desired frequency.

Thus, the energy gap of indium arsenide phosphide ($\text{InAs}_{1-x}\text{P}_x$), for example, can be varied between 0.35 and 1.35 eV, which corresponds to a variation of the peak response from 3.5 micrometers to 0.92 micrometers. Thus, $\text{InAs}_{1-x}\text{P}_x$ detectors can be tailor-made to provide peak response in the nightglow region and for several specific types of laser—namely, helium-neon (He-Ne), (1.15 and 3.39 micrometers), neodymium-doped yttrium aluminum garnet (Nd-YAG) (1.06 micrometers), and the eye-safe erbium (Er) (1.54 micrometers) and holmium (Ho) (2.13 micrometer) lasers. The laser systems, of course, can be used for illumination, target designation, ranging and communications. One application is satellite laser communication systems. The system which appears best at present would use a gallium aluminum arsenide (GaAlAs) pumped Nd:YAG laser which has an output at 1.06 micrometers. This system is detector limited in that there is

no detector available that has good quantum efficiency (> 2 percent) and a quiet gain mechanism. Silicon avalanche detectors are currently being considered; however, they have low quantum efficiency at the required bandwidth. Consequently, indium arsenide phosphide appears to be a good candidate for this detector. A second application is military target detection, where an important target is the CO_2 recombination radiation common to both jet and rocket exhausts. This radiation is at 2.7 micrometers and currently lead sulfide (PbS) and indium arsenide (InAs) are used for its detection. However, PbS detectors are too slow for many cases while InAs, although fast enough, gives optimum detectivity at 3.5 micrometers, resulting in excess noise from the background and excess cooling requirements (required operating temperature drops as the peak wavelength gets longer). Thus, shifting to the 2.7 micrometer peak via InAsP rather than the 3.5 micrometer peak of InAs could allow operating temperatures as much as 30 degrees K higher, and would allow entirely passive cooling of such a detector in a satellite.

An entire range of compositions of thin films of indium arsenide phosphide have been tailor made. Deposited layers of $\text{InAs}_{1-x}\text{P}_x$ on InAs and GaAs substrates over the entire range of $x(0-1)$ were successfully prepared. The results obtained are applicable to three different groups of devices.

A 1-mil layer of n-type $\text{InAs}_{0.27}\text{P}_{0.63}$ followed by a 1 micrometer layer of p-type $\text{InAs}_{0.27}\text{P}_{0.63}$ was grown on a p-type InAs substrate. Mesas with good geometry were etched, and two samples with etched mesas were delivered to the Device Physics Branch for use as near infrared photodiodes.

Six samples of $\text{InAs}_{1-x}\text{P}_x$ over the (0-1) range were prepared on GaAs substrates for use in optical transmission studies de-

signed to determine the band gap of the alloy system as a function of x. With chemical polishing, approximately 50 percent transmission (close to the theoretical maximum) was obtained for the band gap measurements.

Samples of $\text{InAs}_{1-x}\text{P}_x$ on InAs substrates were grown and provided to other researchers for the Advanced Research Projects Agency. They will be used in a basic properties study before being used as IR detectors in the 0.92 to 3.2 micrometer range. The transport data gathered will support Device Physics Branch detector design studies.

LASER MATERIALS: Current Air Force utilization of Q-switched, Nd-doped laser devices in operations which require target illumination or designation have demonstrated a need for a medium gain/energy storage laser material. Materials such as yttrium aluminum garnet (YAG), which has high efficiency and high gain, experience problems because they saturate at a low energy per Q-switched pulse. Low-gain materials such as glass provide high energy per Q-switched pulse at the expense of efficiency and repetition rate.

AFCRL has investigated the germanate family of materials to prepare a solid crystal which can satisfy the requirements for a medium gain laser. Emphasis has centered on bismuth germanate (known as BIG), with promising results.

Bismuth germanates had previously been prepared in other laboratories for investigations of their electro-optical and electro-mechanical properties. As part of the medium-gain laser program, crystals doped with neodymium or erbium, with or without ytterbium, have now been pulled by the Czochralski process. Undoped bismuth germanate single crystals about 38 mm long by 15 mm in diameter and of good optical quality, have been pulled. Good crystal quality was also obtained in

bismuth germanate crystals containing 0.5 to 1.0 weight percent neodymium. Crystals containing erbium were also grown.

Excitation and emission bands of these crystals have widths intermediate to glasses and YAG and may be a good compromise between threshold and power capability. Strong fluorescent emission in the 1.50-1.58 micrometer region for the erbium-doped bismuth germanate suggests the possibility of a 1.54 micrometer crystal laser. In addition to a strong, relatively narrow line in the 1.06 micrometer region, the neodymium-doped bismuth germanate has the added advantage of strong infrared excitation bands in the CW tungsten pumping region.

MICROWAVE ACOUSTIC MATERIALS: Certain materials exhibit complex internal coupling between electric (microwave) and acoustic fields. The materials are generally high optical quality single crystals of light mass atoms which possess complex crystallographic structure. The microwave acoustic crystals selected for device application usually exhibit a high Debye temperature, thermal conductivity, and low acoustic attenuation at microwave frequencies and at room temperature. Present and future Air Force applications include surface wave acoustic delay lines, signal analysis and processing, surface wave acoustic frequency filters, microwave memories, and microwave amplifier devices.

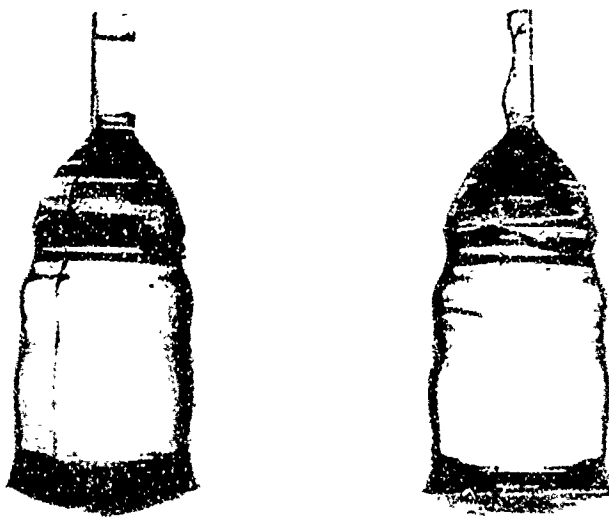
High optical quality crystals, mostly of lithium niobate and lithium tantalate, have been synthesized for application by the Microwave Physics Laboratory. More recently, a program to synthesize large (10 mm cube), high optical quality aluminum nitride (AlN) was substituted for growth of niobate and tantalate single crystals. Experiments on thin films have shown that AlN is a surface wave acoustic material with a high figure of merit. Large AlN single crystals are needed for tensor anal-

yses so that the electro-acoustic properties can be optimized.

Although the chemistry of AlN is similar to other III-V and IV-IV compounds, single crystals of satisfactory quality have not been synthesized in spite of 70 years of research. AFCRL studies indicate the best way to grow these crystals is to crystallize them from solution. However, little information is available, and aluminum nitride is inert to most solvents. Preliminary solvent identification and growth experiments at AFCRL have produced tiny but highly perfect crystals of aluminum ni-

tride. They were identified by X-ray diffraction, and possess the expected color and transparency. Laboratory scientists will attempt to grow larger crystals.

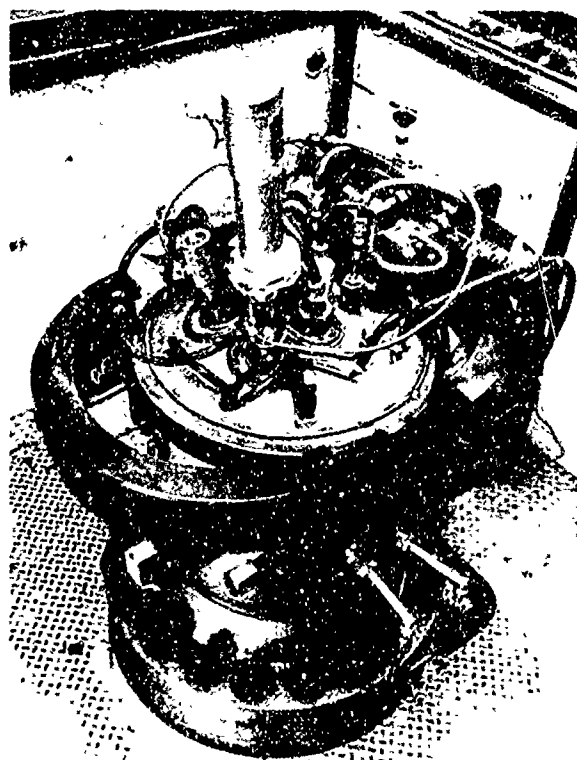
SILICON CARBIDE: The trend toward solid state optical and opto-electronic devices and applications increased the importance of refractory materials with band gaps of 2 to 3 electron volts. Although the controlled preparation of silicon carbide presents severe technical difficulties, no other material appears to have its potential in a wide range of important devices. During



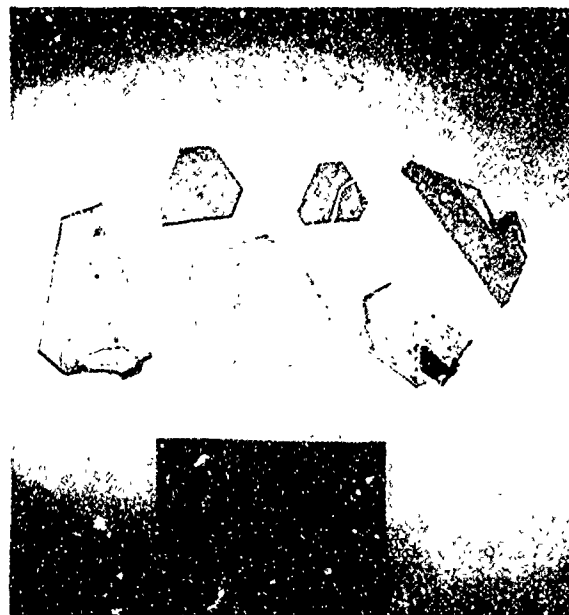
Lithium niobate and lithium tantalate single crystals grown by the Solid State Sciences Laboratory for evaluation and possible exploitation by the Microwave Physics Laboratory as microwave acoustic materials.

this reporting period, a new furnace was designed, built, tested, and began limited operation, growing alpha silicon carbide under controlled conditions. In spite of difficulties in control of temperatures, temperature gradients, purity, and stability of heaters, crystals of good chemical and physical perfection have been grown. This success indicates that experiments can be performed with this furnace to lead to a clear understanding of the growth mechanism in silicon carbide and the growth conditions needed to prepare crystals in adequate numbers, quality, and uniformity for device application research.

A liquid epitaxy technique for growing junctions of alpha silicon carbide on alpha



High-temperature, high-pressure furnace designed for growing alpha silicon carbide crystals. It has a temperature capability of above 2800 C degrees and a pressure capability of more than 60 atmospheres at maximum temperature.



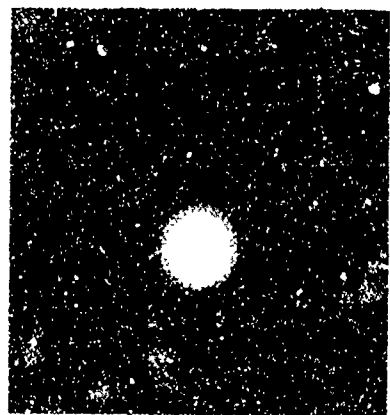
Early silicon carbide single crystals grown in new high-temperature, high-pressure furnace.

silicon carbide substrates has been developed.

A chemical vapor deposition (CVD) process has been developed for far greater control in preparing beta silicon carbide thin films. In the previous process, methyltrichlorosilane was used. In that process, the by-product (HCl) etched many of the desired substrates when conditions were right for deposition. By using silane and toluene lower temperatures could be used, and addition of a controlled amount of chlorine achieved the proper amount of substrate cleaning so that single crystal thin films would be deposited.

One of the major problems in growing silicon carbide is that it exists in many closely related forms known as polytypes. Crystal growth and thermal annealing experiments have clarified the nature of polytypism and methods to control it.

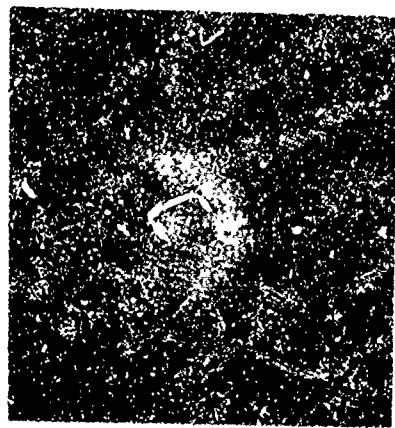
HALIDE IR WINDOWS: The increasingly higher average power of modern lasers has



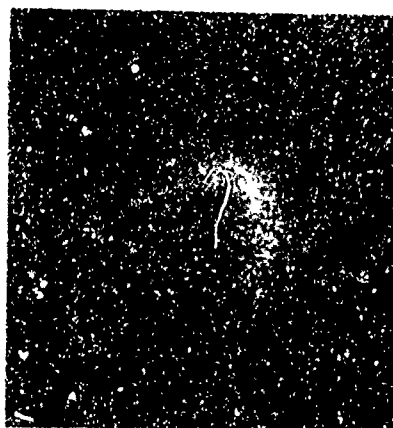
0 Sec



1/2 Sec



1-1/2 Sec



3-1/2 Sec

Thermal distortion of a 50 W CO₂ laser beam by Irtran-6 (CdTe), as a function of laser beam exposure time.

increased demands both on the laser itself, and on the support elements of the optical system. One support element, the window between the laser system and the environment, has been made the subject of a major investigation at AFCRL.

There are many criteria for window materials selection but the most important is extremely low optical absorption at the desired wavelength (10.6 micrometers for a CO₂ laser). Other important properties are good mechanical strength, high thermal conductivity, compatible thermal expansion, a minimum of electronic carriers and resistance to radiation damage.

One important objective was selecting, developing, and improving alkali halides to improve their suitability for window use. Since poor mechanical strength is the principal disadvantage of these materials, methods were investigated to improve their strength without impairing their optical properties. Three types of growth were used for preparing crystals. Czochralski growth was used with a variety of atmospheres. A furnace without metal parts was designed so that a hydrogen chloride (HCl) atmosphere could be used. Bridgman growth was used for most of the other crystals, and a few solution growth experiments accounted for the rest of the crystals.

The first method tested for improving hardness was to add a group II impurity. Tests showed no significant increase for potassium chloride (KCl). Adding 1/10 percent calcium caused a slight increase in hardness, but 7/10 percent calcium caused less increase in hardness than 1/10 percent, and 1/2 percent OH caused about the same increase in hardness as 7/10 percent calcium.

The second hardening method is based on solid state immiscibility. For example, equal parts KCl and NaCl would form a solid solution crystal when first grown, but on cooling, the solid solution would decompose into two immiscible solids of varying



Growth of ALQLOY crystal in air using the Czochralski process.

concentration. The result is similar to polycrystallizing the sample. As part of this approach, Czochralski crystals were grown at concentrations varying from 5 to 75 percent NaCl. An increase in hardness did develop, the hardness maximum occurring in the region of the immiscibility gap, where the greatest disorder would be expected. The optical absorption of the resulting material, however, was quite high.

Both potassium chloride and potassium bromide (KBr) have very low absorption at 10.6 micrometers, and thus appear to be promising candidates for a CO₂ laser window material. They are, however, quite soft. The third method for obtaining stronger materials with adequately low absorption was tested by growing several mixed potassium chloride-potassium bromide crystals by the Czochralski process. The hardness of solid solution crystals is double that of pure KCl and almost triple that of KBr. Optical absorption tests

showed that the halide was strengthened without loss of optical quality. This material is now designated ALQLOY 1.

The final hardening method employed was the use of grain boundary production to strengthen the material. Grain boundaries were produced by applying pressure for specific lengths of time to heated single crystals or boules of the material. This Pressure Induced Recrystallization (PIR) process produced polycrystallinity without producing impurities at the grain boundaries. Initial results with KCl indicated that optical quality was not impaired in the process in spite of a grain size near 10.6 micrometers.

Of the several methods for hardening halides investigated, the most desirable are solid solution hardening and polycrystallization. Present studies involve the combination of these two methods.

SECOND-GENERATION WINDOW MATERIALS: Although the pressure-recrystallized alkali halides will be one acceptable material for high power window materials, they

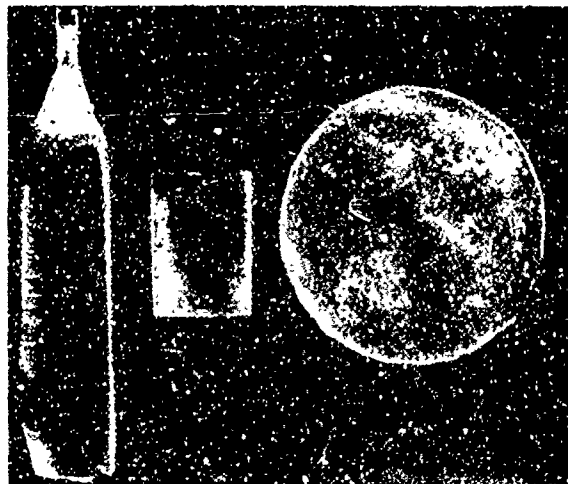
cannot perform at higher powers or more extreme conditions. Consequently, a search is underway in cooperation with other laboratories for other superior materials, or combinations of materials. Three major material categories are being studied at AFCRL: advanced halides, chalcogenides, and pnictides.

Although the common alkali halides have been thoroughly investigated, other halide systems remain relatively unknown. One such series, consisting of compounds of alkali halides with alkaline earth halides, is being studied within the Laboratory. A preliminary assessment of one such system, that between KCl and CaCl₂, indicates that a one-to-one compound does exist. In initial experiments, the material proved to be very hygroscopic and would probably require an environmental protective coating for window use. Other systems of this series are also under study in order to identify and produce less hygroscopic compounds.

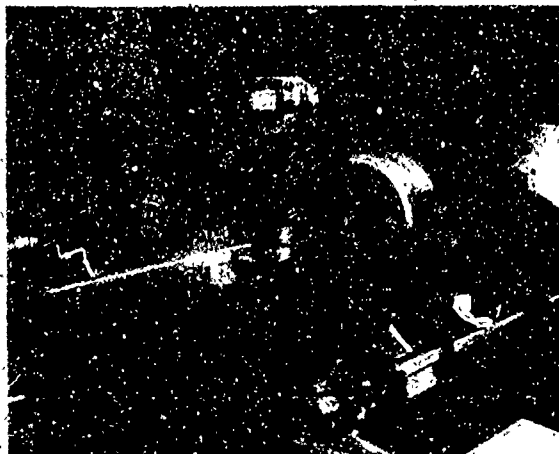
The chalcogenides appear to be the most promising candidates for second-generation window materials, although their growth problems are more severe. Research is proceeding in two areas. First is the study of solid solutions of II-VI compounds, principally cadmium selenide-cadmium telluride, which is expected to form uniform crystals. Preparation of these will be by growth from a melt. The proportion of cadmium selenide will range up to about 20 percent.

The second research area is a study of ternary chalcogenides. The sulfo-salts, which include proustite and pyrargyrite, will be prepared and studied.

Studies of the pnictides initially emphasized gallium phosphide (GaP) and indium phosphide (InP). However, work on the GaP-InP solutions originally selected will not be pursued since they do not look promising. Boron phosphide and boron arsenide have been obtained and crystals of these will be grown and evaluated.



The PIR process. KBr crystal on left is cut into cylinder (center) and reconstituted as a hardened window, on the right, by the use of properly controlled high-temperature, high-pressure processing.



Fluorescence spectrometers, coupled with laser sources developed at AFCRL, have been used to evaluate new laser materials containing transition metal and rare earth ion sensitizers and activators. The monochromatic lines available in lasers allow selective excitation of specific impurities, and the directionality of laser radiation facilitates scanning of small regions of materials for impurity concentration and distribution.

CHARACTERIZATION OF MATERIALS: Continuing quality control is required to ensure that the material being produced is exactly the material specified. Defect or trace element chemistry as well as chemical and structural properties are studied on a continuing basis. Emission spectroscopy is used for routine analysis, spark source mass spectroscopy for studies of defect chemistry at the parts per billion level, and neutron activation analysis techniques for those systems in which matrix effects obscure the defect chemistry.

Often, when a crystal has been selectively or gradient doped, or when processing or material usage has resulted in an undesirable dopant distribution, the electron microprobe is used to determine the content and geometry of selected impurities.

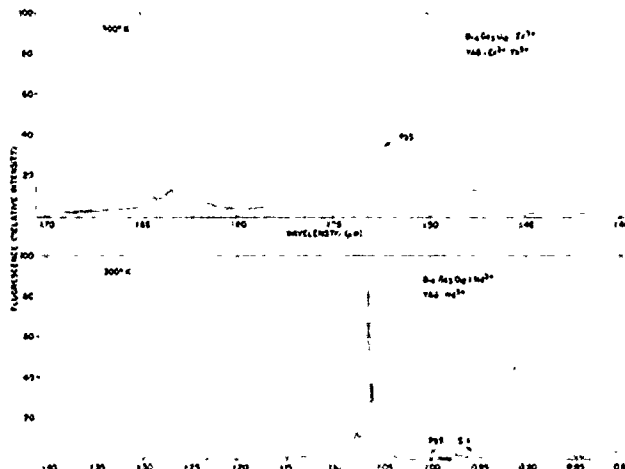
Defect chemistry is only one facet of characterization. Crystalline phase, structure, and crystallinity are also necessary for complete understanding of the material. X-ray powder diffraction, and electron

diffraction coupled with computer simulation of X-ray Laue patterns are used to determine crystalline structure and whether the materials are single or polycrystalline.

The evolution of a new or improved material also requires an understanding of the defect distribution. In particular, the distribution of dislocations, which are linear defects in the crystal, is important in determining the electrical and optical properties of these materials, since the dislocations act as traps for free carriers or as mobility barriers. Proper manipulation of dislocations by judicious selection of thermodynamic variables can sometimes strengthen a material by increasing the number of grain boundaries.

Linear defects can be studied directly by transmission electron microscopy or X-ray topographic techniques. Often, the application of these methods, particularly to dielectric and semiconducting crystals, requires the development of new methodologies and techniques. An example of this is X-ray Differential Depth Topography in which the crystal orientation, Bragg reflection, and wavelength of the X-rays used control the depth from which the X-rays are reflected in the crystal.

OPTICAL SPECTROSCOPY: Optical transmission and reflection measurements are a standard method used at AFCRL for determining energy band gaps, impurity levels and lattice vibrations of semiconducting and insulating materials. Fluorescent band spectra provide information on excited impurity levels, effect of the host lattice, conversion efficiencies, and other characterization parameters. New techniques developed in the Laboratory use CW lasers instead of conventional lamp sources and have improved the sensitivity and extended the capability of fluorescence spectroscopy. Coincidences between laser lines and impurity absorption bands exist throughout the ultraviolet, visible



On the basis of line width and excitation capability determined from this type of measurement, Nd³⁺: Bi₄Ge₃O₁₂ has been selected as a potential medium gain laser material.

and near infrared, so that the high power of laser radiation can be used to excite fluorescence from even very weak impurity absorptions. Fluorescence spectrometers coupled with laser sources have been used to evaluate new laser materials containing transition metal and rare earth ion sensitizers and activators. The monochromatic lines available from lasers allow selective excitation of specific impurities, and the directionality of laser radiation facilitates scanning of small regions of materials for impurity concentration and distribution. This type of measurement was used in selection of neodymium doped bismuth germanate as a potential medium gain laser material.

DEFECT CHARACTERIZATION OF SEMICONDUCTORS: Defects in semiconductors, either in the crystal as grown or irradiation induced, were characterized by localized vibrational mode absorption. Electron irradiation can compensate the dopant even for heavily doped materials, which have large free carrier absorptions, and increase the infrared optical transmission to the point where it will be lattice rather than

free carrier absorption limited. This reveals the localized vibrational mode spectra, without the complications introduced by diffusion of a second impurity system. Aluminum, silicon, and phosphorus impurities in gallium arsenide were studied by this means. Absorption bands corresponding to these impurities were identified, and their strength correlated with impurity concentration. The technique was also used to study the characteristics of ion implants. Aluminum, silicon, and phosphorus (Al⁺, Si⁺, and Pi⁺) were each implanted into GaAs and the localized mode bands were investigated as a function of heat treatment. The percentage of interstitial and substitutional ions were determined this way as a function of anneal temperature. N⁺ implanted into GaAs also revealed an absorption band. Previously, this impurity could not be detected in GaAs. Infrared optical transmission measurements have proved to be a rapid characterization technique for identifying various impurities and defects introduced during crystal growth, irradiation, or implantation procedures.

NEUTRON DAMAGE IN GALLIUM ARSENIDE: Heavily doped GaAs has been increasingly used in semiconductor lasers and diodes for Air Force weapons and guidance systems. These GaAs devices rely on high carrier concentration, typically 10¹⁸ to 10¹⁹ carriers per cubic centimeter. Previous radiation damage studies on less heavily doped GaAs have shown that high-energy electron and fast neutron bombardment drastically reduces both the carrier concentration and the mobility. These quantities are usually calculated from measurements of resistivity and Hall coefficient. The latter becomes difficult or unreliable in heavily doped material. To overcome this obstacle, the technique of determining the electrical properties from the infrared optical reflectivity spectrum was developed.

Samples of n-type GaAs, with 6×10^{18} donors per cubic centimeter, were irradiated with 1 MeV electrons or reactor neutrons. Optical measurements showed that with increasing fluence the free carrier reflectivity edge moves toward longer wavelength, indicating a decrease in the carrier concentration. Simultaneously, the slope of this edge decreased, a combined effect of carrier removal and mobility reduction. A computer program fit of this data yields the carrier concentration and mobility.

The removal rates in n-type GaAs are three carriers per electron and ten carriers per neutron. In addition, neutron irradiation of p-type GaAs with 4×10^{19} holes per cubic centimeter removed 40 holes per neutron. The mobility deteriorated about ten times more rapidly under neutron irradiation than under electron irradiation. The mobility decrease is due to an increase in scattering centers with fluence. This increase is exponential for electrons, linear with neutrons in n-type GaAs, and shows saturation at low fluence levels with p-type GaAs. Isochronal annealing experiments after electron irradiation show one major recovery stage between 170 and 230 degrees C. No such stage was found after neutron irradiation.

Infrared optical measurements can be used to determine the electrical properties of other semiconductor materials whenever heavy doping impedes the use of electrical measurements.

LENSING IN IR WINDOW MATERIALS: The significance of thermal distortion effects in limiting the performance of windows for high power lasers became widely known during this reporting period. Therefore, in conjunction with its overall program to develop and characterize high power laser window materials, the Laboratory has begun an extensive program of theoretical and experimental investigation of thermal distortion effects. Early theoretical investi-

gations identified the distortion mechanism as absorption of laser energy, leading to non-uniform heating of the window by the beam. The heating leads, in turn, to non-uniform refractive index changes, and bulging of the window faces. As a result, the window acts as an aberrating lens with ill-defined focal properties, an effect referred to as "thermal lensing."

Thermal lensing effects were observed in a variety of experiments. For the initial qualitative measurements, a CO₂ laser beam passed through a window and impinged on a thermal phosphor screen. Motion pictures of the spot visible on the screen provided a vivid demonstration of lensing effects. Quantitative results were also obtained by direct measurement of the beam profile, utilizing a beam scanner and pyroelectric detectors.

A simplified theoretical basis for predicting lensing effects and competitively rating candidate window materials was desired as soon as possible. A geometrical optics approach was developed. Materials were rated on the basis of the length of time they could maintain a diffraction limited spot in the far field. Predictions showed that alkali halides were, in general, substantially superior to semiconductors and glasses. The theory not only provided ratings, but also allowed identification of the crucial material and configurational parameters influencing lensing. Small absorption coefficients and changes of the refractive index with temperature, and high thermal conductivities were found most desirable to reduce lensing. The theory also showed that lensing could become the dominant failure mechanism in many laser windows, even at relatively low operating powers.

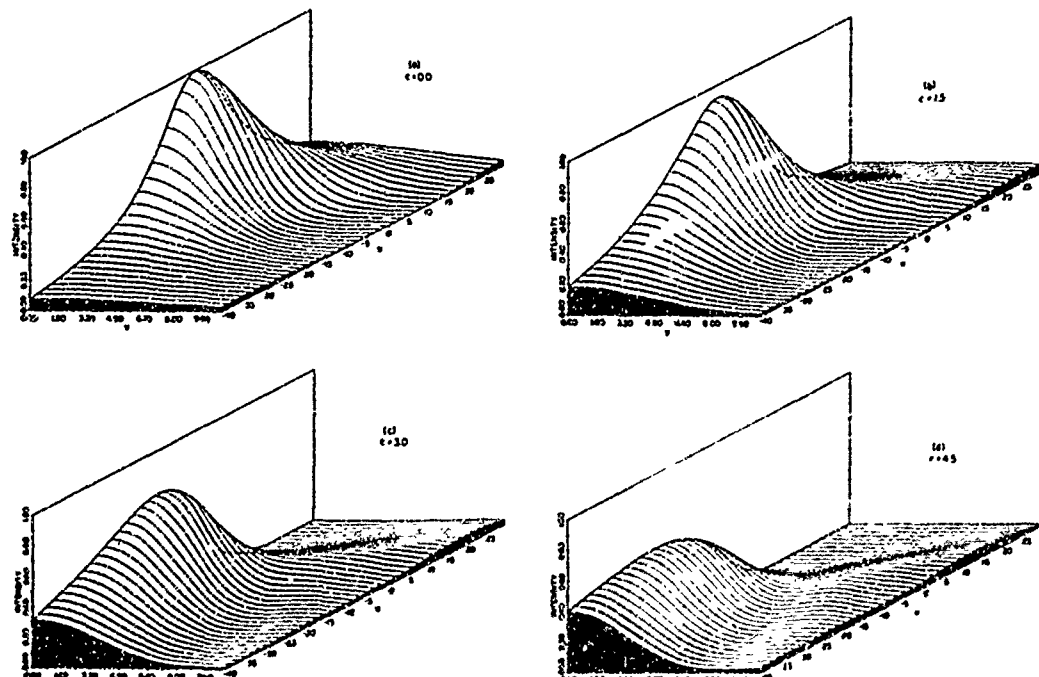
Because lensing is important, a more rigorous and elaborate theory was formulated, to account for interference and diffraction effects. The theory, employing a vector Kirchhoff diffraction approach, provides a detailed prediction of the transmit-

ted intensity throughout space and for all times, once the system parameters have been specified. To compute the lensing at arbitrary times, it was necessary to solve the equation for heat flow in the window. Various computer programs were developed to do this. These programs were then interfaced with specially developed computer programs for vector diffraction optics. Detailed studies of lensing in a wide variety of materials were carried out using these programs.

The theoretical program successfully made quantitative predicted ratings of the performance of candidate window materials, as a basis for their selection in actual

applications. In the regime where the temperature of the sample is linear with time, one may rate materials by comparing how long it takes for the maximum in the transmitted intensity to decrease to some specified fraction of the initial value. The longer the time required for this degradation, the better the material performance.

Interferometry was also used to investigate lensing. This sensitive technique enabled direct observation of the thermally induced changes in the optical path length in the window. The number of fringes moving past a reference point can be counted to provide a quantitative measure of the path length change. Interferometry



Transmitted intensity in the focal region versus abstract on-axis coordinate U and radial off-axis coordinate V , for a narrow Gaussian beam incident on a thin circular lens of an optically isotropic material. The four figures correspond to increasing abstract time C . The degradation and focal shifting with increasing time are evident.

OPTICAL PERFORMANCE EVALUATION OF
LASER WINDOW MATERIALS AT 10.6 MICROMETERS
($P_0 = 500 \text{ W/cm}^2$, $L_0 = 2 \text{ cm}$)

	Characteristic degradation time t_{10} (sec)		
	Amplitude proportional to		
	$e^{-1/2r^2/a_0^2}$	e^{-r^2/a_0^2}	e^{-3r^2/a_0^2}
KBr	3220	2450	1680
KCl	83	68	63
NaCl	190	104	47
KI	125	78	38
CsI	36	16	6
CsBr	27	12	4
CdTe	16	7	3
KRS-5	7	3	1
ZnSe	2	.9	.3
GaAs	2	.6	.2
InSb	.6	.2	.1
Ge	.6	.2	.1
Tl Glass #1173	1	.5	.2
Tl Glass #20	1	.4	.1
Irtran-4	.6	.4	.1
Irtran-6	.1	.1	.02

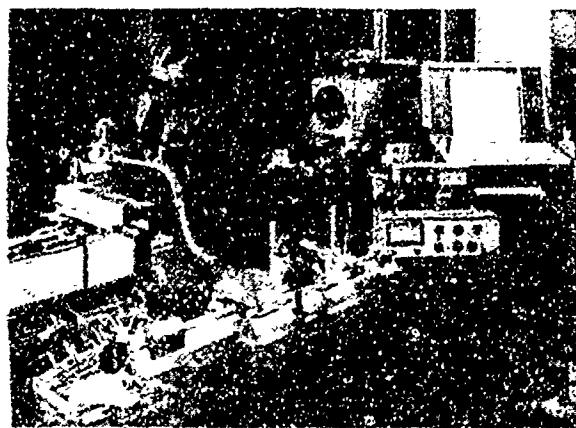
has been found useful in studying absorption coefficients and stress-optic coefficients as well as in direct evaluation of the merit of window materials.

CALORIMETRIC MEASUREMENTS: A very small non-uniform change in window temperature, well below that necessary to cause structural damage, produces enough variation in index of refraction to result in thermal lensing and eventual defocusing of the laser beam from a target. Materials with absorption coefficients of less than 0.001 per cm are required. Absorption coefficients in this range cannot be measured by conventional transmission spectroscopy, which is limited to values greater than 0.01 per cm for a sample one inch long.

Calorimetry is used at AFCLR for measuring small absorption coefficients at 10.6 micrometers. The calorimeter consists of a large aluminum cylinder with feed-throughs for thermocouples, evacuation ports, and mounts for windows. A special

feature is a bellows sample mount which allows accurate positioning of samples so that different parts of the sample can be placed in the beam. A 5-watt stable CO₂ laser is directed either through apertures to limit the beam or through a germanium-focusing lens. Both the initial laser power and the power transmitted through the sample are measured with a disc type calorimetric power meter. Thermocouple voltages measured during thermal rise and decay periods are amplified by a dc nanovoltmeter and recorded. The equipment was designed for evacuated adiabatic calorimetry, but the windows can be removed and measurements made in air. When both rise and decay rates are properly considered, comparative measurements give identical results in vacuum and air. Also, elimination of windows removes the possibility of scattering laser radiation from window surfaces and allows a more sensitive determination of bulk or surface scattering occurring within the crystal.

Sample surfaces are prepared either by polishing or cleaving. The results are most reproducible when the thermocouples are attached either to optically polished or as-grown surfaces. Thermocouples are usually placed on opposite sides of the sample equidistant from the laser beam. The pres-



Calorimetry equipment for measurement of small absorption coefficients.

ence of scattered laser radiation which produces direct heating of the thermocouple is evidenced by a steep slope in the thermal rise curve just after laser turn-on and a corresponding slope in the decay curve after turn-off. Good agreement of thermal rise and decay rates for thermocouples placed on opposite sides of the sample is also an indication that directional scattering is not present.

Typically, exponential rise and decay curves are obtained when the laser heats the sample for a given period of time and then is turned off. The heat absorbed in the sample is determined from the sum of the rise and decay slopes measured over the same temperature interval. For most samples the sum of the rise and decay slopes are nearly constant over the temperature range of measurement unless some other mechanism such as scattering is operative.

One important aspect of characterization is the measurement of small samples and small regions of larger samples to determine homogeneity. The calorimetric measurement equipment has been developed to do this, and measurements have demonstrated that imperfections can produce scattering of the laser radiation and regions of higher absorption in a crystal. Sections of a relatively pure KCl crystal of 0.003 per cm absorption were found to

have a value of 0.008 per cm near an imperfection. A CdTe sample used in a study to compare calorimetric values obtained by different laboratories was scanned and found to have variations from 0.10 per cm at the center to 0.03 per cm only 5 mm below the center.

Some of the absorption coefficients determined here have been tabulated. The absorption coefficients given are for sections of samples which do not contain flaws or other localized regions of strong absorption or scattering. The condition of the reflecting surface is also tabulated.

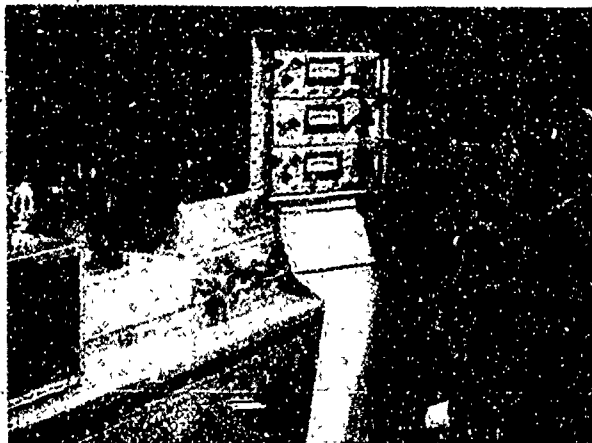
INFRARED DETECTOR RESEARCH

Studies of basic detection mechanisms, detector material development, integrated optics, radiation effects, and sensor system hardening, all contribute to development of advanced detectors for the Air Force. Physical phenomena which may provide detection mechanisms must be investigated, a current knowledge of the state of the art in infrared devices and their operational environments must be maintained, user organizations must be alerted to projected threats, and research to eliminate detector-caused problems must be carried out.

Absorption Coefficients of Present State-of-the-Art Window Materials

Sample	Surface Condition	Absorption Coefficient $\beta A/cm^{-1}$
KCl*	Polished	0.0007
KCl (Polytran)	"	0.002
KCl _{.32} KBr _{.68} (AFCRL)	Cleaved	0.002
KBr	Polished	0.003
CdTe	"	0.003
CdSe (ARL)	"	0.016
ZnSe	"	0.05
GaAs	"	0.12

*High Purity Sample



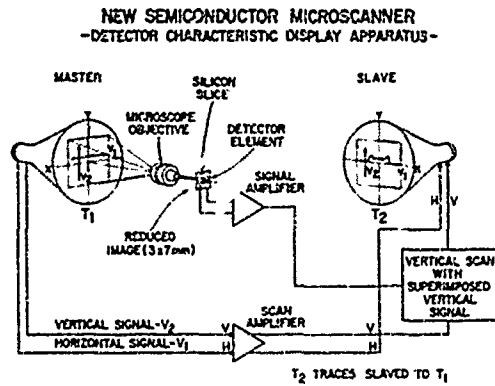
System for measuring detector spectral responsivity.

Guidance for the program comes from several sources. System Program Offices at Wright-Patterson AFB, Ohio, the Space and Missile Systems Organization, Los Angeles, California, and especially knowledgeable individual scientists and engineers are contacted regularly. Environmental programs at AFCRL are often limited by the state of the art in sensors. Guidance has been derived from both the Rocket Readiness Program and Project Hi-Star. Laboratory personnel are members of the Special Devices Working Group, which coordinates imaging device development research for the Director of Defense Research and Engineering, the National Materials Advisory Board Committee for Electromagnetic Detection Devices and the DNA Basic Mechanisms Working Group (Optical Systems), also gives program guidance. Finally, Laboratory scientists forecast future Air Force detector problems and possible solutions, based on in-house studies in detection physics, materials, and radiation effects.

Although available detectors often operate within a factor of 2 or 3 of their theoretical maxima, there are still critical needs for continued detector research to meet future requirements. System reliability, radiation hardness, and ability to operate with a minimum of cooling must be

improved. Because most detectors lose sensitivity rapidly as the signal frequency increases, they cannot be used in high speed, high resolution reconnaissance systems or optical communications systems. Detectors are too expensive for some large scale uses, such as passive interdiction systems or "smart" rockets and bombs. Tactical systems could benefit greatly from advanced detectors because factories, truck engines and even men emit significant amounts of infrared energy, making covert and nighttime operations possible. Ideally, tactical aircraft should have a forward-looking passive imaging system to achieve first pass night attack capability. The "front end" of such a system would consist of 100 to 500 detector-amplifier channels scanned across the scene in front of the aircraft with a moving mirror system. Typical detector costs today are \$500 to \$1,000 each or \$50,000 to \$500,000 per "front end" focal plane, so that cost alone can limit significant deployment. Finally, many detectors are sensitive to radiation effects such as those produced by weapons or trapped particles of the Van Allen belts. Other detectors are easily degraded by relatively low level laser radiation. Thus, there is a need for innovative work leading to low cost, increased reliability detectors that can lead to such results as long range, high reliability missile detection, large forward-looking infrared (FLIR) systems, nighttime "smart" bombs, and passive detection modes for RPV's. AFCRL has initiated a detector program to develop new detector concepts, develop new detector materials, develop integrated optics, study radiation effects in detectors, and study sensor hardening so that we will have a basis for such a technology.

DETECTOR CHARACTERIZATION: To evaluate overall detector performance, to study operational mechanisms, and to communicate with the manufacturers and users of infrared detectors, one must know many characteristics of the device in question.



System for measuring microscopic uniformity of photoresponse.

Spectral response, rise time, noise signature, temperature dependence, and equivalent circuit parameters are some of the important characteristics. In addition, in a program studying radiation effects, there must be a capability for fabricating special samples as well as a capability for measuring radiation-induced defects and their secondary modifications of detector characteristics. Sample preparation at the Laboratory may include epitaxial growth, integrated circuit techniques, ion implantation, and vacuum evaporation processing. The first three are discussed in other parts of this chapter. Vacuum evaporation is used to apply metallic contacts to semiconductor substrates, to form microscopically thin surface alloys and form surface interconnection patterns. Metallic contacts may be ohmic for simple electrical connection or they may form barriers at the surface which are electrically active. The latter contact is known as a Schottky barrier and has been studied in detail at AFCRL because of our belief that it can be exploited in producing high performance, low cost, reproducible detectors. Schottky contacts can be used to form electrical junctions on semiconductors which do not allow p-n junction formation, they can be formed at room temperature, which is important because many detector yield problems are caused by high temperature processing, and finally, they allow the photoresponse

of silicon-based detectors to be extended to longer wavelengths.

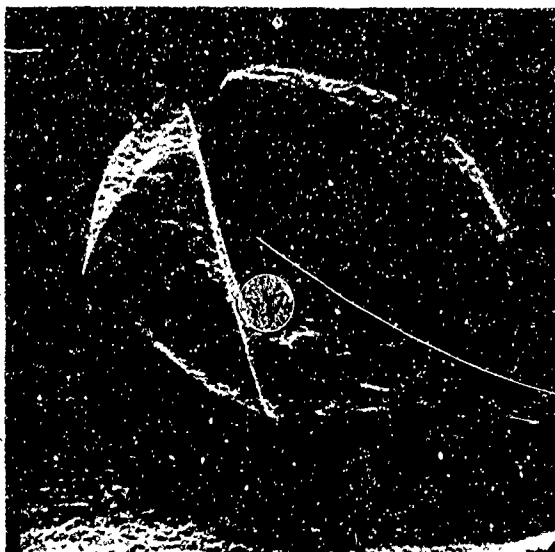
To produce barrier contacts, the surface of a sample is carefully prepared by etch polishing, washing, and final oxide removal etches, done in laminar flow clean benches. Samples are then placed in an ultra-clean high vacuum system where metals are evaporated through a precision mask. To prevent contamination, the vacuum system is oil-free and rough pumped with liquid nitrogen sorption pumps. Precision metal masks or standard photolithographic techniques are used to define the device geometry. Electron beam, thermal, or sputtering metal sources are used.

Detector spectral response is determined using a monochromator system with a split optical output beam which compares the device under test with a calibrated thermocouple. The ratio of the two signals gives the detector spectral responsivity. A computer has been interfaced with the system to record and analyze detector data automatically.

Noise data are taken in a special screen room facility which is both electromagnetic and induction shielded. High resolution current-voltage and capacitance-voltage characteristics are measured. Microscopic uniformity of photoresponse can be measured. An example of a response contour caused when a processing defect resulted in reduced efficiency extending into the central region of the detector is shown.

Two powerful tools for determining the details of radiation-induced defects are thermally stimulated current measurements and thermal capacitance transient measurements. The number of induced defects in the crystal, their energy level and their capture and emission cross sections can be determined from these measurements.

NEW DETECTOR CONCEPTS: State-of-the-art detectors have low yields, poor within-array uniformities, low reliability, and very high costs. In addition, very few de-



Typical response contour measured on microscopic response system.

tectors have wide bandwidth electrical capabilities. Most of these difficulties are caused by the use of critically balanced semiconductor materials that cannot be prepared reproducibly and which are very easy to damage during processing. Therefore, in a radical departure from conventional detector design, the infrared photoresponse of metal barriers on silicon substrates was investigated. These detectors differ from conventional devices in that photoabsorption occurs in a metal rather than in a semiconductor. Uniformity, high reliability, low cost, compatibility with silicon integrated circuits, performance equal to state-of-the-art detectors, and very fast response, were the advantages sought. These advantages were possible because the devices were based on silicon technology, the basic operating mechanism did not depend on silicon or metal impurity densities, and they operated only by majority carrier processes. Majority carrier operation eliminates most of the processing-dependent degradation mechanisms which have plagued other detectors.

This program has now achieved all but

one of its research goals. Schottky photodiodes are very reliable, reproducible, and uniform. It is also clear that they could be produced at low cost. Also, they can be fabricated both singly and in very large arrays, as integral parts of silicon monolithic circuits.

The program has accomplished several important objectives: The cutoff wavelength of a silicon photodiode has been extended from 1 to 5 micrometers, and the response could be extended to 20 micrometers. A room-temperature single element detectivity of $4 \times 10^{10} \text{ cm-Hz}^{1/2} \text{ watt}^{-1}$ has been achieved. A theoretical model of the photoabsorption process including thin film and phonon scattering effects has been developed. The first reported silicon avalanche detector has operated beyond 1.2 micrometers wavelength. Finally, 2 GHz optical modulation has been successfully detected.

An elemental quantum efficiency comparable to those in state-of-the-art devices is the only program goal which has not been achieved. The highest efficiency measured in the Laboratory for a metal-photoabsorption device is 3.5 percent. Optimization might give an additional factor of 2. Typical quantum efficiencies are 0.2 to 1 percent. Conventional detectors have typical quantum efficiencies ranging from 1 percent to 70 percent with typical values in the 20 to 30 percent range, although it is difficult to get large arrays with efficiencies higher than 10 percent because of processing uniformity limitations.

In spite of this limitation, Schottky detectors may exceed the performance of state-of-the-art detectors when used in large arrays. This optimism is based on two important properties of these detectors: their photoresponse is more uniform than for present conventional detectors, and they have already been developed and can be applied immediately to silicon integrated circuits. These factors will allow construction of large element density two-dimensional arrays. These arrays could be

the retina of an electron beam accessed vidicon or could be an all solid state array which would be read out by any of several integrated circuit techniques.

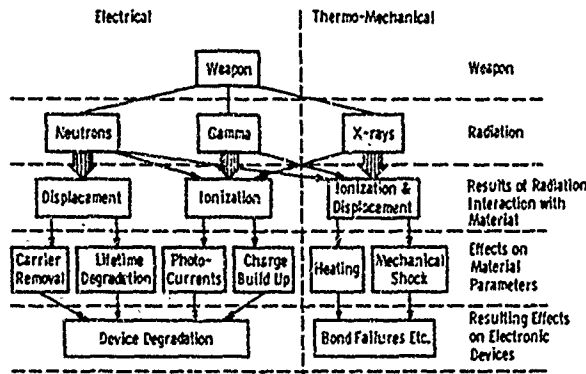
If we assume a state-of-the-art FLIR system having 30 percent quantum efficiency and a square array Schottky barrier system having 0.3 percent quantum efficiency we can compare overall efficiencies. We assume equal sized detector elements and equal flux densities at the focal plane of each system. If the output is a standard television raster, we require 512 lines with 512 resolution elements per line. The Schottky barrier system would use a square detector matrix which stares at the target, while the conventional FLIR system uses 512 detectors in a line, and a spinning mirror scans the scene across the detector line, so that each target is sampled for a dwell time equal to the frame time divided by 512. If the system is either background or shot noise limited, the signal-to-noise ratio will be proportional to the square root of the number of particles counted per frame for each element. The comparative signal-to-noise ratio would be 512 times the Schottky detector quantum efficiency, divided by the conventional detector quantum efficiency, and this is expected to be about 2. The overwhelming advantage of the proposed Schottky barrier system would be its lower cost. Savings factors as great as 100 may be possible with equal performance. The front end of the Schottky barrier system would be one camera tube or one integrated circuit, as opposed to 512 individual detector-amplifier pairs. Also, the moving mirror system would be eliminated, further reducing system weight and complexity. The basic device studies are complete; what remains is the exploitation of their special properties.

INTEGRATED OPTICS: Studies in integrated optics are concerned with the generation, modulation, directing of flow, and detection of optical wavelength energy in

solid structures. Operating devices are made using both linear integrated circuit processing techniques and laminar epitaxial crystal growth. The resulting structures are functionally analogous and geometrically similar to the highly successful microwave acoustic devices.

Our first effort in this area is the Zone Plate Photodetector study which is using silicon monolithic processing to fabricate a zone plate lens on a silicon Schottky barrier device. These devices are expected to focus energy from a large input aperture to a small electrical aperture on the same semiconductor chip, resulting in a signal gain. Focusing of energy from a large to a small aperture has been demonstrated using a collimated infrared microscope. Losses, apparently due to geometrical tolerances, and much more importantly, due to attenuation of the 1.15 micrometer beam in the silicon substrate, have prevented realization of the expected signal gains. The dominance of loss by attenuation was demonstrated by cooling the detector, which increased the semiconductor energy gap and in turn decreased the absorption cutoff wavelength, resulting in a 40 percent increase of the zone plate detector response in relation to a reference detector. New designs which will circumvent these problems must be evolved. Theoretical zone plate studies have shown the possibility of using more complex metallization filters for coding and identification. One example is a detector which delivers a peak signal when two preselected wavelengths are coincident on the detector. The theoretical effort in the study has shown that the zone plate structure is analogous to a multi-element antenna where properties such as directivity can be defined and controlled. A second phase of the program in which laminar optical waveguides will be grown epitaxially has been initiated.

BASIC RADIATION EFFECTS IN DETECTOR AND SENSOR HARDENING: These studies seek to determine the basic mechanisms by



Principal effects of nuclear radiation on electronic devices.

which ionizing radiations affect detectors that operate in the 10-micrometer spectral region and the modifications caused by permanent radiation damage. Studies include theoretical modeling and experimental verification. Emphasis is placed on determination of signal loss mechanisms and experimental verification, the relationship of ionizing noise spectra to defect density, energy and cross-section parameters. The results of these studies are used to analyze the radiation sensitivity of AFCRL environmental sensors and to make these sensors as radiation-resistant as the state of the art will permit.

RADIATION EFFECTS AND DEVICE HARDENING

All solid state sensors are vulnerable to ionizing radiations from nuclear weapons. The proliferation of solid state devices has aggravated the problems which the Air Force must overcome to keep vital systems operational even after exposure to nuclear radiation. Devices used on satellites are exposed to radiation in space. The Laboratory program fills gaps in the knowledge of radiation effects on solid state devices to

support Air Force development of radiation-hardened electronic systems.

DISPLACEMENT EFFECTS: When a semiconductor material is subjected to energetic radiation, two types of radiation effects can occur. Lattice atoms may be displaced, causing permanent effects, and ionization and excitation events can cause transient effects.

Lithium-doped silicon shows promise for use in radiation-resistant solar cells. The Laboratory studies the unconventional permanent displacement effects in this material, to develop a physical model which will explain the electrical behavior of the material in terms of lithium-defect interactions. A model was developed on the basis of Hall effect and resistivity measurements made before and after both irradiation and heat treatment. Infrared absorption measurements also support this model and provide microscopic detail. Results are consistent with a precipitation-like interaction between lithium and neutron-produced defect clusters. The most important determination was that, for every neutron per square centimeter impinging on silicon, approximately 200 lithium atoms per cubic centimeter are required to neutralize the damage.

CHARACTERIZATION OF DEFECTS: Simple displacement damage occurs when a lattice atom is displaced from its normal position, leaving a vacancy. A defect complex is formed when an impurity atom in the crystal combines with the vacancy to form a relatively stable structure. These defect structures are effective charge carrier trapping centers, and cause a general degradation of the crystal electronic properties. The irradiation damage in a crystal can be determined by measuring charge trapped by defects in a manner analogous to the measurement of charge stored in a parallel plate capacitor. Using this capacitance measurement technique, defect structures have been characterized accord-

ing to introduction rates, ionization energy, and charge carrier capture parameters. These characteristics determine the trapping effectiveness of the defect, and the susceptibility of semiconductor devices to the effects of radiation.

RADIATION-INDUCED ELECTRON TRANSPORT EFFECTS: When a beam of X-rays or gamma rays passes through a solid it produces energetic recoil electrons. Most of these are projected in the same direction as the primary photon beam, carrying both energy and charge away from the initial interaction site. Any given electron travels only a short distance before it loses all its energy and comes to rest. However, since electrons are continuously generated along the entire path of the primary beam, the net result can be viewed as a continuous flow of charge and energy throughout the solid. The magnitude of the secondary electron current varies from one material to another due to differences in the probability that a photon of a given energy will first release an electron and second, that the electron will scatter in the backward direction. Since the scattered electrons possess more than a million times as much energy as ordinary conduction electrons,

customary classifications of materials as insulators or conductors are not reliable guides to the magnitude of radiation-induced currents generated in solids. For example, at high photon energies (more than one million electron volts), the radiation-induced current in silicon dioxide, which is normally considered an excellent insulator, can be several times greater than that in gold or copper. At X-ray energies, the radiation-induced currents in materials may differ by as much as a factor of 1000.

This difference in radiation-induced currents can produce a number of very damaging effects in electronic devices. When induced currents in adjacent materials are very different, there will be a net flow of both energy and charge into or out of the region near the boundary between them. Thus, the energy deposited in the transition region can differ markedly from that deposited in the material away from the boundary. An accurate estimate of the energy deposited in the material by radiation is the starting point for predictions concerning the response of electronic systems.

When one of the materials at a boundary is an insulator, large charge densities may build up. The electric field resulting from this process can seriously interfere with the operation of electronic devices. Finally, at a solid-vacuum boundary, an electron current will be projected into the normally insulating vacuum space, thereby providing leakage paths which can interfere with electronic systems not directly exposed to the primary radiation. Near the end of this reporting period, a Laboratory program of experiments and calculations produced the first reliable assessments of the nature and magnitude of secondary electron transport effects of this type.

Energy deposition, electron emission, and charge accumulation were studied in some detail. The conventional experimental and computational techniques for determining these radiation-induced trans-

	Radiation Effects To Be Minimized	Techniques For Minimization	Resulting Device Design Constraints	Resulting Non-Radiation Electrical Compromises
Neutron Induced Permanent Charge	Resistivity Increase	High Majority Carrier Doping	Long Thin Geometry	
	JFET Gain Decrease	High Majority Carrier Doping	Very Thin Channels	Decrease in Reverse Breakdown Voltage
	Bipolar Gain Decrease	Cold Doping Thin Base Widths	Very Thin Base Widths Extra Processing Step	Decrease in Gain
	Diode Characteristic Changes	Cold Doping High Majority Carrier Doping	Extra Processing Steps	Decrease in Breakdown Voltage
Ionizing Radiation Induced Transient Permanent	Transient Photo Currents	Cold Doping Dielectric Isolation Small Geometry High Majority Carrier Doping	Extra Processing Steps, Thin Geometry	Decreased Breakdown Voltage
	Charge Trapping In Dielectric	Research on Trap Free Dielectrics	New Processing Techniques	Possible Temperature Instabilities, Reduced Breakdown Voltage, and Hysteresis Effects

Table of device hardening techniques and their resulting design and electrical characteristic compromises.

port phenomena ignored boundary effects and yielded results applicable only to material more than an electron range away from any boundary. This was done even though solid state devices have dimensions such that critical device elements are always within the transition region where transport effects dominate. The boundary effects were not accounted for because experimental data and reliable theoretical calculations were lacking. Laboratory scientists developed experimental techniques and applied them to a wide variety of material combinations and incident photon energies to relieve this situation. One finding is that the energy deposited in a low atomic number material adjacent to one of higher atomic number can be more than a factor of 10 greater than that obtained by the usual dosimetry methods. It was also found that the energy deposition profiles in a given pair of materials change radically with beam direction, that micron-thick layers of high atomic number materials are sufficient to produce an effect in adjacent low atomic number materials, and that the deposition profile observed is extremely sensitive to the incident primary photon spectrum. Computational techniques were developed which seem to predict most of these effects. The practical consequences of electron transport phenomena are now being studied.

Experimental data were needed to verify existing electron emission calculations. Little information was available because the measurements were difficult to make. Electron yields are low at the X-ray intensities available in the laboratory, necessitating considerable judgment in the selection and design of instrumentation. The first absolute measurements of electron distributions over the X-ray energy range were made in this Laboratory. Initial comparisons with computer calculations indicate that differences exist. The studies are now directed towards resolving these discrepancies.

Investigation of the third transport phe-

nomenon, charge accumulation at material boundaries, is still in its early theoretical and experimental stages. The information available is still insufficient to allow a determination of the degree of agreement between theory and experiment, and experimental techniques to examine certain facets of the theory are still being developed. However, several interesting observations have been made. In boundary regions where excess energy is deposited, the injected charge is negative, and in energy-depleted regions, the charge is positive. The sign of the injected charge may change more than once as a boundary region is traversed; e.g., positive-negative-positive. Although these effects will have a strong influence on dielectric behavior, detailed knowledge of this phenomenon and its effect on systems response must still be gained.

HARDENING OF QUARTZ: When a precision quartz oscillator is subjected to energetic radiation, it will shift in frequency and may even cease to oscillate. For certain space and missile applications, the transient and permanent frequency shifts of commercially available oscillators are not within acceptable limits.

At the request of SAMS/Aerospace Corporation, the Laboratory began research to develop quartz crystals which can be made into radiation-resistant oscillators, to devise non-destructive and non-irradiative test procedures, and to achieve some understanding of the physical mechanisms involved in the radiation processes.

Eight different types of quartz materials were investigated. The frequency changes of the 5 MHz, 5th overtone, AT-cut, temperature-controlled oscillators were monitored as a function of 10 MeV electron irradiation to a dose of 10^6 rads. Electro-diffused, swept, electronic grade quartz was found to be the hardest to radiation. Acoustic loss, or reciprocal Q, measurements were performed on resonators between 4.2 and 500 degrees K, before and

after irradiation, and changes in frequency were correlated with changes in Q spectra.

A 3⁺ charge impurity substituted for an oxygen atom in the quartz (SiO_2) lattice needs a 1⁺ ion for charge compensation. This could be provided by hydrogen, sodium, lithium, or potassium. Both during the sweeping and irradiation processes, the original charge compensation is disturbed resulting in changes in Q spectra and in frequency response during irradiation. For radiation hardness, in addition to sweeping and the elimination of sodium and lithium impurities, it is necessary to include potassium within the crystal. This large ion blocks the channels along certain crystallographic directions and prevents motion by the smaller ions. Usually, uncontrolled or even controlled impurities in a crystal are detrimental to device operation, but in this unusual situation, the controlled addition of specific impurities is essential to the successful operation of the device.

Infrared absorption spectra in the 2.5 to 3.5 micrometer region reveal vibrational complexes, substitutional and interstitial impurities, changes caused by irradiation, and changes caused by sweeping. Distinguishing features in the optical spectra were measured for all types of quartz. Various types of quartz can be distinguished by their IR signature, and a non-irradiative and non-destructive test of sweeping is now possible.

RADIATION SERVICES AND DOSIMETRY: Operating conditions for solid-state devices can include exposure to radiation. Laboratory simulation of space and nuclear radiation environments is an important aspect of the radiation effects program. The radiation facilities of the Solid State Sciences Laboratory were designed to meet basic research needs, and to simulate radiation environments of specific interest to the electronic system designer.

Simulation of nuclear weapons environments is difficult because many parameters can vary in a nuclear event. These would

include: type of radiation, energy distribution, time dependence, and relative intensity. Field tests utilizing actual nuclear detonations would be ideal, but are usually not available when needed and are expensive. For these reasons, the approach has been to supply relatively monoenergetic sources of specific types of radiation, in order to sort out the effects of various component parts of the total environment.

In accordance with this approach the various sources listed in the table satisfy different simulation requirements. The Van de Graaff serves as a 1.5 MeV neutron source, the Pulserad simulates intense pulsed X-ray environments in the 1-2 MeV range, and the linear accelerator is a pulsed 10 MeV electron accelerator which can be used to simulate gamma radiations. Steady state gamma requirements are satisfied with the Co-60 source and steady state electron requirements are met with the 1.5 MeV Dynamitron. Electrons are commonly used for simulation purposes even though there are no primary electrons in the nuclear environment. The assumption is made that if the same amount of energy is deposited in the test sample in the same time interval, then simulation is achieved. This has proved to be a reasonable assumption. However, care must be exercised when dealing with new devices and modified environments.

The radiation facilities in the Laboratory constitute the most complete simulation facilities available in the Department of Defense for in-house researchers, defense contractors, and other DOD agencies to perform laboratory experiments. Many groups used these facilities extensively to satisfy system requirements for radiation hardness. Programs directly related to Advanced Ballistic Reentry Systems (ABRES), Poseidon and Hardened Power Supply projects have been performed here. The linear accelerator fulfilled the radiation requirements for most of this work, and the Co-60 source was used for back-up dosimetry and steady state gamma re-

AFTRL RADIATION SOURCES

RADIATION SOURCE	TYPE OF RADIATION	ENERGY	OUTPUT
Van de Graaff	Electrons, Protons & Heavy Ions Neutrons via nuclear reactions	1.5-3.0 MeV 1-14 MeV	0.500 μ A
Dynamitron	Electrons	0.3-1.5 MeV	10 ma
LINAC	Electrons/X-Rays	3-23 MeV	2 amps pulsed or 0.4 ma (avg)
Flash X-Ray Sources: Febatron Pulserad Cobalt-60 Source	X-Rays Electrons/X-Rays Gamma Rays	300 keV 2 MeV 1.25 MeV	5000 amps 20,000 amps 12,000 curies (Aug. 72)
Positive Ion Accelerator	Electrons, Positive Ions	300 keV	

quirements. Approximately 80 percent of the available radiation time is used for in-house programs. These programs include radiation effects studies on experimental electronic devices, electron-induced emission studies, impurity effects in neutron-irradiated semiconductor materials, and ion implantation studies.

Facility personnel are also conducting a radiation dosimetry program. The response of Co-60 irradiated N/P silicon solar cells was measured as a function of the atomic number of the medium adjacent to the cell and the direction of the gamma ray beam. Previous work in this Laboratory has demonstrated dose perturbations at the interface of materials of different atomic number. Placing various thicknesses of aluminum between the adjacent material and a silicon solar cell had the effect of moving the cell to various locations in an approximate monatomic numbered medium. The solar cell response was determined with this technique at various distances from the interface for gold and

beryllium. Results agreed with predictions based on ionization chamber measurements of dose perturbations in aluminum made in this Laboratory, within 5 percent. Also predicted and demonstrated was a strong response dependence on the direction of the gamma ray beam.

HARDENING OF ELECTROMAGNETIC DEVICES: Few electronic devices were originally designed and tested for radiation resistance, but many military systems must function in a space or nuclear weapons environment. Thus, the great gains in reliability and decreased size resulting from the use of solid-state devices were partially offset by a much greater sensitivity to all kinds of radiation.

Semiconductor devices are sensitive to radiation because they depend on a delicate charge balance, high crystalline perfection, or both, for proper operation. Because both of these qualities are altered at relatively low radiation levels, electronic systems may malfunction at much lower

radiation levels than would be required to cause structural damage to a missile or satellite. A transistor radio made with wide-base, low-frequency transistors would stop playing after a radiation dose which would not incapacitate a man until several days later, even though it would probably be fatal. Fortunately, most of these hardening problems can be solved, if they are known to exist. Shielding, which would effectively eliminate the problem, is usually too heavy to apply to all systems. More sophisticated approaches must be used.

AFCRL is taking long-term and short-term approaches to hardening semiconductor devices. The long-term approach seeks to modify materials and material interfaces so they are less affected by radiation. Before this can be done, a basic understanding must be gained of why material parameters are affected by radiation. The short-term approaches are to design semiconductor devices so that they are less affected by material property changes, and to find and use in circuits these semiconductor devices which are electrically useful and resistant to radiation.

To meet present and future Air Force needs, all semiconductor devices should be hardened to the maximum practical extent, or at least the theory and techniques to harden them should be developed, since devices which seem sufficiently hard may not be adequate in harsher environments in the future. Not only are design radiation levels increasing, but requirements on the allowable degradation of devices at the present levels are also becoming more stringent. Recent requirements imposed on the Zener diode, which had been considered very radiation resistant, specified such small allowable changes in electrical characteristics under radiation that hardening of the device became necessary, and theory and techniques did not exist. Therefore, theory and techniques should be developed, not only to meet today's

radiation requirements, but also for meeting future contingencies in an efficient manner.

PHYSICS OF DEVICE HARDENING: The science of electronic device hardening seeks to design devices so that they depend as little as possible on materials properties that are sensitive to radiation. The changes in operating characteristics induced by radiation vary considerably with the type of device and the nature of the radiation.

Transistors display all three principal categories of radiation damage: displacement, ionization, and thermomechanical. The principal cause of displacement damage is fast neutrons, which cause minority carrier lifetime reduction and carrier removal. They also cause mobility reduction, a second-order effect. X-rays and gamma rays cause permanent ionization damage by causing charge to build up in the oxide and transient effects by generating photocurrents. The transient effects caused by very high dose rates are usually handled by circumvention techniques in the electronic system. The extent of transistor degradation due to displacement and ionization depends strongly on the transistor type, while the extent of thermomechanical damage does not depend on the transistor type, but depends mainly on packaging and metallization, which are common to all transistor types.

When bulk material parameters are modified to decrease their sensitivity to radiation, changes in the geometry of the structure are usually required as well, either to maintain the same electrical characteristics as before the device was redesigned or at least to ensure that the electrical characteristics are still useful.

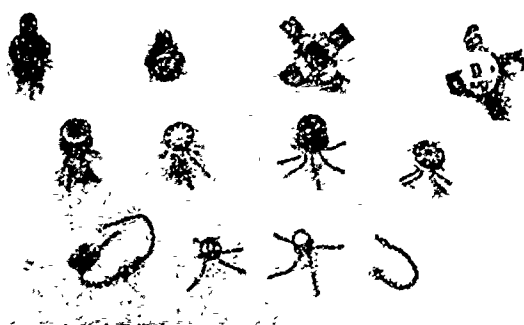
Fortunately, hardening against one type of radiation actually assists in hardening against another type. For instance, gold doping a bipolar transistor to minimize neutron-induced permanent gain degradation also reduces gamma-induced transient

photocurrents. Further, most device hardening techniques lead to a better understanding of device materials and processing techniques, and to better, more reliable devices. For example, very small base width bipolar transistors, needed for radiation hardening, are being investigated for extending the frequency response of bipolars.

AFCRL scientists have studied the numerous requirements, the numerous radiation environments, the feasibility of shielding against some types of radiation, the necessity of circumventing high dose rate-induced transients, the radiation sensitivity of existing devices, and their hardening potential (based on a detailed comparative study). It was found that the most serious deficiencies existed in devices and integrated circuits hardened against neutrons and gamma rays and designed to operate at the two extreme power levels, high power and micro-power, and also in linear integrated circuits. These are still the most serious problems, but the AFCRL program has significantly lessened the deficiencies in research and exploratory development.

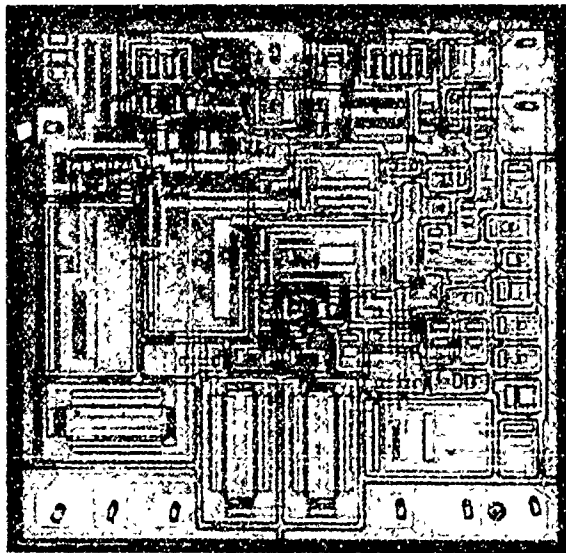
HARDENED POWER TRANSISTOR: Considerable design and testing effort at AFCRL was applied to optimum design and parameter testing of bipolar transistors to handle

high power. Silicon power transistors require many design compromises, even if radiation effects are not considered. High-current devices are usually designed with thick base regions and large junction areas to dissipate large amounts of heat when necessary. However, bipolar devices hardened to neutron irradiation must have low minority carrier lifetimes in the base regions, so that even for low frequency operation, the base must be thin, if the device is to have useful gain. Thus, a uniform, thin, large area base region is a requirement for radiation-hardened power transistors, and the designer faces a difficult problem. Satisfactory solutions have been achieved by very careful design and balancing of various fabrication parameters. This has necessarily involved improved process control. As the power dissipation of a transistor increases, the related problem of second-breakdown becomes more critical, since thermal generation of carriers in the base region is involved. Neutron irradiation aggravates this situation, since it causes lower current gain with its resulting decrease in efficiency, further increasing the power dissipation for a given power output. Although transistors have been developed that satisfy most specifications, there are still problems. Power bipolar transistors had previously been designed for optimum neutron hardness. However, there are still serious burnout problems associated with internally generated photocurrents caused by high dose rate ionizing radiation.



A collection of radiation-hardened devices developed in the Solid State Sciences Laboratory.

LINEAR INTEGRATED CIRCUITS: Commercially available linear integrated circuits are much more sensitive to radiation than digital devices. Because linear circuits are usually designed for very high amplification, they operate at lower current levels, and active elements with high gain and long minority carrier lifetimes are required, which result in "inherently soft" devices. Typically, non-standard current



This is the first radiation-hardened integrated circuit. This operational amplifier is unique, not only because it is hardened, but also because it is the only successful example of a monolithic MIS device with mixed JFET and bipolar technology applied to the same chip.

elements such as lateral p-n-p transistors, supergain transistors, pinched base resistors, collector resistors, and collector junction FET's are used. The most obvious method for hardening the devices is first to eliminate the circuit elements with the greatest susceptibility to radiation, such as lateral p-n-p junctions, and then apply other standard hardening techniques. The Type 770 Operational Amplifier, developed by AFCRL and one of its subcontractors, is the only balanced hardened operational amplifier (hardened against gamma rays, gamma dose rate, and neutron flux) known to the Laboratory.

This operational amplifier employs SiO_2 dielectric isolation, thin film resistors, photocurrent compensation techniques, and junction field effect transistors to achieve radiation hardness. The 770 is, in 1972, the only monolithic MIS device which employs JFET and bipolar technology to obtain optimum electrical and hardness characteristics from both device technologies.

The epitaxial junction field effect devices which were used in the first model of this device did not have the very closely matched characteristics desired for the input differential amplifier stage. Ion implantation is currently being employed to deposit a diffusion source for the input JFET's and has yielded devices with the desired matched characteristics and amplifiers with offset voltages of less than 5 mv.

HIGH TOTAL DOSE EFFECTS: Most studies of radiation effects on semiconductor devices have used dosages of less than 10^6 rads. The Laboratory has attempted to understand theoretically and determine experimentally the permanent degradation effects in bipolar transistors due to ionizing dose levels up to 10^8 rads. The radiation degradation due to ionizing radiation was characterized as a function of collector current (injection level) for a number of bipolar devices. In many devices there was more than 90 percent degradation in current gain for a total gamma dose of 10^8 rads for collector current near the maximum current gain.

Numerous bipolar device types were exposed to Co-60 gamma radiation in the AFCRL cobalt source. The devices were irradiated passively without bias to three dose levels, 10^6 , 10^7 , and 10^8 rads, in silicon. DC current gain as a function of collector current and base-emitter voltage as a function of collector current were measured. These measurements were made using special test equipment which records the log of the current gain, and the base-to-emitter voltage versus the log of the collector current directly. Extensive total dose tests have been performed on Metal-Insulator-Semiconductor (MIS) and JFET devices to radiation levels of more than 10^8 rads gamma and to 10^{16} neutrons per square centimeter.

ZENER DIODES: Because diodes operating in avalanche are used for voltage regula-

tors in many military systems and because avalanche diode oscillators have great future potential, experimental and theoretical information was needed on the transient radiation response of diodes operating in avalanche breakdown. The usual diode response model does not apply, because a diode in avalanche behaves like a voltage source, rather than the current source it resembles under other operating conditions.

Silicon diodes with breakdown voltages from 5.7 to 85 volts were exposed to ionizing dose rates from 10^7 to 8×10^9 rads per second for a wide variety of bias conditions near and in avalanche breakdown. The effectiveness of various hardening techniques was determined experimentally. The transient response of specially designed, neutron-hardened, temperature-compensated, voltage-reference diodes was determined to evaluate the consistency of permanent neutron and transient ionizing hardening techniques. The effect of the temperature compensating junction on transient current was determined for zero-temperature-compensated diodes. The transient response of voltage regulating diodes was evaluated as a function of the circuit providing bias current to the diodes as well as the impedance of the circuit that the reference diode drives. A model appropriate to diodes operating in avalanche breakdown and in an ionizing radiation environment was formulated.

OTHER EFFECTS: Our efforts thus far have been directed primarily toward hardening particular general-purpose semiconductor devices which preliminary analysis indicated could be hardened by standard semiconductor technology. By applying available knowledge of the effects of radiation on general-purpose semiconductor devices and silicon material, semiconductor physicists have now approached the silicon device hardening limits for some of the primary radiation effects. But, problems such

as EMP, both external and internal, and very high dose rate effects, are not sufficiently well documented or understood for devices hardened against them to be developed.

PROCESSING TECHNOLOGY

Experimental solid-state device research requires an up-to-date processing facility. Crude prototypes made for research purposes simply cannot provide meaningful data. For this reason, the Laboratory maintains a state-of-the-art semiconductor processing capability and also works to advance the state of the art.

Silicon and GaAs single crystal slices are readily obtainable from commercial vendors; therefore, the Laboratory does not work on developing processing technology for these materials. Epitaxial layers on single crystal slices are also available commercially; therefore, the experimental vapor phase epitaxial growth reactor in the Laboratory is used to work on special processing problems. At the end of this reporting period, it was being used to study epitaxial growth in windows, areas where the epitaxial deposit is masked by oxide and occurs only where the oxide has been etched off. Since very thin layers (less than 0.5 micrometer) are not available commercially, they are also being studied with this reactor. The Laboratory system has been designed for versatility. For example, by changing the incoming gases and the growth temperature, we can clean the silicon slice by etch removal of a thin layer and then, without removing the slice from the reaction chamber, deposit n- or p-doped silicon and also pyrolytically deposit an oxide or nitride film to cover the silicon if this is necessary in device processing. When epitaxy is used in the latter stages of device fabrication, it is important that both etching and growth take place at as

low a temperature as possible to minimize redistribution of dopants already present. Either high purity liquid silicon tetrachloride or gaseous silane is used for silicon epitaxy. Hydrogen is normally used for dilution and as a carrier gas for silicon tetrachloride. However research into the thermodynamics of the epitaxial reaction has shown that when high purity helium replaces part of the hydrogen, the reaction temperature for both etching and deposition can be reduced.

PHOTOLITHOGRAPHY: The use of light-sensitive, etch-resistant emulsions to define minute areas is the basis of modern semiconductor device processing. While most devices can be processed with the state-of-the-art capability of about 2.5 micrometers line width, two devices, microwave acoustic delay lines and the zone plate detector, require control of dimensions to 1 micrometer. This has been done for acoustic delay lines by pressure contacting and processing one device at a time. The zone plate detector, described in the section on infrared detector research, places a radically new control requirement on photolithographic processing. The zone plate requires alternate rings of equal area so that in the photoresist exposure, both wide and very narrow (1 micrometer), lines must be defined at the same exposure setting. To achieve the result shown in the picture, every step from the initial artwork through each reduction has required separate optimization of exposure times. Five ring zone plates with appropriate ring width have been achieved, but further compensation and optimization will be needed to achieve structures with greater light-gathering power.

ION IMPLANTATION: This technique for precise doping of semiconductors has been used here for studies with both silicon and gallium arsenide. So-called second-order effects, such as lifetime degradation and



Oxide pattern for zone-plate photodetector.

recovery, and the introduction of defect levels in the forbidden band were studied for silicon. First-order problems such as the relationship between implant energy, dose, ion species, implant temperature, anneal temperature, ion distribution and electrical conductivity in silicon have been discussed in past reports. In gallium arsenide it is these first-order effects which are being investigated.

Phosphorus-diffused diode structures are used to investigate lifetime degradation and defect level introduction in silicon. The diodes are implanted at sufficiently high energies so that the ions penetrate to the region immediately beyond the junction. Minority carrier lifetime is measured with the diode reverse recovery technique. Carbon ions were used to study damage effects, because the atomic mass of carbon is close to that of boron, which is the common p-type dopant in silicon, and the carbon itself is non-doping so that the

diode changes are related only to the damage and not to additional doping. For doses below 3×10^{13} ions per cubic centimeters, recovery of minority carrier lifetimes is accomplished at temperatures which are well below the diffusion temperature. For large doses, minority lifetime is permanently degraded. Since carrier lifetime is primarily controlled by energy states near mid-gap, these measurements indicate that mid-gap defect levels will anneal out at 650 degrees C in silicon. Other defect levels introduced in the ion implantation process can be observed by measuring thermally stimulated currents. These usually anneal out at temperatures somewhat above 500 degrees C. This was demonstrated using non-doping sulfur ions to simulate the mass of phosphorus, the common n-type dopant in silicon. The experiments demonstrated that annealing at temperatures from 500 to 650 degrees C will restore the silicon crystal to such order that very sensitive parameters, such as lifetime, are regained.

Gallium arsenide is rapidly becoming an important semiconductor material. One limiting factor in fabrication of GaAs devices is the inability to form thin, heavily doped n-type regions. Ion implantation offers one approach. Other methods of doping GaAs have not been very successful. Possible causes of failure are that the ions do not become located at the desired lattice sites, and defect compensation. Defects resulting from the ion irradiation appear not to be totally removed during post-implantation annealing. The severity of defect compensation in GaAs is suggested by the tendency of implanted junctions to exhibit p-i-n rather than p-n behavior.

Experiments to establish the degree of compensation occurring when non-dopant ions are implanted, as well as the behavior of these defects on annealing, are presently underway. Emphasis is on differential capacitance measurements, using Schottky diodes for depleting through the ion-dam-

aged GaAs. Epitaxial GaAs with a <100> orientation grown in-house is used. Initial results show that most of the initial carrier concentration can be recovered on annealing if the dose implanted was within the $10^{12} - 10^{13}$ ions per square centimeter region, by annealing to about 650 degrees C. Heavier doses ($10^{13} - 10^{14}$) do not recover at such temperatures and studies to solve this problem will continue.

JOURNAL ARTICLES JULY 1970 - JUNE 1972

ARMINGTON, A. F., and O'CONNOR, J. J.

Gel Growth of Iodide Crystals
Mat. Res. Bull., Vol. 6, No. 8 (August 1971)

ARMINGTON, A. F., STARKS, R. J., and BUFORD, J. T.
(Eagle-Picher Res. Lab., Miami, Okla.)

The Determination of Carbon in Iodide Boron
Book, BORON, Vol. 3 (Pub: PQN, Polish
Scient.-1970)

BENDOW, B.

*Theory of Indirect Excitation of Sound by
Light*
Phys. Rev. B., Vol. 4, No. 10 (15 November 1971)

BENDOW, B., HORDVIK, A. (Optical Physics Lab.),
LIPSON, H. and SKOLNIK, I.,
*Optical Evaluation of CO₂ Laser Windows
Materials at AFCRL*
Proc. of 5th Conf. on Laser Tech., Vol. 1 (1972)

BENDOW, B., JASPERSE, J. R., and GIANINO, P. D.
*Kirchhoff Diffraction Theory of Thermal
Lensing in Solids*
Opt. Comm., Vol. 5, No. 2 (May 1972)

BENDOW, B., and YING, SEE-CHEN (Brown Univ.,
Providence, R. I.)
*Quantum Theory of Desorption of Adatoms from
Solid Surfaces*
J. of Vacuum Sci. and Tech., Vol. 9, No. 2 (March-
April 1972)

BERMAN, I., and COMER, J.

*A Resistance Furnace for the Heteroepitaxial
Growth of Single Crystal Beta SiC Through a
Molten Metal Intermediate*
Book, Chem. Vapor Deposition (Pub: Electrochem,
Soc.-1970)

- BERMAN, I., and RYAN, C. E.
The Growth of Silicon Carbide Needles by the Vapor-Liquid-Solid Method
J. Cryst. Growth, Vol. 9 (1971)
- BIRNBAUM, M. M., and FINCHER, C. L. (Aerospace Corp., Los Angeles, Calif.) DUGGER, C. O., GOODRUM, J. W., CAPT., and LIPSON, H. G.
Laser Characteristics of Neodymium-Doped Lithium Germanate Glass
J. of Appl. Phys., Vol. 41, No. 6 (May 1970)
- BLOOM, J. H., and SHEPHERD, F. D., JR.
Inexpensive and Sensitive Laser Beam Aligner for Use During Film Evaporation
J. of Vacuum Sci. and Techn., Vol. 7, No. 4 (July/August 1970)
- BUCHANAN, B., SHEDD, W., ROOSILD, S., and DOLAN, R.
Hardening Electronic Devices Against Very High Dose Radiation Environments
Proc. of Natl. Symp. on Nat. and Manmade Rad. in Sp. (January 1972)
- BURKE, E. A., CAPPELLI, J. R., LOWE, L. G., and WALL, J. A.
Solar Cell Radiation Response Near the Interface of Different Atomic Number Materials
Proc. of Natl. Symp. on Nat. and Manmade Rad. in Sp. (January 1972)
- BURKE, E. A., WALL, J. A., and FREDERICKSON, A. F.
Radiation-Induced Low Energy Electron Emission from Metals
IEEE Trans. on Nuc. Sci., Vol. NS-17, No. 6 (December 1970)
- CAPONE, B. R., KAHAN, A., BROWN, R. N., and BUCKMELTER, J. R., CAPT.
Quartz Crystal Radiation Effects
IEEE Trans. on Nuc. Sci., Vol. NS-17, No. 6 (December 1970)
- CAPONE, B., KAHAN, A., and SAWYER, B. (Res. Prods., Eastlake, Ohio)
^o
Evaluation of Cultured Quartz for High Precision Resonators
Proc. 25th Ann. Symp. on Freq. Cont. (August 1971)
- COMER, J. J.
Domain Formation in Synthetic Quartz
Proc. of 29th Ann. Mtg. of the Electron Microscopy Soc. of Am. (1971)
Electron Microscopy and Diffraction of Thermally Decomposed β -Silicon Carbide Whiskers
J. of Appl. Crystallog., Vol. 4, Part 1 (1 February 1971)
- CZERLINSKY, E. R., and MAC MILLAN, R. A.
Cation Distribution in Aluminum-Substituted Yttrium Iron Garnets by Mossbauer Effect Spectroscopy
Phys. Status Solidi, Vol. 41 (1970)
- DAVIES, D. E., and ROOSILD, S. A.
Minority Carrier Lifetime in Ion Implanted and Annealed Silicon
Appl. Phys. Lett., Vol. 17, No. 3 (1 August 1970)
Energy Levels of Defects in Ion Implanted Silicon
Book, Ion Implantation in Semicond. (Pub.: Springer-Verlag - 1971)
Residual Electrically Active Defects After Lattice Re-Ordering in Ion Implanted Silicon
J. of Appl. Phys. Lett., Vol. 18, No. 12 (15 June 1971)
Irradiation Defects and the Electrical Quality of Ion Implanted Silicon
Solid State Elect., Vol. 14, No. 10 (October 1971)
- DICKINSON, S. K., HILTON, R. M., and LIPSON, H. G.
Czochralski Synthesis and Properties of Rare-Earth-Doped Bismuth Germanate ($Bi_4Ge_3O_{12}$)
Mater. Res. Bull., Vol. 7, No. 3 (March 1972)
- DONOVAN, R. P., LITTLEJOHN, M. A. (N. C. State Univ.) and ROOSILD, S. A.
Piezoresistive Properties of Ion Implanted Layers in Silicon
Book, Ion Implantation in Semicond. (Pub.: Springer-Verlag - 1971)
- DREVINSKY, P. J., ET AL
Impurity Effects on Annealing of Radiation Defects in p-Type Silicon
Appl. Phys. Lett., Vol. 17, No. 10 (15 November 1970)
- DREVINSKY, P. J., and KIMERLING, L. C., CAPT.
Carrier Removal Effects in Neutron Irradiated Lithium-Doped Silicon
Proc. of the IEEE Trans. on Nuc. Sci., Vol. NS-18, No. 6 (December 1971)
- EULER, F., and VAN HOOK, H. J. (Raytheon Res. Div., Waltham, Mass.)
Magnetic Anisotropy of Vanadium-Indium Substituted YIG
J. of Appl. Phys., Vol. 41, No. 8 (July 1970)
- FREDERICKSON, A. R.
Hemispherical Triode: A Device and Technique for Measuring Electron Emission
Proc. 7th Natl. Conf. on Electron Probe Anal. (1972)
- FREDERICKSON, A. R., and BURKE, E. A.
Ionization, Secondary Emission, and Compton Currents at Gamma Irradiated Interfaces

- IEEE Trans. on Nuc. Sci., Vol. NS-18, No. 6 (December 1971)
- FRIEDMAN, J. D.
Linac X-Ray and Electron Dosimetry Using a Remote Control Pin Diode
IEEE Trans. on Nuc. Sci., Vol. NS-18, No. 3 (June 1971)
- GOODRUM, J. W., CAPT.
Top-seeded Flux Growth of Tetragonal GeO_2
J. of Crys. Growth, Vol. 7, No. 2 (September/October 1970)
Solution Top-Seeding: Growth of GeO_2 Polymorphs
J. of Crys. Growth, Vol. 18/14 (May 1972)
- GRANT, W. J.
Role of Rate Equations in the Theory of Luminescent Energy Transfer
Phys. Rev., B, Vol. 4, No. 2 (15 July 1971)
- HUNT, M. H.
The Analysis of Non-Conducting Solids by Spark Source Mass Spectrography
18th Ann. Conf. on Mass Spectromet. and Allied Topics (1970)
- JASPERSE, J. R.
A Method for One Particle Bound to Two Identical Fixed Centers. Application to H_2^+
Phys. Rev. A, Vol. 2, No. 6 (December 1970)
- JASPERSE, J. R., and GIANINO, P. D.
Thermal Lensing in Infrared Laser Window Materials
J. of Appl. Phys., Vol. 43, No. 4 (April 1972)
- KAHAN, A., BOUTHILLETTE, L., and DE ANGELIS, H. M.
Electron Irradiation of Heavily Doped GaAs: Si and GaAs: Te
Rad. Eff. J., Vol. 9, No. 1 and 2 (May 1971)
- KAHAN, A., GOODRUM, J. W., CAPT., and SINGH, R. S., MITRA, S. S. (Univ. of R. I.)
Polarized Reflectivity Spectra of Tetragonal GeO_2
J. of Appl. Phys., Vol. 42, No. 11 (October 1971)
- KENNEDY, J. K., and POTTER, W. D.
Epitaxial Deposition of Degenerate n-Type Layers of Ge on GaAs
J. of Crys. Growth, Vol. 13/14 (May 1972)
- KHAMBATTI, F. B., GIRLIFFE, P. J., and WILSON, M. P., JR., (Univ. of R. I.) ADAMSKI, J. A., and SAHAGIAN, C. S.
Initial Thermal Model of the Flame Fusion Crystal Growth Process
J. of Crys. Growth, Vol. 13/14 (May 1972)
- KIMERLING, L. C., CAPT.
Radiation Effects Studies in n-Type Silicon Semiconductors
Proc., AFSC 1971 Sci. and Eng. Symp., Vol. 1 (5-7 October 1971)
- KIMERLING, L. C., CAPT., and CAENES, C. P., CAPT.
Annealing of Electron Irradiated n-Type Silicon II. Illumination and Fluence Dependence
J. of Appl. Phys., Vol. 42, No. 9 (August 1971)
- KIMERLING, L. C., CAPT., DE ANGELIS, H. M., and CAENES, C. P., CAPT.
Annealing of Electron Irradiated n-Type Silicon I. Donor Concentration Dependence
Phys. Rev. B, Vol. 3, No. 2 (15 January 1971)
- KRISHNA, P., and MARSHALL, R. C.
X-Ray Investigation of 2H-3C Phase-Transformation in Silicon Carbide Single Crystals
Book, Adv. in X-Ray Anal., Vol. 14 (Pub: Plenum Press - 1971)
- KRISHNA, P., MARSHALL, R. C., and RYAN, C. E.
The Structure, Perfection and Annealing Behavior of SiC Needles Grown by VLS Mechanism
J. of Crys. Growth, Vol. 9 (May 1971)
Direct Transformation from the 2H to the 3H Structure in Single-Crystal Silicon Carbide
J. of Crys. Growth, Vol. 11, No. 2 (November 1971)
- LIPSON, H. G.
Lasers in Fluorescence Spectroscopy
Laser Focus (September 1970)
- LIPSON, H. G., BUCKMELTER, J. R., and FITZGERALD, J. R.
Comparison of Optical Fluorescence, Electron Microprobe, and Neutron Activation Methods for Chromium Analysis in Ruby
Book, Devel. in Appl. Spectros., Vol. 9, (Pub.: Plenum Press - 1971)
- MAGEE, T. J., and COMER, J. J.
Ion Implantation in Silicon
Proc. of 29th Ann. Mtg. of Electron Microscopy Soc. of Am. (1971)
- MAGEE, T. J., COMER, J. J., and KIMERLING, L. C., CAPT.
Lithium Precipitation in Silicon
Proc. of 29th Ann. Mtg. of Electron Microscopy Soc. of Am. (1971)

- O'CONNOR, J. J., and ARMINGTON, A. F.
Preparation and Properties of Cuprous Iodide
Mat. Res. Bull., Vol. 6, No. 8 (August 1971)
- PLENDL, J. N.
Characteristic Energy Absorption Spectra of Solids
 Book, Far Infr. Properties of Solids (Pub.: Plenum Press-1970)
Characteristic Spectra of Energy Absorption for Dielectric Solids
Appl. Opt., Vol. 9, No. 12 (December 1970)
Damping of Lattice Vibrations in Solids
Appl. Opt., Vol. 10, No. 1 (January 1971)
Atomistic Interpretation of Solid Solution Hardening from Spectral Analysis
Appl. Opt., Vol. 10, No. 5 (May 1971)
- PLENDL, J. N., and GIELISSE, P. J. (Univ. of R. I.)
Polymorphism of Solids as a Function of Pressure & Temperature
 Book, Les Propriétés Physiques des Solides sous Pression, (Pub.: Colloques Internationaux du Centre National de la Recherche Scientifique - 1970)
Compressibility and Polymorphism of the Elements
Physica Status Solidi, Vol. 42, No. 2 (1 December 1970)
- PLENDL, J. N., GIELISSE, P. J. (Univ. of R. I.), MANSUR, L. C., MITRA, S. S. (Univ. of R. I.) and SMAKULA, A. (Mass. Inst. of Tech., Cambridge, Mass.), TARTE, P. C. (Univ. of Liege, Belgium)
Interpretation of Solid Solution Hardening with Vibrational Spectra
Appl. Opt., Vol. 10, No. 5 (May 1971)
- PLENDL, J. N., GIELISSE, P. J., PLENDL, H. S., KROMHOUT, R. A., (Univ. of R. I.) MANSUR, L. C.
Lattice Vibration Spectra and Physical Characteristics of Metals with Cubic Structure
Appl. Opt., Vol. 10, No. 6 (June 1971)
- PLENDL, J. N., and MANSUR, L. C.
Anomalous Thermal Expansion with Infrared Spectroscopy
Appl. Opt., Vol. 11, No. 5 (May 1972)
- POSEN, H., ARMINGTON, A., and BRUCE, J.
The Selection and Improvement of Alkali Halide Materials for High Power 10.6 μm Windows
Proc. of 5th Conf. on Laser Tech., Vol. 1 (1972)
- POSEN, H., NIKULA, J. V., HUNT, M. H., and VICKERS, V. E.
The LAAFS System and Its Implementation in the Laboratory Automation of a Plate Reader and a Single Crystal X-Ray System
- Proc. of COMMON Mtg., Chicago, Ill., April 1972 (1972)
- SAMPSON, J. L.
Double-Chamber Powder Container for Flame-Fusion Crystal Growth
Rev. of Sci. Instr., Vol. 42, No. 2 (February 1971)
- SCHWUTKE, G. H., BRACK, K., and GOREY, E. F., (IBM, East Fishkill Labs. Hopewell Junc., N. Y.), KAHAN, A., and LOWE, L. F.
Resistivity and Annealing Properties of Implanted Si:H⁺
Rad. Eff. J., Vol. 6, No. 1 and 2 (1970)
- SHEDD, W., BUCHANAN, B., and DOLAN R.
Transient Radiation Effects in Silicon Diodes Near and In Avalanche Breakdown
IEEE Trans. on Nuc. Sci., Vol. NS-18, No. 6 (December 1971)
- SHEPHERD, F. D.
Detectors for Laser Systems
 #70C15 IEEE Paper 6C. 1 (1970)
- SHEPHERD, F. D., JR., YANG, A. C., and TAYLOR, R. W.
A 1 to 2 μm Silicon Avalanche Photodiode
Proc. of the IEEE (Ltr.), Vol. 58, No. 7 (July 1970)
- SKOLNIK, L. H., SPITZER, W. G. (Univ. of So. Calif., Los Angeles), KAHAN, A., EULER, F., and HUNSPERGER, R. G. (Hughes Res. Labs., Malibu, Calif.)
Localized Vibrational Mode Absorption of Ion-Implanted Silicon in GaAs
J. of Appl. Phys., Vol. 43, No. 5 (1972)
- SKOLNIK, L. H., SPITZER, W. G. (Univ. of So. Calif., Los Angeles), KAHAN, A., and HUNSPERGER, R. G. (Hughes Res. Labs., Malibu, Calif.)
Infrared Localized Vibrational-Mode Absorption of Ion-Implanted Aluminum and Phosphorus in Gallium Arsenide
J. of Appl. Phys., Vol. 42, No. 13 (December 1971)
- TAYLOR, R. W., SHEPHERD, F. D., JR., and YANG, A. C.
Silicon Microcircuit Compatible Detectors for the Near Infrared Lasers
Govt. Microcircuit Appl. Conf. Dig. of Pap. (October 1970)
- VICKERS, V. E.
A Model of Schottky Barrier Hot-Electron-Mode Photo-detection
Appl. Opt., Vol. 10, No. 9 (September 1971)
- WALL, J. A., and BURKE, E. A.
Gamma Dose Distributions at and Near the Interface of Different Materials

IEEE Trans. on Nuc. Sci., Vol. NS-17, No. 6
(December 1970)

**PAPERS PRESENTED AT MEETINGS
JULY 1970-JUNE 1972**

ARMINGTON, A. F.

Materials Aspect of the AFCRL Window Program
5th Ann. Conf. on High Power Infr. Laser Window Mats., Bedford, Mass. (27-28 October 1971)

ARMINGTON, A. F., DI PIETRO, M. A. and O'CONNOR, J. J.

Gel Growth of Iodate Crystals
Intl. Conf. on Crys. Growth, Marseille, Fr. (5-9 July 1971)

BENDOW, B.

Theory of Indirect Excitation of Solids by Light
Am. Phys. Soc. Mtg., San Francisco, Calif. (31 January-3 February 1972)

BENDOW, B., and BIKMAN, J. L. (N. Y. Univ.)
Polariton Theory of Resonance Properties of Exciton-Mediated Raman Scattering
2nd Intl. Conf. on Light Scattering in Solids, Paris, Fr. (19-23 July 1971)

BENDOW, B., and GANINO, P. D.

Theory of Thermal Lensing of Laser Beams by Solids
Am. Phys. Soc. Mtg., Albuquerque, N. M. (5-7 June 1972)

BENDOW, B., HORDVÍK, A. (Opt. Phys. Lab.), LIPSON, H., and SKOLNIK, L.
Optical Evaluation of CO₂ Laser Window Materials at AFCRL
5th Class. Conf. on Laser Techn., U.S. Nav. Postgrad. Sch., Monterey, Calif. (25-27 April 1972)

BENDOW, B., and YING, SEE-CHEN. (Brown Univ., Providence, R. I.)

Quantum Theory of Desorption of Atoms from Solid Surfaces
Intl. Surface Sci. Conf., Boston, Mass. (11-15 October 1971)

BERMAN, I.

Annealing of Beta Thin Film Silicon Carbide
Electrochem. Soc. Mtg., Houston, Tex. (7-12 May 1972)

BERMAN, I., and RYAN, C. E.

The Growth of Silicon Carbide Needles by the Vapor-Liquid-Solid Method
Conf. on Crys. Growth and Epitaxy from the Vapor Phase, Eidgenössische, Technische Hochschule, Zurich, Switz. (23-25 September 1970)

BERMAN, I., RYAN, C. E., MARSHALL, R. C. and LITTLE, J. R.

Stability of Thin Film Beta SiC
Intl. Conf. on Vapor Growth & Epitaxy, Jerusalem, Isr. (23-25 May 1972)

BUCHANAN, B. L., and SHEDD, W. M.

Analysis, Design, and Testing of Radiation Hardened Semiconductor Devices
ESD/AFCRL Sci. & Eng. Mtg., L. G. Hanscom Fld., Mass. (3 November 1970)

BUCHANAN, B., SHEDD, W., ROOSILD, S., and DOLAN, R.
Hardening Electronic Devices Against Very High Total Dose Radiation Environments
Natl. Symp. on Nat. and Manmade Rad. in Space, Las Vegas, Nev. (2-5 March 1971)

BURKE, E. A., CAPELLI, J. R., LOWE, L. F., and WALL, J. A.

Solar Cell Radiation Response Near the Interface Between Material of Different Atomic Number
Natl. Symp. on Nat. and Manmade Rad. in Space, Las Vegas, Nev. (2-5 March 1971)

BURKE, E. A., WALL, J. A., and FREDERICKSON, A. R.
Radiation-Induced Low Energy Electron Emission from Metals
1970 IEEE Ann. Conf. on Nuc. and Space Rad. Effects, San Diego, Calif. (21-23 July 1970)

CAPONE, B. R., KAHAN, A., and BROWN, R. N.
Radiation Effects on Frequency and Q of Quartz Resonators

1970 IEEE Ann. Conf. on Nuc. and Space Rad. Effects, San Diego, Calif. (21-23 July 1970)

CAPONE, B. R., KAHAN, A., and SAWYER, B. (Sawyer Res. Prod., Eastlake, Oh.)

Evaluation of Cultured Quartz for High Precision Resonators

25th Ann. Freq. Control Symp., Atlantic City, N. J. (26-28 April 1971)

COMER, J. J.

Domain Formation Twins in Synthetic Quartz
29th Ann. Mtg. of the Elec. Microsc. Soc. of Am., Boston, Mass. (9-18 August 1971)

DAVIES, D. E., and ROOSILD, S.

Energy Levels of Defects in Ion Implanted Silicon

- 2nd Intl. Conf. on Ion Impl. in Semicond., Bavaria, Ger. (24-28 May 1971)
- DICKINSON, S. K., HILTON, R. M., and LIPSON, H. G.
Synthesis of $A_1 B_3 O_{12}$ -Type Materials Containing Rare Earth Dopeants
Intl. Conf. on Crys. Growth, Marseille, Fr. (5-9 July 1971)
- DONOVAN, R. P. (Res. Triangle Inst., N. C.)
LITTLEJOHN, M. A. (N. C. State Univ.), and ROOSILD, S. A.
Piezoresistive Properties of Ion Implanted Layers in Silicon
2nd Intl. Conf. on Ion Impl. in Semicond., Bavaria, Ger. (24-28 May 1971)
- DREVINSKY, P. J., and KIMERLING, L. C. CAPT.
Carrier Removal in Li-Doped Si Irradiated With 5-MeV Neutrons
Am. Phys. Soc. Mtg., Wash., D. C. (25-29 April 1971)
Carrier Removal Effects in Neutron Irradiated Lithium-Doped Silicon
1971 IEEE Ann. Conf. on Nuc. and Sp. Rad. Eff., Durham, N. H. (20-23 July 1971)
- FREDERICKSON, A. R., and BURKE, E. A.
Ionization, Secondary Emission, and Compton Currents at γ - and α -Irradiated Interfaces
1971 IEEE Ann. Conf. on Nuc. and Sp. Rad. Eff., Durham, N. H. (20-23 July 1971)
- FRIEDMAN, J. D.
Linac X-Ray and Electron Dosimetry Using a Remote Control Pin Diode
1971 Particle Accel. Conf., Accel. Eng. and Tech., Chicago, Ill. (1-3 March 1971)
- GARTH, J. C.
Energy-Dependent Boltzmann Model for Far UV Photoemission
Am. Phys. Soc. Mtg., Cleveland, Oh. (29 March-1 April 1971)
- GOODRUM, J. W., CAPT.
Solution Top-Seeding, Growth of GeO_2 Polymorphs
Intl. Conf. on Crys. Growth, Marseille, Fr. (5-9 July 1971)
- HUNT, M. H., NIKULA, J. V., OSEN, H., and VICKERS, V. E.
The AFCRL Automated Photoplate Data Acquisition and Reduction System
20th Ann. Conf. on Mass. Spectrom and Allied Top., Dallas, Tex. (4-9 June 1972)
- KAHAN, A., BOUTHILLETT, L., and DE ANGELIS, H. M.
Radiation Damage of Heavily Doped n-Type GaAs
Intl. Conf. on Rad. Eff. in Semicond., State Univ. of N. Y. at Albany, N. Y. (24-26 August 1970)
- KAHAN, A., EULER, F. K., and WATLEY, T. (Appl. Res. Labs., Sunland, Calif.), SPITZER, W. G. (Univ. of So. Calif., Los Angeles, Calif.)
Ion Implanted Nitrogen in GaAs
Am. Phys. Soc. Mtg., San Francisco, Calif. (31 January-3 February 1972)
- KAHAN, A., GOODRUM, J. W., CAPT., and SINGE, R. S., MITRA, S. S. (Univ. of R. I.)
Lattice Infrared Reflectivity of Tetragonal GeO_2
Am. Phys. Soc. Mtg., Cleveland, Oh. (29 March-1 April 1971)
- KENNEDY, J. K., and POTTER, W. D.
Epitaxial Deposition of Degenerate N-Type Layers of Ge on GaAs
Intl. Conf. on Crys. Growth, Marseille, Fr. (5-9 July 1971)
- KHAMBATTA, F. B., GIELISSE, P. J. (Univ. of R. I.)
ADAMSKI, J. A., and SAHAGIAN, C. S.
Initial Thermal Model of the Flame Fusion Crystal Growth Process
Intl. Conf. on Crys. Growth, Marseille, Fr. (5-9 July 1971)
- KIMERLING, L. C., CAPT.
Radiation Effects Studies in N-Type Silicon Semiconductors
1971 AFSC Sci. and Eng. Symp., Dayton, Oh. (5-7 October 1971)
- KRISHNA, P., and MARSHALL, R. C.
X-Ray Investigation of 2H-3C Phase-Transformation in Silicon Carbide Single Crystals
Conf. on Appl. of X-Ray Anal., Denver, Colo. (5-7 August 1970)
The Structure, Perfection and Annealing Behavior of SiC Needles Grown by a VLS Mechanism
Conf. on Crys. Growth and Epitaxy from the Vapor Phase, Eidgenoessische Technische Hochschule, Zurich, Switz. (23-25 September 1970)
Direct Transformation from the 2H to the δ H Structure in Single-Crystal Silicon Carbide
Intl. Conf. on Crys. Growth, Marseille, Fr. (5-9 July 1971)
- LIPSON, H. G., DICKINSON, S. K., and DUGGER, C. O.
Optical Properties of Neodymium-Doped Germanate Crystals
Am. Phys. Soc. Mtg., Mass. Inst. of Tech., Cambridge, Mass. (27-29 December 1971)
- MAGEE, T. J., and COMER, J. J.
Ion Implantation in Silicon
29th Ann. Mtg. of Elec. Micros. Soc. of Am., Boston, Mass. (9-13 August 1971)

- MAGEE, T. J., COMER, J. J., and KIMERLING, L. C., CAPT.
Lithium Precipitation in Silicon
 29th Ann. Mtg. of Elec. Micros. Soc. of Am., Boston, Mass. (9-13 August 1971)
- O'CONNOR, J. J., and ARMINGTON, A. F.
Preparation and Properties of Cuprous Iodide
 Intl. Conf. on Crys. Growth, Marseille, Fr. (5-9 July 1971)
- POSEN, H.
Physical Properties Measurements at AFCRL
 5th Ann. Conf. on High Power Infr. Laser Window Ma's., Bedford, Mass. (27-28 October 1971)
- POSEN, H., ARMINGTON, A. F., and BRUCE, J.
Some Physical Properties of High Power Laser Window
 6th Class. Conf. on Laser Techn., U. S. Nav. Postgrad. Sch., Monterey, Calif. (25-27 April 1972)
- POSEN, H., NIKULA, J. V., HUNTER, M. H., and VICKERS, V. E.
The LAAFS System and Its Implementation in the Laboratory Automation of a Plate Reader and a Single Crystal X-Ray System
 COMMON Mtg., Symp. on Lab. Auton., Chicago, Ill. (4-6 April 1972)
- SAHAGIAN, C. S.
Crystallography
 Concord Rot. Club Concord, Mass. (30 July 1970)
Crystal Growth Science and Technology
 RESA Mtg., Holloman AFB, N. M. (14 September 1970)
- SHEDD, W., BUCHANAN, B., and DOLAN, R.
Transient Radiation Effects in Silicon Diodes Near and in Avalanche Breakdown
 1971 IEEE Ann. Conf. on Nuc. and Sp. Rad. Eff., Durham, N. H. (20-23 July 1971)
- SHEPHERD, F. D., and YANG, A. C.
A New Silicon Avalanche Infrared Photodetector for the 1 to 2 μ Region
 ESD/AFCRL Sci. & Eng. Mtg., L. G. Hanscom Fld., Mass. (3 November 1971)
- SKOLNIK, L., and SPITZER, W. (Univ of So. Calif., Los Angeles), KAKUN, A. and HUNSPERGER, R. (Hughes Res. Labs., Malibu, Calif.)
Infrared Localized Vibrational Mode Absorption of Ion Implanted Silicon in Gallium Arsenide.
 Am. Phys. Soc. Mtg., Seattle, Wash. (25-27 August 1971)
- TAYLOR, R. W., SHEPHERD, F. D., and YANG, A. C.
Silicon Microcircuit Compatible Detectors for the Near Infrared Lasers
- 1970 Gov. Microcirc. Appl. Conf., U. S. Army Elec. Com., Ft. Monmouth, N. J. (6-8 October 1970)
- TURNER, C. D.
Radiation Effects Research at AFCRL
 Mtg. of the Am. Soc. for Testing and Mat., Univ. of Ct., San Diego, Calif. (23-24 July 1970)
- WALL, J. A., and BURKE, E. A.
Gamma Dose Distributions at and Near the Interface of Different Materials
 1970 IEEE Ann. Conf. on Nuc. and Space Rad. Effects, San Diego, Calif. (21-23 July 1970)
- YING, SEE-CHEN (Brown Univ., Providence, R. I.), and BENDOW, B.
Theory of Desorption at Low Temperatures: Angular and Energy Distributions
 Am. Phys. Soc. Mtg., Atlantic City, N. J. (27-30 March 1972)
- ## TECHNICAL REPORTS JULY 1970 - JUNE 1972
- ARMINGTON, A. F.
Materials Aspect of the AFCRL Window Program
 Conf. on High Power Infr. Laser Window Mats., AFCRL-71-0592 (18 December 1971)
- BENDOW, B., HORDVIK, A., LIPSON, H. and SKOLNIK, L.
Some Aspects of Optical Evaluation of CO₂ Laser Window Materials at AFCRL
 AFCRL-72-0404 (30 June 1972)
- BOUTHILLETTE, L. O., and LOWE, L. F.
High Flux Electron Irradiations
 AFCRL-74-0398 (26 June 1972)
- BUCHANAN, B., and SHEDD, W.
Analysis, Design and Testing of Radiation Hardened Semiconductor Devices
 Proc. of L. G. Hanscom Fld. Sci. and Eng. Awards Mtg., AFCRL-70-0706 (16 December 1970)
- BURKE, E. A., CAPPELLI, J. R., LOWE, L. F., and WALL, J. A.
Solar Cell Radiation Response Near the Interface of Different Atomic Number Materials
 AFCRL-72-0045 (24 November 1971)

- CARNES, C. P., CAPT., DEANGELIS, H. M., PENCZER, R. E., CAPT., and DREVINSKY, P. J.
Damage and Recovery in Electron Irradiated Silicon Heavily Doped with Phosphorus
 AFCRL-70-0423 (3 August 1970)
- DICKINSON, S. K.
Investigations of the Synthesis of Diamonds
 AFCRL-70-0628 (6 November 1970)
Ionic, Covalent, and Metallic Radii of the Chemical Elements
 AFCRL-70-0727 (1 December 1970)
- EYGES, L. J.
Permeable Matter and the Vector H
 AFCRL-70-0536 (2 October 1970)
Dielectric Matter and the Vector D
 AFCRL-70-0537 (5 October 1970)
- FREDERICKSON, A. R., JASPERSE, J. R. and GROSSBAUD, N. (Boston Coll., Chestnut Hill, Mass.)
The Electrostatic Potential Inside a Hemisphere: Its Use as an Electron Energy Analyzer and as a Triode Electronic Device
 AFCRL-71-0369 (23 June 1971)
- FREDERICKSON, A. R., and MATTHEWSON, A.
Backemission of Electrons from Metals Irradiated by 0.2 MeV to 1.4 MeV Electrons
 AFCRL-71-0514 (22 September 1971)
- GIANINO, P. D., and JASPERSE, J. R.
Thermal Lensing in Infrared Laser Window Materials
 AFCRL-72-0202 (23 March 1972)
- GOODRUM, J. W., CAPT.
Some Reactions of Tungsten (VI) Oxide and Molybdenum (VI) Oxide With Liquid Sulfur
 AFCRL-70-0417 (23 July 1970)
Growth and Characterization of Tetragonal (Rutile) GeO_2 Crystals
 AFCRL-71-0187 (12 March 1971)
- LIPSON, H. G.
Optical Properties of Rare-Earth-Doped Germanate Glasses
 AFCRL-70-0612 (23 October 1970)
- POSEN, H.
Physical Properties Measurements at AFCRL
Conf. on High Power Infr. Laser Window Mats.
 AFCRL-71-0592 (13 December 1971)
- POSEN, H., and BRUCE, J. A.
X-Ray Topographic Observations of Slip Distributions in Alpha Silicon Carbide
 AFCRL-72-0225 (30 March 1972)
- SARAGIAN, C. S., and PITHA, C. A. (Ed'ors)
Conference on High Power Infrared Laser Window Materials
 AFCRL-71-0592 (13 December 1971)
- SHEPHERD, F. D., and YANG, A. C.
A New Silicon Avalanche Infrared Photodetector for the 1- to 2- μ Region
Proc. of the L. G. Hancom Fd. Sci. and Eng. Awards Mtg., AFCRL-70-0706 (15 December 1970)

Appendix A

AFCRL PROJECTS BY PROGRAM ELEMENT

Program Element	Project Number, Title and Agency
61101F	IN-HOUSE LABORATORY INDEPENDENT RESEARCH ILIR Laboratory Director's Fund
61102F	DEFENSE RESEARCH SCIENCES AFCRL 5620 Growth and Characterization of Advanced Electromagnetic Materials 5621 Physics of Solid State Phenomena 5631 Ionospheric Radio Physics 5634 Research in Quantum Electronics 5635 Electromagnetic Radiation, Sensors, and Microwave Acoustics 5638 Research on Solid State Electronics 8600 Energetic Particle Environment 8601 Geomagnetism 8603 Infrared and Optical Techniques 8604 Meteorological Research 8605 Upper Atmosphere Structure 8607 Earth Sciences and Technology 8608 Solar Plasma Dynamics 8617 Electrical Structure of Aerospace 8620 Cloud Physics 8627 Spectroscopic Studies of Upper Atmospheric Processes 8658 Infrared Non-Equilibrium Radiative Mechanisms 8659 Energy Conversion Research
62101F	ENVIRONMENT AFCRL 4603 Generation and Propagation of Low Frequency Radio Waves 4642 Alleviation Techniques for Reentry Plasmas 4643 Aerospace Radio Propagation 6670 Atmospheric Sensing Techniques 6672 Weather Radar Techniques 6687 Aerospace Composition 6688 Solar Ultraviolet Radiation 6690 Aerospace Density 6698 Satellite Meteorology 7600 Geodesy for Navigation 7601 Electric and Magnetic Fields 7605 Weather Modification 7621 Atmospheric Optics 7628 Geophysical and Geokinetic Effects 7635 Upper Atmosphere Chemical Processes 7639 Wave Propagation Studies 7649 Solar Environmental Effects 7655 Micrometeorology 7659 Aerospace Research Instrumentation 7661 Polar Atmospheric Processes 7663 Ionospheric Characteristics 7670 IR Properties of the Environment 8624 Variability of Meteorological Elements 8628 Mesoscale Weather Forecasting 8666 Space Environment Observing and Forecasting Techniques 8682 Millimeter Wave Propagation

Appendix A**AFCRL PROJECTS BY PROGRAM ELEMENT**

Program Element	Project Number, Title and Agency
62204F	<i>AEROSPACE AVIONICS</i> AFAL 6095 Electronic Device and Circuitry Techniques 6100 Laser Technology
62601F	<i>ADVANCED WEAPONS AND APPLICATIONS</i> AFWL 3326 Laser Application
62702F	<i>GROUND ELECTRONICS</i> RADC 4600 Electromagnetic Radiation Techniques

In addition to the above continuing Air Force funded projects, AFCRL participates in joint programs supported by the following agencies:

- 1) U. S. Air Force:
 - Air Force Weapons Laboratory
 - Electronic Systems Division
 - Air Force Materials Laboratory
 - Space and Missile Systems Organization
 - Air Weather Service
 - Air Force Technical Applications Center
 - Air Force Flight Test Center
- 2) Advanced Research Projects Agency
- 3) National Aeronautics and Space Administration
- 4) Atomic Energy Commission
- 5) Defense Nuclear Agency
- 6) Defense Mapping Agency
- 7) Army Material Command
- 8) Department of Transportation
- 9) U. S. Navy

AFCRL ROCKET AND SATELLITE PROGRAM: JULY 1970 - JUNE 1972

Date	Launch Site	Vehicle	Experiment	Scientist	Results
26 Jul 70	WSMR	Aerobee 170	MAP II IR	R. Walker	Success
12 Aug 70	WSMR	Aero 150	Solar EUV	H. Hinteregger	Failure (P)
12 Aug 70	WSMR	Aerobee 170	Solar EUV	H. Hinteregger	Success
21 Aug 70	CRR	Black Brant IV	VLF Propagation	R. Harvey	Failure (V)
20 Nov 70	ADTC	Niro	Atmospheric Density (Chemical Release)	N.W. Rosenberg	Success
20 Nov 70	ADTC	Niro	Atmospheric Density and Composition (Chemical Release)	N.W. Rosenberg	Success
20 Nov 70	ADTC	Niro	Atmospheric Composition (Neutral Mass Spectrometer)	C. Philbrick	Success
20 Nov 70	ADTC	Niro	Atmospheric Composition (Positive Ion Mass Spectrometer)	R. Nardisi	Success
20 Nov 70	ADTC	Niro	Atmospheric Composition (Chemical Release)	N.W. Rosenberg	Success
20 Nov 70	ADTC	Niro	Atmospheric Composition (Chemical Release)	N.W. Rosenberg	Success
24 Nov 70	Wallops Island	Trailblazer II	Plasma Diagnostics (Reentry)	W. Rotman	Success
2 Dec 70	WSMR	Aerobee 170	IR Horizons	R. Walker	Success
8 Jan 71	WSMR	Niro	Atmospheric Density - "7" Falling Sphere	A. Faire	Success
8 Jan 71	WSMR	Niro	Atmospheric Density - "7" Falling Sphere	A. Faire	Success
11 Mar 71	WSMR	Niro	Atmospheric Density - "7" Falling Sphere	A. Faire	Success
11 Mar 71	WSMR	Niro	Atmospheric Density - "7" Falling Sphere	A. Faire	Partial
16 Mar 71	WSMR	Aerobee 170	Solar EUV	H. Hinteregger	Success
19 Mar 71	CRR	Nike Tomahawk	Magnetic Fields and Charged Particles	R. Vancouver	Success
19 Mar 71	CRR	Niro	Magnetic Fields and Charged Particles	R. Vancouver	Success
22 Mar 71	Thule	Super Areas	Electron and Ion Density	W. Grieder	Success
24 Mar 71	CRR	Black Brant V/C	IR Aurora and Airglow	D. Kimball	Success
3 Apr 71	WSMR	Aerobee 170	IR Stellar Sources	R. Walker	Success
6 Apr 71	Thule	Super Areas	Electron and Ion Density	W. Grieder	Success
6 Apr 71	Thule	Super Areas	Proton Flux - PCA	W. Grieder	Success
6 Apr 71	Thule	Super Areas	Composition (Mass Spectrometer)	R. Narcisi	Success
6 May 71	ADTC	Niro	Positive Ion Composition (Mass Spectrometer)	R. Narcisi	Success
8 May 71	ADTC	Niro	Density Measurements ("7" Falling Sphere and Optical)	A. Faire	Success
18 May 71	ADTC	Niro	Ionspheric Winds (Chemical Release)	N.W. Rosenberg	Success
18 May 71	ADTC	Niro	(Project HAVE GENIE)	N.W. Rosenberg	Success
18 May 71	ADTC	Niro	AO Temperatures (Chemical Release)	N.W. Rosenberg	Success
18 May 71	ADTC	Niro	(Project HAVE GENIE)	N.W. Rosenberg	Success
18 May 71	ADTC	Niro	Density and Chemical Release ("7" sphere and TMA)	N.W. Rosenberg and A. Faire	Success
			(Project HAVE GENIE)		

WSMR — White Sands Missile Range, New Mexico
 CRR — Churchill Rocket Range, Manitoba, Canada
 ADTC — Armament Development Test Center, Eglin AFB, Florida
 WTR — Western Test Range, Vandenberg AFB, California
 PFRR — Poker Flat Rocket Range, Alaska

AFCOR ROCKET AND SATELLITE PROGRAM: JULY 1970 - JUNE 1972

Date	Launch Site	Vehicle	Experiment	Scientist	Results
18 May 71	ADTC	Niro	Density (10" sphere)	A. Faire	Failure
18 May 71	ADTC	Nike Tomahawk	Atomic Oxygen Profile (Chemical Release) (Project HAVE GENIE)	N.W. Rosenberg	Success
18 May 71	ADTC	Niro	Exploratory Studies (Chemical Release)	N.W. Rosenberg	Success
18 May 71	ADTC	Niro	(Project HAVE GENIE)	N.W. Rosenberg	Success
19 May 71	ADTC	Niro	Ionspheric Winds (Chemical Release)	N.W. Rosenberg	Success
21 May 71	AD'C	Niro	(Project HAVE GENIE)	N.W. Rosenberg	Success
25 May 71	WTR	S71-5	ALO Temperature (Chemical Release)	N.W. Rosenberg	Success
7 Jun 71	ORR	Black Brant V	Ionspheric Winds (Chemical Release)	J. McIsaac	Success
29 Jun 71	VAFB	Aerobee 170	Ionization Gauge for Atmospheric Density	R. Harvey	Success
			VLF Ionospheric Absorption	R. Huffman	Success
29 Jun 71	WSMR	Aerobee 170	Project Chaser - Missile Optical Radiation	R. Walker	Success
6 Aug 71	WTR	OVI-21	Measurements	R. Narcisi	Success
			IR Stellar Sources (Project Hi-Star)	and C. Philbrick	Success
			Neutral Composition (Velocity Mass Spectrometer)	K.S.W. Champion	Success
6 Aug 71	WTR	Cannonball II	Low Altitude Density (Accelerometer Technique)	K.S.W. Champion	Success
6 Aug 71	WTR	Musketball	Low Altitude Density (Satellite Drag Technique)	H. Cohen	Failure
21 Sep 71	WSMR	Niro	Density-Brenstrahlung	H. Cohen	Success
27 Sep 71	WSMR	Niro	Density-Brenstrahlung	L. Weeks	Success
5 Oct 71	Wallops Island	Niro	Density Measurements (O ₂ and O ₃)	C. Philbrick	Success
5 Oct 71	Wallops Island	Niro	(Twilight Neutral Studies Program)	A. Faire	Partial
5 Oct 71	Wallops Island	Niro	Density Measurements (O ₂ and O ₃)	A. Faire	Failure (P)
5 Oct 71	Wallops Island	Niro	(Twilight Neutral Studies Program)	C. Philbrick	Success
5 Oct 71	Wallops Island	Niro	Neutral Composition (Mass Spectrometer)	R. Narcisi	Success
5 Oct 71	Wallops Island	Niro	(Twilight Neutral Studies Program)	R. Narcisi	Success
5 Oct 71	Wallops Island	Niro	Density Measurements (" sphere)	R. Narcisi	Success
6 Oct 71	Wallops Island	Niro	(Twilight Neutral Studies Program)	R. Narcisi	Success
6 Oct 71	Wallops Island	Niro	Density Measurements (" sphere)	R. Narcisi	Success
6 Oct 71	Wallops Island	Niro	(Twilight Neutral Studies Program)	R. Narcisi	Success
6 Oct 71	Wallops Island	Niro	Neutral Composition (Mass Spectrometer)	R. Narcisi	Success
6 Oct 71	Wallops Island	Niro	(Twilight Neutral Studies Program)	R. Narcisi	Success
6 Oct 71	Wallops Island	Niro	Positive Ions (Mass Spectrometer)	R. Narcisi	Success
6 Oct 71	Wallops Island	Niro	(Sunrise Ion Composition Studies Program)	R. Narcisi	Success
6 Oct 71	Wallops Island	Niro	Negative Ions (Mass Spectrometer)	R. Narcisi	Partial
6 Oct 71	Wallops Island	Niro	(Sunrise Ion Composition Studies Program)	A. Stair	Success
16 Oct 71	WSMR	Aerobee 150	N ₂ Vibrational Temperature	and R. O'Neill	Success

Appendix B

AFCRL ROCKET AND SATELLITE PROGRAM: JULY 1970 - JUNE 1972

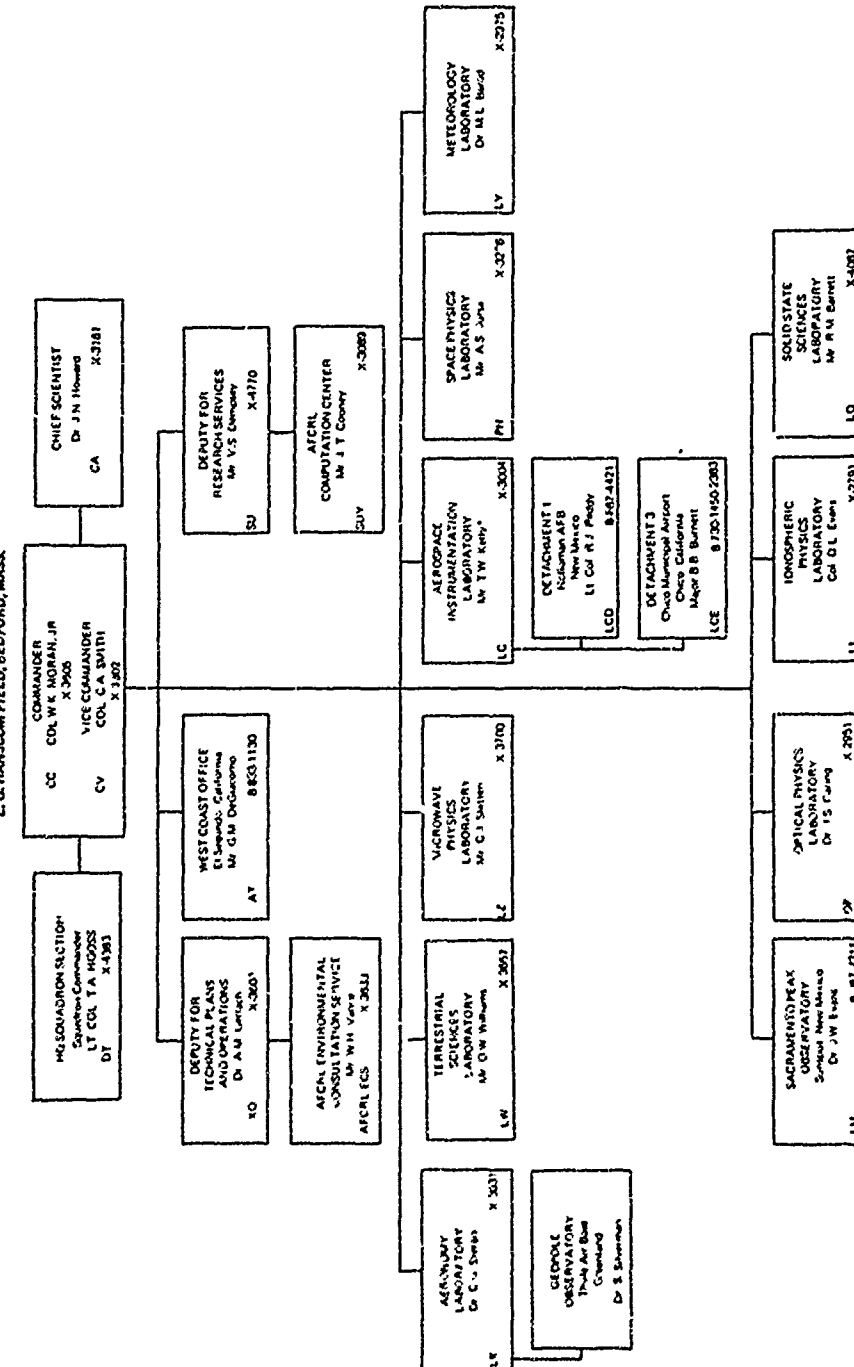
Date	Launch Site	Vehicle	Experiment	Scientist	Results
23 Oct 71	Thule	Super Areas	D-Region Ionization - Daytime	W. Grieder	Success
29 Oct 71	WSMR	Aerobee 170	IR Stellar Sources (Project Hi-Star)	R. Walker	Success
3 Nov 71	WSMR	Aerobee 170	Atmospheric Extinction	R. Penn	Partial
4 Nov 71	Thule	Super Areas	D-Region Ionization - Nighttime	W. Grieder	Success
9 Nov 71	WSMR	Aerobee 150	Solar Extreme Ultraviolet	J. Higgins	Success
9 Nov 71	WSMR	Aerobee 150	Solar Extreme Ultraviolet	J. Manson	Success
16 Nov 71	ADTC	Niro	Chemical Release Studies	N.W. Rosenberg	Success
23 Nov 71	WTR	Aerobee 170	Project Chaser Missile Optical Radiation Measurements	R. Huffman	Success
10 Dec 71	CRR	Niro	Density (7" Sphere)	A. Faire	Success
10 Dec 71	CRR	Nike Tomahawk	Density (10" Sphere)	A. Faire	Failure
10 Dec 71	CRR	Niro	Density (7" Sphere)	A. Faire	Success
17 Jan 72	WSMR	Aerobee 170	IR Stellar Sources (Project Hi-Star)	R. Walker	Success
31 Jan 72	Wallops Island	Niro	Density (7" Sphere)	A. Faire	Success
31 Jan 72	Wallops Island	Niro	Negative Ions (Mass Spectrometer)	R. Narcisi	Failure
6 Feb 72	Wallops Island	Niro	Negative Ions (Mass Spectrometer)	R. Narcisi	Success
6 Mar 72	PFRR	Astrobee D	OH (Photometer)	W. Grieder	Success
9 Mar 72	PFRR	Astrobee D	IR (Circular Variable Filter)	W. Grieder	Success
16 Mar 72	PFRK	Black Brant V A	IR, Ion Composition, Electron Density, Particles	J. Ulwick	Success
4 Apr 72	CRR	Black Brant V C	Electric Field, Charged Particles	R. Sagalyn	Partial
5 Apr 72	ADTC	Niro	Density and Winds Chemical Release	K. Vickery	Success
10 Apr 72	ADTC	Niro	Neutral Composition (A) Chemical Release	K. Vickery	Success
12 Apr 72	ADTC	Niro	Chemical Release (TMA)	K. Vickery	Success
12 Apr 72	ADTC	Niro	Neutral Composition (Mass Spectrometer) (ALADDIN II)	C. Philbrick	Success
12 Apr 72	ADTC	Niro	Neutral Composition (Mass Spectrometer) (ALADDIN II)	C. Philbrick	Success
12 Apr 72	ADTC	Nike Tomahawk	Chemical Release and Density (7" Sphere)	N.W. Rosenberg	Success
12 Apr 72	ADTC	Niro	Chemical Release and Density (7" Sphere)	A. Faire and N.W. Rosenberg	Success
12 Apr 72	ADTC	Niro	Density (7" Sphere)	A. Faire	Success
12 Apr 72	ADTC	Niro	Neutral Oxygen, Wind and Temperature	N.W. Rosenberg	Success
13 Apr 72	ADTC	Niro	Neutral Oxygen, Wind and Temperature	N.W. Rosenberg	Success
13 Apr 72	ADTC	Niro	Neutral Oxygen, Wind and Temperature	N.W. Rosenberg	Success
14 Apr 72	ADTC	Niro	Vertical Winds (Chemical Release)	N.W. Rosenberg	Success
14 Apr 72	ADTC	Patute Tomahawk	Ultraviolet Photoionization Wavelength, Rocket Test	N.W. Rosenberg	Success
14 Apr 72	ADTC	Aerobee 170	IR Stellar Sources (Project Hi-Star)	R. Walker	Success
14 Apr 72	WSMR	Nike Tomahawk	Magnetic Field and Electron Measurements	B. Shuman	Success
1 May 72	CRR	Nike Tomahawk	Magnetic and Electric Field, and Electron Measurements	R. Vancouver	Success
1 May 72	CRR	Niro	Project Chaser - Missile Optical Radiation Measurements	R. Huffman	Failure (V)
20 Jun 72	VAFB	Aerobee 170			

•(P) — Payload
(V) — Vehicle

Appendix C

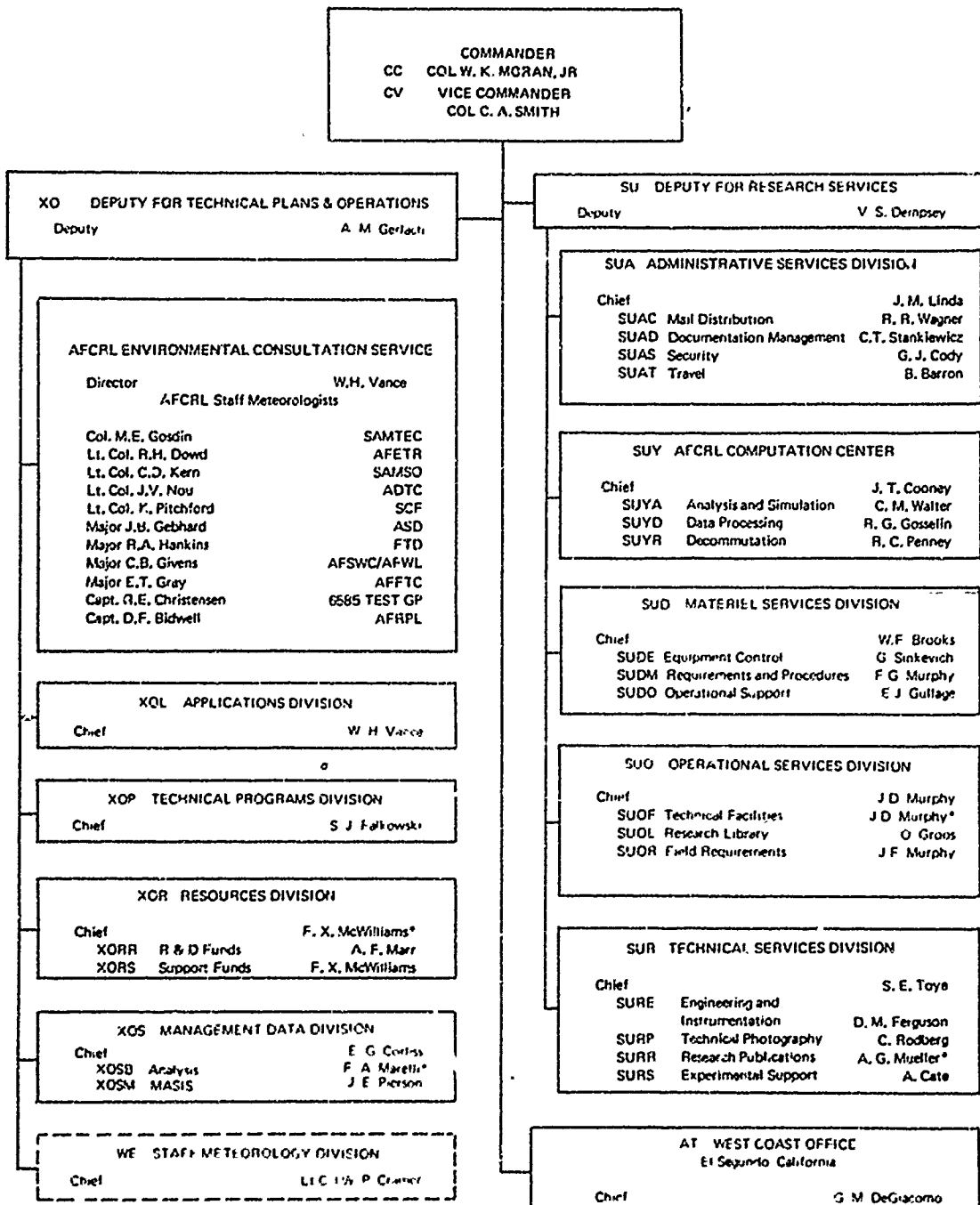
Air Force Cambridge Research Laboratories

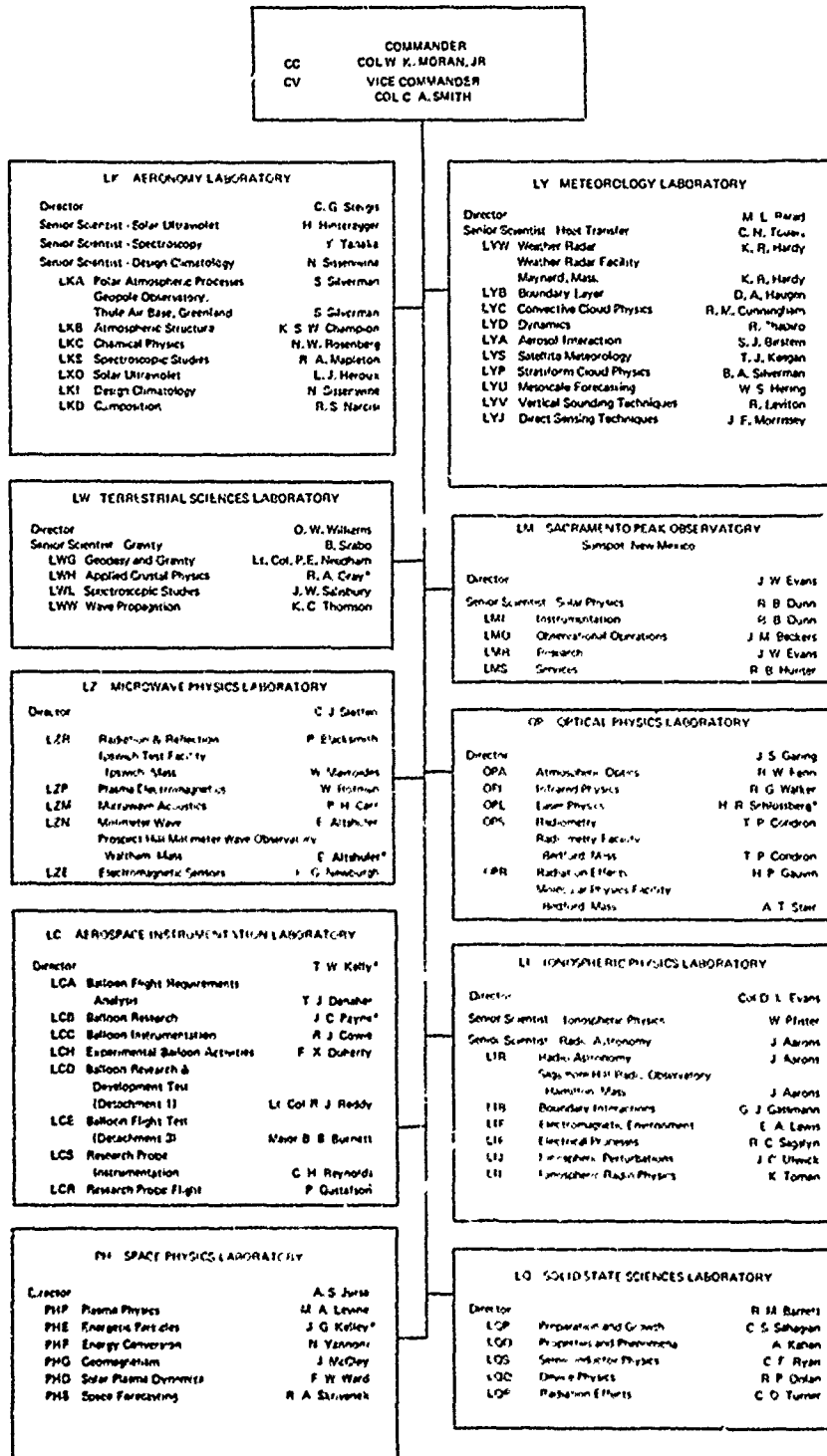
L. G. HANSCOM FIELD, BEDFORD, MASS.



AS OF 30 JUNP 1972

*ACTING





ACKNOWLEDGMENTS

The Editor gratefully acknowledges the support of the Directors of the AFCRL Laboratories who provided the material describing their respective research programs, determined the emphases to be given the research areas, and reviewed material for technical accuracy. Additionally, the Editor gratefully acknowledges the invaluable assistance, understanding and patience of two members of the Office of the Chief Scientist—Paulette Loiselle for typing the many manuscript pages, for collecting, editing and typing of bibliographic material, and for her attention to detail; and Henry Novak for suggesting revisions which brought about improvement in tone, texture and flow of language and dignity of presentation, and for his encouragement when it was so necessary. Special thanks are given to Diane Bouvier and Muriel Cross of the Directorate of Research Services for the many hours unselfishly offered for typing and other special services needed to produce this *Report on Research*.